Christopher
R.J. Fennell

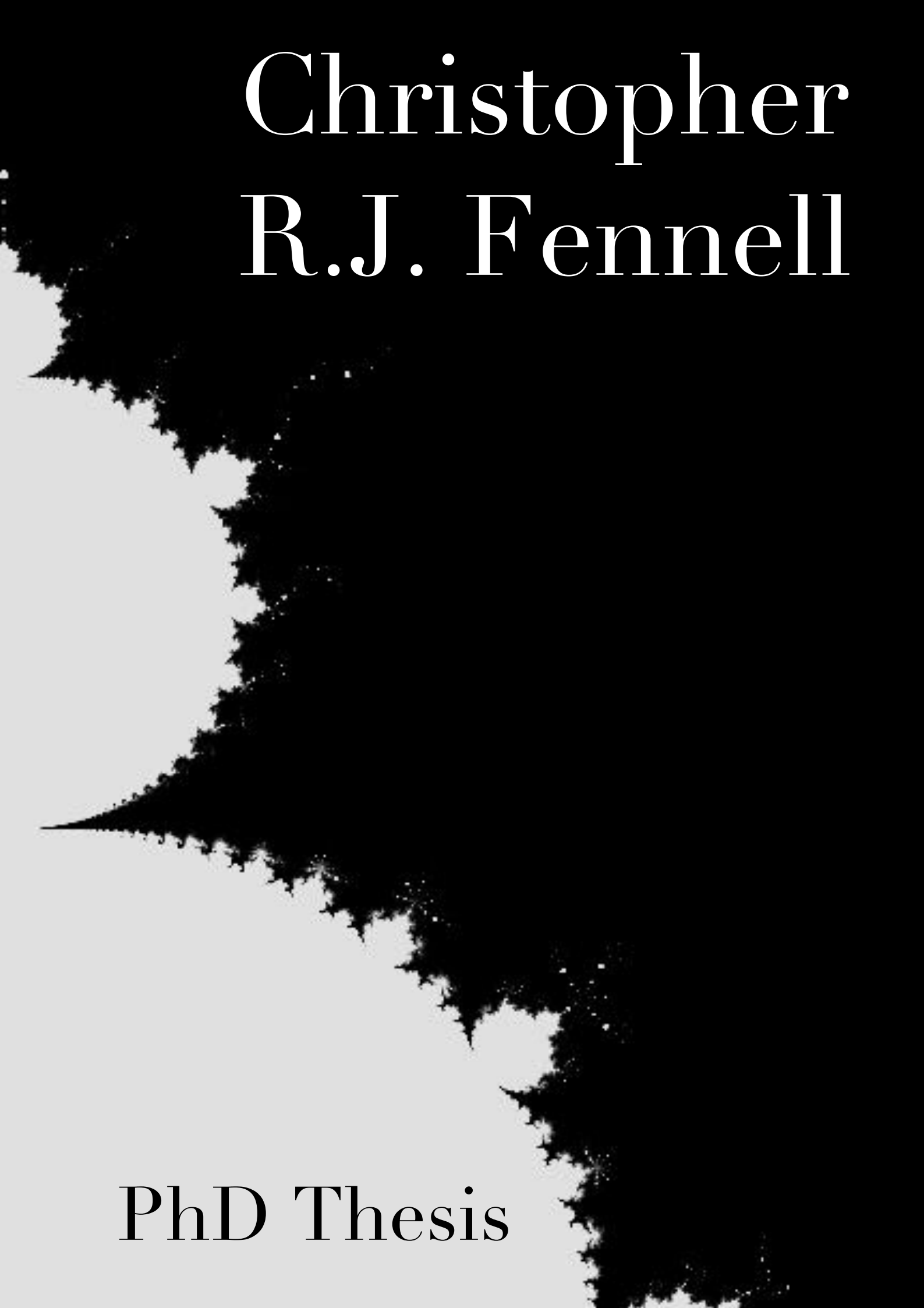

PhD Thesis

Complexities of Ageing

An Investigation of Age-Group Differences in Neuromuscular Complexity.

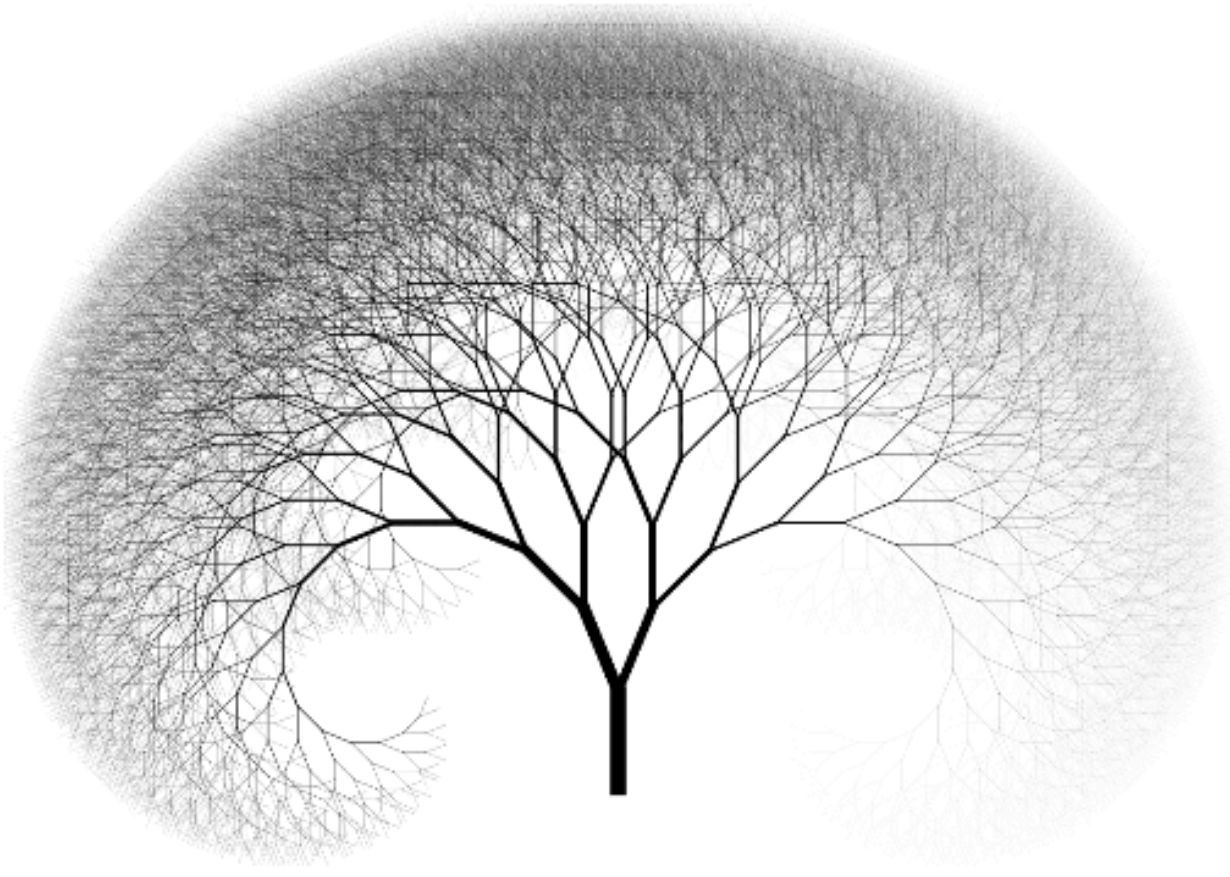

An Investigation of Age-Group Differences in Neuromuscular Complexity.

Christopher R.J. Fennell

A thesis submitted in partial fulfilment of the requirements of the University of Kent for the degree of Doctor of Philosophy

PhD

University of Kent

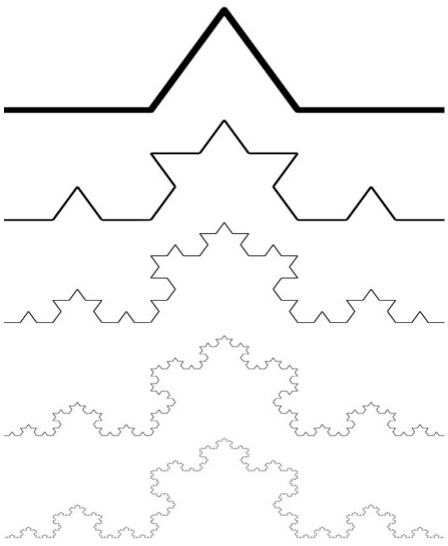

September 2024

Declaration

No part of this thesis has been submitted in support of an application for any degree or other qualification of the University of Kent, or any other University or Institution of learning.

Signed:

Acknowledgements

I would like to express my sincere gratitude to my supervisors, Professor James Hopker and Professor Lex Mauger, for their invaluable guidance throughout my PhD.

I am also thankful to the two hundred and four participants whose time and commitment made the experimental chapters of this thesis possible.

Publications

Fennell, C.R.J., Mauger, A.R., Hopker, J.G. (2024). Alpha band oscillations in common synaptic input are explanatory of the complexity of isometric knee extensor torque signals. *Experimental Physiology*, 1–17. https://doi.org/10.1113/EP092031.

Conferences

Fennell, C.R.J., Mauger, A.R., Hopker, J.G. (2024, July 2-5). *Fatigue-related increases in alpha band common synaptic input is explanatory of alterations in the structure of lower-frequency oscillations in knee extensor torque*. [Oral Presentation]. European College of Sport Science Conference, Glasgow, Scotland, United Kingdom.

Abstract

Neuromuscular complexity quantifies the temporal structure of muscle torque or force signals, providing a non-invasive measure of the neuromuscular system's functionality. Ageing has been identified as a contributing factor to the *loss of neuromuscular complexity,* proposed to reflect an age-related reduction in neuromuscular function, specifically a reduced capacity to effectively control voluntary muscle contractions. Notable gaps remain in the current understanding of how age influences neuromuscular complexity, particularly in knee extensor (KE) muscles and small hand muscles involved in precision pinch grip (PG) tasks. Additionally, the neurophysiological mechanisms underpinning age-related changes in neuromuscular complexity are not yet fully understood, and the functional importance of changes in neuromuscular complexity remains unclear. Therefore, the current thesis investigated age-group differences in the complexity of isometric KE torque and precision PG force signals, as well as the neural mechanism(s) underpinning the complexity of isometric muscle torque signals.

Chapter Four assessed the intra- and inter-day reliability of the complexity of isometric KE muscle torque signals in younger and middle-aged adults. The results indicated that measures of complexity exhibit moderate to excellent intra- and inter-day reliability across both age groups. These findings support neuromuscular complexity as a reliable, non-invasive technique for assessing and monitoring age-group related differences in neuromuscular function.

Chapter Five investigated age-group differences in the complexity of isometric KE muscle torque signals at 40% MVT and MVT. No differences in neuromuscular complexity were observed between middle-aged adults (58.6 ± 5.1 years) and younger adults (21.9 ± 3.7 years). However, age-related changes were evident in the temporal organisation of neuromuscular output, suggesting a possible restructuring of neuromuscular control strategies, that maintains motor performance with age.

Chapter Six investigated the effect of contraction intensity on age-group related differences in the complexity of isometric KE muscle torque signals. The study also examined the relationship between neuromuscular complexity and postural sway. Older adults (64.9 ± 11.3 years) demonstrated lower neuromuscular complexity across a range of contraction intensities (10% to 80% MVT) compared to younger adults (22.5 ± 3.4 years), with the most pronounced

age-group related differences occurring above 20% MVT. These findings suggest that impairments in muscle torque regulation in older age are exacerbated at higher contraction intensities. Additionally, lower neuromuscular complexity was associated with greater postural sway, highlighting the potential functional relevance of complexity.

Chapter Seven investigated age-group differences in the neuromuscular complexity of isometric precision PG force signals. Adults over the age of 70 years exhibited lower neuromuscular complexity than younger adults, aged 18 to 30 years. However, no differences in neuromuscular complexity were observed between younger adults and those aged 50 to 70 years. These findings suggest that measurable changes in hand muscle force regulation begin to emerge in the eighth decade of life, providing insight into the potential time course of age-related changes in hand muscle neuromuscular function.

Chapter Eight investigated the neural mechanism(s) that may underpin the complexity of isometric KE muscle torque signals. Chapter 8A investigated the association between the strength of common synaptic input to the motor neuron pool of the vastus lateralis muscle and the complexity of isometric KE torque in adults aged between 18 and 90 years. Stronger alpha frequency band oscillations in common synaptic input were found to be associated with higher complexity isometric KE torque signals. Chapter 8B investigated whether fatigue-related changes in the strength of common synaptic input to the motor neuron pool could explain fatigue-related changes in isometric KE torque complexity. Fatigue-related changes in the strength of alpha band oscillations in common input accounted for a significant percentage of the fatigue-related changes in isometric KE torque complexity. These findings suggest that the complexity of isometric muscle torque is attributable, in part, to the strength of oscillations in common synaptic input (an adaptive neural response) and is therefore indicative of the neuromuscular system's strategy to adapt muscle torque to meet task demands.

In conclusion, the thesis demonstrates that older adults exhibit lower neuromuscular complexity in both lower and upper extremity muscle groups compared to younger adults. The observed age-related differences in neuromuscular complexity were likely attributable, in part, to alterations in the strength of oscillations in common synaptic input. These findings highlight the potential of neuromuscular complexity as a reliable, functionally relevant, non-invasive biomarker for assessing and monitoring age-related changes in aspects of neuromuscular system function.

Table of Contents

Experimental Chapters

List of Tables

	Appendix	*Page*
Chapter Seven Part A	**Digital filtering of isometric precision pinch grip force signals.**	
Table 7.1a	Descriptive statistics and ANOVA results for the effect of Butterworth filter frequency and contraction intensity on the complexity, entropy and variability of the isometric precision pinch grip force signals.	331

List of Figures

Appendix

Chapter Seven Part A	**Digital filtering of isometric precision pinch grip force signals.**	*Page*

List of Abbreviations and Symbols

ACh	Acetylcholine
αMN	Alpha Motor Neuron
ADLs	Activities of Daily Living
ApEn	Approximate Entropy
ANOVA	Analysis of Variance
AP	Anterior-Posterior
Ca^{2+}	Calcium Ions
CSA	Cross-sectional Area
CApEn	Corrected Approximate Entropy
CV	Coefficient of Variation
CVF	Coefficient of Variation of Force
CVT	Coefficient of Variation of Torque
CV of ISI	Coefficient of Variation of Interspike Intervals
CI	Complexity Index
CI-28	Complexity Index (area) under 28 Coarse-grained Scales
CI-40	Complexity Index (area) under 40 Coarse-grained Scales
CST	Cumulative motor unit spike trains
CoP	Center of Pressure
DF	Dorsiflexors
DFA α	Detrended Fluctuation Analysis Scaling Exponent α
DR	Discharge Rate
EF	Elbow Flexors
ES	Effect Size

EEG	Electroencephalogram
GET	Gas Exchange Threshold
HG	Hand Grip
HD sEMG	High-density Surface Electromyography
iEMG	Intramuscular Electromyography
IFA	Index Finger Abductors
ISI	Interspike Intervals
IET	Incremental Exercise Test
ICC	Intraclass Correlation Coefficient
KE	Knee Extensors
METs	Metabolic Equivalents
MG	Middle Age Group
MSE	Multiscale Entropy
MVT	Maximal Voluntary Torque
MVF	Maximal Voluntary Force
MVC	Maximal Voluntary Contraction
MU	Motor Unit
ML	Medio-Lateral
MEG	Magnetoencephalography
MDC	Minimal Detectable Change
NMJ	Neuromuscular Junction
NCApEn	Normalised Corrected Approximate Entropy
NSampEn	Normalised Sample Entropy
OG	Older Group
OOG	Older-old Group

PF	Plantar Flexors
PG	Pinch Grip
PPS	Pulses Per Second
PSD	Power Spectral Density
PICs	Persistent Inward Currents
RET	Resistance Exercise Training
RMS	Root Mean Square
RMSE	Root Mean Square Error of Torque / Force
RCP	Respiratory Compensation Point
SR	Sarcoplasmic Reticulum
SampEn	Sample Entropy
SD	Standard Deviation
SDF	Standard Deviation of Force
SDT	Standard Deviation of Torque
SEM	Standard Error of Measurement
sEMG	Surface Electromyography
TTF	Time to Task Failure
VL	Vastus Lateralis
$\dot{V}O_{2peak}$	Peak Oxygen Uptake
WE	Wrist Extensors
WF	Wrist Flexors
YG	Younger Age Group

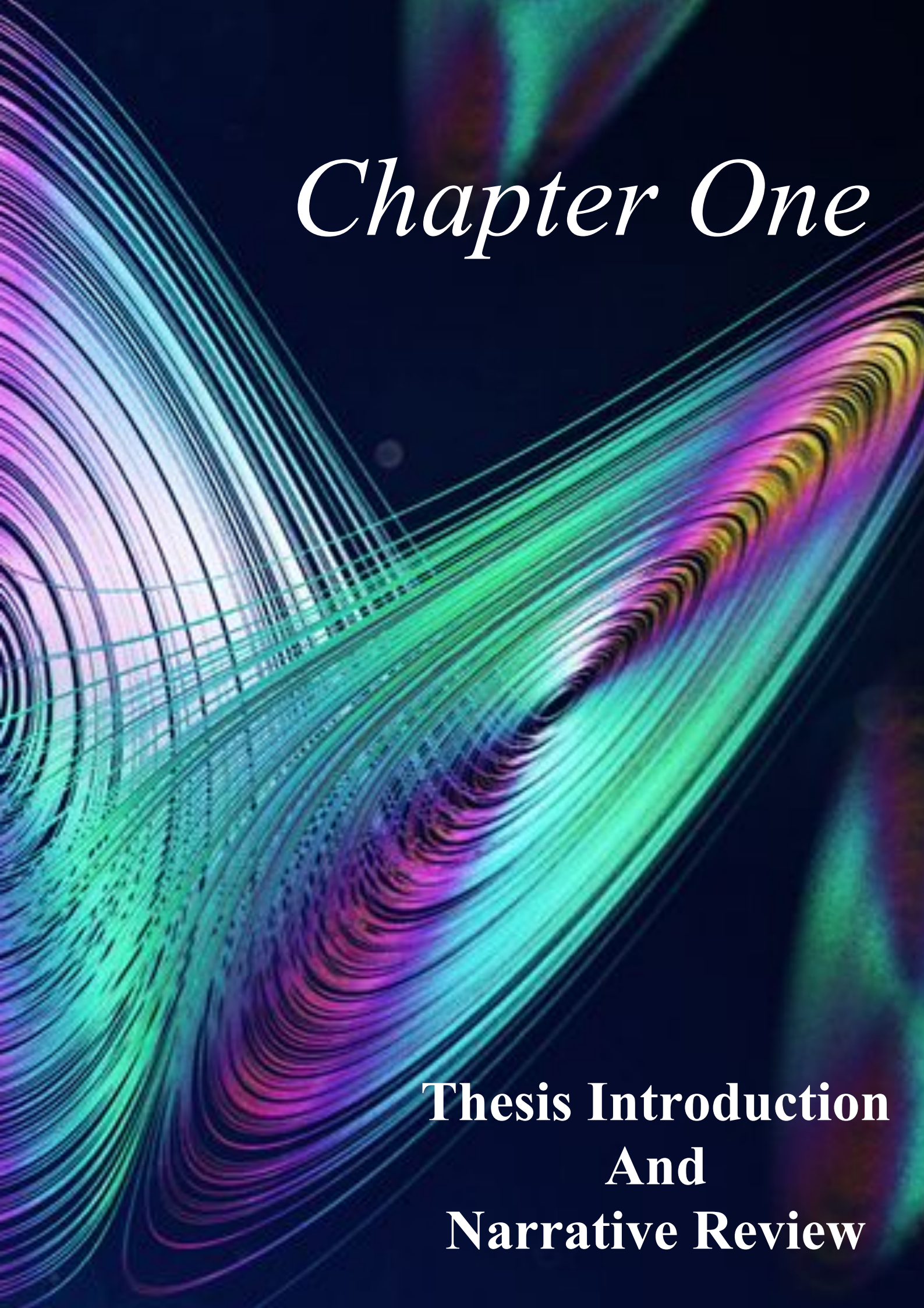

Chapter One

Thesis Introduction And Narrative Review

1.1 - The Ageing Neuromuscular System

"Lack of activity destroys the good condition of every human being, while movement and methodical physical exercise save it and preserve it." Plato.

Mechanisms of Muscle Contraction

Voluntary muscle contractions and thus, human movement is achieved through the complex interaction between the multiple components of the neuromuscular system. Motor units (MU), the smallest functional component of the neuromuscular system, are formed of one alpha motor neuron (αMN) and all the extrafusal muscle fibres it innervates (Eccles & Sherrington, 1930; Sherrington, 1925). The αMN receives synaptic inputs from afferent feedback (from muscle spindles and Golgi tendon organs), descending cortical and reticulospinal pathways, and neuromodulatory pathways from the brain stem (Enoka & Farina, 2021). When synaptic input is sufficiently strong, the αMN reaches its membrane threshold potential and generates an action potential (Heckman & Enoka, 2012). This action potential travels along the αMN's axon to the neuromuscular junction (NMJ; the nerve-muscle synapse), triggering the release of the neurotransmitter acetylcholine (ACh; Heckman & Enoka, 2012). ACh binds to receptor channels on the muscle fibre membrane, making it permeable to sodium (Na^+) and potassium (K^+) ions (Purves et al., 2018). The influx of Na^+ depolarises the membrane, generating a muscle action potential that propagates along the fibre, initiating the contraction of the sarcomeres (Purves et al., 2018).

Sarcomeres, the contractile units of muscle fibres, are formed of thick (myosin) and thin (actin) filaments (Huxley, 1957). Myosin molecular heads attach to binding sites on the actin filaments, forming cross-bridges (Milligan & Flicker, 1987). The propagation of the muscle action potential along the fibre triggers the release of calcium ions (Ca^{2+}) from the sarcoplasmic reticulum (SR; Gordon et al., 2000). Ca^{2+} binds to the troponin-tropomyosin complex, causing a conformational change that exposes the actin binding sites, enabling cross-bridge cycling. This cycle, comprising attachment, power stroke, and detachment of the myosin head from the actin filament is powered by adenosine triphosphate hydrolysis (Gordon et al., 2000). Reuptake of Ca^{2+} into the SR via the Ca^{2+}-ATPase pump terminates the contraction, allowing the muscle to relax. This signalling pathway, known as excitation-contraction coupling, enables muscle contraction and transmission of force via the muscle-tendon complex (Sandow, 1952).

Muscle force is produced through the filtering of neural drive (summation of all MU discharges) with the average twitch force of the active MUs (Farina et al., 2014; Farina & Negro, 2015). Two primary mechanisms determine the amount of muscle force produced: MU recruitment, which involves increasing the number of active MUs, and rate coding, which refers to the frequency of motor neuron action potential discharge (Enoka & Duchateau, 2017; Fuglevand et al., 1993). As synaptic input increases, MUs are recruited sequentially, starting with smaller, low-threshold MUs (αMN innervating the fewest muscle fibres) and progressing to larger, high-threshold MUs (αMN innervating the most muscle fibres). Simultaneously, the discharge rate of all recruited MUs increases, with low-threshold MUs typically firing at higher frequencies than high-threshold MUs (Adrian & Bonk, 1929).

Muscle strength, defined as the maximum voluntary force a muscle or muscle group can generate, is determined by MU recruitment and discharge rate, in addition to muscle fibre composition, and muscle cross-sectional area (CSA; Hunter et al., 2016). Muscle power, the product of force and velocity, is the ability of a muscle or muscle group to generate maximum force in the shortest possible time (Kent, 2006). It is influenced by several factors, including peak force capacity, contraction velocity, myosin content and motility (speed), muscle CSA, fibre composition, and muscle architecture (such as fascicle length and pennation angle; McKinnon et al., 2017; Reid & Fielding, 2012).

The Ageing Neuromuscular System

Ageing is defined as "the process of growing old; or becoming elderly or aged" (OED, Online 2024). According to the World Health Organisation the number of people in the world over 60 years of age was 1 billion in 2019 and is projected to increase to 1.4 billion by 2030 and 2.1 billion by 2050 (data from who.int). Over the next 25 years in the United Kingdom the number of people over 67 years old is projected to increase from 12.3 to 15.9 million and with increases in life expectancy, the number of people over 85 years old is projected to nearly double from 1.6 to 3 million by mid 2043 (data from ons.gov.uk). With a growing ageing population, the deleterious effects associated with an ageing neuromuscular system, such as sarcopenia and dynapenia, that impact daily-living and independence will become ever more prominent. Therefore, it is also of importance that there is continued research and development of methods that can be used in the assessment and monitoring of age-related changes to the neuromuscular system.

Sarcopenia and dynapenia encompass reductions in muscle mass, muscle quality, strength, power and physical function in older age (Allen et al., 2021; Cruz-Jentoft et al., 2019). The age-related reduction in muscle strength begins approximately around the fourth decade of life (Lindle et al., 1997) and has been shown to decline at a rate of 1% to 2% per year after the sixth decade (Frontera et al., 2000; Skelton et al., 1994). By comparison, muscle power exhibits a steeper decline, decreasing at 3.5% per year after the sixth decade, due to the independent influence of ageing on muscle force and contractile velocity (McNeil et al., 2007; Skelton et al., 1994). Functionally, these reductions in muscle strength and power were associated with reduced mobility (Bean et al., 2002), increased incidence and risk of falls (Perry et al., 2007; Skelton et al., 2002; Yeung et al., 2019), loss of independence (Foldvari et al., 2000; Yoshimura et al., 2018) and increased all-cause mortality (Liu et al., 2017; Metter et al., 2004) in older age.

Progressive structural and functional changes to the components of the neuromuscular system (αMNs, NMJ and muscle fibres) underpin the loss of muscle strength and power with ageing (Hunter et al., 2016; McKinnon et al., 2016). The apoptosis of spinal motor neurons and degeneration of distal axons occurs from around the seventh decade and results in a loss of muscle fibre innervation by αMN's (Campbell et al., 1973; Tomlinson & Irving, 1977). Throughout life the collateral re-innervation of orphaned muscle fibres by axonal sprouting of adjacent αMNs helps maintain muscle mass and strength until MU death accelerates and exceeds re-innervation in older age (Gordon et al., 2004; McNeil et al., 2007; Tam & Gordon, 2003). Older adults have been reported to have over 30% fewer MUs across both upper (Campbell et al., 1973; Doherty & Brown, 1993; Power et al., 2012) and lower (Hourigan et al., 2015; Piasecki et al., 2016a) limb muscles than younger adults. The process of denervation with ageing results in fewer, larger surviving MUs, that discharge action potentials at slower more variable rates in upper and lower limb muscles (Barry et al., 2007; Connelly et al., 1999; Kamen et al., 1995; Piasecki et al., 2016b; Tracy et al., 2005).

The age-related loss of MUs leads to the reduction in muscle fibre CSA across all fibres (Type I and II; Lexell et al., 1983), with evidence indicating greater atrophy of Type II muscle fibres that express myosin heavy chain IIa and IIx (MHC IIa and IIx) isoforms (Horwath et al., 2024; Klein et al., 2003; Lexell et al., 1988; Purves-Smith et al., 2014; Sundberg et al., 2025). Loss of MUs, atrophy and loss of individual muscle fibres were the primary cause of the age-related

reduction in whole muscle CSA, and consequently, muscle strength and power (Campbell et al., 1973; Frontera et al., 2000; Lexell, 1995; Lexell et al., 1988; Sundberg et al., 2025). Additionally, older adults have been found to exhibit lower and more variable levels of voluntary activation than young adults, with inadequate activation of surviving MUs potentially contributing to age-related declines in strength and power (De Serres & Enoka, 1998; Knight & Kamen, 2008). Though age-related differences in voluntary activation may be mitigated with practice of maximal isometric contractions (Hunter et al., 2008; Klass et al., 2007; Molenaar et al., 2013).

The lower proportional area of Type II fibres (i.e., greater Type I to II fibre ratio) that express MHC isoforms IIa and IIx in older adults is associated with slower, less powerful muscle fibre contractile speeds (Canepari et al., 2010; D'Antona et al., 2003; Lamboley et al., 2015; Sundberg et al., 2025). Ageing has also been shown to result in alterations to muscle fibre architecture and function, including: a decrease in motor axon conduction velocity (Rivner et al., 2001; Vandervoort, 2002), decreased myosin motility (slowed filament sliding speed) in both Type I and II fibres (Hook et al., 2001), decreased myosin content relative to fibre CSA (fewer actin-myosin interactions; D'Antona et al., 2003), myosteatosis (infiltration of non-contractile connective tissue and adipose; Miljkovic & Zmuda, 2010; Overend et al., 1992), reduced single muscle fibre elasticity (Ochala et al., 2008), decreased tendon stiffness (stretching sarcomeres, decreasing actin-myosin overlap; Narici et al., 2008), and a decrease in Ca^{2+} reuptake into the SR (Hunter et al., 1999). Collectively, the greater whole muscle Type I to II fibre area ratio, along with alterations to muscle fibre architecture and function, contribute to the age-related reduction in muscle force and contractile velocity, and therefore muscle power.

There is indirect evidence of NMJ structural remodelling with human ageing, including a decrease in vesicles in the pre-synaptic terminal, more dispersed postsynaptic endplate area and reduced ACh release (Deschenes, 2011; Jang & Van Remmen, 2011). Ageing has also been shown to result in impaired NMJ transmission in humans (Hourigan et al., 2015; Stalberg & Sonoo, 1994). NMJ transmission is the process involving the release of ACh from the αMN and the binding to the synaptic region of the muscle fibre (Jones et al., 2022) and can be assessed *in vivo* in humans using intramuscular electromyography (iEMG) to measure the variability in a single MU discharge shape, also known as the "jiggle" statistic (Hourigan et

al., 2015; Stalberg & Sonoo, 1994). Greater "jiggle" in older adults compared to younger adults indicates decreased NMJ transmission stability (Hourigan et al., 2015; Stalberg & Sonoo, 1994). These age-related structural and functional changes to the NMJ may lead to less efficient muscle contractions, contributing to the decline in muscle strength and power in older age.

Fatigability with Ageing

Neuromuscular fatigue is an exercise-induced reduction in muscle force and/or power generating capacity (Taylor & Gandevia, 2008). In older adults' greater muscle fatigue could under some circumstances potentially exacerbate the age-related loss of muscle strength and power, further challenging motor function and performance. Indeed, a consequence of the previously discussed age-related changes to the components of the neuromuscular system is the effect on muscle fatigability in older adults, which varies depending on mode (isometric vs. dynamic tasks), intensity, and velocity of contraction (Allman & Rice, 2002; Christie et al., 2011).

During submaximal and maximal isometric contractions older adults (60 to 75 years) were typically less fatigable than younger adults due to slower contractile properties, a shift toward a greater proportion of Type I fibres, and reduced reliance on glycolytic metabolism, leading to lower accumulation of metabolites that impair force generation, such as hydrogen ions and inorganic phosphate (Callahan et al., 2016; Hunter et al., 1999; Hunter et al., 2005; Hunter et al., 2008; Kent-Braun, 2009; Lanza et al., 2007). However, older old adults (> 75 years) appear to exhibit greater fatigability during isometric contractions (Justice et al., 2014). Though the mechanisms underpinning the diminished fatigue resistance to isometric contractions in older old age remain unclear.

For dynamic contractions, especially performed at high velocities, older adults show greater fatigability than younger adults (Callahan & Kent-Braun, 2011; Dalton et al., 2010; Dalton et al., 2012; Wallace et al., 2016), with advanced ageing (> 80 years) leading to even greater fatigability than in older adults aged 60 to 70 years (McNeil & Rice, 2007). By comparison, age-related differences in fatigability were less pronounced for both upper and lower limb muscle groups during slower velocity dynamic contractions (< 180 deg/s; Callahan et al., 2009; Dalton et al., 2012; Yoon et al., 2014). These velocity-dependent differences in fatigability can be attributed to age-related declines in muscle contractile speed and slower shortening

velocities in older adults (Baudry et al., 2010; Callahan & Kent-Braun, 2011; Yoon et al., 2014).

Physical Activity and Neuromuscular Function

The age-related decline in neuromuscular function, including muscle strength and power, can be partially mitigated by undertaking regular physical activity throughout life and into older age (Cartee et al., 2016; Henwood et al., 2008; Moro et al., 2017; Zampieri et al., 2015). Resistance exercise training (RET) is a particularly effective intervention for increasing whole muscle CSA and therefore muscle strength and power in older adults over 60 years of age (Henwood et al., 2008; Hangelbroek et al., 2018; Moro et al., 2017; Stec et al., 2017). Initial improvements in muscle strength and power with RET, not explained by muscle hypertrophy, were likely attributable to neural adaptations, including increased MU discharge rates and lowered MU recruitment thresholds (Christie & Kamen, 2010; Del Vecchio et al., 2019; Kamen & Knight, 2004; Patten et al., 2001).

There is also evidence of chronic exercise enhancing the re-innervation of denervated muscle fibres, through the promotion of axonal sprouting and NMJ formation, which may attenuate the age-related loss of MUs and preserve MU function with ageing (Mosole et al., 2014; Power et al., 2010; Power et al., 2016; Piasecki et al., 2019; Tam & Gordon, 2003). Lifelong endurance exercise training may also have neuroprotective effects, with masters athletes (aged > 60 years) reported to have attenuated age-related declines in MU number, muscle mass and strength (Power et al., 2010; Power et al., 2016; Piasecki et al., 2021a; Wroblewski et al., 2011; Zampieri et al., 2015). However, evidence for the neuroprotective effect of endurance exercise is equivocal, with research finding there to be no preservation of MUs in masters athletes compared with age-matched controls (Piasecki et al., 2016c).

Measuring Neuromuscular Function

The measurement of muscle strength and power can serve as an overall indicator of age-related changes in neuromuscular function (Hunter et al., 2016; McKinnon et al., 2017). However, the investigation of age-related structural and functional changes to individual components of the neuromuscular system (αMNs, NMJ and muscle fibres) in humans requires a diverse array of invasive and non-invasive techniques. High-density surface electromyography (HD sEMG) and iEMG can be used to estimate MU number, muscle action potential, surface MU potential,

and MU size (Piasecki et al., 2016a). The recording of multiple MU discharges with HD sEMG can be used to estimate the strength and variance of common synaptic input to the MU pool (Avrillon et al., 2021; Dideriksen et al., 2018). Functional NMJ transmission stability or "jiggle" can be measured *in vivo* in humans using iEMG by measuring the variability in consecutive MU potentials (Stalberg & Sonoo, 1994) or near fibre MU potentials (Piasecki et al., 2021b). Structural imaging of the NMJ in humans can be achieved with targeted muscle biopsy techniques, where muscle stimulation identifies high density NMJ areas for improved yield (Aubertin-Leheudre et al., 2020).

Age-related changes in total muscle CSA can be evaluated using non-invasive imaging techniques, including ultrasound (Young et al., 1984), computed tomographic imaging (Fiatarone et al., 1994), magnetic resonance imaging (Maden-Wilkinson et al., 2013), and dual-energy X-ray absorptiometry (Maden-Wilkinson et al., 2013). While muscle fibre type, contractile properties, and the regulation of muscle contraction at a single muscle fibre level can be investigated in humans using invasive muscle biopsy techniques (Cristea et al., 2008; D'Antona et al., 2003; Delbono et al., 1997; Fitts et al., 1989; Korhonen et al., 2006; Larsson, 1990; Larsson & Moss, 1993; Yu et al., 2007).

Neuromuscular function can also be assessed by examining the temporal and spatial structure of isometric muscle torque and force signals, by using signal analysis techniques to quantify the *complexity, entropy* and *variability* of the signal (Pethick et al., 2021b). The temporospatial structure inherent to isometric muscle force signals is thought to emerge from the coordinated interactions among the multiple components of the neuromuscular system responsible for the production and control of muscle contractions (Vaillancourt & Newell, 2002; Vieluf et al., 2015). Therefore, age-related structural and functional changes to individual components, along with systemic reorganisation of their interactions within the neuromuscular system, may alter the temporospatial structure of the muscle force signal. Thus, measuring the temporospatial structure of isometric muscle force signals offers a promising, effective non-invasive biomarker for assessing and monitoring age-related changes in neuromuscular system function. The following section of this narrative review discusses the development and application of signal analysis techniques, derived from nonlinear dynamics and information theory, that offer a novel avenue to explore age-related changes in neuromuscular function.

1.2 - Neuromuscular Complexity

"Chaos: When the present determines the future, but the approximate present does not approximately determine the future." Edward Lorenz

History and Background of Physiological Complexity

In the 19th century, French mathematician Henri Poincare noted there was no simple solution to the three-body problem (Poincare, 2017 [Translation]). Poincare had shown that complex dynamical systems had apparently unpredictable behaviours, thus laying the foundations of what would later become known as *Chaos Theory*. In fact, during the latter 20th century there were a collection of scientists from different disciplines concurrently thinking about *Chaos Theory,* although most were unknown to one another. To these scientists, the apparent randomness in the output of a complex system was not arbitrary noise or error, but rather a measurable, deterministic pattern (May, 1976; May & Oster, 1976). Soon thereafter, *Chaos Theory* emerged as a distinct scientific discipline, focusing on the study of dynamical systems that exhibit complex behaviour, and are governed by deterministic laws (Ott, 2012).

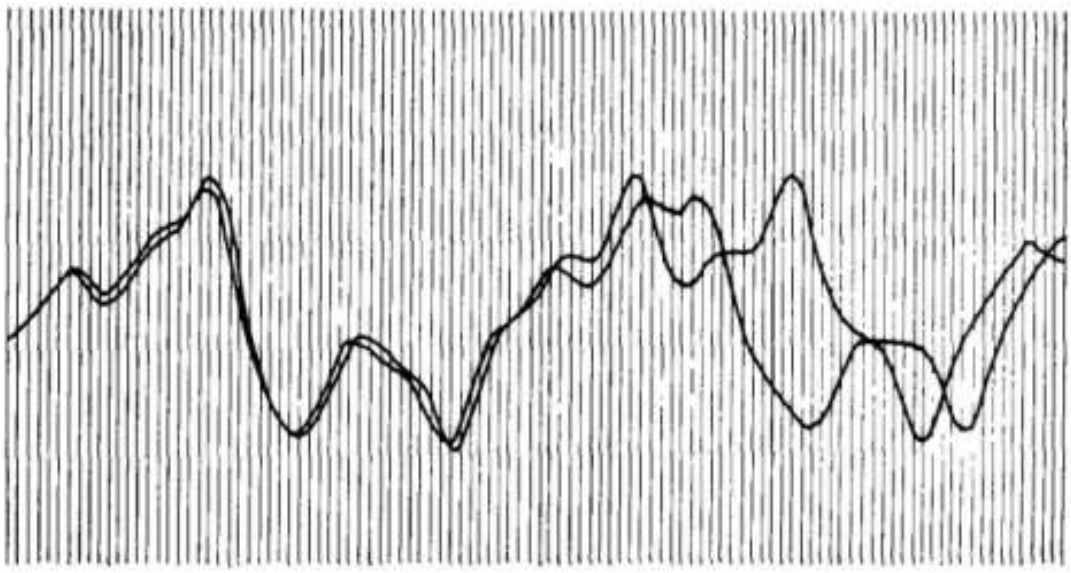

Figure 1.1. Edward Lorenz' weather simulation printout, a seminal moment in the development of Chaos Theory, illustrating the sensitive dependence on initial conditions of a dynamical system. After initially closely following the same path, the weather models diverge, due to small differences caused by a rounding error in the initial starting conditions.

Chaos theory introduced mathematical, numerical, and geometrical techniques that enabled scientists to study the behaviour of complex systems; systems that are inherently dynamic, nonlinear, and nonequilibrium (Ott, 2012). Early pioneers, such as Edward Lorenz, saw that short term predictions could be made of a complex dynamic system like the weather, although long term predictions were no better than guesses due to the sensitivity of the system to initial conditions (Figure 1.1; Lorenz, 1963; Lorenz & Haman, 1996). This illustrates the paradox of complex systems: they exhibit behaviour that is neither entirely random nor completely deterministic, but instead exists along a spectrum, between true randomness to perfect order.

Complex physiological systems, even under resting conditions, produce dynamic nonlinear outputs that are measurable across time, including, blood pressure dynamics (Kaplan et al., 1991), respiratory frequency (Peng et al., 2002), heart rate dynamics (Fennell et al., 2023; Goldberger, 1996; Lipsitz & Goldberger, 1992; Kaplan et al., 1991), and isometric muscle torque or force (Vaillancourt et al., 2002; Vaillancourt et al., 2004). These physiological systems can be described by their *emergent properties* (Delignieres & Marmelat, 2012; Peng et al., 2009). In other words, the whole system is greater than the sum of its parts and therefore cannot be understood by using a traditional reductionist approach (Delignieres & Marmelat, 2012; Peng et al., 2009). To understand the integrative behaviour and functioning of these systems, signal analysis techniques have been developed to quantify the degree of *complexity* of the system by examining the temporal structure of the dynamical nonlinear output (Costa et al., 2002; Pincus, 1991; Peng et al., 1994; Richman & Moorman, 2000). The temporal structure of physiological signals can be quantified by their *complexity;* defined as the degree of self-similarity of the fluctuations in the signal over multiple orders of temporal magnitude (Peng et al., 1994) and their *entropy;* defined as the regularity or randomness of the fluctuations in the signal across time (Richman & Moorman, 2000).

Complexity has been observed in various systems, including ion channel kinetics (Liebovitch et al., 1987), a dripping faucet (Shaw, 1984), the heating of gas inside a cylinder (Libchaber et al., 1982), the dynamics of an animal population (May, 1987; Tang & Chen, 2002) and the pathway to cardiac arrythmia (Garfinkel et al., 1992). Each system demonstrated the period doubling route to chaos; meaning the systems produced fluctuations that were self-repeating in periods of two, then four, and so forth until the periods were no longer regular or self-repeating. The plotting of the doubling periods for each system produces bifurcation diagrams as illustrated in the top image of Figure 1.2. Notably, bifurcation diagrams exhibit fractal-like

characteristics, as the structure is self-similar across multiple levels of magnification. Mathematician Benoit Mandelbrot popularised the term *fractal,* which is used to describe complex geometric structures and shapes that display self-similarity and fractional dimensionality (Eke et al., 2002; Mandelbrot, 1977; Mandelbrot, 1982). The Mandelbrot set depicted in Figure 1.2 is a famous visualisation of complex structure or an escape-time fractal, as it contains progressively finer recursive detail at increasing magnifications, which on the z-axis takes the form of a bifurcation diagram.

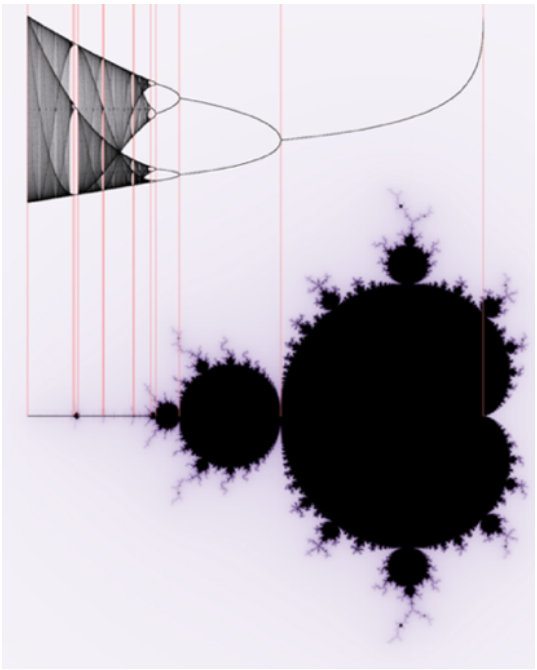

Figure 1.2. (Top) The bifurcation diagram and **(Bottom)** The Mandelbrot Set. The bifurcation diagram is the Mandelbrot Set from the z-axis and demonstrates fractal-like characteristics (i.e., appearing self-similar on multiple scales).

Approximate or statistical fractals are also found across nature, Benoit Mandelbrot proposed the coastline as an example in his work *How Long Is the Coast of Britain? Statistical Self-Similarity and Fractional Dimension* (Mandelbrot, 1967). Further examples of approximate fractal structures in nature include the human bronchial tree (Figure 1.3A; Glenny, 2011; Weibel & Gomez, 1962), river deltas (Figure 1.3B), the neurons of the retina (Caserta et al., 1995) and the His-Purkinje conduction system (Goldberger et al., 1985).

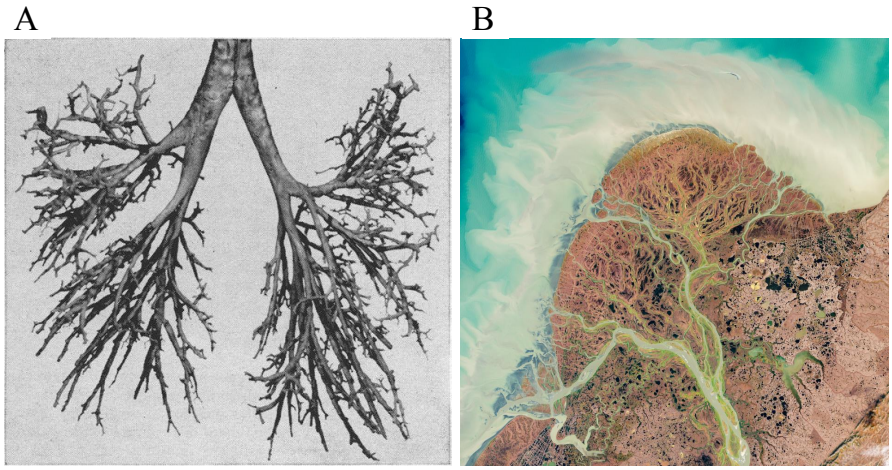

Figure 1.3. Examples of fractal-like geometry and self-similarity in nature **(A)** Image of a human bronchial tree from Weibel & Gomez, (1962), **(B)** Image of the Yukon River delta from earthobservatory.nasa.gov.

Unlike mathematical fractals (e.g., Sierpinski triangle or von-Koch curve) that are exact repeating patterns at different levels of magnification, most natural fractals are statistical fractals (Eke et al., 2002). This means that their self-similarity is only present in between statistical populations of observations of a given feature made at different scales (Eke et al., 2002). Importantly, *complexity* is also seen in physiological signals, with fluctuations in isometric muscle torque or force signals (Vaillancourt & Newell, 2003) and the oscillations in the beat-to-beat intervals of the heart (Figure 1.4; Goldberger, 2006) demonstrating statistical self-similarity over multiple orders of temporal magnitude (i.e., displaying fractal-like characteristics).

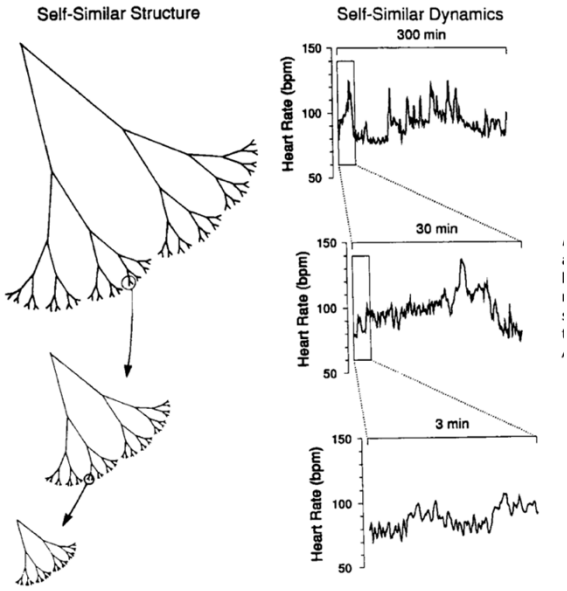

Figure 1.4. **(Left)** Self-similar structure across multiple levels of magnification, **(Right)** Example of self-similar structure in a recording of healthy beat-to-beat intervals of the heart, whereby the heart rate signal is statistically self-similar on different time scales (i.e., the signal demonstrates fractal-like characteristics). From Goldberger, (2006).

In 1948 Claude Shannon published "The mathematical theory of communication" and thus laid the foundation for Information Theory (Shannon, 1948). Central to information theory is the measure of (un)certainty or probability; in essence the greater uncertainty or lower probability of an outcome, the more information that is required to communicate or represent said outcome. The average amount of information required to convey an outcome when considering all possible outcomes was termed *entropy*. In other words, low probability events carry more information and high probability events carry less information.

For example, when taking a card from an unshuffled deck of standard playing cards (i.e., cards grouped in suits) there is more certainty and higher probability in the outcome, when compared to a well-shuffled deck which has more uncertainty and lower probability. As such, the well-shuffled deck carries more information and therefore has a higher *entropy*. Similarly, there is more information content (*entropy*) in the role of a fair six-sided dice, when compared with the flip of a coin. This is due to the greater probability in flipping a head or tail (probability of 1/2), when compared to rolling a specific number on a dice (probability of 1/6). Entropy statistics therefore provide a measure of the rate of new information generated over time in a physiological signal and can be interpreted as the amount of temporal regularity or irregularity in the signal (Pincus, 1991; Seely & Macklem, 2004).

Quantifying the Temporospatial Structure of Physiological Signals

The temporal structure or *complexity* of an isometric muscle force or torque signal can be quantified using the detrended fluctuation analysis (DFA) metric (Peng et al., 1994; Peng et al., 2000). The DFA metric measures the long-range fractal correlations within the signal, or in other words the statistically self-similarity of the signal across multiple temporal scales (Peng et al., 1994; Peng et al., 2000). The DFA analysis produces a scaling exponent α which provides a measure of the noise colour of a physiological signal (i.e., time series data). The DFA scaling exponent α can theoretically range from 0.5, indicating that each data point is random and independent from any previous or future data points (i.e., White noise), to 1.5, indicating a smooth signal with long term memory (i.e., Brownian noise; Goldberger et al., 2002a). The highest *complexity* isometric muscle force or torque signal would produce a scaling exponent α of 1.0 (i.e., 1/f or Pink noise). An α of 1.0 is indicative of a perfectly persistent signal, that is characterised by statistically self-similar fluctuations across multiple temporal scales (Goldberger et al., 2002a). An α between 0.5 and 1 indicates persistent long-

range power-law correlations, so that a large number is more likely to be followed by a large number and vice versa. While an α between 1 and 1.5 indicates correlations exist but were not power-law form (Peng et al., 1995).

Numerous entropy metrics have been developed to study the temporal structure of physiological signals, more common metrics being Approximate Entropy (ApEn) and Sample Entropy (SampEn) which measure the probability of patterns of length *m* and *m*+1 in a time series or the regularity and randomness of the signal (Pincus, 1991; Richman & Moorman, 2000). An ApEn or SampEn value close to 0 would indicate greater regularity or lower complexity in an isometric muscle force or torque signal (low rate of new information being generated over time; Pethick et al., 2021b). By comparison, a value closer to 2 would indicate greater irregularity or higher complexity in an isometric muscle force or torque signal (high rate of new information being generated over time; Pethick et al., 2021b). It is important to note however, that on their own entropy metrics may not strictly indicate changes or differences in the complexity of a physiological signal. For example, white noise, is a random signal with each value in the time series completely independent from previous or future values and is therefore a highly irregular signal. Consequently, white noise produces high ApEn and SampEn values but is not *physiologically* complex and produces a DFA scaling exponent α of 0.5.

Single-scale entropy metrics, such as ApEn and SampEn, only measure the regularity of fluctuations in a signal at one temporal scale, limiting their ability to capture the complex nonlinear behaviour of multi-component biological systems, such as the neuromuscular system (Costa et al., 2002; Costa et al., 2005). The multiscale entropy (MSE) analysis overcomes the limitations of single-scale entropy metrics by assessing the entropy of a physiological signal across multiple temporal scales, providing a more comprehensive understanding of the system's complex behaviour (Costa et al., 2002; Costa et al., 2005). Notably, the scale-to-scale dynamics (i.e., time dependent structure) of a physiological signal revealed by the MSE analysis is postulated to reflect the functioning and nonlinear interaction between different system components that operate on multiple temporal scales (Vieluf et al., 2015). Therefore, the entropy of the signal at specific temporal scales (i.e., regularity of a specific oscillatory frequency in the signal) is suggested to quantify the integrity of specific components and functioning of the systems underlying control processes that operate at the same time scale (Vieluf et al., 2015).

The MSE analysis has been demonstrated to be an efficacious signal analysis technique, able to discriminate between a normal 'healthy' electrocardiogram time series (beat-to-beat intervals of the heart) and an atrial fibrillation electrocardiogram time series (Costa et al., 2002). Furthermore, the MSE analysis has been used to detect age-related differences in electroencephalogram (EEG) and magnetoencephalography (MEG) time series data (McIntosh et al., 2014). The MSE analysis has been shown to be a promising quantitative tool for identifying pathological (Costa et al., 2002) and age-related (McIntosh et al., 2014) changes in physiological time series data. However, only a few studies have utilised the MSE analysis to study age-related changes in the temporal structure of force signals derived from isometric contractions of the upper limb muscles (Knol et al., 2019; Vieluf et al., 2015; Vaillancourt et al., 2004). Therefore, the MSE analysis is used throughout the experimental chapters of the current thesis as a primary *complexity* measure to provide new knowledge regarding the effect of age on the temporal structure of isometric muscle force and torque signals derived from both upper and lower limb contractions.

The spatial structure or *variability* of an isometric muscle force or torque signal can be quantified using the standard deviation of the force signal (SDF) as a measure of absolute signal variability and the coefficient of variation of the force signal (CVF) as a measure of signal variability normalised to the mean of the signal (Pethick et al., 2021b). The combined use of the *complexity* (e.g., DFA and MSE), *entropy* (e.g., SampEn) and *variability* (e.g., CVF and SDF) metrics is necessary for comprehensively assessing the temporospatial structure of an isometric muscle force or torque signal. This multi-metric approach is used in the experimental chapters of the thesis to assess age-group related differences in muscle force and torque signal structure and therefore neuromuscular system function.

Neuromuscular Complexity and Variability with Ageing

Neuromuscular complexity and variability refer to the complexity and variability of a torque or force signal produced by a contracting human skeletal muscle or muscle group. These measures provide valuable insight into the production and control of muscle force by the neuromuscular system and are used as indicators of an individual's ability to produce precise, task-relevant levels of force or torque (Enoka et al., 2003; Hepple & Rice, 2016; Morrison & Newell, 2012; Pethick et al., 2021). Additionally, it has been suggested that an individual's neuromuscular complexity under baseline 'resting state' conditions, typically assessed via the

complexity of a force or torque signal during an unfatigued, constant-load isometric muscle contraction with visual feedback of the target force or torque line, may be indicative of the neuromuscular system's capacity to respond to perturbations; in other words, the system's adaptability (Lipsitz, 2002; Morrison & Newell, 2012; Manor & Lipsitz, 2013; Peng et al., 2009; Vaillancourt & Newell, 2002). Perturbations or task demands relevant to the neuromuscular complexity of lower and upper limb muscles may include sudden changes in external resistance or force demands during voluntary limb movement (e.g., lifting unstable objects or encountering unexpected mechanical resistance), externally applied mechanical disturbances (e.g., unanticipated trip perturbation or support surface translations), and dual-tasking involving cognitive-motor interference. Effective adaptation to such challenges requires dynamic modulation of muscle activity, highlighting the potential functional relevance of neuromuscular complexity in assessing motor adaptability.

Despite these theoretical links, there is currently limited experimental evidence directly connecting baseline neuromuscular complexity to system adaptability. However, baseline complexity in other physiological system outputs has been associated with adaptability, suggesting that neuromuscular complexity may similarly reflect the system's capacity to respond to perturbations or changing task demands (Bigger et al., 1996; Ho et al., 1997; Manor et al., 2010). For example, older adults with lower baseline postural sway complexity demonstrated greater absolute and relative increases in sway speed when transitioning from quiet standing to a cognitively demanding dual-task (i.e., verbalised serial subtractions), indicating reduced adaptability of the postural control system to experimentally induced perturbation (Manor et al., 2010). Likewise, research has demonstrated that the complexity of heart rate fluctuations (i.e., R-R interval complexity) were associated with survival rates in patients with heart failure (Ho et al., 1997) and acute myocardial infarction (Bigger et al., 1996), suggesting that higher physiological complexity may reflect a more adaptable system. These associations suggest that greater physiological complexity reflects an enhanced capacity of the system to adapt and respond effectively to perturbation.

Researchers have supported the postulate that lower neuromuscular complexity reflects a reduced adaptive capacity of the neuromuscular system, suggesting it indicates a diminished ability to adaptively modulate the excitatory and inhibitory properties of neural oscillators that provide amplitude- and frequency-varying input to the motor neuron pool, which regulates muscle force control (Sosnoff et al., 2004). In young adults, neural oscillators operate across

multiple time scales, leading to a more complex force signal, and enabling dynamic adaptability in force production to match the task demand (Kilner et al., 1999; Sosnoff et al., 2004). However, it has been suggested that ageing leads to a shift toward fewer, stronger, and more dominant neural oscillators that operate across fewer time scales, contributing to a more structured force signal of lower complexity (Sosnoff et al., 2004; Vaillancourt & Newell, 2002). Older adults also exhibit a reduced ability to adaptively modulate the multiple neural oscillatory inputs, leading to impaired regulation of muscle force compared to younger adults (Vaillancourt & Newell, 2003). Thus, neuromuscular complexity is thought to serve as an indirect indicator of the neuromuscular system's adaptability in meeting task demands (Sosnoff et al., 2004).

Older adults have typically been found to exhibit worse muscle force control, quantified by a lower neuromuscular complexity and higher neuromuscular variability, than younger adults (Fiogbe et al., 2021; Knol et al., 2019; Pethick, 2023; Galganski et al., 1993; Vaillancourt et al., 2002; Vaillancourt & Newell, 2003). This age-related change in the ability to regulate the production and control of muscle force likely reflects impaired neuromuscular system functionality and adaptability (Manor & Lipsitz, 2013; Peng et al., 2009; Vaillancourt & Newell, 2002; Vieluf et al., 2015). However, age-related changes in neuromuscular complexity and variability were not consistently observed and likely influenced by factors such as contraction intensity and muscle group (Christou & Carlton, 2002; Enoka et al., 2003; Oomen & van Dieen, 2017; Pethick et al., 2022). Chapter Two explores this topic in depth, with a systematic review of the effect of age on the complexity, entropy, and variability of isometric muscle force signals.

Functional Importance of Neuromuscular Complexity and Variability in Ageing

Maintaining the ability to perform activities of daily living (ADLs) throughout life and into older age is essential for independent living (Mlinac & Feng, 2016). The age-associated decline in muscle force control, lower neuromuscular complexity and higher neuromuscular variability, has been shown to contribute to the reduced performance of the fundamental motor skills, manual dexterity, balance, and locomotion, which are essential to a wide range of ADLs (Almuklass et al., 2018a; Camacho-Villa et al., 2025; Feeney et al., 2018; Hirono et al., 2020; Hirono et al., 2021; Marmon et al., 2011a; Marmon et al., 2011b; Mear et al., 2023).

Manual dexterity is defined as the ability to coordinate small movements of the fingers and hands quickly and precisely (Gershon et al., 2010) and is primarily tested using a form of pegboard test (Reuben et al., 2013; Wang et al., 2011). Diminished manual dexterity and hand function has been suggested to be detrimental to basic ADLs (Jette et al., 1990) and can predict a loss of independence in older adults (Falconer et al., 1991; Ostwald et al., 1989). The study of Feeney et al. (2018) found that 58% of the variance in grooved pegboard times could be explained by age and the variability of force at 20% maximal voluntary force (MVF) during a double action wrist extensor (WE) and pinch grip (PG) task. Similarly, the time to complete the grooved pegboard test was found to be significantly associated with muscle force variability of index finger abductors (IFA; Hamilton et al., 2017; Marmon et al., 2011a & 2011b), WE (Almuklass et al., 2016) and the concurrent performance of WE and IFA (Hamilton et al., 2017) for both young and old adults. Supporting these findings, Semmler et al. (2000) demonstrated a concurrent reduction in pegboard performance and increase in the variability of IFA force in older adults.

Being able to maintain balance and postural control is necessary to the performance of ADLs. These activities can range from simple actions such as standing to more complex activities like walking and running on uneven surfaces, that can cause unsteadiness underfoot or unexpected disturbances such as tripping. Notably, the increased incidence of falls in older individuals has been associated with greater postural sway (Kang et al., 2013; Johansson et al., 2017; Melzer et al., 2004; Pajala et al., 2008; Sturnieks et al., 2008). Additionally, older adults with a history of falling have been shown to exhibit increased neuromuscular variability compared with non-fallers (Carville et al., 2007).

The ankle plantar flexor (PF) muscles are important to postural control (Masani et al., 2003) and have consequently been extensively employed when investigating the association between the neuromuscular variability and measures of postural sway. The variability of PF muscle force at 20% MVF was found to be significantly correlated with postural sway during bipedal stance on an unstable platform in older individuals (Hirono et al., 2021) and single-leg stance on an unstable platform in younger individuals (Hirono et al., 2020). In accordance, Oshita & Yano, (2012) demonstrated the variability of PF muscle force at 10% MVF but not 20% MVF, to be significantly associated with postural sway during bipedal stance on a stable and unstable platform in young adults. Moreover, they found that the sustainable time for single-leg stance

was strongly correlated with the variability of PF muscle force at 20% MVF, but not 10% MVF, in young adults (Oshita & Yano, 2010).

Furthermore, postural sway during quiet standing (maintaining an upright, stationary posture without any voluntary movement) was found to be positively correlated with the variability of PF muscle force at an intensity equivalent to the muscle activity required for quiet standing (≥ 5% MVF) in both young and old adults (Kouzaki & Shinohara, 2010). More recently, the complexity (SampEn) of isometric knee extensor (KE) torque signals were found to be explanatory of dynamic balance in healthy adults (Mear et al., 2023). While Davis et al. (2020) found the variability of force from the hip abductor, PF and dorsiflexor (DF) muscles to be the most consistent explanatory variables for postural sway, although no age-related differences were observed in these measures. In contrast, no relationship was found between the variability of PF muscle force at 5 and 10% MVF and postural sway in older women (Barbosa et al., 2018 & 2020).

Locomotion can be clinically measured using walking endurance tests, walking speed tests, chair rise tests and stair ascent and descent tests (Reuben et al., 2013). The variability of PF and DF muscle force at 20% MVF has been found to be significantly correlated with performance on the 6-minute walk test and 25 ft walk test in older individuals with an impaired walking ability due to multiple sclerosis (Almuklass et al., 2018a). A study of non-frail, pre-frail, and frail older adults (aged 75 to 79 years) found that non-frail individuals had faster walking speeds and sit-to-stand test times, when compared with pre-frail and frail individuals (Carnavale et al., 2020). The reduction in functional task performance in the frail group was also accompanied by a significant loss of muscle force control (measured by ApEn and SampEn), when compared with the non-frail group (Carnavale et al., 2020). However, in healthy older adults, no significant associations were found between the variability of PF and DF muscle force at 10 and 20% MVF and performance on the 400 m endurance test, walking speed over 10 m and a chair rise test (Mani et al., 2018). In the study of Seynnes et al. (2005), the variability of isometric KE muscle force at 50% MVF was significantly related to stair climbing and chair rise test performance, but not 6-minute walk test performance in older individuals. Conversely, Manini et al. (2005) found no relationship between the variability of KE muscle force at 50% MVF and the performance on the chair rise test and stair ascent and descent test in older individuals.

Research has shown neuromuscular variability to be associated with the performance of fundamental motor skills, which are essential for ADLs, in both older and younger adults (Almuklass et al., 2018a; Feeney et al., 2018; Hirono et al., 2020; Hirono et al., 2021; Marmon et al., 2011a; Marmon et al., 2011b). However, the limited research on the relationship between fundamental motor skill performance and neuromuscular complexity makes its functional significance unclear (Camacho-Villa et al., 2025). A progressive decline in neuromuscular complexity has been proposed as an indicator of deteriorating system functionality, where a critical loss of complexity may cause an individual to fall below the frailty threshold (Figure 1.5; Lipsitz, 2002). This proposal appears logical given a reduction in neuromuscular complexity may reflect impaired neuromuscular system functionality (Manor & Lipsitz, 2013; Peng et al., 2009; Vaillancourt & Newell, 2002; Vieluf et al., 2015). Therefore, a progressive decline in neuromuscular complexity may also contribute to reduced fundamental motor skill performance and, consequently, a diminished ability to perform ADLs. Further research is required to explore the relationship between the performance of fundamental motor skills and the complexity of isometric muscle force and torque signals. Such research would help clarify the functional impact of age-related changes in the complexity of isometric muscle force and torque signals.

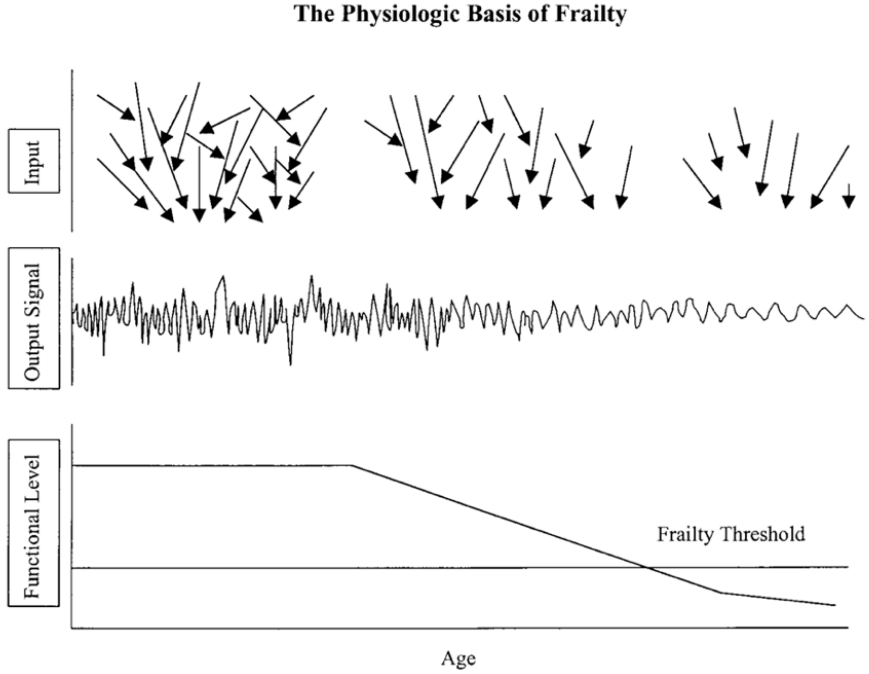

Figure 1.5. The physiologic basis of frailty reproduced from Lipsitz, (2002). **(Top)** Multiple interacting physiologic inputs **(Middle)** produce highly irregular, complex dynamics, **(Bottom)** which impart a high level of functionality on an organism. As the inputs and their connections degrade with age, the output signal becomes more regular and less complex, resulting in functional decline. Ultimately, with continued loss of physiologic complexity, function may fall to the critical level below which an organism can no longer adapt to stress (the frailty threshold).

Mechanisms Underpinning Neuromuscular Complexity and Variability

Total common synaptic input, which comprises the sum of control input, common noise, and independent noise, is transmitted to motor neurons and generates the neural drive to the muscle (Enoka & Farina, 2021; Heckman & Enoka, 2012; Negro & Farina, 2011). Muscle force is produced through the filtering of neural drive with the average twitch force of the active MUs (Farina & Negro, 2015). Independent synaptic inputs (independent noise) are predominantly filtered out by the twitch (temporal) and summation (spatial) filtering effects of the muscle (Dideriksen et al., 2012; Farina & Negro, 2015). Therefore, it is the fluctuations in the common input components (the control input and common noise) that were proposed to be a principal determinant of the spatial structure or *variability* of muscle force signals, with larger fluctuations in common noise resulting in a greater variability in the force signal (Negro et al., 2009; Farina et al., 2012). At lower contraction intensities, the fluctuations of both independent and common noise components likely to contribute to the variability of muscle force resulting in greater variability, with independent noise being progressively filtered out with increasing contraction intensity (Dideriksen et al., 2012; Farina & Negro, 2015).

The study of Feeney et al. (2018), found the variability of isometric muscle force to be significantly correlated with the estimated variance in common synaptic input in both young and older adults. Additionally, an age-related increase in the variability of isometric muscle force was found to be significantly associated with increased fluctuations in common synaptic input, but not with increases in independent synaptic input (Castronovo et al., 2018). Similarly, older adults were found to exhibit greater variability in isometric muscle force during steady voluntary and evoked isometric contractions compared to younger adults, a finding attributed to an increased variance in common synaptic input (Mani et al., 2019).

The properties of the MU population within specific muscles could potentially contribute to age-related changes in muscle force variability, namely the number of MUs, the size of MUs, the twitch and discharge rates of the MUs (Hunter et al., 2016). It has been suggested that muscles with fewer MUs are likely to be affected to a greater extent by the fluctuations transmitted by common noise due to reduced spatial filtering, thus increasing the variability of the muscle force signal (Dideriksen et al., 2012). However, evidence presented by several studies suggests that fewer and larger MUs do not contribute to the age-related increase in

isometric muscle force signal variability (DeFreitas et al., 2011; Keen et al., 1994; McNeil et al., 2005).

Ageing has also been shown to result in slower and more variable MU discharge rates (Orssatto et al., 2022; Soderberg et al., 1991; Taylor et al., 2000; Vaillancourt et al., 2003; Watanabe et al., 2016). Simulation (Moritz et al., 2005; Taylor et al., 2000) and experimental studies (Kallio et al., 2012; Laidlaw et al., 2000) have found greater variability in MU discharge rates to be associated with increased muscle force variability. Conversely, there is evidence to show MU discharge rates do not contribute to the age-related increase in muscle force variability (Barry et al., 2007; Castronovo et al., 2018; Semmler et al., 2000). Therefore, the fluctuations in common synaptic input transmitted by the motor neurons are likely to be one of the principal mechanisms responsible for the age-related increase in the variability of isometric muscle force signals. Although the origins for an age-related change in the variance in common synaptic input are yet to be established.

The research has primarily focused on investigating the mechanisms underlying neuromuscular variability, while the mechanisms governing neuromuscular complexity remain comparatively unexplored. Recent research found that EEG and surface EMG signal complexity could not explain the age-related differences in neuromuscular complexity (Raffalt et al., 2023). Therefore, it was suggested that age-related changes in the peripheral components of the neuromuscular system, specifically the muscle-tendon-skeletal connection, which translates neural signals into movement, may explain the age-related alterations in the temporal and spatial structure of muscle force signals (Raffalt et al., 2023).

With ageing, a decrease in tendon stiffness, an increase in tendon cross-sectional area, and a reduction in the Young's modulus of tendons (slope of the stress-strain relationship; McCrum et al., 2018) may impair the efficient transfer of force from muscle to bone. Additionally, age-related atrophy and the loss of individual muscle fibres (Lexell, 1995; Lexell et al., 1988), along with alterations in sarcomere architecture (D'Antona et al., 2003; Hook et al., 2001), may compromise contractile function and, consequently, muscle force control. Collectively, these changes to the peripheral components of the neuromuscular system may contribute to alterations in neuromuscular complexity and variability, ultimately affecting muscle force control.

Central mechanisms are also likely to determine the temporal structure of isometric muscle force signals, as oscillations in common synaptic input have been demonstrated to closely resemble the oscillations in muscle force signals (Dideriksen et al., 2012; Farina et al., 2014; Negro et al., 2009). It has therefore been speculated that the strength and variance of common synaptic input may be explanatory of the temporal structure or *complexity* of muscle force and torque signals (Pethick et al., 2016; Pethick et al., 2021b).

The exact mechanism(s) and their relative contribution to an age-related difference in neuromuscular complexity and variability are yet to be fully elucidated. However, it is reasonable to hypothesise that the components of the neuromuscular system involved in producing and controlling muscle force during isometric contractions each contribute, to varying degrees, to the age-related differences observed in neuromuscular complexity and variability. Research has demonstrated there to be age-related changes to components of the neuromuscular system, including impairments in component function (e.g., slower and more variable MU discharge rates, increased variability in common synaptic input, and reduced NMJ stability), alterations in component structure (e.g., increased MU size, greater Type I to Type II muscle fibre ratio and change in sarcomere architecture), and a reduction in the number of components (e.g., loss of MUs and individual muscle fibres; Hepple & Rice, 2016; McKinnon et al., 2016; Power et al., 2013; Piasecki et al., 2016a). These age-related structural and functional changes in the force-producing components of the neuromuscular system may be reflected in alterations to the temporospatial structure of the force signal, specifically as a lower signal complexity and a greater signal variability (Fiogbe et al., 2021; Knol et al., 2019; Pethick, 2023; Galganski et al., 1993; Vaillancourt et al., 2002; Vaillancourt & Newell, 2003).

Loss of Complexity Hypothesis

As discussed in the previous section, the exact mechanism(s) underpinning the age-related loss of neuromuscular complexity remains unclear. However, theoretical frameworks, notably the loss of complexity hypothesis, have been postulated to explain the age-related loss or difference in neuromuscular complexity (Figure 1.6; Rey-Robert et al., 2011; Vaillancourt & Newell, 2002; Sleimen-Malkoun et al., 2014). Like all complex dynamical systems, the neuromuscular system has high dimensionality, formed of multiple interacting components (Röhrle et al., 2019). In a well-functioning neuromuscular system, these components work synergistically across multiple temporal scales, resulting in highly complex muscle force signals (Figure

1.6A). An age-related loss of neuromuscular complexity is therefore theorised to result from several factors including: a decrease in the number of components in the system (Figure 1.6B); an alteration in the coupling between components across multiple temporal and spatial scales (functional synergies), being either complete de-coupling or strong mode-locking between components (Figure 1.6C); an increase in the number of components that has a deleterious effect on the efficient functioning of the system (Figure 1.6D; Vaillancourt & Newell, 2002; Sleimen-Malkoun et al., 2014).

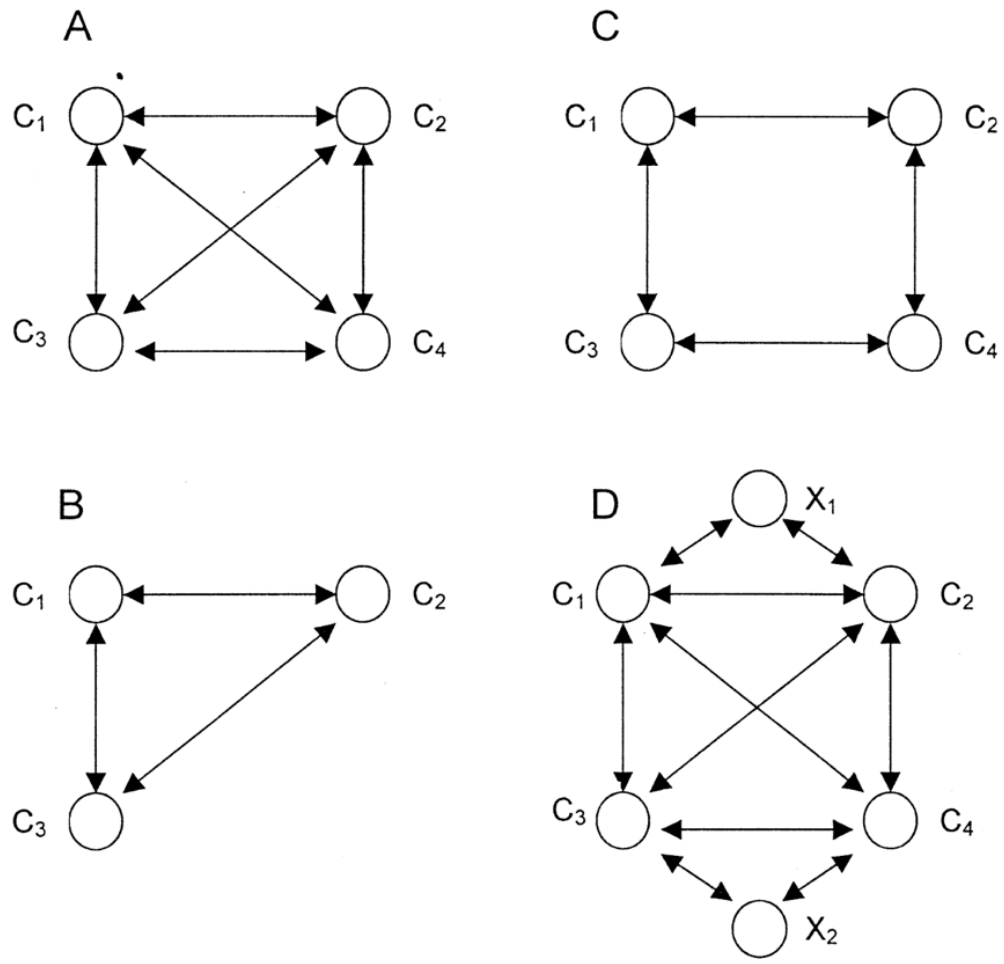

Figure 1.6. Schematic from Vaillancourt & Newell, (2002) illustrating the theoretical framework for a "loss of complexity". **(A)** Highest complexity system, circles represent the systems components, and the arrows represent the coupling between components, **(B)** Illustrates a loss of complexity through the decrease in number of system components, **(C)** Reduction in number of arrows represents a loss of complexity through alterations in the coupling between system components, **(D)** Increase in the number of system components.

The age-related loss of complexity hypothesis is also suggested to be intertwined with the concept of dedifferentiation (Sleimen-Malkoun et al., 2014). Dedifferentiation refers to the process by which structures and mechanisms of behaviour that were once specialised for specific functions lose their specialisation. This results in these structures becoming more simplified, less distinct, or more common across different functions (Baltes & Lindenberger, 1997). Dedifferentiation contributes to the loss of complexity by reducing the specificity and distinctiveness of the system's components (Sleimen-Malkoun et al., 2014). As specialised functions and structures become more generalised with age, their interactions become more homogenised and less capable of producing complex outputs. However, it is crucial to reiterate that due to a lack of empirical evidence the loss of complexity and the process of dedifferentiation remain theoretical concepts in our attempt to understand age-related differences in neuromuscular complexity. Experimental research is needed to validate these theoretical concepts by identifying the specific system components and determining the extent to which age-related structural and functional changes, along with systemic reorganisation of their interactions, contribute to the observed reduction in neuromuscular complexity.

Effect of Fatigue on Neuromuscular Complexity

Neuromuscular fatigue extends beyond a reduction in force-generating capacity (Taylor & Gandevia, 2008) and is also associated with a decline in neuromuscular complexity (Pethick et al., 2015, 2016). Research suggests that the fatigue-induced reduction in neuromuscular complexity is influenced by both central and peripheral mechanisms (Pethick et al., 2018a, 2018b). Evidence for central involvement comes from findings that caffeine ingestion attenuated both the decline in voluntary activation (a marker of central fatigue) and neuromuscular complexity compared to a placebo (Pethick et al., 2018a).

Meanwhile, peripheral mechanisms were highlighted by a study in which circulatory occlusion of the working muscles at task failure prevented the recovery of neuromuscular complexity (Pethick et al., 2018b). Since the occlusion blocked the restoration of the muscle metabolic milieu, the sustained reduction in complexity was attributed, at least in part, to peripheral fatigue (Pethick et al., 2018b). This indicates that both central and peripheral components of the neuromuscular system play a role in determining the complexity and variability of isometric muscle force.

A fatigue-induced decline in neuromuscular complexity may potentially exacerbate the already lower baseline complexity observed in older adults, further impairing motor function and the ability to perform ADLs. However, research has not yet investigated the effect of age on the fatigue-induced change in neuromuscular complexity. Since fatigue in older adults is influenced by factors such as contraction mode, intensity, and velocity (Allman & Rice, 2002; Christie et al., 2011), research is required to being determining how different fatiguing tasks impact age-related changes in neuromuscular complexity.

Physical Activity and Neuromuscular Complexity with Ageing

Central and peripheral adaptations to the neuromuscular system, associated with chronic physical activity, have been suggested to potentially mitigate the age-related decrease in neuromuscular complexity and increase in neuromuscular variability (Pethick & Piasecki, 2022). There is limited human-based research examining how these central and peripheral adaptations in older adults, induced by chronic physical activity, affect neuromuscular complexity and variability. However, research indicates that chronic exercise training (Pethick, 2023), habitual use of dominant limb (Keogh et al., 2006), and acute exercise interventions (Keogh et al., 2007) may improve muscle force control of older adults.

Masters' endurance athletes (aged > 55 years) have been found to exhibit isometric muscle torque control (assessed by CVF, ApEn, and DFA) comparable to younger adults (aged < 35 years) matched for physical activity levels (Pethick, 2023). In contrast, inactive older adults (aged > 55 years) showed significantly higher muscle torque variability compared to both the master athletes and younger adults, although no differences in the complexity of isometric KE torque signals were observed between the three groups (Pethick, 2023). These findings suggest that lifelong physical activity may help offset an age-related decline in neuromuscular variability, but not in complexity (Pethick, 2023).

It has been postulated that the habitual daily use of the dominant limb can affect the age-related differences observed in muscle force control, potentially indicating the sensitivity of muscle force control to differences in physical activity levels. Previous research testing both limbs has demonstrated the variability of isometric muscle force signal to be greater in the non-dominant limb of upper extremity muscles (Critchley et al., 2014; Keogh et al., 2006; Kenway et al., 2016) and lower extremity muscles (Hanson et al., 2022), compared to the dominant limb.

However, only Keogh et al. (2006) has shown that the age-related increase in the variability of muscle force signal was more pronounced in the non-dominant limb compared to the dominant limb. These findings suggest that the habitual daily use of muscles throughout life may mitigate against the expected increase in neuromuscular variability.

Numerous acute exercise intervention studies have explored the potential to counteract the age-related decline in muscle force control, with mixed results. Several RET programs have shown improvements in older adult's muscle force control, by reducing their neuromuscular variability (Bilodeau et al., 2000; Keen et al., 1994; Keogh et al., 2007; Kobayashi et al., 2014; Kavanagh et al., 2016). Unilateral RET has also been shown to increase neuromuscular complexity, as measured by SampEn, in both the trained and untrained limbs of older adults (Keogh et al., 2007), suggesting that both muscular and neural adaptations may contribute to age-related changes in complexity. However, other RET studies have reported no significant reductions in neuromuscular variability among older adults (Bellew, 2002; Tracy et al., 2004; Tracy & Enoka, 2006; Hortobagyi et al., 2001), indicating that the effectiveness of RET may depend on factors such as training protocol, task specificity and/or muscle group trained.

Steadiness task and skills training, such as the novel dexterity skill training by Ranganathan et al. (2001), consistently reduced tri-digit pinch force variability and improved pegboard completion time in older adults, with similar results observed in practice-based interventions like pegboard training (Marmon et al., 2011a). Though the impact of force steadiness practice on neuromuscular complexity and variability remains inconclusive, with research reporting increased complexity and decreased variability in IFA force (Sosnoff & Voudrie, 2009), while others reported no significant change in PF force variability (Holmes et al., 2015).

The age-related decline in muscle strength and power is well-established, and similarly, a decrease in neuromuscular complexity and increase in variability is likely to be inevitable with age, irrespective of physical activity levels. While regular physical activity and acute exercise interventions have the potential to mitigate some age-related changes in neuromuscular function, thereby preserving neuromuscular complexity and variability, there are likely limits to how much these interventions can counteract the decline associated with ageing.

Narrative Review Summary

Neuromuscular function, specifically the production and regulation of muscle torque or force, can be evaluated through the quantification of muscle torque and force signal complexity, entropy and variability (Pethick et al., 2021b; Vieluf et al., 2015). However, notable gaps remain in the current understanding of how age influences neuromuscular complexity and variability. In particular, the neurophysiological mechanisms underpinning age-related changes in neuromuscular complexity are not yet well understood, and the functional importance of changes in neuromuscular complexity remains unclear. Moreover, the effect of age on fatigue-induced changes in neuromuscular complexity has not been investigated. Addressing these knowledge gaps will advance the understanding of how signal analysis techniques, derived from nonlinear dynamics and information theory, can be used to investigate mechanistic and functional age-related changes to the neuromuscular system.

Chapter Two

The effect of age on the complexity, entropy and variability of isometric muscle force signals:

A systematic review and meta-analysis.

2.1 - Introduction

Isometric muscle force or torque signals are nonlinear outputs of the neuromuscular system, characterised by distinct and measurable temporal and spatial structures (Challis, 2006; Vaillancourt et al., 2002; Vaillancourt & Newell, 2003; Goldberger, 1996; Goldberger et al., 1990; Goldberger et al., 2002a). The temporospatial structure of an isometric muscle force signal is thought to emerge from the coordinated interactions of the neuromuscular system's components that regulate muscle contractions (Vaillancourt & Newell, 2002; Vieluf et al., 2015). Ageing causes a progressive alteration in the structure and function of the neuromuscular system's components, which consequently leads to a reduction in neuromuscular function (Hunter et al., 2016; McKinnon et al., 2016) and is therefore postulated to be reflected in the temporospatial structure of the muscle force signal (Vaillancourt & Newell, 2002; Sleimen-Malkoun et al., 2014). Over the past two decades, researchers have used signal analysis techniques from the field of nonlinear dynamics and information theory to examine the effect of age on the temporal (*neuromuscular complexity*) and spatial (*neuromuscular variability*) structure of isometric muscle force signals; providing insights into age-related changes in the production and regulation of muscle force (Challis, 2006; Fiogbe et al., 2021; Knol et al., 2019; Vaillancourt et al., 2002; Vaillancourt & Newell, 2003).

The impact of age on the complexity, entropy and variability of isometric muscle force signals may be influenced by both muscle group and contraction intensity (Christou & Carlton, 2002; Enoka et al., 2003; Oomen & van Dieen, 2017; Pethick et al., 2022). Different muscle groups exhibit distinct physiological characteristics, such as muscle contractile properties, fibre type distribution, MU discharge behaviour and MU innervation ratios (Enoka, 1995; Harridge et al., 1996; Inglis et al., 2025), which may affect how ageing alters neuromuscular function. Indeed, age-related MU loss and remodelling, along with changes in MU recruitment and discharge rates, were not uniform across muscles (Orssatto et al., 2022; Piasecki et al., 2016a). Furthermore, muscles with fewer MUs are likely to be affected to a greater extent by the fluctuations transmitted by synaptic noise due to reduced spatial filtering, increasing the variability of the muscle force signal (Dideriksen et al., 2012). These muscle-specific factors may contribute to differences in how age affects the complexity and variability of force signals.

Age-related differences in neuromuscular variability were influenced by contraction intensity, with effects typically more pronounced at low contraction intensities (Enoka et al., 2003;

Oomen & van Dieen, 2017). A previous meta-analysis found the effect of age on muscle force variability was large and consistent at low contraction intensities (2 to 10% MVF; effect size r = 0.72, 95% CI [0.65; 0.78]; Oomen & van Dieen, 2017). However, at higher contraction intensities (40 to 80% MVF), the effect of age was comparatively smaller and there was larger variance in effect sizes across studies (effect size r = 0.48, 95% CI [0.29; 0.64]; Oomen & van Dieen, 2017). The influence of contraction intensity on age-related differences in neuromuscular variability is likely explained by several mechanisms. At lower contraction intensities, force output is primarily controlled by a smaller pool of low-threshold MUs, making it more susceptible to fluctuations in both independent and common noise components of common synaptic input (Dideriksen et al., 2012; Farina & Negro, 2015).

The age-related loss of motor neurons and compensatory reinnervation of orphaned muscle fibres results in fewer, larger, and less spatially mixed MUs in older adults (Hepple & Rice, 2016). This MU reorganisation potentially results in earlier activation of larger MUs, and greater variability in MU discharge rates (Connelly et al., 1999; Kamen et al., 1995; Tracy et al., 2005). Consequently, older adults exhibit greater muscle force variability than younger adults, particularly at low contraction intensities, as the last recruited MU has the greatest influence on force fluctuations (Enoka et al., 2003; Selen et al., 2005; Tracy et al., 2005). Furthermore, the age-related loss of MUs may attenuate the filtering of synaptic noise, particularly at lower contraction intensities, thereby increasing the variability of the muscle force signal.

At moderate to high contraction intensities (>40% MVF), both force signal variability and age-related differences in force variability were generally smaller than lower contraction intensities (Christou & Carlton, 2002; Oomen & van Dieen, 2017). As contraction intensity increases, the recruitment of additional MUs progressively filters out independent noise, potentially leading to a reduction in force signal variability (Dideriksen et al., 2012; Farina & Negro, 2015). Moreover, as contraction intensity exceeds a MU's recruitment threshold, its discharge rate increases, reducing MU force fluctuations (Fuglevand et al., 1993). This, in turn, diminishes the contribution of individual MUs to force variability, leading to an overall reduction in force signal variability (Allum et al., 1978; Christakos, 1982). The mechanisms underpinning age-related changes in neuromuscular complexity at different contraction intensities requires investigation. Nonetheless, research that has investigated changes in both neuromuscular

complexity and variability across various muscle groups and contraction intensities provide insights into age-related differences in neuromuscular system function.

Previous reviews of the literature have focused on the effect of age on the variability of isometric muscle force signals (Christou, 2011; Enoka et al., 2003; Oomen & van Dieen, 2017). However, these reviews did not include literature which had investigated the effect of age on the complexity of isometric muscle force signals. A more recent scoping review by Pethick et al. (2022) provided a detailed examination of age-related differences in both isometric muscle force signal complexity and variability; however, it did not employ a systematic review methodology. Without a structured methodology for study selection and evaluation, scoping reviews are susceptible to selection bias, potentially overlooking or underrepresenting relevant studies. To address this gap, the current chapter aimed to provide a systematic review and meta-analysis of studies investigating the effect of age on the complexity, entropy and variability of isometric muscle force signals. Additionally, the review also aimed to assess the impact of muscle group and contraction intensity on age-related differences in the complexity, entropy and variability of isometric muscle force signals.

The systematic review aimed to address the following questions:

1) Does the current literature demonstrate there to be an effect of age on the complexity, entropy and variability of isometric muscle force signals?

2) Is there an effect of contraction intensity and muscle group on the age-related differences in the complexity, entropy and variability of isometric muscle force signals?

2.2 - Methods

2.2.1. Literature Search.

The literature search was made using PubMed on 15th July 2022. The search terms (force OR torque OR muscle) AND (steadiness OR variability OR fluctuations OR complexity) AND (ageing) AND (young OR old) were used. The search terms were used to systematically check for new studies every month between 15th July 2022 and 1st August 2024.

The reference lists of the included studies after the initial search were checked for further eligible studies. The included studies were also entered into connected papers (www.connectedpapers.com) to check for additional studies.

2.2.2. Inclusion Criteria.

1. The study was comparing isometric muscle force signal variability AND/OR complexity between at least two healthy adult participant groups characterised by age (i.e., younger and older groups).
2. The study participants were human, in full health and not from a patient population (studies with a patient population were included if there were also a comparison between a healthy younger and healthy older participant groups).
3. There was a muscle force control task performed by fresh muscle with visual feedback of the target force line. Force control task was defined as a submaximal continuous isometric contraction performed to achieve a constant contraction intensity using any muscle of either the upper or lower extremities. Studies with only sinusoidal force tasks were removed.
4. CVF [1]AND/OR root mean square error (RMSE) were reported as an outcome measure of force variability and accuracy OR there was a measure of entropy or complexity (e.g., ApEn, SampEn, MSE or DFA). Studies with other measures of steadiness or complexity were accepted if it allowed for a clear comparison of force steadiness between age groups. Studies with only SDF were not included.
5. The study was an original research article and NOT a review article, systematic review, or *meta*-analysis.

[1] For consistency throughout the systematic review (Chapter Two) muscle force will also be used to define muscle torque. For example, the coefficient of variation of force will be used to describe the coefficient of variation of torque.

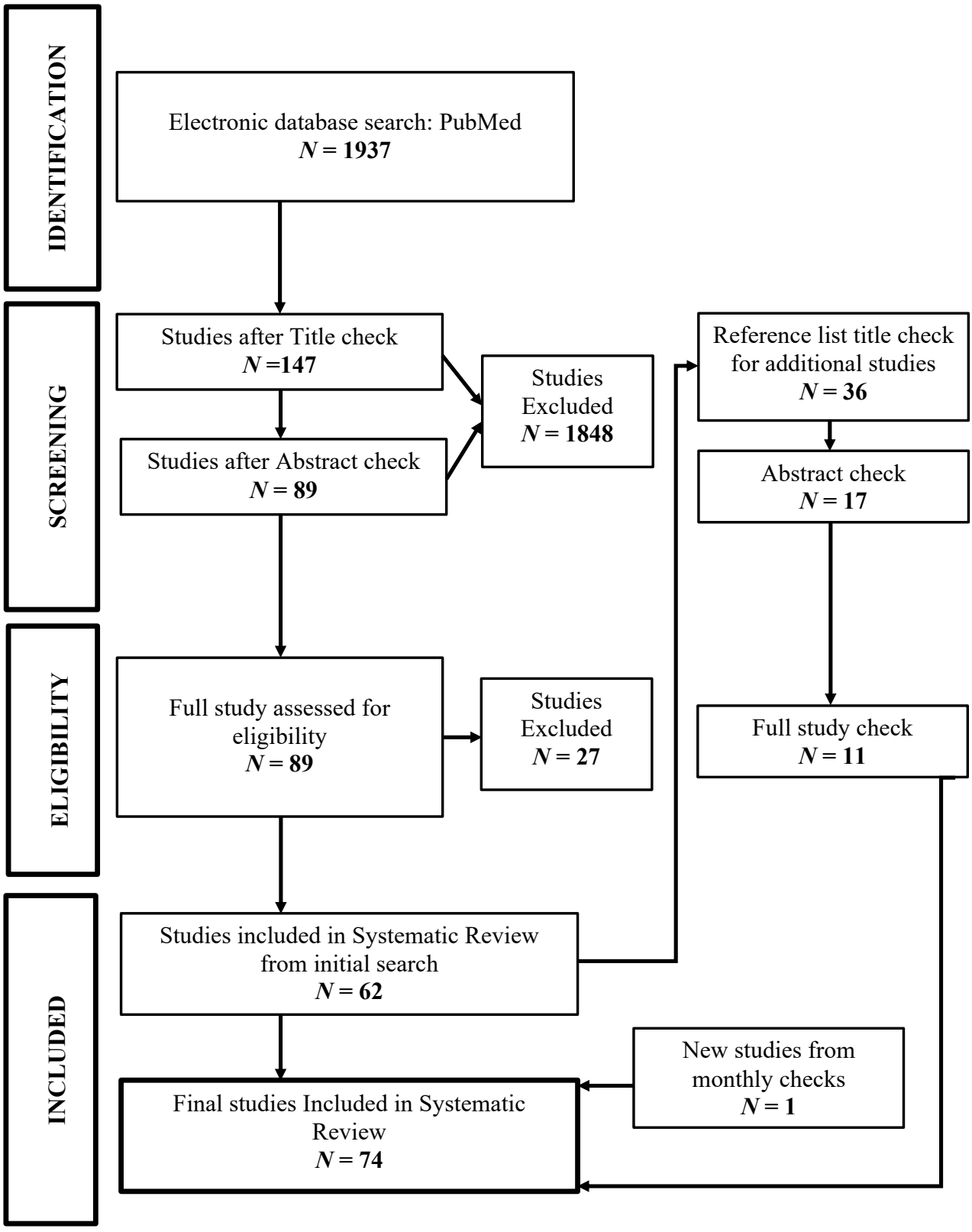

Figure 2.1. Literature search and study inclusion flow-chart.

2.2.3. Data Extraction.

To allow for the calculation of effect sizes, the means and SDs of the CVF, RMSE of force, ApEn and SampEn of force were extracted from fifty studies presented in Table 2.1.A and 2.1.B (studies marked with an asterisk after publication date were used in effect size analysis). When the mean and SD data were not presented in the study text, the data were digitally extracted from figures using plot digitising software (plotdigitizer.com). There were sixteen studies reporting the CVF but mean and SD data could not be acquired for the following reasons: data were not presented in text and there were no suitable figures for digitising; data were combined across contraction intensities; data were combined across age groups; or the study did not use percentage of MVF to prescribe contraction intensity.

The effect sizes were only calculated from isometric tasks under controlled conditions with visual feedback of target force line. Isometric tasks with potentially confounding factors were not included, such as tasks with no visual feedback of target force line, changes in visual scaling or feedback of target force line, steadiness task after fatiguing exercise or steadiness tasks with a cognitive challenge.

The following data were also extracted from the studies and presented in Tables 2.1.A and 2.1.B: first author name, publication date, participant sample size of both younger and older groups, participant age of both younger and older groups, participant physical activity levels, complexity and variability metrics used for analysis, muscle groups used for isometric task, target contraction intensity as a percentage of MVF used for isometric tasks (or other target contraction intensity prescription) and the main outcome results of the study.

2.2.4. Effect Size Calculations.

The effect size Hedges' *g* was calculated by dividing the difference in groups means by the pooled weighted SD. In the seven studies where there were two older groups, the data of the two groups were combined for the calculation of effect size. The upper and lower 95% confidence intervals and Z-scores were also calculated for each effect size estimate.

The effect sizes were pooled using a random effects model, to account for random error within studies and the true variation in effect size between studies. The CVF effect sizes were pooled in four ways: pooling all effect size estimates, pooling effect sizes by muscle groups studied, and pooling effect sizes by target contraction intensity.

Effect sizes were interpreted according to Cohen, (1988): $g \geq 0.20$ small effect, $g \geq 0.50$ medium effect and $g \geq 0.80$ large effect. Effect sizes were coded as positive when a higher CVF and RMSE or a lower entropy (SampEn and ApEn) was reported in the older participants compared with the younger participants.

2.3 - Results

2.3.1. Study Inclusion.

The initial PubMed search yielded $N = 1937$ studies. These studies were filtered down to $N = 147$ after checking the study titles, which were then filtered further to $N = 89$ after checking the study abstracts. These final studies went through a full-paper review to check all inclusion criteria were met, which filtered the studies to $N = 62$ to be included in the systematic review.

The reference lists of the sixty-two included studies were then checked and connected papers used to find further studies which may be relevant but were missed by the initial search. The search yielded $N = 36$ studies based on their titles. These studies were then filtered to $N = 17$ after checking the studies abstracts. These final studies went through a full-paper review to check all inclusion criteria were met, which filtered the studies to $N = 11$ to be included in the systematic review. From the monthly systematic check for new studies, $N = 1$ study was found and included in the systematic review.

The final number of studies included in the systematic review were $N = 74$. These studies were divided into two groups, with one group containing studies with measures of complexity ($N = 18$ papers; Table 2.1.A) and the other group containing studies with variability and steadiness measures only ($N = 56$ papers; Table 2.1.B).

The number of studies removed and the reason for removal at the full-paper review stage were as follows: $N = 4$ studies removed for not meeting inclusion criteria 1, $N = 17$ studies removed for not meeting inclusion criteria 3, $N = 10$ studies removed for not meeting inclusion criteria 4 and $N = 1$ study removed for not meeting inclusion criteria 5.

2.3.2. Demographics.

Fifty-four studies contained both male and female participants in both the younger and older age groups. Fifty-two studies reported the exact distribution of male to female participants, with a mean of 11 ± 7 older females, 10 ± 5 older males, 9 ± 5 younger females and 9 ± 5 younger males in each study. Of the remaining twenty studies, six contained only male participants, three studies contained only female participants and eleven did not state the sex of participants. The participants in all studies were reported to be in full health with no contraindications to performing the specific isometric contractions required for the study. The studies of Carville et al. (2007), Carville et al. (2006) and Vaillancourt et al. (2002) contained a faller group, Parkinson patient group and hormone replacement therapy groups respectively and comparisons to these groups were excluded from the systematic review.

The studies included were published between 1993 and 2023, with a relatively even distribution in publications between those years. Thirty-three studies were published prior to 2010, and forty-one studies were published after 2010.

2.3.3. Sample Size.

The total sample size of the studies ranged from 14 to 108, with a mean sample size of 36 ± 18 (sample size data does not include the participants from the middle-aged groups of three studies or the faller, hormone replacement therapy and Parkinson patient groups in Carville et al., 2007, Carville et al., 2006 and Vaillancourt et al., 2002 respectively). The sum of participants from all studies was 2640, with 1438 older participants and 1202 younger participants.

In all but fourteen studies, the number of participants were divided approximately equally between the younger and older age groups. In all fourteen cases the older group had a greater sample size in comparison to the younger group.

Across all studies the total sample size of the older groups ranged from 7 to 60 with a mean sample size of 19 ± 11 (studies with two older groups had the sample of both groups combined for the purpose of analysis). The sample size of the younger groups ranged from 7 to 49 with a mean sample size of 16 ± 9.

2.3.4. Age Groups

All studies included at least one group of young adults, with a mean age across all studies of 23.9 ± 2.1 years and one group of older adults, with a mean age across all studies of 71.1 ± 4.1 years (studies with two older groups had the mean age of both groups combined for the purpose of analysis).

Ten studies had two older groups, of which seven divided the old group based on age with an old group (aged between 60 and 70 years) and older old group (aged over 70 years). Vieluf et al. (2018), split the older group into novices and experts based on their experience preforming highly dexterous tasks, while Marchini et al., (2017) divided the older group based on training level (i.e., trained, and untrained). Similarly, Pethick, (2023) recruited a group of master athletes (i.e., highly active older adults) and an inactive older adult group. Three studies had three age groups, with the addition of a middle-aged group (mean age 48 to 52 years; Holmes et al., 2015; Lavender & Nosaka, 2007; Marmon et al., 2011).

2.3.5. Physical Activity Levels.

Thirty studies provided information on the physical activity levels of their participants, while forty-four studies did not provide any information on participant physical activity levels. Of the thirty studies which provided physical activity information, only four studies provided quantitative data of the participants physical activity levels using metabolic equivalents (METs). Twenty studies simply stated that all their participants were self-reported to be physically active and/or undertaking regular light to moderate exercise, with nine of these studies requiring participants to have not performed strength training for a specified period.

One study reported their participants to be matched for active days per week (Hanson et al., 2022), while another divided the older group into trained and untrained, with the trained group having one year training experience (Marchini et al., 2017). Justice et al. (2014) included participants in their younger age group if they performed light and moderate physical activity but did not state any physical activity requirements for their older age group. Pethick, (2023) measured participant physical activity using actigraphy. While Carville et al. (2006) reported daily weekly exercise hours for both age group and Carville et al. (2007) only reported the daily exercise levels for the older age group.

2.3.6. Muscle Groups.

The included studies assessed the force complexity and/or variability of nine muscle groups. The most studied muscle group were the index finger abductors (IFA) which were tested in twenty-nine studies. Fifteen studies tested the knee extensor muscles (KE), ten studies tested the elbow flexor muscles (EF) and seven studies tested ankle dorsiflexor muscles (DF). Twelve studies tested a form of pinch grip (PG), five studies tested ankle plantar flexor muscles (PF), two studies tested wrist extensor muscles (WE), and another two studies tested hand grip force (HG). Finally, one study tested wrist flexor muscles (WF).

Nine studies tested more than one muscle group. Tracy et al. (2007b) tested three muscle groups the KE, EF, and IFA. The following studies tested two muscle groups: Tracy, (2007) tested the DF and PF, Sosnoff & Newell, (2006b) tested the IFA and PG, Bazzucchi et al. (2004) tested the KE and EF, Tracy et al. (2007a) tested the KE and EF, Baweja et al., (2012) tested the IFA and DF, Feeney et al. (2018) tested the WE and PG, Marmon et al. (2011b) tested IFA and PG and Sosnoff & Newell, (2011) tested IFA and PG.

For the purposes of this review, the IFA, EF, PG, WE, WF, and HG were categorised as upper extremity muscle groups and the KE, DF, and PF were categorised as lower extremity muscle groups.

2.3.7. Contraction Intensity Prescription.

The target contraction intensities of sixty-four studies were prescribed as a percentage of the individual participants MVF, with contraction intensities ranging from 2 to 100% MVF. Forty-one of the studies which used percentage of MVF tested more than one contraction intensity, with twenty-three studies testing only one contraction intensity. Of the ten studies not prescribing contraction intensity based on percentage of MVF, five studies prescribed contraction intensity in newtons, two studies prescribed contraction intensity as a percentage of a one repetition maximum of the target muscles and three studies prescribed contraction intensity based upon a percentage of the individual participants motor unit (MU) recruitment threshold. For the purposes of this review, contraction intensities prescribed as percentages of MVF were arbitrarily categorised as: Low (≤ 10% MVF), Moderate (≥ 15% and ≤ 40% MVF) and High (≥ 50% and ≤ 100% MVF).

2.3.8. Complexity, Entropy and Variability Analysis.

In all but ten studies the variability metric, CVF was used as a measure of relative force variability. Of the ten studies which did not report the CVF, four studies reported complexity metrics (Sosnoff & Newell, 2008; Vieluf et al., 2018; Vaillancourt & Newell, 2003; Vaillancourt et al., 2002), five studies reported the RMSE of the force signal (Chen et al., 2017; Baweja et al., 2012; Keogh et al., 2006; Kwon & Christou, 2018; Marchini et al., 2017), and one study reported the arithmetic mean of absolute deviation values of the force signal (Berger et al., 2020). Most studies also report the SDF, which provides a measure of absolute variability in the force signal.

It is important to note that in all cases throughout this review the CVF was defined as the variability of the measured individual force or torque signals, calculated as the SD of the force signal divided by the mean of the force signal, multiplied by one hundred. To maintain consistency throughout the review the CVF will be used to also define the coefficient of variation of torque (CVT).

The CVF was selected as the main variability metric of interest in the current review as it accommodates for differences in strength, as commonly observed between the younger and older age groups. Moreover, the CVF was utilised by the majority of studies and therefore allows for a detailed effect size analysis. A greater CVF indicates decreased force steadiness or an increased magnitude of variability in the force signal. Force accuracy was quantified using the RMSE of force, which measures the error between the force produced by the participant and the target force. Thirteen studies reported the RMSE of force.

As noted previously, the studies were divided into two groups, with a group of eighteen studies containing measures of isometric force signal complexity (Table 2.1.A). The complexity and entropy metrics used across the eighteen studies were, ApEn, SampEn, DFA α, MSE, corrected approximate entropy (CApEn), normalised sample entropy (NSampEn) and normalised corrected approximate entropy (NCApEn). These entropy and complexity metrics were derived from the field of nonlinear dynamics and quantify the irregularity, randomness, and long-range fractal correlations of the force signal, thus, providing additional information on the temporal structure of the muscle force signal.

In the case of the entropy metrics ApEn, SampEn, MSE, CApEn, NSampEn, NCApEn, a low value indicates lower complexity with a higher value indicating higher complexity. The DFA α exponent values can theoretically range from 0.5 (white noise) through to 1.5 (brown noise), with a value of 1.0 (pink noise) being the highest complexity signal that exhibits statistically self-similar fluctuations. Further detail on the entropy and complexity metrics can be found in Chapter Three - General Methods.

Table 2.1.A Summary of studies included in systematic review which investigate the effect of age on the complexity of isometric muscle force signals.

Paper	Participant Groups	Physical Activity Levels	Complexity, Entropy and Variability Metrics	Muscle Group and Contraction Intensity	Main Study Results
Pethick, (2023)	YG N = 14 (23.9±4.7y) OG Active N = 14 (60.4±4.4y) OG Inactive N = 13 (61.1±3.9y)	Physical activity determined using Actigraphy.	ApEn DFA CVF	KE at 10, 20 and 40% MVF.	↔ ApEn and DFA between each group at all intensities. ↑ CVF, OG inactive vs. YG and OG active at all contraction intensities.
Fiogbe et al., (2021) * **[CVF – & SampEn +]**	YG N = 8 (24±2.8y) OG N = 13 (63±2.8y)	Not Reported	SampEn CApEn NCApEn NSampEn CVF	KE at 15, 30 and 40% MVF for 30s with 10 min rests.	↓ SampEn, CApEn, NCApEn, and NSampEn. ↔ CVF.
Knol et al., (2019) * **[CVF & SampEn +]**	YG N = 18 (6F, 12M; 24.9±3.56y) OG N = 12 (8F, 4M; 76.69±6.41y)	Not Reported	SampEn MSE CVF RMSE SDF	Right-handed index-thumb PG at 10 and 30% MVF for 22s.	↓ SampEn and MSE at both force levels. ↑ CVF, RMSE and SDF at both force levels.
Vieluf et al., (2018)	YG N = 14 (9F, 5M; 22.64±1.82y) *Novices in performing highly dexterous tasks OG(N) N = 12 (7F, 5M; 58.17±2.95y) *Novices in performing highly dexterous tasks OG(E) N = 14 (8F, 6M; 57.93±2.91y) *Experts in performing highly dexterous tasks	Not Reported	MSE SDF	PG at 7 N for 30s, with left, right and both hands.	↓ MSE (main effect of age $P < 0.01$). ↑ SDF in OG(N), than YG and OG(E) (main effect of age $P = 0.01$).
Vieluf et al., (2015) * **[CVF +]**	YG N = 11 (5F, 6M; 23±2.2y) OG N = 11 (6F, 5M; 67±1.7y)	Participants self-reported to be physically active.	MSE CVF SDF	IFA (right-hand) at 10, 20, 40, 60 and 80% MVF for 15s.	↔ MSE ($P = 0.34$). ↑ CVF at all force targets ($P = 0.03$). ↔ SDF ($P = 0.18$).
Jordan et al., (2013)	YG N = 12 (4F, 8M; 25.8±4.5y) OG N = 10 (5F, 5M; 76.5±6.4y)	Not Reported	DFA CVF SDF RMSE	IFA at 1-5% above recruitment threshold force of the MUs for 60s.	↔ DFA ($P = 0.39$). ↑ CVF ($P < 0.05$). ↑ SDF ($P < 0.001$). ↔ RMSE ($P = 0.80$).
Hu & Newell, (2011)	YG N = 11 (5F, 6M; 20-24y) OG (65-69y) N = 11 (7F, 5M) OG (75-79y) N = 11 (7F, 4M)	Not Reported	ApEn CVF RMSE	IFA at 20% MVF using both index fingers (the sum of finger forces used to match force target line).	↔ ApEn ($P = 0.239$). ↑ CVF in both OG vs. YG ($P = 0.001$). ↑ RMSE in both OG vs. YG ($P = 0.001$).
Ofori et al., (2010) * **[ApEn & CVF +]**	YG N = 16 (21.9±2.6y) OG N = 16 (71.0±3.6y)	Not Reported	ApEn CVF SDF	IFA at 5, 10 and 20% MVF for 30s.	↓ ApEn ($P < 0.05$). ↑ CVF ($P < 0.05$).

Sosnoff & Voudrie, (2009) * **[ApEn & CVF +]**	YG N = 36 (18F, 18M; 22.9±3.4y) OG N = 36 (19F, 17M; 72.1±4.5y)	Not Reported	ApEn CVF	IFA at 15% MVF for 20s with 30s rest.	↓ ApEn ↑ CVF ($P < 0.001$).
Sosnoff & Newell, (2008) * **[ApEn +]**	YG N = 12 (22.7±3.7y) OG N = 13 (67.9±1.3y)	Not Reported	ApEn RMSE	IFA at 10% MVF for 25s.	↓ ApEn ↑ RMSE
Sosnoff & Newell, (2007) * **[ApEn +]**	20year YG: N = 16 (24.5±2.3y) 60year OG: N = 17 (66.0±3.0y) 70year OG: N = 14 (75.0±2.6y)	Not Reported	ApEn CVF	IFA at 5 and 25% MVF for 25s with 30s rest.	↓ ApEn, 70year vs. YG at 25% MVF. ↔ ApEn, YG vs. both OG at 5% MVF. ↑ CVF, YG vs. both OG at 5 and 25% MVF.
Challis, (2006) * **[CVF - & ApEn +]**	YG N = 10 (23.8±2.8y) OG N = 12 (73.7±3.2y)	Not Reported	ApEn CVF	PF at MVF for 3 x 10s with 2min rest	↓ ApEn ↔ CVF
Sosnoff & Newell, (2006a) * **[ApEn & CVF +]**	20year old group: N = 15 (24.9±3.8y) 60year old group: N = 15 (65.7±3.1y) 70year old group: N = 18 (75.2±4.2y)	Not Reported	ApEn CVF	IFA at 5 and 25% MVF for 25s with 30s rest.	↓ ApEn, 70yr vs. 20yr and 60yr.
Sosnoff & Newell, (2006b) * **[ApEn & CVF +]**	20year YG: N = 16 (7F, 9M; 24.9±3.8y) 60year OG: N = 16 (8F, 8M; 65.7±3.1y) 70year OG: N = 16 (9F, 7M; 75.2±2.7y)	Not Reported	ApEn CVF	IFA, two-digit PG (index finger to thumb) and three-digit PG (index and middle finger to thumb) at 5% MVF for 20s or 30s.	↓ IFA ApEn**,** YG vs. both OG. ↔ PG ApEn. ↑ CVF, both OG vs. YG for all tasks.
Sosnoff & Newell, (2006c) * **[ApEn & CVF +]**	YG N = 15 (6F, 9M; 24.9±3.8y) OG N = 33 (18F, 15M; 70.9±5.6y)	Not Reported	ApEn CVF	IFA at 5 and 25% MVF for 25s with 30s rest.	↓ ApEn ↑ CVF
Sosnoff & Newell, (2006d)	20year YG: N = 16 (9F, 7M; 24.2±2.2y) 60year OG: N = 16 (7F, 9M; 64.9±3.1y) 70year OG: N = 16 (8F, 8M; 75.4±2.8y)	Not Reported	DFA CVF	IFA at 5 and 25% MVF for 25s with 20s rest.	↔ DFA between all groups ($P = 0.14$). ↑ CVF, 70yr OG vs. YG and 60yr OG.
Vaillancourt & Newell, (2003) * **[ApEn +]**	YG N = 10 (5F, 5M; 22±1y) OG N = 10 (5F, 5M; 67±2y) OOG N = 10 (5F, 5M; 82±5y)	Moderately Active (Highly active excluded)	ApEn DFA RMSE	IFA at 5, 10, 20 and 40% MVF for 25s with 100s rest.	↓ ApEn**,** both OG vs. YG. ↑ DFA, both OG vs. YG. ↑ RMSE, both OG vs. YG.
Vaillancourt et al., (2002)	YG N = 7 (25±2.7y) OG N = 7 (72.5±5.1y)	Not Reported	Cross-ApEn RMSE SDF	PG (index finger to thumb) at 5, 25 and 50% MVF for 20s.	↓ Cross-ApEn at all contraction intensities ($P < 0.05$). ↑ RMSE at all contraction intensities ($P < 0.01$). ↑ SDF at all contraction intensities ($P < 0.05$).

Abbreviations and Symbols: ↓ = OG produced a significantly lower metric value compared with YG; ↑ = OG produced a significantly higher metric value compared with YG; ↔ = no significant difference between age groups; * = studies marked with an asterisk were used for ApEn, SampEn and/or CVF effect size estimates; [+] = studies with only positive effect sizes; [-] = studies with only negative effect sizes; [±] = studies with both positive and negative effect sizes; ApEn = approximate entropy; CApEn = corrected approximate entropy; CVF = coefficient of variation of force; DFA = detrended fluctuation analysis; MSE = multiscale entropy; MVF = maximal voluntary force; NCApEn = normalised corrected approximate entropy; NSampEn = normalised sample entropy; OOG = older-old group; OG = older age group; RMSE = root mean square error; SampEn = sample entropy; SDF = standard deviation of force; YG = younger age group; y = years.

Table 2.1.B Summary of studies included in systematic review which investigate the effect of age on the variability of isometric muscle force signals.

Paper	Participant Groups	Physical Activity Levels	Variability Metric	Muscle Group and Contraction Intensity	Main Study Results
Hanson et al., (2022) * **[+]**	YG N = 16 (6F, 10M; 27±9.8y) OG N = 16 (6F, 10M; 72±5.2y)	Groups matched: 4.23 to 4.57 active days per week	CVF RMSE	KE at 15% MVF for 2 minutes, once on each leg.	↔ CVF and RMSE.
Berger et al., (2020)	YG N = 16 (16M; 25.44±1.93y) OG N = 16 (16M; 56.75±4.71y)	Not Reported	Arithmetic mean of absolute deviation values	PG at 7.5 N, 6 times for 30s with 30s rest.	↑ inaccuracies ($P = 0.02$).
Wu et al., (2019a) * **[+]**	YG N = 16 (8F, 25.5±3.7y; 8M, 24.3±2.7y) OG N = 17 (8F, 69.3±3.8y; 8M, 70.0±3.7y)	In past 5y not performed competitive sports or S&C training.	CVF	KE at 20% MVF for 15s.	↑ CVF.
Wu et al., (2019b) * **[±]**	YG N = 22 (11F, 23.8±2.4; 11M, 24.2±2.0) OG N = 22 (10F, 68.4±2.7; 12M, 70.2±1.9)	In past 5y not performed competitive sports or S&C training.	CVF	KE at 20, 50 and 80% MVF for 15s, with 5-10minute rest.	↑ CVF at 20% MVF ($P < 0.01$). ↔ CVF at 50% and 80% MVF.
Pereira et al., (2019) * **[+]**	YG N = 49 (25F, 21.6±2.5y; 24M, 22.1±3.1y) OG N = 36 (19F, 66.8±5.9y; 15M, 68.5±5.6y)	Reported as MET-h/wk. YG 54.1-65 h/wk and OG 30.4-31.5 h/wk	CVF	EF at 5% MVF for 45s.	↑ CVF ($P < 0.001$).
Mani et al., (2019) * **[+]**	YG N = 13 (8F, 5M; 25±4y) OG N = 12 (5F, 7M; 78±5y)	Not Reported	CVF	WE (right arm) at 10% MVF for 30s	↑ CVF ($P = 0.002$).
Walker et al., (2019) * **[-]**	YG N = 13 (10F, 3M; 25±4y) OG N = 11 (6F, 5M; 69±3y)	Not Reported	CVF	KE at 20 and 70% MVF.	↔ CVF at 20 and 70% MVF.
Kwon & Christou, (2018)	YG N = 11 (6F, 5M; 22.6±4.1y) OG N = 12 (5F, 7M; 74.1±5.7)	Moderately Active	RMSE SDF	DF (right ankle) at 15% MVF for 31s.	↔ RMSE. ↑ SDF
Pereira et al., (2018) * **[+]**	YG N = 48 (24F, 21.6±2.6y; 24M, 22.1±3.1y) OG N = 60 (34F, 68.2±6.4y; 26M, 69.6±5.5y)	Reported as MET-h/wk. YG 55.6-66.1h/wk and OG 31.5-37.5h/wk	CVF	EF at 5% MVF for 40s.	↑ CVF ($P < 0.01$).
Feeney et al., (2018)	YG N = 13 (8F, 5M; 25±4y) OG N = 12 (5F, 7M; 78±5y)	Not Reported	CVF	WE and thumb-index finger PG at 10 and 20% MVF for 30s.	↑ CVF, for both WE and thumb-index finger PG (main effect $P = 0.03$).
Blomkvist et al., (2018)	YG N = 10 (5F, 5M; 24±3y) OG N = 30 (19F, 11M; 67±8y)	Not Reported	CVF	HG at 5, 10 and 25% MVF for 17s, with left and right hand.	↑ CVF at all contraction intensities for both left and right hand ($P < 0.05$).

Smart et al., (2018) * **[+]**	YG N = 9 (9M; 23±2y) OG N = 9 (9M; 77±5y)	Not Reported	CVF	EF at 2.5, 5, 10, 20, 40, 60 and 80% MVF for 10s.	↑ CVF at all contraction intensities ($P < 0.01$).
Castronovo et al., (2018)	N = 20 (7F, 13M; 18-75y)	Not Reported	CVF	DF at 20% MVF for 30s.	↑ CVF ($P < 0.001$).
Keenan et al., (2017)	YG N = 20 (11F, 9M; 21.4±6.1y) OG N = 23 (12F, 11M; 76±10y)	Not Reported	CVF	PG (thumb to index finger on dominant hand) at 1 N.	↑ CVF ($P = 0.001$).
Marchini et al., (2017)	YG N = 10 (2F, 8M; 28.4±4.4y) OG(T) N = 10 (8F, 2M; 66±6.3y) *Trained group OG(UT) N = 12 (12F; 67.7±5.7y) *Untrained group	Two older groups divided into groups based on exercise experience. Trained group with minimum of 1 year training experience.	RMSE SDF	DF at 5 N with both feet at the same time, for 23s.	↑ SDF, OG(T) and OG(UT) vs. YG ($P < 0.05$). ↑ RMSE, OG(T) and OG(UT) vs. YG ($P < 0.05$).
Chen et al., (2017)	YG N = 14 (7F, 7M; 24.9±0.7y) OG N = 14 (8F, 6M; 68.2±1.0y)	Not Reported	RMSE	IFA at 20% MVF for 34s.	↑ RMSE ($P = 0.009$).
Arellano et al., (2016) * **[+]**	YG N = 9 (3F, 6M; 23.6±2.9y) OG N = 9 (5F, 4M; 76.3±7y)	Not Reported	CVF	WF at 10% MVF.	↔ CVF ($P = 0.177$).
Kenway et al., (2016) * **[+]**	YG N = 15 (6F, 9M; 25±4y) OG N = 18 (9F, 9M; 71±6y)	Not Reported	CVF	IFA at 5, 10, 20 and 30% MVF for 10s with both hands simultaneously and with one hand.	↑ CVF during bilateral tasks at 5 and 10% MVF ($P < 0.001$). ↑ CVF during unilateral tasks at 10% MVF ($P = 0.025$).
Tracy et al., (2015) * **[±]**	Study 1: YG N = 27 (15F, 12M; 22.7±3.3y) OG N = 14 (7F, 7M; 71.9±4.8y) Study 2: YG N = 27 (15F, 12M; 22.7±3.3y) OG N = 14 (9F, 5M; 75.1±5.02y)	All participants were regular exercisers performing a minimum of <3h per week of low to moderate intensity exercise, and no strength training for at least 1 year	CVF SDF	IFA (non-dominant hand) at 2.5, 30 and 65% MVF for 20s with either 30s or 60s rest (depending on task intensity).	↑ Pooled CVF across contraction intensities ($P < 0.05$). *Data pooled from both studies.
Pereira et al., (2015) * **[+]**	YG N = 36 (18F, 20.6±1.1y; 18M, 20.6±1.8y) OG N = 30 (17F, 70.3±6.2y; 13M, 70.5±5.6y)	Reported as MET-h/wk. YG 57.2-77.6 h/wk and OG 33.7-39.5 h/wk	CVF	EF at 5, 30 and 40% MVF for 40s.	↑ CVF at 5% MVF ($P < 0.001$). ↔ CVF at 30 and 40% MVF.
Holmes et al., (2015)	YG N = 11 (6F, 5M; 24.5±3y) MG N = 9 (3F, 6M; 52.3±8y) OG N = 9 (5F, 4M; 78.2±4y)	Not Reported	CVF	PF at 10% MVF for 3min.	↔ CVF between all groups ($P = 0.714$)

Critchley et al., (2014) * **[+]**	YG N = 31 (17F, 14M; 19.7±0.9y) OG N = 31 (16F, 15M; 65.1±8.1y)	Not Reported	CVF RMSE	PG at 10% MVF for 20s.	↑ CVF and RMSE ($P < 0.05$)
Justice et al., (2014) * **[+]**	YG N = 26 (14F, 12M; 22.1±3.7y) OG (65-75y) N = 27 (12F, 15M; 70.3±2.7y) OG (76-90y) N = 25 (15F, 10M; 80.0±4.1y)	YG included if performing light and moderate physical activity. OG not reported.	CVF	DF at 5 and 20% of 1 rep max for 60s.	↔ CVF between YG, OG (65-70y) and OG (76-90y) at 5% of 1 rep max. ↑ CVF, OG (76-90y) vs. YG and OG (65-75y) at 20% of 1 rep max.
Vanden Noven et al., (2014) * **[+]**	YG N = 16 (8F, 8M; 20.4±2.1y) OG N = 17 (8F, 9M; 68.8±4.4y)	Reported as MET-h/wk. YG 59.5±38.3 h/wk and OG 22.0±21.8 h/wk	CVF	DF at 5% MVF for 40s.	↑ CVF ($P = 0.002$).
Fox et al., (2013) * **[+]**	YG N = 10 (5F, 5M; 25±4y) OG N = 10 (6F, 4M; 71±5y)	Not Reported	CVF	IFA (non-dominant left hand) at 2% MVF for 35s.	↑ CVF.
Kallio et al., (2012) * **[+]**	YG N = 8 (8M; 27.1±3.2y) OG N = 9 (9M; 70.2±4.1y)	YG and OG reported to perform moderate to strenuous exercise 3 times per week or more.	CVF	PF at a target force that would produce sEMG activation corresponding to 10 and 20% MVF of soleus muscle.	↑ CVF at 10% ($P < 0.001$) and 20% MVF ($P < 0.05$).
Baweja et al., (2012)	YG N = 12 (7F, 5M; 18-35y) OG N = 10 (6F, 4M; 65-85y)	Not Reported	RMSE SDF	IFA and DF at 10% of 1 rep max for 15s.	↑ RMSE ($P < 0.001$). ↑ SDF ($P = 0.003$).
Arjunan et al., (2012) * **[+]**	YG N = 20 (10F, 10M; 20-30y) OG N = 20 (10F, 10M; 55-70y)	All groups were moderately active, performing non-strenuous exercise 3-5 times per week.	CVF	EF at 100% MVF.	↑ CVF.
Marmon et al., (2011b) * **[+]**	YG N = 25 (11F, 14M; 25.8±4.4y) MG N = 25 (17F, 8M; 50.6±5.6y) OG N = 25 (17F, 8M; 74.5±6.3y)	Not Reported	CVF	IFA and precision PG (index finger to thumb) at 5% MVF for 60s.	↑ CVF, OG vs. YG and MG during both IFA ($P < 0.001$) and precision PG ($P < 0.003$). ↔ CVF, YG vs. MG during both IFA and precision PG ($P > 0.05$).
Kennedy & Christou, (2011)	YG N = 10 (5F, 5M; 25±4y) OG N = 10 (6F, 4M; 71±5y)	Not Reported	CVF	IFA (non-dominant left hand) at 2 and 30% MVF for 35s.	↔ CVF ($P = 0.07$).
Sosnoff & Newell, (2011) * **[+]**	YG N = 16 (7F, 9M; 24.9±3.8y) 60year OG N = 16 (8F, 8M; 65.7±3.1y) 70year OG N = 16 (9F, 7M; 75.2±2.7y)	Not Reported	CVF	IFA (dominant hand), two-digit grip (index finger to thumb) and three-digit grip (index and middle finger to thumb) at 5% MVF for 30s.	↑ CVF, both OG vs. YG during all tasks (main effect of age $P < 0.05$).

Kouzaki & Shinohara, (2010) * **[+]**	YG N = 20 (20M; 28.1±4.0y) OG N = 20 (20M; 69.7±2.8y)	Not Reported	CVF	PF at 2.5, 5, 10, 15 and 20% MVF for 40s.	↑ CVF at 2.5 and 5% MVF. ↔ CVF at 10, 15 and 20% MVF.
Carville et al., (2007) * **[±]**	YG N = 44 (26F, 18M; 29.3±0.6y) OG N = 44 (29F, 15M; 75.9±0.6y) *non-faller group	Only reported for OG, 27.6±3.2 min/day of moderate PA.	CVF	KE at 10, 25 and 50% MVF for 10s with 60s rest.	↔ CVF at all contraction intensities.
Lavender & Nosaka, (2007) * **[±]**	YG N = 10 (10M; 20.4±2.0y) MG N = 12 (12M; 48.0±7.3y) OG N = 10 (10M; 70.5±4.1y)	Participants reported to not be involved in resistance training and only undertaking light recreational exercise.	CVF	EF at 30, 50 and 80% MVF.	↔ CVF between all groups at all contraction intensities.
Welsh et al., (2007)	YG N = 16 (7F, 9M; 23±4y) OG N = 16 (8F, 8M; 74±7y)	Participants reported to perform less than 3h/week of low to moderate exercise and no strength training for one year.	CVF	KE at 2% MVF above the pre-determined MU recruitment threshold.	↔ CVF.
Dewhurst et al., (2007) * **[+]**	YG N = 15 (15F; 23.6±3.4y) OG N = 11 (11F; 68.6±5.7y)	Participants reported to be moderately active, performing PA no more than twice per week.	CVF	DF at 5, 10 and 15% MVF for 30s with 3min rest.	↑ CVF at all contraction intensities ($P < 0.001$).
Tracy, (2007) * **[±]**	YG N = 11 (5F, 6M; 22.7±2.7y) OG N = 10 (5F, 5M; 72.8±5.5y)	Participants reported to perform less than 3h/week of low to moderate exercise and no strength training for one year.	CVF SDF	DF and PF at 2.5, 5, 10, 30, 50 and 80% MVF.	↔ CVF at all contraction intensities during DF ($P > 0.05$). ↑ CVF during PF at 2.5% ($P = 0.03$) and 5% MVF ($P = 0.04$). ↔ CVF during PF at 10, 50 and 80% MVF ($P > 0.05$). ↓ CVF during PF at 30% MVF ($P = 0.012$).
Tracy et al., (2007a) * **[±]**	YG N = 22 (22.9±3.3y) OG N = 23 (74.0±7.1y)	Participants reported to perform no more than 3h/week of moderate PA and no strength training in preceding year.	CVF SDF	KE and EF at 2.5, 30 and 65% MVF.	↑ CVF at 2.5% MVF for both KE and EF. ↓ CVF at 30 and 65% MVF for both KE and EF. ↓ SDF at 65% MVF for both KE and EF. ↔ SDF at 2.5 and 30% MVF for both KE and EF.
Tracy et al., (2007b) * **[±]**	YG N = 10 (10M; 21.7±3.4y) OG N = 10 (10M; 72.1±3.9y)	Participants reported to perform no more than 3h/week of moderate PA and no strength training in preceding year.	CVF SDF	KE, EF and IFA at 2.5, 5, 10, 30 and 50% MVF.	↔ Pooled CVF data across muscles and contraction intensities ($P = 0.90$). ↑ CVF during IFA at 2.5% MVF only ($P = 0.04$). ↔ Pooled SDF data across muscles and contraction intensities ($P = 0.62$).

Voelcker-Rehage et al., (2006) * **[+]**	YG N =15 (6F, 9M; 19.9±1.6y) OG N = 14 (6F, 8M; 69.9±3.5y)	Not Reported	CVF	Bi-digit PG at 20% MVF.	↑ CVF.
Keogh et al., (2006)	YG N = 13 (23.8±4.7y) OG N = 14 (75.7±2.5y)	Not Reported	RMSE SDF	Tri-digit finger-pinch at 20 and 40% MVF.	↑ RMSE and SDF ($P < 0.01$).
Carville et al., (2006) * **[-]**	YG N = 16 (16F; 27.4±5.6y) OG N = 14 (14F; 70.5±5.8y)	OG reported to perform 2.5±2.4 hours of exercise per week and the YG 4.6±2.6 hours per week.	CVF	KE (both legs) at 10, 25, 50 and 100% MVF.	↔ CVF at all contraction intensities ($P > 0.05$).
Tracy et al., (2005)	YG N = 11 (4F, 7M; 22.3±3.5y) OG N = 14 (5F, 8M; 74.9±5.7y)	Participants reported to perform no more than 3h/week of moderate PA and no strength training in preceding year.	CVF SDF	IFA at 3% MVF above the MU recruitment threshold, for 10-25s with 60s rest. Forces produced split into three bins: 0-5% MVF, 5.1-10% MVF and 10.1-15% MVF.	↔ CVF when target forces not split into bins ($P > 0.05$). ↑ CVF at 0-5% MVF only ($P < 0.05$). ↑ SDF at all target force bins ($P < 0.05$).
Shinohara et al., (2005)	YG N = 10 (5F, 5M; 24.1±5.3y) OG N = 10 (5F, 5M; 72.5±4.9y)	Participants reported to perform no more than minimal levels of PA on a regular basis.	CVF	IFA (both hands) at 2.5, 10 and 40% MVF for 20s.	↔ CVF for both hands and at all contraction intensities ($P > 0.05$).
Bazzucchi et al., (2004) * **[+]**	YG N = 8 (8F; 24.2±4.2y) OG N = 8 (8F; 70.6±2.6y)	Participants reported moderate PA, but not in systematic training.	CVF	KE and EF at 20, 50 and 80% MVF for 30s.	↑ CVF at 20% MVF during EF only. ↑ CVF at 80% MVF during EF and KE.
Vaillancourt et al., (2003) * **[+]**	YG N = 10 (5F, 5M; 22±1y) OG N = 10 (5F, 5M; 67±2y) OOG N = 10 (5F, 5M; 82±5y)	Not Reported	CVF	IFA at 5, 10, 20 and 40% MVF for 25s with 100s rest.	↑ CVF, OG and OOG vs. YG.
Tracy & Enoka, (2002) * **[±]**	YG N = 20 (10F, 10M; 22.1±2.2y) OG N = 20 (10F, 10M; 71.5±4.3y)	Participants reported to perform no more than 3h/week of moderate PA and no strength training in preceding year.	CVF SDF	KE at 2, 5, 10 and 50% MVF for 10-12s.	↑ CVF at 2, 5 and 10% MVF. ↔ CVF at 50% MVF. ↓ SDF at 5, 10 and 50% MVF. ↔ SDF at 2% MVF.
Ranganathan et al., (2001) * **[+]**	YG N = 27 (14F, 13M; 27.7y) OG N = 28 (16F, 12M; 70.5y)	Not Reported	CVF	PG (thumb to index or middle finger with dominant hand) at 5, 10 and 20% MVF.	↑ CVF at 5 and 10% MVF for both index finger ($P < 0.001$) and middle finger PG ($P < 0.05$). ↔ CVF at 20% MVF for both index finger and middle finger PG.
Christou & Carlton, (2001)	YG N = 24 (12F, 12M; 25.3±2.8y) OG N = 24 (12F, 12M; 73.3±5.5y)	Participants reported to engage in moderate to intense regular PA.	CVF SDF	KE at 5, 10, 20, 35, 50, 65, 80 and 90% MVF for 10-15s with 120s rest.	↑ CVF at all contraction intensities. ↑ SDF at all contraction intensities.

Hortobagyi et al., (2001)	YG N = 10 (21.1±1.2y) OG N = 30 (72±4.7y)	Participants reported to have not exercised more than once a week during preceding 3 years.	CVF SDF	KE at 25 N.	↔ CVF and SDF.
Burnett et al., (2000) * **[+]**	YG N = 14 (9F, 5M; 23±0.9y) OG N = 15 (7F, 8M; 74±1.5y)	Not Reported	CVF SDF	IFA (non-dominant left hand) at 2.5, 5, 20, 50 and 75% MVF.	↑ CVF at all contraction intensities. ↑ SDF at 2.5, 5 and 50% MVF. ↔ SDF at 20 and 75% MVF.
Semmler et al., (2000) * **[+]**	YG N = 11 (6F, 5M; 24.1±4.1y) OG N = 14 (6F, 8M; 70.4±5.9y)	Participants reported to be moderately active on daily basis.	CVF	IFA (non-dominant left hand) at 2.5, 5, 7.5 and 10% MVF.	↑ CVF at 2.5 and 5% MVF. ↔ CVF at 7.5 and 10% MVF.
Graves et al., (2000)	YG N = 17 (10F, 7M; 22.9±3.5y) OG N = 15 (8F, 7M; 71.2±7.8y)	Participants reported to be sedentary to moderately active, with no strength training in preceding 6 months.	CVF	EF (non-dominant left arm) at 5, 10, 20, 35, 50 and 65% MVF.	↔ CVF at all contraction intensities.
Laidlaw et al., (2000) * **[+]**	YG N = 8 (4F, 4M; 26.6±0.57y) OG N = 14 (8F, 6M; 73.4±1.63y)	Not Reported	CVF	IFA (non-dominant left hand) at 2.5, 5, 7.5 and 10% MVF for 30s.	↑ CVF at all contraction intensities.
Keen et al., (1994) * **[+]**	YG N = 10 (5F, 5M; 23y) OG N = 11 (6F, 5M; 65y)	Not Reported	CVF SDF	IFA at 2.5, 5, 20 and 50% MVF for 20s with 30-60s rest.	↑ CVF at all contraction intensities.
Galganski et al., (1993) * **[+]**	N = 22 (6F, 16M) divided into two age groups. YG (avg age 28y) OG (avg age 67y)	Not Reported	CVF	IFA (non-dominant left hand) at 5, 20, 35 and 50% MVF.	↑ CVF at all contraction intensities.

Abbreviations and Symbols: ↑ = OG produced a significantly higher metric value compared with YG; ↓ = OG produced a significantly lower metric value compared with YG; ↔ = no significant difference between age groups; * = studies marked with an asterisk were used for coefficient of variation of force effect size estimates; [+] = studies with only positive effect sizes; [-] = studies with only negative effect sizes; [±] = studies with both positive and negative effect sizes; CVF = coefficient of variation of force; METS = metabolic equivalents; MG = middle age group; MVF = maximal voluntary force; OG = older age group; PA = physical activity; RMSE = root mean square error; SDF = standard deviation of force; YG = younger age group; y = years.

2.3.9. Effect of age on the complexity of isometric muscle force signals.

The effect sizes of ApEn were calculated from the data of eight studies, providing a total of 13 estimates of the effect of age on the complexity of isometric muscle force signal (Table 2.2). The effect sizes of SampEn were calculated from the data of two studies providing a total of 5 estimates of the effect of age on the complexity of isometric muscle force signal (Table 2.2).

Table 2.2 Pooled Hedges' *g* for the effect of age on the approximate and sample entropy of the isometric muscle force signal.

	Pooled *g*	Lower 95% CI	Upper 95% CI	Z-score	*N*
ApEn Random Effects Model	0.57	0.44	0.71	8.42	13
SampEn Random Effects Model	1.37	1.18	1.56	14.1	5

The ApEn random effect model revealed a medium positive effect, while the SampEn random effect model revealed a large positive effect (i.e., greater ApEn and SampEn in the younger group in comparison to the older group).

In total, there were 8 large positive effect sizes ($g \geq 0.8$), 5 medium to large positive effect sizes ($g > 0.5$ to 0.8) and 4 small to medium positive effect sizes ($g > 0.2$ to 0.5). The 95% confidence intervals of nine effect size estimates crossed zero, which indicates the possibility of finding a negative effect size if the population were sampled again (i.e., greater ApEn and SampEn in the older group in comparison to the younger group).

Of the seven studies not included in the effect size analysis, five studies found no significant difference between the younger and older groups in the complexity metrics used to analyse the muscle force signal (all $P > 0.05$). The remaining two studies found ageing to result in a statistically significant loss of muscle force complexity (all $P < 0.05$).

2.3.10. Effect of age on the variability of isometric muscle force signals.

The effect sizes of the CVF were calculated from the data of forty-seven studies, providing a total of 151 estimates of the effect of age on the variability of isometric muscle force signals (Table 2.3). Pooled effect sizes of all 151 estimates revealed a medium effect of age on the variability of isometric muscle force signal (Table 2.3).

Table 2.3 Pooled Hedges' *g* for the effect of age on the coefficient of variation of force of the isometric muscle force signal.

Random Effect Model Pooled *g*	Lower 95% CI	Upper 95% CI	Z-score	*N*	+'ve ES	-'ve ES
0.52	0.37	0.67	6.59	151	114	37

In total, there were 114 positive effects found (i.e., larger CVF in older group, in comparison to the younger group) and 37 negative effects found (i.e., smaller CVF in older group, in comparison to the younger group). There were 58 large positive effects ($g \geq 0.8$), 26 medium to large positive effects ($g > 0.5$ to 0.8) and 21 small to medium positive effects ($g > 0.2$ to 0.5). Nine of the positive effect sizes were between 0 and 0.2. There were 5 large negative effects ($g \leq -0.8$), 13 medium to large negative effects ($g < -0.5$ to -0.8) and 10 small to medium negative effects ($g \leq -0.2$ to -0.5). Nine of the negative effect sizes were between 0 and -0.2.

The 95% confidence intervals of forty-six positive effect size estimates zero, which indicates the possibility of finding a negative effect size if the population were sampled again (i.e., greater CVF in the younger group in comparison to the older group).

Of the forty-six studies included in the effect size analysis, thirty-four studies had positive effect sizes only, four studies had negative effect sizes only and eight studies had both positive and negative effect sizes.

Effect sizes were pooled for each muscle group. Table 2.4 presents the effect sizes, along with 95% confidence intervals, Z-score, the number of estimates for each muscle group, the mean age of the participants in the older and younger groups who performed the steadiness tasks for each muscle group and the percentage difference in MVF for each muscle group between the younger and older groups. There were large positive pooled effect sizes for the IFA muscle group. The PG, WE and EF muscle groups showed a medium to large positive effect size. The PF muscle group showed a small to medium positive effect size, while the KE and DF muscle groups showed a negative effect.

Table 2.4 Pooled Hedges' *g* for the effect of age on the coefficient of variation of force for each muscle group.

Muscle Group	Random Effect Pooled *g*	Lower 95% CI	Upper 95% CI	Z-score	*N*	+'ve ES	-'ve ES	OG Age (y)	YG Age (y)	% Dif MVF
IFA	0.93	0.65	1.22	6.40	54	52	2	71.0±2.7	24.3±1.7	17.3±18.8
PG	0.61	0.10	1.11	2.37	12	12		70.5±4.8	23.1±3.9	19.5±12.8
WE / WF	0.66	-0.61	1.92	1.01	2	2		77.2±1.2	24.3±1.0	14.9±36.3
EF	0.67	0.28	1.06	3.36	25	19	6	71.4±3.0	22.1±1.3	16.0±11.6
KE	-0.06	-0.39	0.28	-0.33	32	13	19	70.1±3.6	25.5±2.3	23.8±21.0
PF	0.33	-0.19	0.84	1.25	14	10	4	71.2±2.2	26.3±2.3	40.0±8.8
DF	-0.13	-0.99	0.73	-0.30	12	6	6	71.3±3.2	22.2±1.3	46.3±31.6
UP Muscle	0.80	0.59	1.00	7.54	98	85	8			
LO Muscle	0.04	-0.23	0.31	0.30	58	29	29			

Abbreviations: DF = dorsiflexors; EF = elbow flexors; ES = effect size; IFA = index finger abductors; KE = knee extensors; LO = lower extremity muscles; MVF = maximal voluntary force; OG = older group; PF = plantar flexors; PG = pinch grip; UP = upper extremity muscles; WE = wrist extensors; WF = wrist flexors; YG = younger group; y = years.

Effect sizes were pooled for each target contraction intensity. Table 2.5 presents the effect sizes, along with 95% confidence intervals, Z-score, and the number of estimates for each target contraction intensity. There were large positive pooled effect sizes at 2, 2.5, 5, and 7.5% MVF (Pooled $g \geq 0.8$), medium to large positive pooled effect sizes at 10, 15, 20, 40, and 100% MVF (Pooled $g \geq 0.5$ to 0.8) and small to medium positive effect sizes at 25, 60, and 80% MVF (Pooled $g \geq 0.2$ to 0.5). There was a small negative pooled effect size at 30% MVF (Pooled $g < -0.20$). At 35, 65, 70, and 75% MVF only one effect size estimate was available, as such no pooling was performed.

Table 2.5 Pooled Hedges' *g* for the effect of age on the coefficient of variation of force for each target contraction intensity.

Contraction Intensity (% MVF)	Random Effect Pooled *g*	Lower 95% CI	Upper 95% CI	Z-score	*N*	+'ve ES	-'ve ES
2	0.88	-0.82	2.59	1.02	2	2	
2.5	0.90	0.06	1.74	2.11	14	12	2
5	0.84	0.49	1.19	4.69	33	30	3
7.5	0.93	-2.11	3.97	0.60	2	2	
10	0.62	0.22	1.02	3.01	23	19	4
15	0.53	-0.25	1.31	1.33	5	4	1
20	0.79	0.35	1.23	3.49	18	17	1
25	0.31	-0.51	1.13	0.74	4	3	1
30	-0.27	-0.85	0.31	-0.92	12	4	8
35*	1.07	0.17	1.96		1	1	
40	0.51	-0.24	1.25	1.33	4	3	1
50	0.05	-0.51	0.61	0.16	15	8	7
60	0.21	-0.62	1.04	0.50	4	2	2
65*	-0.21	-0.74	0.32		1		1
70*	-0.75	-1.58	0.08		1		1
75*	0.77	0.02	1.53		1	1	
80	0.20	-0.48	0.88	0.58	8	5	3
100	0.67	-0.36	1.70	1.28	3	1	2
Low (≤ 10%MVF)	0.76	0.51	1.01	6.01	74	65	9
Moderate (≥15% to ≤40%MVF)	0.43	0.15	0.70	3.03	44	32	12
High (≥50% to ≤100%MVF)	0.15	-0.19	0.50	0.87	33	17	16

Abbreviations: ES = effect size; MVF = maximal voluntary force; * Denotes only one effect size estimate for the target contraction intensity and no pooling was performed.

Figures 2.2 and 2.3 presents the distribution of effect size estimates for the effect of age on the CVF across target contraction intensities and muscle groups. There were 74 effect size estimates made on low contraction intensities (≤ 10% MVF), 44 effect size estimates made on moderate contraction intensities (≥ 15% and ≤ 40% MVF) and 33 effect size estimates made on high contraction intensities (≥ 50% and ≤ 100% MVF).

There were 85 positive effects and 8 negative effects for the upper extremity muscles. There was a large positive pooled effect for the upper extremity muscles at low target contraction intensities (Hedges' g = 0.85, 95% CI [0.56: 1.14]), with 49 positive effects and 2 negative effects. There was a medium positive pooled effect for the upper extremity muscles at moderate target contraction intensities (Hedges' g = 0.79, 95% CI [0.42: 1.15]), with 22 positive effects and 3 negative effects. There was a medium positive pooled effect for the upper extremity muscles at high target contraction intensities (Hedges' g = 0.67, 95% CI [0.18: 1.16]), with 14 positive effects and 3 negative effects.

There were 29 positive effects and 29 negative effects for the lower extremity muscles. There was a medium positive pooled effect for the lower extremity muscles at low target contraction intensities (Hedges' g = 0.54, 95% CI [0.07: 1.01]), with 16 positive effects and 7 negative effects. There was a negative pooled effect for the lower extremity muscles at moderate target contraction intensities (Hedges' g = -0.06, 95% CI [-0.49: 0.36]), with 10 positive effects and 9 negative effects. There was a small negative pooled effect for the lower extremity muscles at high target contraction intensities (Hedges' g = -0.37, 95% CI [-0.86: 0.13]), with 3 positive effects and 13 negative effects.

The sixteen studies not included in the effect size analysis found varying effects of age on the CVF. Seven studies found a significant effect of age (all $P < 0.05$) with the older group having a higher CVF in comparison to the younger group, across various muscle groups (WE, PG, DF, PG, and IFA). In contrast, seven studies found no effect of age (all $P > 0.05$) with the older group having a similar CVF to the younger group, across various muscle groups (KE, EF, PF, and IFA). Of the final two studies, one study found the CVF to be significantly higher in the older group only when target contraction intensity was between 0 and 5% MVF (Tracy et al., 2005) and the other study found the CVF to be significantly higher in the 70-year older group in comparison to the younger group, but not the 60-year older group (Sosnoff et al., 2006d).

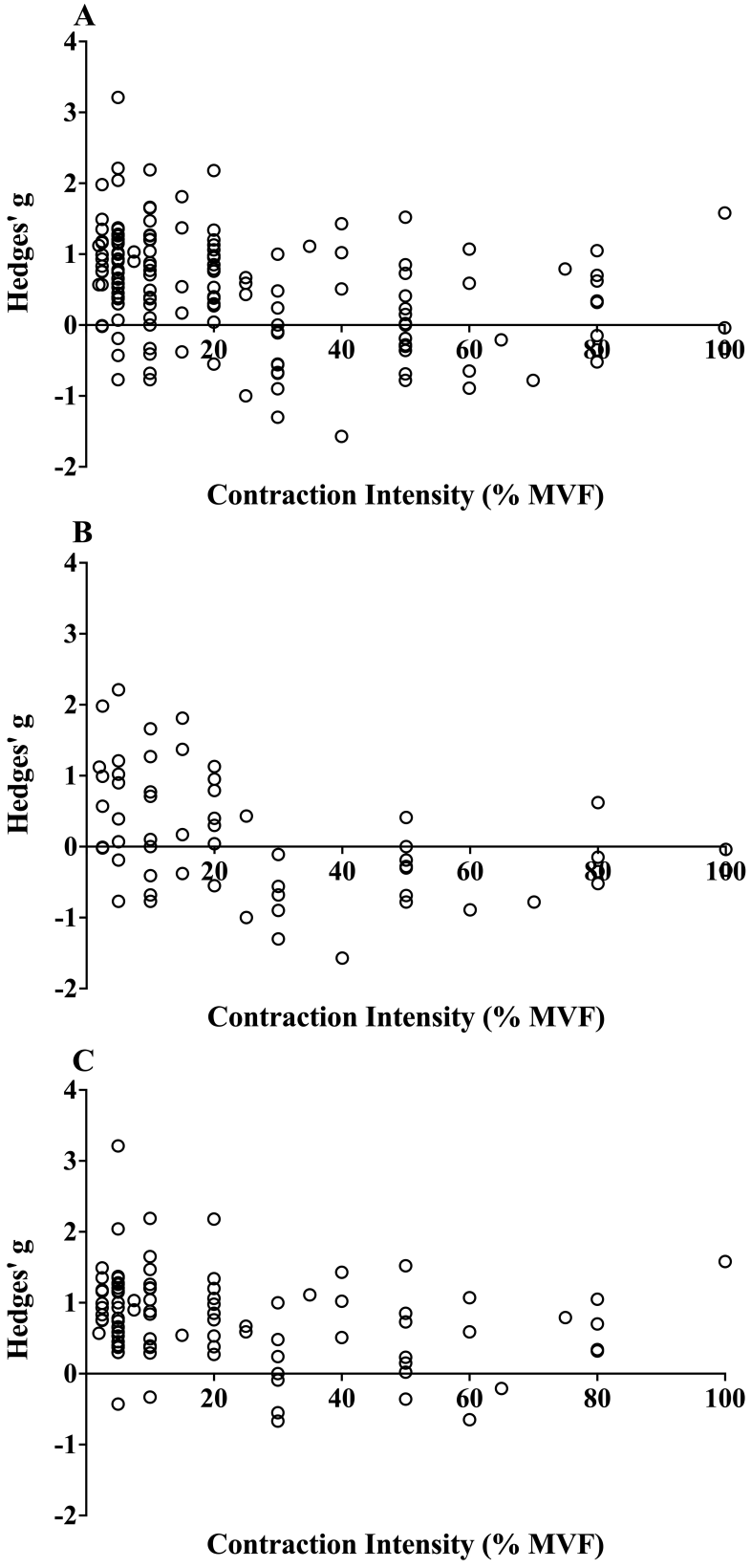

Figure 2.2. Distribution of Hedges' g effect sizes for the effect of age on the coefficient of variation of force of the isometric muscle force signals across target contraction intensities **(A)** All muscle groups, **(B)** Lower extremity muscle groups, **(C)** Upper extremity muscle groups (MVF = maximal voluntary force).

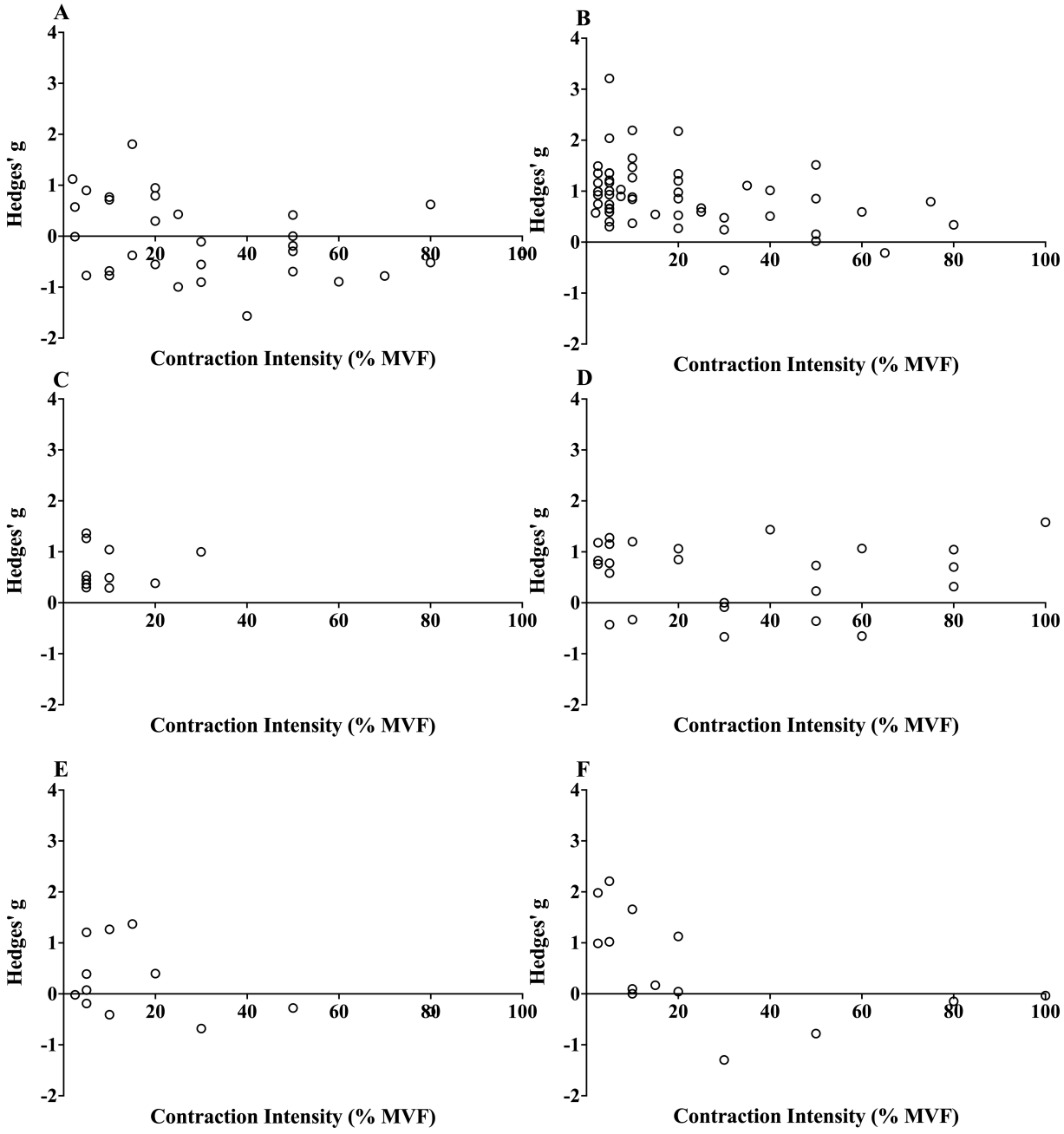

Figure 2.3. Distribution of Hedges' g effect sizes for the effect of age on the coefficient of variation of force of the isometric muscle force signals across target contraction intensities **(A)** Knee extensors, **(B)** Index finger abductors, **(C)** Pinch Grip, **(D)** Elbow flexors, **(E)** Dorsiflexors, **(F)** Plantar flexors (MVF = maximal voluntary force).

2.3.11. Effect of age on the accuracy of isometric muscle force.

The effect sizes of the RMSE of force were calculated from the data of six studies, providing a total of 11 estimates of the effect of age on the accuracy of isometric muscle force (Table 2.6). Pooled effect sizes of all 11 estimates revealed a large positive effect of age on the accuracy of isometric muscle force (Table 2.6).

Table 2.6 Pooled Hedges' *g* for the effect of age on the root mean square error of isometric muscle force.

Random Effect Model Pooled *g*	Lower 95% CI	Upper 95% CI	Z-score	*N*	+'ve ES	-'ve ES
1.43	0.67	2.19	3.69	11	11	0

2.4 - Discussion

2.4.1. Effect of age on the complexity and entropy of isometric muscle force signals.

The effect size analysis conducted in this review provides evidence that older adults generate isometric muscle force signals with lower complexity and entropy compared to younger adults. Individual effect sizes ranged from 0.03 to 0.95 for ApEn and from 0.88 to 2.08 for SampEn. In all cases, the effect sizes were positive, indicating that the older participants exhibited lower ApEn and SampEn values than the younger participants in the studies analysed. When pooled using the random-effect model analysis, ApEn and SampEn demonstrated medium and large effects, respectively (Table 2.2). The lower ApEn and SampEn of the older participants indicates a more regular and predictable force signal structure, whereas the higher values observed in younger adults reflect greater signal irregularity or randomness.

There are numerous entropy and complexity metrics which can be employed when studying the complexity of physiological time-series data (Pethick et al., 2021). To truly characterise and understand the complexity of physiological time-series data, it may be necessary to apply several entropy and complexity metrics (Goldberger et al., 2002b). However, researchers have commonly focused on applying one complexity or entropy metric, as was the case with fourteen of the eighteen studies presented in the current review (see Table 2.1.A).

The most utilised metrics by the studies in the current review and in the effect size analysis were the entropy metrics, ApEn and SampEn. Both quantify the similarity probability of patterns of length m and m+1 in a data series or the regularity and randomness of the signal (Pincus, 1995), the only difference being SampEn removes the bias found in ApEn resulting from self-matching in the data (Richman & Moorman, 2000). Theoretically, low entropy values close to 0 should indicate low *physiological complexity* and high entropy values close to 2 should indicate high *physiological complexity*. The caveat being some signals, such as white noise produce high entropy values (i.e., highly irregular signal), but are not *physiologically* complex.

On their own single-scale ApEn and SampEn may not strictly indicate changes or differences in the complexity of a physiological signal and their use to quantify signal complexity has been questioned (Yentes & Raffalt, 2021). Indeed, this potentially constrains the interpretability of

studies which have solely used these single-scale entropy metrics (Challis, 2006; Hu & Newell, 2011; Ofori et al., 2010; Sosnoff & Newell, 2006a, 2006b & 2006c; Sosnoff & Newell, 2007; Sosnoff & Newell, 2008; Sosnoff & Voudrie, 2009; Vaillancourt et al., 2002). However, this does not invalidate the findings of the studies solely using ApEn and SampEn, given the size of the effects found across multiple studies (Table 2.2) and the support of studies using the complexity metrics (DFA and MSE) that also found an age-related reduction in neuromuscular complexity (Knol et al., 2019; Vaillancourt & Newell, 2003; Vieluf et al., 2018). Nonetheless, this does illustrate the need for future research to have a combination of multiple entropy (e.g., SampEn) and complexity (e.g., DFA and MSE) metrics to provide a more comprehensive insight into the effect of age on the complexity of isometric muscle force and torque.

The pooled random effect size analysis appears to offer a clear picture of the effect of age on the complexity and entropy isometric muscle force. However, there were additional data and studies not included in the effect size analysis that require discussion to provide a comprehensive review of the literature. The prevailing direction of the literature indicates an age-related loss of isometric muscle force complexity and entropy, however, there were five studies which did not find an effect of age on isometric muscle force complexity (Hu & Newell, 2011; Jordan et al., 2013; Pethick, 2023; Sosnoff & Newell, 2006d; Vieluf et al., 2015).

Notably, no effect of age was observed on the ApEn of isometric IFA force (Hu & Newell, 2011). Furthermore, research employing the MSE analysis found there to be no effect of age on the complexity of isometric IFA force across a range of contraction intensities (Vieluf et al., 2015). Similarly, three studies using the DFA analysis found there to be no significant effect of age on the complexity of isometric KE force (Pethick, 2023) and isometric IFA force (Jordan et al., 2013; Sosnoff & Newell, 2006d). There was a trend towards a lower complexity (higher scaling exponent α) in the 70-year-old participants when compared with the young and 60-year-old participants, although significance was not reached (Sosnoff & Newell, 2006d). These findings were important as the MSE and DFA analysis, unlike the entropy analysis (ApEn and SampEn), characterise the *complexity* of the physiological signal (Pethick et al., 2021). Briefly, the DFA α metric captures the long-range fractal-like correlations in the signal (Peng et al., 1994; Seely & Macklem, 2004) and the MSE analysis measures the regularity or irregularity of the signal across multiple temporal scales (Costa et al., 2002). Collectively, this evidence suggests that older adults do not consistently exhibit lower isometric muscle force complexity

compared to younger adults (Hu & Newell, 2011; Jordan et al., 2013; Pethick, 2023; Sosnoff & Newell, 2006d; Vieluf et al., 2015).

On the contrary, research employing both entropy and complexity metrics found older adults to have a higher DFA scaling exponent α and a lower ApEn (i.e., loss of muscle force complexity) during isometric IFA contractions than younger adults (Vaillancourt & Newell, 2003). Similarly, another study by Vieluf and colleagues, also utilising the MSE analysis, found older adults to have a significantly reduced isometric PG force complexity than younger adults (Vieluf et al., 2018). This finding was supported by the study of Knol et al. (2019) which also found the complexity of isometric PG force, assessed using the MSE analysis, to be significantly lower in older adults compared to younger adults.

There is differing evidence as to the effect of age on the complexity of isometric muscle force. Although there may only be five studies which go against the predominant direction of the literature, the relative paucity of research in area of age and isometric muscle force complexity necessitates that these few studies were given due consideration. The discrepancies in findings across studies are likely attributable to factors such as the specific muscle group examined, and the contraction intensity employed during isometric tasks. These factors will be examined in detail in the following sections of this review, with the aim of providing a comprehensive understanding of how age influences the complexity of isometric muscle force signals.

In summary, addressing the first question of this review, the effect size analysis and existing literature suggest that older adults produce isometric muscle force signals with lower complexity and entropy than younger adults. However, some evidence indicates that older and younger adults isometric muscle force signals may not differ in complexity or entropy. To date, there has been paucity of research into the effect of age on the complexity of isometric muscle force, particularly of the muscle groups involved in KE and PG tasks. Notably, most of these studies have only employed a single complexity or entropy metric, which is unlikely to fully capture the temporal structure (*complexity*) of the muscle force signal. Therefore, further research is needed to examine the effect of age on isometric muscle force complexity using a combination of complexity and entropy metrics.

2.4.2. Effect of age on the variability of isometric muscle force signals.

The random effect size analysis of the CVF revealed a medium effect of age (Hedges' g = 0.52, 95% CI [0.37: 0.67]; Table 2.3), indicating that when data were pooled across studies, older adults exhibit a higher CVF than younger adults. However, individual effect sizes reveal conflicting results, with some studies showing a negative effect of age (lower muscle force signal variability in older adults compared to younger adults) and others showing no difference in muscle force signal variability between younger and older groups (Figures 2.2 and 2.3).

A total of 151 effect size estimates were derived from 47 studies. Of these, 114 showed positive effect sizes, indicating higher CVF in older adults compared to younger adults, while 37 were negative, indicating lower CVF in older adults compared to younger adults. These individual effect sizes are notable, as they indicate that isometric muscle force control may, in many instances, remain stable or even improve with age. However, caution is needed when drawing such conclusions due to the cross-sectional study designs and potential confounding factors, including differences in physical activity levels, training experience, and whether the dominant or non-dominant limb was used for the task. The pooled random effect size analysis by muscle group (Table 2.4) and contraction intensity (Table 2.5) further suggests that both muscle group and contraction intensity may influence age-related differences in CVF, contributing to the contrasting findings across studies.

Consistent with the complexity literature, most studies indicate that older adults produce isometric muscle force signals with greater variability than younger adults. However, studies not included in the effect size analysis must also be considered for a comprehensive understanding of the literature. Sixteen studies were not included in the effect size analysis. Of these, seven found no significant age-related effect on the CVF across various muscle groups and contraction intensities (Christou & Carlton, 2001; Graves et al., 2000; Holmes et al., 2015; Hortobágyi et al., 2001; Kennedy & Christou, 2011; Shinohara et al., 2005; Welsh et al., 2007). Two additional studies found both significant and non-significant effects, which were attributed to different contraction intensities (Tracy et al., 2005) or age-related differences between the 70-year-old and 60-year-old groups (Sosnoff et al., 2006d).

Interestingly, eight studies included in the effect size analysis had both positive and negative effect sizes. In these studies, the contrasting findings were due to the use of multiple contraction

intensities (Lavendar & Nosaka, 2007; Tracy & Enoka, 2002; Tracy et al., 2007a & 2007b; Tracy et al., 2015; Wu et al., 2019b) or muscle groups (Tracy, 2007; Tracy et al., 2007b). While four studies found only negative effects (Carville et al., 2006; Challis, 2006; Fiogbe et al., 2021; Walker et al., 2019). In total, 19 studies found no age-related effect on the CVF.

Eight studies not included in the effect size analysis demonstrated a significant effect of age on the CVF, with older adults showing higher CVF across various muscle groups (Castronovo et al., 2018; Blomkvist et al., 2018; Feeney et al., 2018; Hu & Newell, 2011; Jordan et al., 2013; Keenan et al., 2017; Pethick, 2023; Sosnoff et al., 2006c). When combined with 34 studies reporting positive effect sizes and 8 studies with both positive and negative effects, a total of 50 studies found that age affects the CVF. The conflicting evidence regarding the effect of age on neuromuscular variability likely stems from factors also identified in the complexity literature, notably differences in the muscle groups and contraction intensities used across studies.

The CVF measures the variation of a signal around a fixed mean, providing insight into the variability or steadiness of force production. Unlike complexity and entropy metrics, variability metrics do not capture the temporal structure of a physiological signal or how it evolves over time. This distinction is crucial because fluctuations in isometric muscle force signals are not purely random and independent, but exhibit complexity (Slifkin & Newell, 1999). To fully characterise the temporal and spatial structure of muscle force signal fluctuations, it is recommended that variability metrics are used in conjunction with complexity and entropy metrics (Pethick et al., 2021; Pincus & Goldberger, 1994; Slifkin & Newell, 1999).

The importance of combining entropy and variability metrics was first highlighted by Lipsitz & Goldberger (1992), who compared the heart rate time series of a younger (22-year-old) and an older (73-year-old) individual. While both time series had the same mean and standard deviation, the entropy of the younger individual was higher (ApEn = 1.09 vs. 0.48). Similarly, the age-related differences in neuromuscular complexity have been observed in the absence of significant differences in the neuromuscular variability (Challis, 2006; Fiogbe et al., 2021). This suggests that complexity and entropy metrics may be more sensitive to age-related changes in the structure of physiological signals. However, studies have also shown age-related differences in the neuromuscular variability without differences in neuromuscular complexity (Hu & Newell, 2011; Jordan et al., 2013). Ultimately, no single complexity, entropy, or

variability metric can fully capture the age-related changes in the temporospatial structure of physiological signals. This highlights the importance of incorporating a combination of complexity, entropy, and variability metrics in future research to better understand subtle age-related differences in the temporospatial structure of physiological signals.

In summary, addressing the first question of this review, the effect size analysis and wider literature suggest that older adults produce isometric muscle force signals of greater variability than younger adults. However, evidence also indicates that the variability of isometric muscle force signals may not differ between older and younger adults. Differences between and within studies may be influenced by factors such as the muscle group and contraction intensity used in isometric tasks, as discussed later in the review. Future research on age-related differences in isometric muscle force signal structure, should incorporate variability, complexity, and entropy metrics to fully capture the signal's temporospatial structure.

2.4.3. Effect of age on the accuracy of isometric muscle force.

The measure of force accuracy, RMSE, has not been widely utilised in the current literature, with only thirteen of the seventy-four studies presented in Tables 2.1.A and 2.1.B reporting the metric. Despite its limited use, RMSE remains a useful and important metric as it quantifies the difference between the target force and the actual force produced by the participants during the isometric force matching task. This indicates whether the participants were closely meeting the prescribed contraction intensity. Given that age-related changes in muscle force variability depend on contraction intensity (see section "*Effect of contraction intensity on the complexity, entropy, and variability of isometric muscle force signals*"), it is essential to determine whether participants were accurately achieving the intended contraction intensity. While reporting the mean of the actual force output can confirm that the target contraction intensity was achieved, it may obscure important details about how the force was generated. Reporting the root mean square error (RMSE) of force offers two key advantages: it provides a precise measure of output accuracy and demonstrates the consistency with which the target intensity was maintained throughout the isometric task.

Due to the limited use of the RMSE metric, only 11 effect sizes were pooled for the random effect analysis. This analysis produced a large positive effect (Table 2.6), indicating a significant age-related loss of isometric muscle force accuracy (i.e., greater RMSE of force in

the older group, when compared with the younger group). The effect size data was supported by five additional studies not included in the analysis, all of which reported that ageing leads to a loss of isometric muscle force accuracy across a range of contraction intensities (Chen et al., 2017; Baweja et al., 2012; Hu & Newell, 2011; Marchini et al., 2017; Vaillancourt et al., 2002). Contrary to this evidence, there were two studies that did not find an effect of ageing on the accuracy of isometric muscle force (Jordan et al., 2013; Kwon & Christou, 2018).

Despite the limited research, the prevailing evidence indicates an age-related loss of isometric muscle force accuracy, contributing to the evidence demonstrating an age-related increase in the variability and decrease in the complexity of isometric muscle force. The RMSE of force should be reported when investigating the effects of age on the complexity and variability of isometric muscle force signals, as it provides valuable insight into age-related changes in force control.

2.4.4. Effect of muscle group on the complexity, entropy and variability of isometric muscle force signals.

As highlighted in the two preceding sections (*"Effect of age on the complexity and entropy of isometric muscle force signals"* and *"Effect of age on the variability of isometric muscle force signals"*), a potential factor contributing to the differences in findings between studies was the muscle group used for the isometric force matching tasks. There were nine muscle groups used across all the studies presented in Tables 2.1.A and 2.1.B. Of these, four muscle groups were examined in the complexity and entropy of isometric muscle force effect size analysis (IFA, PF, PG, and KE) and eight muscle groups were examined in the variability of isometric muscle force effect size analysis (IFA, PG, WE, WF, EF, KE, PF and DF).

It is important to note that due to the limited number of effect sizes for each muscle group in the complexity and entropy of isometric muscle force analysis, the effect sizes were not pooled for a random effect analysis based on muscle group, as was done for the variability of isometric muscle force effect sizes (Table 2.4). This limitation underscores the need for more research to obtain sufficient data for a comprehensive analysis regarding how the temporal structure or complexity of isometric muscle force signals from different muscle groups is influenced by age.

When the CVF effect size estimates were pooled by lower and upper extremity muscles in the random effect analysis, the lower extremity muscles demonstrated no effect of age on the variability of isometric muscle force, while the upper extremity muscles demonstrated a large effect of age on the variability of isometric muscle force (Table 2.4). The current literature demonstrates, unequivocally, that the variability of isometric muscle force was significantly higher in the upper extremity muscles of older adults compared to their younger counterparts. Conversely, the effect of age on the variability of isometric muscle force in the lower extremity muscles was equivocal, with an equal number of positive and negative effect sizes reported (Table 2.4).

Although lower extremity muscles appear to be less affected by age at high contraction intensities (≥ 50% and ≤ 100% MVF), the distribution of contraction intensities used in the studies does not fully account for the absence of an age-related effect on the variability of isometric force of the lower extremity muscles, as there were positive and negative effects observed across all contraction intensity categories (Figure 2.2B). In contrast, contraction intensity had a negligible effect on the variability of isometric force of the upper extremity muscles, with predominantly positive effects at the low, moderate, and high contraction intensity categories (Figure 2.2C). This suggests that the neuromuscular mechanisms responsible for the age-related differences in the variability of isometric force may disproportionately affect the upper extremity muscles when compared to the lower extremity muscles.

The most studied upper extremity muscle group were the IFA, which were tested in twenty-nine studies. Eighteen of these studies were included in the variability of isometric muscle force effect size analysis, yielding fifty-four effect sizes, fifty-two of which were positive effects and two were negative effects (Table 2.4; Figure 2.3B). The random effect analysis revealed a large effect (Hedges' g = 0.93, 95% CI [0.65: 1.22]; Table 2.4), indicating a significant age-related increase in the variability of IFA force. Additionally, six studies provided ten effect sizes of ApEn of force for the IFA, ranging from 0.03 to 0.95. These effect sizes collectively suggest that older adults produce isometric IFA muscle force signals of greater variability and lower entropy than younger adults.

Research not included in the effect size analysis presents contradictory evidence. For instance, studies found no effect of age on the complexity of the IFA force using MSE (Vieluf et al., 2015), DFA (Jordan et al., 2013; Sosnoff & Newell, 2006d), and ApEn (Hu & Newell, 2011). Furthermore, Kennedy & Christou, (2011) and Shinohara, (2005), whose data were not included in the effect size analysis found there to be no significant effect of age on the CVF of IFAs. Despite these exceptions, the preponderance of evidence supports the conclusion that that older adults produce isometric IFA muscle force signals of greater variability and lower entropy than younger adults.

Along with the IFAs, the variability of WE, WF and PG muscle force has been shown to be associated with clinical measures of manual dexterity (Almuklass et al., 2016; Feeney et al., 2018; Hamilton et al., 2017; Marmon et al., 2011a; Semmler et al., 2000). Therefore, understanding how age effects the force control of these muscle groups is of functional importance. Nine studies provided fourteen effect sizes for the CVF of the WE, WF and PG muscles. In all cases, the effect sizes were positive, with the random effect analysis producing a medium effect for these muscle groups (*note,* WE and WF effect sizes were combined; Table 2.4). Additionally, three other studies not included in the effect size analysis found a significant effect of age on the variability of isometric muscle force produced during thumb to index finger PG tasks (Feeney et al., 2018; Keenan et al., 2017), tri-digit finger-pinch tasks (Keogh et al., 2006), and WE tasks (Feeney et al., 2018). There were four SampEn and ApEn effect sizes produced for PG tasks, ranging from 0.36 to 1.17. These entropy effect size data are supported by Vieluf et al. (2018) and Knol et al. (2019), who found the complexity of older adults' isometric PG force to be significantly lower than younger adults. Similarly, RMSE and SDF were all found to be significantly greater in older adults compared with younger adults during a PG task (Vaillancourt et al., 2002).

Based on the effect size data and research discussed, there is strong evidence showing that older adults produce isometric muscle force signals (WE, WF, and PG) with greater variability and lower complexity than younger adults. Notably, the smaller upper extremity muscles, which are crucial for fine motor control and dexterous tasks, appear to be particularly affected by age. It is probable that smaller muscles were affected to a greater extent by the age-related reorganisation of MUs that leads to fewer and larger MUs (Hepple & Rice, 2016). In older adults, this MU reorganisation may result in larger MUs being activated earlier and at lower more variable firing rates, making the muscle force output more variable in comparison to that

of young adults. This age-related reorganisation of MUs would likely have a larger effect on the variability of force signal of smaller muscles, as there would potentially be a larger relative increase in muscle fibres per surviving MU, when compared to larger muscles (Hepple & Rice, 2016). Additionally, it has been suggested that muscles with fewer MUs were likely to be more susceptible to the fluctuations transmitted by common noise due to reduced spatial filtering, thus increasing the variability of the muscle force signal (Dideriksen et al., 2012). Further research is needed to identify the exact mechanisms and determine the extent to which each contributes to the age-related changes in neuromuscular variability in different muscle groups.

There were ten studies investigating the effect of age on the variability of isometric EF muscle force signals. Nine of these studies were included in the effect size analysis, providing twenty-five effect sizes, of which nineteen were positive effects and six were negative effects (Table 2.4; Figure 2.3D). The random effect analysis produced a medium effect (Hedges' g = 0.67, 95% CI [0.28: 1.06]; Table 2.4), indicating that older adults produce isometric EF muscle force signals of greater variability than younger adults. Findings which were consistent with the other upper extremity muscle groups. The one study not included in the effect size analysis found there to be no significant effect of age on the CVF (Graves et al., 2000). The six negative effect sizes were found in three studies, which can be attributed the use of several contraction intensities, as positive effects were also found in the same studies (Lavender et al., 2007; Tracy et al., 2007a & 2007b).

As indicated by the random effect size analysis of lower extremity muscles, evidence regarding the effect of age on isometric force variability in larger muscle groups involved in locomotion and balance tasks was inconclusive. The KEs were the second most studied muscle group in the literature, having been tested in fifteen studies. Eleven of these studies were included in the variability of isometric muscle force effect size analysis, providing thirty-two effect sizes, of which thirteen were positive effects and nineteen were negative effects (Table 2.4; Figure 2.3A). The random effect analysis produced a negative effect (Hedges' g = -0.06, 95% CI [-0.39: 0.28]; Table 2.4), indicating there was no effect of age on the variability of isometric KE force. Similarly, the studies not included in the effect size analysis all found no statistically significant effect of age on the CVF of the KE muscles (Christou & Carlton, 2001; Hortobagyi et al., 2001; Welsh et al., 2007).

Contraction intensity appears to contribute to the divergent effect sizes, with most positive effects found at lower contraction intensities and mainly negative effects found at higher contraction intensities (Figure 2.3A). The research of Fiogbe et al. (2021) and Pethick, (2023) were currently the only published evidence demonstrating the effect of age on both the variability, complexity and entropy of isometric KE muscle force. Interestingly, all entropy metrics were found to be higher in the younger group in comparison to the older group, however, the CVF was similar between groups at all contraction intensities (Fiogbe et al., 2021). Conversely, Pethick (2023) found older adults CVF to be significantly greater than younger adults, however, no significant differences in the DFA α and ApEn were observed between age groups (Pethick, 2023). The effect of age on the complexity and variability of isometric KE force remains unclear. Further research employing complexity, entropy and variability metrics is needed to establish the impact of age on the force control of the KE muscles.

The variability of isometric PF muscle force was examined in five studies, while the variability of isometric DF muscle force was examined in seven studies. Eight studies (four for each muscle group) were included in the variability of isometric muscle force effect size analysis, providing fourteen effect sizes for the PF (Table 2.4; Figure 2.3F) and twelve effect sizes for the DF (Table 2.4; Figure 2.3E). The random effect analysis of the PF produced a small positive effect (Hedges' $g = 0.33$, 95% CI [-0.19: 0.84]; Table 2.4), indicating that older adults typically produce isometric PF force signals of greater variability than younger adults. In contrast, the random effect analysis of the DF produced a negative effect (Hedges' $g = -0.13$, 95% CI [-0.99: 0.73]; Table 2.4), indicating there was no effect of age found for the variability of isometric DF force. Additionally, two studies not included in the effect size analysis found no effect of age on isometric DF force accuracy (Kwon & Christou, 2018) or isometric PF force variability (Holmes et al., 2015). Conversely, force variability and accuracy of the DF were found to be impaired by age in another two studies (Castronovo et al., 2018; Marchini et al., 2017).

The variability of both isometric DF and PF muscle force has been found to correlate with measures of postural sway, a key indicator of an individual's ability to maintain postural control and balance (Davis et al., 2020; Hirono et al., 2020 & 2021; Masani et al., 2003). Therefore, from a functional perspective, it was encouraging that evidence indicates there to

be a maintenance of isometric force variability of these muscle groups in older age. However, the findings were mixed, with both positive and negative effects reported for the DF and PF muscles, with most negative effects found at moderate and high contraction intensities (Figures 2.3E & 2.3F). This indicates that contraction intensity influences the variability of force of these muscles. Only one study has assessed the complexity of isometric PF force was (Challis, 2006). While the CVF was found to be similar between the younger (22.0 ± 21.1%) and older group (21.3 ± 17.9%), the ApEn of the force signal was significantly greater in the younger group (0.240 ± 0.052) when compared with the older group (0.191 ± 0.079). In accordance with the findings of Fiogbe et al. (2021), this evidence necessitates the use of both entropy and complexity metrics when investigating the effect of age on the temporal structure of force signals, as this structure remains undetected by variability metrics.

In summary and in answer to question two of the review, age-related changes in the variability of isometric muscle force signals appear to disproportionately affect the muscles of the upper extremities when compared to the muscles of the lower extremities. There was clear and robust evidence demonstrating upper extremity muscles required for fine motor control and dexterous tasks to be greatly affected by age. In contrast, the larger lower extremity muscles necessary for locomotion and balance appear to be less affected by age. However, there is limited research investigating the effect of age on the complexity of isometric muscle force signals across all muscle groups. Consequently, the extent to which the complexity of isometric force of both lower and upper extremity muscles is affected by age is not so well understood. Therefore, further research into the effect of age on the complexity of isometric force signals across all muscle groups is warranted.

2.4.5. Effect of contraction intensity on the complexity, entropy and variability of isometric muscle force signals.

The effect of age on both neuromuscular complexity and variability is greatly dependent on the contraction intensity used for the isometric force matching task (Table 2.5; Figures 2.2 & 2.3). In the current systematic review, researchers predominantly set the contraction intensity as a percentage of each participant's MVF, a method adopted by sixty-three studies. Contraction intensity can be prescribed at absolute force levels; however, age can affect muscle strength (Frontera et al., 2000) and in turn muscle strength can affect muscle force control (Christou et al., 2002). Thus, using absolute target contraction intensity may confound comparisons

between younger and older age groups. While studies utilising different contraction intensity prescription methods were included in Tables 2.1.A and 2.1.B to ensure a comprehensive review of the literature, the effect size analysis focused only on those studies using percentage of MVF to ensure comparisons could be made between studies. Throughout the literature a range of eighteen contraction intensities were employed, from 2 to 100% MVF. As detailed in the results section, these target contraction intensities were categorised as: Low (≤ 10% MVF), Moderate (≥ 15% and ≤ 40% MVF) and High (≥ 50% and ≤ 100% MVF).

When effect sizes were pooled by contraction intensity category (Low, Moderate and High) for a random effect analysis, the dependence of contraction intensity on the age-related differences in muscle force variability were evident. The effect of age on muscle force variability was greatest at low contraction intensities with the random effect analysis producing a medium effect (Hedges' g = 0.76, 95% CI [0.51: 1.01]; Table 2.5). This indicates that older adults exhibit significantly greater variability in isometric muscle force than younger adults. Similarly, at moderate contraction intensities, although the effect size was slightly smaller, the random effect analysis also revealed a medium effect (Hedges' g = 0.43, 95% CI [0.15: 0.70]; Table 2.5). This again indicates that the variability of the force signal was significantly greater the older adults compared with younger adults. Lastly, when high contraction intensities were pooled, the random effect analysis produced a smaller positive effect than at both the low and moderate contraction intensity categories (Hedges' g = 0.15, 95% CI [-0.19: 0.50]; Table 2.5), indicating a lesser impact of age on muscle force signal variability.

The pooling of effect sizes by contraction intensity category demonstrates that age-related differences in the variability of isometric muscle force predominantly occur at low contraction intensities, typically between 2 and 10% MVF. The oscillations in MU force when the MU is initially recruited and discharged at low rates were greater in older adults (Kudina, 1999; Westgaard & De Luca, 2001) and is therefore speculated to be a mechanism responsible for the larger age-related difference in force variability at low contraction intensities. In addition, MU size is thought to be related to the achievable level of fine control, in other words, smaller MUs, with fewer fibres, generate finer movements (Azevedo et al., 2020). Therefore, an age-related increase in the fibre ratio of lower-threshold MUs (Deschenes, 2011; Piasecki et al., 2016a), may explain why larger age-related differences were observed at lower contraction intensities (< 10% MVF).

As highlighted in the preceding section ("*Effect of muscle group on the complexity, entropy and variability of isometric muscle force signals*") there was an interaction between muscle group and contraction intensity. At low contraction intensities, the upper extremity muscles produced a large positive effect (Hedges' g = 0.85, 95% CI [0.56: 1.14]), while at moderate (Hedges' g = 0.79, 95% CI [0.42: 1.15]) and high (Hedges' g = 0.67, 95% CI [0.18: 1.16]) contraction intensities a medium positive effect of age on the variability of the force signal was observed. This random effect analysis of muscle group by contraction intensity category demonstrates that the age-related differences in force variability were significant across contraction intensities for the upper extremity muscles. Conversely, the effect of age on the variability of force of the lower extremity muscles appears to be more dependent on contraction intensity. There was a medium positive effect found for the lower extremity muscles at low contraction intensities (Hedges' g = 0.54, 95% CI [0.07: 1.01]). However, at moderate (Hedges' g = -0.06, 95% CI [-0.49: 0.36]) and high (Hedges' g = -0.37, 95% CI [-0.86: 0.13]) contraction intensities negative effects were found by the random effect analysis. This suggests that as contraction intensity was increased beyond 10% MVF the effect of age on the force variability of lower extremity muscles becomes less evident.

Maintaining force control with all muscle groups and at all contraction intensities is important throughout life, as the performance of ADLs requires many muscle groups and a range of force generating capacities. However, muscle force control is of particular importance at low contraction intensities as most ADLs performed by older individuals were undertaken at low contraction intensities (Tikkanen et al., 2016). Therefore, it is understandable that the literature has commonly focused on testing low contraction intensities with 74 effect sizes, while moderate and high contraction intensities produced 44 and 33 effect sizes respectively.

The complexity of isometric muscle force has also been examined across various contraction intensities. However, due to the limited number of effect sizes available, pooling by contraction intensity was not performed. Research has revealed an age-related difference in isometric muscle force complexity across a range of contraction intensities, from 5% MVF (Ofori et al., 2010; Sosnoff & Newell, 2006a, 2006b & 2006c; Vaillancourt et al., 2002; Vaillancourt & Newell, 2003) to 100% MVF (Challis, 2006). Research by Knol et al. (2019) and Fiogbe et al. (2021) also found age-related differences in neuromuscular complexity across a range of contraction intensities, from 15 to 40% MVF. In contrast, studies have also found there to be no effect of age on the complexity of isometric muscle force at low (Jordan et al., 2013; Sosnoff

& Newell, 2006d; Sosnoff & Newell, 2007), moderate (Sosnoff & Newell, 2006d; Vieluf et al., 2015) and high (Vieluf et al., 2015) contraction intensities.

Due to the limited number of studies investigating the effect of age on isometric muscle force complexity, there was inevitably limited data at each contraction intensity for each muscle group. Therefore, it was not possible to make clear conclusions as to the effect of contraction intensity on the age-related differences in the complexity of isometric muscle force. Notably there is a lack of research on isometric muscle force complexity using contraction intensities above 40% MVF. Future research should aim to use a broad range of contraction intensities when assessing the effect of age on neuromuscular complexity, to build a greater understanding of the interaction between contraction intensity and muscle group.

In summary, and addressing the second question of the review, the current literature indicates that age-related differences in neuromuscular variability depend on the contraction intensity used in isometric force matching tasks. The dependence of contraction intensity on neuromuscular variability explains, in part, the difference in effect sizes and findings between and within the studies presented in the current review. The largest age-related differences in neuromuscular variability, as measured by the CVF, were observed at lower contraction intensities. Although age-related differences in neuromuscular variability were also seen across a range of contraction intensities, from 2 to 100% MVF. There was also an interaction between contraction intensity and muscle group, with upper extremity muscles effected by age similarly across contraction intensities, whereas the lower extremity muscles were primarily affected by age at low contraction intensities (≤ 10% MVF). The paucity of research and equivocal findings makes drawing clear conclusions as to the effect of contraction intensity on the age-related difference in neuromuscular complexity difficult. Therefore, all future research should endeavour to use a comprehensive range of contraction intensities when investigating the effect of age on the complexity of isometric muscle force signals.

2.5 - Conclusion

The review examined how age affects the complexity, entropy, and variability of isometric muscle force signals, and assessed how these effects are influenced by muscle group and contraction intensity. Overall, the evidence suggests that older adults exhibit isometric muscle force signals of lower complexity and higher variability than younger adults. Smaller upper extremity muscles appear more susceptible to age-related changes in neuromuscular variability than larger lower extremity muscles (Table 2.4). These age-related differences in neuromuscular variability were most pronounced at low contraction intensities, with these differences being less pronounced at higher intensities (Table 2.5). Furthermore, upper extremity muscles showed consistent age-related differences in neuromuscular variability across all contraction intensities (Figure 2.2C), whereas lower extremity muscles were primarily affected at lower contraction intensities (Figure 2.2B).

The paucity of research makes it challenging to elucidate the effects of contraction intensity and muscle group on age-related differences in neuromuscular complexity, particularly of the KE muscles and the muscles involved in precision PG tasks. Future research should investigate a wider range of contraction intensities to advance current understanding of the age-related changes in the complexity, entropy, and variability of force signals in both upper and lower extremity muscle groups. This is crucial to fully characterise age-related differences in neuromuscular complexity and variability, and by extension, in neuromuscular function and the regulation of muscle force under varying task demands.

Statement of Thesis Purpose

To investigate whether there are age-group related differences in the complexity, entropy and variability of muscle torque and force signals derived from isometric knee extension contractions and isometric precision pinch grip contractions.

Statements of Research Aims and Hypotheses

Chapter Four - Intra- and inter-day reliability of the complexity, entropy and variability metrics derived from isometric knee extensor muscle torque signals.

Aim: To assess the intra- and inter-day reliability of the complexity, entropy and variability metrics derived from isometric KE torque signals of younger and middle-aged adults. **Hypothesis:** The complexity, entropy and variability metrics derived from isometric KE torque signals would demonstrate good to excellent intra- and inter-day reliability in both young and middle-aged adults.

Chapter Five - Effect of age-group on the temporal and spatial structure of isometric knee extensor muscle torque signals.

Aim: To investigate age-group differences in the complexity, entropy and variability of isometric KE torque signals. **Hypothesis:** Middle-aged adults would demonstrate lower complexity and entropy and greater variability in isometric KE torque signals compared to younger adults.

Chapter Six - Effect of contraction intensity on age-group related differences in the complexity, entropy and variability of isometric knee extensor torque signals.

Aims:

(1) To investigate the effect of contraction intensity on the age-group related differences in the complexity, entropy and variability of isometric KE torque signals.

(2) To identify the contraction intensities at which the complexity, entropy and variability of isometric KE torque signals were most strongly associated with performance in postural sway and locomotion tasks.

Hypotheses:

(1) Age-group related differences in the complexity, entropy and variability of isometric KE torque signals would be greatest at lower contraction intensities, with age-group related differences being smaller at higher contraction intensities.

(2) Isometric KE torque signals of lower complexity and entropy, and greater variability would be associated with increased postural sway and worse locomotion task performance.

Chapter Seven - Effect of age-group on the neuromuscular complexity and variability of hand muscle force signals.

Aims: To investigate age-group differences in the complexity, entropy, and variability of isometric precision PG force signals across contraction intensities, and to examine whether the complexity and entropy of isometric precision PG force signals are associated with the performance of the manual dexterity tasks. **Hypotheses:** Older adults would produce isometric precision PG force signals of lower complexity and entropy and greater variability across all contraction intensities compared to younger adults. Force signals of lower complexity and entropy of would be associated with worse performance of manual dexterity tasks.

Chapter Eight A - Neural mechanisms underpinning the complexity, entropy and variability of isometric knee extensor torque signals of younger and older adults.

Aim: To investigate the association between the strength and variability of common synaptic input to the motor neuron pool innervating the VL muscle and the complexity of isometric KE torque of adults aged between 18 and 90 years. **Hypothesis:** Stronger and more variable common synaptic input to the motor neuron pool innervating the VL muscle would be associated with an isometric KE torque signal of lower complexity and greater variability.

Chapter Eight B - Neural mechanisms underpinning fatigue-related alterations in the complexity, entropy and variability of isometric knee extensor torque signals.

Aims:

(1) To investigate whether the fatigue-related changes in the strength of common synaptic input to the VL muscle is explanatory of fatigue-related changes in the complexity, entropy and variability of isometric KE torque signals.

(2) To establish whether fatigue-related changes in the complexity and variability of isometric KE torque were accompanied by changes in the complexity and variability of low-pass filtered CSTs and interference HD sEMG signals from the VL muscle.

(3) To determine the strength of association between the effective neural drive to the VL muscle and fluctuations in isometric KE torque during fresh and fatigued contractions.

Hypotheses:

(1) Fatigue would increase the strength of common synaptic input to the VL muscle and would be explanatory of a fatigue-related decrease in the complexity and entropy and increase in the variability of isometric KE torque signals.

(2) The fatigue-related decrease in the complexity and entropy and increase in the variability of isometric KE torque signals will be associated with a decrease in the complexity and entropy and increase in the variability of the CST and interference HD sEMG signals.

(3) Effective neural drive would be strongly cross-correlated with isometric KE torque during fresh and fatigued contractions.

Chapter Three

General Methods.

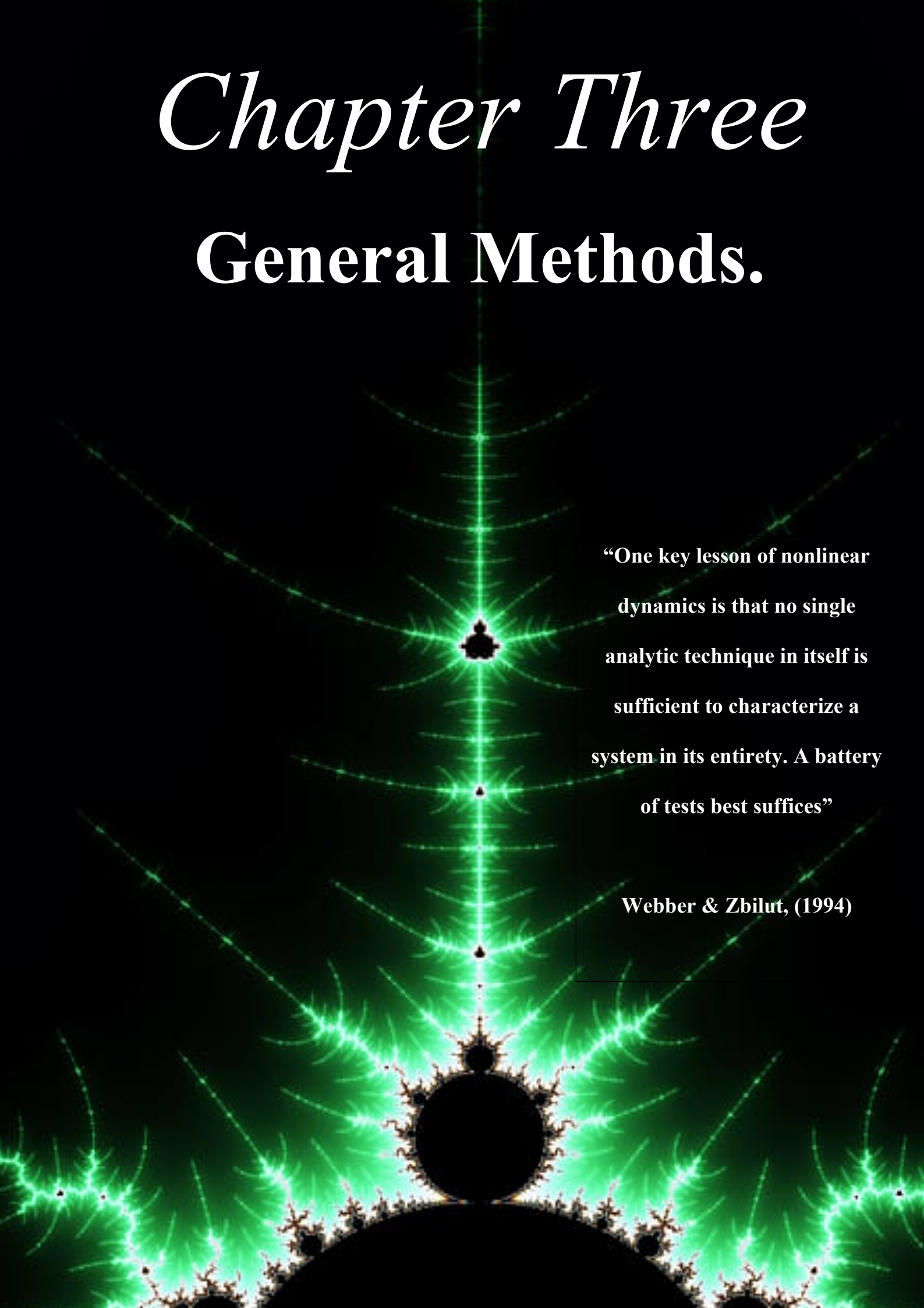

"One key lesson of nonlinear dynamics is that no single analytic technique in itself is sufficient to characterize a system in its entirety. A battery of tests best suffices"

Webber & Zbilut, (1994)

Introduction

This chapter outlines the general methods used in the experimental studies of the thesis. Methods specific to individual studies were included in the relevant experimental chapters.

3.1 - Health and Safety.

All equipment and procedures performed in the experimental studies of the thesis were covered by individual risk assessments, which were consulted and signed prior to completing data collection.

3.2 - Ethical approval and informed consent.

All studies within this thesis were completed with full ethical approval of the University of Kent Research Ethics Committee according to the 1964 Declaration of Helsinki standards and its later amendments (without being registered). Prior to participating in the research studies participants provided written informed consent. All participants also consented to having research findings published in academic journals and presented at conferences.

3.3 - Participant recruitment and screening.

Participants were primarily recruited from the local community in Kent, England, and surrounding counties. The younger age groups were also made up of participants recruited from the University of Kent student population. All participants were assigned with an alpha-numerical code (e.g., Y01) to ensure confidentiality and to anonymise subsequent data relating to each participant.

All participants completed a health and physical activity questionnaire prior to completing any testing to confirm they were in full health and met the inclusion/exclusion criteria for participation in the research. Specific individual study inclusion and exclusion criteria were detailed in the methods of each experimental chapter.

Across all studies participants were regular exercisers, and self-reported to have performed above the World Health Organisation guidelines for ≥ 2years (i.e., 2.5 to 5 hours of moderate exercise per week; Bull et al., 2020).

3.4 - Familiarisation.

Prior to completing the experimental data collection all participants were familiarised with the laboratory surroundings, equipment, and protocols. In all cases participants were provided with a pre-defined practice period for the muscle force control tasks, to ensure all participants were similarly well practiced in the tasks prior to completion of the experimental torque or force control tasks of the specific study. Participants were closely guided through all protocols verbally and using a digital protocol timer to ensure precise replication of the protocols across participants.

3.5 - Experimental controls.

In studies with repeated visits participants attended the laboratory at the same time of day (±1 hour). Visits were conducted on non-concurrent days with a minimum gap of two full days and maximum gap of five full days between visits. In all studies participants were instructed to refrain from any exercise in the day prior to testing and intense exercise in the two days prior. Participants were instructed to arrive euhydrated and in a post-prandial state, having eaten at least 4-hours prior to testing. Participants were told to not consume caffeine within 8-hours and alcohol within 24-hours of testing.

3.6 - Knee extensor torque measurement.

Isometric KE torque (units: Nm) was measured using an isokinetic dynamometer (Cybex HUMAC Norm; CSMi, Stoughton, MA, USA), initialised and calibrated (accepted error < 0.2%) before commencing data collection and then quarterly thereafter according to the manufacturer's instructions.

In all cases the participant's right leg was securely attached to the lever arm of the dynamometer with a padded Velcro strap, with their lateral epicondyle of the right femur in line with the axis of rotation of the lever arm. Participants knee angle was set at 90 degrees, with full extension being 0 degrees. Participants wore an over shoulder and waist seat belt to prevent unwanted movement and use of hip extensors during the contractions. The contralateral limb (left leg) was stabilised using a fixed input adapter and thigh stabiliser strap. The computer monitor (60 cm diameter) displaying the instantaneous torque was positioned 1 m in front of the participants eye line. The positioning of the knee extensor input adapter, dynamometer rotation, dynamometer height, chair-back angle, chair fore/aft, chair rotation, and chair

monorail position were recorded in all experimental studies to ensure precise replication of the participants' set up on an isokinetic dynamometer.

During the isometric maximal voluntary contraction (MVC) trials, participants were instructed to exert maximal instantaneous effort against the dynamometer lever arm and to not pace the effort. Standardised verbal encouragement was provided at regular intervals to encourage maximal effort and consistency across trials. To maintain encouragement consistency, the same phrases, tone, and timing were used for all participants and trials. Real-time feedback was provided in the form of the previous maximal voluntary torque (MVT) value, and participants were encouraged to exceed their previous effort.

During the submaximal constant load torque matching tasks participants were instructed to match their instantaneous torque output to a horizontal thin line (1 mm thick) superimposed on the computer monitor. The Y axis of the display was scaled to the participants MVT, ensuring the superimposed line was located at the same position on the monitor for all participants. The dynamometer was programmed to automatically correct the torque signal for the effect of gravity before data collection.

The isometric KE torque data were recorded at 1000 Hz (unless specified otherwise) via a 16-bit analogue-to-digital converter (ADC; CED Micro 1401-3; Cambridge Electronic Design, Cambridge, United Kingdom), interfaced with a personal desktop computer, with data collected (Spike2, Cambridge Electronic Design) and exported at 1000 Hz for analysis offline in MATLAB (R2023a, The MathWorks, Natick, MA, USA). The dynamometer produces a torque signal with a range of ±0.1 V, within the ±10 V input range of the ADC. The ADC converts the input voltage to a 16-bit digital value in approximately 2 μs, resolving the signal into 65,536 discrete levels. For a ±10 V input range, the resolution was approximately 305 μV per step, which corresponds to a torque resolution of approximately 0.03 Nm (or 30 mNm), assuming a linear relationship between the voltage and the applied torque. This setup ensures high sensitivity and accurate measurement of small torque variations.

The dynamometer model (Cybex HUMAC Norm; CSMi, Stoughton, MA, USA), along with the ADC (CED Micro 1401-3; Cambridge Electronic Design, Cambridge, United Kingdom) and data recording software (Spike2, Cambridge Electronic Design), were selected to replicate the setup used in a substantial body of research on isometric muscle torque signal complexity

and variability (Pethick et al., 2015, 2016, 2018a, 2018b, 2019). Additionally, in line with standard practice for isometric KE torque signal complexity analysis, the torque signal was exported at 1000 Hz without digital filtering (Pethick et al., 2015).

3.7 - Precision pinch grip force measurement.

Isometric precision PG force (units: N) was measured using a miniature button load cell system (CDFT, Capacity 0-250 N, Accuracy ± 0.25%; Applied Measurements Ltd, Berkshire, UK), which was initialised, and calibrated with a strain gauge amplifier / signal conditioner (Bandwidth 6 kHz max unfiltered; Applied Measurements Ltd, Berkshire, UK) by the manufacturers for collection of compression force, prior to data collection. The load cell was calibrated weekly during data collection for Chapter Seven using 12 known weights ranging from 50 g to 2000 g. These weights correspond to forces of approximately 0.49 N to 19.62 N. This calibration ensured accurate force measurements across the expected experimental range.

When completing isometric precision PG force matching tasks participants were seated on a chair in front of a table with the computer monitor (60 cm diameter) displaying their real-time force output 80 cm in front of their eye-line. The participants upper arm of the dominant hand was bent at 120 degrees at the elbow, with the forearm supported on an arm rest and held in a neutral (supination/pronation) position. The centre of the thumb and index finger of the dominant hand were positioned to grip the miniature button load cell. The distance between the thumb and index finger was 10 mm. During the submaximal constant load force matching tasks participants were instructed to match their instantaneous force output to a horizontal thin line (1 mm thick) superimposed on the computer monitor. The Y axis of the display was scaled to the participants MVF, ensuring the superimposed line was located at the same position on the monitor for all participants.

To record the pinch grip force data the miniature button load cell system was connected via BNC cable to an ADC (CED Micro 1401-3; Cambridge Electronic Design, Cambridge, United Kingdom), interfaced with a personal desktop computer, with force data collected (Spike2, Cambridge Electronic Design) and exported at 1000 Hz for analysis offline in MATLAB (R2023a, The MathWorks, Natick, MA, USA).

3.8 - Quantification of Neuromuscular Variability.

Prior to the calculation of the muscle torque or force signal variability the steadiest epoch of each contraction was identified as the epoch with the lowest SD (note, the duration of the epoch was specified in individual experimental chapters). The absolute variability of the torque or force signal was quantified using the variability metric SDT/SDF. The variability metric CVT/CVF (CVF = [SDF/mean force] x 100) was calculated to quantify the variability in the participant's torque or force signal normalised to the mean of the torque or force signal. The accuracy of torque or force signal during submaximal constant load tasks (i.e., contractions at a % MVT/MVF) was quantified by calculating the RMSE between the target torque or force and the participant's instantaneous torque or force. All calculations of muscle torque or force signal variability were performed with custom written MATLAB code (R2023a, The MathWorks, Natick, MA, USA).

3.9 - Quantification of Neuromuscular Complexity.

Prior to the calculation of the muscle torque or force signal complexity the steadiest epoch of each contraction was identified as the epoch with the lowest SD (note, the duration of the epoch was specified in individual experimental chapters). The complexity and entropy of the torque and force signals were measured with the time domain analyses: SampEn, DFA and MSE. All calculations of muscle torque and force signal complexity and entropy were performed with custom written MATLAB code (R2023a, The MathWorks, Natick, MA, USA).

Sample entropy

SampEn quantifies the conditional probability that a template length of m and $m + 1$ data points are repeated during the time series within a tolerance of r (set at a % of the time series SD; Richman & Moorman, 2000). In other words, SampEn indicates the predictability of future values in a time series based on previous values. For time series data that is ordered templates are often similar for m and m+1 points, thus the conditional probability approaches 1 and the entropy of the signal approaches 0. Therefore, entropy values closer to 0 indicate greater regularity and high predictability of a time series, while a value closer to 2 indicates greater irregularity and lower predictability of a time series. Figure 3.1. below provides a visual illustration of the calculation of SampEn.

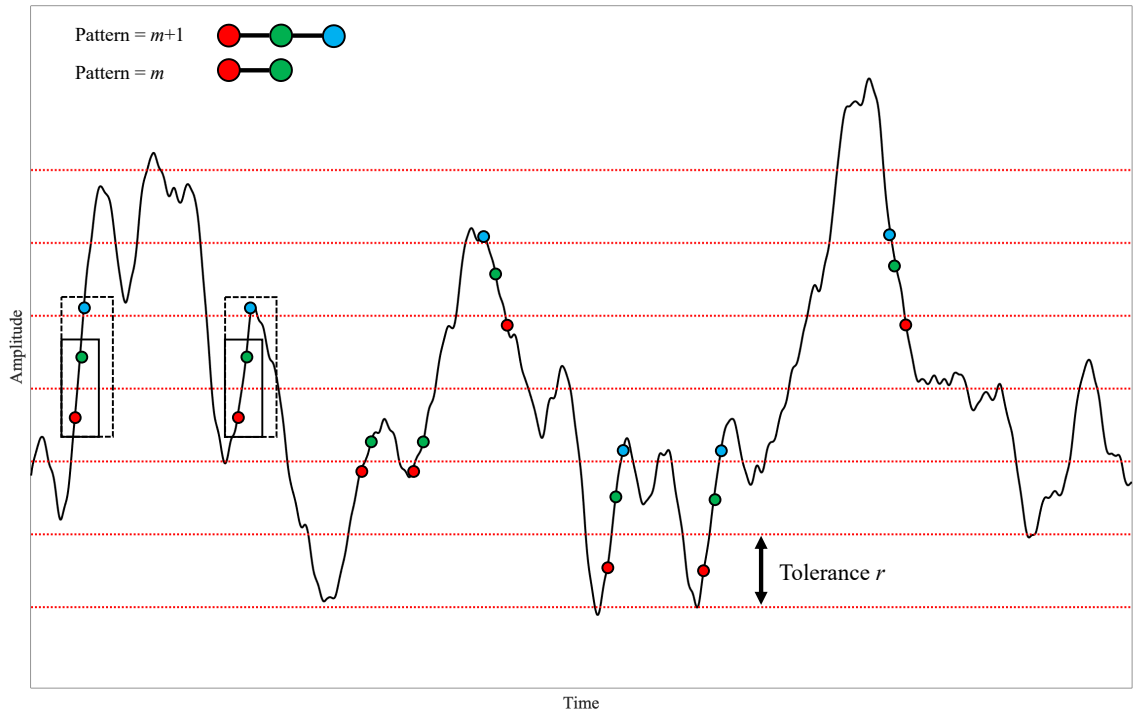

Figure 3.1. Schematic illustration of SampEn estimation where the template length *m* was set at 2 (denoted by the red and green circles). The tolerance for accepting matches was *r* (denoted by the dotted red lines). In this example, two templates to the far left of the Figure (enclosed by the solid box) match, and the *m*+1st points also match (enclosed by the dashed box). Therefore, *A* and *B* both increment by 1.

In the current thesis template length was set at $m = 2$ and tolerance $r = 10\%$ of the SD of the torque and force signal for SampEn analysis. The equation for calculating SampEn [1] is shown below, where N was the number of data points in the time series, m was the length of the template, Ai was the number of matches of the ith template of length $m + 1$ data points, and Bi was the number of matches of the ith template of length m data points:

$$[1]\ SampEn(m, r, N) = -\log\left(\frac{\sum_{i=1}^{N-m} A_i}{\sum_{i=1}^{N-m} B_i}\right) = -\log\binom{A}{B}$$

SampEn was used instead of ApEn, as it avoids counting self-matches by taking the logarithm after averaging, thus reducing the inherent bias existing within the ApEn calculation. In addition, for long time series, such as isometric muscle force signals (i.e., > 5000 data points) both SampEn and ApEn produce similar values. As such, their combined use is redundant when studying the temporal structure of isometric muscle torque and force signals.

Multiscale entropy analysis

The MSE analysis of the torque and force signals were performed as outlined by Costa et al. (2002), providing a measure of neuromuscular complexity over multiple time scales (i.e., the time-dependent structure of the torque and force signals). The MSE analysis addresses the limitations of single-scale SampEn, which measures the regularity of a physiological signal on a single time scale and fails to fully capture its structural and dynamical behaviour (Costa et al., 2002). Consequently, single-scale entropy may overlook critical physiological information and temporal structures linked to the function and interactions between multiple system components operating across multiple time scales (Knol et al., 2019; Vieluf et al., 2015).

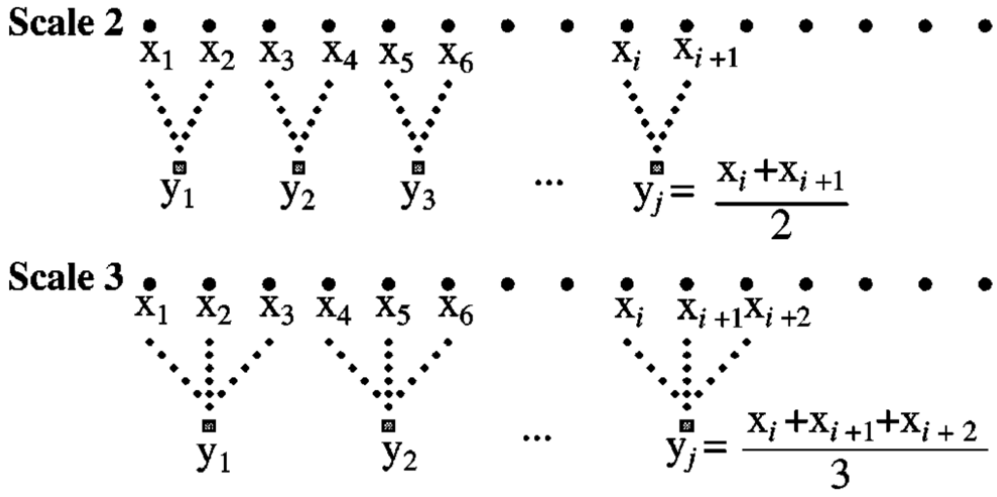

Figure 3.2. Schematic illustration of the multiscale entropy analysis coarse-graining procedure (reproduced from Costa et al., 2002).

From the one-dimensional discrete time series, $\{\chi_1,\ldots, \chi_I,\ldots, \chi_N\}$, coarse-grained time series were constructed, $\{y^{(\tau)}\}$, determined by the scale factor, τ. The original time series was divided into non-overlapping widows of length τ, and then the data points inside each window were averaged, as shown by Figure 3.2 reproduced from Costa et al. (2002). The coarse-grained time series was calculated according to equation [2], where τ = the scale factor, j = time index, N = number of data points and i = index variable used to iterate through the data points:

$$[2]\ y_j^{(\tau)} = \frac{1}{\tau} \sum_{i-(j-1)\tau+1}^{j\tau} \chi_{i'},\ 1 \leq j \leq N/\tau$$

At one scale, the time series $\{y^{(1)}\}$ was the original time series length (example Figure 3.3A). The length of the coarse-grained time series was equal to the length of the original time series divided by the scale factor, τ, with each coarse-grained time series capturing the regularity of the torque signal at different scales. In the current thesis the torque and force time series were coarse-grained up to scale 28, to ensure the coarsest time series contained enough data points for a reliable estimate of SampEn (Costa et al., 2002). Figure 3.3 provides an illustrative example of the coarse graining of a precision PG force signal, with Figure 3.3A being the original time series and Figures 3.3B to 3.3E being the signal coarse-grained at different time scales.

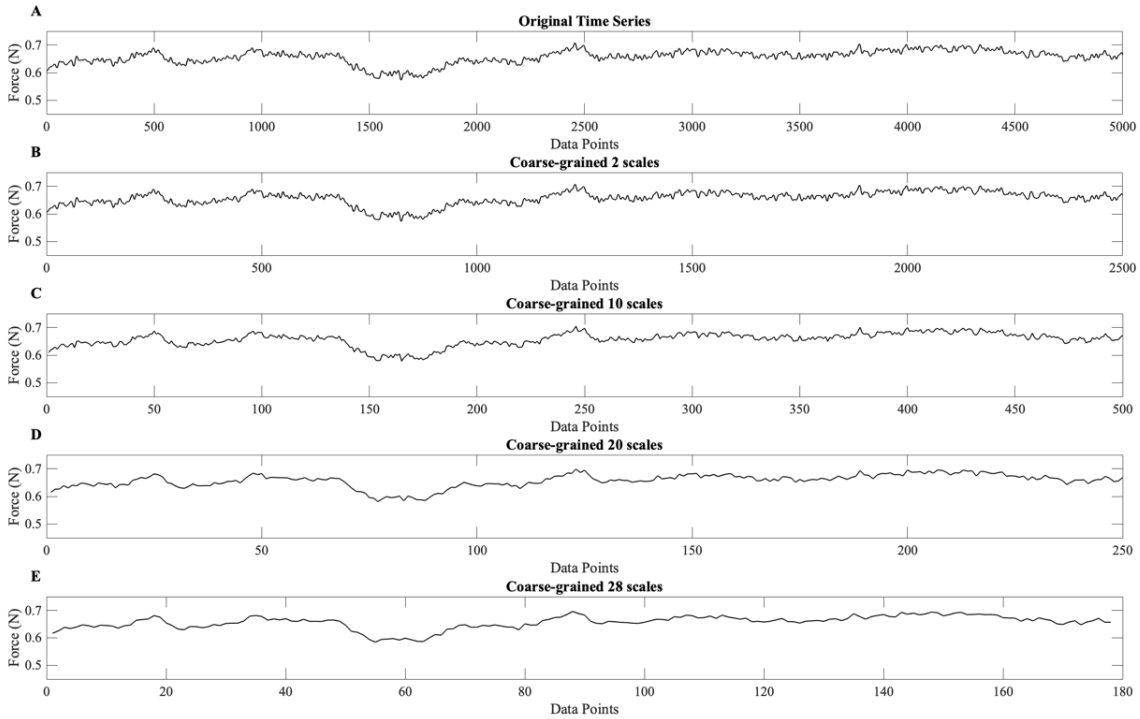

Figure 3.3. Isometric precision pinch grip force signal coarse-grained at different time scales **(A)** Original force signal with no coarse graining, **(B)** Coarse-grained force signal at time scale 2, **(C)** Coarse-grained force signal at time scale 10, **(D)** Coarse-grained force signal at time scale 20, **(E)** Coarse-grained force signal at time scale 28.

The SampEn for each coarse-grained time series was calculated and plotted against the scale factor, τ, producing a MSE curve (Figure 3.4 provides an example of a MSE curve). The SampEn of each coarse-grained time series was computed using equation [1] and a template length set at m = 2 and r = 10% of the SD of the torque or force signal. The areas under the MSE curve were calculated from scales 1 to 28 using equation [3]:

$$[3]\ CI = \sum_{i=1}^{\tau} SampEn(i)$$

The area under the MSE curve was defined as the complexity index (CI), with higher CI values indicating greater complexity of the physiological signal. For example, if the area under MSE curve from scales 1 to 28 were calculated this metric would be termed, CI-28.

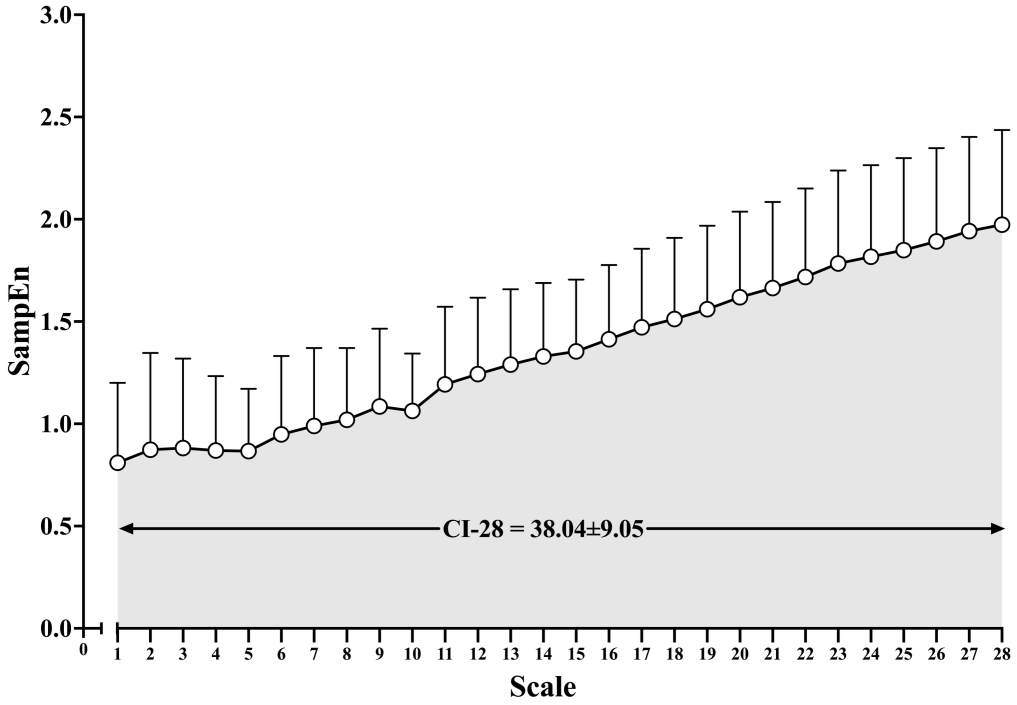

Figure 3.4. Example multiscale entropy curve from N = 140 individuals performing isometric knee extension contractions at 40% of maximal voluntary torque. Each open circle represents the sample entropy of the torque signal at each coarse-grained scale. Note the asymptotic behaviour of the MSE curve, with SampEn continuing to increase with increasing scales. Such asymptotic behaviour indicates the presence of long-range correlations, or new "physiological information" and "complex structures" being revealed across the frequency components of the torque signal that were captured by the coarse graining process.

The coarse-graining procedure of the MSE computation acts as a low-pass filter on the time series (attenuating high frequency components of the time series), in addition to downsampling the original time series (the coarse-grained time series data length is equal to the original time series divided by the scale factor τ) providing a measure of time series (ir)regularity over multiple scales. Therefore, the SampEn at shorter coarse-grained scales captures the regularity of the higher frequency components of the signal, and as the scales become longer (coarser) the regularity of the lower frequency components of the signal were captured.

When using the MSE analysis, it is important to consider that SampEn is sensitive to time series length (Costa et al., 2002; Richman & Moorman, 2000). As the scale factor increases and the series shortens, the statistical reliability of SampEn decreases. Therefore, MSE may not be suitable for time series with fewer than 5000 data points.

Detrended fluctuation analysis

The DFA algorithm was used, as outlined by Peng et al. (1994), to measure the fractal scaling (self-similarity) of the torque and force time series. The DFA algorithm allows for the detection of long-range correlations embedded in seemingly non-stationary physiological time series data. The torque and force time series (denoted as *For*) were first integrated, using equation [4]:

$$[4]\ y(k) = \sum_{i=1}^{k} (For_i - \overline{For}), \qquad k = 1, \ldots, N$$

The integrated time series were then divided into boxes of equal length, *n*. Within each box of length *n*, a straight line was fitted to the data using least squares, denoting the local trend in each box, $y_n(k)$. The integrated time series y(k) was then detrended by subtracting the local trend, $y_n(k)$, within each box. The root-mean-square fluctuation of the integrated and detrended time series was calculated by equation [5]:

$$[5]\ F(n) = \sqrt{\frac{1}{N} \sum_{k=1}^{N} [y(k) - y_n(k)]^2}$$

The DFA computation [5] was repeated across all box sizes to provide a relationship between *F(n)*, the average fluctuation as a function of box size, and the box size, *n*, the number of data points in a box (Peng et al., 1995). The logarithm of box size, log *n*, and the logarithm of the average fluctuation as a function of box size, log *F(n),* were plotted to produce the double logarithmic plot. The slope of the double logarithmic plot, log *F*(*n*) vs log *n,* determines the scaling exponent α. In all cases (unless specified otherwise in experimental chapters) DFA α of the torque and force signals was calculated with 57 box sizes ranging from 1250 to 4 data points as recommended by Pethick et al. (2015). Figure 3.5 presents an example precision pinch grip force output time series and the integrated force output time series with the local trend in each box represented by a red line.

Figure 3.5. (A) Example precision pinch grip force signal time series data (60% MVF), **(B)** The integrated force output time series, with the least-squares fit representing the "trend" in each box (red lines) and the vertical lines indicating the box size of n = 250 data points.

The DFA analysis produces a scaling exponent α. An α = 0.5 indicates that all values of the time series were completely uncorrelated from all previous and future values (i.e., unpredictable white noise; indicative of a very rough time series). An α = 1.5 indicates Brown noise (integral of white noise) and a loss of long-range correlations (i.e., a smooth output with long term memory). A perfectly persistent physiological time series would have a scaling exponent α of 1.0 (i.e., 1/f or pink noise), suggestive of a physiological output of high complexity, that is statistically self-similar with long range-correlations. An α between 0.5 and 1 indicates persistent long-range power-law correlations, so that a large number is more likely to be followed by a large number and vice versa. While an α between 1 and 1.5 indicates correlations exist but were not power-law form (Peng et al., 1995).

Both MSE and DFA analyses assess signal complexity, raising the question of potential redundancy in using both metrics. However, MSE offers an additional advantage by providing SampEn measures at each scale, allowing for scale-to-scale differentiation in signal regularity through MSE curves (i.e., the temporal dynamics of signal structure). In contrast, DFA typically yields a single complexity value for the entire signal, the scaling exponent α.

3.10 - High density surface electromyography.

HD sEMG: Setup and signal acquisition

HD sEMG signals were recorded from the participants vastus lateralis (VL) muscle of the right leg using semi-disposable 64-electrode grids (5 rows x 13 columns; 4 mm electrode diameter; 8 mm interelectrode distance; GR08MM1305; OT Bioelettronica, Torino, Italy; Figure 3.6). Prior to the placement of the electrode grid, the skin of VL muscle was clean shaven, firmly rubbed with medical grade abrasive paste (Spes Medica, Battipaglia, Italy), and cleansed with a 70% ethanol wipe.

The electrode grids were attached to the skin using disposable adhesive foam interfaces (F0A08MM1305; OT Bioelettronica, Torino, Italy), and the holes of the foam interfaces filled with conductive paste to ensure skin-electrode contact (Spes Medica, Battipaglia, Italy). The electrode grids were further secured with kinesiology tape (Kinesio Precut, Albuquerque, NM, USA). The electrode grid was aligned longitudinally with the estimated orientation of the muscle fibres (proximal to distal) on the centre of the right VL muscle belly, individualised for each participant through palpitation. Skinfold thickness at the site of application of the electrode grid was determined before attachment using Harpenden skinfold callipers (British indicators Ltd, Burgess Hill, UK).

The reference electrode was placed on the patella of the right leg and connected to the HD sEMG pre-amplifier. Six ground electrodes (Ag/AgCl, 37.5 x 37.5 mm; Ambu WhiteSensor 4831Q) were attached to the participant and isokinetic dynamometer (Cybex HUMAC Norm; CSMi, Stoughton, MA, USA) to reduce baseline HD sEMG signal noise (Hunter, 2023; Martinez-Valdes et al., 2016). Three ground electrodes were attached to the participant, on the patella of the right leg, the styloid process of the ulna on the right arm, and the malleolus of the right leg. Three further ground electrodes were attached directly around the base of the dynamometer chair.

HD sEMG signals were recorded in monopolar mode, sampled at 2048 Hz, and converted to digital data by a 12-bit analogue-to-digital converter (EMG-USB2+, 64-channel EMG amplifier; OT Bioelettronica, Torino, Italy; 3 dB; Figure 3.6), band-pass filtered (10-500 Hz) and recorded in OTBioLab+ software (v1.5.9, OT Bioelettronica, Torino, Italy). All HD sEMG signals were amplified using a gain of 1000.

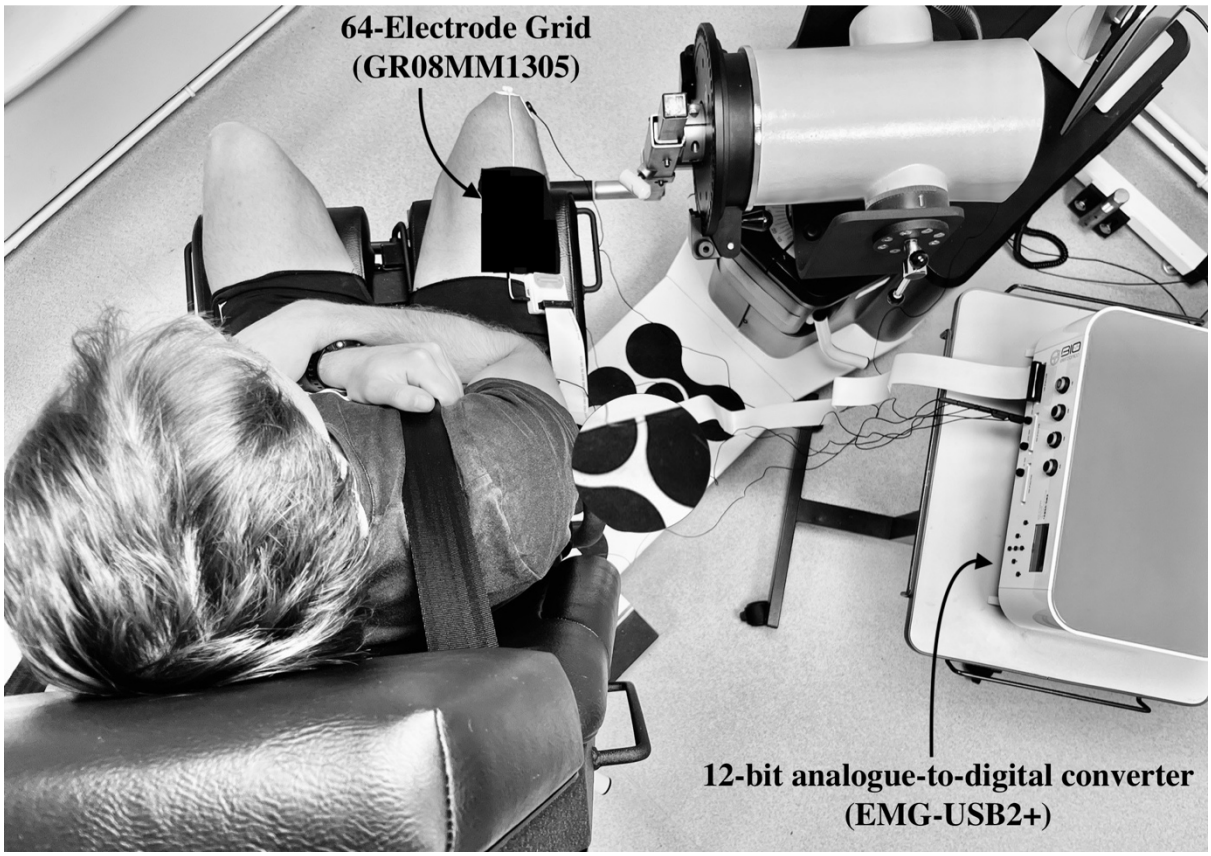

Figure 3.6. HD sEMG 12-bit analogue-to-digital converter (EMG-USB2+, 64-channel EMG amplifier; OT Bioelettronica, Torino, Italy) and isokinetic dynamometer (Cybex HUMAC Norm; CSMi, Stoughton, MA, USA) set up for the recording of interference EMG signals from the participants vastus lateralis muscle of the right leg during isometric knee extension contractions using semi-disposable 64-electrode grids (5 rows x 13 columns; 4 mm electrode diameter; 8 mm interelectrode distance; GR08MM1305; OT Bioelettronica, Torino, Italy) secured with kinesiology tape (Kinesio Precut, Albuquerque, NM, USA).

HD sEMG: Motor unit decomposition

The HD sEMG signals were decomposed offline using the *Decomponi* feature of the OT BioLab+ software (v1.5.9, OT Bioelettronica, Torino, Italy), which is based on convolution blind-source separation (Negro et al., 2016a). Figure 3.7 illustrates the decomposition process of interference EMG signals recorded during the isometric KE contractions to binary MU spike trains. Electrode channels exhibiting poor signal-to-noise or artefacts were removed before decomposition.

The estimated MU spike trains were assessed against a silhouette measure (SIL), which represents the silhouette of the detected MU and was used as a normalised index of reliability (Negro et al., 2016a). The SIL was initially set at 0.90 and then reduced to 0.85 to increase MU yield. Due to the use of a lower SIL value (0.85) to discriminate MUs, additional inclusion

criteria for MU acceptance were implemented (Feeney et al., 2018). Only MUs that met the following criteria were accepted for further analysis: (1) pulse-to-noise ratio ≥ 28 dB; (2) a mean interspike interval (ISI) between 20 and 200 ms; (3) CV of ISI < 30%; (4) a skewness for the ISI distribution < 2; and (5) an observable waveform in bipolar differential recordings (Feeney et al., 2018). A single experienced investigator visually inspected all decomposition results and excluded all erroneous MUs and discharge times (Del Vecchio et al., 2020; Martinez-Valdes et al., 2023).

The binary representations of MU spike trains for all 20 second isometric KE contractions (see example Figure 3.7D) performed by each participant were exported from the OT BioLab+ software (v1.5.9, OT Bioelettronica, Torino, Italy) for analysis offline in MATLAB (R2023a; The MathWorks, Natick, MA, USA). Before further analysis of the binary MU spike trains, the steadiest 10 second epoch of muscle torque signal from each 20 second isometric KE contraction was identified as the epoch with the lowest SD (see example Figure 3.7D and 3.7E). The binary MU discharges from the same 10 second epoch were extracted for further analysis.

Calculation of motor unit discharge characteristics

The spike trains of each active MU during the steadiest 10 second epoch of the isometric KE contractions were analysed to derive the following MU discharge characteristics: mean MU discharge rate in pulses per second (PPS), CV of ISI, and mean ISI.

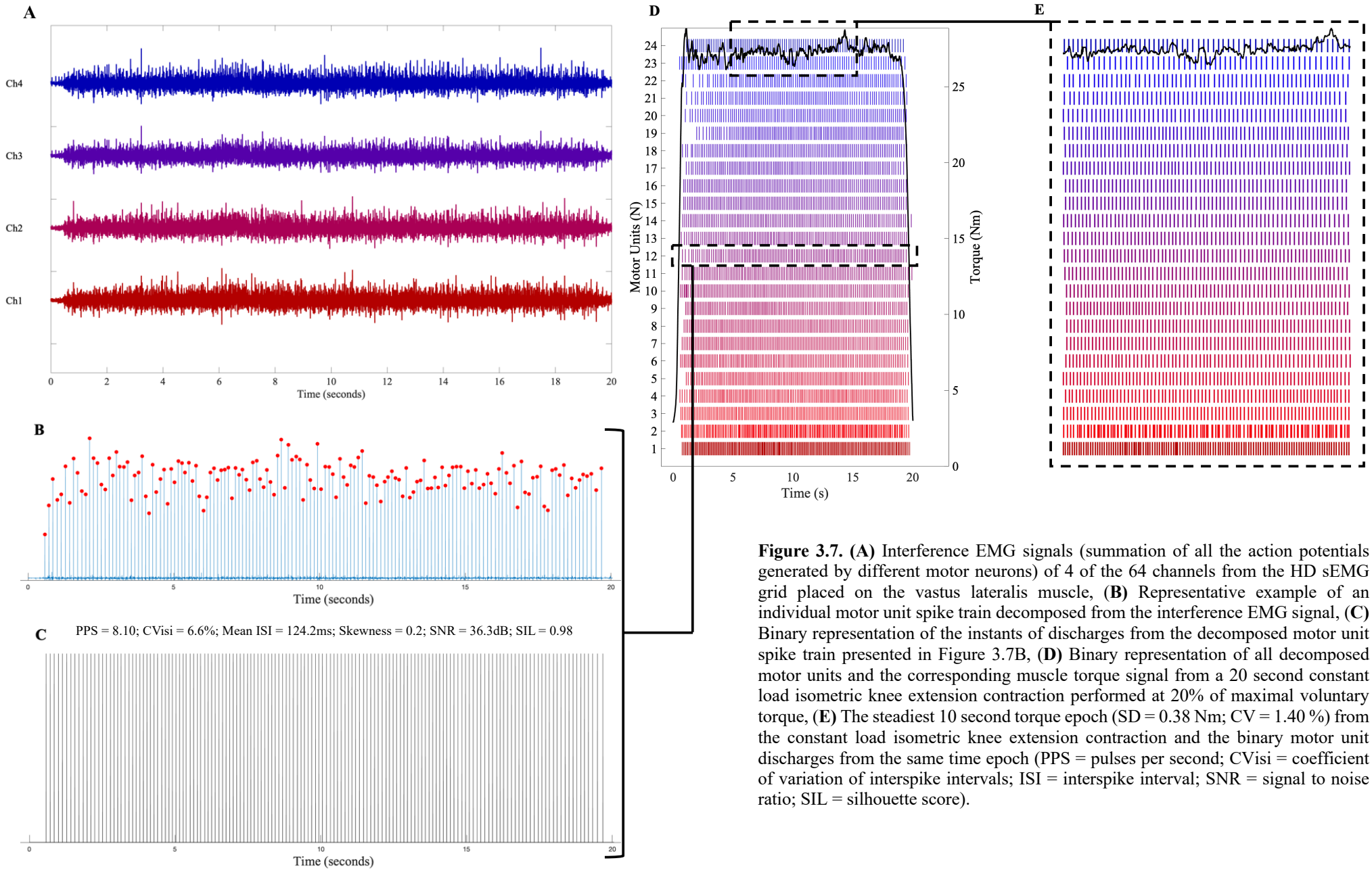

Figure 3.7. (A) Interference EMG signals (summation of all the action potentials generated by different motor neurons) of 4 of the 64 channels from the HD sEMG grid placed on the vastus lateralis muscle, **(B)** Representative example of an individual motor unit spike train decomposed from the interference EMG signal, **(C)** Binary representation of the instants of discharges from the decomposed motor unit spike train presented in Figure 3.7B, **(D)** Binary representation of all decomposed motor units and the corresponding muscle torque signal from a 20 second constant load isometric knee extension contraction performed at 20% of maximal voluntary torque, **(E)** The steadiest 10 second torque epoch (SD = 0.38 Nm; CV = 1.40 %) from the constant load isometric knee extension contraction and the binary motor unit discharges from the same time epoch (PPS = pulses per second; CVisi = coefficient of variation of interspike intervals; ISI = interspike interval; SNR = signal to noise ratio; SIL = silhouette score).

Calculation of smoothed motor unit cumulative spike trains

The binary spike trains of all active MUs during the steadiest 10 second epoch of the isometric contraction were summed to produce a cumulative spike train (CST). To extract the low-frequency components of effective neural drive to the muscle, representative of torque fluctuation dynamics, the CSTs were smoothed with a 400-ms Hann window (Figure 3.8).

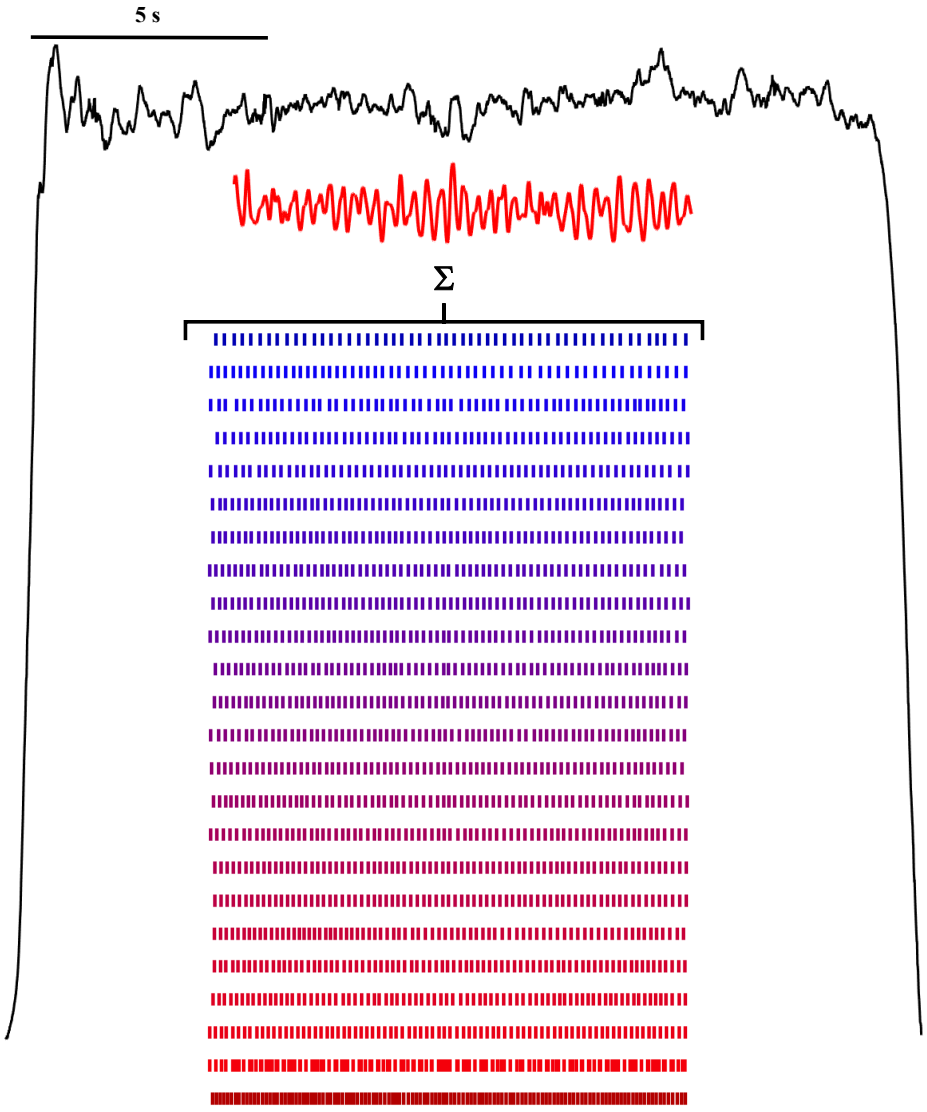

Figure 3.8. Illustration of the individual motor unit spike trains from the 10 second epoch (Figure 3.7E) being summed to generate a cumulative spike train, which has been low pass filtered to produce the smoothed cumulative spike train (depicted by the red trace). The torque signal trace from the 20 second isometric knee extension contraction from which the motor unit spike trains were derived is depicted by the black line.

The complexity and variability of the smoothed CSTs was then determined using, SampEn, DFA, MSE, CV and SD, as outlined in General Methods - Sections 3.8 and 3.9.

Estimation of within-muscle motor unit coherence

Within-muscle (intra-muscle) frequency domain coherence analysis was used to assess the neural connectivity between MUs of the same muscle (Myers et al., 2004). The coherence value at a given frequency represents the correlation between two signals (i.e., two CSTs of equal number of MUs) ranging from 0 (no correlation) to 1 (perfect correlation).

The within-muscle coherence was performed on two equal-sized groups of unfiltered CSTs (derived from the steadiest 10 second epoch of the isometric KE contraction). To estimate coherence, the magnitude-squared coherence was calculated using Welch's averaged periodogram method with 1 second non-overlapping windows. The number of MUs in each of the two groups of CSTs ranged from 1 to the maximum of half the number of detected MUs during the isometric contraction. For each coherence function iteration, 100 random permutations were performed on CSTs of varying number of MUs (Figure 3.9). The averaged value of coherence was computed from all permutations (Negro et al., 2016b; Hug et al., 2021).

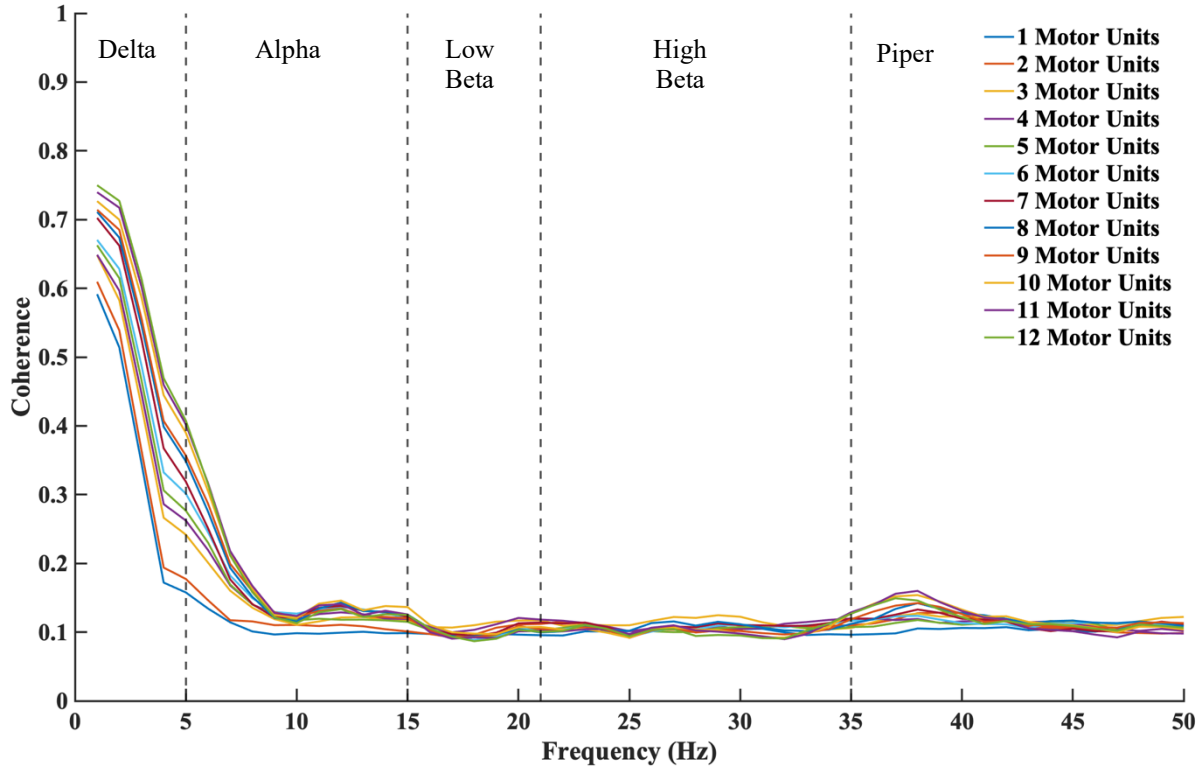

Figure 3.9. Example of an individual coherence analysis between two cumulative spike trains of different numbers of motor units from 0 to 50 Hz. Each estimation of coherence is the average of 100 random combinations of the original spike trains.

Coherence was calculated in the low-frequency delta bandwidth (0-5 Hz), which has been shown to be the dominant frequency of voluntary control in muscle torque or force output and represents common neural drive to the muscle (Farina & Negro 2015). Coherence was also calculated across the frequency bands: Alpha (5-15 Hz), Low beta (15-21 Hz), High beta (21-35 Hz), Piper (35-50 Hz) and Gamma (32-100 Hz; Dideriksen et al., 2018).

The higher the coherence value, for the same number of MUs involved in the coherence estimation, indicates a greater strength of common synaptic input to the motor neuron pool (Negro & Farina, 2011). As shown in Figure 3.10 coherence monotonically increases with the number of MUs used to generate the CSTs, therefore only contractions with a minimum of 6 MUs were subject to the within-muscle coherence analysis (Dideriksen et al., 2018; Lecce et al., 2023).

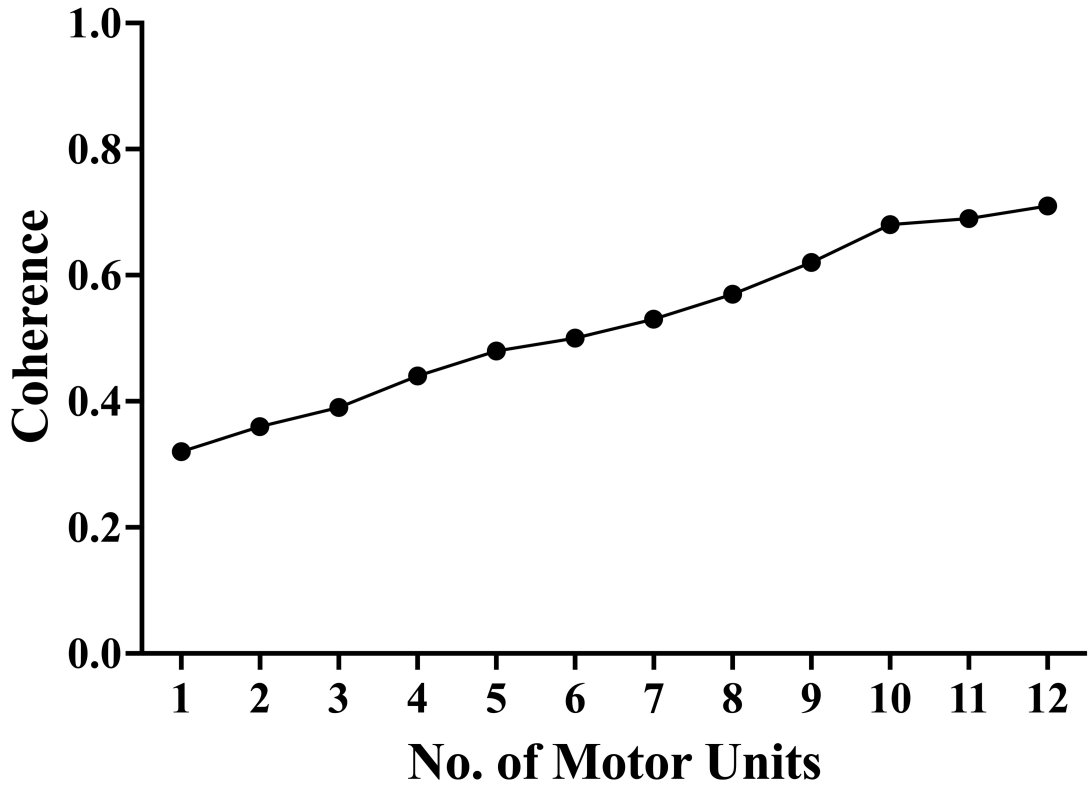

Figure 3.10. The coherence in the delta bandwidth (0-5 Hz) monotonically increases with the number of motor units used to derive the unfiltered cumulative spike trains (summation of individual motor unit spike trains of different number of motor units).

The coherence estimates were also transformed into standard Z-scores using equation [6] below, where *COH* is the raw coherence values, *L* is the number of time segments used in the coherence analysis (e.g., for 10 second, *L* = 10 as the analysis was performed on a 10 second window), *atanh* returns the inverse hyperbolic tangent of the square root of COH, and the *bias* is calculated empirically as the mean *z*-score between 100 and 500 Hz where no coherence is expected.

$$[6]\ z = \sqrt{2L} \times \operatorname{atanh}\left(\sqrt{COH}\right) - bias$$

The standard Z-transform is an empirical method for removing bias from the signals that were uncorrelated within the specified range (Del Vecchio et al., 2019a; Laine & Valero-Cuevas, 2017; Rossato et al., 2022). The transformed coherence values can be considered significantly greater than zero at a value of 1.65 (one-sided 95% confidence level).

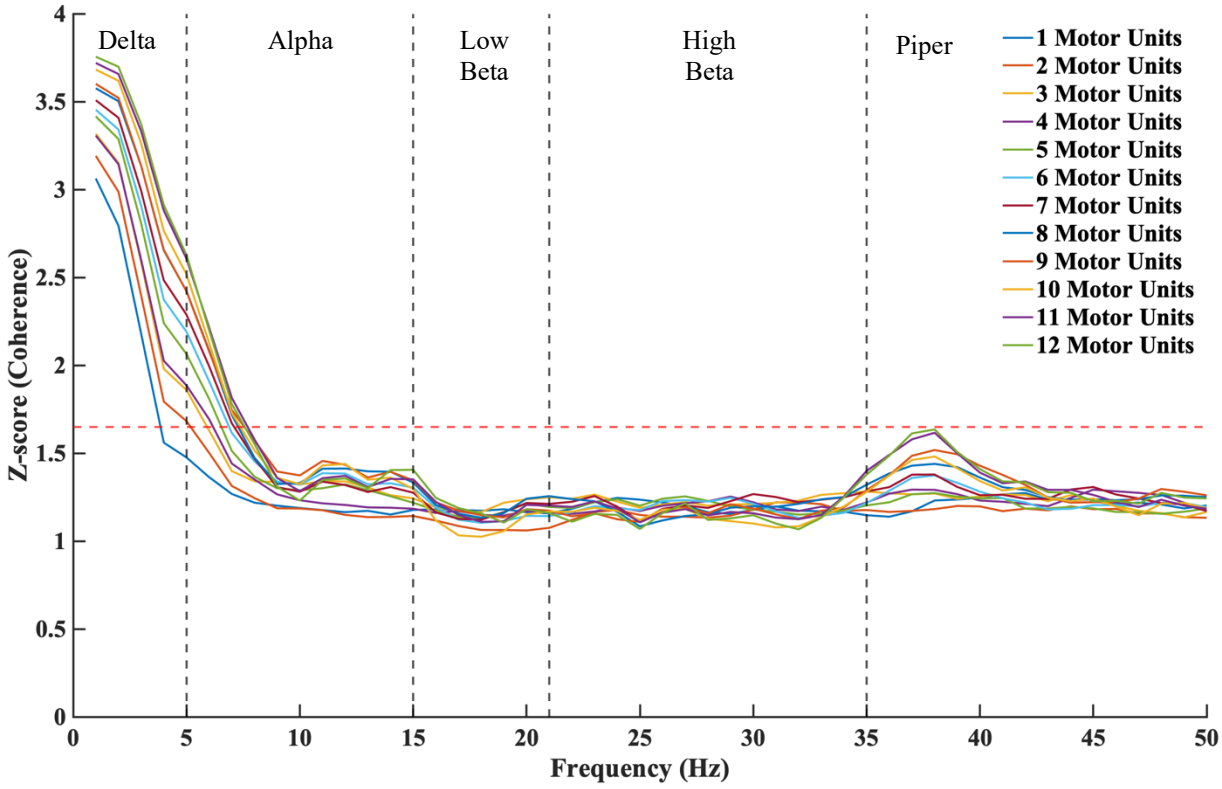

Figure 3.11. Example coherence data from Figure 3.9 which has been standard Z-transformed (red dashed line = one-sided 95% confidence level).

Interference EMG signal processing and analysis

The interference EMG signals of all 64 channels from the HD sEMG grid (see example signals Figure 3.7A) for all isometric KE contractions performed by each participant were exported from the OT BioLab+ software (v1.5.9, OT Bioelettronica, Torino, Italy) for analysis offline in MATLAB (R2023a; The MathWorks, Natick, MA, USA).

The interference EMG signals from the channels were summed to generate a single interference EMG signal representing the global neural drive to the VL muscle (summation of all the action potentials recorded by the HD sEMG grid). Channels exhibiting poor signal-to-noise or artefacts were removed before summation. Before further analysis a 10 second epoch of the summed interference EMG signal was extracted, corresponding to the steadiest 10 second epoch of muscle torque time series from each 20 second isometric KE contraction.

The summed interference EMG signals were full-wave rectified and filtered with a 4th order Butterworth filter with low-pass cut-off frequency of 500 Hz. The rectified and filtered interference EMG signals were then subjected to the complexity and variability analysis, SampEn, DFA, MSE, CV and SD as outlined in General Methods - Sections 3.8 and 3.9.

The power spectral density (PSD) was estimated from the summed interference EMG signals (filtered with a 4th order Butterworth filter with low-pass cut-off frequency of 500 Hz) using a non-overlapping linear Hanning window (window size 512 samples), creating 4 Hz frequency bins. The frequency bin with the greatest power density was used to determine the dominant frequency of the interference EMG signal. Total power was calculated as the total power between the frequency range of 0 and 200 Hz. The relative power in each 4 Hz frequency bin was calculated as follows: power in frequency bin divided by total power multiplied by 100.

3.11 - Statistical analyses.

Data were presented as individual values or mean ± SD (unless specified otherwise). Statistical analyses were conducted using IBM SPSS Statistics 29 (IBM, Armonk, New York, USA). Visual inspection of Q-Q plots and Shapiro-Wilk statistics were used to assess whether data were normally distributed. The statistical significance level was set at $P < 0.05$ in all cases.

Experimental Chapters

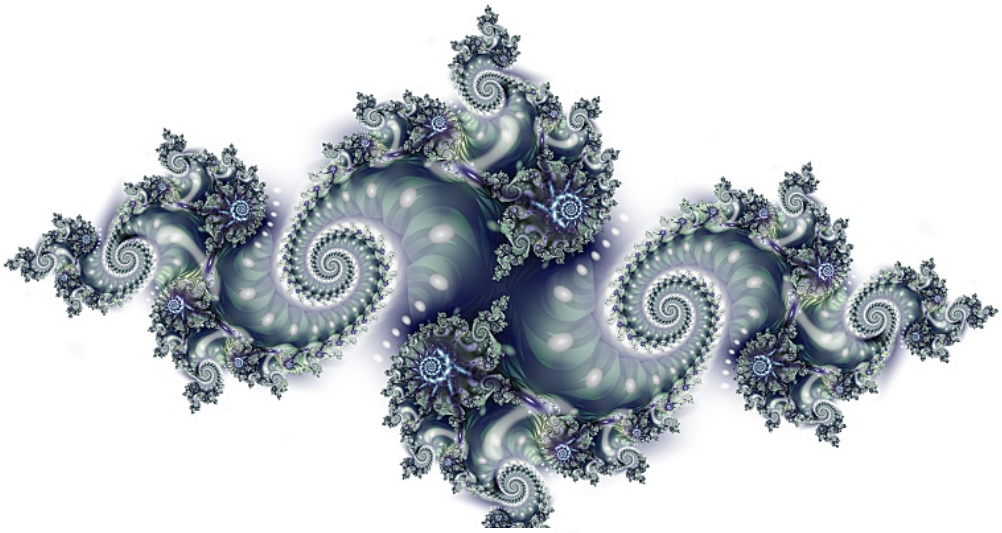

Chapter Four

Intra- and inter-day reliability of the complexity, entropy and variability metrics derived from isometric knee extensor muscle torque signals.

4.1 - Introduction

Measurement of the temporospatial structure of isometric muscle torque signals has the potential to be an effective non-invasive tool for assessing and monitoring changes in neuromuscular function and motor control. This can be achieved using signal analysis techniques to quantify the *complexity, entropy* and *variability* of the muscle torque signal (Pethick et al., 2021b). In the forthcoming experimental chapters, the complexity, entropy and variability metrics will be used to investigate age-group differences in the neuromuscular function of the KE muscles (Chapters Five, Six, Eight A, and Eight B). Therefore, knowledge of the metrics intra- and inter-day reliability is required to delineate between expected systematic and/or random variation and that of 'real age-related' changes. Moreover, reliability data can be used to estimate the required sample size to detect differences or changes in the metrics beyond measurement error.

Intra-day reliability is defined as the degree to which measurement results were consistent over time, it is typically evaluated by having the same individuals perform the measurement on multiple occasions on the same day, under the same conditions (Koo & Li, 2016). Inter-day reliability quantifies the stability of measurements taken on different days (Atkinson & Nevill, 1998). It is crucial in contexts where systematic error (e.g., learning effects, transient changes in fatigue or motivation) and random error (e.g., inconsistencies in the measurement protocol, inherent biological variation or technical/mechanical variation) could affect the results (Atkinson & Nevill, 1998). Reliable measurements are therefore critical for detecting *true* changes in a variable of interest, rather than measurement artifacts or random variations.

Reliability can be quantified using both relative and absolute measures (Atkinson & Nevill, 1998; Hopkins, 2000). Relative reliability, often measured by the intraclass correlation coefficient (ICC), is an index of both correlation and agreement between repeated measurements (Bartko, 1966). ICC values range from 0 to 1, with higher values indicating stronger reliability (Koo & Li, 2016; McGraw & Wong, 1996). Absolute reliability assesses the consistency of individual measurement scores, considering the magnitude of measurement error. Common absolute reliability measures include the standard error of measurement (SEM), coefficient of variation (CV) and minimal detectable change (MDC). SEM reflects the precision of individual scores by estimating the amount of error in a measurement and is derived from the standard deviation of test scores and the correlation coefficient (Atkinson &

Nevill, 1998; Harvill, 1991; Weir, 2005). CV is defined as the ratio of the SD to the mean, and it expresses the extent of variability in relation to the mean of the population (Atkinson & Nevill, 1998). MDC indicates the smallest amount of change in a measurement that reflects a real change beyond measurement error and is often used to determine the clinical significance of changes in a measurement (Beckerman et al., 1996; Beckerman et al., 2001; Weir, 2005).

Previous research has investigated the reliability of the variability of isometric KE muscle torque in younger adults (mean age < 32 years; Singh et al., 2010; Spiering et al., 2011). The intra-day reliability of the variability of isometric KE muscle torque was found to be excellent at 15% MVT (ICC = 0.91) and good at 20% MVT (ICC = 0.82; Singh et al., 2010). Similarly, inter-day reliability was found to be good at 15% MVT (ICC = 0.82) and 20% MVT (ICC = 0.79; Singh et al., 2010). In contrast, another study reported poor intra-day reliability for the variability of isometric KE muscle torque at 5% MVT (ICC = 0.20; Spiering et al., 2011). Research on other muscle groups has shown that older adults (aged 67 ± 8 years) exhibit good reliability for the variability of isometric HG muscle force at 5% MVF (ICC = 0.81), 10% MVF (ICC = 0.77), and 25% MVF (ICC = 0.77; Blomkvist et al., 2018). Young individuals (aged 12.8 ± 3.1 years) demonstrated good to excellent inter-day reliability for the variability of DF and PF muscle torque (ICCs = 0.86 to 0.91; Bandholm et al., 2008). Likewise, younger adults (aged 20.9 ± 0.7 years) exhibited good intra-day reliability for the variability of isometric PF force at 25% MVF (ICC = 0.88; CV = 6.96%; Clark et al., 2005).

The current research suggests that the intra- and inter-day reliability of isometric muscle torque and force signal variability at low contraction intensities is generally good to excellent. However, a notable gap remains due to the absence of established reliability statistics for complexity and entropy metrics derived from submaximal (i.e., 40% MVT) and maximal (i.e., MVT) isometric KE torque signals in both younger (18 to 30 years) and middle aged (50 to 70 years) adults. These metrics were suggested to provide deeper insights into neuromuscular function (Pethick et al., 2021a; Pethick et al., 2021b), yet their reliability has not been evaluated. To address this gap, the present study aimed to assess the intra- and inter-day reliability of complexity, entropy, and variability metrics derived from isometric KE torque signals of younger and middle-aged adults. It was hypothesised that the complexity, entropy and variability metrics derived from isometric KE torque signals would demonstrate good to excellent intra- and inter-day reliability in both young and middle-aged adults.

4.2 - Methods

4.2.1. Participants.

Sixty-six healthy individuals (50 male; 16 female) were recruited to participate in the study. Participants were recruited to be in two age groups, the younger age group (YG) were aged 18 to 30 years (N = 22; 16M, 6F) and the middle age group (MG) were aged 50 to 70 years (N = 44; 34M, 10F). The same participants data were presented in Chapter Five, where the data was analysed to assess the effect of age on the isometric KE torque signal complexity, entropy and variability.

Before being allowed to participate in the study all potential participants completed a health questionnaire to ensure they were in full health. Participants were required to be non-obese, non-smokers, not have previous or current circulatory disorders, have no known or signs/symptoms of cardiovascular, neuromuscular, renal, or metabolic conditions, and not be physically impaired (i.e., able to perform maximal exercise). All participants were regular exercisers, having performed above the World Health Organisation guidelines for ≥ 2 years (i.e., 2.5 to 5 hours of moderate exercise per week; Bull et al., 2020). Participant height was measured using a portable stadiometer (Seca 217; Seca GmbH & Co. KG, Hamburg, Germany), body mass measured using a mechanical flat scale (Seca 760; Seca GmbH & Co. KG, Hamburg, Germany) and body composition (fat mass percentage and lean body mass) measured using a Seca mBCA 525 (Seca GmbH & Co. KG, Hamburg, Germany).

Participants provided written informed consent at the first visit. The study was completed with full ethical approval of the University of Kent Research Ethics Committee (Proposal number: 21_2020_21), according to Declaration of Helsinki standards (but without being registered).

4.2.2. Experimental Design.

Each participant completed three visits to the laboratory at the same time of day (± 1 hour). Visit one being participant screening, laboratory familiarisation and the measurement of isometric MVT of the KE muscles. At visits two and three, participants completed the repeated measurements of isometric KE muscle torque control at 40% MVT and MVT, from which the torque signal complexity, entropy and variability metrics were calculated. The submaximal (40% MVT) and maximal (MVT) intensities were selected to assess the intra- and inter-day reliability of the complexity, entropy, and variability in isometric knee extensor torque signals,

representing two contraction intensities with distinct neuromuscular demands (Inglis et al., 2025).

4.2.3. Measurement of isometric knee extensor maximal voluntary torque (visit one).

Participants were set up on an isokinetic dynamometer (Cybex HUMAC Norm; CSMi, Stoughton, MA, USA), as outlined in Chapter Three - General Methods - Section 3.6. Once set up on the dynamometer, participants performed a warm-up of ten submaximal contractions of increasing effort after which a series of brief (6 second) MVCs were performed to establish the MVT. MVCs were repeated (separated by 60 seconds rest) until a plateau in peak torque was reached (i.e., until three consecutive peak torques were within 5% of each other). The highest torque value from a 2 second epoch was recorded as the participant's MVT, which was then used to set the isometric exercise intensity (40% MVT) for the constant load isometric KE contractions in visits two and three.

Participants were then familiarised with the torque control tasks by performing five 10 second constant load contractions at 20% MVT followed by five 10 second constant load contractions at 40% MVT, with self-selected rest periods between contractions.

4.2.4. Repeated measurement of isometric knee extensor torque control (visits two and three).

Visits two and three involved the repeated measurement of isometric KE muscle torque control. Participants were seated and set up on the isokinetic dynamometer as recorded in visit one. Participants then completed a brief warm-up of isometric contractions consisting of five 10 second constant load contractions at 20% MVT, followed by five 10 second constant load contractions at 40% MVT, with 10 second rest periods.

After the warmup, participants completed four 6 second MVCs with 60 seconds recovery between each MVC. The MVCs were then followed by 10 minutes rest after which participants completed six 10 second constant load contractions at 40% MVT with 60 seconds recovery between each contraction. During the 40% MVT torque matching tasks participants were instructed to match their instantaneous torque output to a thin line (1 mm thick) superimposed on the computer monitor. The Y axis of the display was scaled to the participants MVT, ensuring the superimposed line was located at the same position on the monitor for all participants.

4.2.5. Torque signal complexity, entropy, and variability metric analysis.

Prior to the calculation of the muscle torque complexity, entropy and variability metrics, the steadiest 5 seconds of each contraction (i.e., the four MVCs and six 40% MVT contractions performed at visits 2 and 3) were identified as the 5 seconds with the lowest SD. The SDT, CVT and RMSE which quantify the variability and accuracy of torque signal were calculated as outlined in Chapter Three - General Methods - Section 3.8. The complexity and entropy metrics, SampEn, DFA and CI-28 were calculated as outlined in Chapter Three - General Methods - Section 3.9.

To calculate intra-day reliability at 40% MVT, the complexity, entropy and variability metrics were derived from the two most accurate contractions performed during visit 2, identified as the contractions with the lowest RMSE. To calculate intra-day reliability at MVT, the complexity, entropy and variability metrics were derived from the two steadiest contractions performed during visit 2, identified as the contractions with the lowest SDT.

To calculate inter-day reliability at 40% MVT, the complexity, entropy and variability metrics were derived from the two most accurate contractions performed during visits 2 and 3, identified as the contractions with the lowest RMSE. For each visit, the mean of these two contractions was calculated for each metric, providing the metrics value for day 1 and day 2. To calculate inter-day reliability at MVT, the complexity, entropy and variability metrics were derived from the two steadiest contractions performed during visits 2 and 3, identified as the contractions with the lowest SDT. For each visit, the mean of these two contractions was calculated for each metric, providing the metrics value for day 1 and day 2.

4.2.6. Statistical analysis.

The intra- and inter-day reliability analysis was conducted using the combined data from all participants ($N = 66$) as well as separately on the YG ($N = 22$) and MG ($N = 44$).

Paired samples *t*-test was performed to determine if there was a significant difference in the complexity, entropy and variability metrics between day (day 1 vs. day 2) and within day (contraction 1 vs. contraction 2).

Relative intra- and inter-day reliability of the complexity, entropy and variability metrics was assessed through two-way random $ICC_{2,1}$ for absolute agreement (Shrout & Fleiss, 1979).

Based on the ICCs, relative reliability was defined as: poor = ICC < 0.5, moderate = ICC ≥ 0.5 to < 0.75, good = ICC ≥ 0.75 to < 0.90 and excellent = ICC ≥ 0.90 (Koo & Li, 2016).

Absolute intra- and inter-day reliability of the complexity, entropy and variability metrics was assessed by the SEM which was calculated using equation [1] and MDC using equation [2]:

$$[1]\ SEM = SD\ x\ \sqrt{1 - ICC}$$

$$[2]\ MDC = SEM\ x\ 1.96\ x\ \sqrt{2}$$

Intra- and inter-day CV was calculated using equation [3]:

$$[3]\ CV = \left(\frac{Mean}{SD}\right) x\ 100$$

Based on the CV, absolute reliability was defined as: poor = CV ≥ 30%, moderate = CV ≥ 20% to < 30%, good = CV ≥ 10% to < 20% and excellent = CV < 10%.

The estimation of sample size for a two-tailed test for each complexity, entropy and variability metric was performed using Equation [4]. In this equation, N = estimated sample size, Δ = MDC, α = significance level set at 0.05, β = power set at 90% and σ = standard deviation of the data. The MDC was selected to estimate the sample size required to detect a statistically significant change in the metric beyond the measurement error.

$$[4]\ N = \frac{2 \cdot \left(Z_{\left(1-\frac{\alpha}{2}\right)} + Z_{\beta}\right)^2 \cdot \sigma^2}{\Delta^2}$$

The significance level was set at $P < 0.05$ in all cases. Statistical analyses were performed in IBM SPSS statistics 29 (IBM Corp., Armonk, NY, United States).

4.3 - Results

4.3.1. Participant characteristics and anthropometrics.

Data from forty-four middle aged adults (34M; 10F) and twenty-two younger adults (16M; 6F) were included in the analysis. Table 4.1 presents the participant characteristics and anthropometrics.

Table 4.1 Participant characteristics and anthropometrics.

	Middle Age Group	Younger Age Group
N	44 (34M; 10F)	22 (16M; 6F)
Age (years)	58.6 ± 5.1	21.9 ± 3.7
Height (cm)	173.8 ± 8.6	177.3 ± 9.8
Mass (kg)	72.3 ± 12.1	74.1 ± 12.1
Fat Mass (%)	22.0 ± 7.2	16.1 ± 9.1
Lean Body Mass (%)	78.0 ± 7.2	83.9 ± 9.1
Lean Body Mass (kg)	56.3 ± 10.1	61.9 ± 10.9
Lean Body Mass Index ($kg.m^2$)	18.5 ± 2.1	19.3 ± 1.9
Systolic BP (mmHg)	131 ± 8	126 ± 6
Diastolic BP (mmHg)	80 ± 10	73 ± 8

Abbreviations: BP = blood pressure; data are mean ± SD..

4.3.2. Intra-day reliability of isometric knee extensor torque signal complexity, entropy and variability metrics.

Table 4.2 presents the intra-day reliability statistics of the isometric KE torque signal complexity, entropy and variability metrics at 40% MVT. SampEn demonstrated good to excellent relative reliability (ICC = 0.83 to 0.91). Absolute reliability of SampEn was good to excellent (CV = 9.83% to 17.23%). Estimated sample size for SampEn ranged from 17 to 32. The complexity metrics, DFA α (ICC = 0.66 to 0.71) and CI-28 (ICC = 0.68 to 0.72) demonstrated moderate relative reliability. Absolute reliability of DFA α and CI-28 was good to excellent (CV = 5.13% to 12.70%). Estimated sample size for DFA α and CI-28 ranged from 8 to 10.

The variability metrics, CVT (ICC = 0.65 to 0.73) and RMSE (ICC = 0.64 to 0.72) demonstrated moderate relative reliability. SDT demonstrated good to excellent relative reliability (ICC = 0.77 to 0.91). Absolute reliability of the variability metrics was moderate to excellent (CV = 14.74% to 30.20%). Estimated sample size for the variability metrics (SDT, CVT and RMSE) ranged from 8 to 32.

Table 4.3 presents the intra-day reliability statistics of the isometric KE torque signal complexity, entropy and variability metrics at MVT. SampEn demonstrated good to excellent relative reliability (ICC = 0.87 to 0.90). However, the absolute reliability of SampEn was poor (CV = 33.47% to 33.89%). Estimated sample size for SampEn ranged from 22 to 29. The complexity metric, DFA α demonstrated poor to moderate relative reliability (ICC = 0.48 to 0.69), but exhibited excellent absolute reliability (CV = 4.89% to 5.02%). CI-28 demonstrated moderate to good relative reliability (ICC = 0.63 to 0.77) and moderate absolute reliability (CV = 22.89% to 29.72%). Estimated sample size for DFA α and CI-28 ranged from 7 to 13.

The variability metrics, CVT (ICC = 0.20 to 0.44) and SDT (ICC = 0.41 to 0.68) demonstrated poor to moderate relative reliability. Absolute reliability of the CVT (CV = 28.19% to 29.79%) and SDT (CV = 27.87% to 28.84%) was moderate. Estimated sample size for CVT and SDT ranged from 4 to 9.

4.3.3. Inter-day reliability of isometric knee extensor torque signal complexity, entropy and variability metrics.

Table 4.2 presents the inter-day reliability statistics of the isometric KE torque signal complexity, entropy and variability metrics at 40% MVT. SampEn demonstrated good to excellent relative reliability (ICC = 0.85 to 0.90). Absolute reliability of SampEn was moderate to excellent (CV = 9.62% to 20.15%). Estimated sample size for SampEn ranged from 19 to 28. The complexity metrics, DFA α (ICC = 0.71 to 0.77) and CI-28 (ICC = 0.77 to 0.78) demonstrated moderate to good relative reliability. Absolute reliability of DFA α and CI-28 was excellent (CV = 4.46% to 9.52%). Estimated sample size for DFA α and CI-28 ranged from 10 to 13.

The variability metrics, SDT (ICC = 0.85 to 0.94), CVT (ICC = 0.75 to 0.84) and RMSE (ICC = 0.61 to 0.88) demonstrated moderate to excellent relative reliability. Absolute reliability of

the variability metrics was moderate to good (CV = 12.49% to 24.42%). Estimated sample size for the variability metrics ranged from 8 to 45.

Table 4.3 presents the inter-day reliability statistics of the isometric KE torque signal complexity, entropy and variability metrics at MVT. SampEn demonstrated moderate to good relative reliability (ICC = 0.70 to 0.82) and moderate absolute reliability (CV = 28.16% to 28.17%). Estimated sample size for SampEn ranged from 10 to 16. The complexity metric, DFA α demonstrated moderate to good relative reliability (ICC = 0.73 to 0.82), but exhibited excellent absolute reliability (CV = 3.51% to 3.84%). CI-28 demonstrated moderate relative reliability (ICC = 0.63 to 0.67) and moderate absolute reliability (CV = 21.02% to 24.41%). Estimated sample size for DFA α and CI-28 ranged from 8 to 15.

The variability metrics, CVT (ICC = 0.38 to 0.55) and SDT (ICC = 0.67 to 0.88) demonstrated poor to good relative reliability. Absolute reliability of the CVT (CV = 22.22% to 24.54%) and SDT (CV = 21.51% to 21.88%) was moderate. Estimated sample size for CVT and SDT ranged from 5 to 23.

Table 4.2 Intra- and inter-day reliability of isometric knee extensor torque signal complexity, entropy and variability metrics at 40% MVT.

		Inter-day reliability						Intra-day reliability					
		P	$ICC_{2,1}$	CV (%)	SEM	$MDC_{95\%}$	Est. Sample Size (*N*)	*P*	$ICC_{2,1}$	CV (%)	SEM	$MDC_{95\%}$	Est. Sample Size (*N*)
SDT (Nm)	All (*N*=66)	0.034	0.94	14.54	0.21	0.57	45	0.438	0.91	15.90	0.25	0.70	32
	MG (*N*=44)	0.728	0.85	12.49	0.12	0.32	19	0.215	0.77	14.74	0.15	0.41	12
	YG (*N*=22)	0.026	0.94	18.63	0.29	0.80	43	0.839	0.89	18.24	0.37	1.04	25
CVT (%)	All (*N*=66)	0.019	0.83	14.85	0.29	0.81	16	0.440	0.73	16.07	0.40	1.11	11
	MG (*N*=44)	0.605	0.75	12.91	0.21	0.58	11	0.064	0.69	14.82	0.24	0.67	9
	YG (*N*=22)	0.010	0.84	18.72	0.38	1.05	18	0.833	0.65	18.58	0.60	1.66	8
RMSE (%)	All (*N*=66)	0.009	0.67	22.23	0.93	2.59	9	0.338	0.71	27.59	1.14	3.17	10
	MG (*N*=44)	0.095	0.61	24.42	1.08	2.98	8	0.423	0.72	30.20	1.22	3.38	10
	YG (*N*=22)	0.001	0.88	17.85	0.49	1.36	24	0.610	0.64	22.37	0.98	2.72	8
SampEn	All (*N*=66)	0.976	0.90	13.13	0.14	0.38	28	0.421	0.91	12.29	0.13	0.37	32
	MG (*N*=44)	0.444	0.87	9.62	0.14	0.38	21	0.193	0.89	9.83	0.13	0.35	26
	YG (*N*=22)	0.277	0.85	20.15	0.14	0.39	19	0.745	0.83	17.23	0.15	0.41	17
DFA α	All (*N*=66)	0.543	0.74	4.52	0.07	0.19	11	0.493	0.69	5.70	0.08	0.23	9
	MG (*N*=44)	0.466	0.77	4.46	0.06	0.18	12	0.226	0.71	5.13	0.07	0.20	10
	YG (*N*=22)	0.951	0.71	4.64	0.08	0.21	10	0.773	0.66	6.82	0.10	0.27	8
CI-28	All (*N*=66)	0.450	0.77	8.90	4.28	11.86	13	0.612	0.69	11.44	5.69	15.78	9
	MG (*N*=44)	0.337	0.78	8.59	4.16	11.54	13	0.243	0.68	10.93	5.52	15.29	9
	YG (*N*=22)	0.990	0.77	9.52	4.35	9.52	13	0.444	0.72	12.70	5.85	16.21	10

Abbreviations: All = all participants combined; CV = coefficient of variation; CVT = coefficient of variation of torque; CI-28 = complexity index under 28 scales; DFA = detrended fluctuation analysis scaling exponent α; Est. = Estimated; ICC = intraclass correlation coefficient; MDC = minimal detectable change; MVT = maximal voluntary torque; MG = middle age group; RMSE = root mean square error of torque; SDT = standard deviation of torque; SampEn = sample entropy; SEM = standard error of measurement; YG = younger age group.

Table 4.3 Intra- and inter-day reliability of isometric knee extensor torque signal complexity, entropy and variability metrics at MVT.

		Inter-day reliability						Intra-day reliability					
		P	$ICC_{2,1}$	CV (%)	SEM	$MDC_{95\%}$	Est. Sample Size (*N*)	*P*	$ICC_{2,1}$	CV (%)	SEM	$MDC_{95\%}$	Est. Sample Size (*N*)
SDT (Nm)	All (*N*=66)	0.936	0.80	21.63	2.86	7.92	14	0.535	0.59	28.19	4.28	11.86	7
	MG (*N*=44)	0.300	0.88	21.51	1.66	4.60	23	0.692	0.68	27.87	2.98	8.25	9
	YG (*N*=22)	0.531	0.67	21.88	4.33	12.02	9	0.318	0.41	28.84	6.14	17.02	5
CVT (%)	All (*N*=66)	0.933	0.49	22.99	1.72	4.77	6	0.596	0.34	28.72	2.15	5.97	5
	MG (*N*=44)	0.626	0.55	22.22	1.37	3.80	7	0.647	0.44	28.19	1.79	4.95	5
	YG (*N*=22)	0.609	0.38	24.54	2.27	6.28	5	0.260	0.20	29.79	2.74	7.59	4
SampEn	All (*N*=66)	0.777	0.74	28.17	0.11	0.31	11	0.709	0.88	33.75	0.08	0.22	23
	MG (*N*=44)	0.527	0.70	28.16	0.13	0.36	10	0.567	0.87	33.89	0.09	0.25	22
	YG (*N*=22)	0.274	0.82	28.17	0.05	0.15	16	0.588	0.90	33.47	0.04	0.12	29
DFA α	All (*N*=66)	0.063	0.73	3.62	0.06	0.17	11	0.016	0.57	4.93	0.09	0.26	7
	MG (*N*=44)	0.042	0.68	3.51	0.06	0.17	9	0.048	0.48	4.89	0.09	0.25	6
	YG (*N*=22)	0.719	0.82	3.84	0.06	0.17	15	0.182	0.69	5.02	0.10	0.27	9
CI-28	All (*N*=66)	0.883	0.65	22.15	5.34	14.79	8	0.044	0.69	27.74	5.74	15.92	9
	MG (*N*=44)	0.489	0.63	21.02	4.75	13.15	8	0.021	0.63	29.72	5.65	15.66	8
	YG (*N*=22)	0.347	0.67	24.41	6.28	17.42	9	0.860	0.77	22.89	5.71	15.83	13

Abbreviations: All = all participants combined; CV = coefficient of variation; CVT = coefficient of variation of torque; CI-28 = complexity index under 28 scales; DFA = detrended fluctuation analysis scaling exponent α; Est. = Estimated; ICC = intraclass correlation coefficient; MDC = minimal detectable change; MVT = maximal voluntary torque; MG = middle age group; SDT = standard deviation of torque; SampEn = sample entropy; SEM = standard error of measurement; YG = younger age group.

4.4 - Discussion

The aim of the current chapter was to assess the intra- and inter-day reliability of complexity, entropy, and variability metrics derived from isometric KE torque signals at 40% MVT and MVT in younger and middle-aged adults. Findings indicate that at 40% MVT, all metrics show moderate to excellent intra- and inter-day reliability across the entire participant group and within each age group when analysed separately (ICCs from 0.61 to 0.94; Table 4.2). At MVT, intra- and inter-day reliability ranged from poor to excellent across the entire participant group and within each age group (ICCs from 0.20 to 0.90; Table 4.3).

This was the first study to examine the intra- and inter-day reliability of complexity (DFA and CI-28), and entropy (SampEn) metrics derived from submaximal (40% MVT) and maximal (MVT) isometric KE torque signals in both younger (18 to 30 years) and middle aged (50 to 70 years) adults. These metrics all demonstrated moderate to excellent intra- and inter-day absolute and relative reliability at 40% MVT across the entire participant group and within each age group (ICCs from 0.66 to 0.91; CVs from 4.46% to 20.15%; Table 4.2). While at MVT, absolute and relative intra- and inter-day reliability was poor to excellent across the entire participant group and within each age group (ICCs from 0.48 to 0.90; CVs from 3.51% to 33.89%; Table 4.3).

These findings suggest that complexity and entropy metrics provide a reliable method for assessing and monitoring neuromuscular function at submaximal intensities (40% MVT) across different age groups. However, the lower and more variable reliability at MVT indicates that maximal contractions may not provide a consistent signal for assessing neuromuscular function using complexity and entropy analyses. Therefore, submaximal contraction intensities may be preferable when comparing neuromuscular function across age groups while minimising the influence of systematic and random error.

For younger adults, the variability metrics (SDT and CVT) demonstrated moderate to excellent intra- and inter-day reliability at 40% MVT (ICCs $\geq$ 0.65; CVs $\leq$ 18.72%; Table 4.2). These results were consistent with those reported in prior research in younger populations that assessed the reliability of the variability of isometric KE torque at submaximal intensities (ICCs $\geq$ 0.79; Singh et al., 2010). Importantly, this study extends the intra- and inter-day

reliability data for SDT and CVT to middle-aged adults for the first time, suggesting that these measures were reliable across age groups (ICCs ≥ 0.69; CVs ≤ 14.82%; Table 4.2).

At MVT, the CVT exhibited poor to moderate intra- and inter-day reliability across the entire participant group and within each age group (ICCs ≤ 0.55; CVs ≥ 22.22%; Table 4.3). This lower reliability was likely due to the method of performing MVCs, where a constant target torque was not maintained. Instead, substantial deviations in torque production typically occur during the contraction. This results in larger differences in the torque signal variability across contractions, contributing to the lower reliability. As such, these findings suggest that CVT may not be a reliable measure for assessing neuromuscular function at MVT.

The estimated sample sizes were determined based on detecting changes that exceed measurement error. These estimates not only indicate the number of participants needed to observe significant within-subject changes but can also guide sample size decisions for detecting differences between groups or intervention-related changes. For instance, the estimated sample size required to detect a within-subject change in the complexity metrics DFA and CI-28 at 40% MVT was between 9 and 13 participants (see Table 4.2). Researchers can use these estimates as a guide for determining appropriate sample sizes, ensuring sufficient power to detect meaningful changes within individuals.

Alternatively, for between-group comparisons, a total sample size of 26 participants (13 per group) may be appropriate for comparing group differences in both the DFA and CI-28 metrics. This assumes that variability was similar within each group and that the effect size was comparable to the MDC. However, if between-group differences were expected to be smaller, a larger sample size may be required to detect significant effects. Conversely, if expected differences were larger, a smaller sample size may be sufficient.

For example, the sample size estimation for SampEn at 40% MVT ranged from 17 to 26, indicating in a required total sample size of 34 to 52 (Table 4.2). In comparison, a sample size estimation using data from a prior study investigating the effect of age on isometric KE torque complexity indicates a sample size of 18 (9 per age group group) would be suitable to detect an age-related difference in SampEn at an alpha level of 0.05 and power of 90% (Fiogbe et al.,

2021). Therefore, researchers should also consider conducting a formal power analysis to refine sample size estimates based on anticipated effect sizes and specific study parameters.

The intra- and inter-day reliability statistics in Tables 4.2 and 4.3 provide a reference for researchers when assessing whether differences or changes in the complexity, entropy and variability of isometric KE muscle torque signals were greater than the expected change due to systematic or random error. However, further research is required to extend the reliability of these metrics across different muscle groups, contraction intensities and populations. Expanding this research would enhance the practical applicability of these metrics in research and clinical settings.

4.4.1. Limitations.

Achieving reasonable precision in estimates of reliability typically requires a sample size of approximately 50 participants (Hopkins, 2000). In this study, the YG and MG included 22 and 44 participants, respectively. This discrepancy in sample size likely affects the precision of the reliability estimates for the YG, potentially affecting the robustness and generalisability of the findings. Conversely, the larger sample size of the MGs provides a more reliable estimate, closer to the recommended threshold, thereby increasing the confidence in the reliability estimates for this group.

4.5 - Conclusion

In summary, the current chapter has presented, for the first time, both relative and absolute intra- and inter-day reliability data for complexity, entropy, and variability metrics calculated from isometric KE torque signals. All metrics demonstrated moderate to excellent intra- and inter-day reliability at 40% MVT, with all ICCs exceeding 0.60 and all CVs below 20%. These findings demonstrate the reliability of complexity, entropy, and variability metrics in quantifying the temporal and spatial structure of submaximal isometric muscle torque signals. As such, these metrics provide a reliable non-invasive technique for assessing and monitoring age-related differences in neuromuscular function and muscle torque control. Furthermore, the reliability data provides a basis for estimating appropriate study sample sizes.

Chapter Five

Effect of age-group on the temporal and spatial structure of isometric knee extensor muscle torque signals.

5.1 - Introduction

The neuromuscular system exhibits emergent phenomena, meaning its function is greater than the sum of its individual components (Delignieres & Marmelat, 2012; Peng et al., 2009). Consequently, age-related changes in neuromuscular function and muscle torque control cannot be fully understood through a reductionist approach that examines individual components in isolation. Instead, the integrative functioning and nonlinear interactions between multiple components of the neuromuscular system is thought to be reflected in the temporal and spatial structure of the fluctuations in the torque output of an isometric muscle contraction (Vieluf et al., 2015; Vaillancourt et al., 2004).

The temporospatial structure of the fluctuations in isometric muscle torque signals can be quantified using non-invasive signal analysis techniques derived from the field of nonlinear dynamics and information theory (Clark et al., 2023; Pethick et al., 2021a; Pethick et al., 2021b; Seely & Macklem, 2004). Therefore, in recent decades, researchers have increasingly studied the temporospatial structure of these signals to assess the impact of age on neuromuscular function and muscle torque control (Christou, 2011; Enoka et al., 2003; Oomen & van Dieen, 2017; Pethick et al., 2022).

A comprehensive assessment of the effects of age on the temporospatial structure of isometric muscle torque signals requires the combined use of complexity (e.g., DFA and MSE), entropy (e.g., SampEn), and variability (e.g., CVF and SDF) metrics (Clark et al., 2023; Pethick et al., 2021a; Pethick et al., 2021b; Seely & Macklem, 2004). However, as discussed in Chapter Two, most research on isometric KE torque signals has primarily focused on analysing the spatial structure or variability of signal fluctuations.

To date, only two studies have specifically investigated the effect of age on the temporal structure or complexity of isometric KE torque signals, producing contrasting findings (Fiogbe et al., 2021; Pethick, 2023). One study found no significant age-related differences in complexity of isometric KE torque signals (assessed by ApEn and DFA; Pethick, 2023). In contrast, the other study reported older adults to exhibit lower complexity (assessed by ApEn and SampEn) than younger adults (Fiogbe et al., 2021). Both studies examined younger (24±2.8 and 23.9±4.7 years) and older adult (63±2.8 and 60.4±4.4 years) groups with similar mean ages and utilised comparable contraction intensities (10 to 40% MVT) during isometric

KE torque matching tasks, minimising these factors as potential explanations for their differing findings (Fiogbe et al., 2021; Pethick, 2023). Given the limited number of studies investigating the effect of age on isometric KE torque complexity, drawing definitive conclusions remains challenging. Further studies are needed to advance our understanding of how age influences the complexity of these torque signals.

Notably, the MSE analysis has not yet been used to quantify the effect of age on the complexity of isometric KE torque signals, despite being demonstrated to be an efficacious signal analysis technique (Costa et al., 2002; Costa et al., 2005; McIntosh et al., 2014; Vaillancourt et al., 2004). It has been shown to identify pathological (Costa et al., 2002) and age-related (McIntosh et al., 2014; Vaillancourt et al., 2004) changes in physiological time series data. The MSE analysis reveals the scale-to-scale dynamics (i.e., time-dependent structure) of an isometric muscle torque signal, which is thought to reflect the functioning and nonlinear interactions of different neuromuscular system components operating across multiple temporal scales (Vieluf et al., 2015). The current study was the first to use the MSE analysis to investigate how age influences the temporal structure of isometric KE muscle torque signals, providing novel insights into age-related changes in neuromuscular complexity.

The current study recruited middle-aged adults (50 to 70 years) to investigate the early changes in neuromuscular function, an age when declines in strength and power also begin to occur (Lindle et al., 1997; Skelton et al., 1994). These functional declines were underpinned by progressive structural and functional changes in the components of the neuromuscular system (Hunter et al., 2016; Larsson et al., 2019; McKinnon et al., 2017). Furthermore, since the key changes, such as the apoptosis of spinal motor neurons and the decline in MU reinnervation accelerate around the seventh decade (Campbell et al., 1973; Tomlinson & Irving, 1977), targeting a middle-aged population provides insight into the early stages of neuromuscular ageing, before more pronounced impairments begin to occur.

Two contraction intensities, 40% MVT and MVT, were selected to examine age-related differences in the complexity, entropy, and variability of isometric KE torque signals in the current study. 40% MVT provides a sustainable, submaximal load for assessing neuromuscular function and regulation of muscle torque. This intensity has also been used in prior research on age-related changes in isometric KE torque signals, allowing for comparison

with existing findings (Fiogbe et al., 2021; Pethick, 2023). While MVT represents maximal torque-generating capacity, where age-related deficits typically become evident from around the fourth decade of life onwards (Lindle et al., 1997). Examining both submaximal and maximal intensities enables the evaluation of age-related differences in neuromuscular function and muscle torque regulation across different task demands.

The current study aims to fill a critical gap in the literature by using the MSE analysis, alongside entropy and variability metrics, to investigate age-group differences in the temporal and spatial structure of isometric KE torque signals. This approach will advance the current understanding of how age influences neuromuscular function and muscle torque control.

Aim and Hypothesis.

The aim of the current experimental chapter was to investigate age-group differences in the complexity, entropy and variability of isometric KE torque signals. It was hypothesised that middle-aged adults would demonstrate lower complexity and entropy and greater variability in isometric KE torque signals compared to younger adults.

5.2 - Methods

5.2.1. Participants.

Sixty-six healthy individuals (50 male; 16 female) were recruited to participate in the study. Participants were recruited to be in two age groups, the YG were aged 18 to 30 years (N = 22; 16M, 6F) and the MG were aged 50 to 70 years (N = 44; 34M, 10F).

Before being allowed to participate in the study all potential participants completed a health questionnaire to ensure they were in full health. Participants were required to be non-obese, non-smokers, not have previous or current circulatory disorders, have no known or signs/symptoms of cardiovascular, neuromuscular, renal, or metabolic conditions, and not be physically impaired (i.e., able to perform maximal exercise). All participants were regularly undertaking endurance exercise, and reported to perform have performed above the World Health Organisation guidelines for ≥ 2 years (i.e., 2.5 to 5 hours of moderate exercise per week; Bull et al., 2020). At visit one prior to exercise testing all participants completed a long form international physical activity questionnaire, which was used to derive an estimate of MET hours per week and exercise time per week (Craig et al., 2003). Participant height was measured using a portable stadiometer (Seca 217; Seca GmbH & Co. KG, Hamburg, Germany), body mass measured using a mechanical flat scale (Seca 760; Seca GmbH & Co. KG, Hamburg, Germany) and body composition (fat mass percentage and lean body mass) measured using a Seca mBCA 525 (Seca GmbH & Co. KG, Hamburg, Germany).

Participants provided written informed consent at the first visit. The study was completed with full ethical approval of the University of Kent Research Ethics Committee (Proposal number: 21_2020_21), according to Declaration of Helsinki standards (but without being registered).

5.2.2. Experimental Design.

Each participant completed three visits to the laboratory at the same time of day (±1 hour). Visit one being participant screening, laboratory familiarisation, measurement of isometric MVT of the KE muscles and performance of a maximal incremental exercise test (IET). At visits two and three, participants completed the measurements of isometric KE muscle torque control at 40% MVT and at MVT, from which the torque signal complexity, entropy and variability metrics were calculated.

5.2.3. Measurement of isometric knee extensor maximal voluntary torque and aerobic capacity (visit one).

Participants were set up on an isokinetic dynamometer (Cybex HUMAC Norm; CSMi, Stoughton, MA, USA), as outlined in Chapter Three - General Methods - Section 3.6. Once set up on the dynamometer, participants performed a warm-up of ten submaximal contractions of increasing effort after which a series of brief (6 second) MVCs were performed to establish the MVT. MVCs were repeated (separated by 60 seconds rest) until a plateau in peak torque was reached (i.e., until three consecutive peak torques were within 5% of each other). The highest torque value from a 2 second epoch was recorded as the participant's MVT, which was then used to set the isometric exercise intensity (40% MVT) for the constant load isometric KE contractions in visits two and three. Participants were familiarised with the torque control tasks by performing five 10 second constant load contractions at 20% MVT followed by five 10 second constant load contractions at 40% MVT, with self-selected rest periods between contractions.

Participants then rested for 30 minutes before commencing the IET. The IET protocol was performed on an electro-magnetically braked ergometer (Excalibur Sport, Lode BV, Groningen, The Netherlands). Participants completed a 10-minute warm-up at 50 W, after which the required cycling power output increased by 25 W every minute (i.e., 1 W every 2.4 seconds) until they reached volitional exhaustion (operationally defined as a cadence of < 60 revolutions/min for > 5 seconds, despite strong verbal encouragement).

During the IET, respiratory gas exchange data were assessed using online breath-by-breath gas analysis (Metalyzer 3B; CORTEX Biophysik GmbH, Leipzig, Germany). Prior to all testing the gas analyser was calibrated according to the manufacturer recommendations using with ambient air and known concentrations of oxygen and carbon dioxide. The bidirectional turbine (flow meter) was calibrated with a 3-litre calibration syringe.

5.2.4. Gas exchange data analysis.

The participant's peak oxygen uptake ($\dot{V}O_{2peak}$) was assessed as the highest oxygen uptake that was attained during a 1-minute period in the test. Participants gas exchange threshold was determined as the breakpoint in carbon dioxide production and oxygen consumption (i.e., the point at which the carbon dioxide production begins to increase out of proportion to the oxygen

consumption). This breakpoint also coincided with the increase in both ventilatory equivalent of oxygen and end-tidal pressure of oxygen with no concomitant increase in ventilatory equivalent of carbon dioxide (Beaver et al., 1986; Pallares et al., 2016). The respiratory compensation point was determined as an increase in both the ventilatory equivalent of oxygen and ventilatory equivalent of carbon dioxide and a decrease in partial pressure of end-tidal carbon dioxide (Whipp et al., 1989; Lucia et al., 1999).

5.2.5. Measurement of isometric knee extensor torque control (visits two and three).

Visits two and three involved the repeated measurement of isometric KE muscle torque control. Participants were seated and set up on the isokinetic dynamometer as recorded in visit one. Participants then completed a brief warm-up of isometric contractions consisting of five 10 second constant load contractions at 20% MVT followed by five 10 second constant load contractions at 40% MVT, with 10 second rest periods.

After the warmup, participants completed four 6 second MVC with 60 second recovery between each MVC. The MVCs were then followed by 10 minutes rest after which participants completed six 10 second constant load contractions at 40% MVT with 60 seconds recovery between each contraction. During the 40% MVT matching tasks participants were instructed to match their instantaneous torque output to a thin line (1 mm thick) superimposed on the computer monitor. The Y axis of the display was scaled to the participants MVT, ensuring the superimposed line was located at the same position on the monitor for all participants.

5.2.6. Torque signal complexity, entropy, and variability metric analysis.

Prior to the calculation of the isometric KE muscle torque complexity, entropy and variability metrics, the steadiest 5 seconds of each contraction (i.e., the four MVCs and six 40% MVT contractions performed at visits 2 and 3) was identified as the 5 seconds with the lowest SD. The SDT, CVT and RMSE which quantify the variability and accuracy of torque output were calculated as outlined in Chapter Three - General Methods - Section 3.8. The complexity and entropy metrics, SampEn, DFA, MSE and CI-28 were calculated as outlined in Chapter Three - General Methods - Section 3.9. For each day, the two most accurate contractions at 40% MVT on each day (identified as the contractions with the lowest RMSE) and two steadiest MVCs on each day (identified as the contractions with the lowest SDT) were selected. The mean of these two contractions was then calculated and used as the participant's complexity, entropy, and variability metric values for statistical analysis.

5.2.7. Statistical analysis.

Age-group related differences in physical activity (Exercise time per week and MET hours), IET data, and MVT were assessed using independent samples *t*-test.

The effect of age-group on the scale-to-scale behaviour of the MSE curves was assessed using a mixed-design two-way ANOVA, with age group (YG vs. MG) as the between-subjects factor and coarse-grained scale (1 to 28) as the within-subjects factor.

The effect of age-group on the SDT, CVT, SampEn, DFA and CI-28 was assessed using a mixed-design ANOVA, with day (Day 1 vs. Day 2) as the within-subjects factor and age group (YG vs. MG) as the between-subjects factor.

Hedges' g (interpreted as: 0.2 to 0.5 small effect, 0.5 to 0.8 medium effect, ≥ 0.8 large effect) and partial eta squared (η_p^2; interpreted as: 0.01 small effect, 0.06 medium effect, 0.14 large effect) were used to assess effect sizes. Hedges' g effect sizes were coded as positive when the MG presented with a higher CVT, SDT or RMSE OR a lower SampEn, DFA or CI-28, when compared with the YG.

Bonferroni *post hoc* comparisons were used when a main effect or interaction was significant. The significance level was set at $P < 0.05$ in all cases. Statistical analyses were performed in IBM SPSS statistics 29 (IBM Corp., Armonk, NY, United States).

5.3 - Results

5.3.1. Participant characteristics and anthropometrics.

Incremental exercise test and physical activity data

Data from forty-four middle age adults (34 male; 10 female) and twenty-two younger adults (16 male; 6 female) were included in the analysis. Table 5.1 presents participant characteristics, anthropometrics, physical activity and IET data.

Table 5.1 Participant characteristics, anthropometrics and IET data.

	Middle Age Group	Younger Age Group	*t*-test results (MG vs. YG)
N	44 (34M; 10F)	22 (16M; 6F)	
Age (years)	58.6 ± 5.1	21.9 ± 3.7	***P* < 0.001**
Height (cm)	173.8 ± 8.6	177.3 ± 9.8	*P* = 0.136
Mass (kg)	72.3 ± 12.1	74.1 ± 12.1	*P* = 0.582
Fat Mass (%)	22.0 ± 7.2	16.1 ± 9.1	***P* = 0.005**
Lean Body Mass (kg)	56.3 ± 10.1	61.9 ± 10.9	***P* = 0.040**
Lean Body Mass Index ($kg.m^2$)	18.5 ± 2.1	19.3 ± 1.9	*P* = 0.108
Systolic BP (mmHg)	131 ± 8	126 ± 6	***P* = 0.024**
Diastolic BP (mmHg)	80 ± 10	73 ± 8	***P* = 0.001**
Relative $\dot{V}O_{2peak}$ ($ml.kg^{-1}.min^{-1}$)	40.9 ± 7.6	47.2 ± 12.8	***P* = 0.015**
Power at $\dot{V}O_{2peak}$ (W)	277 ± 68	318 ± 94	***P* = 0.048**
Relative $\dot{V}O_2$ at GET ($ml.kg^{-1}.min^{-1}$)	27.2 ± 6.7	31.5 ± 10.3	***P* = 0.046**
Power at GET (W)	162 ± 48	193 ± 72	***P* = 0.041**
Relative $\dot{V}O_2$ at RCP ($ml.kg^{-1}.min^{-1}$)	34.3 ± 7.1	38.4 ± 10.9	*P* = 0.074
Power at RCP (W)	215 ± 57	242 ± 80	*P* = 0.117
Exercise time per week (hours)	9.9 ± 4.7	13.2 ± 4.8	***P* = 0.021**
MET hours per week	85.9 ± 49.4	104.1 ± 52.4	*P* = 0.220

Abbreviations: BP = blood pressure; GET = gas exchange threshold; MET = metabolic equivalents; MG = middle age group; RCP = respiratory compensation point; $\dot{V}O_{2peak}$ = peak oxygen uptake; $\dot{V}O_2$ = oxygen uptake; YG = younger age group; Significant *P* values highlighted by bold font; data are mean ± SD.

Maximal isometric knee extensor torque data (visit 1)

Table 5.2 presents the MVT data collected at visit one and used to derive the participants' target torque for the 40% MVT tasks. The YG presented with significantly higher isometric MVT, than the MG ($P < 0.001$; Table 5.2). When isometric MVT was normalised to body mass (Nm/kg) and lean body mass (Nm/LBM.kg) the YG exhibited a significantly higher torque to mass ($P < 0.001$; Table 5.2) and torque to lean body mass ($P < 0.001$; Table 5.2), than the MG.

Table 5.2 Visit one maximal voluntary isometric knee extensor torque data.

	Middle Age Group	Younger Age Group
MVT (Nm)	150.1 ± 51.3	216.9 ± 77.1*
Target 40% MVT (Nm)	60.0 ± 20.5	86.8 ± 30.9*
Torque/Mass (Nm/kg)	2.1 ± 0.6	2.9 ± 0.8*
Torque/LBM (Nm/kg)	2.6 ± 0.7	3.4 ± 0.8*

Abbreviations: MVT = maximal voluntary torque; LBM = lean body mass; data are mean ± SD; * = $P < 0.001$.

5.3.2. Effect of age-group on isometric knee extensor torque signal complexity, entropy and variability.

Multiscale entropy curve results

There was no significant main effect of age ($F_{(1, 64)} = 0.128$; $P = 0.721$; $\eta_p^2 = 0.002$), but there was a significant main effect of coarse-grained ($F_{(27, 1728)} = 107.817$; $P < 0.001$; $\eta_p^2 = 0.628$) and a significant age by coarse-grained interaction ($F_{(27, 1728)} = 22.176$; $P < 0.001$; $\eta_p^2 = 0.257$) for SampEn calculated across 28 coarse-grained scales during the constant load tasks at 40% MVT (Figure 5.1A). At shorter scales (≤ scale 7) the MG exhibited significantly higher SampEn ($P < 0.05$), compared with the YG (Figure 5.1A). At longer (coarser) scales (scales 17 to 28) YG exhibited significantly higher SampEn ($P < 0.05$), compared with the MG (Figure 5.1A).

There was no significant main effect of age ($F_{(1, 64)} = 0.549$; $P = 0.461$; $\eta_p^2 = 0.009$), but there was a significant main effect of coarse-grained scale ($F_{(27, 1728)} = 165.584$; $P < 0.001$; $\eta_p^2 = 0.721$) and a significant age by coarse-grained interaction ($F_{(27, 1728)} = 6.843$; $P < 0.001$; $\eta_p^2 = 0.097$) for SampEn calculated across 28 coarse-grained scales at MVT (Figure 5.1B). At shorter scales (≤ scale 2) the MG exhibited significantly higher SampEn (all $P < 0.05$), compared with

the MG (Figure 5.1B). At longer (coarser) scales (scales 19 to 28) YG exhibited significantly higher SampEn (all $P < 0.05$), compared with the MG (Figure 5.1B).

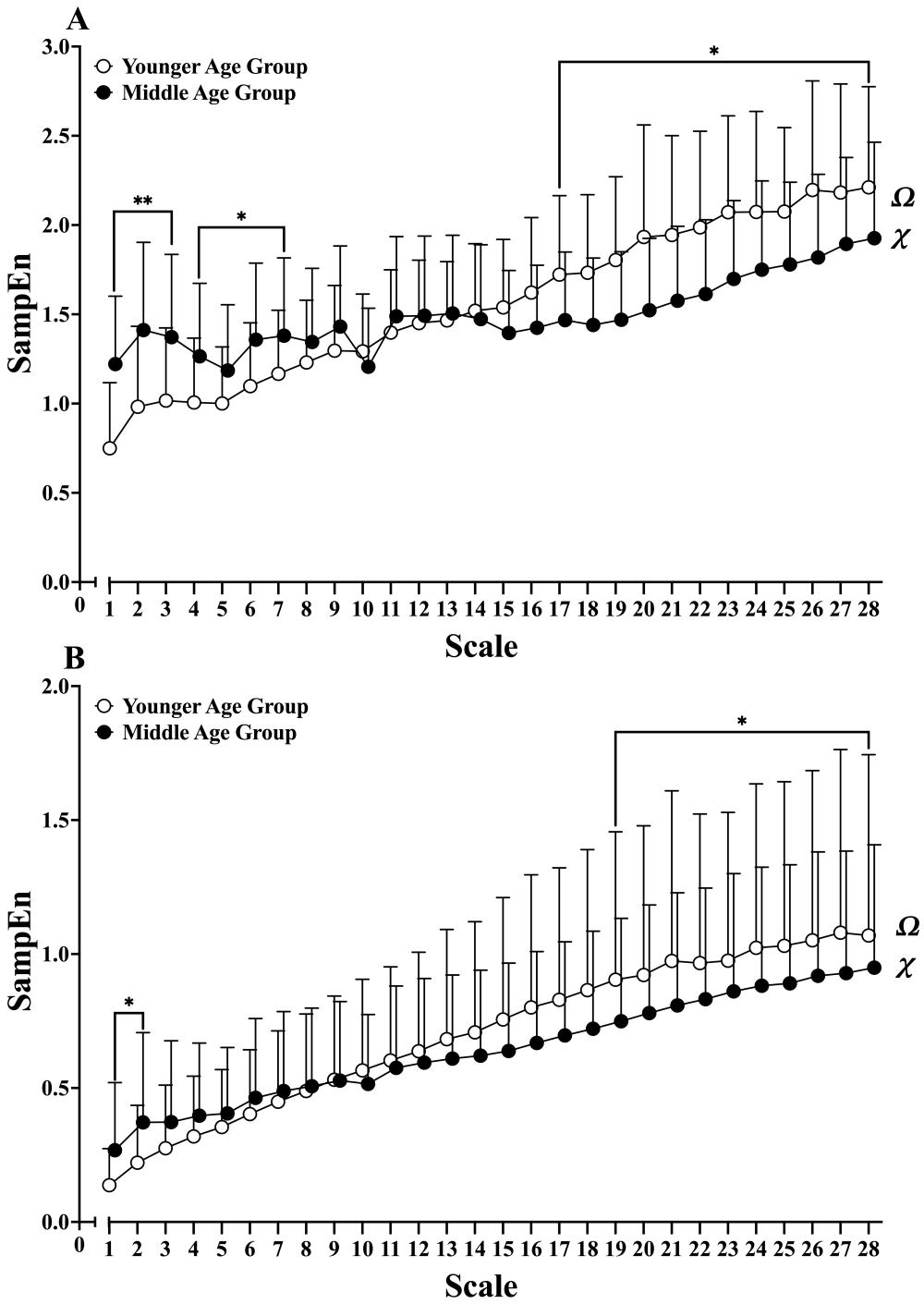

Figure 5.1. (A) Multiscale entropy curves calculated from isometric knee extensor torque signals of the younger and middle age groups at 40% MVT, **(B)** Multiscale entropy curves calculated from isometric knee extensor torque signals of the younger and middle age groups at MVT (open circles = younger age group; closed circles = middle age group; Ω = significant main effect of coarse-grained scale; χ = significant age group by coarse-grained scale interaction; * = significant difference between age groups $P < 0.05$; ** = significant difference between age groups $P < 0.001$).

Table 5.3 and 5.4 present the descriptive statistics, effect sizes and ANOVA results for the effect of age-group on the complexity, entropy and variability of the torque signals at 40% MVT and MVT, respectively.

Complexity index results

There was no significant effect of age on the CI-28 metric derived from the torque signals at 40% MVT (Table 5.3) and at MVT (Table 5.4).

Detrended fluctuation analysis results

There was no significant effect of age on the DFA α metric derived from the torque signals at 40% MVT (Table 5.3) and at MVT (Table 5.4).

Sample entropy results

The MG had a significantly higher SampEn derived from the torque signals at 40% MVT (Table 5.3) and at MVT (Table 5.4), when compared with the YG.

Variability metric results

The YG had a significantly higher SDT and CVT derived from the torque signals at 40% MVT, when compared with the MG (Table 5.3). There was no significant effect of age on the RMSE derived from the torque signals at 40% MVT (Table 5.3). The YG had a significantly higher SDT and CVT derived from the torque signals at MVT, when compared with the MG (Table 5.4).

Table 5.3 Descriptive statistics, effect sizes and ANOVA results for the effect of age-group on the complexity, entropy and variability of the isometric knee extensor torque signals at 40% MVT.

	YG $N = 22$ (mean ± SD)	MG $N = 44$ (mean ± SD)	Hedges' g	Hedges' g Lower 95% CI	Hedges' g Upper 95% CI	F, P and η_p^2 values	Main effect of Age	Main effect of Day	Age by Day interaction
SDT (Nm)	1.70±1.13	0.74±0.29	-1.38	-1.95	-0.82	F	28.139	9.533	8.333
						P	**<0.001**	**0.003**	**0.005**
						η_p^2	0.305	0.130	0.115
CVT (%)	1.91±0.92	1.30±0.39	-0.99	-1.53	-0.45	F	14.335	11.326	8.500
						P	**<0.001**	**0.001**	**0.005**
						η_p^2	0.183	0.150	0.117
RMSE (%)	2.92±1.37	2.68±1.49	-0.16	-0.68	0.35	F	0.401	6.990	0.113
						P	0.529	**0.010**	0.738
						η_p^2	0.006	0.098	0.002
SampEn	0.73±0.35	1.23±0.36	-1.41	-1.97	-0.84	F	20.074	0.243	1.932
						P	**<0.001**	0.624	0.169
						η_p^2	0.312	0.004	0.029
DFA α	1.22±0.13	1.22±0.13	-0.02	-0.53	0.49	F	0.007	0.191	0.088
						P	0.936	0.664	0.767
						η_p^2	<0.001	0.003	0.001
CI-28	42.69±8.60	42.14±8.50	0.06	-0.45	0.58	F	0.087	0.279	0.305
						P	0.769	0.599	0.582
						η_p^2	0.001	0.004	0.005

Abbreviations: CVT = coefficient of variation of torque; CI-28 = complexity index under 28 scales; DFA = detrended fluctuation analysis scaling exponent α; MG = middle age group; MVT = maximal voluntary torque; RMSE = root mean square error of torque; SDT = standard deviation of torque; SampEn = sample entropy; YG = younger age group; Significant P values highlighted by bold font.

Table 5.4 Descriptive statistics, effect sizes and ANOVA results for the effect of age-group on the complexity, entropy and variability of the isometric knee extensor torque signals at MVT.

	YG $N = 22$ (mean ± SD)	MG $N = 44$ (mean ± SD)	Hedges' g	Hedges' g Lower 95% CI	Hedges' g Upper 95% CI	F, P and η_p^2 values			
							Main effect of Age	Main effect of Day	Age by Day interaction
SDT (Nm)	12.05±6.98	6.61±4.66	-0.98	-1.52	-0.45	F	14.225	0.211	1.315
						P	**<0.001**	0.648	0.256
						η_p^2	0.182	0.003	0.020
CVT (%)	5.56±2.39	4.31±1.81	-0.62	-1.14	-0.10	F	5.640	0.116	0.620
						P	**0.021**	0.734	0.434
						η_p^2	0.081	0.002	0.010
SampEn	0.13±0.13	0.27±0.22	-0.68	-1.21	-0.16	F	6.769	<0.001	0.800
						P	**0.012**	0.987	0.374
						η_p^2	0.096	<0.001	0.012
DFA α	1.52±0.13	1.52±0.10	-0.04	-0.56	0.47	F	0.033	2.244	0.707
						P	0.856	0.139	0.404
						η_p^2	0.001	0.034	0.011
CI-28	19.44±10.15	17.97±7.12	0.18	-0.34	0.69	F	0.462	0.324	1.668
						P	0.499	0.571	0.201
						η_p^2	0.007	0.005	0.025

Abbreviations: CVT = coefficient of variation of torque; CI-28 = complexity index under 28 scales; DFA = detrended fluctuation analysis scaling exponent α; MG = middle age group; MVT = maximal voluntary torque; SDT = standard deviation of torque; SampEn = sample entropy; YG = younger age group; Significant P values highlighted by bold font.

5.4 - Discussion

5.4.1. The effect of age-group on the complexity, entropy and variability of isometric knee extensor torque signals.

The aim of the current experimental chapter was to investigate age-group differences in the complexity, entropy and variability of isometric KE torque signals. Main findings indicate no age-group related differences in the complexity (DFA and CI-28) of the torque signal at 40% MVT and MVT (Tables 5.3 and 5.4). However, the novel application of MSE analysis revealed an age-related cross-over in SampEn in the MSE curves (Figure 5.1), indicating alterations in the temporal structure of the torque signal that may reflect changes in neural control strategies rather than a reduction in neuromuscular function. Contrary to the hypothesis, the MG exhibited torque signals of higher entropy (SampEn) and lower variability (SDT and CVT) than the YG at 40% MVT and MVT (Tables 5.3 and 5.4).

The current study's findings align with those of Pethick (2023), as no significant age-related differences were observed in the complexity of isometric KE torque signals, as assessed by the DFA analysis. Both the current study and Pethick (2023) recruited *older* participants who regularly engaged in endurance exercise, a factor that may have contributed to the preservation of neuromuscular complexity in this age group (Pethick & Piasecki, 2022). Lifelong endurance training has been suggested to exert neuroprotective effects, with masters athletes (aged >60 years) exhibiting attenuated age-related declines in MU number, muscle mass, and strength (Power et al., 2010; Power et al., 2016; Piasecki et al., 2021a; Wroblewski et al., 2011; Zampieri et al., 2015).

One proposed mechanism for this preservation in neuromuscular function is the enhancement of MU reinnervation, as chronic exercise has been shown to promote axonal sprouting and NMJ formation, potentially mitigating MU loss and maintaining MU function with age (Mosole et al., 2014; Power et al., 2010; Power et al., 2016; Piasecki et al., 2019; Tam & Gordon, 2003). However, evidence for this neuroprotective effect remains inconclusive, as research has reported no significant differences in MU preservation between masters athletes and age-matched controls (Piasecki et al., 2016c). Nevertheless, it may be possible that regular endurance exercise in middle age preserves neuromuscular complexity by delaying the onset

of age-related structural and functional changes to the components of the neuromuscular system.

The current study was the first to use the MSE analysis to quantify the effect of age on the temporal structure of isometric KE torque signals (Figure 5.1). As originally outlined by Costa et al. (2002), the MSE analysis provides a measure of complexity of a physiological signal over multiple time scales. Thus, overcoming the limitations of SampEn which only measures the regularity or randomness of a physiological signal on one scale, and therefore does not capture the multiple different temporal structures present within the signal (Costa et al., 2002; McIntosh et al., 2014; Vaillancourt et al., 2004).

The CI-28 metric (area under the MSE curve) derived from the MSE analysis showed no significant difference between age groups, suggesting, similar to the DFA analysis, that torque signal complexity remained unchanged with age at both 40% MVT and MVT (Tables 5.3 and 5.4). However, CI-28 does not account for interactions between age and coarse-grained scales, which led to a distinct cross-over phenomenon in the MSE curves (Figure 5.1). Specifically, YG exhibited significantly lower SampEn at shorter time scales compared to the MG (≤ scale 7 at 40% MVT, Figure 5.1A; ≤ scale 2 at MVT, Figure 5.1B). Conversely, at longer (coarser) time scales, the MG exhibited significantly lower SampEn compared to the YG (≥ scale 17 at 40% MVT, Figure 5.1A; ≥ scale 19 at MVT, Figure 5.1B). This cross-over captures an age-related change in the regularity of torque signal fluctuations across different time scales, in other words, a change in the regularity of the different frequency components present within the torque signal (Vieluf et al., 2015).

Complex biological systems, such as the neuromuscular system, produce outputs with structure across multiple temporal scales through the integrative functioning of system components that operate over different time scales (Vaillancourt & Newell, 2002; Sleimen-Malkoun et al., 2014). The MSE algorithm was specifically designed to capture this temporal structure (Costa et al., 2002; Costa et al., 2005). A cross-over in the MSE curves, although speculative, may indicate age-related changes in the frequency patterns of multiple neural oscillators, which provide frequency- and amplitude-varying input to the motor neuron pool, inputs that were crucial for coordinating and controlling muscle contractions (Sosnoff et al., 2004).

Despite potential changes in neural control, task performance of the MG remained unaffected as evidenced by similar RMSE values across age groups (Table 5.3). This may suggest that the middle-aged adults were still able to effectively modulate neural oscillatory inputs to the motor neuron pool. Raising the possibility that the scale-to-scale entropic behaviour of the MSE curves, that reflects alterations in the temporal structure of the torque signal, may be linked to age-related adaptations in neural control strategies that ensure task demands were met. Further research using HD sEMG to measure the discharge times of multiple concurrently active MUs is needed to clarify the relationship between MSE curve behaviour and the neural mechanisms underlying the temporal structure of different frequency components in the torque signal.

Notwithstanding the cross-over in SampEn, both age groups MSE curves also demonstrated similar asymptotic behaviour, with SampEn continuing to increase with increasing time scales (Figure 5.1). Such asymptotic behaviour indicates that there was new physiological information being revealed at all scales and indicating that the torque signal was not dominated by a single time constant. This MSE curve behaviour was a characteristic suggested to be reflective of a complex, healthy and well-functioning physiological system, absent of any pathology (Costa et al., 2005).

The age-related cross-over behaviour of MSE curves is not a new phenomenon and has previously been observed in EEG and MEG time series data (McIntosh et al., 2014). Similar to the findings of the present study, older adults exhibited higher SampEn at shorter time scales, with a cross-over point where younger adults demonstrated higher SampEn at longer (coarser) time scales (McIntosh et al., 2014). This age-dependent shift in the temporal structure of EEG and MEG signals has been suggested to reflect a transition from long-range correlations (coarser time scales) to greater local processing (shorter time scales) with ageing (McIntosh et al., 2014), highlighting the potential of the MSE analysis in capturing functionally relevant age-related changes in physiological signals.

A similar cross-over in the entropy of electrocardiogram signals was reported in the seminal MSE study by Costa et al. (2002), where beat-to-beat intervals from individuals with atrial fibrillation exhibited higher entropy at shorter time scales (≤ 6 scales) but showed a white noise-like monotonic decrease at longer scales. In contrast, healthy beat-to-beat time series displayed a gradual increase in entropy, with higher values at longer scales (> 7 scales; Costa et al., 2002). This cross-over pattern characterised differences in cardiac dynamics and the

degradation of control mechanisms due to pathology, physiological information that would have been obscured by calculating entropy at a single scale (Costa et al., 2002).

Likewise, in the present study, the MG exhibited significantly higher SampEn at scale one (i.e., no coarse graining) compared to the YG (Figures 5.1A and 5.1B). If considered in isolation, SampEn at a single scale would have provided a misleading characterisation of the neuromuscular system's physiological complexity, given the nuanced findings of the MSE analysis and the absence of age-related differences in other complexity metrics (DFA and CI-28). The scale-to-scale entropic behaviour observed in the MSE curves may capture subtle, progressive changes to neuromuscular system components that were not detected by traditional complexity measures (SampEn and DFA), changes that may precede declines in neuromuscular function. These findings reinforce the necessity for future research to examine the scale-to-scale dynamics of torque signals using MSE analysis to gain a more comprehensive understanding of neuromuscular complexity.

The MG demonstrated lower torque signal variability (SDT and CVT) than the YG (Tables 5.3 and 5.4), contrary to previous research reporting greater neuromuscular variability in older adults (Bazzucchi et al., 2004; Pethick, 2023; Tracy et al., 2007; Tracy & Enoka, 2002; Wu et al., 2019a; Wu et al., 2019b). However, the pooled Hedges' *g* effect size from the thesis meta-analysis indicates that older adults often exhibit lower KE torque signal variability (Chapter Two, Table 2.4), supporting present findings.

One primary mechanism thought to underpin torque signal variability is the variance in common synaptic input to motor neurons, which modulates the discharge behaviour of MUs (Castronovo et al., 2018; Feeney et al., 2018). Accordingly, the higher torque signal variability observed in the YG may indicate greater variance in common synaptic input during isometric contractions at submaximal and maximal intensities than the MG. However, the specific mechanisms governing neuromuscular variability and complexity and the age-related changes remain to be fully elucidated. Given the evidence from multiple studies showing neuromuscular complexity can change independently of variability, and vice versa (Challis, 2006; Fiogbe et al., 2021; Hu & Newell, 2011; Jordan et al., 2013), it is plausible that the neural processes governing neuromuscular complexity and variability were distinct yet interrelated. Further research is needed to clarify these mechanisms.

5.4.2. Limitations.

The MG were aged 58.6 ± 5.1 years (range 50 to 70 years) and were therefore unlikely to reflect the effect of *older* age (> 70 years) on neuromuscular function and muscle torque control. Accordingly, caution is advised not to generalise the findings to much older age groups. Future research should aim to investigate the impact of age on neuromuscular complexity in individuals aged over 70 years, where structural and functional changes to the components of the neuromuscular system may become more pronounced (Hunter et al., 2016; McKinnon et al., 2016).

The use of only two contraction intensities (40% MVT and MVT) was a notable limitation of the current chapter. Research has shown the torque variability of the lower extremity muscles to be dependent on target torque (Chapter Two). However, due to the paucity of research, the effect of contraction intensity on KE torque signal complexity remains unclear. As such, the effect of contraction intensity on age-related differences in isometric KE torque complexity will be addressed experimentally in the subsequent chapters of this thesis (see Chapters Six and Eight A).

5.5 - Conclusion

The current study found no age-group related differences in neuromuscular complexity, as assessed by DFA and CI-28. However, the MSE analysis revealed an age-related cross-over in SampEn, suggesting that age may alter the temporal organisation of the neuromuscular output rather than causing a uniform decline in complexity. Furthermore, there were no differences between age-groups in the accuracy of task performance, potentially indicating that the MSE analysis reveals an age-related restructuring of neuromuscular control strategies that helps preserve muscle control before noticeable changes occur. The cross-over pattern observed in the MSE curves underscores the importance of assessing the multiple temporal structures inherent to muscle torque signals, rather than relying solely on single-scale entropy metrics.

Chapter Six

Effect of contraction intensity on age-group related differences in the complexity, entropy and variability of isometric knee extensor torque signals.

6.1 - Introduction

6.1.1. The effect of contraction intensity on age-group related differences in the complexity, entropy and variability of isometric knee extensor torque signals.

The performance of lower extremity fundamental motor skills, such as locomotion and balance (Newell, 2020), requires lower extremity muscle torque regulation across various contraction intensities. However, age-related changes in lower extremity muscle torque regulation appear to be contraction intensity dependent (Christou & Carlton, 2002). Specifically, the age-related increase in the variability in isometric KE torque signals occurs predominantly at lower contraction intensities (≤ 10% MVT), whereas this effect diminishes as contraction intensity increases (≥ 15% MVT; Chapter Two, Table 2.5).

This increased torque variability at low intensities may be attributed to greater oscillations in MU force during initial recruitment and low-rate discharge in older adults (Kudina, 1999; Westgaard & De Luca, 2001). Additionally, the age-related MU reorganisation results in fewer, larger MUs that are recruited at lower intensities and discharge at slower, more variable rates (Connelly et al., 1999; Kamen et al., 1995; Piasecki et al., 2016b; Tracy et al., 2005). The reduction in smaller MUs, which are critical for fine motor control (Azevedo et al., 2020), coupled with increased discharge variability, likely exacerbates the variability of torque fluctuations in older adults. This effect was particularly pronounced at lower contraction intensities (e.g., ≤ 10% MVT), where each MU has a greater contribution to the net torque (Fuglevand et al., 1993).

Due to limited research, the systematic review and meta-analysis of Chapter Two could not assess how contraction intensity influences age-related differences in isometric KE torque complexity. Similarly, Chapter Five was unable to provide insight into the influence of contraction intensity as it only assessed the effect of age at two intensities (40% MVT and MVT). Existing studies on the effect of age on the complexity of isometric KE torque have primarily examined intensities ≤ 40% MVT (Fiogbe et al., 2021; Pethick, 2023). One study found that complexity (measured by ApEn and DFA) decreased with increasing contraction intensity (10 to 40% MVT) in both younger and older adults, with no significant age-related differences observed (Pethick, 2023). In contrast, the other study reported lower complexity (measured by ApEn and SampEn) in older adults compared to younger adults, with complexity increasing from 15 to 40% MVT in both groups (Fiogbe et al., 2021). These conflicting results

underscore the need for further research to determine how age influences KE torque signal complexity across a comprehensive range of contraction intensities (e.g., 10 to 80% MVT).

The neuromuscular system regulates torque output by adjusting MU recruitment and discharge rates, with higher contraction intensities necessitating a greater strength of common synaptic input to motor neurons to facilitate both the increase in the number of recruited MUs and their discharge rates (Contessa et al., 2009; Castronovo et al., 2015; Fuglevand et al., 1993; McManus et al., 2016). As contraction intensity increases, the concurrent increase in the strength of common synaptic input (Castronovo et al., 2015) leads to a strengthened correlated discharge of APs, known as MU synchronisation (Farina & Negro, 2015). Theoretically, greater MU synchronisation may result in more uniform and predictable oscillations in the common input signal, reducing its complexity (Pethick et al., 2016; Pethick et al., 2021b). Since the oscillations in common synaptic input (i.e., common neural drive) closely resemble the structure of the muscle torque signal (Dideriksen et al., 2012; Mazzo et al., 2022; Negro et al., 2009; Thompson et al., 2018), this reduction in complexity may be transmitted to the torque signal. Consequently, as contraction intensity increases, a corresponding decline in torque complexity may be expected (Pethick et al., 2016; Pethick et al., 2021b).

Older adults have been shown to exhibit a greater strength of common synaptic input for the same relative level of torque production, contributing to increased neuromuscular variability compared to younger adults (Castronovo et al., 2018). The increased strength of common synaptic input could result in less complex oscillatory patterns in neural drive and a corresponding reduction in torque signal complexity in older age (Pethick et al., 2016; Pethick et al., 2021b). Functionally, greater strength of common synaptic input could also become a neural constraint, limiting the ability to redistribute neural drive across muscles, reducing precision in movement (Baker et al., 1999) and adaptability to disturbances, such as fatigue (Rossato et al., 2022). Assuming muscle torque signal complexity (i.e., temporal structure) largely reflects the oscillations in common synaptic input (Dideriksen et al., 2012; Mazzo et al., 2022; Negro et al., 2009; Thompson et al., 2018), age-related differences in complexity may indicate changes in the neuromuscular systems functionality and adaptability.

Since higher contraction intensities impose greater neuromuscular demands, including increased neural drive to recruit higher-threshold MUs and enhance rate coding, restricting analysis to ≤ 40% MVT may overlook critical age-related changes in neuromuscular control

(Inglis et al., 2025; Orssatto et al., 2022). Expanding research to a wider intensity range (e.g., 10 to 80% MVT) is essential to fully characterise the effect of age on isometric KE torque complexity, and by extension, muscle torque regulation across different task demands. Therefore, the first aim of the current experimental chapter was to investigate the effect of contraction intensity on the age-group related differences in the complexity, entropy and variability of isometric KE torque signals.

6.1.2. The relationship between isometric knee extensor signal complexity and fundamental motor skill performance.

The voluntary control of postural muscles is an important mechanism in maintaining postural stability, during standing and locomotion. Notably, the torque steadiness of lower limb muscles during voluntary isometric contractions has been found to be significantly associated with postural control in both younger and older individuals (Davis et al., 2020; Hirono et al., 2020; Hirono et al., 2021; Kouzaki & Shinohara, 2010; Oshita & Yano, 2010). Additionally, research has shown that a loss of lower limb muscle control was accompanied by a reduction in locomotion task performance in older adults (Almuklass et al., 2018a; Carnavale et al., 2020; Seynnes et al., 2005).

The quadriceps femoris muscles are well known for their crucial role in functional locomotor activities, such as walking (Martien et al., 2015). These muscles also contribute to maintaining postural control during standing (Krishnamoorthy et al., 2003; Krishnamoorthy et al., 2004; Laughton et al., 2003), with their function being particularly important in preventing falls (Ahmadiahangar et al., 2018). However, quadricep muscle function was highly susceptible to the effect of ageing (Abe et al., 2011; Abe et al., 2014; Fuchs et al., 2023). Indeed, age-related declines in quadriceps function, assessed by neuromuscular complexity and variability of their torque signals, may explain impairments in both postural control and locomotion in older age.

Older adults with a history of falling have been shown to exhibit reduced force steadiness of the quadriceps than non-fallers (Carville et al., 2007). Furthermore, a lower entropy of isometric KE torque (measured by ApEn and SampEn) has been linked to worse performance in functional locomotion tasks among frail older adults, compared to their non-frail counterparts (Carnavale et al., 2020). More recently, the CVT and SampEn derived from isometric KE contractions were found to be correlated with dynamic balance in healthy adults

(Mear et al., 2023). However, there has been paucity of research examining the relationship between the complexity of isometric KE torque, postural control, and locomotion performance across different age groups. Investigating the functional significance of postural muscle torque complexity is essential for understanding how specific muscle groups contribute to postural control and locomotion with age. Such research would elucidate the broader functional significance of neuromuscular complexity.

It is also important that the contraction intensities used to derive the torque complexity metrics align with the requirements of the postural control and locomotion tasks (Mear et al., 2023). Therefore, the second aim of the current study was to identify the contraction intensities at which the complexity, entropy and variability of isometric KE torque signals were most strongly associated with postural sway and locomotion task performance.

6.1.4. Aims and Hypotheses.

The two aims of the current experimental chapter were:

(1) To investigate the effect of contraction intensity on the age-group related differences in the complexity, entropy and variability of isometric KE torque signals.
(2) To identify the contraction intensities at which the complexity, entropy and variability of isometric KE torque signals were most strongly associated with performance in postural sway and locomotion tasks.

It was hypothesised that:

(1) Age-group related differences in the complexity, entropy and variability of isometric KE torque signals would be greatest at lower contraction intensities, with age-group related differences being smaller at higher contraction intensities.
(2) Isometric KE torque signals of lower complexity and entropy, and greater variability would be associated with increased postural sway and worse locomotion task performance.

6.2 - Methods

6.2.1. Participants.

Forty healthy individuals (28 male; 12 female) were recruited to participate in the study. Participants were recruited to be in two age groups, the YG were aged 18 to 30 years (N = 20; 14M, 6F) and the older group (OG) were aged 50 to 85 years (N = 20; 14M, 6F).

Before being allowed to participate in the study all potential participants completed a health questionnaire to ensure they were in full health. Participants were required to be non-obese, non-smokers, not have previous or current circulatory disorders, have no known or signs/symptoms of cardiovascular, neuromuscular, renal, or metabolic conditions. Participants were required to be living independently and able to perform active daily living tasks. All participants were regular exercisers, having performed above the World Health Organisation guidelines for ≥ 2 years (i.e., 2.5 to 5 hours of moderate exercise per week; Bull et al., 2020). Participant height was measured using a Seca portable stadiometer (Seca 217; Seca GmbH & Co. KG, Hamburg, Germany) and body mass measured using a Seca mechanical flat scale (Seca 760; Seca GmbH & Co. KG, Hamburg, Germany).

Participants provided written informed consent at the first visit. The study was completed with full ethical approval of the University of Kent Research Ethics Committee (Proposal number: 22_20_23), according to Declaration of Helsinki standards (but without being registered).

6.2.2. Experimental Design.

Each participant completed two visits to the laboratory at the same time of day (± 1 hour). Visit one being participant screening, laboratory familiarisation and the measurement of isometric MVT of the KE muscles. At visit two, participants completed the measurements of isometric KE muscle torque control at 10, 20, 30, 40, 50, 60, 70 and 80% MVT, from which the torque signal complexity, entropy and variability metrics were calculated. During visit two, participants also completed the postural sway and locomotion tasks.

6.2.3. Measurement of isometric knee extensor maximal voluntary torque (visit one).

Participants were set up on an isokinetic dynamometer (Cybex HUMAC Norm; CSMi, Stoughton, MA, USA), as outlined in Chapter Three - General Methods - Section 3.6. Once set up on the dynamometer, participants were familiarised with the dynamometer by performing a

series of torque matching tasks at 20 Nm of torque, before commencing the measurement of MVT.

After familiarisation, participants performed a warm-up of ten submaximal contractions of increasing effort after which a series of brief (6 second) MVCs were performed to establish MVT. MVCs were repeated (separated by 60 seconds rest) until a plateau in peak torque was reached (i.e., until three consecutive peak torques were within 5% of each other). The highest torque value from a 2 second epoch was recorded as the MVT, which was then used to set the relative constant load isometric contraction intensities of 10, 20, 30, 40, 50, 60, 70 and 80% MVT to be used in the torque control tasks in visit two.

6.2.4. Postural sway tests (visit two).

At the start of visit two, participants stood barefoot on a force plate (BP400600HF; AMTI, Watertown, MA, USA; the force plate was embedded in the concrete laboratory floor), with their feet shoulder-width apart and arms crossed over their chest. The participant's foot placement was marked with tape before the first postural sway test, to ensure precise placement in following tests. Participants were instructed to stand as still as possible in a bipedal stance with eyes open for 45 seconds. The test was completed four times.

The CoP data on the Fx (Anterior-Posterior [AP] sway; see example Figure 6.1B) and Fy axis (Medio-Lateral [ML] sway; see example Figure 6.1C) were sampled at 240 Hz. Force plate CoP data was then exported at 240 Hz for analysis offline using custom written code in MATLAB (R2023a; The MathWorks, Natick, MA, USA). Prior to the calculation of postural sway metrics, the AP and ML CoP time series were band-passed between 0.2 and 20 Hz using a 4^{th} order Butterworth filter. This was done to isolate physiologically relevant sway signals by removing low-frequency drift and high-frequency noise. The first 10 seconds and last 5 seconds of the CoP time series was removed prior to further analysis.

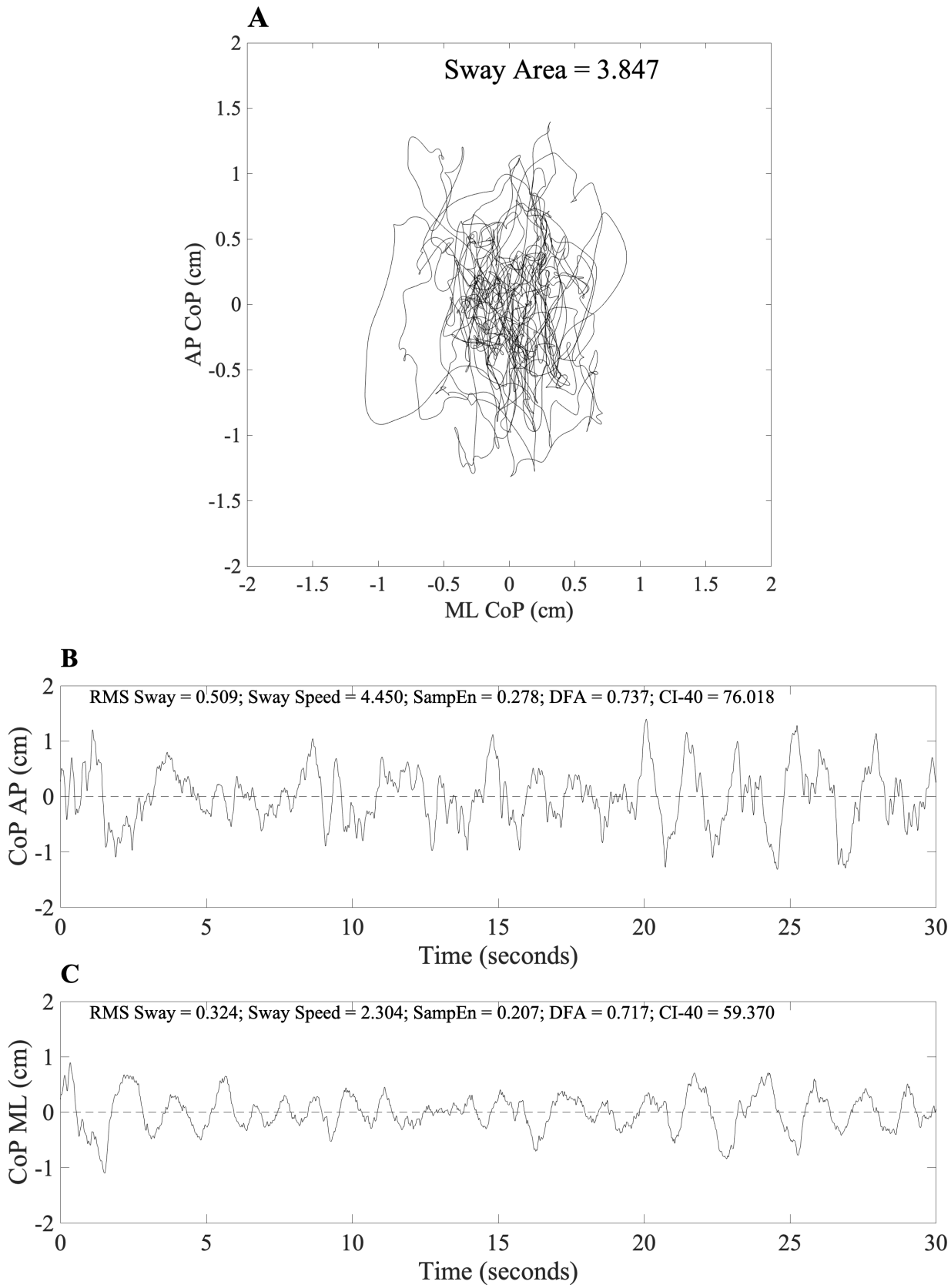

Figure 6.1. Example of an older adult's centre of pressure time series from a 30 second postural sway test **(A)** Sway area, **(B)** Anterior-posterior centre of pressure time series, **(C)** Medio-lateral centre of pressure time series.

Postural sway metrics calculated from AP and ML CoP time series were the RMS sway (cm; calculated as the square root of the mean of the squared deviations of the CoP data from its mean position over time), sway speed (cm/s; calculated by dividing the total displacement of the CoP by the duration of the test), sway area (cm^2; calculated as the area enclosed by the CoP trajectory; Figure 6.1A; Jiang et al., 2013), and sway amplitude (cm; calculated by applying the Fast Fourier Transform to the CoP data. The resulting amplitude spectrum was normalised, the DC component (zero-frequency) was set to zero to remove any offset, and the average of the maximum values of the normalised spectrum was taken as the sway amplitude).

6.2.5. Measurement of isometric knee extensor torque control (visit two).

After completing the postural sway tests participants were set up on the dynamometer as determined in visit one. The muscle torque control tasks required participants to match their instantaneous knee extensor torque output to a thin line (1 mm thick) superimposed on the computer monitor at the relative contraction intensities of 10, 20, 30, 40, 50, 60, 70 and 80% MVT. The Y axis of the display was scaled to the participants MVT, ensuring the superimposed line was located at the same position on the monitor for all participants.

The participants performed four 10 second contractions at each intensity starting at 10% MVT and progressing to 80% MVT. To ensure participants were not fatigued during the protocol, recovery durations between contractions were increased as contraction intensity increased. Recovery between the 10, 20 and 30% MVT contractions were 30 seconds, recovery between the 40 and 50% MVT contractions were 60 seconds, recovery between the 60 and 70% MVT contractions were 90 seconds, and recovery between the 80% MVT contractions were 120 seconds. As neuromuscular fatigue can reduce signal complexity (Pethick et al., 2015), complexity measures were examined across the four repeated contractions at each intensity using a repeated measures ANOVA to confirm their stability and rule out fatigue-related effects.

6.2.6. Locomotion tasks (visit two).

After completing the isometric KE contractions, participants rested for 30 minutes, before completing in a randomised order; the 30 second sit-to-stand test, timed up and go test, and 10 m walk test. These tasks were chosen to reflect the use of the lower limbs in daily living tasks. Participants were provided with 5 minutes rest between tests. Each task was repeated four times to improve measurement reliability by averaging out individual performance variability. All

tasks were initiated by a verbal ‘go’ instruction from the researcher, and completion time was recorded using a digital stopwatch.

30 second sit-to-stand test: The participant was seated in a chair with their feet flat on the floor and their arms crossed over their chest. The participant was then asked to stand up from the chair and return to a seated position as many times as possible within 30 seconds. The test was completed four times with the average number of successful stand-up and sit-down repetitions recorded as the test score. Participants rested for at least 2 minutes between each sit-to-stand test, with individuals allowed more recovery if required.

Timed up and go test: The participant was seated in a chair with their feet flat on the floor. The participant was then asked to stand and walk 3 meters to a turnaround point and return to the chair, as quickly as possible by walking. The test was completed four times with the average time taken to complete the task recorded as the test score. Participants rested for at least 2 minutes between each timed up and go test, with individuals allowed more recovery if required.

10 m walk test: The participant was stood at the start of a 10 m empty corridor. The participant was then asked to complete the 10 m distance as quickly as possible by walking. The test was completed four times (twice in each direction) with the average time taken to complete the walk taken as the test score. Participants rested for at least 2 minutes between each 10 m walk test, with individuals allowed more recovery if required.

6.2.7. Torque signal complexity, entropy, and variability metric analysis.

Prior to the calculation of the muscle torque complexity, entropy and variability metrics, the steadiest 5 seconds of each contraction was identified as the 5 seconds with the lowest SD, from which the complexity, entropy and variability metrics were then calculated.

The SDT, CVT and RMSE which quantify the variability and accuracy of torque signal were calculated as outlined in Chapter Three - General Methods - Section 3.8. The complexity and entropy metrics, SampEn, DFA, MSE and CI-28 were calculated as outlined in Chapter Three - General Methods - Section 3.9. For each contraction intensity, the two most accurate contractions (identified as the contractions with the lowest RMSE) were selected. The mean of these two contractions was then calculated and used as the participant’s complexity, entropy and variability metric values for statistical analysis.

6.2.8. Statistical analysis.

Age-group related (YG vs. OG) differences in MVT were assessed using an independent samples *t*-test.

The effect of age-group on the scale-to-scale behaviour of the MSE curves at each contraction intensity was assessed using a mixed-design two-way ANOVA, with age group (YG vs. OG) as the between-subjects factor and coarse-grained scale (1 to 28) as the within-subjects factor.

The effects of age-group (YG vs. OG) and contraction intensity (10, 20, 30, 40, 50, 60, 70, and 80% MVT) on torque signal complexity, entropy, and variability metrics were assessed using a mixed-design two-way ANOVA, with age group as the between-subjects factor and contraction intensity as the within-subjects factor.

Age-group related (YG vs. OG) differences in all postural sway metrics and locomotion test outcomes were assessed using an independent samples *t*-test.

The relationship between the performance outcomes of the fundamental motor skill tasks (postural sway metrics and locomotion tests) and the isometric KE torque signal complexity, entropy and variability metrics at each target torque (10, 20, 30, 40, 50, 60, 70 and 80% MVT) were established using a Pearson's bivariate two-tailed correlation. Due to the multiple correlation calculations, the level of statistical significance for the correlation coefficients was adjusted to $P < 0.01$. Following this, stepwise, multiple, linear regression analyses were conducted for each postural sway metric and locomotion test. Participant age and MVT were entered in the first step as independent covariates, while the correlated torque signal complexity and entropy metrics were entered stepwise as primary independent variables to identify the metrics that could explain significant variance in the dependent variables, being the postural sway metrics and locomotion tests. To account for the risk of Type I error due to multiple comparisons (the maximum number of primary independent variables included in any regression analysis was three), a Bonferroni correction was applied to the regression analyses to adjust the significance threshold ($\alpha = 0.05$).

Statistical assumptions of linearity, additivity, homoscedasticity, multicollinearity, independence of residuals, and normality of residuals were checked and accepted unless otherwise stated. Multicollinearity among the independent variables was identified using the

variance inflation factor. Multicollinearity was considered acceptable if the variance inflation factor was between 1 and 5 (Frost, 2019) and the condition index was < 10.

Cohens' d (interpreted as: 0.2 to 0.5 small effect, 0.5 to 0.8 medium effect, ≥ 0.8 large effect) and partial eta squared (η_p^2; interpreted as: 0.01 small effect, 0.06 medium effect, 0.14 large effect) were used to assess effect sizes. Cohens' d effect sizes were coded as positive when the OG presented with a higher CVT, SDT, RMSE and DFA or a lower SampEn and CI-28, when compared with the YG.

Bonferroni *post hoc* comparisons were used when a main effect or interaction was significant. The significance level was set at $P < 0.05$ in all cases. Statistical analyses were performed in IBM SPSS statistics 29 (IBM Corp., Armonk, NY, United States).

6.3 - Results

6.3.1. Participant characteristics.

Data from twenty older adults (14 male; 6 female) and twenty younger adults (14 male; 6 female) were included in the analysis. Table 6.1 presents participant characteristics. The YG produced significantly higher MVT than the OG ($P = 0.005$; Table 6.1).

Table 6.1 Participant characteristics.

	Younger Group	Older Group
N	20 (14M, 6F)	20 (14M, 6F)
Age (years)	22.5 ± 3.4	64.9 ± 11.3
Height (cm)	174.6 ± 9.6	171.2 ± 8.6
Mass (kg)	66.2 ± 8.4	70.0 ± 8.8
MVT (Nm)	190.1 ± 73.0	134.6 ± 41.3
Torque/Mass (Nm/kg)	2.9 ± 1.1	1.9 ± 0.6

Abbreviations: MVT = maximal voluntary torque; data are mean ± SD.

6.3.2. Effect of contraction intensity on age-group related differences in the complexity, entropy and variability of isometric knee extensor torque signals.

Multiscale entropy curve results

Figure 6.2 presents the comparison of the younger and older age groups MSE curves at each isometric knee extensor contraction intensity. There was a main effect of age-group on the MSE curves at 30% MVT ($F_{(1, 38)} = 5.361$; $P = 0.026$; $\eta_p^2 = 0.124$; Figure 6.2C), 40% MVT ($F_{(1, 38)} = 4.963$; $P = 0.032$; $\eta_p^2 = 0.116$; Figure 6.2D), 50% MVT ($F_{(1, 38)} = 4.696$; $P = 0.037$; $\eta_p^2 = 0.110$; Figure 6.2E), 60% MVT ($F_{(1, 38)} = 8.910$; $P = 0.005$; $\eta_p^2 = 0.190$; Figure 6.2F), 70% MVT ($F_{(1, 38)} = 10.790$; $P = 0.002$; $\eta_p^2 = 0.226$; Figure 6.2G), and 80% MVT ($F_{(1, 38)} = 5.959$; $P = 0.020$; $\eta_p^2 = 0.139$; Figure 6.2H). There was no main effect of age-group on the MSE curves at 10% MVT ($F_{(1, 38)} = 3.000$; $P = 0.092$; $\eta_p^2 = 0.075$; Figure 6.2A) and 20% MVT ($F_{(1, 38)} = 1.333$; $P = 0.255$; $\eta_p^2 = 0.034$; Figure 6.2B).

There was a significant main effect of coarse-grained scale at 10% MVT ($F_{(27, 1026)} = 35.669$; $P < 0.001$; $\eta_p^2 = 0.491$), 20% MVT ($F_{(27, 1026)} = 96.500$; $P < 0.001$; $\eta_p^2 = 0.717$), 30% MVT ($F_{(27, 1026)} = 155.598$; $P < 0.001$; $\eta_p^2 = 0.804$), 40% MVT ($F_{(27, 1026)} = 250.319$; $P < 0.001$; $\eta_p^2 = 0.868$), 50% MVT ($F_{(27, 1026)} = 296.001$; $P < 0.001$; $\eta_p^2 = 0.886$), 60% MVT ($F_{(27, 1026)} = 366.578$; $P < 0.001$; $\eta_p^2 = 0.906$), 70% MVT ($F_{(27, 1026)} = 463.585$; $P < 0.001$; $\eta_p^2 = 0.926$), and 80% MVT ($F_{(27, 1026)} = 405.338$; $P < 0.001$; $\eta_p^2 = 0.916$).

There was a significant age group by coarse-grained scale interaction at 20% MVT ($F_{(27, 1026)} = 4.086$; $P = 0.043$; $\eta_p^2 = 0.097$), 30% MVT ($F_{(27, 1026)} = 4.369$; $P = 0.035$; $\eta_p^2 = 0.103$), 40% MVT ($F_{(27, 1026)} = 4.332$; $P = 0.032$; $\eta_p^2 = 0.102$), 50% MVT ($F_{(27, 1026)} = 4.966$; $P = 0.017$; $\eta_p^2 = 0.116$), 60% MVT ($F_{(27, 1026)} = 7.864$; $P = 0.002$; $\eta_p^2 = 0.171$), 70% MVT ($F_{(27, 1026)} = 9.544$; $P < 0.001$; $\eta_p^2 = 0.205$), and 80% MVT ($F_{(27, 1026)} = 5.123$; $P = 0.013$; $\eta_p^2 = 0.122$). There was no age group by coarse-grained scale interaction at 10% MVT ($F_{(27, 1026)} = 0.272$; $P = 0.648$; $\eta_p^2 = 0.007$).

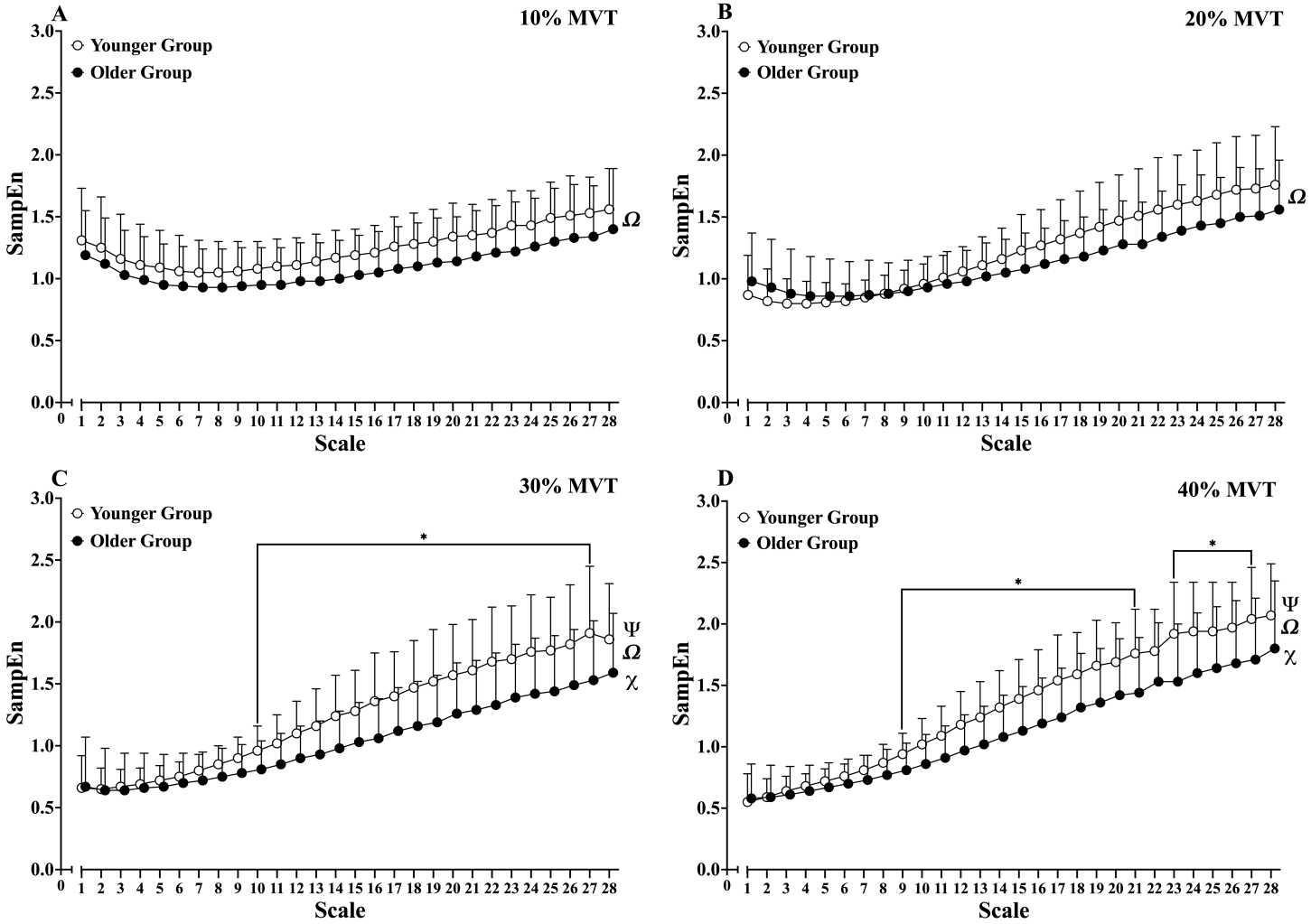

Figure 6.2. Multiscale entropy curves calculated from isometric knee extensor torque signals of the younger and older groups at **(A)** 10% MVT, **(B)** 20% MVT, **(C)** 30% MVT, **(D)** 40% MVT (Younger group = open circles; Older group = closed circles; MVT = maximal voluntary torque; SampEn = sample entropy; Ψ = significant main effect of age group; Ω = significant main effect of coarse-grained scale; χ = significant age group by coarse-grained scale interaction; *Post hoc* pairwise comparisons between age groups at each coarse-grained scale of the multiscale entropy curves are denoted by significance * in each plot; * = $P < 0.05$).

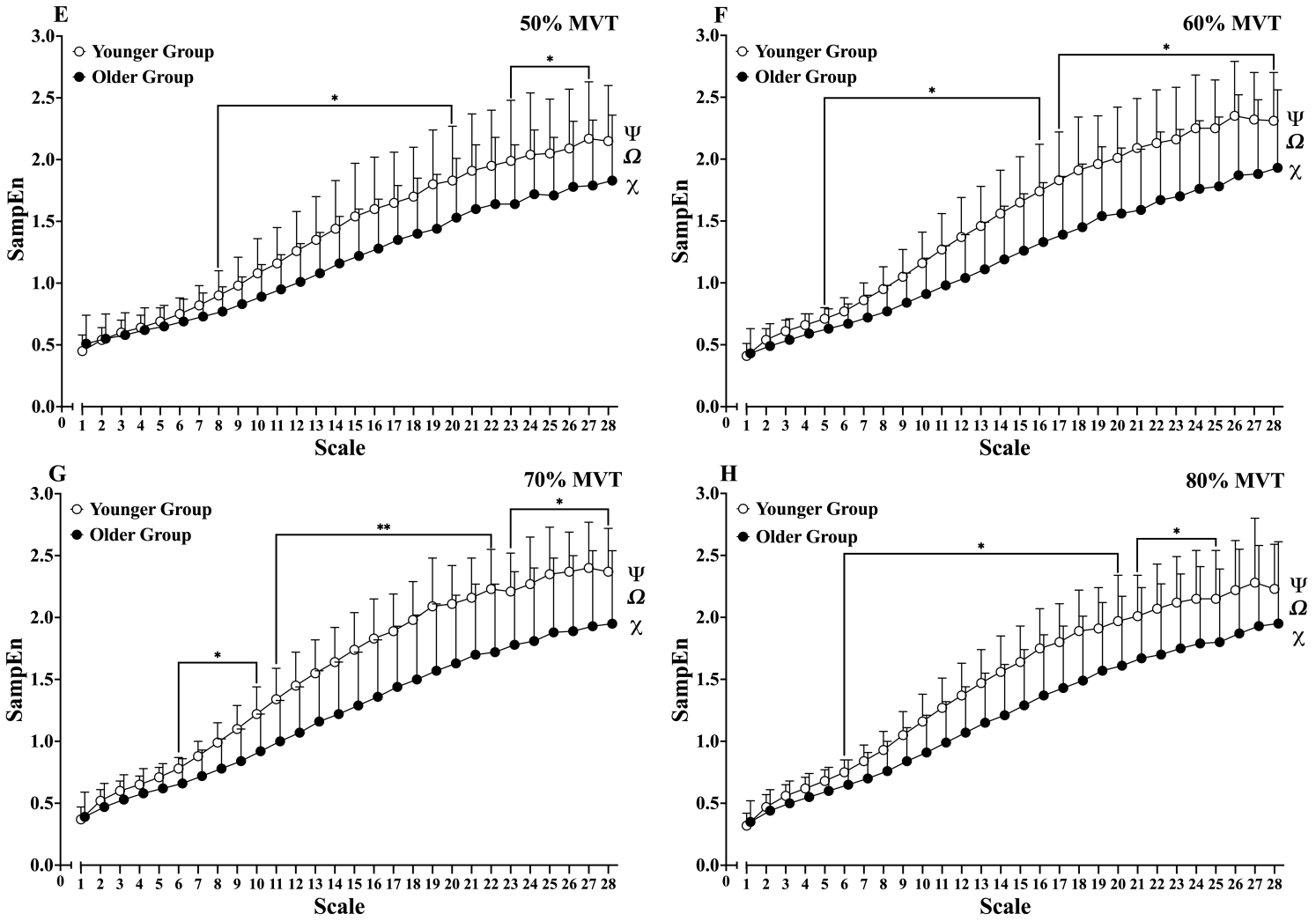

Figure 6.2. Continued. Multiscale entropy curves calculated from isometric knee extensor torque signals of the younger and older groups at **(E)** 50% MVT, **(F)** 60% MVT, **(G)** 70% MVT, **(H)** 80% MVT (Younger group = open circles; Older group = closed circles; MVT = maximal voluntary torque; SampEn = sample entropy; Ψ = significant main effect of age group; Ω = significant main effect of coarse-grained scale; χ = significant age group by coarse-grained scale interaction; *Post hoc* pairwise comparisons between age groups at each coarse-grained scale of the multiscale entropy curves are denoted by significance * in each plot; * = $P < 0.05$; ** = $P < 0.001$).

Table 6.2 presents the descriptive statistics and ANOVA results for the effect of age-group and contraction intensity on the complexity, entropy and variability of the isometric knee extensor torque signals. Table 6.3 presents the Cohens' d for the effect of age-group on the complexity, entropy and variability of the isometric knee extensor torque signals at each contraction intensity.

Complexity index results

There was a significant main effect of age group for the CI-28 metric, with the OG presenting with a lower CI-28 metric in comparison to the YG (P = 0.008; Table 6.2). *Post hoc* pairwise comparisons revealed the OG to have a lower CI-28 in comparison to the YG at 30% MVT (P = 0.013), 40% MVT (P = 0.034), 50% MVT (P = 0.037), 60% MVT (P = 0.003), 70% MVT (P = 0.005) and 80% MVT (P = 0.033).

Detrended fluctuation analysis results

There was a significant main effect of age group for the DFA α metric, with the OG presenting with a higher DFA α in comparison to the YG (P = 0.009; Table 6.2). *Post hoc* pairwise comparisons revealed the OG to have a higher DFA α in comparison to the YG at 30% MVT (P = 0.038), 40% MVT (P = 0.044), 60% MVT (P = 0.003), and 70% MVT (P = 0.019).

Sample entropy results

There was no main effect of age group for SampEn (Table 6.2). There was a significant main effect of contraction intensity but no age group by contraction intensity interaction for SampEn (Table 6.2).

Variability metric results

There was a significant main effect of age group on the RMSE, with the OG presenting with a higher RMSE in comparison to the YG (P = 0.041; Table 6.2). There was a significant main effect of contraction intensity and a significant age by contraction intensity interaction for RMSE (Table 6.2). *Post hoc* pairwise comparisons revealed the OG to have a higher RMSE in comparison to the YG at 10% MVT (P = 0.004).

There was no main effect of age group on the CVT and SDT (Table 6.2). There was a significant main effect of contraction intensity and a significant age by contraction intensity

interaction for the CVT (Table 6.2). *Post hoc* pairwise comparisons revealed the OG to have a higher CVT in comparison to the YG at 10% MVT ($P = 0.014$). There was a significant main effect of contraction intensity and a significant age by contraction intensity interaction for the SDT (Table 6.2). *Post hoc* pairwise comparisons revealed the OG to have a lower SDT in comparison to the YG at 50% MVT ($P = 0.015$), 60% MVT ($P = 0.019$) and 80% MVT ($P = 0.030$).

Table 6.2 Descriptive statistics and ANOVA results for the effect of age-group and contraction intensity on the complexity, entropy and variability of the isometric knee extensor torque signals.

		Contraction Intensity								*F, P* and η_P^2 values			
		10% MVT	20% MVT	30% MVT	40% MVT	50% MVT	60% MVT	70% MVT	80% MVT		Main effect of Age	Main effect of Intensity	Age by Intensity Interaction
SDT (Nm)	YG	0.41±0.20	0.66±0.26	0.98±0.43	1.27±0.60	γ 1.65±0.75	γ 2.03±0.98	2.55±1.41	γ 2.88±1.42	*F*	3.305	65.231	4.994
	OG	0.48±0.23	0.58±0.29	0.95±0.58	1.05±0.60	1.12±0.46	1.38±0.53	1.71±1.19	1.88±1.10	*P*	0.077	**<0.001**	**0.009**
										η_P^2	0.084	0.644	0.122
CVT (%)	YG	γ 2.25±0.94	1.85±0.60	1.82±0.72	1.71±0.50	1.84±0.67	1.86±0.74	1.97±0.82	2.00±0.79	*F*	1.345	9.605	4.886
	OG	3.32±1.52	2.15±0.89	2.38±1.29	1.99±1.00	1.72±0.56	1.79±0.64	1.83±1.09	1.73±0.80	*P*	0.254	**<0.001**	**0.003**
										η_P^2	0.036	0.211	0.120
RMSE (%)	YG	γ 4.01±1.82	2.67±1.19	2.44±1.22	2.26±0.71	2.23±0.92	2.20±0.90	2.36±0.98	2.38±0.91	*F*	4.487	27.233	6.795
	OG	7.33±4.56	3.33±1.48	3.40±2.08	2.82±1.42	2.31±0.82	2.19±0.67	2.41±1.63	2.40±1.43	*P*	**0.041**	**<0.001**	**0.004**
										η_P^2	0.111	0.431	0.159
SampEn	YG	1.31±0.42	0.87±0.32	0.66±0.26	0.55±0.23	0.45±0.13	0.41±0.10	0.37±0.10	0.32±0.10	*F*	0.047	141.947	1.265
	OG	1.19±0.36	0.98±0.39	0.67±0.40	0.58±0.28	0.51±0.23	0.43±0.20	0.39±0.20	0.35±0.17	*P*	0.829	**<0.001**	0.261
										η_P^2	0.001	0.798	0.034
DFA α	YG	1.32±0.08	1.34±0.06	γ 1.33±0.13	γ 1.31±0.10	1.28±0.13	γ 1.23±0.13	γ 1.25±0.11	1.28±0.11	*F*	7.552	5.482	1.296
	OG	1.35±0.09	1.38±0.11	1.40±0.10	1.38±0.10	1.35±0.11	1.35±0.14	1.36±0.14	1.36±0.14	*P*	**0.009**	**<0.001**	0.275
										η_P^2	0.173	0.132	0.035
CI-28	YG	34.98±6.19	34.13±6.65	γ 34.90±7.67	γ 37.18±6.67	γ 38.99±8.53	γ 42.36±7.82	γ 43.62±6.30	γ 41.17±6.84	*F*	7.846	11.894	1.282
	OG	30.63±9.28	31.34±7.82	28.99±8.44	31.54±9.16	32.94±9.45	33.55±10.46	34.42±11.01	33.89±11.19	*P*	**0.008**	**<0.001**	0.283
										η_P^2	0.179	0.248	0.034

Abbreviations: CI-28 = complexity index under 28 scales; CVT = coefficient of variation of torque; DFA = detrended fluctuation analysis scaling exponent α; MVT = maximal voluntary torque; OG = older age group; RMSE = root mean square error; SampEn = sample entropy; SDT = standard deviation of torque; YG = younger age group; Significant *P* values highlighted by bold font; γ = significant difference between YG and OG $P < 0.05$; data are mean ± SD.

Table 6.3 Cohens' d for the effect of age-group on the complexity, entropy and variability of the isometric knee extensor torque signal at each contraction intensity.

		Contraction Intensity							
		10% MVT	20% MVT	30% MVT	40% MVT	50% MVT	60% MVT	70% MVT	80% MVT
SDT (Nm)	Cohens' d [95% CI]	0.31 [-0.32, 0.93]	-0.30 [-0.92, 0.32]	-0.06 [-0.68, 0.56]	-0.37 [-0.99, 0.26]	-0.83 [-1.48, -0.19]	-0.81 [-1.45, -0.16]	-0.63 [-1.27, 0.00]	-0.78 [-1.42, -0.13]
CVT (%)	Cohens' d [95% CI]	0.83 [0.19, 1.48]	0.39 [-0.24, 1.02]	0.52 [-0.11, 1.15]	0.35 [-0.28, 0.97]	-0.18 [-0.80, 0.44]	-0.10 [-0.72, 0.52]	-0.15 [-0.77, 0.47]	-0.33 [-0.95, 0.29]
RMSE (%)	Cohens' d [95% CI]	0.94 [0.29, 1.59]	0.48 [-0.14, 1.11]	0.55 [-0.08, 1.18]	0.49 [-0.14, 1.11]	0.09 [-0.53, 0.71]	-0.02 [-0.64, 0.60]	0.04 [-0.58, 0.66]	0.01 [-0.61, 0.63]
SampEn	Cohens' d [95% CI]	0.31 [-0.31, 0.94]	-0.30 [-0.92, 0.32]	-0.04 [-0.66, 0.58]	-0.10 [-0.72, 0.52]	-0.30 [-0.93, 0.32]	-0.11 [-0.73, 0.51]	-0.12 [-0.74, 0.50]	-0.20 [-0.83, 0.42]
DFA α	Cohens' d [95% CI]	0.36 [-0.27, 0.98]	0.43 [-0.20, 1.06]	0.59 [-0.04, 1.22]	0.64 [0.00, 1.27]	0.55 [-0.08, 1.18]	0.92 [0.27, 1.57]	0.83 [0.18, 1.48]	0.61 [-0.03, 1.24]
CI-28	Cohens' d [95% CI]	0.54 [-0.09, 1.17]	0.38 [-0.25, 1.00]	0.72 [-0.08, 1.36]	0.69 [-0.05, 1.33]	0.66 [-0.02, 1.30]	0.93 [-0.28, 1.59]	1.01 [-0.35, 1.66]	0.77 [-0.13, 1.41]

Abbreviations: CI-28 = complexity index under 28 scales; CVT = coefficient of variation of torque; DFA = detrended fluctuation analysis scaling exponent α; MVT = maximal voluntary torque; RMSE = root mean square error; SampEn = sample entropy; SDT = standard deviation of torque.

6.3.3. Postural Sway results.

The OG presented with a significantly greater AP RMS sway ($P < 0.001$; d = 1.221, 95% CI [0.537: 1.892]; Figure 6.3A), AP sway speed ($P < 0.001$; d = 1.221, 95% CI [0.541: 1.897]; Figure 6.3B), AP sway amplitude ($P < 0.001$; d = 1.199, 95% CI [0.517: 1.868]; Figure 6.3C) and sway area ($P < 0.001$; d = 0.764, 95% CI [0.117: 1.403]; Figure 6.3D), in comparison to the YG. There was no difference between the YG and OG in ML RMS sway ($P = 0.286$; d = 0.465, 95% CI [-0.167: 1.090]; Figure 6.3A), ML sway speed ($P = 0.504$; d = -0.213, 95% CI [-0.833: 0.410]; Figure 6.3B) and ML sway amplitude ($P = 0.314$; d = 0.323, 95% CI [-0.303: 0.945]; Figure 6.3C).

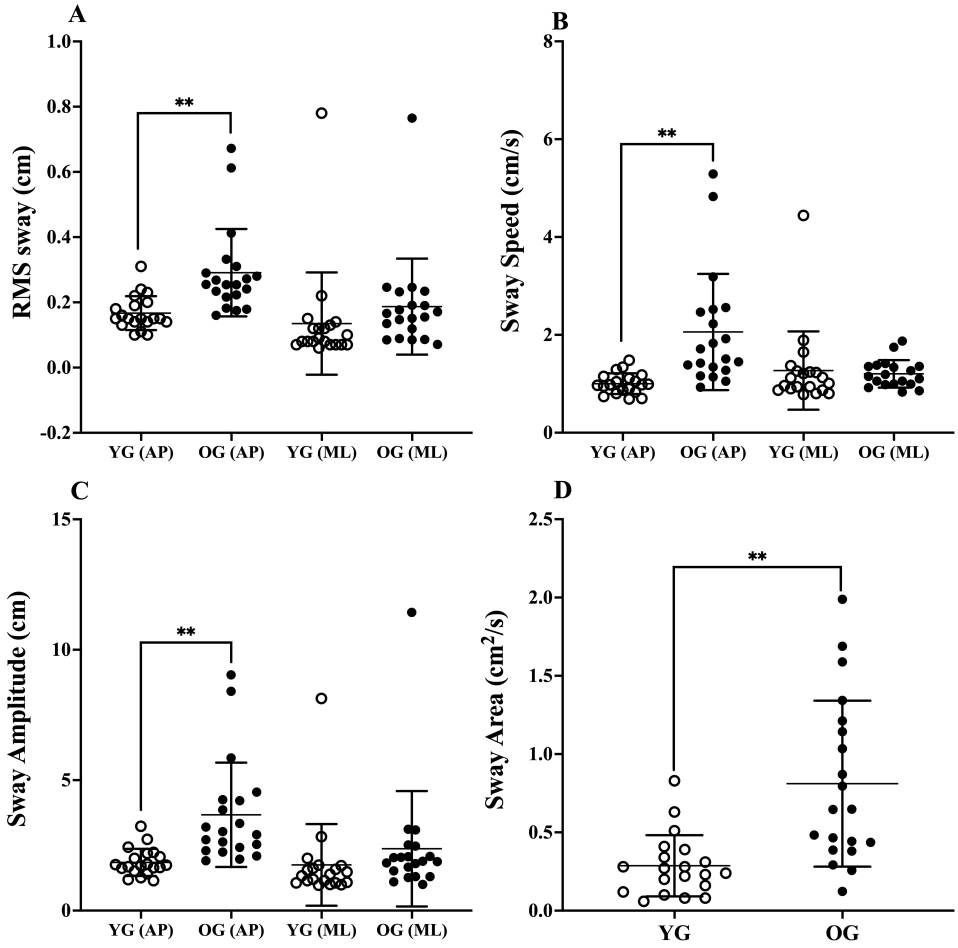

Figure 6.3. (A) Root mean square sway, calculated from the anterior-posterior and medio-lateral centre of pressure data of the younger and older groups, **(B)** Sway speed, calculated from the anterior-posterior and medio-lateral centre of pressure data of the younger and older groups, **(C)** Sway amplitude, calculated from the anterior-posterior and medio-lateral centre of pressure data of the younger and older groups, **(D)** Sway area, calculated from the anterior-posterior and medio-lateral centre of pressure data of the younger and older groups (AP = anterior-posterior; ML = medio-lateral; OG = older group; YG = younger group;** = $P < 0.001$).

6.3.4. Locomotion task results.

The YG completed the Up and Go tests significantly faster than the OG ($P = 0.008$; d = 0.87, 95% CI [0.22: 1.52]; Figure 6.4A). There was no difference between the YG and OG in the time taken to complete the 10 m walk test ($P = 0.926$; d = -0.03, 95% CI [-0.65: 0.59]; Figure 6.4B). The YG completed a significantly higher number of sit-to-stands in comparison to the OG ($P = 0.004$; d = -0.95, 95% CI [-1.60: -0.29]; Figure 6.4C).

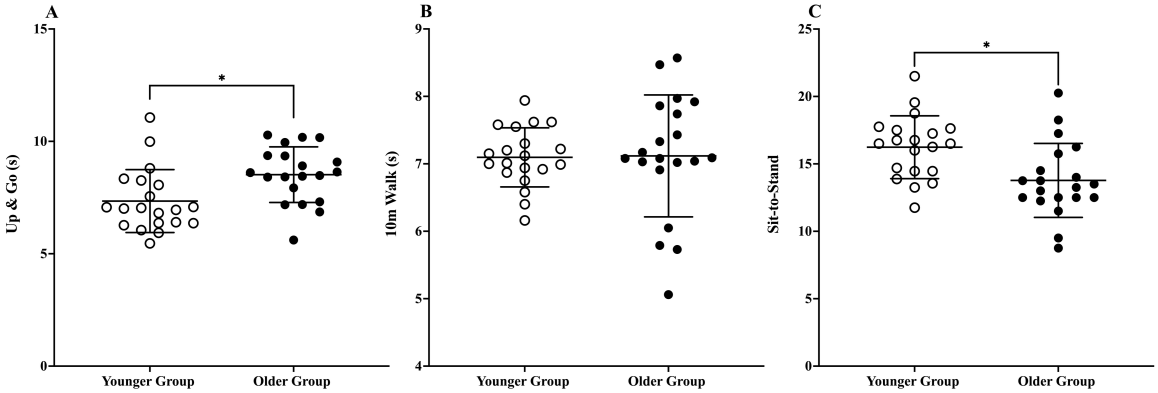

Figure 6.4. (A) Up and Go test, **(B)** 10 m walk test, **(C)** Sit-to-stand test (* = $P < 0.05$).

6.3.5. Relationship between fundamental motor skill performance and the complexity, entropy and variability of isometric knee extensor torque signals.

Pearson's bivariate two-tailed correlation analysis revealed: CI-28 at 10% (r = -0.536; R^2 = 0.287; $P < 0.001$) and 20% (r = -0.441; $R^2 = 0.195$; $P < 0.01$) of MVT to be correlated with AP RMS sway; CI-28 at 50% (r = -0.433; $R^2 = 0.188$; $P < 0.01$), DFA α at 50% (r = 0.413; R^2 = 0.170; $P < 0.01$), and SampEn at 50% (r = -0.410; $R^2 = 0.168$; $P < 0.01$) of MVT to be correlated with ML RMS sway; CI-28 at 10% MVT to be correlated with AP sway speed (r = -0.507; R^2 = 0.258; $P < 0.001$); CI-28 at 50% (r = -0.322; $R^2 = 0.104$; $P < 0.01$) and DFA α at 50% (r = 0.319; $R^2 = 0.102$; $P < 0.01$) of MVT to be correlated with ML sway speed; CI-28 at 10% MVT to be correlated with AP sway amplitude (r = -0.531; $R^2 = 0.281$; $P < 0.001$); CI-28 at 50% (r = -0.382; $R^2 = 0.146$; $P < 0.01$) and DFA α at 50% (r = 0.368; $R^2 = 0.136$; $P < 0.01$) of MVT to be correlated with ML sway amplitude; and SampEn at 70% MVT to be correlated with 10 m walk time (r = 0.424; $R^2 = 0.179$; $P < 0.01$). These isometric KE torque signal complexity and entropy metrics were then entered into the stepwise, multiple, linear regression analyses.

Table 6.4 presents the isometric KE torque signal complexity and entropy metrics that explained a significant proportion of variance in the AP postural sway metrics and 10 m walk time, when participant age and MVT were included as independent co-variates. CI-28 at 10% MVT was found to explain between 5.4% and 9.1% of the variance in the AP postural sway metrics (Table 6.4). SampEn at 70% MVT was found to explain 10.6% of the variance in 10 m walk time (Table 6.4).

Table 6.4 Relationship between fundamental motor skill performance and the complexity and entropy of isometric knee extensor torque signals.

Dependent Variables	Independent Covariates: Age and MVT		Independent Predictor Variables				
	R	R^2		ΔR^2	β	ΔF	Sig. Δ*F*
AP RMS Sway (cm)	0.723	0.522	CI-28 10%	0.091	-0.330	8.154	0.007
AP Sway Speed (cm/s)	0.722	0.522	CI-28 10%	0.054	-0.254	4.382	0.044
AP Sway Amp. (cm)	0.734	0.539	CI-28 10%	0.074	-0.298	6.652	0.014
10m Walk	0.341	0.116	SampEn 70%	0.106	0.345	4.783	0.036

Abbreviations: Amp = amplitude; AP = anterior-posterior; CI-28 = complexity index under 28 scales; MVT = maximal voluntary torque; RMS = root mean square; SampEn = sample entropy.

DFA α at 50% MVT was found to explain a significant proportion of variance in the ML postural sway metrics. However, these results were not reported due to the presence of strong collinearity between DFA and the covariate MVT, as indicated by a condition index exceeding 10. This level of collinearity makes it difficult to distinguish the contribution of DFA from that of MVT in the model.

6.4 - Discussion

6.4.1. Effect of contraction intensity on age-group related differences in the complexity, entropy and variability of isometric knee extensor torque signals.

The first aim of the current experimental chapter was to investigate the effect of contraction intensity on the age-group related differences in the complexity, entropy and variability of isometric KE torque signals. Main findings indicate that, across a wide range of contraction intensities (10 to 80% MVT), older adults exhibit lower neuromuscular complexity than younger adults, as assessed by DFA and CI-28 (Table 6.2). As evidenced by the consistent medium to large effect sizes (Table 6.3) and significant *post hoc* pairwise comparisons (Table 6.2), the impact of age-group on neuromuscular complexity (DFA and CI-28) was most pronounced at contraction intensities exceeding 20% MVT. These findings are contrary to the hypothesis and suggest that impairments in muscle torque regulation in older age are exacerbated at higher contraction intensities. Notably, older adults exhibited lower SampEn across multiple time scales of the MSE curves than younger adults (Figure 6.2), suggesting that age-group related differences in neuromuscular complexity may result from changes in both the function of individual components and their interactions within the neuromuscular system.

The current study was the first to employ the MSE analysis to examine age-group related differences in the temporal structure of isometric KE torque signals across a range of contraction intensities (10 to 80% MVT). The CI-28 complexity metric, derived from the MSE analysis, was consistently lower in older adults compared with younger adults across contraction intensities ranging from 30 to 80% MVT (Table 6.2). There were also age-related differences in the DFA α of the torque signals across contraction intensities (Table 6.2). Both age groups DFA α was found to depart from $1/f$ noise ($\alpha = 1.0$), being the highest complexity signal, towards Brownian noise ($\alpha = 1.5$). However, the older adults exhibited a scaling exponent α closer to 1.5, indicative of a lower complexity signal, compared to the younger adults. These findings align with previous research showing that older adults exhibit lower neuromuscular complexity at 15% to 40% MVT than younger adults (Fiogbe et al., 2021). Importantly, the current study expands on this by demonstrating that age-related differences in neuromuscular complexity persist across a broader range of contraction intensities (30% to 80% MVT).

Collectively, the DFA and MSE analyses indicate older adults to have a lower neuromuscular complexity than younger adults. These findings may be explained by the greater strength of common synaptic input required by older adults to achieve the same relative level of torque production compared to younger adults (Castronovo et al., 2018). As a consequence, there would be greater MU synchronisation, and therefore less complex temporal oscillatory patterns in neural drive (Pethick et al., 2016; Pethick et al., 2021b). This reduced complexity common input signal may then be reflected in a lower complexity torque signal (Pethick et al., 2016; Pethick et al., 2021b; Negro et al., 2009; Thompson et al., 2018). The older adult's lower neuromuscular complexity across a wide range of contraction intensities (30 to 80% MVT) potentially indicates an impairment in neuromuscular function and torque regulation across different task demands.

The older adult's lower CI-28 at derived from contractions at 30 to 80% MVT were attributable to the lower SampEn at longer (coarser) time scales of the MSE curves compared to the younger adults (Figure 6.2). The neuromuscular system's high dimensionality, consisting of multiple interacting components, may explain this age-related suppression of SampEn across the coarser time scales (Rohrle et al., 2019; Vieluf et al., 2015). The functioning and nonlinear interaction between different system components is suggested to determine the temporal structure of the torque signal at multiple time scales (Vieluf et al., 2015). Therefore, it is plausible to speculate that the age-dependent scale-to-scale entropic behaviour of the torque signal, reflects changes in both the function of individual components and their interaction within the neuromuscular system operating at their specific time scales (Vieluf et al., 2015).

Notably, there was no age-related differences in SampEn at time scale one of the MSE curves at all contraction intensities (Figure 6.2). The MSE curve behaviour highlights the importance of examining the entropic behaviour of muscle torque signals across multiple time scales, rather than relying on single-scale entropy, particularly when investigating age-related differences in neuromuscular complexity. However, research is still required to elucidate the mechanisms determining the behaviour of the MSE curves. If the mechanisms underpinning the temporal structure of torque signal can be established, the MSE analysis would become an effective, easily applied, surrogate measure for assessing specific mechanistic alterations to the functioning and behaviour of the neuromuscular system on a component level.

Older adults exhibited significantly greater neuromuscular variability (CVT) at 10% MVT than younger adults (Table 6.2), with the effect of age less evident at higher contraction intensities (≥ 20% MVT; Tables 6.2 and 6.3). This greater neuromuscular variability at low contraction intensities (10% MVT) may result from greater oscillations in MU force during initial recruitment, fewer and larger MUs with slower and more variable discharge rates, and the loss of smaller MUs essential for precise motor control (Azevedo et al., 2020; Connelly et al., 1999; Fuglevand et al., 1993; Kudina, 1999; Kamen et al., 1995; Piasecki et al., 2016b; Tracy et al., 2005; Westgaard & De Luca, 2001). The observed age-related difference in neuromuscular complexity, but not in neuromuscular variability at higher intensities (≥ 20% MVT) suggests that the temporal and spatial structure of muscle torque signals may be influenced by distinct mechanisms and was therefore investigated in Chapter Eight.

The effect size analysis in Chapter Two revealed an effect of contraction intensity and muscle group on the age-related differences in neuromuscular variability. Specifically, the variability of upper extremity isometric muscle force signals (CVF) was negatively affected by age across all contraction intensity categories (Figure 2.2C). In comparison, the variability of lower extremity isometric muscle force signals were primarily affected by age at lower contraction intensities (Figure 2.2B). However, it was not possible to analyse the effect of contraction intensity and muscle group on the age-related differences in neuromuscular complexity. This was because of the limited number of available effect sizes for both upper and lower extremity muscles at multiple contraction intensities in the current literature (Chapter Two). The current chapter has provided the first data regarding the effect of contraction intensity on the age-related differences in the complexity of lower extremity muscle torque signals (Tables 6.2 and 6.3). Therefore, the next experimental chapter (Chapter Seven) will examine the effect of contraction intensity on age-related differences in the complexity of upper extremity muscle force signals (i.e., isometric precision PG force signals).

6.4.2. Relationship between fundamental motor skill performance and the complexity, entropy, and variability of isometric knee extensor torque signals.

The second aim of the current experimental chapter was to identify the contraction intensities at which the complexity, entropy and variability of isometric KE torque signals were most strongly associated with the performance in postural sway and locomotion tasks. Findings show the complexity of the isometric KE torque signal at 10% MVT to be significantly

explanatory of the variance in the RMS, speed and amplitude of AP postural sway during bipedal standing (Table 6.4). The complexity metric that consistently explained a significant proportion of variance in AP postural sway, when controlling for participant age and MVT, was CI-28 (Table 6.4).

As hypothesised, individuals who presented with a lower complexity torque signal exhibited a greater RMS, speed and amplitude of postural sway. When accounting for age and MVT, CI-28 at 10% MVT explained between 5.4% to 9.1% of additional variance in the AP postural sway metrics (Table 6.4). Current findings extend previous research that has shown the neuromuscular variability of PF and DF muscle force at low contraction intensities (between 5% and 20% MVT) to be associated with postural control (Hirono et al., 2020; Hirono et al., 2021; Kouzaki & Shinohara 2010; Oshita & Yano, 2012). Taken together, these findings underscore the functional significance of neuromuscular complexity and variability. They further suggest that maintaining postural stability necessitates precise neuromuscular control of lower extremity muscles, particularly at low contraction intensities.

The SampEn of the isometric KE torque signal at 70% MVT was found to be associated with the performance of the 10 m locomotion task (Table 6.4). This extends findings of previous research that demonstrated the variability of isometric KE torque at 50% MVT to be significantly related to stair climbing and chair rise test performance (Seynnes et al., 2005). In contrast, research has shown also found there to be no relationship between the variability of isometric KE torque at 50% MVT and the performance of chair rise and stair ascent and descent tests (Manini et al., 2005). Although the KE muscles are crucial to locomotion performance, the sustained isometric contractions used to derive the complexity and variability metrics in the current and previous studies were not directly representative of the neuromuscular demands of the locomotion tasks. Hence the equivocal findings and limited association with the isometric KE torque signal complexity and variability metrics in the current and previous studies.

Postural control during standing and locomotion is achieved through a complex process, involving the coordinated multi-directional action of postural muscles around the lower-limb joints (Hagio & Kouzaki, 2015; Kutch et al., 2008; Monte et al., 2024), in addition to, sensory inputs from the vestibular system, proprioceptive receptors (i.e., muscle spindles and Golgi tendon organs), and visual cues (Elias et al., 2014; Luu et al., 2012; Peterka, 2018). Indeed, the

KE muscles were only one component in the complex postural control system. This likely explains the very limited, albeit significant, association between neuromuscular complexity and postural control.

6.4.3. Limitations.

In Chapter Five, the *younger* mean age of the MG was a limitation. The current study sought to address this by expanding the age range of the OG in the current study to between 50 and 85 years. Although the OG were *older* than the MG of Chapter Five, it could be speculated that they were still too *young* to start observing the age-related changes in neuromuscular function attributable to older-old age. The *younger* age of the OG can be attributed, in part, to difficulties in recruiting high numbers of older adults (> 70 years), in the absence of medical conditions and impairments to lower limb function.

The current chapter was limited to assessing neuromuscular complexity during sustained isometric contractions. However, postural control during standing and locomotion involves dynamic and repetitive muscle contractions. Therefore, it is possible sinusoidal or "ramp-up ramp-down" torque matching tasks may be more comparable to the demands of lower extremity fundamental motor skills. Future research should explore the relationship between these torque matching tasks and fundamental motor skill performance in a range of populations.

6.5 - Conclusion

Older adults exhibit lower neuromuscular complexity (DFA and CI-28) compared to younger adults across a range of contraction intensities (10 to 80% MVT), with the most pronounced age-group related differences occurring above 20% MVT. These findings suggest that impairments in muscle torque regulation in older age are exacerbated at higher contraction intensities. Additionally, older adults exhibit lower SampEn across multiple time scales of the MSE curves than younger adults. This indicates that age-group related differences in neuromuscular complexity may result from changes in both individual component function and their interaction within the neuromuscular system across multiple time scales. Furthermore, this study provides evidence that, when accounting for age and MVT, lower neuromuscular complexity was associated with worse performance of the postural sway tasks.

Chapter Seven

Effect of age-group on the neuromuscular complexity and variability of hand muscle force signals.

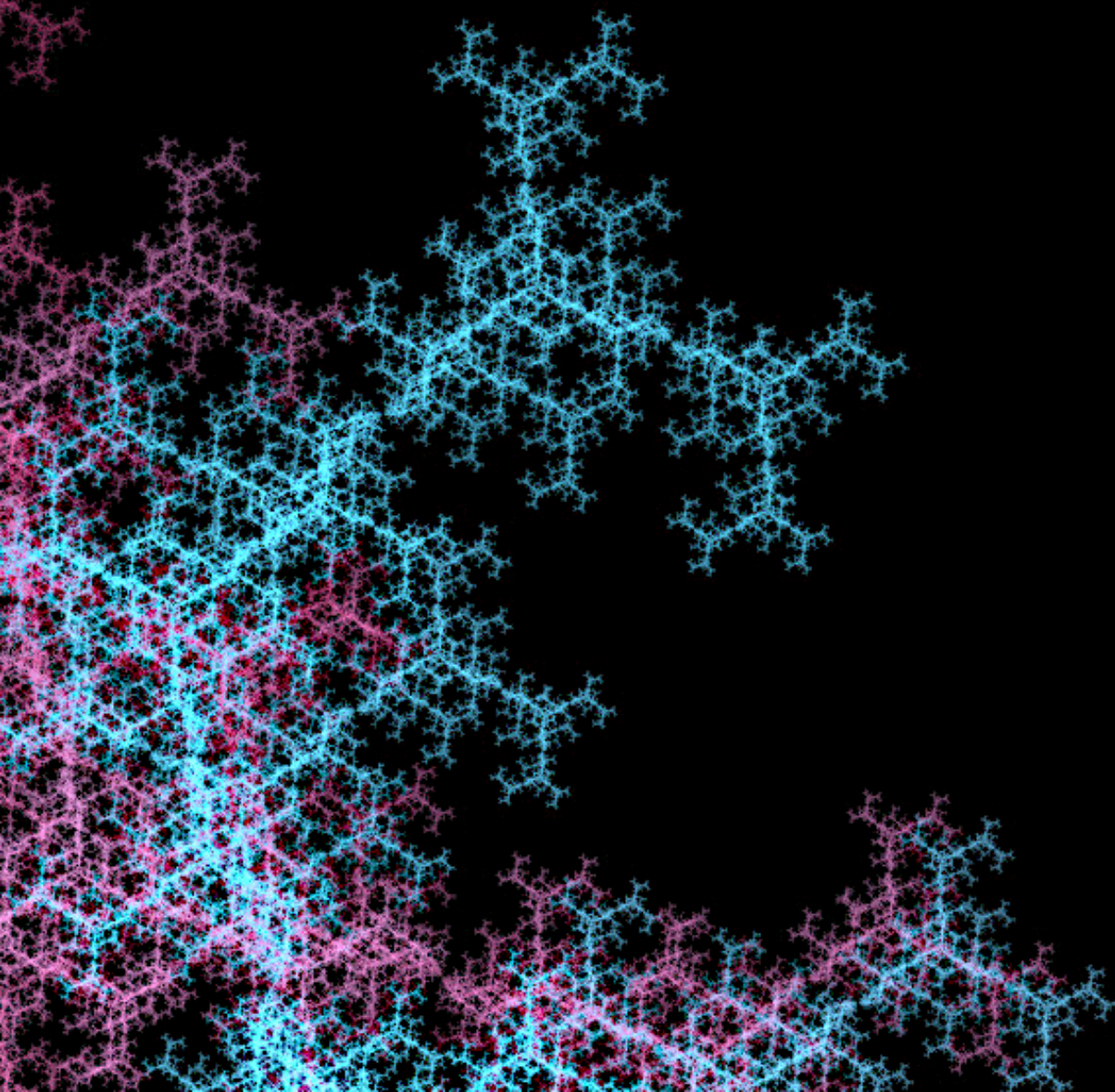

7.1 - Introduction

Manual dexterity is a marker of motor function and neurological health and can be defined as the ability to make precise, coordinated hand and finger movements to grasp and manipulate objects (Gershon et al., 2010; Reuben et al., 2013). It has been suggested that diminished manual dexterity and consequently hand muscle function were detrimental to basic ADLs (Jette et al., 1990; Williams et al., 1982) and can predict a loss of independence in older individuals (Ostwald et al., 1989; Falconer et al., 1991). Manual dexterity is commonly assessed using a form of pegboard test (Ranganathan et al., 2001; Reuben et al., 2013; Wang et al., 2011), the performance of which requires muscle strength, tactile perception, cognitive processing speed, attentional processing, coordination, and *muscle force control* (Ashendorf et al., 2009; Almuklass et al., 2016; Carey et al., 1997; Carmeli et al., 2003; Ebaid et al., 2017; Feeney et al., 2018; Huddleston et al., 2014; Lawrence et al., 2015; Marmon et al., 2011a; Marmon et al., 2011b; Seidler et al., 2002).

Effective regulation of hand and wrist muscle force control, quantifiable through measures neuromuscular complexity and variability, is essential to the successful performance of tasks requiring manual dexterity (Camacho-Villa et al., 2025). Feeney et al. (2018) reported that age and the variability of muscle force at 20% MVF during a double action WE and precision PG tasks accounted for 58% of the variance in grooved pegboard test times. Similarly, force variability of the IFA and WE muscles, both individually and in combination, was significantly associated with pegboard performance across young and older adults (Almuklass et al., 2016; Daneshgar et al., 2024; Hamilton et al., 2017). Additionally, reduced pegboard performance in older adults has been associated with the increased variability in IFA muscle force (Semmler et al., 2000). While the role of neuromuscular variability of hand and wrist muscles in tasks requiring manual dexterity has been investigated, the contribution of neuromuscular complexity remains unclear. Furthermore, the effects of age-group on the neuromuscular complexity of upper limb muscles, especially during isometric precision PG tasks, are not well understood.

Older adults consistently exhibit greater isometric precision PG force signal variability than younger adults across contraction intensities, 5 to 40% MVF (Critchley et al., 2014; Dottor et al., 2025; Feeney et al., 2018; Keogh et al., 2006; Keenan et al., 2017; Marmon et al., 2011b; Ranganathan et al., 2001; Sosnoff & Newell, 2011), likely due, in part, to increased strength

and variance in common synaptic input to the motor neurons (Castronovo et al., 2018; Feeney et al., 2018). Comparatively, the influence of age on the complexity and entropy of isometric precision PG force signals remains unclear (Knol et al., 2019; Sosnoff & Newell, 2006b; Vaillancourt et al., 2002; Vieluf et al., 2018). Sosnoff and Newell (2006b) found no age-related difference in single-scale ApEn at 5% MVF. By comparison, Vaillancourt et al. (2002) reported lower cross-ApEn in older adults compared to younger adults at 5, 25 and 50% MVF. However, as demonstrated by the MSE analysis in Chapters Five and Six, single-scale entropy analysis fails to fully characterise the effect of age on the multi-scale temporal structure inherent to muscle force signals.

The temporal structure of muscle force signals, as revealed by the scale-to-scale entropic behaviour of the MSE curve analysis, is postulated to reflect the neuromuscular system's control processes and the integrative functioning of its components (Knol et al., 2019; Vieluf et al., 2015). This analysis therefore offers deeper insights into age-related differences in neuromuscular function and muscle force regulation than those provided by signal scale entropy measures alone. However, only one study has investigated the scale-to-scale entropic behaviour of precision PG force signals, finding that older adults exhibited lower SampEn across all temporal scales at 10% and 30% MVF compared to younger adults (Knol et al., 2019). By assessing scale-to-scale entropic behaviour of precision PG force signals across a wider range of contraction intensities (10 to 60% MVF), the current study aims to provide a comprehensive understanding of age-group related differences neuromuscular complexity and by extension hand muscle function and force regulation across different task demands.

Aims and Hypotheses.

To investigate age-group differences in the complexity, entropy, and variability of isometric precision PG force signals across contraction intensities, and to examine whether the complexity and entropy of isometric precision PG force signals are associated with the performance of the manual dexterity tasks.

It was hypothesised that older adults would produce isometric precision PG force signals of lower complexity and entropy and greater variability across all contraction intensities compared to younger adults. Furthermore, it was hypothesised that force signals of lower complexity and entropy of would be associated with worse performance of manual dexterity tasks.

7.2 - Methods

7.2.1. Participants.

Sixty-four healthy individuals (38 male; 26 female) were recruited to participate in the study. Participants were recruited to be in four age groups, the YG were aged 18 to 30 years (N = 16; 10M, 6F), the 50 year old group were aged 50 to 59 years (N = 16; 6M, 10F), the 60 year old group were aged 60 to 69 years (N = 16; 10M, 6F) and the 70 year old group were aged 70 to 85 years (N = 16; 12M, 4F).

Before being allowed to participate in the study all potential participants provided written informed consent and completed a health questionnaire to ensure they were in full health. Participants were required to be non-obese, non-smokers, not have previous or current circulatory disorders, have no known or signs/symptoms of cardiovascular, neuromuscular, renal, or metabolic conditions, and not have arthritis of the hand or injuries to the muscles or tendons of the hand, wrist, elbow, or shoulder. Participants were required to be living independently and able to perform active daily living tasks. The study was completed with full ethical approval of the University of Kent Research Ethics Committee (Proposal number: 22_20_23), according to Declaration of Helsinki standards (but without being registered).

7.2.2. Experimental Design.

Each participant completed one experimental session. Firstly, participants completed a familiarisation of the isometric precision PG force control task by performing a series of force matching tasks at 1 N. Secondly, the participants' isometric precision PG MVF was measured to establish relative isometric contraction intensities for the subsequent precision PG force control tasks. Participants then performed the isometric precision PG force control tasks at 5, 10, 15, 20, 30, 40, 50 and 60% MVF. From the isometric precision PG force control tasks the force signal complexity, entropy and variability metrics were calculated. Lastly, participants completed the Purdue Pegboard and Moberg Pick-up manual dexterity tests.

7.2.3. Measurement of isometric precision pinch grip maximal voluntary force.

Participants were set up with the miniature button load cell (Applied Measurements Ltd, Berkshire, UK), as outlined in Chapter Three - General Methods - Section 3.7.

Prior to commencing the measurement of MVF participants were familiarised with the miniature button load cell by performing a series of force matching tasks at 1 N of force. Participants then performed a warm-up of 10 second submaximal contractions with 10 second rest periods, after which a series of brief (6 second) MVCs were performed to establish the MVF. MVC trials were repeated (separated by 60 seconds rest) until a plateau in peak force is reached (i.e., until three consecutive peak forces were within 5% of each other). The highest force value from a 2 second epoch was recorded as the participant's MVF, which was then used to set the relative constant load isometric exercise intensities of 5, 10, 15, 20, 30, 40, 50 and 60% MVF to be used in the force control tasks.

All force data were recorded at a 1000 Hz (CED Micro 1401-3, Cambridge Electronic Design, Cambridge, United Kingdom), interfaced with a personal desk top computer, with data collected (Spike2, Cambridge Electronic Design) and exported at 1000 Hz for analysis offline in MATLAB (The MathWorks, Natick, MA, USA).

7.2.4. Measurement of isometric precision pinch grip force control.

Upon completing the measurement of isometric precision PG MVF, participants rested for 20 minutes before commencing the muscle force control task which required participants to match their instantaneous precision PG force output to a thin line (1 mm thick) superimposed on the computer monitor at relative contraction intensities of 5, 10, 15, 20, 30, 40, 50 and 60% MVF. The Y axis of the display was scaled to the participants MVF, ensuring the superimposed line was located at the same position on the monitor for all participants.

The participants performed four 10 seconds contractions at each intensity starting at 5% MVF and progressing to 60% MVF. To ensure participants were not fatigued during the protocol, as fatigue has been shown to change the complexity of muscle force output (Pethick et al., 2015), recovery durations between contractions were increased as contraction intensity increased. Recovery between the 5, 10 and 15% MVF contractions were 30 seconds, recovery between 20, 30 and 40% MVF contractions were 60 seconds and recovery between 50 and 60% MVF contractions were 90 seconds. There was a 120 second recovery between each contraction intensity set. As neuromuscular fatigue can reduce signal complexity (Pethick et al., 2015), complexity measures were examined across the four repeated contractions at each intensity using a repeated measures ANOVA to confirm their stability and rule out fatigue-related effects.

7.2.5. Manual dexterity tasks.

After completing the isometric precision PG force control tasks, a 20-minute rest was observed. Participants then completed the Purdue Pegboard test and Moberg pick-up test, chosen to reflect the use of the hand in daily living tasks requiring fine dexterity. Participants were provided with two practice attempts at the Purdue Pegboard and Moberg Pick-up test before completing the actual tests. Each task was repeated four times to improve measurement reliability by averaging out individual performance variability.

Purdue Pegboard test (Tiffin & Asher, 1948): The participants were seated at a table with the pegboard placed directly in front. The participants were then instructed to pick up each peg (using an index finger to thumb PG) situated next to the board individually and place as many pegs as possible into the board in 30 seconds. The participants completed the pegboard four times with their dominant hand, with the average number of pegs placed across the four tests taken as the test score. Two minutes rest was observed between Purdue Pegboard test repeats.

Moberg Pick-up test (Amirjani et al., 2007): The participants were seated at a table with a set of 12 small everyday metal objects placed directly in front (5 cm fine screw, 2.3 cm wide screw, 3.3 cm and 2.8 cm paper clip, 1.4 cm diameter ring, 3.8 cm safety pin, two small nuts, one wing nut, 2.8 cm and 2.2 cm diameter coin and 5.5 cm key). The participants were instructed to pick up the objects (using an index finger to thumb PG) one at a time and place them into a container (dimensions 3x8x5 cm) as quickly as possible. The participants completed the test four times with their dominant hand, with the average time across the four repeats taken as the test score. Two minutes rest was observed between Moberg pick-up test repeats.

7.2.6. Force signal complexity, entropy, and variability metric analysis.

Prior to the calculation of the complexity, entropy and variability metrics a 2nd order Butterworth filter with a low pass cut off at 40 Hz was applied to the force signal as determined by Chapter Seven - Part A (see Appendix). The steadiest 5 seconds of each contraction was then identified as the 5 seconds with the lowest SD from which the complexity, entropy and variability metrics were calculated.

The SDF, CVF and RMSE which quantify the variability and accuracy of force signal were calculated as outlined in Chapter Three - General Methods - Section 3.8. The complexity and entropy metrics, SampEn, DFA, MSE and CI-28 were calculated as outlined in Chapter Three

- General Methods - Section 3.9. For each contraction intensity, the two most accurate contractions (identified as the contractions with the lowest RMSE) were selected. The mean of these two contractions was then calculated and used as the participant's complexity, entropy and variability metric values for statistical analysis.

7.2.7. Statistical analysis.

Age-group related differences in MVF and manual dexterity tests performances were assessed using a one-way ANOVA (YG vs. 50 year vs. 60 year vs. 70 year). The effect of age-group on the scale-to-scale behaviour of the MSE curves at each contraction intensity was assessed using a mixed-design two-way ANOVA, with age-group (YG vs. 50 year vs. 60 year vs. 70 year) as the between-subjects factor and coarse-grained scale (1 to 28) as the within-subjects factor.

The effects of age-group (YG vs. 50 year vs. 60 year vs. 70 year) and contraction intensity (5, 10, 15, 20, 30, 40, 50 and 60% MVF) on force signal complexity, entropy, and variability metrics were assessed using a mixed-design two-way ANOVA, with age-group as the between-subjects factor and contraction intensity as the within-subjects factor.

The relationship between the performance outcomes of the Purdue Pegboard and Moberg Pick-up tests and the isometric precision PG force signal complexity and entropy metrics at each target force (5, 10, 15, 20, 30, 40, 50 and 60% MVF) were established using a Pearson's bivariate two-tailed correlation. Due to the multiple correlation calculations, the level of statistical significance for the correlation coefficients was adjusted to $P < 0.01$. No significant correlation coefficients were found; therefore, stepwise, multiple, linear regressions were not conducted.

Cohens' d (interpreted as: 0.2 to 0.5 small effect, 0.5 to 0.8 medium effect, ≥ 0.8 large effect) and partial eta squared (η_p^2; interpreted as: 0.01 small effect, 0.06 medium effect, 0.14 large effect) were used to assess effect sizes. Cohens' d effect sizes were coded as positive when the 70-year group presented with a higher CVF, SDF, RMSE or DFA OR a lower SampEn or CI-28, when compared with the YG. Bonferroni *post hoc* comparisons were used when a main effect or interaction was significant. The significance level was set at $P < 0.05$ in all cases. Statistical analyses were performed in IBM SPSS statistics 29 (IBM Corp., Armonk, NY, United States).

7.3 - Results

7.3.1. Participant characteristics.

Data from forty-eight older adults (28M; 20F) and sixteen younger adults (10M; 6F) were included in the analysis. There was no significant difference between age groups in MVF (all $P > 0.05$; Table 7.1). Table 7.1 presents participant characteristics.

Table 7.1 Participant characteristics.

	Younger Group	50 year Group	60 year Group	70 year Group
N	16 (10M, 6F)	16 (6M, 10F)	16 (10M, 6F)	16 (12M, 4F)
Age (years)	23.8 ± 3.5	53.6 ± 3.3	64.9 ± 2.7	75.8 ± 4.4
Handedness (R, L)	14 R, 2 L	16 R	14 R, 2 L	13 R, 3 L
MVF (N)	13.0 ± 5.1	11.7 ± 3.6	11.9 ± 3.6	11.6 ± 3.9

Abbreviations: MVF = maximal voluntary force.

7.3.2. Effect of age-group on isometric precision pinch grip force signal complexity, entropy and variability.

Multiscale entropy curve results

Figure 7.1 presents the comparison of the younger and older age groups MSE curves at each isometric precision pinch grip contraction intensity. There was a main effect of age group on the MSE curves at 10% MVF ($F_{(3, 60)} = 2.770$; $P = 0.049$; $\eta_p^2 = 0.122$; Figure 7.1B), 15% MVF ($F_{(3, 60)} = 5.580$; $P = 0.002$; $\eta_p^2 = 0.218$; Figure 7.1C), 20% MVF ($F_{(3, 60)} = 3.982$; $P = 0.012$; $\eta_p^2 = 0.166$; Figure 7.1D), 30% MVF ($F_{(3, 60)} = 4.168$; $P = 0.010$; $\eta_p^2 = 0.172$; Figure 7.1E), 40% MVF ($F_{(3, 60)} = 5.056$; $P = 0.003$; $\eta_p^2 = 0.202$; Figure 7.1F), 50% MVF ($F_{(3, 60)} = 2.836$; $P = 0.046$; $\eta_p^2 = 0.128$; Figure 7.1G), and 60% MVF ($F_{(3, 60)} = 3.399$; $P = 0.024$; $\eta_p^2 = 0.150$; Figure 7.1H). There was no main effect of age group on the MSE curve at 5% MVF ($F_{(3, 60)} = 1.703$; $P = 0.176$; $\eta_p^2 = 0.078$; Figure 7.1A),

There was a significant main effect of coarse-grained scale at 5% MVF ($F_{(27, 1620)} = 399.520$; $P < 0.001$; $\eta_p^2 = 0.869$), 10% MVF ($F_{(27, 1620)} = 403.107$; $P < 0.001$; $\eta_p^2 = 0.870$), 15% MVF ($F_{(27, 1620)} = 335.745$; $P < 0.001$; $\eta_p^2 = 0.848$), 20% MVF ($F_{(27, 1620)} = 280.233$; $P < 0.001$; $\eta_p^2 = 0.824$), 30% MVF ($F_{(27, 1620)} = 231.110$; $P < 0.001$; $\eta_p^2 = 0.794$), 40% MVF ($F_{(27, 1620)} = 265.408$; $P < 0.001$; $\eta_p^2 = 0.816$), 50% MVF ($F_{(27, 1620)} = 312.172$; $P < 0.001$; $\eta_p^2 = 0.843$), and 60% MVF ($F_{(27, 1620)} = 398.390$; $P < 0.001$; $\eta_p^2 = 0.873$).

There was no age group by coarse-grained scale interaction at 5% MVF ($F_{(27, 1620)} = 1.057$; $P = 0.346$; $\eta_p^2 = 0.050$), 10% MVF ($F_{(27, 1620)} = 1.025$; $P = 0.418$; $\eta_p^2 = 0.049$), 15% MVF ($F_{(27, 1620)} = 1.580$; $P = 0.158$; $\eta_p^2 = 0.073$), 20% MVF ($F_{(27, 1620)} = 1.123$; $P = 0.353$; $\eta_p^2 = 0.053$), 30% MVF ($F_{(27, 1620)} = 0.844$; $P = 0.510$; $\eta_p^2 = 0.041$), 40% MVF ($F_{(27, 1620)} = 1.152$; $P = 0.338$; $\eta_p^2 = 0.054$), 50% MVF ($F_{(27, 1620)} = 0.988$; $P = 0.424$; $\eta_p^2 = 0.049$), and 60% MVF ($F_{(27, 1620)} = 1.424$; $P = 0.237$; $\eta_p^2 = 0.069$).

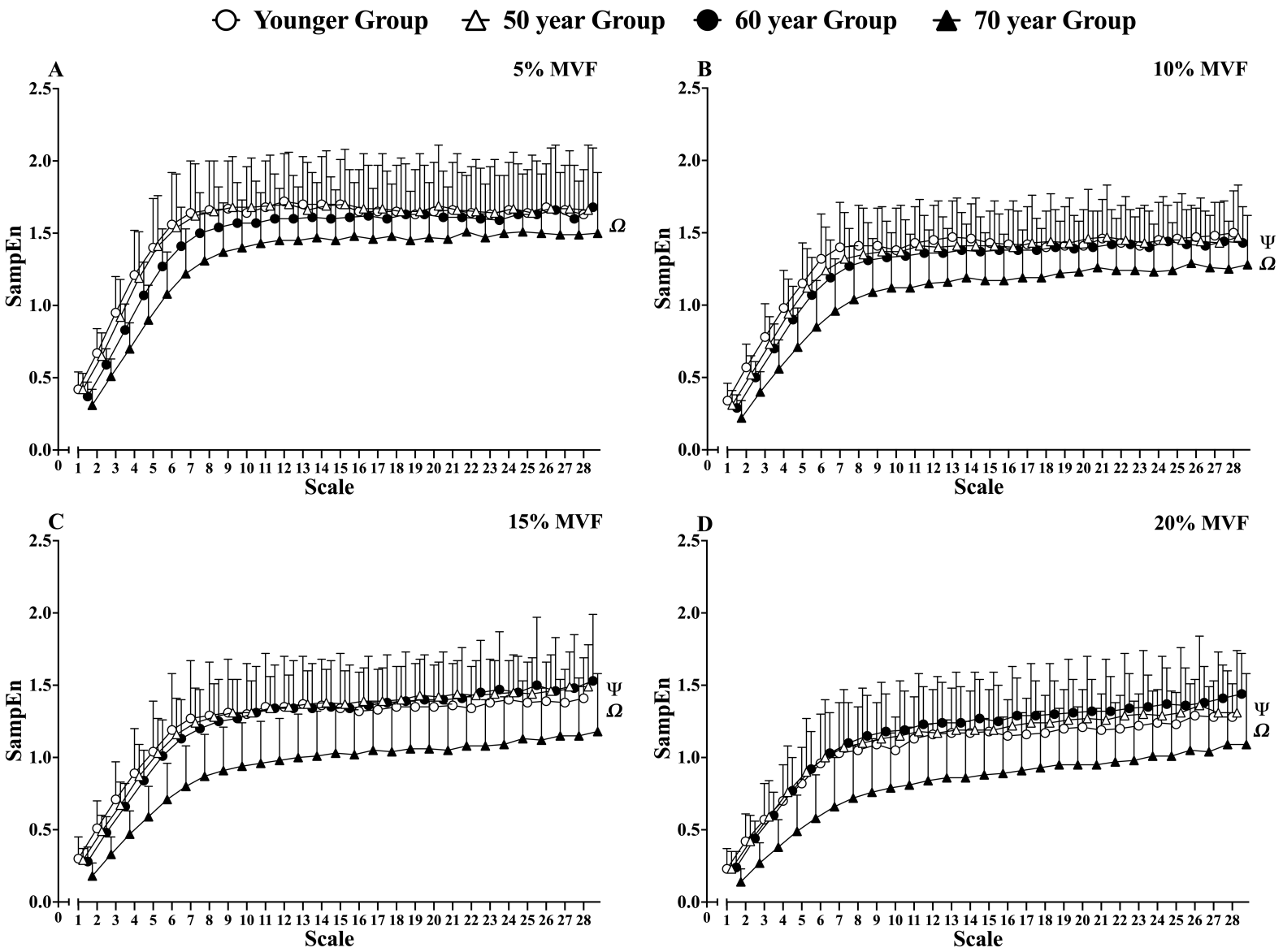

Figure 7.1. Multiscale entropy curves calculated from the isometric precision pinch grip force signals of the younger and older age groups at **(A)** 5% MVF, **(B)** 10% MVF, **(C)** 15% MVF, **(D)** 20% MVF (Younger group = open circles; 50 year group = open triangles; 60 year group = closed circles; 70 year group = closed triangles; MVF = maximal voluntary force; SampEn = sample entropy; Ψ = significant main effect of age group; Ω = significant main effect of coarse-grained scale).

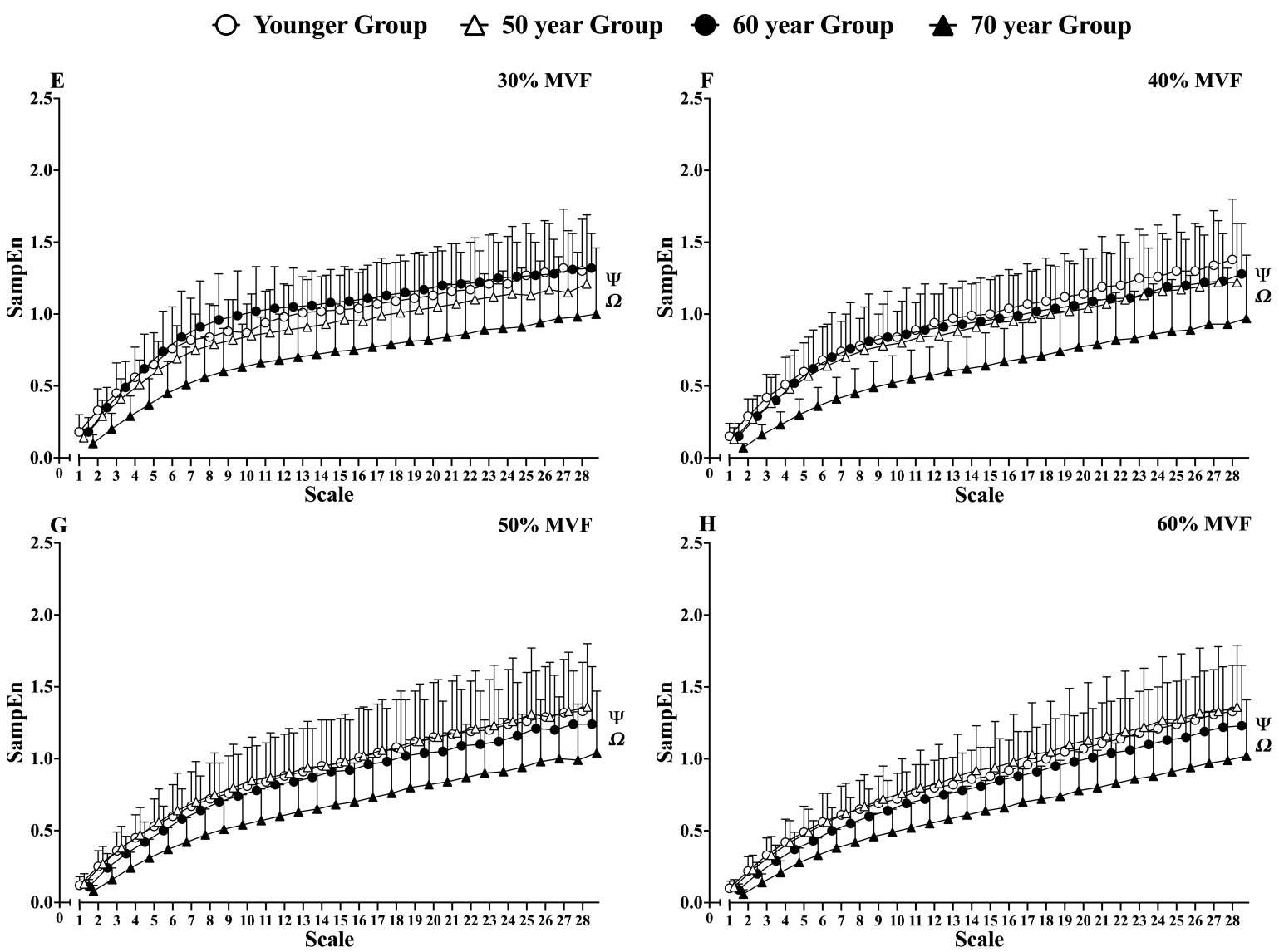

Figure 7.1. Continued. Multiscale entropy curves calculated from the isometric precision pinch grip force signals of the younger and older age groups at **(E)** 30% MVF, **(F)** 40% MVF, **(G)** 50% MVF, **(H)** 60% MVF (Younger group = open circles; 50 year group = open triangles; 60 year group = closed circles; 70 year group = closed triangles; MVF = maximal voluntary force; SampEn = sample entropy; Ψ = significant main effect of age group; Ω = significant main effect of coarse-grained scale).

Table 7.2 presents the descriptive statistics and ANOVA results for the effect of age-group and contraction intensity on the complexity, entropy and variability of the isometric precision PG force signals. Table 7.3 presents the Cohens' d effect sizes for the effect of age-group (younger group versus 70-year age group) on the complexity, entropy and variability of the isometric precision PG force signals at each contraction intensity.

Complexity index results

There was a significant main effect of age group for the CI-28 metric (Table 7.2). *Post hoc* pairwise comparisons revealed the 70 year group to have a significantly lower CI-28 metric, in comparison to the YG ($P = 0.003$) the 50 year group ($P = 0.005$), and 60 year group ($P = 0.007$). There was no significant difference in CI-28 between the YG and 50 year group ($P > 0.05$), YG and 60 year group ($P > 0.05$) and 50 year and 60 year group ($P > 0.05$). There was significant main effect of contraction intensity, but no age group by contraction intensity interaction for CI-28 (Table 7.2).

Detrended fluctuation analysis results

There was a significant main effect of age group for the DFA α metric (Table 7.2). *Post hoc* pairwise comparisons revealed the 70 year group to have a significantly higher DFA α in comparison to the YG ($P = 0.020$), the 50 year group ($P = 0.021$) and the 60 year group ($P = 0.012$). There was no significant difference in DFA α between the YG and 50 year group ($P > 0.05$), YG and 60 year group ($P > 0.05$) and 50 year and 60 year group ($P > 0.05$). There was significant main effect of contraction intensity, but no age group by contraction intensity interaction for DFA α (Table 7.2).

Sample entropy results

There was a significant main effect of age group for SampEn (Table 7.2). *Post hoc* pairwise comparisons revealed the 70 year group to have a significantly lower SampEn in comparison to the YG ($P = 0.0012$), the 50 year group ($P = 0.022$) and the 60 year group ($P = 0.042$). There was no significant difference in SampEn between the YG and 50 year group ($P > 0.05$), YG and 60 year group ($P > 0.05$) and 50 year and 60 year group ($P > 0.05$). There was significant main effect of contraction intensity and an age group by contraction intensity interaction for SampEn (Table 7.2).

Variability metric results

There was a significant main effect of age group for the SDF (Table 7.2). *Post hoc* pairwise comparisons revealed the 70 year group to have a significantly higher SDF in comparison to the YG ($P = 0.008$), the 50 year group ($P = 0.013$), and the 60 year group ($P = 0.012$). There was no significant difference in the SDF between the YG and 50 year group ($P > 0.05$), YG and 60 year group ($P > 0.05$) and 50 year and 60 year group ($P > 0.05$). There was significant main effect of contraction intensity, but no age group by contraction intensity interaction for the SDF (Table 7.2).

There was a significant main effect of age group for the CVF (Table 7.2). *Post hoc* pairwise comparisons revealed the 70 year group to have a significantly higher CVF in comparison to the YG ($P < 0.001$), the 50 year group ($P < 0.001$) and the 60 year group ($P < 0.001$). There was no significant difference in the CVF between the YG and 50 year group ($P > 0.05$), YG and 60 year group ($P > 0.05$) and 50 year and 60 year group ($P > 0.05$). There was significant main effect of contraction intensity, but no age group by contraction intensity interaction for the CVF (Table 7.2).

There was a significant main effect of age group for RMSE (Table 7.2). *Post hoc* pairwise comparisons revealed the 70 year group to have a significantly higher RMSE in comparison to the YG ($P < 0.001$) and the 60 year group ($P < 0.001$). There was no significant difference in RMSE between the YG and 50 year group ($P > 0.05$), YG and 60 year group ($P > 0.05$), 50 year and 60 year group ($P > 0.05$), and 50 year and 70 year group ($P > 0.05$). There was significant main effect of contraction intensity and an age group by contraction intensity interaction for RMSE (Table 7.2).

Table 7.2 Descriptive statistics and ANOVA results for the effect of age-group and contraction intensity on the complexity, entropy and variability of the isometric precision pinch grip force signals.

		Contraction Intensity									*F, P* and η_p^2 values		
		5% MVF	10% MVF	15% MVF	20% MVF	30% MVF	40% MVF	50% MVF	60% MVF		Main effect of Age	Main effect of Intensity	Age by Intensity Interaction
SDF (N)	YG	0.03±0.02	$ 0.04±0.01	$ 0.05±0.02	$ 0.07±0.04	Z K 0.10±0.07	Z 0.14±0.08	0.17±0.08	0.20±0.06	*F*	5.442	101.052	1.827
	50yr	0.03±0.01	0.04±0.02	0.05±0.02	0.06±0.04	0.11±0.06	0.14±0.08	0.15±0.08	0.20±0.12	*P*	**0.002**	**<0.001**	0.089
	60yr	0.03±0.01	0.04±0.01	0.05±0.02	0.06±0.02	0.08±0.04	0.14±0.11	0.18±0.12	0.21±0.13	η_p^2	0.220	0.635	0.086
	70yr	0.04±0.02	0.06±0.02	0.07±0.02	0.10±0.05	0.15±0.06	0.21±0.07	0.27±0.18	0.31±0.14				
CVF (%)	YG	Z K 4.87±1.67	Z K 3.30±1.47	$ 2.76±1.16	$ 2.70±0.73	$ 2.72±0.93	$ 2.86±0.94	I K 3.16±1.17	3.12±1.37	*F*	14.671	43.210	1.079
	50yr	6.74±3.05	4.05±1.99	2.91±1.23	2.85±1.24	3.25±1.69	3.11±1.46	2.70±1.25	2.99±1.56	*P*	**<0.001**	**<0.001**	0.379
	60yr	5.77±1.57	3.68±1.20	2.81±1.15	2.47±0.60	2.40±0.65	2.72±1.30	3.04±1.48	3.17±1.98	η_p^2	0.431	0.427	0.053
	70yr	8.87±3.38	5.62±1.96	4.59±1.23	4.70±1.49	4.57±1.53	5.00±1.81	4.90±2.85	4.62±1.85				
RMSE (%)	YG	Z Σ K 11.21±7.35	Z 5.84±2.73	Z K 5.03±2.75	Z K 4.04±1.59	Z K 3.67±1.45	Z K 4.03±1.26	4.24±1.66	5.34±5.79	*F*	8.339	64.799	3.313
	50yr	21.50±11.60	11.04±5.63	7.02±3.99	5.83±2.38	5.29±3.14	4.91±2.58	4.14±2.12	4.59±2.80	*P*	**<0.001**	**<0.001**	**0.002**
	60yr	11.86±5.83	8.23±4.05	5.46±2.56	4.64±2.19	3.89±1.92	3.85±1.47	4.46±2.74	5.25±6.54	η_p^2	0.301	0.528	0.146
	70yr	23.40±11.31	13.32±9.37	8.80±3.41	7.88±2.47	6.36±2.23	6.54±2.21	6.39±3.64	6.34±3.90				
SampEn	YG	Z I 0.42±0.12	Z 0.34±0.12	Z I 0.30±0.15	0.23±0.14	0.18±0.12	Z 0.15±0.09	0.12±0.06	I 0.10±0.05	*F*	5.591	176.429	1.836
	50yr	0.42±0.11	0.31±0.10	0.29±0.08	0.23±0.12	0.14±0.06	0.13±0.08	0.13±0.07	0.11±0.05	*P*	**0.002**	**<0.001**	**0.045**
	60yr	0.37±0.10	0.29±0.09	0.28±0.10	0.24±0.11	0.18±0.10	0.15±0.09	0.11±0.05	0.09±0.04	η_p^2	0.224	0.753	0.087
	70yr	0.31±0.11	0.22±0.12	0.18±0.09	0.14±0.09	0.10±0.06	0.07±0.03	0.08±0.04	0.06±0.03				
DFA α	YG	1.31±0.11	1.39±0.09	1.43±0.09	1.48±0.10	1.52±0.09	Z 1.52±0.09	I 1.53±0.09	Z I 1.53±0.06	*F*	3.102	118.603	0.964
	50yr	1.32±0.09	1.40±0.08	1.44±0.07	1.47±0.10	1.54±0.09	1.54±0.11	1.52±0.10	1.52±0.10	*P*	**0.033**	**<0.001**	0.507
	60yr	1.28±0.10	1.40±0.07	1.41±0.13	1.45±0.09	1.52±0.08	1.55±0.08	1.55±0.09	1.56±0.10	η_p^2	0.138	0.672	0.048
	70yr	1.32±0.11	1.44±0.10	1.48±0.11	1.52±0.12	1.59±0.11	1.62±0.11	1.61±0.10	1.63±0.09				
CI-28	YG	42.75±8.02	Z 36.72±6.06	$ 34.31±7.76	$ 29.57±6.49	Z K 26.68±6.27	$ 26.31±6.00	Z I 25.22±7.43	Z I 23.71±5.53	*F*	6.357	95.453	0.729
	50yr	42.77±9.56	36.07±7.88	35.10±5.73	30.95±10.28	24.53±8.80	24.17±8.22	25.80±8.29	24.70±8.10	*P*	**<0.001**	**<0.001**	0.804
	60yr	40.85±7.82	35.10±6.19	34.80±8.09	32.32±5.97	28.28±5.88	25.27±7.45	23.83±8.24	22.09±7.43	η_p^2	0.247	0.622	0.036
	70yr	36.80±8.89	30.01±8.82	26.00±7.83	22.83±10.06	19.44±8.71	17.45±6.59	18.52±7.23	17.51±5.88				

Abbreviations: CI-28 = complexity index under 28 scales; CVF = coefficient of variation of force; DFA = detrended fluctuation analysis scaling exponent α; MVF = maximal voluntary force; RMSE = root mean square error; SampEn = sample entropy; SDF = standard deviation of force; YG = younger age group; Significant *P* values highlighted by bold font; $ = significant difference between 70yr and all other groups $P < 0.05$; Z = significant difference between 70yr and YG $P < 0.05$; Σ = significant difference between 50yr and YG $P < 0.05$; I = significant difference between 70yr and 50yr $P < 0.05$; K = significant difference between 70yr and 60yr $P < 0.05$; data are mean ± SD.

Table 7.3 Cohens' d for the effect of age-group (younger group versus 70 year age group) on the complexity, entropy and variability of the isometric precision pinch grip force signals at each contraction intensity.

		Contraction Intensity							
		5% MVF	10% MVF	15% MVF	20% MVF	30% MVF	40% MVF	50% MVF	60% MVF
SDF (N)	Cohens' d [95% CI]	0.41 [-0.29, 1.11]	1.38 [0.61, 2.15]	1.20 [0.45, 1.95]	0.85 [0.13, 1.58]	0.68 [-0.03, 1.39]	0.86 [0.13, 1.58]	0.68 [-0.03, 1.39]	1.07 [0.33, 1.81]
CVF (%)	Cohens' d [95% CI]	1.46 [0.68, 2.24]	1.30 [0.54, 2.07]	1.49 [0.70, 2.27]	1.67 [0.86, 2.47]	1.42 [0.64, 2.19]	1.45 [0.67, 2.23]	0.80 [0.06, 1.50]	0.89 [0.17, 1.62]
RMSE (%)	Cohens' d [95% CI]	1.25 [0.49, 2.00]	1.06 [0.32, 1.80]	1.19 [0.43, 1.94]	1.80 [0.98, 2.62]	1.39 [0.62, 2.17]	1.36 [0.59, 2.13]	0.74 [0.02, 1.46]	0.20 [-0.50, 0.89]
SampEn	Cohens' d [95% CI]	1.03 [0.29, 1.77]	0.96 [0.23, 1.69]	1.00 [0.26, 1.73]	0.75 [0.03, 1.47]	0.77 [0.05, 1.49]	1.10 [0.36, 1.84]	0.82 [0.10, 1.54]	0.92 [0.19, 1.65]
DFA α	Cohens' d [95% CI]	0.06 [-0.63, 0.76]	0.50 [-0.21, 1.20]	0.48 [-0.22, 1.19]	0.37 [-0.33, 1.07]	0.70 [-0.02, 1.41]	0.99 [0.26, 1.72]	0.81 [0.09, 1.53]	1.18 [0.43, 1.93]
CI-28	Cohens' d [95% CI]	0.68 [0.03, 1.40]	0.86 [0.14, 1.59]	1.04 [0.30, 1.78]	0.78 [0.06, 1.49]	0.93 [0.20, 1.66]	1.37 [0.60, 2.14]	0.89 [0.16, 1.62]	1.06 [0.32, 1.80]

Abbreviations: CI-28 = complexity index under 28 scales; CVF = coefficient of variation of force; DFA = detrended fluctuation analysis scaling exponent α; MVF = maximal voluntary force; RMSE = root mean square error; SampEn = sample entropy; SDF = standard deviation of force.

7.3.4. Manual dexterity task results.

During the Purdue pegboard test the 70 year group placed significantly fewer pegs, in comparison to the YG ($P < 0.001$; d = -2.96, 95% CI [-3.96: -1.96]), 50 year group ($P < 0.001$; d = -1.91, 95% CI [-2.74: -1.07]) and 60 year group ($P = 0.049$; d = -0.94, 95% CI [-1.67: -0.21]; Figure 7.2A). The 60 year group placed significantly fewer pegs, in comparison to the YG ($P < 0.001$; d = -1.44, 95% CI [-2.22: -0.66]; Figure 7.2A).

The 70 year group completed the Moberg Pick-up test significantly slower than the YG ($P = 0.002$; d = 1.14, 95% CI [0.40: 1.89]), 50 year group ($P = 0.002$; d = 1.14, 95% CI [0.39: 1.89]) and the 60 year group ($P = 0.009$; d = 0.99, 95% CI [0.25: 1.72]; Figure 7.2B).

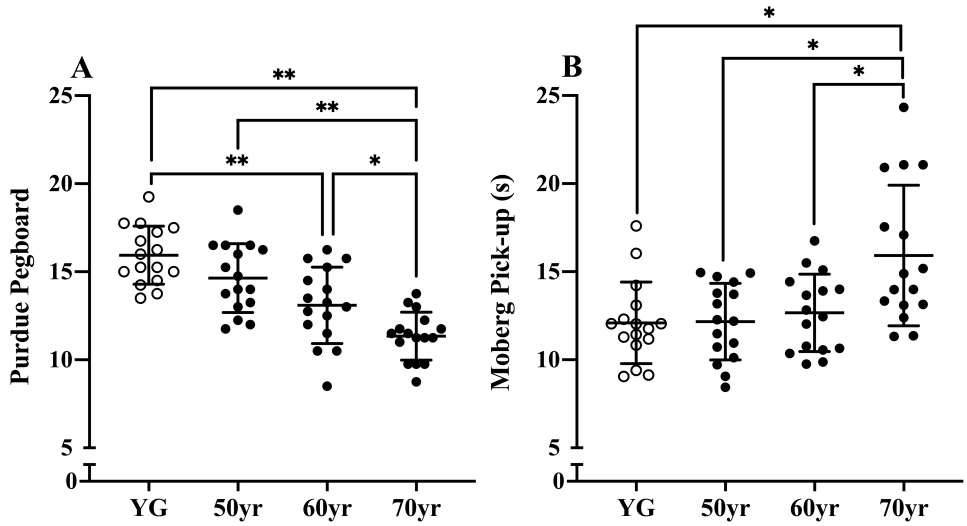

Figure 7.2. Manual dexterity test results **(A)** Purdue pegboard, **(B)** Moberg pick-up (* = $P < 0.05$ and ** = $P < 0.001$).

7.3.5. Relationship between the complexity and entropy of isometric precision pinch grip force and manual dexterity task performance.

No significant correlations were found between the complexity and entropy of isometric precision PG force signals and the performance of Purdue Pegboard and Moberg Pick-up tests (all $P > 0.01$).

7.4 - Discussion

7.4.1. Effect of age-group on isometric precision pinch grip force signal complexity, entropy and variability.

The first aim of the current experimental chapter was to investigate age-group differences in the complexity, entropy and variability of isometric precision PG force signals across contraction intensities. Consistent with the hypothesis, main findings indicate that adults over 70 years exhibit lower neuromuscular complexity (CI-28), and greater neuromuscular variability (CVF and SDF) than younger adults, aged 18 to 30 years (Table 7.2). These age-related differences in neuromuscular complexity and variability were observed across contraction intensities (10 to 60% MVF), as supported by consistent medium to large effect sizes (Table 7.3). However, no differences in neuromuscular complexity or variability were observed between the younger adults and those aged 50 to 70 years (Table 7.2). These findings suggest that measurable age-related changes in neuromuscular function, and consequently hand muscle force regulation likely occur in the eighth decade of life but remains largely preserved in the sixth and seventh decades.

The current findings align with previous research showing neuromuscular complexity (DFA α) of another small hand muscle, the IFA, to be lower in a 70 year group ($\alpha = 1.35$) compared to a younger group ($\alpha = 1.29$) and 60 year group ($\alpha = 1.27$; Sosnoff & Newell, 2006d). Similarly, neuromuscular variability (CVF) was greater in the 70 year group compared with both the younger group and 60 year group (Sosnoff & Newell, 2006d). Consistent with present findings, this suggests that a measurable change in hand muscle force control begins in the eighth decade of life (Sosnoff & Newell, 2006d). However, such conclusions can only be confirmed with longitudinal data of changes in neuromuscular complexity and variability across the life span.

Effective motor control can be achieved through MU recruitment and modulation MU discharge rates of the muscles involved in a task (Hepple & Rice, 2016; Piasecki et al., 2016a). Therefore, current findings of maintained neuromuscular function and hand muscle control may be explained, in part, by the relatively constant number of MUs up to approximately 60 years of age, after which a progressive loss of MUs occurs (Campbell et al., 1973; Tomlinson & Irving, 1997). In older adults (63 to 81 years), the thenar muscles, which play a key role in

precision PG force control, contain approximately 50% fewer MUs compared to younger adults (21 to 28 years; Doherty & Brown, 1993).

Ageing also results in a continuous cycle of MU denervation and reinnervation, leading to MU remodelling and fibre type grouping (Hepple & Rice, 2016). This process increases the MU-to-muscle fibre ratio (Jones et al., 2022; Hepple & Rice, 2016; Piasecki et al., 2016b). Consequently, muscle contractions in older adults involve the recruitment of fewer (Doherty & Brown, 1993), larger (Dalton et al., 2008; Galea, 1996) MUs, which discharge at slower (Kamen et al., 1995) and more variable rates (Tracy et al., 2005). This loss of MUs and MU pool remodelling in small hand muscles has been demonstrated to reduce the precision with which older adults can control and coordinate muscle contractions (Galganski et al., 1993; Erim et al., 1999). Additionally, greater strength and variance in common synaptic input to the motor neurons may also explain the lower neuromuscular complexity and greater variability of the 70 year group (Castronovo et al., 2018; Feeney et al., 2018; Pethick et al., 2016; Pethick et al., 2021b; Negro et al., 2009; Thompson et al., 2018).

MSE curve analysis revealed that the 70 year group exhibited lower SampEn across all 28 coarse-grained scales at 10 to 60% MVF than younger, 50 year, and 60 year groups (Figure 7.1). These findings build upon previous research showing that younger adults (24.9 ± 3.6 years) had higher SampEn across all 25 coarse-grained scales of the MSE curves derived from isometric PG force signals at 10% and 30% MVF than older adults (76.7 ± 6.4 years; Knol et al., 2019). By assessing scale-to-scale entropic behaviour of force signals across a wider range of contraction intensities, the present study extends these findings, providing a more comprehensive understanding of age-related changes in neuromuscular complexity.

The observed age-related differences in the scale-to-scale entropic behaviour of the MSE curves indicates that the force signals of older adults (70 year group) exhibit greater temporal regularity across multiple oscillatory frequencies than those of younger adults. This suggests that an age-related decline in neuromuscular complexity (CI-28), and by extension neuromuscular function, may result from both an impairment in the function of individual components and their interactions within the neuromuscular system (Vieluf et al., 2015). Further research is needed to experimentally test this integrative theoretical framework and establish whether the behaviour of MSE curves reflects age-dependent differences in the neuromuscular system at the component level.

To the authors' knowledge, this study is the first to use the DFA analysis to examine the effect of age on the fractal scaling (self-similarity) of isometric precision PG force signals. The force signals of all age groups deviated from 1/f noise (α = 1.0, representing the high complexity) toward Brown noise, indicating low complexity, with all α values approaching 1.5 (Table 7.2). However, a main effect of age was observed, with the 70 year group exhibiting a higher DFA α than the younger, 50 year, and 60 year groups (Table 7.2). This higher DFA α (i.e., ≥ 1.5) may reflect age-related reductions in the efficiency of motor information transmission and processing capacity, particularly in integrating visual, proprioceptive, and cutaneous inputs (Cerella & Hale, 1994; Sosnoff & Newell, 2006d; Vieluf et al., 2018).

Functionally, the observed age-related difference in neuromuscular function of the hand muscles may impair the ability to perform ADLs, such as writing, typing, buttoning clothes, cooking, using electronic devices and manipulating small objects; tasks which are essential for maintaining independence and quality of life in older age (Mlinac & Feng, 2016). Furthermore, from an applied perspective, the analysis methods used in this study could complement traditional maximal grip force tests in geriatrics, offering a broader assessment and monitoring tool for clinicians to better evaluate hand muscle force control deficits. However, additional research is required to examine the efficacy and sensitivity of these methods in monitoring and detecting clinically meaningful changes in neuromuscular function across the lifespan and in response to various acute and chronic intervention strategies.

7.4.2. Relationship between the complexity and entropy of isometric precision pinch grip force and manual dexterity task performance.

The second aim of the study was to investigate whether the complexity and entropy of isometric precision PG force was associated with the performance of manual dexterity tasks. Contrary to the hypothesis, lower complexity (DFA and CI-28) and entropy (SampEn) of isometric precision PG force signals were not associated with worse manual dexterity performance.

The performance of both manual dexterity tests (Purdue Pegboard and Moberg Pick-up test) was determined by the quick and precise movement of small metal objects using a precision PG (index finger to thumb PG). Therefore, it is likely that an individual's performance is mostly explained by their tactile perception, cognitive processing speed, attentional processing, and

coordination (Carmeli et al., 2003; Ebaid et al., 2017; Huddleston et al., 2014; Lawrence et al., 2015; Seidler et al., 2002).

The study found that the 70 year group performed worse on the Purdue Pegboard and Moberg Pick-Up tests than the YG, 50 year, and 60 year groups (Figure 7.2). These results align with previous research demonstrating age-related declines in performance on the Purdue Pegboard (Stijic et al., 2023) and Moberg Pick-Up (Amirjani et al., 2007) tests. Ageing is characterised by a decline in tactile perception (Decorps et al., 2014), cognitive processing speed (Ebaid et al., 2017; Hong et al., 2015), attentional processes (Huddleston et al., 2014; Walters et al., 2021) and coordination (Almuklass et al., 2018b; Seidler et al., 2002). Thus, a combination of these factors likely explains most of the variance in the age-related differences in the performance of the manual dexterity tasks, not explained by the complexity and entropy metrics.

These findings should not diminish the potential efficacy of complexity and entropy metrics for assessing functional changes to neuromuscular system. Instead, these findings simply show that the complexity metrics derived from isometric precision PG force signals during constant load contractions do not determine the performance of two manual dexterity tasks. Therefore, current findings may just reflect the force matching tasks, from which the complexity metrics were derived, not matching the requirements of these specific manual dexterity tasks. Future research endeavours should use different force matching methodologies (e.g., sinusoidal force matching tasks), PG contractions (e.g., tri-digit PG) or double action tasks (e.g., concurrent WE and PG contractions) to establish a measure of neuromuscular complexity for comparison to manual dexterity tasks.

7.4.3. Limitations.

The performance of manual dexterity tasks in everyday living involves the use of different digits of both hands. However, the current study only assessed the neuromuscular complexity and variability of isometric force produced by an index finger to thumb contraction of the dominant hand (i.e., precision PG). Additionally, the manual dexterity tasks were also performed using the index finger and thumb PG of the dominant hand. Force control between the other digits of the hand will require the activation of, and synergy between, different hand and forearm muscles. Therefore, caution is advised if extrapolating and/or comparing current

neuromuscular complexity and variability values to muscle force control values derived from PG contractions performed between other digits of the hands.

The effect of biological sex on neuromuscular complexity and variability was not directly addressed in this study. By normalising contraction intensity to each participant's MVF, differences in maximal PG force between men and women were controlled (Haward & Griffin, 2002). However, previous research has reported sex-related differences in neuromuscular function (Guo et al., 2025) and specifically, in hand muscle force control (Dottor et al., 2025; Shim et al., 2004). Additionally, females experience a reduction in neuromuscular function earlier in the lifespan, with a faster rate of deterioration observed beyond the age of 80 compared to males (Haynes et al., 2020; Kim et al., 2018). Therefore, the uneven distribution of men and women, particularly of the 50 year group (Table 7.1), may have influenced the differences between age groups.

7.5 - Conclusion

Adults over 70 years exhibit lower neuromuscular complexity, greater neuromuscular variability and worse manual dexterity than younger adults, aged 18 to 30 years. However, no differences in neuromuscular complexity or variability were observed between the younger adults and those aged 50 to 70 years. The change in the temporospatial structure of the force signal beyond 70 years suggests a degradation in the functioning of the neuromuscular system's control processes, along with reduced efficiency in motor information transmission and processing capacity during fine motor tasks. Collectively, these findings suggest that measurable changes in hand muscle force regulation emerge in the eighth decade of life, providing insight into the potential time course of age-related changes in hand muscle neuromuscular function.

Chapter Eight

Part A

Neural mechanisms underpinning the complexity, entropy and variability of isometric knee extensor torque signals of younger and older adults.

8.1a - Introduction

The current thesis has demonstrated that older adults exhibit lower neuromuscular complexity (DFA and CI-28) across a range of contraction intensities (10 to 80% MVT) than younger adults (Chapter Six). Furthermore, the MSE analysis has revealed the scale-to-scale entropic behaviour (temporal structure) of the torque signal to be influenced by age-group (Chapters Five and Six); suggesting age-related changes in the neuromuscular system's control processes and the integrative functioning of its components across multiple time scales (Knol et al., 2019; Vieluf et al., 2015). However, the mechanisms underpinning these age-group related differences in neuromuscular complexity have yet to be fully explored experimentally. Though, existing research suggests that neuromuscular complexity may be attributable, in part, to the collective behaviour of the MU pool (Farina & Negro, 2015).

The MU is the smallest functional unit of the neuromuscular system; consisting of a motor neuron and all the muscle fibres it innervates (Eccles & Sherrington, 1930; Sherrington, 1925). Motor neurons receive synaptic inputs (originating from afferent feedback, descending cortical and reticulospinal pathways, and neuromodulatory pathways from the brain stem; Enoka & Farina, 2021) which generate the effective neural drive to the muscle (Negro & Farina, 2011). Muscle force is then produced through the filtering of neural drive with the average twitch force of the active MUs. The independent synaptic inputs are predominantly filtered out by the twitch (temporal) and summation (spatial) filtering effects of the muscle (Dideriksen et al., 2012; Farina & Negro, 2015). Therefore, it is the common input components (the control input and common noise) received by the motor neurons that makes muscle force control possible and determines the structural characteristics of the torque output (Dideriksen et al., 2012; Farina & Negro, 2015).

Notably, the low-frequency oscillations (< 10 Hz) in common synaptic input have been demonstrated to be a principal determinant of muscle torque variability and closely resemble the structure of the muscle torque signal (Dideriksen et al., 2012; Farina et al., 2014; Negro et al., 2009). It has therefore been speculated that common synaptic input may also be explanatory of the temporal structure (*complexity*) of the muscle torque signal (Pethick et al., 2016; Pethick et al., 2021b).

The measurement of coherence between CSTs, derived from discharge times of multiple concurrently active MUs, can be used to estimate the strength of common synaptic input within and between muscles during isometric contractions (Avrillion et al., 2021; Dideriksen et al., 2018). Coherence between CSTs is typically calculated in distinct frequency bands, delta (0-5 Hz), alpha (5-15 Hz), low beta (15-21 Hz), high beta (21-35 Hz), piper (35-50 Hz) and gamma (32-100 Hz; Dideriksen et al., 2018). These frequency bands represent the influence of different sources of synaptic input on muscle torque control (Farmer et al., 1993; McAuley et al., 1997; Vaillancourt & Newell, 2000; Watanabe & Kohn, 2015). However, due to the low pass filtering effects of the muscle's contractile properties, it is primarily the delta and alpha band oscillations that are transmitted to the torque signal (Farina et al., 2014; Negro et al., 2009).

The magnitude of coherence between CSTs is associated with the relative proportion of common synaptic input with respect to the independent inputs (Negro & Farina, 2015). In other words, for the same number of MUs in the coherence analysis, a greater coherence between CSTs indicates a greater strength of common synaptic input to the motor neuron pool. Alternatively, a lower coherence between CSTs indicates a reduction in the strength of common synaptic input to the motor neuron pool (De La Rocha et al., 2007; Negro & Farina, 2012).

Through assessing coherence between CSTs, older adults have been shown to exhibit greater strength of common synaptic input during sustained isometric contractions at 20% MVT, compared to younger adults (Castronovo et al., 2018). Moreover, the relative strength of common synaptic input has been found to increase with higher isometric contraction intensities (Castronovo et al., 2015). The increase in common input strength was accompanied by greater variability in muscle torque signal (Castronovo et al., 2015; Castronovo et al., 2018). However, no studies to date have investigated whether changes in the complexity of isometric KE torque signals are associated with the strength of common synaptic input to the motor neuron pool.

Aims and Hypothesis.

The main aim of the current chapter was to investigate the association between the strength and variability of common synaptic input to the motor neuron pool innervating the VL muscle and the complexity of isometric KE torque of adults aged between 18 and 90 years. To achieve this, the study used HD sEMG to record discharge times of multiple concurrently active MUs from the VL muscle during isometric KE contractions at 10 to 80% MVT. This allowed for the

strength of common synaptic input to be estimated by within-muscle (intra-muscle) frequency domain coherence analysis. In addition, the chapter aimed to assess the complexity and variability of smoothed CSTs, providing a measure of the complexity and variability of common synaptic input (Hunter, 2023). It was hypothesised that stronger and more variable common synaptic input to the motor neuron pool innervating the VL muscle would be associated with an isometric KE torque signal of lower complexity and greater variability.

8.2a - Methods

8.2.1. Participants.

Sixty healthy participants (56 male; 4 female) aged between 18 and 90 were recruited to participate in the study. Participants were recruited to be in three age groups, the YG were aged 18 to 30 years (N = 20; 17M, 3F), the MG were aged 31 to 49 years (N = 20; 19M, 1F), and the OG were aged 50 to 90 years (N = 20; 20M, 0F).

Before being allowed to participate in the study all potential participants provided written informed consent and completed a health questionnaire to ensure they were in full health. Participants were required to not have previous or current circulatory disorders, have no known or signs/symptoms of cardiovascular, neuromuscular, renal, or metabolic conditions. Participants were required to be living independently and able to perform active daily living tasks. All participants were regular exercisers, having performed above the World Health Organisation guidelines for ≥ 2 years (i.e., 2.5 to 5 hours of moderate exercise per week; Bull et al., 2020). Participant height was measured using a Seca portable stadiometer (Seca 217; Seca GmbH & Co. KG, Hamburg, Germany) and body mass measured using a Seca mechanical flat scale (Seca 760; Seca GmbH & Co. KG, Hamburg, Germany).

The study was completed with full ethical approval of the University of Kent Research Ethics Committee (Proposal number: 32_20_23), according to Declaration of Helsinki standards (but without being registered).

8.2.2. Experimental Design.

Each participant completed one experimental session. The participants' isometric KE MVT was first measured to establish the relative isometric contraction intensities for the subsequent KE torque control tasks. Participants were then familiarised with the KE torque control tasks by performing isometric KE contractions at 10 and 20% MVT. After familiarisation, participants performed the KE torque control tasks at the relative contraction intensities of 10, 20, 30, 40, 50, 60, 70 and 80% MVT, from which the torque signal complexity, entropy and variability metrics were calculated. HD sEMG signals were recorded from the VL muscle during all isometric contractions of the KE torque control tasks.

8.2.3. Measurement of isometric knee extensor maximal voluntary torque.

Participants were set up on an isokinetic dynamometer (Cybex HUMAC Norm; CSMi, Stoughton, MA, USA), as outlined in Chapter Three - General Methods - Section 3.6. Once set up on the dynamometer participants performed a warm-up of ten submaximal contractions of increasing effort, after which four (6 second) MVCs (each MVC separated by 60 second rest) were performed to establish MVT. The highest torque value from a 2 second epoch was recorded as the MVT, which was then used to set the relative constant load isometric contraction intensities of 10, 20, 30, 40, 50, 60, 70 and 80% MVT to be used in the torque control tasks.

8.2.4. Measurement of isometric knee extensor muscle torque control.

Prior to commencing the muscle torque control tasks, participants rested for 20 minutes and were then familiarised with matching their instantaneous KE torque output to a thin line (1 mm thick) superimposed on the computer monitor at 10 and 20% MVT.

After familiarisation, participants performed the KE torque control tasks, which required the participant to match their instantaneous KE torque signal to a thin line (1 mm thick) superimposed on the computer monitor at the relative contraction intensities of 10, 20, 30, 40, 50, 60, 70 and 80% MVT. The Y axis of the display was scaled to the participant's MVT, ensuring the superimposed line was located at the same position on the monitor for all participants.

The participants performed three 20 second contractions at each intensity starting at 10% MVT and progressing to 80% MVT, with recovery between all contractions set at 120 seconds. All contractions at each intensity were analysed to derive the torque signal complexity, entropy and variability metrics (see section 8.2.7.). As neuromuscular fatigue can reduce signal complexity (Pethick et al., 2015), complexity measures were examined across the three repeated contractions at each intensity using a repeated measures ANOVA to confirm their stability and rule out fatigue-related effects.

8.2.5. High density surface electromyography data collection.

Prior to the torque control tasks participants were set up with a HD sEMG array on the right VL muscle as outlined in Chapter Three - General Methods - Section 3.10 - *HD sEMG: Setup and signal acquisition*. The HD sEMG signals were recorded throughout each 20 second

isometric contraction of the KE torque control tasks, as outlined in Chapter Three - General Methods - Section 3.10 - *HD sEMG: Setup and signal acquisition*.

8.2.6. High density surface electromyography data analysis.

HD sEMG: Motor unit decomposition

The HD sEMG signals were decomposed offline into MU spike trains, as outlined in Chapter Three - General Methods - Section 3.10 - *HD sEMG: Motor unit decomposition.* Before further analysis of the binary MU spike trains, the steadiest 10 second epoch of muscle torque time series from each 20 second isometric KE contraction was identified as the epoch with the lowest SD. The binary MU discharges from the same 10 second epoch were extracted for further analysis.

Estimation of within-muscle motor unit coherence

To assess the neural connectivity between MUs of the VL muscle during the isometric KE torque control tasks, within-muscle (intra-muscle) coherence was estimated from the decomposed MU spike trains. Within-muscle coherence was estimated as outlined in General Methods - Section 3.10 - *Estimation of within-muscle motor unit coherence* and reported as the transformed Z-scores.

The coherence value at a given frequency represents the correlation between two signals (i.e., two CSTs of equal number of MUs). Coherence was calculated in the low-frequency delta bandwidth (0-5 Hz), which has been shown to be the dominant frequency of voluntary control in the muscle torque output and represents common neural drive to the muscle (Farina & Negro, 2015). Coherence was also calculated across the frequency bands: Alpha (5-15 Hz), Low beta (15-21 Hz), High beta (21-35 Hz), Piper (35-50 Hz) and Gamma (32-100 Hz). Higher coherence values, for the same number of MUs involved in the coherence estimation, indicates a greater strength of common synaptic input to the motor neuron pool.

Calculation of smoothed motor unit cumulative spike trains

The spike trains of each active MU during the steadiest 10 second epoch of the 20 second isometric KE contractions were summed to produce a CST. To extract the low-frequency components of effective neural drive to the muscle, representative of torque fluctuation dynamics, the CSTs were smoothed with a 400-ms Hann window (see Chapter Three - General Methods - Section 3.10 - *Calculation of smoothed motor unit cumulative spike trains*). The

complexity, entropy and variability of the smoothed CST signals was then determined using, SampEn, DFA, CI-28, SD and CV as outlined in General Methods - Sections 3.8 and 3.9. The DFA α of the smoothed CST signals were calculated with 76 box sizes ranging from 2000 to 4 data points.

Interference EMG signal processing and analysis

As outlined in full detail in General Methods - Section 3.10 - *Interference EMG signal processing and analysis,* the interference EMG signals from the accepted channels were summed to generate a single interference EMG signal representing the global neural drive to the VL muscle (summation of all the action potentials recorded by the HD sEMG grid). Before further analysis a 10 second epoch of the summed interference EMG signal was extracted, corresponding to the steadiest 10 second epoch of muscle torque time series from each 20 second isometric KE contraction. The PSD of the 10 second epoch of the summed interference EMG signal (filtered with a 4^{th} order Butterworth filter with low-pass cut-off frequency of 500 Hz) was then calculated.

8.2.7. Torque signal complexity, entropy, and variability metric analysis.

Prior to the calculation of the muscle torque complexity, entropy and variability metrics, the steadiest 10 seconds of each contraction was identified as the 10 seconds with the lowest SD from which the complexity, entropy and variability metrics were then calculated.

The SDT, CVT and RMSE which quantify the variability and accuracy of the torque signal were calculated as outlined in Chapter Three - General Methods - Section 3.8. The complexity and entropy metrics, SampEn, DFA, MSE and CI-28 were calculated as outlined in Chapter Three - General Methods - Section 3.9.

8.2.8. Statistical analysis.

For each isometric contraction intensity, the effects of age-group (YG, MG and OG) and coherence frequency band (delta, alpha, low beta, high beta, piper, and gamma) were assessed using a mixed-design two-way ANOVA, with age group as the between-subjects factor and frequency band as the within-subjects factor.

The effects of contraction intensity (10, 20, 30, and 40% MVT) and frequency band (delta, alpha, low beta, high beta, piper, and gamma) on within-muscle coherence were assessed using a two-way repeated measures ANOVA to examine within-subject effects.

The effect of age-group on the scale-to-scale behaviour of the MSE curves at each contraction intensity was assessed using a mixed-design two-way ANOVA, with age-group (YG, MG and OG) as the between-subjects factor and coarse-grained scale (1 to 28) as the within-subjects factor.

The effect of age-group (YG, MG, and OG) and contraction intensity (10, 20, 30, 40, 50, 60, 70, 80% MVT) on torque signal complexity, entropy, and variability metrics and the total power of the interference HD sEMG signal were assessed using a mixed-design two-way ANOVA, with age-group as the between-subjects factor and contraction intensity as the within-subjects factor.

For each relative contraction intensity (10 to 80% MVT) the relationship between coherence Z-scores at each frequency band (delta, alpha, low beta, high beta, piper and gamma) and the torque signal complexity, entropy and variability metrics (DFA, MSE, CI-28, SampEn, CVT, SDT and RMSE) were established using a Pearson's bivariate two-tailed correlation. Following this, a hierarchical, multiple, linear regression analysis for each relative contraction intensity (10 to 80% MVT) was conducted to assess the relationship between alpha band coherence Z-scores and the torque signal metrics (DFA, MSE, CI-28, CVT, SDT and RMSE). Participant age was entered in the first step as an independent covariate, and the alpha band coherence Z-scores were added in the second step as the primary independent variable to explain variance in each dependent variable (DFA, MSE, CI-28, CVT, SDT and RMSE) separately.

For each relative contraction intensity (10 to 80% MVT) the relationship between the smoothed CST signal metrics (DFA, CI-28, SampEn, CV and SD) and the corresponding torque signal complexity, entropy and variability metrics (DFA, CI-28, SampEn, CVT and SDT) were established using a Pearson's bivariate two-tailed correlation. Following this, a hierarchical, multiple, linear regression analysis for each relative contraction intensity (10 to 80% MVT) was conducted to assess the relationship between the CV of smoothed CST signals and the CVT. Participant age was entered in the first step as an independent covariate, and the CV of

smoothed CST signals were added in the second step as the primary independent variable to explain variance the dependent variable, CVT.

Statistical assumptions of linearity, additivity, homoscedasticity, multicollinearity, independence of residuals, and normality of residuals were checked and accepted unless otherwise stated. Multicollinearity among the independent variables was identified using the variance inflation factor. Multicollinearity was considered acceptable if the variance inflation factor was between 1 and 5 (Frost, 2019) and the condition index was < 10.

Bonferroni *post hoc* comparisons were used when a main effect or interaction was significant. The significance level was set at $P < 0.05$ in all cases. Statistical analyses were performed in IBM SPSS statistics 29 (IBM Corp., Armonk, NY, United States).

8.3a - Results

8.3.1. Participant characteristics and anthropometrics.

The characteristics of all sixty participants were presented in Table 8.1a. These participants provided data for the results sections 8.3.4. and 8.3.7.

Table 8.1a Participant characteristics *N* = 60.

	All Participants	Younger Group	Middle Group	Older Group
N	60 (56M, 4F)	20 (17M, 3F)	20 (19M, 1F)	20 (20M, 0F)
Age (years)	42.7 ± 17.6	23.9 ± 4.2	40.9 ± 3.8	63.3 ± 10.2
Height (cm)	177.7 ± 7.2	178.7 ± 6.2	178.4 ± 8.8	176.1 ± 6.4
Mass (kg)	74.1 ± 10.8	67.8 ± 8.4	77.5 ± 12.3	77.1 ± 8.6
VL Skinfold (mm)	7.8 ± 3.2	8.0 ± 3.5	8.4 ± 2.7	6.9 ± 3.4
MVT (Nm)	186.14 ± 61.19	216.57 ± 62.19	199.77 ± 63.27	142.06 ± 26.95

Abbreviations: MVT = maximal voluntary torque; VL = vastus lateralis muscle.

8.3.2. Motor unit characteristics.

Table 8.2a presents the MU characteristics of all participants who provided two or more MU during the isometric KE contractions of the torque control tasks. In total, 11,050 MUs were decomposed and accepted across all isometric KE contractions performed by all participants.

Table 8.2a Characteristics of all detected motor units.

		Contraction Intensity							
		10% MVT	20% MVT	30% MVT	40% MVT	50% MVT	60% MVT	70% MVT	80% MVT
Participant *N*	All	59	60	59	57	55	48	40	35
	YG	19	20	20	18	16	12	9	5
	MG	20	20	19	19	19	16	12	11
	OG	20	20	20	20	20	20	19	19
Participant Age (years)	All	42.9±17.6	42.7±17.6	42.6±17.7	43.4±17.5	44.0±17.5	46.3±17.3	47.5±17.1	50.5±15.8
	YG	23.5±4.0	23.9±4.2	23.9±4.2	24.2±4.3	23.9±4.3	25.0±4.4	24.8±4.2	26.6±2.6
	MG	40.9±3.8	40.9±3.8	40.7±3.8	40.7±3.8	40.7±3.8	41.1±3.9	41.0±4.5	40.7±4.6
	OG	63.3±10.2	63.3±10.2	63.3±10.2	63.3±10.2	63.3±20.3	63.3±10.2	62.4±9.7	62.4±9.7
Total MUs	All	1870	1885	1839	1662	1384	1057	781	572
	YG	613	554	522	380	240	156	74	30
	MG	626	648	627	587	458	313	208	114
	OG	631	683	690	695	686	588	499	428
Mean MUs per Contraction	All	10.61±3.98	10.51±4.27	10.51±4.15	9.78±4.24	8.48±4.76	7.45±4.34	6.54±4.08	5.50±4.12
	YG	10.75±3.07	9.34±2.77	8.70±3.33	7.23±3.54	5.33±3.04	4.58±3.23	2.89±1.97	2.00±0.94
	MG	10.57±3.85	10.80±4.68	11.00±4.26	10.30±3.58	8.04±4.03	6.66±2.75	5.78±1.98	3.58±1.73
	OG	10.52±4.97	11.38±4.96	11.87±4.32	11.58±4.46	11.43±4.89	9.80±4.81	8.75±4.44	7.54±4.49
DR (PPS)	All	10.08±1.70	10.35±1.61	10.91±1.85	11.24±1.73	12.10±2.10	12.85±2.98	13.59±2.32	14.41±3.28
	YG	10.79±1.61	10.59±1.48	11.67±1.79	11.35±1.73	11.98±1.69	12.40±1.67	14.28±1.66	16.29±2.00
	MG	10.23±1.37	10.89±1.31	11.21±1.67	11.74±1.42	13.72±1.73	14.60±3.70	14.88±1.90	15.13±3.37
	OG	9.26±1.79	9.58±1.78	9.85±1.65	10.67±1.91	11.14±2.29	11.72±2.34	12.45±2.35	13.50±3.32

Abbreviations: DR = discharge rate; MU = motor unit; MVT = maximal voluntary torque; MG = middle age group; OG = older age group; PPS = pulses per second; YG = younger age group.

8.3.3. Motor unit within-muscle coherence results.

Table 8.3a presents the MU characteristics of all participants who provided six or more MUs during the isometric KE contractions during the torque control tasks. These MU data were analysed for the results sections 8.3.3., 8.3.5., and 8.3.6.

Table 8.4a presents the two-way ANOVA statistics for the effect of age-group and frequency band on within-muscle coherence Z-scores at each contraction intensity. There was no main effect of age-group at 10, 20, 30, 40%, 60%, 70% and 80% MVT for within-muscle coherence (Table 8.4a), indicating that overall, coherence Z-scores (all frequency bands) were not significantly different across age groups. There was main effect of age group on within-muscle coherence at 50% MVT (Table 8.4a), indicating that overall, the YG had higher coherence Z-scores in comparison to the MG and OG.

The effect of contraction intensity on within-muscle coherence was only assessed from 10 to 40% MVT, due to the notably lower sample sizes above 40% MVT. There was no significant main effect of contraction intensity on within-muscle coherence Z-scores ($F_{(3, 147)}$ = 1.111; P = 0.347; η_p^2 = 0.025), indicating that overall, coherence Z-scores (all frequency bands) were not different across contraction intensities from 10 to 40% MVT.

Table 8.3a Characteristics of motor units used in the within-muscle coherence analysis.

		Contraction Intensity							
		10% MVT	20% MVT	30% MVT	40% MVT	50% MVT	60% MVT	70% MVT	80% MVT
Participant *N*	All	55(51M, 4F)	58(54M, 4F)	56(53M, 3F)	50(48M, 2F)	44(42M, 2F)	33(32M, 1F)	25(24M, 1F)	17(16M, 1F)
	YG	19(16M, 3F)	20(17M, 3F)	18(16M, 2F)	13(12M, 1F)	9(8M, 1F)	4(4M, 0F)	1(1M, 0F)	N/A
	MG	19(18M, 1F)	19(18M, 1F)	18(17M, 1F)	18(17M, 1F)	15(14M, 1F)	12(11M, 1F)	9(8M, 1F)	4(3M, 1F)
	OG	17(17M, 0F)	19(19M, 0F)	20(20M, 0F)	19(19M, 0F)	20(20M, 0F)	17(17M, 0F)	15(15M, 0F)	13(13M, 0F)
Participant Age (years)	All	41.6±17.4	42.3±17.7	43.6±17.6	44.8±16.8	48.0±17.0	50.1±15.0	53.7±14.0	57.3±12.3
	YG	23.5±4.0	23.9±4.2	24.3±4.2	24.3±4.1	25.1±4.4	26.8±3.0	26.0±0.0	N/A
	MG	40.7±3.8	40.7±3.8	40.9±3.7	40.9±3.7	41.3±4.0	41.3±4.5	42.1±4.3	42.8±5.6
	OG	62.9±10.6	63.5±10.4	63.2±10.2	62.4±9.7	63.3±10.2	61.8±9.8	62.5±10.1	61.8±10.1
Total MUs	All	1830	1867	1808	1595	1302	955	655	438
	YG	613	554	501	336	189	103	20	N/A
	MG	612	639	617	578	427	285	178	65
	OG	605	674	690	681	686	567	459	373
Mean MUs per Contraction	All	11.14±3.57	10.77±4.10	10.89±3.90	10.63±3.80	9.91±4.22	9.65±3.38	8.73±3.57	8.76±3.71
	YG	10.75±3.07	9.34±2.77	9.28±2.95	8.62±3.18	7.20±2.71	8.58±2.17	6.67±0.00	N/A
	MG	10.88±3.69	11.21±4.43	11.43±3.94	10.78±3.07	9.49±3.13	7.92±1.69	6.52±1.69	6.17±0.33
	OG	11.86±4.05	11.82±4.67	11.87±4.32	11.95±4.26	11.43±4.89	11.12±3.89	10.20±3.79	9.56±3.92
DR (PPS)	All	10.25±1.55	10.34±1.56	10.94±1.89	11.23±1.77	11.78±2.06	12.13±2.25	13.23±2.30	13.54±2.60
	YG	10.79±1.61	10.59±1.48	11.78±1.86	11.52±1.95	11.52±1.85	12.43±0.86	16.28±0.00	N/A
	MG	10.21±1.41	10.78±1.24	11.32±1.65	11.81±1.43	12.80±1.48	13.42±2.30	14.53±1.86	15.60±2.95
	OG	9.69±1.52	9.63±1.81	9.85±1.65	10.48±1.76	11.14±2.29	11.15±2.01	12.24±2.07	12.90±2.23

Abbreviations: DR = discharge rate; MU = motor unit; MVT = maximal voluntary torque; MG = middle age group; OG = older age group; PPS = pulses per second; YG = younger age group.

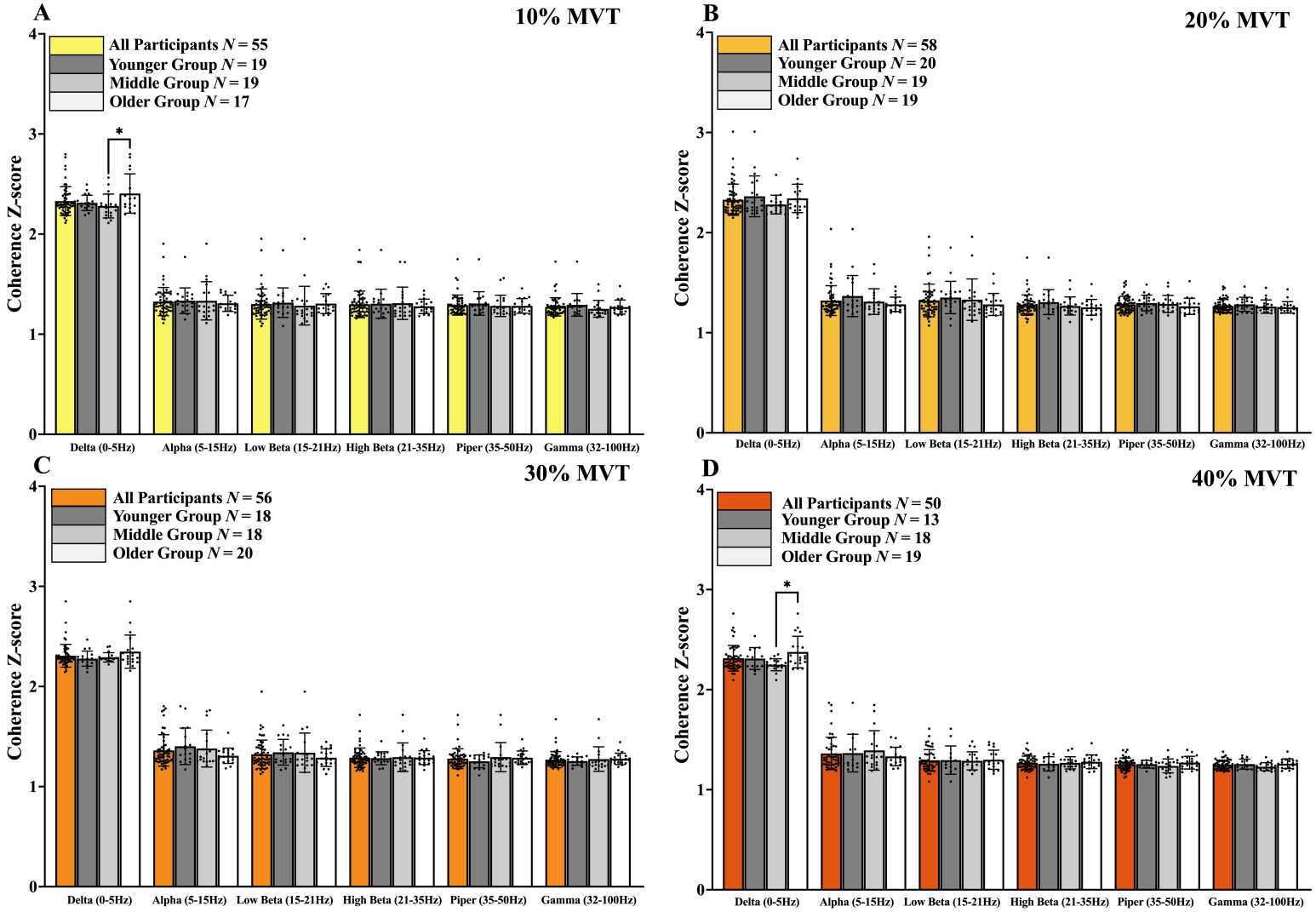

Figure 8.1a. The younger, middle and older age groups within-muscle coherence Z-scores in the delta (0-5Hz), alpha (5-15Hz), low beta (15-21Hz), high beta (21-35Hz), piper (35-50Hz) and gamma (32-100Hz) frequency bands, derived from the isometric knee extensor contractions at **(A)** 10% MVT, **(B)** 20% MVT, **(C)** 30% MVT, **(D)** 40% MVT (MVT = maximal voluntary torque; * = $P < 0.05$).

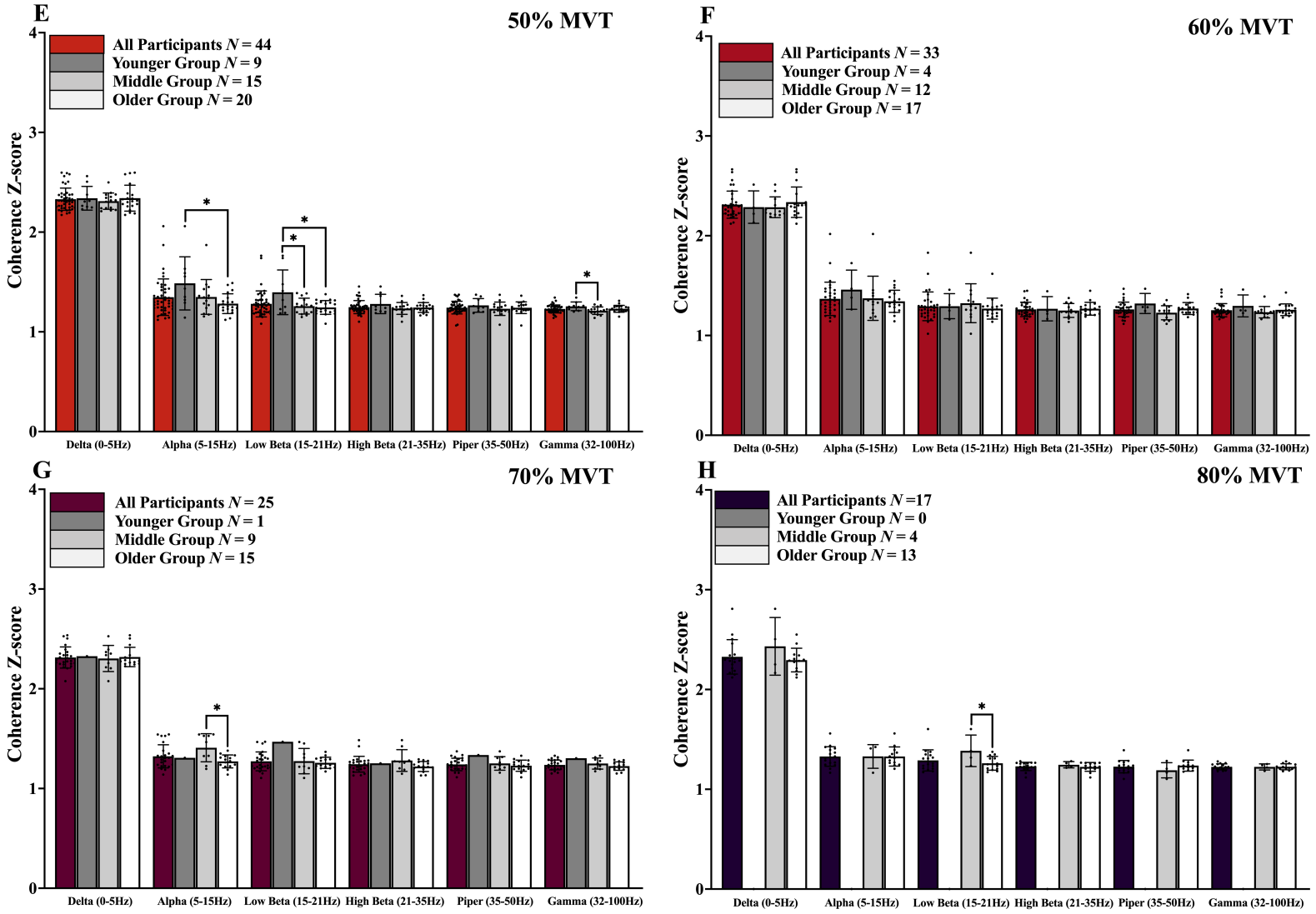

Figure 8.1a Continued. The younger, middle and older age groups within-muscle coherence Z-scores in the delta (0-5Hz), alpha (5-15Hz), low beta (15-21Hz), high beta (21-35Hz), piper (35-50Hz) and gamma (32-100Hz) frequency bands, derived from the isometric knee extensor contractions at **(E)** 50% MVT, **(F)** 60% MVT, **(G)** 70% MVT, **(H)** 80% MVT (MVT = maximal voluntary torque; * = $P < 0.05$).

Table 8.4a Two-way ANOVA statistics for the effect of age-group and frequency band on within-muscle coherence Z-scores at each contraction intensity.

		Contraction Intensity							
		10% MVT	20% MVT	30% MVT	40% MVT	50% MVT	60% MVT	70% MVT	80% MVT
Main effect of Age	*F*	0.233	1.667	0.115	0.833	5.088	0.394	2.729	2.281
	P	0.793	0.198	0.891	0.441	**0.011**	0.678	0.087	0.152
	η_p^2	0.009	0.057	0.004	0.034	0.199	0.026	0.199	0.132
Main effect of Frequency band	*F*	1187.500	1096.450	1142.033	1058.180	846.227	397.359	250.671	306.572
	P	**<0.001**	**<0.001**	**<0.001**	**<0.001**	**<0.001**	**<0.001**	**<0.001**	**<0.001**
	η_p^2	0.958	0.952	0.956	0.957	0.954	0.930	0.919	0.953
Age by Frequency band interaction	*F*	2.045	0.925	2.415	2.124	2.583	1.038	2.031	2.104
	P	**0.029**	0.510	**0.009**	**0.023**	**0.006**	0.415	**0.037**	0.074
	η_p^2	0.073	0.033	0.084	0.083	0.112	0.065	0.156	0.123

Abbreviation: MVT = maximal voluntary torque; Significant *P* values highlighted by bold font.

8.3.4. Effect of age-group on the complexity, entropy and variability of isometric knee extensor torque signals (*N* = 60).

Multiscale entropy curve results

Figure 8.2a presents the comparison of the younger, middle and older age groups MSE curves at each isometric knee extensor contraction intensity. There was a main effect of age group on the MSE curves at 40% MVT ($F_{(2, 57)}$ = 9.126; P = 0.022; η_p^2 = 0.126; Figure 8.2a.D), 50% MVT ($F_{(2, 57)}$ = 5.680; P = 0.006; η_p^2 = 0.166; Figure 8.2a.E), and 60% MVT ($F_{(2, 57)}$ = 3.306; P = 0.044; η_p^2 = 0.104; Figure 8.2a.F). There was no main effect of age group on the MSE curves at 10% MVT ($F_{(2, 57)}$ = 0.533; P = 0.590; η_p^2 = 0.018; Figure 8.2a.A), 20% MVT ($F_{(2, 57)}$ = 0.843; P = 0.436; η_p^2 = 0.029; Figure 8.2a.B), 30% MVT ($F_{(2, 57)}$ = 2.938; P = 0.061; η_p^2 = 0.093; Figure 8.2a.C), 70% MVT ($F_{(2, 57)}$ = 0.481; P = 0.621; η_p^2 = 0.018; Figure 8.2a.G), and 80% MVT ($F_{(2, 57)}$ = 0.662; P = 0.520; η_p^2 = 0.024; Figure 8.2a.H),

There was a significant main effect of coarse-grained scale at 10% MVT ($F_{(27, 1539)}$ = 55.086; P < 0.001; η_p^2 = 0.491), 20% MVT ($F_{(27, 1539)}$ = 157.763; P < 0.001; η_p^2 = 0.735), 30% MVT ($F_{(27, 1539)}$ = 386.688; P < 0.001; η_p^2 = 0.872), 40% MVT ($F_{(27, 1539)}$ = 491.643; P < 0.001; η_p^2 = 0.896), 50% MVT ($F_{(27, 1539)}$ = 630.039; P < 0.001; η_p^2 = 0.917), 60% MVT ($F_{(27, 1539)}$ = 877.984; P < 0.001; η_p^2 = 0.939), 70% MVT ($F_{(27, 1539)}$ = 907.969; P < 0.001; η_p^2 = 0.944), and 80% MVT ($F_{(27, 1539)}$ = 957.116; P < 0.001; η_p^2 = 0.947).

There was a significant age group by coarse-grained scale interaction at 20% MVT ($F_{(27, 1539)}$ = 5.584; P = 0.004; η_p^2 = 0.164), 30% MVT ($F_{(27, 1539)}$ = 7.324; P < 0.001; η_p^2 = 0.204), 40% MVT ($F_{(27, 1539)}$ = 6.494; P = 0.001; η_p^2 = 0.186), 50% MVT ($F_{(27, 1539)}$ = 6.908; P < 0.001; η_p^2 = 0.195), and 60% MVT ($F_{(27, 1539)}$ = 4.493; P = 0.005; η_p^2 = 0.136). There was no age group by coarse-grained scale interaction at 10% MVT ($F_{(27, 1539)}$ = 2.579; P = 0.079; η_p^2 = 0.083), 70% MVT ($F_{(27, 1539)}$ = 1.951; P = 0.127; η_p^2 = 0.067), and 80% MVT ($F_{(27, 1539)}$ = 1.380; P = 0.254; η_p^2 = 0.049).

Table 8.5a presents the descriptive statistics and ANOVA results for the effect of age-group and contraction intensity on the complexity, entropy and variability of the isometric knee extensor torque signals.

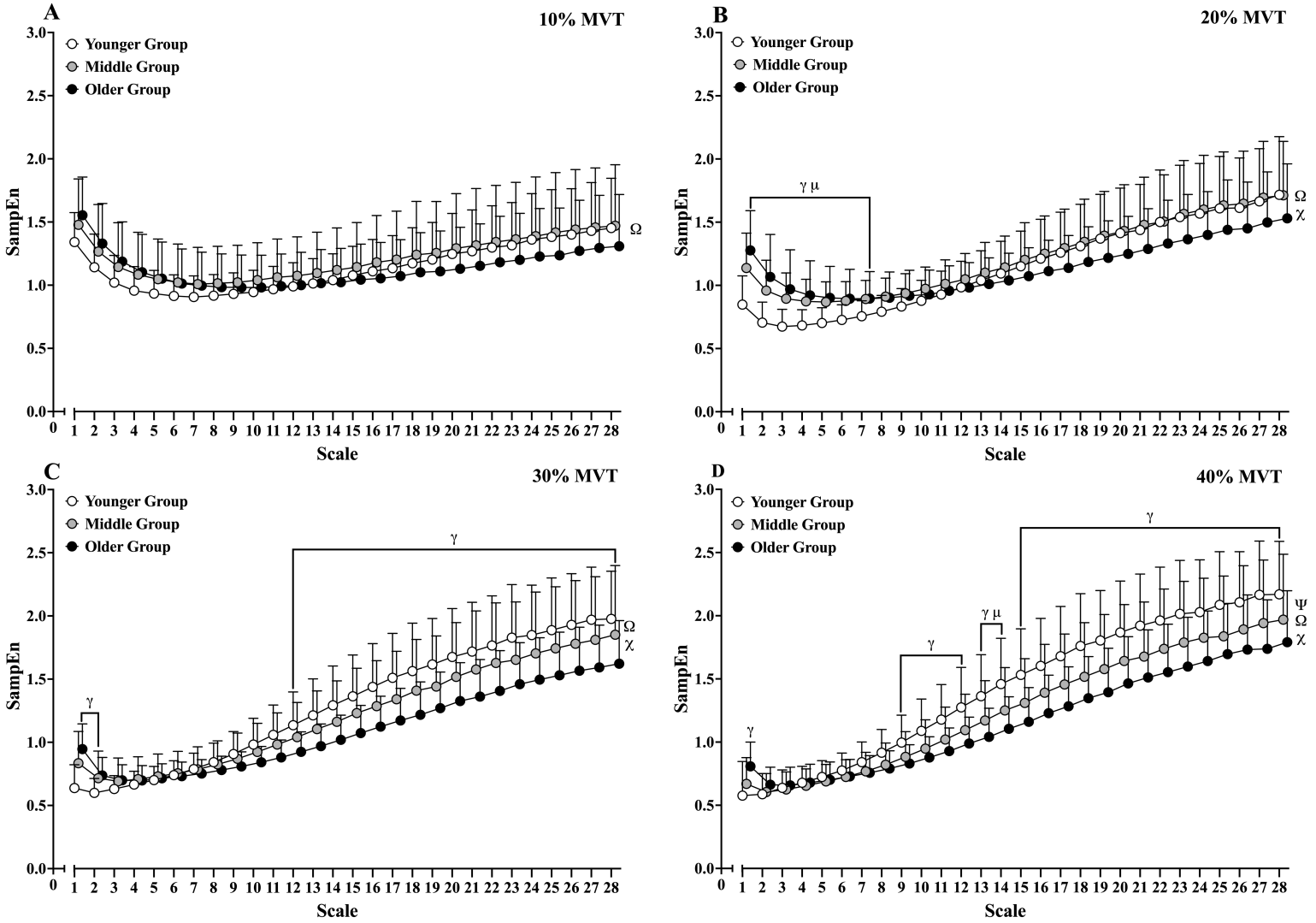

Figure 8.2a. Multiscale entropy curves calculated from the isometric knee extensor torque signals of the young, middle and older age groups at each contraction intensity **(A)** 10% MVT, **(B)** 20% MVT, **(C)** 30% MVT, **(D)** 40% MVT (Younger age group = open circles; Middle age group = grey circles; Older age group = closed circles; MVT = maximal voluntary torque; SampEn = sample entropy; Ψ = significant main effect of age group; Ω = significant main effect of coarse-grained scale; χ = significant age group by coarse-grained scale interaction; γ = significant difference between YG and OG $P < 0.05$; μ = significant difference between YG and MG $P < 0.05$).

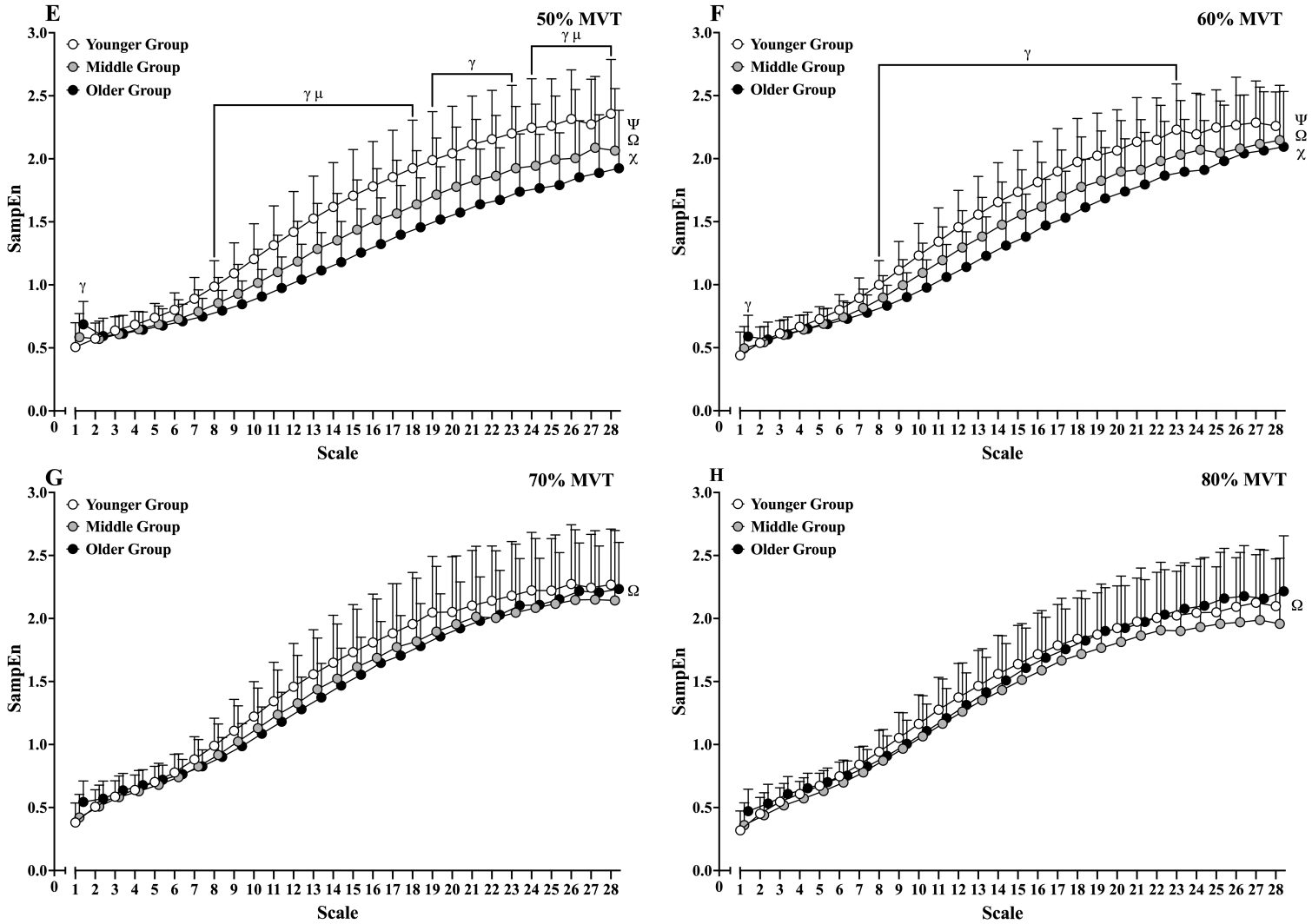

Figure 8.2a Continued. Multiscale entropy curves calculated from the isometric knee extensor torque signals of the young, middle and older age groups at each contraction intensity **(E)** 50% MVT, **(F)** 60% MVT, **(G)** 70% MVT, **(H)** 80% MVT (Younger age group = open circles; Middle age group = grey circles; Older age group = closed circles; MVT = maximal voluntary torque; SampEn = sample entropy; Ψ = significant main effect of age group; Ω = significant main effect of coarse-grained scale; χ = significant age group by coarse-grained scale interaction; γ = significant difference between YG and OG $P < 0.05$; μ = significant difference between YG and MG $P < 0.05$).

Table 8.5a Descriptive statistics and ANOVA results for the effect of age-group and contraction intensity on the complexity, entropy and variability of the isometric knee extensor torque signals.

		Contraction Intensity								*F*, *P* and η_p^2 values			
		10% MVT	20% MVT	30% MVT	40% MVT	50% MVT	60% MVT	70% MVT	80% MVT		Main effect of Age	Main effect of Intensity	Age by Intensity Interaction
SDT (Nm)	YG	0.47±0.15	γ μ 0.85±0.28	γ μ 1.22±0.48	γ μ 1.64±0.79	γ μ 2.10±1.00	γ μ 2.71±1.24	γ 3.32±1.60	γ 3.67±1.56	*F*	9.149	65.993	3.582
	MG	0.41±0.17	0.61±0.21	0.92±0.32	1.20±0.49	1.60±0.73	1.99±0.93	2.86±2.71	3.35±3.00	*P*	**<0.001**	**<0.001**	**0.019**
	OG	0.37±0.12	0.50±0.16	0.71±0.16	0.87±0.26	1.12±0.39	1.33±0.49	1.52±0.56	1.88±0.76	η_p^2	0.253	0.550	0.117
CVT (%)	YG	2.24±0.68	2.04±0.65	1.98±0.86	2.01±1.15	2.04±1.10	2.23±1.26	2.44±1.68	2.32±1.39	*F*	2.295	6.153	2.099
	MG	2.08±0.56	1.59±0.40	1.62±0.55	1.57±0.59	1.68±0.78	1.69±0.69	2.07±1.48	2.13±1.45	*P*	0.111	**<0.001**	0.061
	OG	2.53±0.81	1.87±0.48	1.70±0.31	1.55±0.43	1.62±0.61	1.58±0.55	1.55±0.56	1.69±0.73	η_p^2	0.078	0.102	0.072
RMSE (%)	YG	γ 4.28±2.12	2.87±0.87	2.60±1.08	2.39±1.29	2.37±1.26	2.66±1.51	2.77±1.77	2.78±1.49	*F*	0.039	41.740	3.555
	MG	5.51±2.43	3.07±1.28	2.67±1.24	2.35±0.97	2.16±0.90	2.31±1.06	2.42±1.55	2.86±1.88	*P*	0.961	**<0.001**	**0.010**
	OG	6.95±4.25	3.25±1.38	2.52±0.64	2.21±0.56	2.08±0.65	2.02±0.74	2.03±0.85	2.26±1.02	η_p^2	0.001	0.436	0.116
SampEn	YG	1.34±0.23	γ μ 0.85±0.23	γ μ 0.64±0.18	γ 0.58±0.27	γ 0.51±0.19	γ 0.44±0.19	γ 0.38±0.15	γ 0.32±0.15	*F*	9.354	320.372	2.603
	MG	1.48±0.36	1.14±0.28	0.83±0.25	0.67±0.21	0.58±0.19	0.49±0.17	0.42±0.18	0.36±0.18	*P*	**<0.001**	**<0.001**	**0.018**
	OG	1.55±0.30	1.28±0.31	0.95±0.20	0.81±0.19	0.69±0.18	0.59±0.17	0.54±0.17	0.47±0.17	η_p^2	0.257	0.856	0.088
DFA α	YG	1.29±0.09	1.32±0.11	1.28±0.12	1.25±0.13	1.22±0.12	1.22±0.12	1.26±0.14	1.32±0.11	*F*	0.067	6.221	2.016
	MG	1.27±0.10	1.27±0.12	1.27±0.16	1.27±0.16	1.24±0.18	1.21±0.16	1.25±0.19	1.28±0.18	*P*	0.935	**<0.001**	**0.016**
	OG	1.27±0.08	1.31±0.09	1.34±0.10	1.30±0.13	1.29±0.14	1.26±0.14	1.23±0.14	1.24±0.14	η_p^2	0.002	0.103	0.069
CI-28	YG	31.87±6.10	32.01±6.78	36.28±7.34	γ 39.80±7.97	γ 43.22±7.59	43.30±6.75	42.94±8.75	40.21±7.11	*F*	1.703	24.024	2.365
	MG	33.99±9.49	34.38±6.86	34.10±8.69	35.49±8.59	37.71±9.31	39.62±8.03	40.43±10.82	37.66±10.77	*P*	0.192	**<0.001**	**0.023**
	OG	31.60±8.04	31.94±6.59	30.72±5.54	32.70±7.07	34.34±8.23	37.13±8.09	40.52±7.09	40.61±7.29	η_p^2	0.059	0.308	0.081

Abbreviations: CI-28 = complexity index under 28 scales; CVT = coefficient of variation of torque; DFA = detrended fluctuation analysis scaling exponent α; MVT = maximal voluntary torque; MG = middle age group; OG = older age group; RMSE = root mean square error of torque; SampEn = sample entropy; SDT = standard deviation of torque; YG = younger age group; Significant *P* values highlighted by bold font; γ = significant difference between YG and OG $P < 0.05$; μ = significant difference between YG and MG $P < 0.05$; δ = significant difference between MG and OG $P < 0.05$; (data are mean ± SD).

8.3.5. Relationship between within-muscle coherence and the isometric knee extensor torque signal complexity, entropy and variability metrics.

Pearson's correlation analysis revealed alpha band coherence Z-scores to be significantly correlated with SampEn across the coarse-grained scales of the MSE curves for the contraction intensities, 20 to 60% MVT. There were no significant correlations found between the other coherence frequency bands (delta, low beta, high beta, piper and gamma) and SampEn across the coarse-grained scales of the MSE curves. When controlling for age, the hierarchical regression model revealed alpha band coherence Z-scores to be significantly associated with SampEn at scales 10 to 28 of the coarse-grained torque signals during the isometric KE contractions at 20, 30, 40, 50 and 60% MVT (Figure 8.3a).

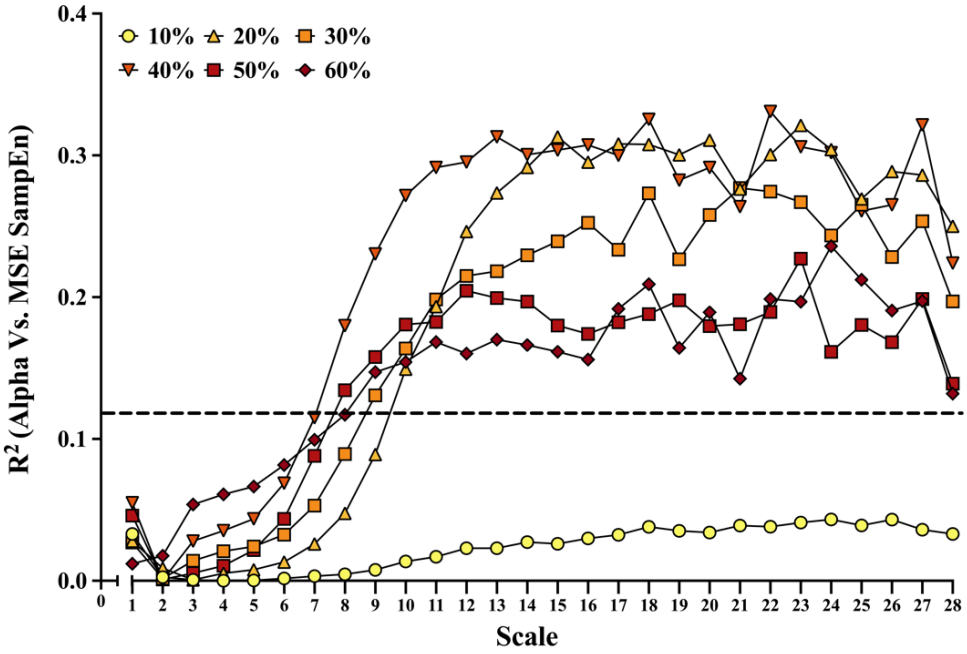

Figure 8.3a. Relationship (R^2 values) between the alpha band coherence Z-scores and the sample entropy at each coarse-grained scale of the multiscale entropy analysis of isometric knee extension contractions at 10 to 60% of maximal voluntary torque (dashed line = significant correlation $P < 0.05$).

Alpha band coherence Z-scores were not significantly associated with SampEn at scale 1 (i.e., SampEn of the original torque signal) at all isometric KE contraction intensities (all $P > 0.05$; Figure 8.3a; Table 8.6a). Pearson's correlation analysis revealed alpha band coherence Z-scores to be the only frequency band significantly correlated with the torque complexity, entropy and variability metrics. Tables 8.6a and 8.7a present the statistics from the hierarchical, multiple, linear regression models, that assessed the relationship between alpha band coherence Z-scores and the torque signal metrics (DFA, SampEn1, SampEn28, CI-28, CVT, SDT and RMSE), with participant age as an independent covariate.

Table 8.6a Statistics from the hierarchical, multiple, linear regression analyses of the torque complexity metrics.

Contraction Intensity (% MVT)	Dependent Variables	Independent Covariate: Participant Age				Independent Predictor Variable: Alpha Band Coherence			
		R	R^2	β	*P*	ΔR^2	β	*P*	ΔF
10% (*N* = 55)	DFAα	0.007	0.000	-0.011	0.959	0.002	-0.045	0.948	0.104
	CI-28	0.103	0.011	-0.092	0.454	0.021	0.145	0.434	1.124
	SampEn 1	0.229	0.052	0.227	0.093	0.001	-0.025	0.243	0.034
	SampEn 28	0.219	0.048	-0.205	0.107	0.033	0.183	0.110	1.880
20% (*N* = 58)	DFAα	0.018	0.000	-0.117	0.895	0.330	-0.590	**<0.001**	27.119
	CI-28	0.152	0.023	-0.041	0.253	0.224	0.486	**<0.001**	16.396
	SampEn 1	0.482	0.233	0.443	**<0.001**	0.028	-0.170	**<0.001**	2.047
	SampEn 28	0.280	0.079	-0.163	**0.033**	0.250	0.514	**<0.001**	20.523
30% (*N* = 56)	DFAα	0.206	0.042	0.053	0.127	0.293	-0.562	**<0.001**	23.351
	CI-28	0.348	0.121	-0.238	**0.009**	0.151	0.404	**<0.001**	11.032
	SampEn 1	0.485	0.235	0.438	**<0.001**	0.027	-0.171	**<0.001**	1.949
	SampEn 28	0.380	0.145	-0.255	**0.004**	0.197	0.461	**<0.001**	15.860
40% (*N* = 50)	DFAα	0.096	0.009	0.029	0.507	0.272	-0.526	**<0.001**	17.820
	CI-28	0.301	0.091	-0.239	**0.034**	0.233	0.486	**<0.001**	16.160
	SampEn 1	0.333	0.111	0.302	**0.018**	0.055	-0.236	**0.014**	3.077
	SampEn 28	0.326	0.106	-0.264	**0.021**	0.224	0.478	**<0.001**	15.742
50% (*N* = 44)	DFAα	0.201	0.041	0.052	0.190	0.127	-0.386	**0.023**	6.242
	CI-28	0.345	0.119	-0.220	**0.022**	0.089	0.323	**0.008**	4.600
	SampEn 1	0.292	0.085	0.201	0.055	0.046	-0.233	0.056	2.179
	SampEn 28	0.339	0.115	-0.183	**0.024**	0.139	0.404	**0.002**	7.634
60% (*N* = 33)	DFAα	0.278	0.078	0.164	0.117	0.283	-0.545	**0.001**	13.301
	CI-28	0.406	0.165	-0.333	**0.019**	0.113	0.345	**0.008**	4.713
	SampEn 1	0.116	0.014	0.092	0.519	0.012	-0.114	0.675	0.379
	SampEn 28	0.332	0.110	-0.253	0.059	0.132	0.372	**0.016**	5.245
70% (*N* = 25)	DFAα	0.176	0.031	0.017	0.401	0.102	-0.357	0.207	2.600
	CI-28	0.250	0.063	-0.066	0.227	0.138	0.415	0.085	3.804
	SampEn 1	0.039	0.002	0.074	0.854	0.005	0.080	0.929	0.114
	SampEn 28	0.136	0.019	-0.009	0.517	0.066	0.287	0.379	1.582
80% (*N* = 17)	DFAα	0.378	0.143	0.297	0.135	0.178	-0.429	0.067	3.664
	CI-28	0.369	0.136	-0.295	0.145	0.146	0.390	0.098	2.853
	SampEn 1	0.077	0.006	-0.089	0.768	0.003	-0.059	0.939	0.048
	SampEn 28	0.285	0.081	-0.198	0.268	0.202	0.458	0.098	3.942

Abbreviations: DFAα = detrended fluctuation analysis scaling exponent α; CI-28 = complexity index under 28 coarse-grained scales of the torque multiscale entropy curves; SampEn 1 = sample entropy at coarse-grained scale 1 of the multiscale entropy analysis; SampEn 28 = sample entropy at coarse-grained scale 28 of the multiscale entropy analysis; MVT = maximal voluntary torque of the knee extensors; Significant *P* values highlighted by bold font.

Table 8.7a Statistics from the hierarchical, multiple, linear regression analyses of the torque variability metrics.

Contraction Intensity (% MVT)	Dependent Variables	Independent Covariate: Participant Age				Independent Predictor Variable: Alpha Band Coherence			
		R	R^2	β	*P*	ΔR^2	β	*P*	ΔF
10% (*N* = 55)	CVT	0.194	0.038	0.210	0.156	0.042	0.205	0.116	2.371
	SDT	0.220	0.049	-0.204	0.106	0.046	0.214	0.076	2.625
	RMSE	0.131	0.017	0.115	0.341	0.043	-0.208	0.200	2.372
20% (*N* = 58)	CVT	0.018	0.000	0.009	0.892	0.013	0.118	0.689	0.733
	SDT	0.476	0.226	-0.386	**<0.001**	0.146	0.392	**<0.001**	12.749
	RMSE	0.378	0.143	-0.312	**0.003**	0.080	0.291	**<0.001**	5.695
30% (*N* = 56)	CVT	0.073	0.005	-0.009	0.594	0.051	0.236	0.213	2.888
	SDT	0.493	0.243	-0.371	**<0.001**	0.186	0.448	**<0.001**	17.284
	RMSE	0.422	0.178	-0.268	**0.001**	0.299	0.568	**<0.001**	30.291
40% (*N* = 50)	CVT	0.079	0.006	-0.019	0.587	0.211	0.464	**0.003**	12.695
	SDT	0.428	0.183	-0.356	**0.002**	0.307	0.558	**<0.001**	28.248
	RMSE	0.349	0.122	-0.276	**0.013**	0.320	0.570	**<0.001**	26.913
50% (*N* = 44)	CVT	0.123	0.015	0.262	0.425	0.109	0.358	0.066	5.097
	SDT	0.359	0.129	-0.135	**0.017**	0.286	0.580	**<0.001**	20.072
	RMSE	0.331	0.110	-0.129	**0.028**	0.234	0.524	**<0.001**	14.581
60% (*N* = 33)	CVT	0.084	0.007	0.206	0.641	0.321	0.579	**0.003**	14.322
	SDT	0.396	0.157	-0.273	**0.023**	0.323	0.581	**<0.001**	18.628
	RMSE	0.364	0.133	-0.270	**0.037**	0.191	0.447	**0.003**	8.447
70% (*N* = 25)	CVT	0.008	0.000	-0.027	0.971	0.005	-0.078	0.947	0.109
	SDT	0.355	0.126	-0.389	0.081	0.005	-0.075	0.214	0.115
	RMSE	0.231	0.054	-0.216	0.266	0.001	0.033	0.540	0.021
80% (*N* = 17)	CVT	0.332	0.110	0.355	0.193	0.014	0.118	0.396	0.216
	SDT	0.062	0.004	0.009	0.812	0.136	0.376	0.348	2.213
	RMSE	0.134	0.018	-0.080	0.607	0.080	0.287	0.487	1.235

Abbreviations: CVT = coefficient of variation of torque; SDT = standard deviation of torque; RMSE = root mean square error of torque; MVT = maximal voluntary torque of the knee extensors; Significant *P* values highlighted by bold font.

Alpha band coherence was significantly associated with the torque signal complexity metrics DFA α and CI-28; and was able to explain between 12.7% to 33.0% of the variance in DFA α and 8.9% to 23.3% of the variance in CI-28 during the isometric KE contractions at intensities from 20 to 60% MVT (Table 8.6a). The standardised beta coefficients indicate that higher alpha band coherence Z-scores were associated with lower DFA α values and higher CI-28 values (i.e., increased torque complexity).

Alpha band coherence was significantly associated with the torque signal variability metrics SDT and RMSE of torque; and was able to explain between 14.6% to 32.3% of the variance in the SDT and 8.0% to 32.0% of the variance in the RMSE of torque signal during the isometric KE contractions at intensities from 20 to 60% MVT (Table 8.7a). The standardised beta coefficients indicate that higher alpha band coherence Z-scores were associated with higher SDT and RMSE values (i.e., increased torque variability).

8.3.6. Relationship between the variability of smoothed cumulative motor unit spike train signals and isometric knee extensor torque signal variability.

The smoothed CST signal complexity metrics (proposed to be measures of common synaptic input complexity; Hunter, 2023) were not significantly associated with the corresponding isometric KE torque signal complexity metrics (all $P > 0.05$).

The CV of smoothed CST signals was found to explain a significant amount of variance in the CVT at 20% MVT ($r = 0.346$; $R^2 = 0.119$; $P = 0.009$), 30% MVT ($r = 0.310$; $R^2 = 0.096$; $P = 0.021$), and 40% MVT ($r = 0.535$; $R^2 = 0.286$; $P < 0.001$).

8.3.7. Effect of age-group and contraction intensity on the power spectral density of the interference HD sEMG signals.

There was a significant main effect of age-group for total interference HD sEMG power ($F_{(2, 57)}$ = 6.697; P = 0.03; η_p^2 = 0.199) and a significant age group by contraction intensity interaction ($F_{(14, 413)}$ = 4.644; P < 0.001; η_p^2 = 0.147). *Post hoc* pairwise comparisons revealed the YG to have a significantly higher total power across all contraction intensities (10 to 80% MVT) when compared to the OG (all P < 0.05). No differences were found between the YG and MG or the MG or OG for total power across all contraction intensities (all P > 0.05). There was a significant main effect of contraction intensity for total interference HD sEMG power ($F_{(7, 413)}$ = 24.176; P < 0.001; η_p^2 = 0.309; Figure 8.4a). *Post hoc* pairwise comparisons revealed total power to significantly increase with increasing contraction intensity (all P < 0.01).

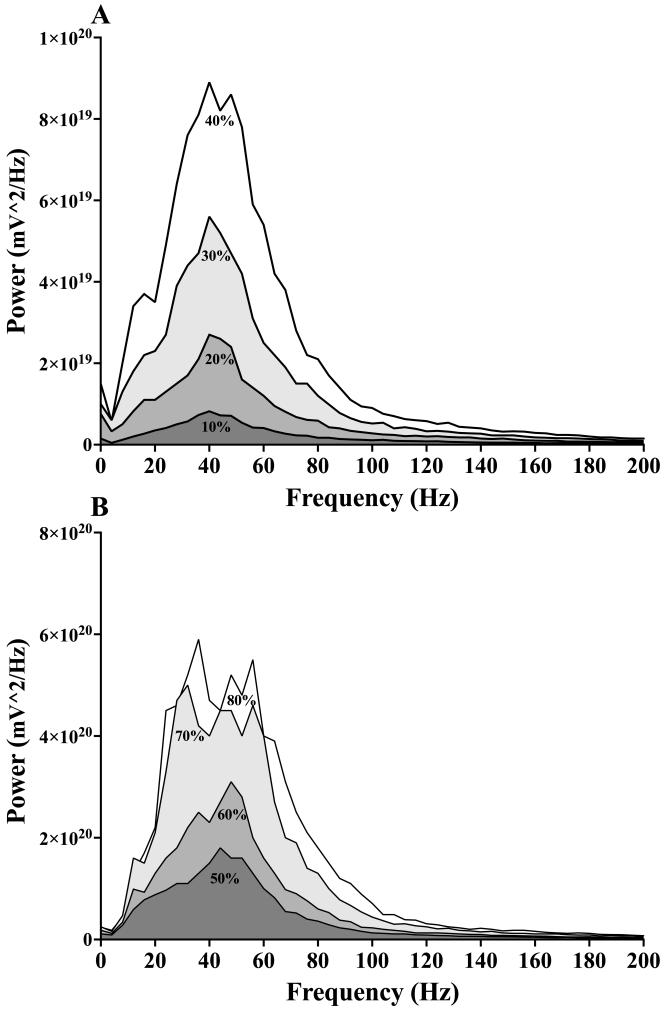

Figure 8.4a. (A) Power density spectrum for interference HD sEMG signals from contractions at 10, 20, 30 and 40% MVT, **(B)** Power density spectrum for interference HD sEMG signals from contractions at 50, 60, 70 and 80% MVT.

8.4a - Discussion

The current study investigated whether the estimated strength of common synaptic input, assessed by the within-muscle coherence of CSTs, was explanatory of KE torque signal complexity and variability during fresh submaximal isometric contractions across a range of intensities (10 to 80% MVT), in adults aged from 18 to 90 years. The main findings revealed significant associations between common input in the alpha band (5 to 15 Hz) and muscle torque signal complexity metrics, CI-28, DFA α (Table 8.6a), as well as SampEn at scales 10 to 28 of the MSE curves (Figure 8.3a) at 20% to 60% MVT. However, contrary to the current hypothesis and those of previous researchers (Pethick et al., 2016, 2021b), participants with stronger common input in the alpha band exhibited muscle torque signals of higher complexity (i.e., a higher CI-28 and a DFA α closer to 1.0), and greater irregularity (i.e., a higher SampEn).

8.4.1. Effect of age-group and isometric contraction intensity on the strength of common synaptic input.

The current study found there to be no effect of age-group on the estimated strength of common synaptic input at 10, 20, 30, 40%, 60%, 70% and 80% MVT (Table 8.4a; Figure 8.1a). Current findings corroborate previous research that also found no age-related differences in common synaptic input of the motor neurons innervating the VL muscle, in the delta, alpha and beta frequency bands during sustained isometric contractions at 25% MVT (Guo et al., 2024). In contrast, older adults have been found to exhibit greater strength of common synaptic input to the tibialis anterior (TA) muscle in the delta frequency band during sustained isometric contractions at 20% MVT, than younger adults (Castronovo et al., 2018). Although, no age-related differences were found in common synaptic input in the alpha and beta frequency bands (Castronovo et al., 2018). The effect of age on the estimated strength of common synaptic input remains unclear and warrants further investigation.

Age-related changes in each of the frequency bands is likely dependent on the extent to which ageing has affected the different sites within the neuromuscular system from which synaptic inputs originate (Erim et al., 1999; Hunter et al., 2016). For example, with advancing age there is often cortical atrophy (McGinnis et al., 2011; Salat et al., 2004; Ward, 2006), and a reduction in the ability of Ia afferents to discharge motor neurons (Baudry et al., 2014). Consequently, there is an increase in cortical activity (Seidler et al., 2010) and cortical excitability (Baudry et al., 2014) when older adults perform motor tasks. Furthermore, ageing is associated with the

degeneration of the dopaminergic system (Seidler et al., 2010). Therefore, the extent to which the *older* study participants were affected by these factors would have an influence on the strength of common inputs in the alpha, beta, and piper frequency bands; which were thought to be partly dependent on Ia afferent feedback (Christakos et al., 2006; Lippold, 1970), cortical activity (Conway et al., 1995; Feige et al., 2000) and dopamine (McAuley et al., 2000), respectively.

The effect of contraction intensity on the estimated strength of common synaptic input was only assessed from 10% to 40% MVT, due to the notably lower participant sample sizes at contraction intensities above 40% MVT (Table 8.3a). The lower participant sample size with increasing isometric contraction intensity is attributable to the inability to identify the minimum of six MUs required for the within-muscle coherence analysis (Dideriksen et al., 2018). Previous researchers have also observed large reductions in identifiable MUs with increasing contraction intensity (Del Vecchio & Farina, 2019). This reduction in MU yield is likely a consequence of greater MU action potential superposition in the interference HD sEMG signal (Del Vecchio et al., 2019b).

It has previously been shown that delta and alpha band coherence increases (i.e., relative increase in the proportion of common synaptic input with respect to independent input) when the net excitatory input to the motor neurons increases, due to increases in the intensity of the muscle contraction (Castronovo et al., 2015). In the current study, the incremented increase in KE muscle contraction intensity from 10% to 40% MVT, was found to significantly increase the excitatory neural drive to the muscle (Figure 8.4a). However, this was not accompanied by a relative increase in the strength of common input in the delta and alpha frequency bands.

Previous researchers found common synaptic input to be significantly higher at 75% MVT, when compared to 20% and 50% MVT (Castronovo et al., 2015). Notably, common synaptic input was not found to be higher at 50% MVT, when compared to 20% MVT (Castronovo et al., 2015). Taken together with current study findings, this may suggest that an observable relative increase in the strength of common synaptic input only occurs above a threshold in motor neuron excitation. In this instance the net excitatory input to the motor neuron is influenced by the contraction intensity. When compared to lower contraction intensities, higher contraction intensities necessitate greater MU recruitment, rate coding and consequently MU synchronisation (Avrillion et al., 2023; Fuglevand et al., 1993; Henneman et al., 1965; Milner-

Brown et al., 1973). This would likely explain a relative increase in the proportion of common synaptic input with respect to independent input, as contraction intensity is increased beyond a certain threshold.

8.4.2. Effect of age-group and contraction intensity on the complexity, entropy and variability of isometric knee extensor torque signals.

No age-group related differences in isometric KE torque signal complexity were observed across the range of contraction intensities (10 to 80% MVT), as assessed by DFA α and CI-28 (Table 8.5a). These findings contrast with those presented in Chapter Six, where participants of a similar age range were studied, and older adults exhibited significantly lower isometric KE torque complexity than younger adults. However, as observed in Chapter Five, an age-related cross-over in the MSE curves was also evident in the current chapter (Figure 8.2a). This cross-over behaviour, discussed in detail in Chapter Five, reflects age-related differences in the temporal structure of the torque signal. Specifically, older adults exhibit increased irregularity in higher-frequency components and increased regularity in lower-frequency components than younger adults.

The current chapter also builds upon the findings of Chapter Six by demonstrating a progressive age-related suppression of SampEn at coarser time scales (at 10 to 60% MVT; Figures 8.2a.A to 8.2a.F). These findings suggest a gradual decline in SampEn, indicative of increasing regularity in low-frequency torque signal components, across the adult lifespan, with reductions evident from young to middle-aged adults and further into older age. Collectively, these results highlight the sensitivity of MSE analysis for capturing progressive, age-group related changes in neuromuscular complexity, and by extension neuromuscular function and the regulation of muscle torque control.

8.4.3. Relationship between the strength of common synaptic input and isometric knee extensor torque signal complexity, entropy and variability.

This chapter presents the first evidence establishing a relationship between the strength of common synaptic input and the complexity measures used to analyse the temporal structure of torque signals during isometric contractions. Specifically, when controlling for age, the strength of alpha band oscillations in common synaptic input was found to predict up to 23.3% and 33.0% of the variance in the CI-28 and DFA α isometric KE torque complexity metrics, respectively, at contraction intensities ≤ 40% MVT (Table 8.6a). The involuntary oscillations

in the alpha frequency band were associated with physiological tremor (Lippold, 1971; McAuley & Marsden, 2000), and can be attributed, in part, to proprioceptive (Ia) afferent feedback from the active muscles that project to the motor neuron pool (Christakos et al., 2006; Lippold, 1970; Laine et al., 2016; Mehrkanoon et al., 2014). Therefore, it can be inferred that the complexity of a submaximal isometric KE torque signal might be indicative of the amount of Ia afferent feedback and the ability to modulate Ia presynaptic inhibition.

The comparable DFA α and CI-28 isometric KE torque complexity metrics between age groups (Table 8.5a; specifically for contractions ≤ 40% MVT, because of the low sample size of the YG above 40% MVT), may be explained by the similarity in the strength of common synaptic input between age groups (Table 8.4a). Although, this interpretation is made cautiously due to study limitations, as discussed in section 8.4.5. Limitations. The contrasting findings between Chapters Six and Eight A suggests that an age-related loss of isometric KE torque complexity may not inevitable. However, as highlighted in previous chapters (Chapters Five and Six), the equivocal findings of the current thesis were likely attributable to differences in the age of the older groups, where participants may be *too* young to observe a difference in complexity. Further research is required to establish the involvement of common synaptic input when age-related changes in isometric KE torque complexity are more likely to be present, such as in much older individuals (aged > 80 years).

In previous chapters (see Chapters Five and Six), it was speculated that the age-dependent scale-to-scale differences in the MSE curves may reflect the behaviour of the multiple components of the neuromuscular system that operate over multiple temporal scales and therefore determine the structural characteristics of the muscle torque signal (Dideriksen et al., 2012; Farina et al., 2014; Negro et al., 2009; Farina & Negro, 2015). This chapter provides an initial step towards explaining the behaviour of the MSE curves, as current findings demonstrate alpha band oscillations in common synaptic input to be significantly associated with SampEn at coarse-grained scales 10 to 28, during the isometric KE contractions at intensities from 20% to 60% MVT (Figure 8.3a).

The current study is unable to directly explain the age-related cross-over phenomenon, or the scale-to-scale entropic behaviour observed in the MSE curves. However, it is possible to speculate that this MSE curve behaviour may be related to age-associated changes in the

strength of common synaptic input. If so, the higher SampEn observed at the longer (coarser) time scales in younger adults, compared with middle-aged and older adults (Figure 8.2a), could reflect a greater strength of common synaptic input in the younger group. The absence of differences in the estimated strength of common synaptic input between age groups may, however, be due to limitations in capturing a representative sample of MUs at each contraction intensity (see Section 8.4.5. Limitations). Therefore, increasing the yield of MU recordings is essential to verify the involvement of common synaptic input in the age-related scale-to-scale entropic behaviour observed in the MSE curves.

It is notable that there was no association between common input in the alpha frequency band and the SampEn of all coarse-grained scales of the MSE curve at 10% MVT (Figure 8.3a). Similarly, common input in the alpha frequency band was not associated with any of the isometric KE torque complexity (DFA and CI-28; Table 8.6a) and variability (CVT, SDT and RMSE; Table 8.7a) metrics at 10% MVT. These findings suggest that at 10% MVT, common input in the alpha band does not predominate the temporal irregularity and structure of the torque signal, captured specifically by these complexity metrics (MSE, DFA and CI-28). The steadiness (low CVT and SDT) and limited targeting errors (low RMSE) at 10% MVT (Table 8.5a), likely explains the lack of association between the torque variability metrics (CVT, SDT and RMSE) and common synaptic input in the alpha band (Mehrkanoon et al., 2014). However, torque control at 10% MVT is likely to still be determined predominantly by low-frequency common neural drive to the muscle and not greatly influenced by synaptic noise (Dideriksen et al., 2012).

The absence of a relationship between the delta frequency band (0 to 5 Hz) and the torque complexity metrics is notable, particularly considering that low-frequency components (< 10 Hz) of neural drive are typically transformed into muscle torque (Farina & Negro, 2015). This may suggest that complexity metrics used in this study, namely MSE, DFA and CI-28, were unable to capture the temporal structure of the torque signal produced by common synaptic input below 5 Hz. The alpha frequency band (5 to 15 Hz), in contrast, encompasses the frequencies of effective neural drive as well as higher frequency common inputs (Farina & Negro, 2015).

It is theoretically plausible, based upon the principles of nonlinear dynamics, amplitude [frequency] modulation, and the established relationships between neural activity and muscle

torque output, that these higher frequency components may be embedded as common irregularities within lower-frequency oscillations in common neural drive through nonlinear amplitude modulation (Watanabe & Kohn, 2015). These irregularities in common neural drive might then be transmitted into the muscle torque signal, if the input is common to a sufficient number of motor neurons (Farina & Negro, 2015). This nonlinear transmission might explain why stronger alpha frequency band oscillations in common synaptic input were associated with more irregular and complex torque signals (Figure 8.3a; Table 8.6a). The presence of these irregularities suggests that nonlinear interactions between the different frequency bands of common input may contribute to the overall complexity of the muscle torque signal. However, the strength of alpha band oscillations accounted for only part of the variance in torque signal complexity, further research is required to elucidate the additional mechanisms underlying the unexplained variance.

Stronger coherence between CSTs in the alpha frequency band (physiological tremor band) is suggested to be associated with error corrections and overshoots in movement during tasks of muscle torque control (Cabral et al., 2024; Mehrkanoon et al., 2014). In line with this, when controlling for age, the current study found that stronger alpha band oscillations in common synaptic input was significantly associated with greater targeting errors (i.e., higher RMSE) and greater absolute variability (i.e., higher SDT) of the torque signals (Table 8.7a). Furthermore, by increasing the target torque, participants made greater targeting errors (i.e., higher RMSE) and exhibited torque signals of greater absolute variability (i.e., higher SDT; Table 8.5a). Importantly, the variance in the RMSE and SDT explained by alpha band coherence increased from 4.3% and 4.6% at 10% MVT to 32.0% and 30.7% at 40% MVT, respectively (Table 8.7a). These findings highlight the involvement of oscillations in the alpha frequency band (physiological tremor band) in modulating the precision of muscle torque output across different contraction intensities.

8.4.4. Relationship between the variability of common synaptic input and isometric knee extensor torque signal variability.

The current chapter also assessed the complexity and variability of smoothed CSTs; proposed to be a measure of the temporal and spatial structure of common synaptic input to the motor neurons innervating the VL muscle (Hunter, 2023). The study found no significant association between neuromuscular complexity and the complexity of the smoothed CST. These findings

suggest that the temporal structure of common synaptic input to the VL muscle, may not directly influence the complexity of isometric KE muscle torque.

When controlling for age, greater variability of smoothed CSTs (i.e., greater variability in common synaptic input to the motor neurons) was significantly associated with greater neuromuscular variability (i.e., CVT) during contractions at 20% to 40% MVT. The variability in common synaptic input was able to explain between 9.6% and 28.6% of the variance in the CVT. These findings corroborate previous research, that has also found greater variability in common synaptic input to be significantly associated with greater WE and PG muscle force variability during fresh isometric contractions (Feeney et al., 2018). The current chapter is the first to demonstrate the relationship between the variability in common synaptic input to the VL muscle and the variability in isometric KE torque signals. It provides further evidence supporting the transmission of low-frequency common neural drive into the spatial structure of isometric KE muscle torque.

The reduced MU yield at higher contraction intensities (≥ 50% MVT; Table 8.3a) and consequently a lower number of MUs within the smoothed CSTs, would result in a less reliable estimate of the variability in common synaptic input. This likely explains why the variability of common synaptic input was not significantly associated with the CVT at higher contraction intensities (≥ 50% MVT). The current study estimated the variability in common synaptic input by smoothing CSTs with a 400-ms Hann window, to extract the low-frequency components of neural drive, and then calculated the variability of the smoothed CSTs (Hunter, 2023; see Chapter Three - General Methods). In the study of Feeney et al., (2018) a state-space model was used to estimate the variability in common synaptic input. It was not possible to implement the state-space model in the current study. However, it is likely the state-space model method provides a more reliable estimate of the variability in common synaptic input (Feeney et al., 2017). This likely accounts for the stronger association observed between the variability in common synaptic input and muscle force steadiness by previous researchers ($R^2 = 0.31$ to 0.39; Feeney et al., 2018).

8.4.5. Limitations.

The predominant limitation of the current study is the low MU yield across all contraction intensities, but most notably at the higher contraction intensities (≥ 50% MVT; Table 8.2a).

Although, the number of detected MU is comparable to previous research (Dideriksen et al., 2018; Laine et al., 2015). The inability to identify the minimum of six MUs required for the within-muscle coherence analysis for many participants at higher contraction intensities, limited the comparisons that could be made between contraction intensities. In addition, the disproportionally low MU yield from the younger adults at the higher contraction intensities (Table 8.3a), restricted the ability to assess the interaction between age-groups and contraction intensity on the estimated strength of common synaptic input. All the data and results for all contraction intensities have been reported. However, the discussion of within-muscle coherence focussed primarily on the results at the contractions performed at ≤ 40% MVT, because of the more comparable participant sample sizes and MU yield.

There are a greater number of active MUs at higher contraction intensities, when compared with lower contraction intensities (Avrillion et al., 2023). Therefore, even if the minimum of six MUs were identified at the higher intensities, this still represents a smaller proportion of the total number of active MUs. Thus, it is probable that the estimates of the strength of common synaptic input at ≥ 50% MVT were *not* sufficiently representative of the actual strength of common synaptic input. This may also explain the diminished association between common synaptic input and the complexity and variability of isometric KE torque at ≥ 50% MVT (Tables 8.6a and 8.7a). Irrespective of contraction intensity, the optimal coherence analysis would use CSTs of as many MUs as possible, to provide the nearest estimate of the strength of common synaptic input.

The detection of a larger number of active MUs was constrained, at the time of data collection, by the compatibility of electrode-grids comprised of only 64-electrodes (5 rows x 13 columns; 4 mm electrode diameter; 8 mm interelectrode distance; GR08MM1305; OT Bioelettronica, Torino, Italy) with the 12-bit analogue-to-digital converter (EMG-USB2+, 64-channel EMG amplifier; OT Bioelettronica, Torino, Italy; 3 dB). However, the development of larger, and denser HD sEMG electrodes (Caillet et al., 2023) and high-density magnetomyography (Klotz et al., 2023) will allow future investigations to identify a greater and more representative sample of active MUs, thus allowing for a closer estimation of the actual strength of common synaptic input. A closer estimation of actual strength of common synaptic input may also increase the amount of variance that can be explained in the isometric torque complexity metrics.

Isometric KE torque is produced through the co-activation of multiple muscles. However, in the current study, HD sEMG signals were only recorded from VL muscle. The complexity metrics derived from the isometric KE torque signal likely reflects both the intra-muscle and inter-muscle common synaptic input of all KE muscles. The intra-muscle and inter-muscle common synaptic input to the motor neuron pools of the other KE muscles may also explain additional variance in the complexity metrics (SampEn at each coarse-grained scale, CI-28 and DFA α), not explained by the common synaptic input to the motor neuron pool of the VL muscle.

The current study only investigated the neural mechanisms underpinning isometric KE torque complexity and variability. There is evidence to show the same mechanisms (i.e., strength and variability of common synaptic input) underpin the torque or force variability of other muscle groups (Castronovo et al., 2018; Feeney et al., 2018; Mani et al., 2019), such as the variability of isometric precision PG force, that was assessed in Chapter Seven (Feeney et al., 2018). It is also highly probable that the strength of common synaptic input is explanatory of the torque or force complexity of other muscle groups. However, as shown in Chapter Seven, the MSE curves derived from isometric precision PG force did not demonstrate the same age-dependent scale-to-scale entropic behaviour as the isometric KE torque MSE curves. Thus, research is required to explore the mechanisms that determine the complexity of torque or force of other muscle groups.

8.5a - Conclusion

The current chapter provides the first evidence demonstrating an association between the strength of common synaptic input in the alpha (physiological tremor) band and the neuromuscular complexity of the KE muscles. Stronger common input in the alpha band was found to be associated with muscle torque signals of higher complexity (i.e., a higher CI-28 and a DFA α closer to 1.0), and greater irregularity (i.e., a higher SampEn). Furthermore, greater variability in common synaptic input was significantly associated with greater neuromuscular variability.

Overall, current findings indicate that the temporospatial structure (neuromuscular *complexity* and *variability*) of muscle torque is determined, in part, by the strength and variability of oscillations in common synaptic input. Importantly, this study provides experimental data that shows the complexity measures derived from isometric muscle torque signals were indicative of adaptive neural responses, and thus, the neuromuscular system's strategy to meet task demands. These findings also support the theoretical framework of physiological complexity, that proposes the changes in a system on a component level (i.e., change in the strength and variability of common synaptic input), were reflected on a behavioural level in the *complexity* of a systems output (Vaillancourt & Newell, 2002; Sleimen-Malkoun et al., 2014).

Chapter Eight

Part B

Neural mechanisms underpinning fatigue-related alterations in the complexity, entropy and variability of isometric knee extensor torque signals.

8.1b - Introduction

Neuromuscular fatigue extends beyond a reduction in torque-generating capacity (Taylor & Gandevia, 2008); it is also characterised by a decline in neuromuscular complexity (Pethick et al., 2015, 2016). This reduction in complexity has been consistently observed in KE torque signals during isometric contractions, as demonstrated by numerous studies employing diverse methodological approaches (see Pethick et al., 2021b; Pethick & Tallent, 2022, for reviews). Similarly, age-related declines in neuromuscular complexity have been reported across various muscle groups, including the KE muscles (Fiogbe et al., 2021). Consistent with these findings, the current thesis also observed a lower neuromuscular complexity in the KE muscles of older adults compared to younger adults (Chapter Six).

The fatigue and age-related reductions in neuromuscular complexity is suggested to reflect a reduction in the functionality and adaptability of the neuromuscular system (Lipsitz & Goldberger, 1992; Manor & Lipsitz, 2013; Peng et al., 2009). As such, a reduction in muscle torque complexity is suggested to have functional implications for the performance of fundamental motor skills (Pethick et al., 2022). Indeed, the current thesis has demonstrated that lower KE torque signal complexity may partly explain worse performance of fundamental motor skills, as such impaired balance (i.e., increased postural sway; Chapter Six). Although fatigue-related reductions in locomotor muscle torque complexity may have a deleterious impact on motor skills, potentially further increasing fall risk in older adults, the effect of age on changes in isometric KE complexity due to fatigue remains to be established. Moreover, the mechanisms underpinning the fatigue-related loss of isometric KE torque complexity remain unclear.

Maintenance of a constant muscle torque during fatiguing submaximal intermittent isometric contractions requires adaptive neural strategies to compensate for decreases in the torque producing capacity of the muscle (Rossato et al., 2022; Valenčič et al., 2024). These neural strategies include the recruitment of additional MUs and modulation of their discharge rates, which initially remain stable, followed by a progressive increase toward task failure, likely driven by increased common synaptic input to motor neurons innervating the fatiguing muscles (Contessa et al., 2009; Castronovo et al., 2015; McManus et al., 2016; Rossato et al., 2022; Valenčič et al., 2024).

The presence of common synaptic input is required for the effective regulation of muscle torque (Farina & Negro, 2015), however, too much common synaptic input and consequently MU synchronisation, may be deleterious to motor control (Baker et al., 1992; Yao et al., 2009). Indeed, research has found that fatigue-related increases in the low-frequency bands of common synaptic input were explanatory of the increased variability of isometric muscle torque (Contessa et al., 2009; Castronovo et al., 2015; McManus et al., 2016). Likewise, age-related increases in the variability of isometric muscle torque have been associated with the increased strength of low-frequency oscillations in common synaptic input (Castronovo et al., 2018). These findings demonstrate that too common synaptic input, due to age and/or neuromuscular fatigue, may prove maladaptive to motor control.

Research employing cross-correlation analyses has demonstrated that low-frequency oscillations (<10 Hz) in common synaptic input, representing effective neural drive, to closely resemble the structure of the muscle torque signal (Dideriksen et al., 2012; Mazzo et al., 2022; Negro et al., 2009; Thompson et al., 2018). Theoretically, fatigue-induced increases in the strength of common synaptic input and accompanying MU synchronisation, are expected to result in less complex (i.e., smoother and more regular) oscillatory patterns in the common synaptic input. These changes then manifest as a reduction in the complexity of the muscle torque signal. Consequently, it has been postulated that the fatigue-related decrease in isometric KE muscle torque complexity may be attributed, in part, to an increase in common synaptic input to the motor neuron pool (Pethick et al., 2016; Pethick et al., 2021b).

Chapter Eight A presented the first evidence to show that the strength of common synaptic input to the motor neurons innervating the VL muscle was explanatory of fresh isometric KE torque signal complexity. However, in contrast with the hypothesis of previous researchers (Pethick et al., 2016, 2021b), it was found that stronger common synaptic input in the alpha frequency band during fresh isometric KE contractions was associated with higher complexity torque signals (see Chapter Eight - Part A for the full discussion). Nevertheless, it stands to reason that common synaptic input may be able to explain the fatigue-related reduction in isometric KE torque signal complexity. The primary aim of the current study was to investigate whether the fatigue-related changes in the strength of common synaptic input to the VL muscle could explain fatigue-related changes in isometric KE torque signal complexity.

Recent research has shown a concurrent loss of isometric ankle torque complexity and low pass filtered CST complexity derived from the TA muscle during fatiguing contractions (Hunter, 2023). The fatigue-related decrease in ankle torque complexity was suggested to be a consequence of the decrease in CST complexity (Hunter, 2023). However, Chapter Eight A did not find smoothed CST complexity to be associated with KE torque complexity during fresh isometric KE contractions (see Chapter Eight - Part A). Nevertheless, further research is required to substantiate whether a fatigue-related change in CST complexity accompanies a fatigue-related change in muscle torque complexity.

The interference HD sEMG signal represents the global neural drive to the muscle (the summation of all MU action potentials recorded by the HD sEMG electrode grid). Research has shown a fatigue-related decline in sEMG signal complexity derived from the KE muscles (Beretta-Piccoli et al., 2015; Hernandez & Camic, 2019) and the biceps brachii (Cashaback et al., 2013). Notably, the MU synchronisation, that accompanies increased common synaptic input, was implicated in the fatigue-related loss of sEMG complexity (Beretta-Piccoli et al., 2015). The association between fatigue-related changes in the complexity of muscle torque and the complexity of interference HD sEMG signals has not yet been explored. Therefore, the secondary aim of the current study was to establish whether fatigue-related changes in the complexity and variability of isometric KE torque were accompanied by changes in the complexity and variability of low-pass filtered CSTs and interference HD sEMG signals from the VL muscle.

Aims and Hypotheses.

The three aims of the current experimental chapter were:

(1) To investigate whether the fatigue-related changes in the strength of common synaptic input to the VL muscle is explanatory of fatigue-related changes in the complexity, entropy and variability of isometric KE torque signals.
(2) To establish whether fatigue-related changes in the complexity and variability of isometric KE torque were accompanied by changes in the complexity and variability of low-pass filtered CSTs and interference HD sEMG signals from the VL muscle.
(3) To determine the strength of association between the effective neural drive to the VL muscle and fluctuations in isometric KE torque during fresh and fatigued contractions.

It was hypothesised that:

(1) Fatigue would increase the strength of common synaptic input to the VL muscle and would be explanatory of a fatigue-related decrease in the complexity and entropy and increase in the variability of isometric KE torque signals.

(2) The fatigue-related decrease in the complexity and entropy and increase in the variability of isometric KE torque signals will be associated with a decrease in the complexity and entropy and increase in the variability of the CST and interference HD sEMG signals.

(3) Effective neural drive would be strongly cross-correlated with isometric KE torque during fresh and fatigued contractions.

8.2b - Methods

8.2.1. Participants.

Sixty healthy participants (56 male; 4 female) aged between 18 and 90 were recruited to participate in the study. Participants were recruited to be in three age groups, the YG were aged 18 to 30 years (N = 20; 17M, 3F), the MG were aged 31 to 49 years (N = 20; 19M, 1F), and the OG were aged 50 to 90 years (N = 20; 20M, 0F). The sixty participants of the current experimental chapter were the same as the participants of experimental Chapter Eight - Part A.

Before being allowed to participate in the study all potential participants provided written informed consent and completed a health questionnaire to ensure they were in full health. Participants were required to not have previous or current circulatory disorders, have no known or signs/symptoms of cardiovascular, neuromuscular, renal, or metabolic conditions. Participants were required to be living independently and able to perform active daily living tasks. All participants were regular exercisers, having performed above the World Health Organisation guidelines for ≥ 2 years (i.e., 2.5 to 5 hours of moderate exercise per week; Bull et al. 2020). Participant height was measured using a Seca portable stadiometer (Seca 217; Seca GmbH & Co. KG, Hamburg, Germany) and body mass measured using a Seca mechanical flat scale (Seca 760; Seca GmbH & Co. KG, Hamburg, Germany).

The study was completed with full ethical approval of the University of Kent Research Ethics Committee (Proposal number: 32_20_23), according to Declaration of Helsinki standards (but without being registered).

8.2.2. Experimental Design.

Each participant completed one experimental session. The participants' isometric KE MVT was first measured to establish the relative isometric contraction intensities for the subsequent isometric KE fatigue protocol. Participants were then familiarised with the KE torque control tasks by performing isometric KE contractions at 10 and 20% MVT. After familiarisation, participants performed the isometric KE fatigue protocol, while HD sEMG signals were recorded from the VL muscle.

8.2.3. Measurement of isometric knee extensor maximal voluntary torque.

Participants were set up on an isokinetic dynamometer (Cybex HUMAC Norm; CSMi, Stoughton, MA, USA), as outlined in Chapter Three - General Methods - Section 3.6. Once set up on the dynamometer participants performed a warm-up of ten submaximal contractions of increasing effort, after which four (6 second) MVCs were performed to establish MVT (each MVC separated by 60 second rest). The highest torque value from a 2 second epoch was recorded as the participant's MVT, which was then used to set the relative constant load isometric contraction intensities of 20% and 60% MVT to be used in the measurement of fresh and fatigued isometric KE torque control.

The isometric KE torque data were recorded at 2048 Hz via a CED Micro 1401-3 (Cambridge Electronic Design, Cambridge, UK), interfaced with a personal desktop computer, with data collected (Spike2, Cambridge Electronic Design) and exported at 1000 Hz for complexity analysis and at 2048 Hz for cross-correlation analysis offline in MATLAB (R2023a; The MathWorks, Natick, MA, USA).

8.2.4. Isometric knee extensor torque fatigue protocol.

Prior to commencing the muscle torque control tasks participants were familiarised with matching their instantaneous KE torque output to a thin line (1 mm thick) superimposed on the computer monitor at 10 and 20% MVT.

After familiarisation participants performed three 20 second fresh isometric KE contractions at 20% MVT, with 120 seconds recovery between each contraction. Contractions lasting 20 seconds were used to ensure that the target torque (20% MVT) was met for > 10 seconds, while ensuring that the contractions did not induce fatigue.

The fresh isometric contractions were followed by repeated 3 second isometric KE contractions at 60% MVT to task failure, with 2 seconds recovery between contractions. The isometric contraction intensity at 60% MVT was selected to be above the participants' critical torque (Pethick et al., 2016). Task failure was defined as the participant being unable to meet the required torque (60% MVT) for two consecutive contractions. The task also ended if the participant completed 100 contractions. Eight of the sixty participants reached 100 contractions. Immediately (2 seconds) following task failure the participant completed one 20 second isometric KE contraction at 20% MVT, as the measure of fatigued KE torque (Figure

8.1b). The time to task failure (TTF) of the 60% MVT task was recorded as the measure of task performance.

The isometric KE contraction intensity was set at 20% MVT for the measurement of fresh and fatigued KE torque control as this intensity demonstrated the highest yield of MU from the VL muscle in pilot testing when the interference HD sEMG signals were decomposed.

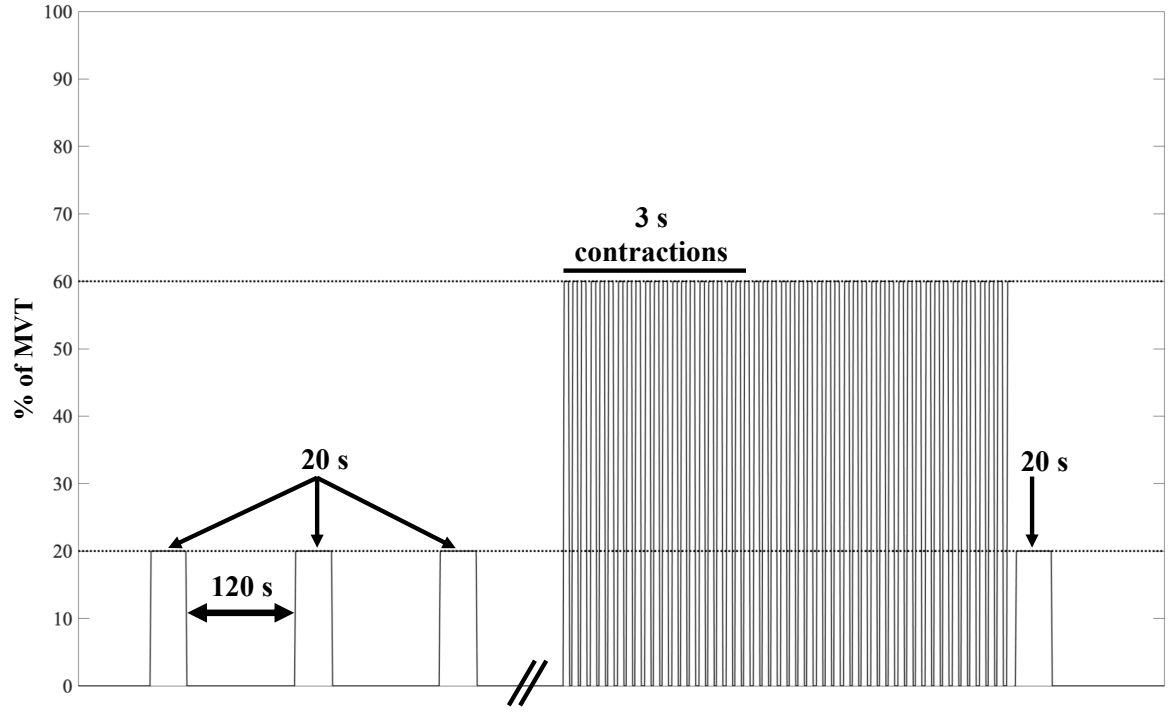

Figure 8.1b. Schematic of the isometric knee extensor fatigue protocol. Participants completed three 20 second fresh isometric knee extensor contractions at 20% MVT with 120 seconds recovery, followed by repeated 3 second isometric knee extensor contractions at 60% MVT to task failure (or completion of 100 repetitions) with 2 seconds recovery between each contraction, immediately (2 second) followed by a 'fatigued' isometric knee extensor contraction at 20% MVT (MVT = maximal voluntary torque).

8.2.5. High density surface electromyography data collection.

Prior to the torque control tasks participants were set up with a HD sEMG array on the right VL muscle as outlined in Chapter Three - General Methods - Section 3.10 - *HD sEMG: Setup and signal acquisition*. The HD sEMG signals were recorded throughout the three fresh and one fatigued 20 second isometric knee extensor contractions at 20% MVT as outlined in Chapter Three - General Methods - Section 3.10 - *HD sEMG: Setup and signal acquisition*.

8.2.6. High density surface electromyography data analysis.

HD sEMG: Motor unit decomposition

The HD sEMG signals were decomposed offline into MU spike trains, as outlined in Chapter Three - General Methods - Section 3.10 - *HD sEMG: Motor unit decomposition.* Before further analysis of the binary MU spike trains, the steadiest 10 second epoch of muscle torque time series from the 20 second fresh and fatigued KE at 20% MVT was identified as the epoch with the lowest SD. The binary MU discharges from the same 10 second epoch were extracted for further analysis.

Fifty-eight participants provided ≥ 6 MU during each of the three fresh isometric KE contractions at 20% MVT. However, only thirty-six of the sixty participants provided the minimum number of MU (≥ 6 MU) required for within-muscle coherence analysis during the fatigued isometric KE contractions at 20% MVT (Dideriksen et al., 2018). As such only these thirty-six participants data were used in all further analysis of the study.

The MUs decomposed during the fresh and fatigued isometric KE contractions at 20% MVT were potentially different, due to increased MU recruitment during the fatigued contraction. Like Castronovo et al. (2015), MUs were not tracked across contractions, because it was demonstrated that coherence estimates were not associated with differences in recruitment threshold. Moreover, only MUs active for the full 20 seconds of the isometric KE contractions were used in the within-muscle MU coherence analysis.

Estimation of within-muscle motor unit coherence

To assess the neural connectivity between MUs of the VL muscle during the fresh and fatigued isometric KE contractions at 20% MVT, within-muscle (intra-muscle) coherence was estimated from the decomposed MU spike trains. Within-muscle coherence was estimated as outlined in General Methods - Section 3.10 - *Estimation of within-muscle motor unit coherence* and reported as the transformed Z-scores.

The coherence value at a given frequency represents the correlation between two signals (i.e., two CSTs of equal number of MUs). Coherence was calculated in the low-frequency delta bandwidth (0-5 Hz), which has been shown to be the dominant frequency of voluntary control in the muscle torque output and represents common neural drive to the muscle (Farina & Negro

2015). Coherence was also calculated across the frequency bands: Alpha (5-15 Hz), Low beta (15-21 Hz), High beta (21-35 Hz) and Piper (35-50 Hz). The higher the coherence value, for the same number of MUs involved in the coherence estimation, indicates a greater strength of common synaptic input to the motor neuron pool.

Calculation of smoothed motor unit cumulative spike trains

The spike trains of each active MU during the steadiest 10 second epoch of the 20 second fresh and fatigued 20% MVT were summed to produce CST. To extract the low-frequency components of effective neural drive to the muscle, representative of torque fluctuation dynamics, the CSTs were smoothed with a 400-ms Hann window (see Chapter Three - General Methods - Section 3.10 - *Calculation of smoothed motor unit cumulative spike trains*). The complexity, entropy and variability of the smoothed CSTs was then determined using, SampEn, DFA, CI-28, SD and CV as outlined in General Methods - Sections 3.8 and 3.9.

Interference EMG signal processing and analysis

As outlined in full detail in General Methods - Section 3.10 - *Interference EMG signal processing and analysis,* the interference EMG signals from the accepted channels were summed to generate a single interference EMG signal representing the global neural drive to the VL muscle (summation of all the action potentials recorded by the HD sEMG grid). Before further analysis a 10 second epoch of the summed interference EMG signal was extracted, corresponding to the steadiest 10 second epoch of muscle torque time series from the 20 second fresh and fatigued KE at 20% MVT.

The PSD of the 10 second epoch of the summed interference EMG signal (filtered with a 4^{th} order Butterworth filter with low-pass cut-off frequency of 500 Hz) was then calculated. The filtered interference EMG signals were also full-wave rectified and subjected to the complexity, entropy and variability analysis; SampEn, DFA, CI-28, SD and CV as outlined in General Methods - Sections 3.8 and 3.9. The DFA α of both smoothed CST and interference EMG signals were calculated with 76 box sizes ranging from 2000 to 4 data points.

8.2.7. Torque signal complexity, entropy, and variability metric analysis.

The most accurate fresh isometric KE contraction at 20% MVT, identified as the contraction with the lowest RMSE, was used for comparison to the fatigued isometric KE contraction at 20% MVT. Prior to the calculation of the KE muscle torque signal complexity, entropy and

variability metrics, the steadiest 10 seconds of fresh and fatigued isometric KE contraction at 20% MVT was identified as the 10 seconds with the lowest SD, as proposed by Pethick et al. (2015).

The SDT, CVT and RMSE which quantify the variability and accuracy of torque signal were calculated as outlined in Chapter Three - General Methods - Section 3.8. The complexity and entropy metrics, SampEn, DFA, MSE and CI-28 were calculated as outlined in Chapter Three - General Methods - Section 3.9.

8.2.8. Cross-correlation analysis of torque and effective neural drive.

The individual binary MU spike trains from the steadiest 10 second epoch of the isometric contraction were summed to produce a CST. To extract the low-frequency components of effective neural drive to the muscle, representative of torque fluctuation dynamics, the CSTs were smoothed with a 400-ms Hann window, and high pass filtered (0.75 Hz, 2^{nd} order zero-lag, Butterworth) to remove trends and isolate the fluctuations in neural drive (Mazzo et al., 2021; Negro et al., 2009; Thompson et al., 2018). The torque signal was low-pass filtered (20 Hz, 4^{th} order, Butterworth) and high-pass filtered (0.75 Hz, 2^{nd} order zero-lag, Butterworth) for comparison with the estimates of neural drive. The cross-correlation (time domain) between the estimates of effective neural drive (the CST) and isometric KE torque was calculated across the entire 10 second contraction (Mazzo et al., 2021; Negro et al., 2009; Thompson et al., 2018).

8.2.9. Statistical analysis.

The effect of age-group (YG, MG, and OG) on TTF was assessed with a one-way ANOVA.

The effects of condition (fresh vs. fatigued) and age-group (YG, MG, and OG) on all MU characteristic metrics, all torque signal complexity, entropy and variability metrics, all CST and interference HD sEMG signal metrics and the total power of the interference HD sEMG signal were assessed using a mixed-design two-way ANOVA, with condition as the within-subjects factor and age-group as the between-subjects factor.

The effect of condition (fresh vs. fatigued) on the within-muscle coherence Z-scores was assessed using a mixed ANOVA, with condition (fresh vs. fatigued) and frequency band (delta,

alpha, low beta, high beta and piper) as the within-subjects factor and age-group (YG, MG, and OG) as the between-subjects factor.

The effect of condition (fresh vs. fatigued) on the scale-to-scale behaviour of the MSE curves of the torque signals was assessed using a mixed ANOVA, with condition (fresh vs. fatigued) and coarse-grained scale (1 to 28) as within-subjects factor and age-group (YG, MG, and OG) as the between-subjects factor.

The relationship between the coherence Z-scores at each frequency band (delta, alpha, low beta, high beta and piper) and the torque signal complexity, entropy and variability metrics (DFA, MSE, SampEn, CVT, SDT and RMSE) were established using a Pearson's bivariate two-tailed correlation. Following this, a hierarchical, multiple, linear regression analysis was conducted to assess the relationship between alpha band coherence Z-scores and the torque signal complexity, entropy and variability metrics (DFA, MSE, CI-28, CVT, SDT and RMSE). Participant age and the absolute intensity at 20% MVT were entered in the first step as independent covariates, and the alpha band coherence Z-scores were added in the second step as the primary independent variable to explain variance in each dependent variable (DFA, MSE, CI-28, CVT, SDT and RMSE) separately.

Hierarchical multiple linear regression analyses were conducted to assess the relationship between fatigue-related changes in alpha band coherence Z-scores and fatigue-related changes in torque signal complexity, entropy, and variability metrics (DFA, MSE, CI-28, CVT, SDT, and RMSE). Participant age and TTF were entered in the first step as independent covariates, and fatigue-related changes in alpha band coherence Z-scores were added in the second step as the primary independent variable to explain variance in each dependent variable (DFA, MSE, CI-28, CVT, SDT and RMSE) separately.

Hierarchical multiple linear regression analyses were conducted to assess the relationship between fatigue-related changes in the torque signal metrics (SampEn, CVT, and SDT) and corresponding changes in the CST signal and interference HD sEMG signal metrics (SampEn, CV, and SD). Participant age and TTF were entered in the first step as independent covariates, and the corresponding CST signal or interference HD sEMG signal metrics were added in the second step as the primary independent variable to explain variance in each dependent variable (SampEn, CVT, and SDT) separately.

Statistical assumptions of linearity, additivity, homoscedasticity, multicollinearity, independence of residuals, and normality of residuals were checked and accepted unless otherwise stated. Multicollinearity among the independent variables was identified using the variance inflation factor. Multicollinearity was considered acceptable if the variance inflation factor was between 1 and 5 (Frost, 2019) and the condition index was < 10.

Bonferroni *post hoc* comparisons were used when a main effect or interaction was significant. The significance level was set at $P < 0.05$ in all cases. Statistical analyses were performed in IBM SPSS statistics 29 (IBM Corp., Armonk, NY, United States).

8.3b - Results

8.3.1. Participant characteristics and anthropometrics.

Of the sixty participants, thirty-six provided enough MUs (≥ 6 MU) required for within-muscle coherence analysis during both the fresh and fatigued isometric KE at 20% MVT. As such, only these thirty-six participants data were used in all further analysis. Table 8.1b presents the participant characteristics of the thirty-six participants.

Table 8.1b Participant characteristics.

	All Participants	Younger Group	Middle Group	Older Group
N	36 (35M, 1F)	9 (9M, 0F)	14 (13M, 1F)	13 (13M, 0F)
Age (years)	44.3 ± 15.4	25.8 ± 3.7	41.0 ± 4.2	60.7 ± 10.3
Height (cm)	177.6 ± 7.0	180.2 ± 2.9	176.5 ± 9.0	176.8 ± 6.5
Mass (kg)	74.2 ± 10.3	69.1 ± 7.9	73.5 ± 10.8	78.7 ± 10.0
VL Skinfold (mm)	7.0 ± 3.1	7.3 ± 3.7	7.7 ± 2.5	6.1 ± 3.1
MVT (Nm)	184.6 ± 61.6	236.9 ± 62.7	185.4 ± 61.3	147.6 ± 28.9
20% MVT (Nm)	36.9 ± 12.3	47.4 ± 12.5	37.1 ± 12.3	29.5 ± 5.8
60% MVT (Nm)	110.8 ± 37.0	142.2 ± 37.6	111.2 ± 36.8	88.6 ± 17.3

Abbreviations: MVT = maximal voluntary torque; VL = vastus lateralis muscle (data are mean ± SD).

TTF was significantly longer for the OG (399.6 ± 116.1 seconds), in comparison to the YG (273.9 ± 157.2 seconds; $P = 0.011$). There was no significant difference in TTF between the MG (310.4 ± 114.1 seconds) and OG ($P = 0.201$) or YG ($P = 1.000$).

8.3.2. Motor unit characteristics.

Table 8.2b presents the MU characteristics and ANOVA results of the thirty-six participants who provided ≥ 6 MU during both the fresh and fatigued isometric KE contractions at 20% MVT. There was no difference in number of MUs decomposed and accepted from the fresh and fatigued isometric KE contractions at 20% MVT ($P = 0.161$; Table 8.2b).

Table 8.2b Motor unit characteristics from the fresh and fatigued contractions.

					F, *P* and η_p^2 values		
		Fresh 20% MVT	Fatigued 20% MVT		Condition	Age Group	Condition by Age
Total MU (*N*)	All	330	314				
	YG	73	65				
	MG	118	112				
	OG	139	137				
MU per Contraction (*N*)	All	9.17 ± 3.31	8.72 ± 3.29	*F*	2.055	3.344	0.354
	YG	8.11 ± 1.36	7.22 ± 1.30	*P*	0.161	**0.048**	0.704
	MG	8.43 ± 2.71	8.00 ± 2.29	η_p^2	0.059	0.169	0.021
	OG	10.69 ± 4.33	10.54 ± 4.35				
DR (PPS)	All	8.80 ± 1.61	8.82 ± 1.74	*F*	0.090	9.515	0.588
	YG	9.88 ± 1.49	10.35 ± 1.82	*P*	0.766	**<0.001**	0.561
	MG	9.01 ± 1.49	8.85 ± 1.42	η_p^2	0.003	0.366	0.034
	OG	7.82 ± 1.32	7.73 ± 1.16				
Mean ISI (ms)	All	114.17 ± 17.74	121.78 ± 22.86	*F*	4.583	10.469	0.585
	YG	102.08 ± 10.06	104.09 ± 19.34	*P*	**0.040**	**<0.001**	0.563
	MG	111.08 ± 17.12	119.10 ± 18.81	η_p^2	0.122	0.388	0.034
	OG	125.88 ± 16.23	136.90 ± 20.01				
CV of ISI (%)	All	19.63 ± 3.45	20.87 ± 4.12	*F*	5.368	4.060	1.227
	YG	21.10 ± 4.12	23.49 ± 2.58	*P*	**0.027**	**0.027**	0.306
	MG	19.82 ± 2.39	21.32 ± 3.68	η_p^2	0.140	0.197	0.069
	OG	18.42 ± 3.72	18.56 ± 4.39				

Abbreviations: CV = coefficient of variation; DR = discharge rate; ISI = interspike interval; MVT = maximal voluntary torque; MU = motor unit; PPS = pulses per second; Significant *P* values highlighted by bold font (data are mean ± SD).

8.3.3. Effect of fatigue and age-group on within-muscle coherence.

There was a significant main effect of condition (fresh vs. fatigued) on within-muscle coherence Z-scores ($F_{(1, 33)} = 11.603$; $P = 0.002$; $\eta_p^2 = 0.260$), indicating that overall, coherence Z-scores (all frequency bands) were higher during the fatigued contractions in comparison to the fresh contractions. *Post hoc* pairwise comparisons revealed the delta ($P = 0.003$), alpha ($P = 0.002$) and low beta ($P = 0.025$) frequency band coherence Z-scores to be significantly higher during the fatigued contraction in comparison to the fresh contractions (Figure 8.2b).

There was no main effect of age group on within-muscle coherence ($F_{(2, 33)} = 0.473$; $P = 0.627$; $\eta_p^2 = 0.028$), indicating that overall, coherence Z-scores (all frequency bands) were not different between the YG, MG, and OG. There was no condition (fresh vs. fatigued) by age

group interaction ($F_{(2, 33)} = 1.443$; $P = 0.251$; $\eta_p^2 = 0.080$), indicating that overall, the effect of age-group on the coherence Z-scores was consistent across both the fresh and fatigued conditions.

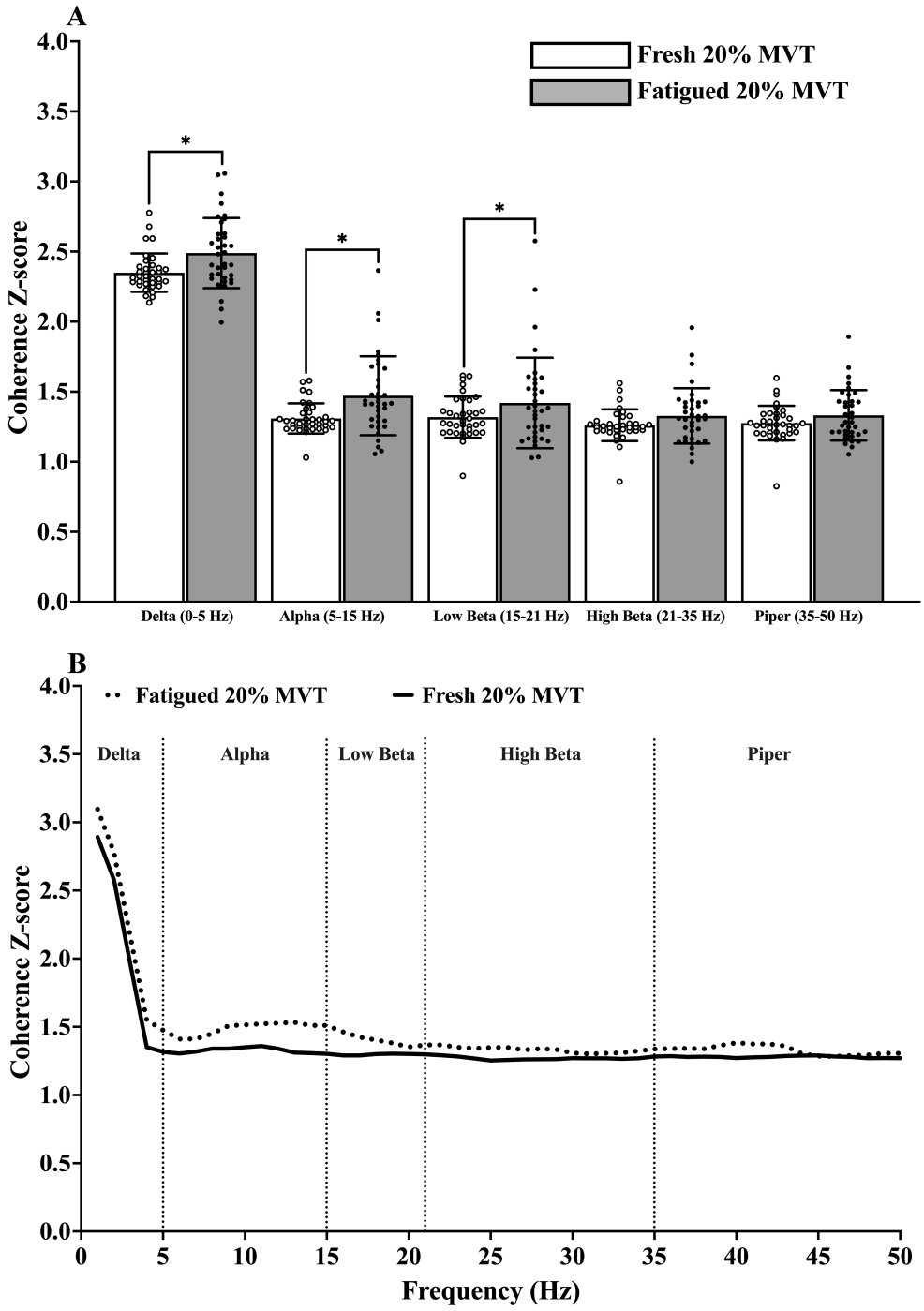

Figure 8.2b. (A) Individual participant ($N = 36$) within-muscle coherence Z-scores at the different frequency bands during the fresh (open circles) and fatigued (closed circles) isometric knee extensor contractions at 20% of maximal voluntary torque, **(B)** The group mean coherence Z-scores from 0 to 50 Hz of the fresh (solid line) and fatigued (dashed line) isometric knee extensor contractions at 20% of maximal voluntary torque (* = $P < 0.05$).

8.3.4. Effect of fatigue and age-group on isometric knee extensor torque signal complexity, entropy and variability.

Multiscale entropy curve results

There was no main effect of condition (fresh vs. fatigued; $F_{(1, 33)} = 1.949$; $P = 0.172$; $\eta_p^2 = 0.056$), no main effect of age group ($F_{(2, 33)} = 1.000$; $P = 0.379$; $\eta_p^2 = 0.057$) and no condition by age group interaction ($F_{(2, 33)} = 0.613$; $P = 0.548$; $\eta_p^2 = 0.036$), for SampEn calculated across the 28 coarse-grained scales of the MSE curve.

There was a main effect of coarse-grained scale ($F_{(27, 891)} = 189.126$; $P < 0.0001$; $\eta_p^2 = 0.851$) and a significant condition (fresh vs. fatigued) by coarse-grained scale interaction ($F_{(27, 891)} = 38.722$; $P < 0.0001$; $\eta_p^2 = 0.540$). *Post hoc* pairwise comparisons revealed at shorter scales (≤ scale 7) the fresh contractions exhibited significantly higher SampEn, in comparison to the fatigued contractions (all $P < 0.05$; Figure 8.3b). At longer (coarser) scales (≥ scale 13) the fatigued contractions exhibited significantly higher SampEn, in comparison to the fresh contractions (all $P < 0.05$; Figure 8.3b).

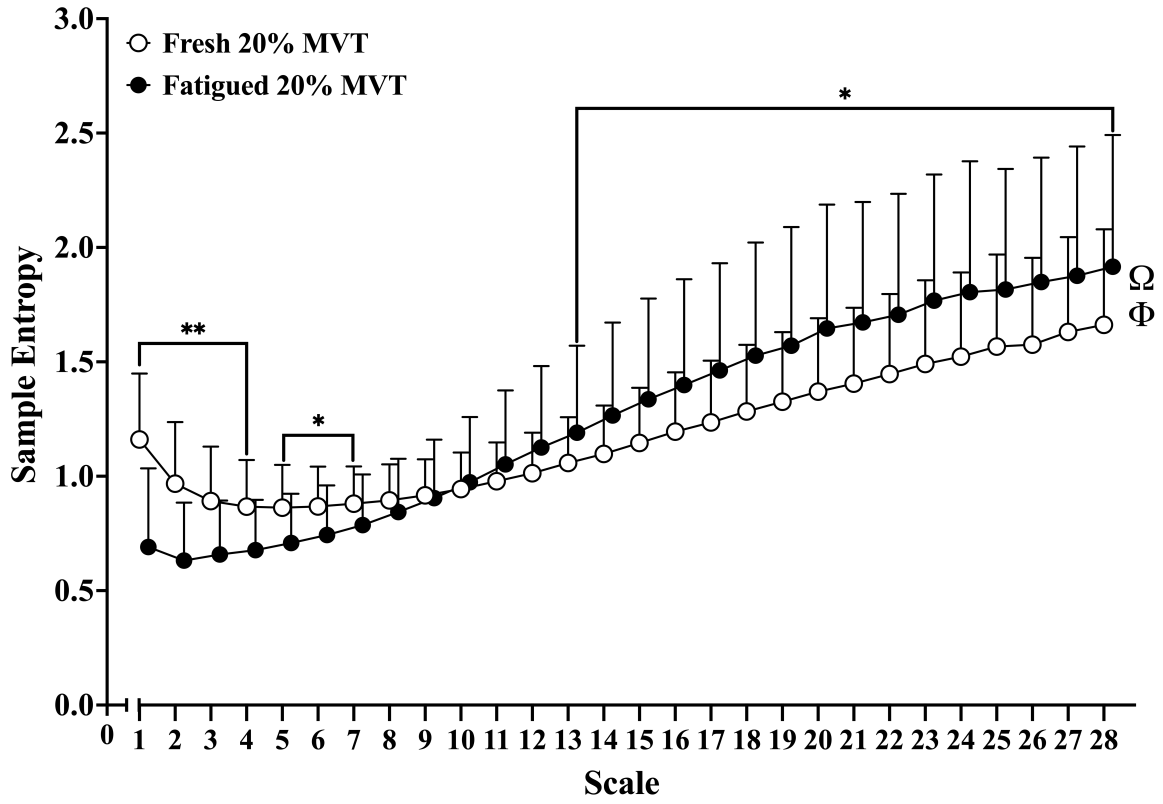

Figure 8.3b. Multiscale entropy curve of sample entropy calculated from the torque signals of the fresh and fatigued isometric knee extensor contractions at 20% of maximal voluntary torque (open circles = fresh 20% MVT; closed circles = fatigued 20% MVT; MVT = maximal voluntary torque; Ω = significant main effect of scale; Φ = significant condition by scale interaction; * = $P < 0.05$; ** = $P < 0.001$).

Complexity index results

There was no main effect of condition (fresh vs. fatigued; $F_{(1, 33)} = 1.950$; $P = 0.172$; $\eta_p^{2.} = 0.056$), no main effect of age group ($F_{(2, 33)} = 1.000$; $P = 0.379$; $\eta_p^{2.} = 0.057$) and no significant condition by age group interaction ($F_{(2, 33)} = 0.613$; $P = 0.548$; $\eta_p^{2.} = 0.036$) for the CI-28 metric (Figure 8.4b.A).

Detrended fluctuation analysis results

There was no main effect of condition (fresh vs. fatigued; $F_{(1, 33)} = 3.560$; $P = 0.068$; $\eta_p^{2.} = 0.097$), no main effect of age group ($F_{(2, 33)} = 0.783$; $P = 0.465$; $\eta_p^{2.} = 0.045$) and no significant condition by age group interaction ($F_{(2, 33)} = 0.207$; $P = 0.814$; $\eta_p^{2.} = 0.012$) for the DFA α metric (Figure 8.4b.B).

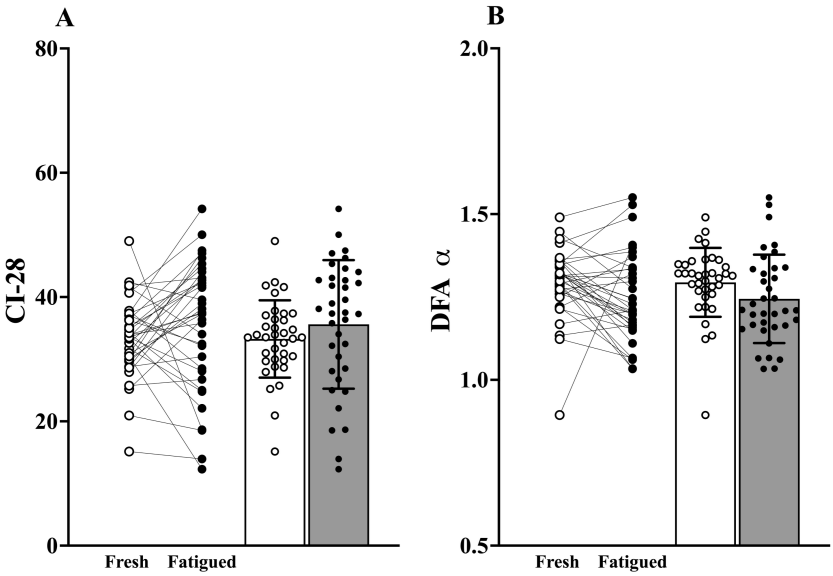

Figure 8.4b. Before-after and bar plots of the complexity metrics calculated from the torque signals of the fresh and fatigued isometric knee extensor contractions at 20% of maximal voluntary torque **(A)** Complexity index under 28 coarse-grained scales, **(B)** Detrended fluctuation analysis scaling exponent α (open circles = fresh of 20% MVT; closed circles = fatigued 20% MVT).

Variability metric results

The CVT (main effect of condition, $F_{(1, 33)} = 43.331$; $P < 0.0001$; $\eta_p^{2.} = 0.568$; Figure 8.5b.A), SDT (main effect of condition, $F_{(1, 33)} = 45.041$; $P < 0.0001$; $\eta_p^{2.} = 0.577$; Figure 8.5b.B) and RMSE of torque (main effect of condition, $F_{(1, 33)} = 22.300$; $P < 0.001$; $\eta_p^{2.} = 0.403$; Figure 8.5b.C) were significantly higher during fatigued isometric KE at 20% MVT in comparison to the fresh isometric KE at 20% MVT.

There was no effect of age group on the CVT ($F_{(2, 33)} = 0.292$; $P = 0.749$; $\eta_p^{2.} = 0.017$), the SDT ($F_{(2, 33)} = 2.031$; $P = 0.147$; $\eta_p^{2.} = 0.110$), and the RMSE of torque ($F_{(2, 33)} = 3.054$; $P = 0.061$; $\eta_p^{2.} = 0.156$). There was no condition by age group interaction for the CVT ($F_{(2, 33)} = 0.833$; $P = 0.444$; $\eta_p^{2.} = 0.048$), the SDT ($F_{(2, 33)} = 1.579$; $P = 0.221$; $\eta_p^{2.} = 0.087$), and the RMSE of torque ($F_{(2, 33)} = 1.270$; $P = 0.294$; $\eta_p^{2.} = 0.071$).

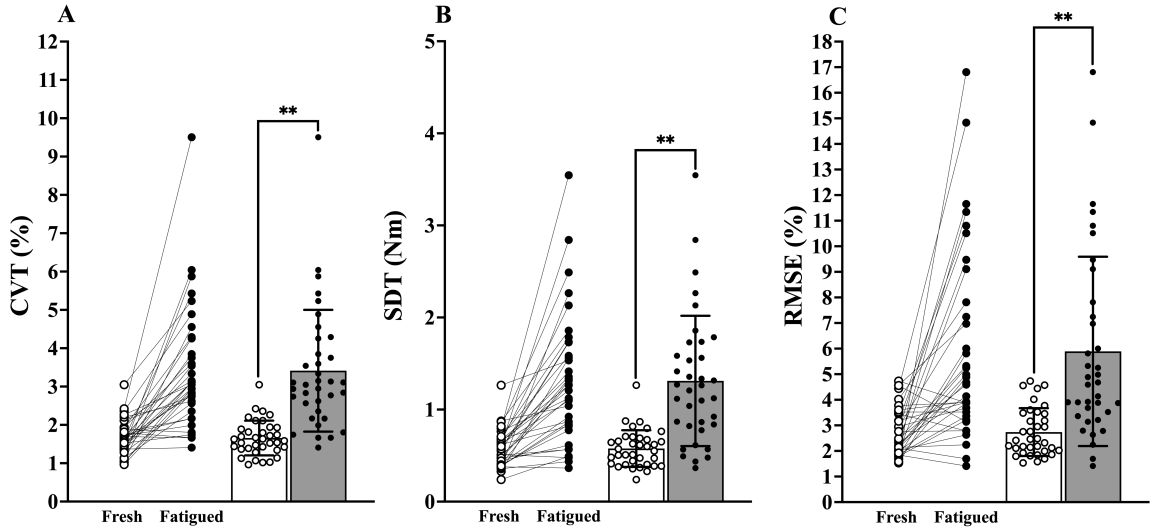

Figure 8.5b. Before-after and bar plots of the variability metrics calculated from the torque signals of the fresh and fatigued isometric knee extensor contractions at 20% of maximal voluntary torque **(A)** Coefficient of variation of torque, **(B)** Standard deviation of torque, **(C)** Root mean square error of torque (open circles = fresh 20% MVT; closed circles = fatigued 20% MVT; main effect of condition ** = $P < 0.001$).

8.3.5. Relationship between within-muscle coherence and the isometric knee extensor torque signal complexity, entropy and variability metrics.

The hierarchical, multiple, linear regression analysis revealed alpha band coherence Z-scores to be significantly associated with SampEn of the coarse-grained torque signal from scales 9 to 28 during both the fresh and fatigued isometric KE at 20% MVT (all $P < 0.05$; Figure 8.6b.A). Alpha band coherence Z-scores were not significantly associated with SampEn at scale 1 (i.e., SampEn of the original torque signal) during both the fresh ($P = 0.883$) and fatigued ($P = 0.399$) isometric KE at 20% MVT (Table 8.3b; Figure 8.6b.A).

Alpha band coherence explained 24.0% of the variance in SampEn at scale 28 during the fresh KE contractions (Table 8.3b; Figure 8.6b.A) and explained 11.9% of the variance in SampEn at scale 28 during the fatigued KE contractions (Table 8.3b; Figure 8.6b.A).

The fatigue-related Δalpha band coherence Z-scores were significantly associated with the fatigue-related ΔSampEn of the coarse-grained torque signal from scales 11 to 28 (all $P < 0.05$; Figure 8.6b.B). The fatigue-related Δalpha band coherence Z-scores were not significantly associated with the fatigue-related ΔSampEn at scale 1 (Table 8.3b; Figure 8.6b.B). In contrast, the fatigue-related Δalpha band coherence explained 11.5% of the variance in the fatigue-related ΔSampEn at scale 28 (Table 8.3b; Figure 8.6b.B).

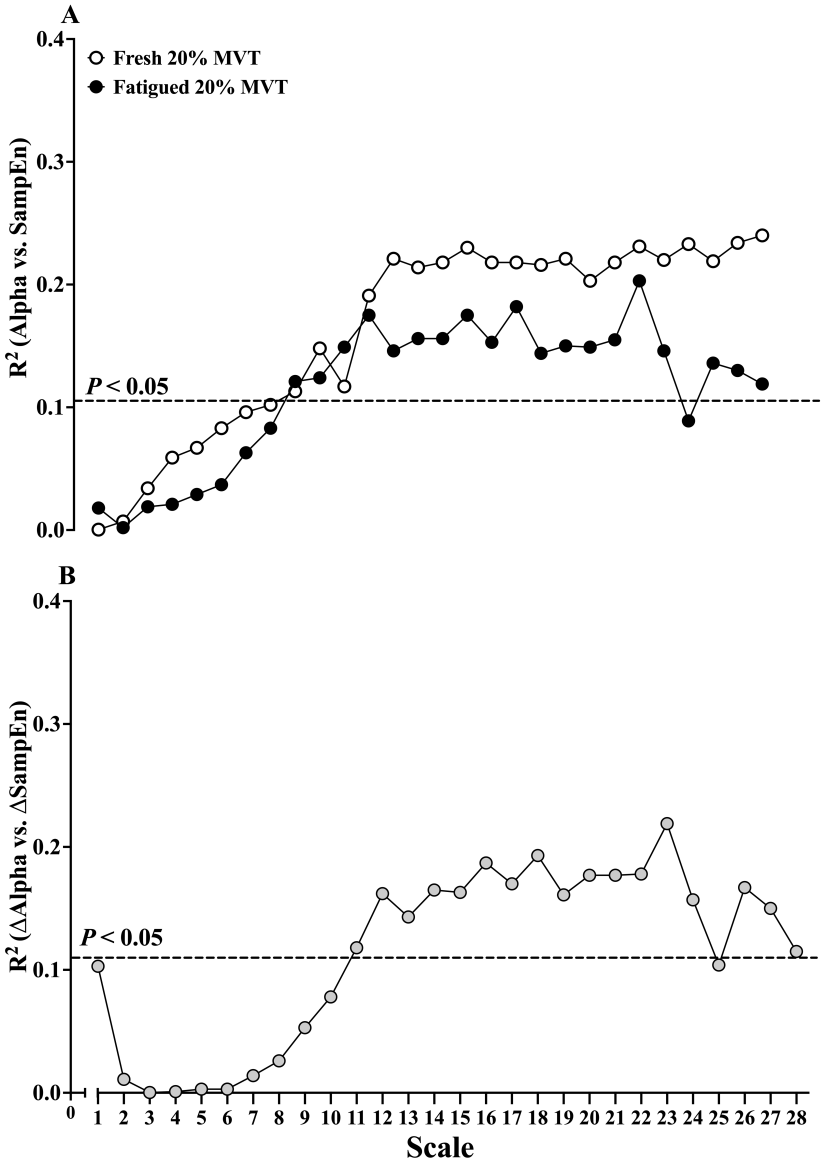

Figure 8.6b. (A) Relationship (R^2 values) between the alpha band coherence Z-scores and the sample entropy at each coarse-grained scale of the multiscale entropy analysis derived from the fresh and fatigued isometric knee extensor contractions at 20% of maximal voluntary torque, **(B)** Relationship (R^2 values) between the fatigued-related change in alpha band coherence Z-scores and the fatigue-related change in sample entropy at each coarse-grained scale of the multiscale entropy analysis (open circles = fresh 20% MVT; closed circles = fatigued 20% MVT; grey circles = ΔAlpha vs. ΔSampEn; MVT = maximal voluntary torque; SampEn = sample entropy; dashed line = significant correlation $P < 0.05$).

Table 8.3b presents the statistics from the hierarchical, multiple, linear regression analysis assessing the relationship between alpha band coherence Z-scores and the complexity (DFA and CI-28), entropy (SampEn) and variability (CVT, SDT and RMSE) of the isometric KE muscle torque signals. Table 8.3b also presents the statistics from the hierarchical, multiple, linear regression analysis assessing the relationship between the fatigue-related change in alpha band coherence Z-scores and the fatigue-related change in the complexity (DFA and CI-28), entropy (SampEn) and variability (CVT, SDT and RMSE) of the isometric KE muscle torque signal.

Alpha band coherence explained 23.1% and 13.6% of the variance in the CI-28 torque metric during the fresh and fatigued KE contractions respectively (Table 8.3b). The fatigue-related Δalpha band coherence explained 11.8% of the variance in the fatigue-related ΔCI-28 torque metric (Table 8.3b)**.** Alpha band coherence explained 31.4% and 12.0% of the variance in DFA α of the torque signal during the fresh and fatigued KE contractions respectively (Table 8.3b). The fatigue-related Δalpha band coherence explained 9.4% of the variance in the fatigue-related ΔDFA α (Table 8.3b).

The fatigued-related Δalpha band coherence could explain 19.0%, 21.7% and 13.6% of the variance in the fatigued-related ΔCVT, ΔSDT and ΔRMSE respectively (Table 8.3b).

Alpha band coherence could explain 15.0% and 13.2% of the variance in the CVT and SDT respectively, during the fatigued KE contractions at 20% MVT. In comparison, alpha band coherence was not associated with the CVT or SDT during the fresh KE contractions at 20% MVT (Table 8.3b).

Table 8.3b Statistics from the hierarchical, multiple, linear regression analyses of the torque signal complexity, entropy and variability metrics.

	Dependent Variables	Independent Predictor Variable: Alpha Band Coherence			
		R^2	β Coef.	*P*	Δ*F*
Fresh 20% MVT	DFA α	0.314	-0.568	**<0.001**	14.938
	CI-28	0.231	0.487	**<0.001**	10.850
	SampEn Scale 1	<0.001	-0.021	0.883	0.022
	SampEn Scale 28	0.240	0.497	**0.001**	13.001
	CVT	0.004	0.020	0.901	0.016
	SDT	0.004	0.064	0.633	0.232
	RMSE	0.002	0.050	0.087	0.096
Fatigued 20% MVT	DFA α	0.120	-0.361	**0.036**	4.787
	CI-28	0.136	0.384	**0.019**	6.080
	SampEn Scale 1	0.018	-0.140	0.399	0.731
	SampEn Scale 28	0.119	0.360	**0.027**	5.353
	CVT	0.150	0.403	**0.024**	5.653
	SDT	0.132	0.378	**0.016**	6.422
	RMSE	0.076	0.287	0.111	2.689

	Dependent Variables	Independent Predictor Variable: Fatigue-related ΔAlpha Band Coherence			
		R^2	β Coef.	*P*	Δ*F*
Fatigue-related change	ΔDFA α	0.094	-0.322	**0.049**	4.184
	ΔCI-28	0.118	0.362	**0.040**	4.584
	ΔSampEn Scale 1	0.103	-0.337	0.064	3.672
	ΔSampEn Scale 28	0.115	0.356	**0.044**	4.388
	ΔCVT	0.190	0.458	**0.009**	7.839
	ΔSDT	0.217	0.491	**0.004**	9.705
	ΔRMSE	0.136	0.388	**0.032**	5.059

Abbreviations: CVT = Coefficient of variation of torque; DFAα = detrended fluctuation analysis scaling exponent α; CI-28 = complexity index under 28 coarse-grained scales of the torque multiscale entropy curves; MVT = maximal voluntary torque of the knee extensors; RMSE = Root mean square error of torque; SDT = Standard deviation of torque; Significant *P* values highlighted by bold font.

8.3.6. Effect of fatigue and age-group on the complexity, entropy and variability of the smoothed cumulative motor unit spike train signals.

Table 8.4b presents the descriptive statistics and ANOVA results for the effect of fatigue and age-group on the complexity, entropy and variability of the smoothed cumulative spike train signals.

Complexity index results

There was no main effect of condition (fresh vs. fatigued) on the CI-28 metric (Table 8.4b). There was a main effect of age group, but no condition by age group interaction on the CI-28 metric (Table 8.4b).

Detrended fluctuation analysis results

The DFA α of the CST signals were significantly higher during the fatigued KE at 20% MVT, in comparison to the fresh KE at 20% MVT (Table 8.4b). There was no main effect of age group and no condition by age group interaction on the DFA α of the CST signals (Table 8.4b).

Sample entropy results

The SampEn of the CST signals were significantly lower during the fatigued KE at 20% MVT, in comparison to the fresh KE at 20% MVT (Table 8.4b). There was no main effect of age group and no condition by age group interaction on the SampEn of the CST signals (Table 8.4b).

There was no association between the fatigue-related decline the CSTs signal SampEn at scale 1 and the fatigue-related decline in KE torque SampEn at scale 1 ($r < 0.001$; $R^2 < 0.001$; $P = 0.971$).

Variability metric results

The CV of the CST signals were significantly higher during the fatigued KE at 20% MVT, in comparison to the fresh KE at 20% MVT (Table 8.4b). There was no main effect of age group and no condition by age group interaction on the CV of the CST signals (Table 8.4b).

There was no main effect of condition (fresh vs. fatigued), no main effect of age group and no condition by age group interaction on the SD of the CST signals (Table 8.4b).

There was a significant relationship between the fatigued-related increase in the CV of the CST and the concurrent fatigue-related increase in the CVT ($r = 0.416$; $R^2 = 0.173$; $P = 0.009$; Figure 8.7b).

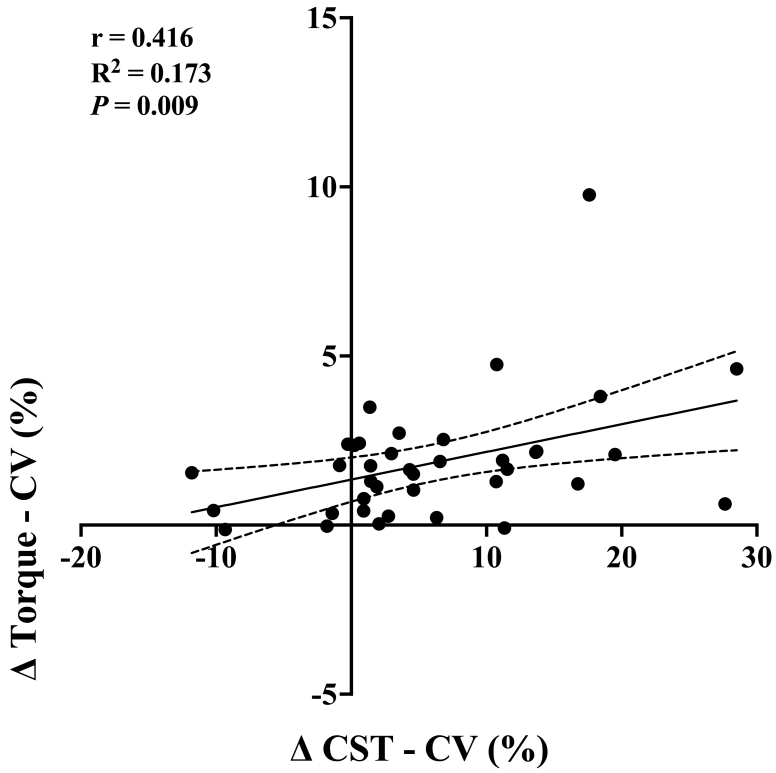

Figure 8.7b. Relationship between the fatigue-related change in the coefficient of variation of the smoothed cumulative spike train signals and the fatigued-related change in the coefficient of variation of torque.

Table 8.4b Descriptive statistics and ANOVA results for the effect of fatigue and age-group on the complexity, entropy and variability of the smoothed cumulative spike train signals.

						F, *P* and η_p^2 values		
		All Participants (*N* = 38)	Younger Group (*N* = 10)	Middle Group (*N* = 15)	Older Group (*N* = 13)		Main effect of condition	Main effect of age	Condition by Age Interaction
SD of CST	Fresh	0.017±0.004	0.017±0.002	0.017±0.004	0.017±0.005	*F*	0.007	0.543	1.710
	Fatigued	0.017±0.004	0.016±0.003	0.017±0.004	0.019±0.006	*P*	0.936	0.586	0.196
						η_p^2	<0.001	0.030	0.089
CV of CST (%)	Fresh	31.39±7.00	30.53±4.95	31.97±9.92	31.38±4.09	*F*	15.956	0.026	0.104
	Fatigued	37.42±9.61	37.70±5.62	37.49±11.51	37.11±10.28	*P*	**<0.001**	0.974	0.901
						η_p^2	0.313	0.001	0.006
SampEn (scale 1)	Fresh	0.17±0.02	0.17±0.02	0.17±0.02	0.17±0.02	*F*	9.335	0.284	0.523
	Fatigued	0.16±0.02	0.16±0.02	0.16±0.02	0.15±0.02	*P*	**0.004**	0.754	0.597
						η_p^2	0.211	0.016	0.029
DFA α	Fresh	1.52±0.03	1.52±0.03	1.52±0.03	1.52±0.04	*F*	12.328	0.192	0.532
	Fatigued	1.54±0.04	1.55±0.04	1.53±0.04	1.54±0.03	*P*	**0.001**	0.826	0.592
						η_p^2	0.260	0.011	0.030
CI-28	Fresh	26.74±1.42	26.95±1.01	27.07±1.96	26.18±0.71	*F*	<0.001	3.902	1.308
						P	0.996	**0.030**	0.283
	Fatigued	26.68±1.94	27.63±1.75	26.99±1.79	25.60±1.85	η_p^2	<0.001	0.182	0.070

Abbreviations: CST = smoothed cumulative spike train; CV = coefficient of variation; CI-28 = complexity index under 28 scales; DFA = detrended fluctuation analysis scaling exponent α; SD = standard deviation; SampEn = sample entropy; Significant *P* values highlighted by bold font (data are mean ± SD).

8.3.7. Effect of fatigue and age-group on the power spectral density of the interference HD sEMG signals.

Total HD sEMG power was significantly higher during the fatigued KE at 20% MVT, in comparison to the fresh KE at 20% MVT (main effect, $F_{(1, 33)} = 45.195$; $P < 0.001$; $\eta_p^2 = 0.442$; Figure 8.8b.B). There was no main effect of age group ($F_{(2, 33)} = 3.129$; $P = 0.051$; $\eta_p^2 = 0.099$) and no condition (fresh vs. fatigued) by age group interaction ($F_{(2, 35)} = 1.655$; $P = 0.200$; $\eta_p^2 = 0.055$).

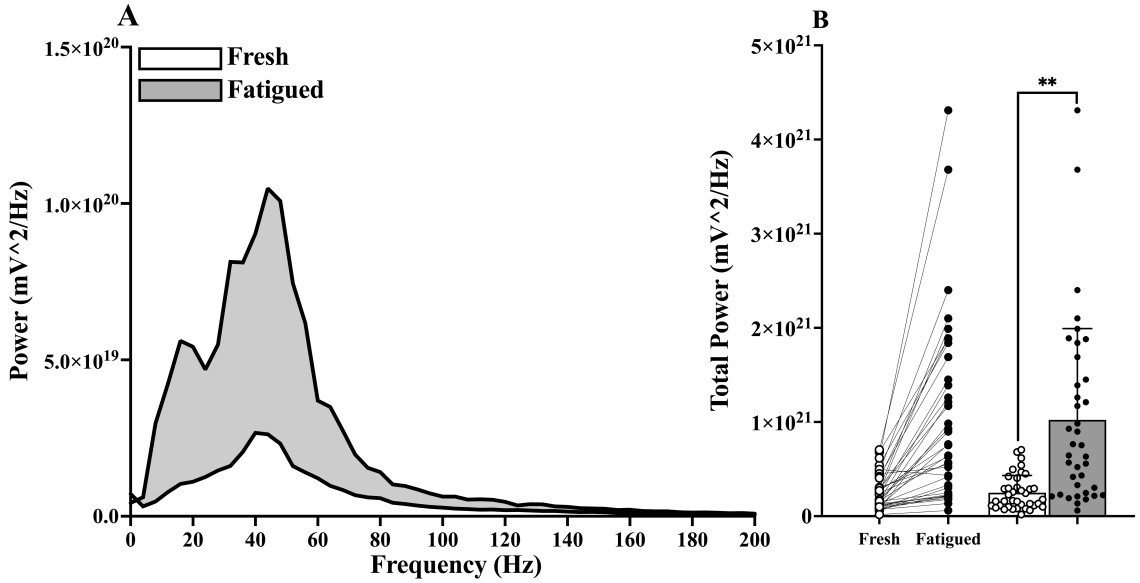

Figure 8.8b (A) Power spectrum of the HD sEMG signals derived from the fresh and fatigued isometric knee extensor contractions at 20% of maximal voluntary torque, **(B)** Before-after and bar plots of the total power of the HD sEMG signals derived from the fresh and fatigued isometric knee extensor contractions at 20% of maximal voluntary torque (open circles = fresh 20% MVT; closed circles = fatigued 20% MVT; ** = $P < 0.001$).

8.3.8. Effect of fatigue and age-group on the complexity, entropy and variability of the interference HD sEMG signals.

Table 8.5b presents the descriptive statistics and ANOVA results for the effect of fatigue and age on the complexity, entropy and variability of the interference HD sEMG signals.

Complexity index results

The CI-28 of the interference HD sEMG signals were significantly higher during the fresh KE at 20% MVT, in comparison to the fatigued KE at 20% MVT (Table 8.5b). There was no main effect of age group and no condition by age group interaction on the CI-28 of the interference HD sEMG signals (Table 8.5b).

Detrended fluctuation analysis results

The DFA α of the interference HD sEMG signals were significantly lower during the fresh KE at 20% MVT, in comparison to fatigued KE at 20% MVT (Table 8.5b). There was a main effect of age group, but there was no condition by age group interaction on the DFA α of the interference HD sEMG signals (Table 8.5b).

Sample entropy results

The SampEn of the interference HD sEMG signals were significantly lower during the fresh KE at 20% MVT, in comparison to the fatigued KE at 20% MVT (Table 8.5b). There was a main effect of age group, but no condition by age group interaction on the SampEn of the interference HD sEMG signals (Table 8.5b). The fatigue-related decline the interference HD sEMG signal SampEn at scale 1 was not associated with the fatigue-related decline in KE torque SampEn at scale 1 ($r = 0.278$; $R^2 = 0.078$; $P = 0.09$).

Variability metric results

There was a main effect of condition (fresh vs. fatigued), with fatigue-related increases in the CV and SD of the interference HD sEMG signals (Table 8.5b). There was a significant relationship between the fatigued-related increases in the CV and SD of the interference HD sEMG signals and the concurrent fatigue-related increases in the CVT and SDT (Figure 8.9b).

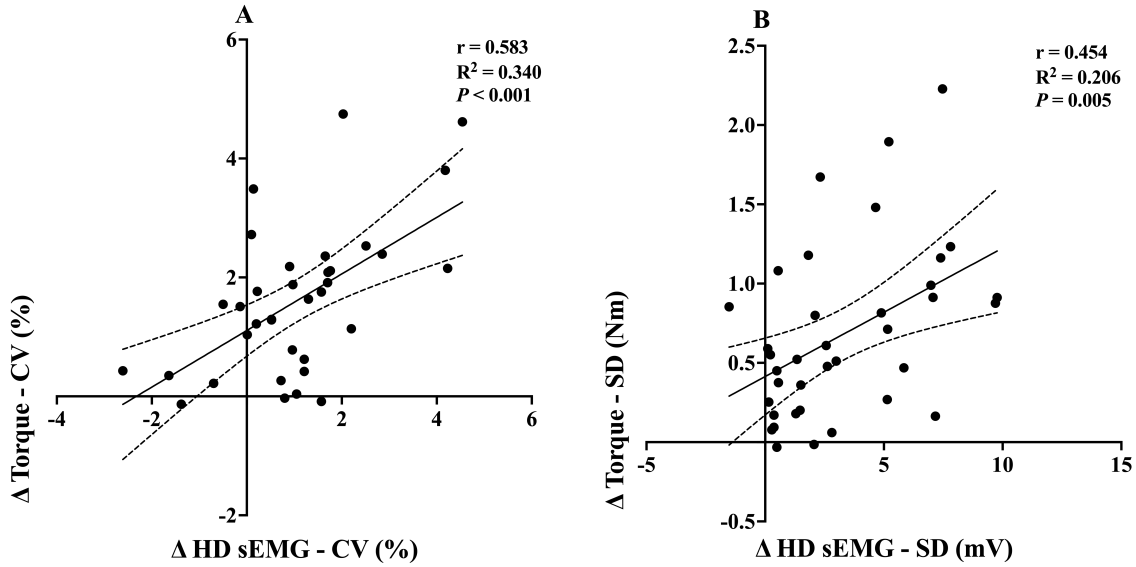

Figure 8.9b. (A) Relationship between the fatigue-related change in the coefficient of variation of the HD sEMG signals and the fatigued-related change in the coefficient of variation of torque, **(B)** Relationship between the fatigue-related change in the standard deviation of the HD sEMG signals and the fatigued-related change in the standard deviation of torque.

Table 8.5b Descriptive statistics and ANOVA results for the effect of fatigue and age-group on the complexity, entropy and variability of the interference HD sEMG signals.

						F, *P* and η_p^2 values			
		All Participants (*N* = 38)	Younger Group (*N* = 10)	Middle Group (*N* = 15)	Older Group (*N* = 13)		Main effect of condition	Main effect of age	Condition by Age Interaction
Mean HD sEMG (mV)	Fresh	7.86±3.06	γ 10.63±2.57	7.91±3.11	5.68±1.07	*F*	46.730	9.951	2.212
	Fatigued	11.89±5.82	16.12±5.05	12.41±5.82	8.08±3.84	*P*	**<0.001**	**<0.001**	0.125
						η_p^2	0.579	0.369	0.115
SD (mV)	Fresh	6.15±2.41	γ 8.29±1.97	6.21±2.48	4.44±0.88	*F*	47.330	9.962	2.223
	Fatigued	9.43±4.62	12.81±3.79	9.80±4.62	6.42±3.24	*P*	**<0.001**	**<0.001**	0.124
						η_p^2	0.582	0.369	0.116
CV (%)	Fresh	77.86±1.45	78.11±1.38	77.42±1.49	78.10±1.45	*F*	17.557	1.023	1.186
	Fatigued	79.05±2.26	79.95±3.27	78.62±1.53	78.79±1.88	*P*	**<0.001**	0.371	0.318
						η_p^2	0.347	0.058	0.067
SampEn (scale 1)	Fresh	1.38±0.19	γ 1.23±0.16	1.37±0.19	1.49±0.15	*F*	59.616	8.509	0.798
	Fatigued	1.19±0.24	1.02±0.13	1.18±0.23	1.36±0.22	*P*	**<0.001**	**0.001**	0.459
						η_p^2	0.637	0.334	0.045
DFA α	Fresh	0.73±0.04	γ 0.75±0.04	0.73±0.04	0.71±0.05	*F*	66.057	5.080	1.134
	Fatigued	0.76±0.05	0.79±0.03	0.78±0.04	0.73±0.05	*P*	**<0.001**	**0.012**	0.334
						η_p^2	0.660	0.230	0.063
CI-28	Fresh	72.97±2.42	72.10±1.73	72.79±3.04	73.83±1.96	*F*	22.905	2.253	0.183
	Fatigued	71.24±2.77	70.11±2.34	70.99±2.31	72.38±3.25	*P*	**<0.001**	0.121	0.834
						η_p^2	0.403	0.117	0.011

Abbreviations: HDsEMG = high-density surface electromyography; CV = coefficient of variation; CI-28 = complexity index under 28 scales; DFA = detrended fluctuation analysis scaling exponent α; SD = standard deviation; SampEn = sample entropy; Significant *P* values highlighted by bold font; γ = significant difference between YG and OG $P < 0.05$; (data are mean ± SD).

8.3.9. Cross-correlation results of torque and effective neural drive.

The estimate of effective neural drive was moderately correlated with the fluctuations in the fresh and fatigued isometric KE torque signals (Figure 8.10b).

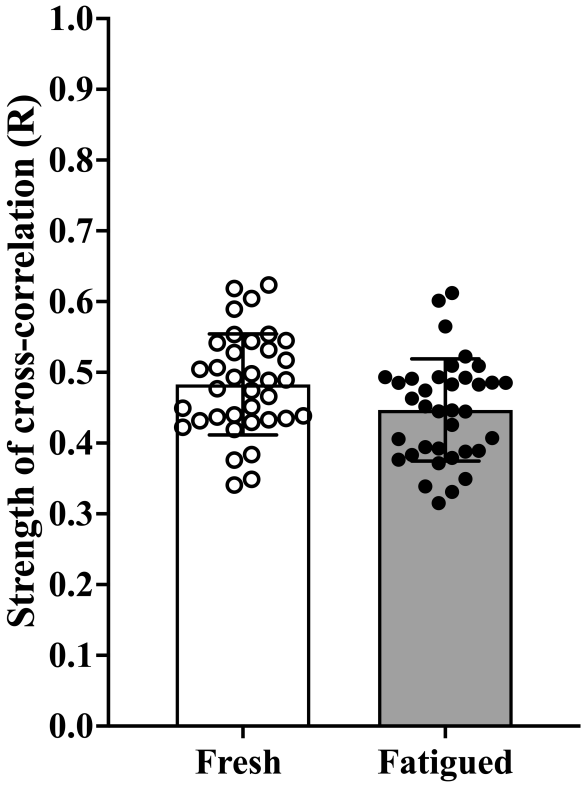

Figure 8.10b. Cross-correlation coefficients for the estimate of effective neural drive and the fluctuations in the fresh and fatigued isometric knee extensor torque signals at 20% of maximal voluntary torque (open circles = fresh 20% MVT; closed circles = fatigued 20% MVT).
.

8.4b - Discussion

The current study investigated whether the strength of oscillations in common synaptic input, assessed by the within-muscle coherence of CSTs, were explanatory of fatigue-related changes in isometric KE torque signal complexity, in adults aged from 18 to 90 years. The main findings were the fatiguing isometric KE protocol resulted in an increase in the strength of common synaptic input, with significant increases in the delta (common drive band), alpha (physiological tremor band) and low beta frequency bands (Figure 8.2b.A). There was a significant fatigue-related increase in torque signal variability (Figure 8.5b), but no significant fatigue-related change in the CI-28 and DFA α (Figure 8.4b) complexity metrics. The fatigue-related change in alpha band coherence was significantly associated with the fatigue-related changes in the CVT, SDT, RMSE, CI-28 and DFA α (Table 8.3b), and the SampEn of the coarse-grained torque signal from scales 11 to 28 of the MSE curve (Figure 8.6b.B).

Contrary to prior hypotheses (Pethick et al., 2016, 2021b), current findings indicate that larger fatigue-related increases in common input in the alpha band were accompanied by larger increases in torque signal complexity (i.e., increase in CI-28 and decrease in DFA α) and signal irregularity (i.e., increase in SampEn). However, in accordance with our hypothesis, participants who demonstrated greater fatigue-related increases in the strength of common input in the alpha band, were also likely to exhibit larger increases in the CVT, SDT and RMSE.

8.4.1. Effect of fatigue on the strength of common synaptic input and isometric knee extensor torque signal complexity, entropy and variability.

In accordance with existing literature, there was an increase in the strength of common synaptic input when the muscle was fatigued (Contessa et al., 2009; Castronovo et al., 2015; McManus et al., 2016; Rossato et al., 2022). The observed increase in the strength of common input at higher oscillatory frequencies (alpha and low beta coherence bands; Figure 8.2b) likely reflects the reduced inhibition of the Ia afferent feedback loop and increased corticospinal excitation and descending drive as the muscle is fatigued (Castronovo et al., 2015; Mehrkanoon et al., 2014). Moreover, the observed fatigue-related increase in the CV of ISI (Table 8.2b) and power of the HD sEMG signal (Figure 8.8b) is indicative of greater input to the motor neurons that is synchronized at a presynaptic level (Schmied & Descarreaux, 2010). This may also be suggestive of a fatigue-related increase in both common and independent synaptic inputs.

Immediately following task failure, participants were able to meet the target torque set at 20% MVT, albeit with a significantly higher torque variability and greater targeting errors in comparison to fresh contractions of a matched intensity (Figure 8.5b). The observed fatigue-related increase in alpha band oscillations in common synaptic input could account for 19.0%, 21.7% and 13.6% of the corresponding increases in the CVT, SDT and RMSE, respectively (Table 8.3b). Current findings corroborate earlier research, which linked fatigue-related increases in the strength of common synaptic input with increases in muscle torque signal variability (Contessa et al., 2009; Castronovo et al., 2015; McManus et al., 2016).

Alpha band oscillations in common synaptic input (common noise) were suggested to be associated with error corrections and overshoots in movement during tasks of muscle torque control (Mehrkanoon et al., 2014). This likely explains the concurrent fatigue-related decrease in muscle torque control and increase in alpha band oscillations, in addition to the significant association between the strength of alpha band oscillations and the torque signal variability during the fatigued contractions (Table 8.3b). The absence of a clear relationship between alpha band oscillations and isometric KE torque control during the fresh contractions at 20% MVT supports this interpretation (Table 8.3b), as participants performed steadier contractions (Figures 8.5b.A & 8.5b.B) and made smaller targeting errors (Figure 8.5b.C). These findings extend upon those of Chapter Eight A, by further highlighting the involvement of alpha frequency band (physiological tremor band) oscillations in modulating the precision of isometric KE muscle torque control.

It is also plausible that because of the repeated contractions at 60% MVT, there may have been a prolongation of dendritic persistent inward currents (PICs; that provide an additional source of excitatory current that amplifies and prolongs synaptic inputs to the motor neurons; Binder et al., 2020), and consequently the sustained discharge of higher threshold MUs during the fatigued KE contraction at 20% MVT. This is possible as the inhibitory input necessary to deactivate PICs of the MUs recruited during the higher intensity contractions at 60% MVT, would likely be compromised by the continued excitatory drive necessary to complete the KE contraction at 20% MVT after the fatiguing protocol (Beauchamp et al., 2023). If this is the case, there would be a greater number of active higher threshold MUs with a larger torque producing capacity, than is required for a muscle contraction at 20% MVT. This would result in a degradation in isometric torque control during the contraction at 20% MVT (i.e., higher CVT, SDT and RMSE of torque). Thus, in the current study, the prolongation of PICs likely

contributed to the fatigue-related reduction in isometric KE torque control, however, research is required to confirm this hypothesis.

There was no effect of fatigue on the complexity metrics CI-28 and DFA α, although notable inter-individual variability in the fatigue-related changes were evident in both metrics (Figure 8.4b). The fatigue-related change in alpha band coherence accounted for a small yet significant percentage of the inter-individual variability in complexity metrics, CI-28 (11.8%) and DFA α (9.4%). Interestingly, during the fresh contractions, common input in the alpha band explained a greater percentage of the variance in CI-28 (23.1% for fresh contractions versus. 13.6% for fatigued contractions) and DFA α (31.4% for fresh contractions versus. 12.0% for fatigued contractions) metrics, in comparison to the fatigued contractions (Table 8.3b). The direction and magnitude of change in torque complexity attributable to fatigue warrants further investigation, because this appears to be driven primarily by neural mechanisms other than the observed increases in the strength of common synaptic input. Indeed, it is plausible that the fatigue-related changes in torque signal complexity does not exclusively originate from neural signals but may also be mediated by neuromuscular system components peripheral in origin (e.g., muscle-tendon interaction; Raffalt et al., 2023).

Consistent with previous research findings (Pethick et al., 2015), fatigue resulted in a significant decrease in SampEn at scale one of the MSE curve, indicating increased regularity of the original torque signal (Figure 8.3b). However, SampEn at scale one fails to describe the regularity of the multiple oscillatory frequencies present in the torque signal, as illustrated by the *cross-over* in the MSE curves derived from the fresh and fatigued contractions. During the fatigued contractions, SampEn was lower at shorter scales (≤ scale 7), and higher at longer (coarser) scales (≥ scale 13) when compared to the fresh contractions (Figure 8.3b).

The cross-over in SampEn at longer (coarser) scales is noteworthy, because the coarse-graining procedure progressively reveals the lower frequency oscillations present in the torque signal (Vaillancourt & Newell, 2003; Vaillancourt et al., 2004; Knol et al., 2019). Current findings indicate that the oscillations contained within the torque signals become progressively more irregular and unpredictable at lower frequencies. Importantly, fatigue appears to alter the temporal structure of torque signal, simultaneously increasing the regularity at shorter scales and decreasing the regularity at longer scales in comparison to fresh torque signals.

Notably, the fatigue-related decreases in SampEn at coarse-grained scales one through to nine were not correlated with the change in common input in the alpha frequency band. However, from the point of cross-over in the MSE curves (scales 11 to 28), the fatigue-related increase in SampEn was associated with the increase in the strength of alpha band oscillations in common synaptic input (Figure 8.6b). Therefore, the MSE curve cross-over might, in part, be attributed to the fatigue-related increases in the strength of alpha band oscillations in common synaptic input. As initially postulated in Chapter Eight A, this might suggest that higher frequency common inputs at or above those of effective neural drive were embedded as irregularities, through nonlinear amplitude modulation, into the lower-frequency oscillations in common neural drive (Watanabe & Kohn, 2015). These irregularities could then potentially be transmitted into the lower-frequency components of the torque signal and captured as a higher SampEn at the longer (coarser) scales of the MSE curves. Thus, the greater irregularity of the fatigued torque signals (i.e., the higher SampEn at longer scales) might be explained, in part, by the fatigue-related increase in the strength of higher frequency oscillations in common synaptic input.

The current experimental chapter findings extend upon those of Chapter Eight A, where SampEn at the longer (coarser) scales were found to be significantly associated with the strength of common oscillations in the alpha band (Chapter Eight A, Figure 8.3a). However, likely due to lower participant sample sizes and low MU yield, common synaptic input in the alpha band was unable to directly explain the age-related cross-over in SampEn, as the KE torque signals were progressively coarse-grained (see Chapter Eight A).

The cross-over in isometric KE torque MSE curves has now been observed due to age (Chapter Five, Six and Eight A) and neuromuscular fatigue (Chapter Eight B). As initially speculated in previous chapters, the current thesis has provided the first evidence that demonstrates the behaviour of the MSE curves may be indicative of the adaptive neural response to the demand of the task. The neural response being the increase in the relative strength of common oscillations in the alpha frequency band. Indeed, further research is required to corroborate and extend current findings to the age-dependent scale-to-scale entropic behaviour of muscle torque signals revealed by the MSE analysis. In addition, research is also required to establish the physiological mechanisms that may explain the remaining variance in the fatigue-induced MSE cross-over phenomenon.

8.4.2. Effect of age-group on fatigue-related changes in the strength of common synaptic input and neuromuscular complexity.

This study represents the first assessment of the effect of age on fatigue-related changes in the estimated strength of common synaptic input and isometric KE torque signal complexity. Age did not emerge as a significant contributing factor to the fatigue-related changes in the strength of common synaptic input or isometric KE torque signal complexity. It is plausible that the participants of the OG were *too young* (aged 60.7 ± 10.3 years; Table 8.1b) to observe any age-related factors, including the increased strength of common synaptic input, which may impair muscle control (Mynark & Koceja, 2001; Shaffer & Harrison, 2007). Additionally, an effect of age on torque control may be attenuated during low-difficulty motor tasks, such as constant isometric contractions (Bootsma et al., 2021; Guo et al., 2024). To elucidate the potential effects of age on fatigue-related changes in common synaptic inputs and torque signal complexity, future studies may need to recruit older participants (> 70 or 80 years) and employ more complex tasks, such as ramp isometric contractions (Guo et al., 2024).

8.4.3. Effect of fatigue on the complexity, entropy and variability of smoothed cumulative spike train signals.

The current chapter also assessed the complexity and variability of smoothed CSTs (proposed to be a measure of the temporal structure of an estimate of common synaptic inputs; Hunter, 2023). Main findings were the fatigue-related loss of complexity and increase in variability of the smoothed CSTs (Table 8.4b). The fatigue-related increase in the regularity (i.e., lower SampEn) of the smoothed CSTs is likely explained by the overall increase in CST coherence because of fatigue (i.e., increase in the strength of common synaptic input relative to the independent input; Figure 8.2b).

Current findings corroborate recent research, that demonstrated the concurrent loss of ankle torque and smoothed CST (derived from the active MUs of the TA muscle) complexity during fatiguing contractions (Hunter, 2023). The researchers suggested the fatigue-related decrease in ankle torque complexity was a consequence of the decrease in CST complexity (Hunter, 2023). In the current study, a fatigue-related decline in KE torque SampEn (scale one of the MSE curve; Figure 8.3b) was also observed. However, no association was found between the fatigue-related decline the smoothed CST SampEn and the decline in KE torque SampEn. Moreover, no other smoothed CST complexity metrics were found to be associated with

fatigue-related alterations in isometric KE torque complexity. Thus, current findings indicate that the fatigue-related alterations in isometric KE torque complexity were not explained by the complexity of common synaptic inputs.

The variability of the smoothed CSTs (measure of the variability in the estimate of common synaptic input) was found to be increased due to fatigue (Table 8.4b). This fatigue-related increase in smoothed CST variability was significantly associated with the fatigue-related increase in isometric KE torque variability (Figure 8.7b). These findings extend upon the findings of Chapter Eight A, in addition to previous research, where it was found that greater variability in the estimate of common synaptic input was significantly associated with worse torque or force steadiness during fresh isometric contractions (Feeney et al., 2018).

8.4.4. Effect of fatigue on the complexity, entropy and variability of interference HD sEMG signals.

The main findings were the fatigue-related reduction in interference HD sEMG signal complexity and increase in interference HD sEMG signal variability (Table 8.5b). Current findings corroborate those of previous researchers, who also observed a fatigue-related decline in sEMG signal complexity of the KE muscles (Beretta-Piccoli et al., 2015).

The interference HD sEMG signal represents the summation of all MU action potentials and is therefore representative of all synaptic inputs to the MU pool. The overall fatigue-related increase in the strength of common synaptic input (Figure 8.2b) and accompanying MU synchronisation, likely explains the increased temporal regularity (i.e., lower SampEn and CI-28) of the interference HD sEMG signal (Table 8.5b). However, fatigue-related decline in the interference HD sEMG signal SampEn could not explain the fatigue-related decline in isometric KE torque SampEn.

Interestingly, the fatigue-related change in coefficient of variation and standard deviation of the interference HD sEMG signal (i.e., signal variability), was able to explain 34.0% and 20.6% of the variance in the fatigue-related change in CVT (Figure 8.9b.A) and SDT (Figure 8.9b.B), respectively. These findings indicate that fatigue increases the variability of global neural drive to the VL muscle, and consequently the increased variability in global neural drive increases the variability in isometric KE torque.

Overall, the current study has observed fatigue-related increase in the: coherence between CSTs (Figure 8.2b), power of the HD sEMG signal (Figure 8.8b), and variability of CSTs (Table 8.4b). Therefore, it can be concluded that the fatigue-related increase in strength and variance of common and independent synaptic inputs were explanatory mechanisms for the deterioration in neuromuscular control of KE muscles during fatiguing isometric contractions.

8.4.5. Cross-correlation between torque and effective neural drive.

The tertiary aim of the study was to determine the strength of association between the effective neural drive to the VL muscle and fluctuations in isometric KE torque during fresh and fatigued contractions. The estimate of effective neural drive (CST) was found to be moderately correlated with the fluctuations in the fresh and fatigued KE torque signals (Figure 8.10b). This suggests that the spatial structure of the fluctuations in isometric KE muscle torque is largely determined by the low-frequency oscillations in effective neural drive. Current findings extend previous experimental research using HD sEMG that has demonstrated the fluctuations in finger abduction force, ankle dorsiflexion torque (Negro et al., 2009; Sahinis et al., 2024) and plantar-flexion torque (Mazzo et al., 2022) to closely resemble the low-frequency oscillations in effective neural drive.

8.4.6. Limitations.

Contraction intensity has been shown to influence torque signal complexity, with a loss of isometric KE torque complexity shown to occur exclusively above critical torque (Pethick et al., 2016). Although the fatigue protocol contractions were performed above critical torque (60% MVT), the comparison of fresh and fatigued torque complexity was derived from contractions below KE critical torque (20% MVT). The lower intensity was selected to maximise the number of MU decomposed from the contraction. However, it is conceivable that fatigue-related changes in torque complexity were influenced by the contraction intensity. Further research is required to elucidate the relationship between fatigue-related changes in torque complexity and common synaptic input derived from fatigue protocols performed at a range of isometric contraction intensities, in addition to different contraction modes (isometric vs. dynamic tasks) and velocities which influence muscle fatigability in older adults (Allman & Rice, 2002; Christie et al., 2011).

The 20% MVT target value was determined in an unfatigued state and the same target torque was used in the post-fatigue condition (Figure 8.1b). Given that MVT will be reduced following

the fatigue-protocol, the unfatigued target torque value would represent a greater relative proportion of MVT in the fatigued condition (e.g., potentially exceeding 20% MVT). This could act as a confounding factor, as it may have influenced neuromuscular complexity, and the strength and variance of common synaptic input measured in the fresh and fatigued conditions. Therefore, differences observed between conditions may partly reflect variations in the relative intensity rather than solely the effects of fatigue.

The study did not measure the development of central and peripheral fatigue induced by the fatigue protocol. Given the contraction intensity certainly exceeded critical torque, it be inferred that both central and peripheral fatigue did occur (Pethick et al., 2016). However, the absence of a quantitative measure of fatigue limits our ability to fully explain the impact of inter-individual levels of fatigue on torque complexity and common synaptic input.

The current chapter also shares the same limitations as outlined in Chapter Eight A (Section 8.4.5. Limitations). The main limitations being the low MU yield and only recording HD sEMG signals from the VL muscle.

8.5b - Conclusion

The ability to modulate common synaptic input to the motor neurons is an adaptive neural strategy required for continued torque production and control when the muscle is fatigued (Rossato et al., 2022). The current chapter provides the first evidence that demonstrates the fatigue-related increase in the strength of common synaptic input in the alpha band (physiological tremor band) to be explanatory of a significant percentage of the fatigue-related changes in isometric KE torque complexity.

Furthermore, the study presents novel evidence of a neuromuscular fatigue-related cross-over in the MSE curves derived from isometric KE torque signals. During the fatigued contractions, SampEn was lower at shorter scales (≤ scale 7), and higher at longer (coarser) scales (≥ scale 13) when compared to the fresh contractions. Importantly, from the point of cross-over in the MSE curves (scales 11 to 28), the fatigue-related increase in SampEn was significantly associated with the fatigue-related increase in the strength of alpha band oscillations in common synaptic input.

These findings suggest that higher frequency oscillations in common synaptic input may be embedded in the low-frequency components of common neural drive and captured as the greater irregularity of the low-frequency components of the fatigued torque signals (i.e., the higher SampEn at longer scales). This supports the interpretation that complexity metrics reflect the neural mechanisms underpinning the modulation of torque control and therefore the neuromuscular system's strategy to meet task demands (Peng et al., 2009; Manor & Lipsitz, 2013).

Chapter Nine

General Discussion.

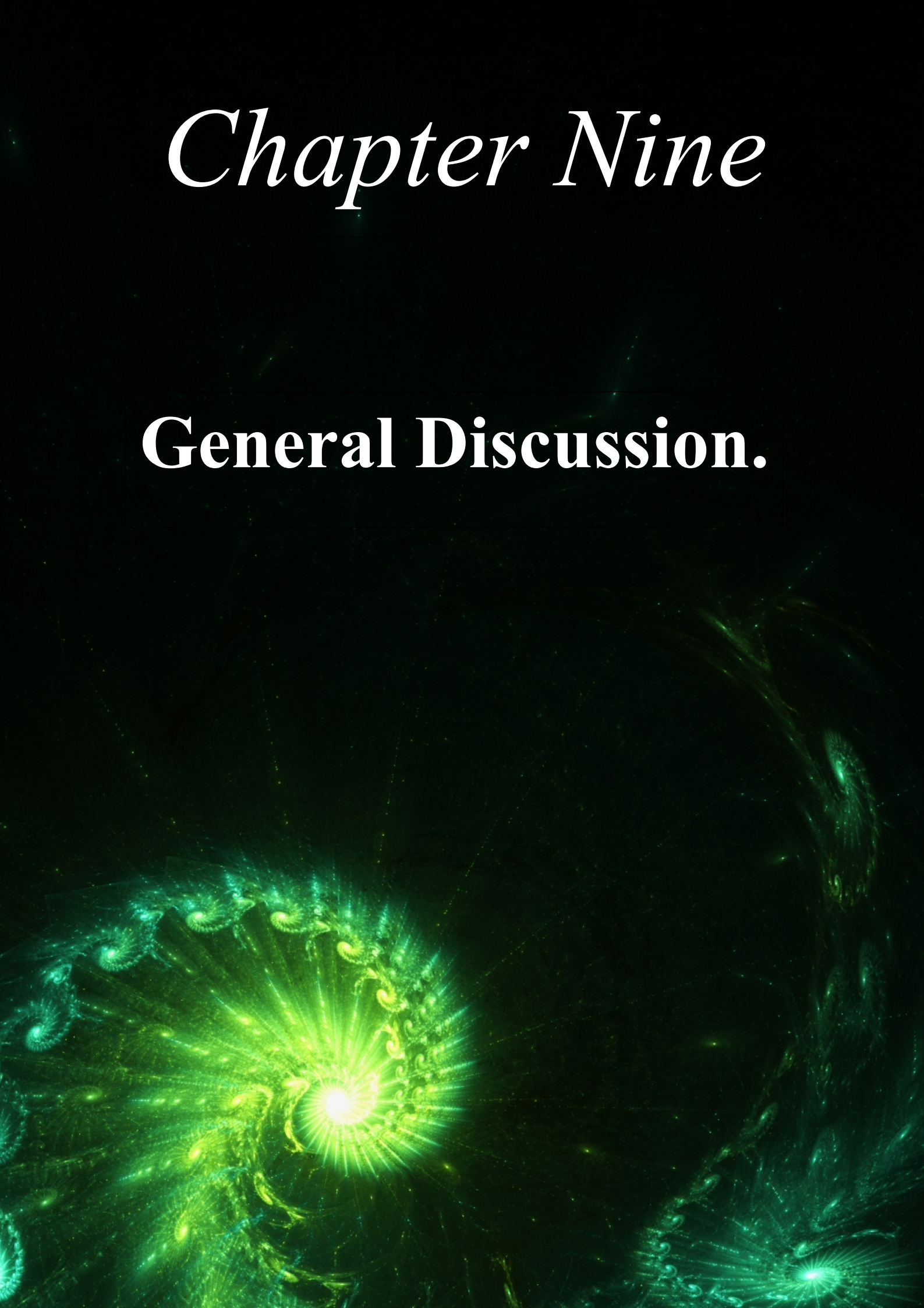

9.1 - Introduction

The primary aim of the thesis was to investigate whether there are age-group related differences in the complexity, entropy and variability of isometric muscle torque and force signals from the lower (knee extensor muscles) and upper (hand muscles) extremities (Chapters Five, Six, Seven, and Eight). By examining the neuromuscular complexity (temporal structure) and variability (spatial structure) of muscle torque and force signals, the research aimed to advance the current understanding of age-related differences in neuromuscular system function, with a specific focus on the production and regulation of muscle torque and force.

The sub themes of the thesis also aimed to address notable gaps in the literature, the most prominent being the neural mechanism(s) underpinning the complexity of isometric muscle torque (Chapters Eight A and Eight B), whether fatigue further exacerbates the age-related loss of neuromuscular complexity (Chapter Eight B), the functional importance of neuromuscular complexity (Chapters Six and Seven), and the effect of contraction intensity and muscle group on the age-related differences in neuromuscular complexity (Chapters Six and Seven).

The experimental chapters have already provided comprehensive discussions regarding chapter specific findings. Therefore, the general discussion will provide a synthesis of the novel findings of the thesis.

9.2 - The effect of age-group on the complexity and entropy of isometric knee extensor muscle torque signals.

Complexities of ageing: *what was known about the effect of age on the complexity of isometric knee extensor torque signals prior to this thesis?*

There was a limited body of research investigating the effects of age on the complexity and entropy of isometric KE torque signals, with existing studies yielding inconsistent results (Fiogbe et al., 2021; Pethick, 2023). For instance, Pethick (2023) reported no significant age-related differences in neuromuscular complexity. In contrast, Fiogbe et al. (2021) observed lower neuromuscular complexity in older adults compared with younger individuals. Consequently, prior to the present thesis, the influence of age on the complexity and entropy of isometric KE torque signals remained unclear. To address this gap in the literature, the current thesis systematically examined age-group related differences in neuromuscular

complexity. Importantly, to enable a comprehensive characterisation of the temporal structure of the torque signal, a range of complementary complexity and entropy (DFA, MSE, and SampEn) metrics were employed across the experimental chapters.

Irregularity of torque: *the effect of age-group on the single scale entropy of isometric knee extensor muscle torque signals.*

The effect of age-group on the (ir)regularity of the isometric KE torque signals was quantified using the commonly employed single scale entropy metric, SampEn (Richman & Moorman, 2000). There was a main effect of age on the single scale entropy of isometric KE torque in Chapters Five and Eight A, with the older age groups found to exhibit more irregular torque signals (i.e., higher SampEn) than the younger age groups. Conversely, in Chapter Six there was no main effect of age on single scale entropy, although older adults typically exhibited more irregular torque signals (i.e., higher SampEn) than younger adults. Collectively, these experimental chapters suggest that older age is characterised by an increase in the irregularity of isometric KE torque signals.

As highlighted throughout the thesis, these single scale entropy metrics do not strictly capture the *complexity* of a physiological signal. Therefore, the higher SampEn does not directly indicate age-related differences in complexity of the muscle torque signal. Indeed, the complexity analyses, DFA and MSE, suggest that the process of ageing is characterised by a nuanced change in the temporal structure of the torque signal, that results in a progressive loss of neuromuscular complexity.

Colours of ageing: *the effect of age-group on the detrended fluctuation analysis scaling exponent of isometric knee extensor muscle torque signals.*

Throughout the experimental chapters of the thesis the effect of age-group on the fractal scaling (i.e., noise colour) of the isometric KE torque signals was assessed using the DFA scaling exponent α. In all chapters, the DFA α of each age groups torque signal was found to depart from $1/f$ noise or pink noise ($\alpha = 1.0$; being the highest complexity signal) towards brown noise (α closer to 1.5). However, compared to younger adults, older adults produced torque signals with higher scaling exponents closer to 1.5, indicating a lower neuromuscular complexity (Chapters Six and Eight A). This is also suggestive of an age-related reduction in the efficiency

of motor information transmission and information processing capacity (Cerella & Hale, 1994; Sosnoff & Newell, 2006d; Vieluf et al., 2018).

Cross-over phenomenon: *the effect of age-group on the time dependent structure of isometric knee extensor muscle torque signals.*

The present thesis was the first to examine the effect of age-group on the time-dependent structure of isometric KE torque signals using the MSE analysis. This approach has yielded novel insights into age-related changes in the temporal structure of isometric KE torque signals, thereby advancing current understanding of the underlying organisation and behaviour of the neuromuscular system's control processes. Notably, the MSE revealed physiologically meaningful information about the signal's temporal structure that was not captured by single-scale entropy measures, offering a more comprehensive assessment of neuromuscular complexity and therefore neuromuscular function.

In Chapter Five, the age-related cross-over in the MSE curves derived from KE muscle torque signals was demonstrated for the first time. Subsequent experimental chapters corroborated this age-related cross-over behaviour (Chapters Six and Eight A). Younger adults exhibited a lower SampEn at shorter time scales than older adults, with a cross-over occurring as the torque signal was coarse-grained. Thereafter, older adults exhibited a lower SampEn at longer (coarser) time scales than younger adults (see example Figure 9.1). In other words, younger adults produce torque signals with higher frequency oscillations (i.e., shorter time scales) of greater regularity and lower frequency oscillations (i.e., longer time scales) of greater irregularity, when compared with older adults. Conversely, older adults produce torque signals with higher frequency oscillations of greater irregularity and lower frequency oscillations of greater regularity, when compared with younger adults.

This age-dependent scale-to-scale entropic behaviour and consequently the cross-over phenomenon of the MSE curves is likely a function of the neuromuscular system's high dimensionality (Rohrle et al., 2019; Sleimen-Malkoun et al., 2014). The scale-to-scale dynamics of the MSE curves suggests that ageing affects the function and structure of individual components and the interaction between components of the neuromuscular system, which operate and produce inputs over multiple temporal scales. These frequency- and amplitude-varying inputs interact non-additively to meet the torque requirements of task

demands, consequently transmitting temporal structure that manifests in the torque signal. Therefore, the age-dependent scale-to-scale dynamics observed in the MSE curves may indicate age-related modifications in the neuromuscular system's strategy for the production and precise control of isometric KE muscle contractions, specifically, its capacity to modulate torque output in accordance with task demands.

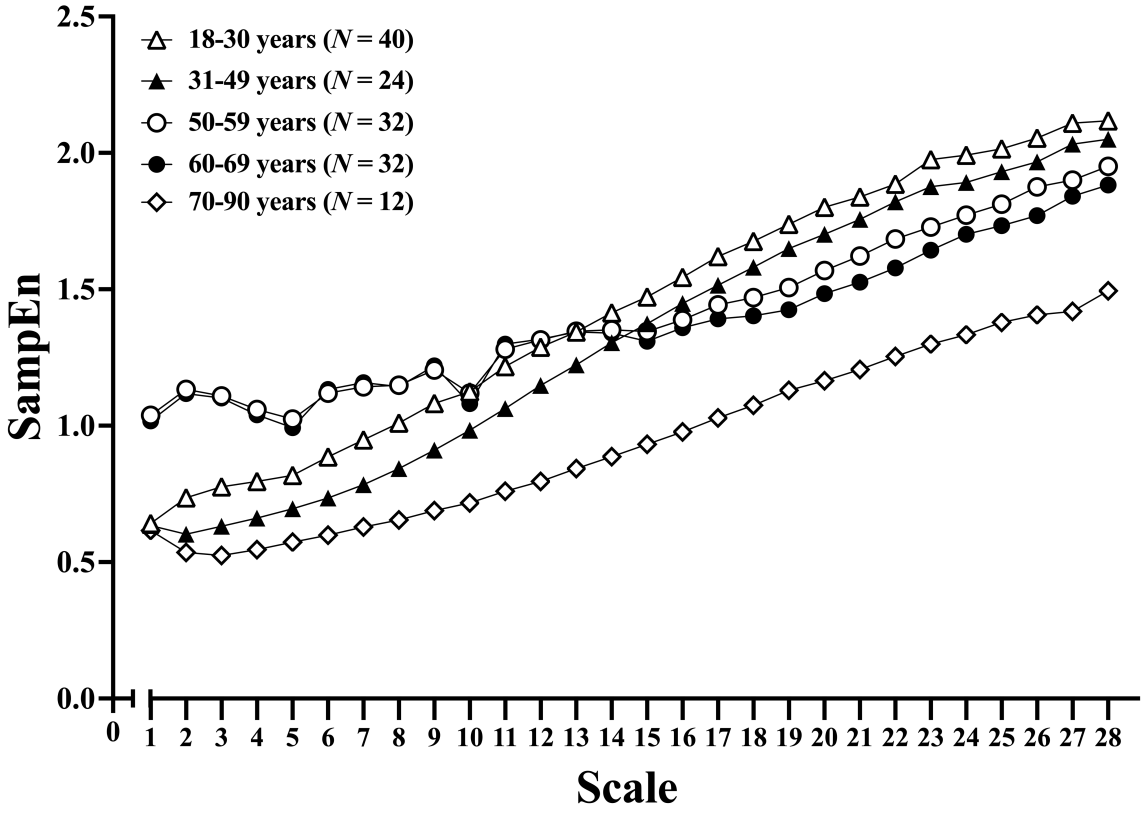

Figure 9.1. Multiscale entropy curves of isometric knee extensor torque signals from contractions performed by adults aged from 18 to 90 years. Note the *cross-over* behaviour of the MSE curves; the younger adults (e.g., 18-30-year group) present with a lower SampEn at shorter scales and a higher SampEn at longer (coarser) scales compared to older adults (e.g., 60-to-69-year group). The *cross-over* is indicative of age-related changes in the (ir)regularity of the different frequency components present in the torque signals (data from $N = 140$ individuals performing isometric knee extension contractions at 40% of maximal voluntary torque; error bars removed for clarity).

The current interpretation of the scale-to-scale dynamics of the MSE curves is speculative; however, it concurs with those made by others (Knol et al., 2019; Vieluf et al., 2015) and aligns with the theoretical framework of physiological complexity (Vaillancourt & Newell, 2002; Sleimen-Malkoun et al., 2014). The current thesis also presents the first experimental data demonstrating the strength of oscillations in common synaptic input to be a system input that can partially explain the regularity of the lower frequency oscillations in the torque signal (Chapters Eight A and Eight B). However, further research is required to unravel the mechanisms that determine the regularity of the multiple frequency components embedded in

the torque signal, thereby explaining the scale-to-scale dynamics of the MSE curves. Moreover, if the mechanisms underpinning the regularity of the oscillatory frequencies in the torque signal can be established, the MSE analysis would be an efficacious measure for assessing specific mechanistic alterations to the neuromuscular system on a component level.

The MSE curves of 140 unique participants from across the studies (Chapters Five, Six and Eight A) were collated and grouped by age to produce Figure 9.1 (*note*, no statistical analysis was performed on this data). This collation of experimental data reinforces the age-related cross-over phenomenon (Figure 9.1). However, a notable exception is the MSE curve of the 70-to-90-year group, which exhibits a lower SampEn across all 28 coarse-grained scales when compared to all younger age groups (groups aged < 69 years; Figure 9.1). Similarly, the age-related cross-over in the MSE curves in Chapters Six and Eight A were less prominent compared with Chapter Five (i.e., the older groups exhibited a lower SampEn across more time scales than younger groups). The ages of the older groups' participants in Chapters Six (64.9 ± 11.3 years; range 50 to 85 years) and Eight A (63.3 ± 10.2 years; range 50 to 90 years) was higher than the older group participants in Chapter Five (58.6 ± 5.1 years; range 50 to 70 years). This suggests that the pathway to senescence may eventually lead to a progressive increase in the regularity of more oscillatory frequencies present in the torque signal and thus an age-related loss of neuromuscular complexity.

It is important to note that the presence of a cross-over in the MSE curves does not directly indicate an age-related loss of complexity, as both age groups may exhibit statistically similar levels of overall signal complexity, as quantified by the area under the MSE curve (i.e., CI-28). In Chapter Five, the cross-over resulted in there being no age-related difference in the CI-28 metric. However, in Chapters Six and Eight A, older adults demonstrated significantly lower CI-28 values than younger adults, which was attributable to lower SampEn across the coarser temporal scales. The progressive increase in the regularity of more oscillatory frequencies and the concomitant loss of torque signal complexity (i.e., reduced CI-28), observed with advancing age, may reflect detrimental structural and functional changes within individual system components, as well as a reorganisation of interactions among components operating across multiple timescales (Sleimen-Malkoun et al., 2014).

9.3 - The effect of age-group on the variability of isometric knee extensor torque signals.

Equivocality of variability: *what was known about the effect of age on the variability of isometric knee extensor torque signals prior to this thesis?*

The literature has presented ambiguous evidence regarding the effect of age on the variability of isometric KE torque signals. This equivocality was demonstrated by the effect size analysis in Chapter Two. Out of the 32 effect sizes for the variability of isometric KE torque (i.e., CVT), 13 indicated a positive effect (i.e., older adults produced torque signals of greater variability than younger adults), while 19 indicated a negative effect (i.e., older adults produced torque signals of lower variability than younger adults). Consequently, the pooled random effects model revealed there to be no effect of age on the variability of isometric KE torque signals (g = -0.06, 95% CI [-0.39: 0.28]; Table 2.4).

In addition to the equivocality of evidence, there had also been paucity of research combining variability metrics (i.e., CVT and SDT) with the complexity and entropy metrics. Therefore, this thesis employed a multi-metric approach, combining complexity, entropy, and variability metrics to ensure a comprehensive characterisation of the temporospatial structure of isometric KE torque signals, and therefore neuromuscular function.

Variable and accurate ageing: *the effect of age-group on the variability and accuracy of isometric knee extensor torque signals.*

The data from the experimental chapters collectively suggests that older adults produce less variable torque signals (i.e., lower CVT and SDT) and make fewer targeting errors (i.e., lower RMSE) during isometric KE torque control tasks than younger adults (Chapters Five, Six and Eight A). Chapter Five revealed significant age-related differences in the CVT and SDT, indicating that older adults had lower neuromuscular variability than younger adults. Conversely, Chapter Six did not show a main effect of age-group on the CVT and SDT. However, there was a tendency for older adults to have less variable and more accurate isometric KE torque at ≥ 50% MVT than younger adults. Similarly, Chapter Eight A found that older adults typically exhibited less variable and more accurate KE torque signals at ≥ 20% MVT, although there was no main effect of age observed in the CVT and RMSE. There was a

main effect of age-group for the SDT, indicating lower neuromuscular variability among older adults compared with younger adults (Chapter Eight A).

The current findings suggest that older age does not result in lower neuromuscular variability of the KE muscles. This appears somewhat incongruent with the observed age-related decline in neuromuscular complexity of the same muscle group. However, based on the present evidence, a plausible interpretation is that age-related declines in neuromuscular complexity may precede measurable impairments in muscle torque steadiness and accuracy. Conceptually, ageing may initiate a gradual decline in torque complexity, reflecting early adaptations in the neuromuscular system's strategy to meet task demands, evident as altered scale-to-scale dynamics in the MSE curves (Figure 9.1), but without impairing task performance (i.e., no age-related decline in muscle steadiness or accuracy; Figure 9.2). As this decline in complexity progresses with advancing age, it may reach a critical threshold, the "frailty threshold" (Lipsitz, 2002). At this point, age-related alterations to the neuromuscular system function and control processes may become more pronounced. These alterations being reflected by a global suppression of the MSE curve across all time scales (Figure 9.1). As a result, the ability to meet task demands becomes compromised, leading to observable impairments in torque steadiness and accuracy (Figure 9.2).

This interpretation is supported by Figure 9.2, which presents the CVT and RMSE for the same 140 unique participants whose MSE data were shown in Figure 9.1. The 70 to 90-year age group, which exhibited lower SampEn across all 28 coarse-grained scales relative to the other age groups, also demonstrated higher CVT and RMSE values, indicative of reduced torque steadiness and accuracy (Figures 9.1 and 9.2). However, further research is needed to confirm and expand upon this observation.

Importantly, the observed age-related differences in the variability and accuracy of isometric KE torque are nuanced. This is evidenced by the significant age by contraction intensity interactions identified for CVT (Chapter Six), as well as for the SDT and RMSE (Chapters Six and Eight A). As initially discussed in Chapter Two, these interactions suggest that the impact of age on KE torque variability and accuracy is task-dependent, varying with the intensity of isometric contraction. This interaction effect may help explain the inconsistency of findings related to KE torque signal variability in the existing literature. Further discussion of the effect of age and contraction intensity on neuromuscular variability is provided in Section 9.4.

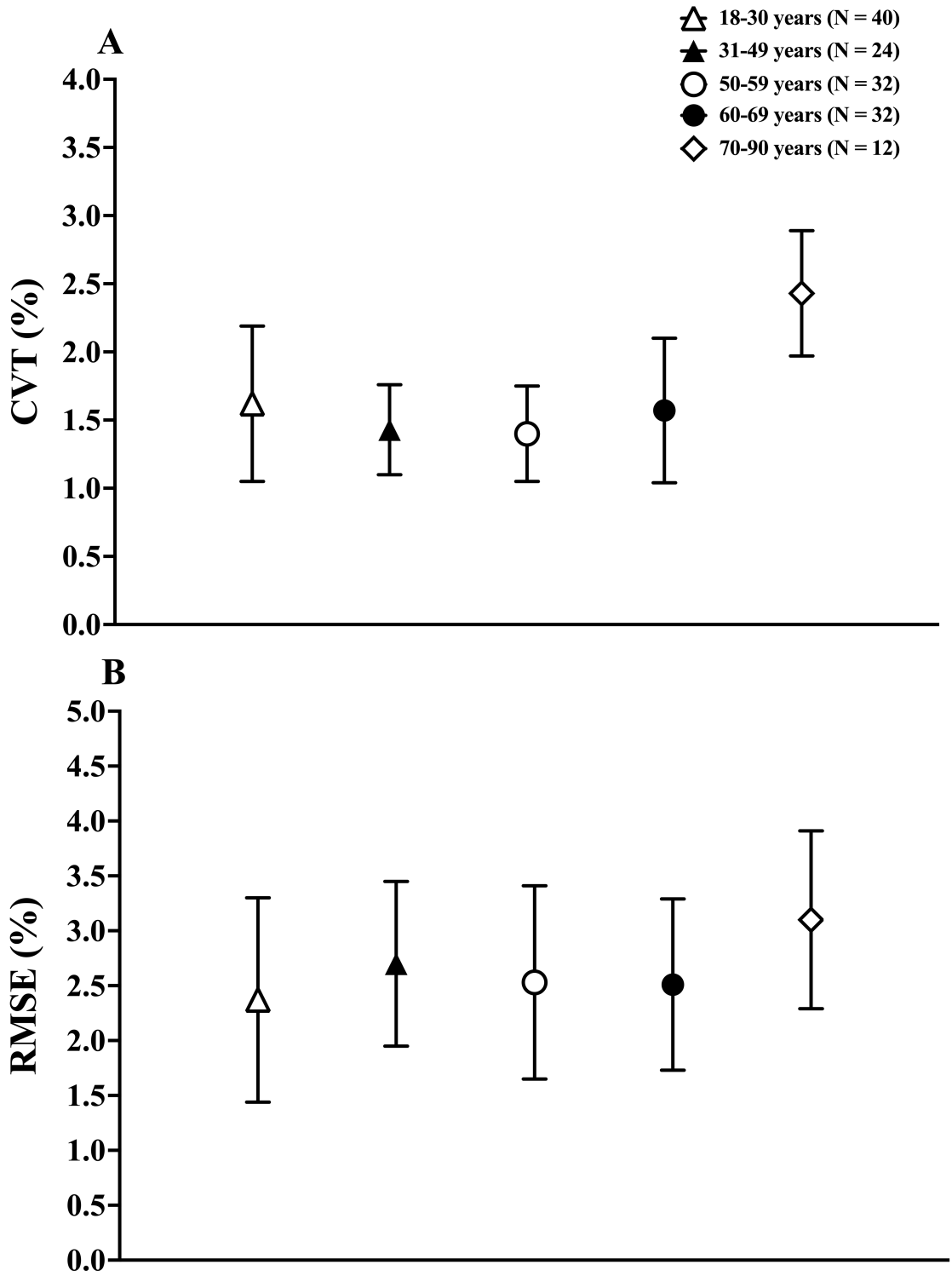

Figure 9.2. (A) Coefficient of variation of torque, **(B)** Root mean square error of torque (data from N = 140 individuals aged between 18 and 90 years performing isometric knee extension contractions at 40% of maximal voluntary torque; data are mean ± SD).

9.4 - The effect of muscle group and contraction intensity on age-related differences in the complexity, entropy and variability of isometric muscle torque and force signals.

The muscle and intensity matter: *the effect of muscle group and contraction intensity on neuromuscular complexity and variability.*

The emphasis of the thesis experimental chapters was on the effect of age-group on the complexity of isometric KE torque signals (Chapters Five, Six, Eight A and Eight B). However, it was also pertinent to investigate the effect of age-group on the complexity, entropy and variability of isometric precision PG force (Chapter Seven). This was predicated by the paucity of research assessing the effect of age on the temporospatial structure of isometric force signals derived from upper extremity muscles which are important to the performance of tasks requiring manual dexterity. In addition to the lack of exploration into the effect of muscle group and contraction intensity on the age-related differences in neuromuscular complexity.

Adults over 70 years of age were found to produce isometric PG force signals, across all contraction intensities (5 to 60% MVF), that exhibited lower complexity and greater variability, than force signals of adults under 70 years of age (Chapter Seven). These findings were suggestive of preserved fine motor control in the sixth and seventh decades of life, with a degradation in neuromuscular function and consequently a reduction in fine motor control into the eighth decade.

To demonstrate the effect of muscle group (KE and PG) and relative contraction intensity (10% to 60% MVT and MVF) on the age-related differences in neuromuscular complexity and variability, Cohens' d effect sizes were estimated from the data collected in Chapters Six (YG vs. OG; see Table 6.1 for group descriptives) and Seven (YG vs. 60yr group and YG vs. 70yr group; see Table 7.1 for group descriptives; Figure 9.3). The effect sizes reveal consistency in the age-related differences in complexity of both isometric KE torque and PG force signals across relative contraction intensities (Figures 9.3A to 9.3C). This suggests that there may be a uniform age-related reduction in neuromuscular function of both the upper and lower extremity muscles across contraction intensities. Functionally, this is of importance as the performance of fundamental motor skills necessitates the neuromuscular function across the muscle's full range of activation.

The effect sizes also reiterate the interaction, first highlighted in Chapter Two, between muscle group and contraction intensity regarding the age-related differences in neuromuscular variability. For the YG versus 70 year group comparison, the variability of isometric precision PG force was negatively affected by age across all contraction intensity categories (Figures 9.3D and 9.3E). By comparison, the negative effect of age on the variability of isometric KE torque occurs primarily at low contraction intensities, with the effect of age progressively less evident at higher contraction intensities (Figures 9.3D and 9.3E). The equivocality of previous research findings partially stems from the use of different contraction intensities across studies, in addition to studies using a limited number of contraction intensities (Chapter Two). Current evidence further underscores the importance of measuring muscle torque or force across a range of contraction intensities when investigating the effect of age on neuromuscular complexity and variability.

It is noteworthy that older adults aged 64.9 ± 11.3 years exhibited a lower isometric KE torque complexity across contraction intensities than younger adults aged 22.5 ± 3.4 years (Figures 9.3A and 9.3B; Chapter Six). Conversely, older adults of a similar age, 64.9 ± 2.7 years (60 year group), did not exhibit a lower isometric precision PG force complexity across contractions intensities than younger adults aged 23.8 ± 3.5 years (Figures 9.3A and 9.3B; Chapter Seven). An age-related difference in isometric precision PG force complexity was only observed when older adults aged 75.8 ± 4.4 years (70 year group) were compared to the younger adults, aged 23.8 ± 3.5 years (Figures 9.3A and 9.3B; Chapter Seven).

Current evidence appears to suggest that an age-related difference in isometric KE torque complexity occurs earlier in life when compared with isometric precision PG force complexity. Although, as discussed previously, this difference in KE torque complexity does not translate into a reduction in task performance, as demonstrated by the limited effect of age on the CVT, SDT and RMSE (Figures 9.3D to 9.3F). Nevertheless, understanding the muscle-specific time course of age-related declines in neuromuscular complexity is essential, particularly when aiming to optimise the timing of interventions designed to mitigate such losses and, by extension, preserve neuromuscular function. However, it is important to acknowledge that different participant cohorts performed the isometric KE and isometric precision PG control tasks. As such, this interpretation should be made with caution. Further research is warranted to determine whether the time course of age-related declines in neuromuscular complexity differs across muscle groups.

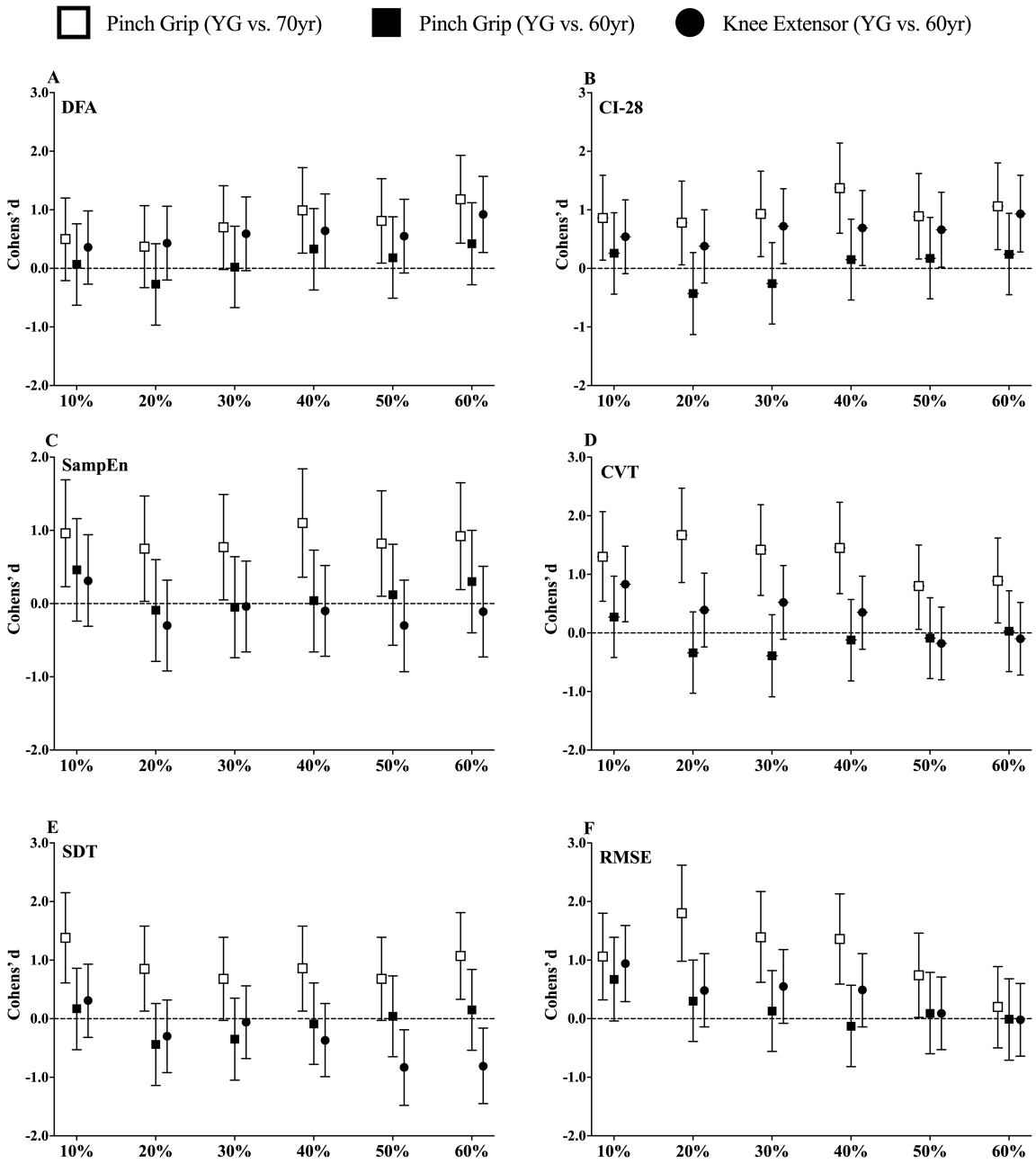

Figure 9.3. Assessment of the effect of muscle group and contraction intensity on the age-group related differences in the complexity, entropy and variability of isometric muscle torque/force using Cohens' d effect sizes produced with the data collected in Chapters 6 and 7 **(A)** Detrended fluctuation analysis, **(B)** Complexity index under 28 coarse-grained scales, **(C)** Sample entropy, **(D)** Coefficient of variation of torque/force, **(E)** Standard deviation of torque/force, **(F)** Root mean square error of torque/force (data are Cohens' d effect sizes with upper and lower 95% confidence limits; Cohens' d effect sizes were coded as positive when the older group presented with a higher CVT, SDT, RMSE or DFA OR a lower SampEn or CI-28, when compared with the younger group).

Topology of curves: *the muscle and contraction intensity dependent scale-to-scale dynamics of multiscale entropy curves.*

Data from Chapters Six and Eight A demonstrated that the temporal structure of isometric KE torque signals depends on the relative intensity of the muscle contraction, as illustrated by the scale-to-scale dynamics in the MSE curves (Figure 9.4A). At shorter scales SampEn decreased with increasing contraction intensity. This trend persisted until around scale 10, at which point a cross-over occurred as the torque signal was coarse-grained further. Subsequently, at longer (coarser) scales SampEn increased with increasing contraction intensity, as illustrated in Figure 9.4A. In other words, increasing the contraction intensity progressively increases the regularity of higher frequency oscillations (i.e., shorter time scales) and increases the irregularity of lower frequency oscillations (i.e., longer time scales) in the torque signal. Alternatively, decreasing the contraction intensity progressively increases the irregularity of higher frequency oscillations and increases the regularity of lower frequency oscillations in the torque signal.

Notably, the experimental chapters have demonstrated the scale-to-scale entropic behaviour of isometric KE torque signals to be attributable to several factors, including age (Chapters Five, Six and Eight A), contraction intensity (Figure 9.4A) and neuromuscular fatigue (Chapter Eight B). Additionally, the contraction intensity related cross-over behaviour of the MSE curves is corroborated by previous researchers studying the effect of age and contraction intensity on the time dependent structure of isometric IFA force (Vieluf et al., 2015). Collectively, these findings strengthen the hypotheses that suggests changes to the temporal structure of a muscle torque signal, as captured by the scale-to-scale dynamics of the MSE curves, is indicative of changes in the neuromuscular systems control processes in response to the specific task requirements.

The MSE curves derived from isometric precision PG force signals exhibited different scale-to-scale behaviour when compared to the MSE curves derived from isometric KE torque signals (Figure 9.4). Notably there was no age or contraction intensity related cross-over in the MSE curves derived from isometric precision PG force signals (Figure 9.4B). The overall behaviour of the MSE curves derived from isometric precision PG force can be described by an initial increase in SampEn across shorter scales, with an eventual stabilisation, or slight increase in SampEn at longer (coarser) scales (Figure 9.4B). For lower contraction intensities, the MSE curves stabilised at shorter scales and higher SampEn values, when compared to

higher contraction intensities. By comparison, higher contraction intensities exhibit MSE curves with lower SampEn values, that progressively increase across the coarse-grained scales, to converge with the SampEn values of lower contraction intensities (Figure 9.4B). These MSE curve profiles were similar to those presented in previous research that assessed the effect of age and contraction intensity of the temporal structure of isometric PG and IFA force signals using the MSE analysis (Knol et al., 2019; Vaillancourt et al., 2004; Vieluf et al., 2015).

The muscle and contraction intensity dependent scale-to-scale dynamics of the MSE curves suggests that there may be muscle specific control strategies required to meet the task demands. Differences in the interactions and coupling within and between (sub)system components, in addition to muscle specific structure and function of individual system components (Vaillancourt & Newell, 2002; Sleimen-Malkoun et al., 2014), would likely result in unique frequency- and amplitude-varying inputs to the muscle. These inputs would potentially manifest as muscle specific temporal structure in the torque and force signals, hence the muscle and contraction intensity dependent scale-to-scale dynamics of the MSE curves. Further experimental research is required to determine whether the muscle dependent behaviour of the MSE curves is indicative of muscle specific differences in the behaviour of the neuromuscular system on a component level.

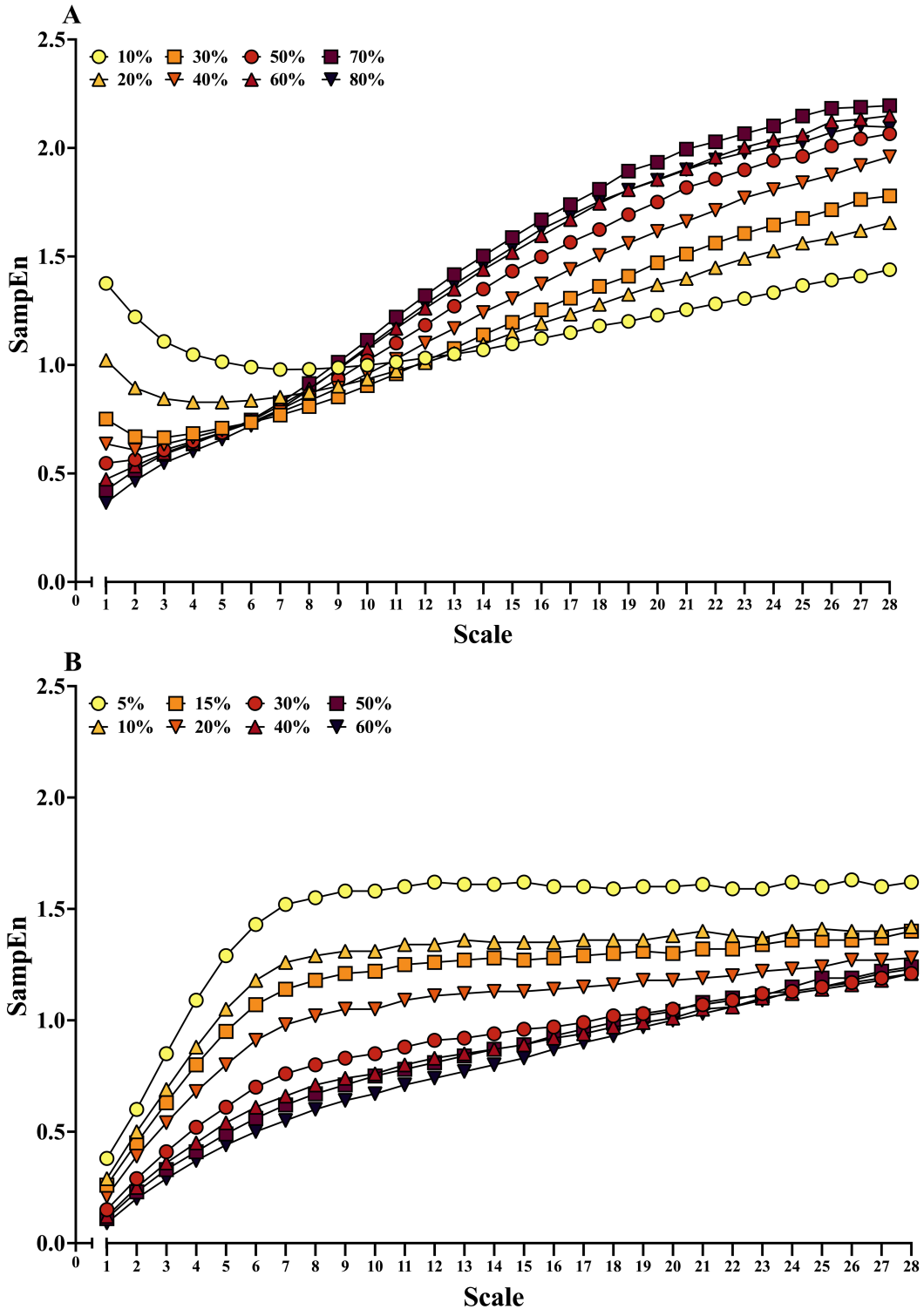

Figure 9.4. (A) Multiscale entropy curves of isometric knee extensor torque at multiple relative contraction intensities. Note the *cross-over* in the MSE curves with lower contraction intensities presenting with higher SampEn values at shorter scales, and higher contraction intensities presenting with higher SampEn at longer (coarser) scales. The *cross-over* is indicative of contraction intensity related alterations in the regularity of the different frequency components present within the torque signals (mean data from $N = 80$ individuals performing isometric knee extension contractions), **(B)** Multiscale entropy curves of isometric precision pinch grip force at multiple relative contraction intensities (mean data from $N = 64$ individuals performing of isometric precision pinch grip contractions).

9.5 - Relationship between fundamental motor skills and the complexity of isometric knee extensor torque signals.

Equilibrium of the inverted pendulum: *the association between complexity of isometric knee extensor torque and the magnitude of postural sway.*

Upright human postural control can be effectively modelled as a simplified inverted pendulum (Winter, 1995; Winter et al., 2003; Loram & Lakie, 2002). The equilibrium of the inverted pendulum (i.e., maintenance of postural control) during standing is achieved through a complex process, involving the integration of sensory inputs from somatosensory, vestibular, and visual system, in addition to the coordinated action of the musculoskeletal system (Luu et al., 2012; Peterka, 2018).

The progressive decline in neuromuscular complexity is postulated to be associated with a concomitant degradation in system functionality, whereby a critical loss of complexity would see individual fall below the frailty threshold (Lipsitz, 2002). However, there has been an absence of experimental research substantiating the functional implications of a loss of neuromuscular complexity. The KE muscles contribute to maintaining postural control during standing (Krishnamoorthy et al., 2004; Laughton et al., 2003). As such, it is plausible that lower neuromuscular complexity of the KE muscles may be associated with worse postural control. Therefore, Chapter Six investigated the association between the complexity of isometric KE torque and the magnitude of postural sway across different age groups.

The thesis presented novel evidence that individuals exhibiting lower neuromuscular complexity in the KE muscles demonstrate a greater magnitude, speed and amplitude of AP postural sway (Chapter Six). When accounting for age and MVT, neuromuscular complexity (CI-28) could explain a significant, albeit small percentage (5.4% to 9.1%) of additional variance in the magnitude, speed and amplitude of AP postural sway. Importantly, this experimental evidence highlights the functional significance of neuromuscular complexity and therefore provides an initial foundation for the use of complexity metrics as monitoring tools for the assessment of functional neurophysiological changes in younger and older adults. However, further research is required to establish the efficacy and sensitivity of these measures in monitoring and detecting clinically meaningful changes to fundamental motor skill performance longitudinally and in response to acute interventions.

9.6 - Neural mechanisms underpinning the neuromuscular complexity and variability of the knee extensor muscles.

Temporal structure of torque: *mechanisms that underpin the complexity of isometric knee extensor torque signals.*

The current thesis presents the first evidence establishing the relationship between the strength of common synaptic input and the complexity measures used to analyse the temporal structure of KE torque signals during isometric contractions (Chapters Eight A and Eight B). Specifically, stronger alpha band oscillations in common synaptic input were found to be significantly associated with higher complexity torque signals during isometric KE contractions (i.e., a higher CI-28 and a DFA scaling exponent α closer to 1.0; Chapter Eight A).

Importantly, the thesis provides an initial step towards explaining the neural mechanisms accountable for the age and fatigue related scale-to-scale dynamics of the MSE curves and therefore the temporal structure of the torque signals (Chapters Eight A and Eight B). In Chapter Eight A, stronger alpha band oscillations in common synaptic input were found to be significantly associated with higher SampEn of the coarse-grained muscle torque signals from scales 10 to 28. Furthermore, Chapter Eight B revealed that fatigue-related increases in the strength of alpha band oscillations in common synaptic input were significantly associated with the fatigue-related increase in the SampEn of the coarse-grained muscle torque signals from scales 11 to 28. These findings suggest that the SampEn of muscle torque signal at longer (coarser) scales may be indicative of the strength of common synaptic input to the motor neurons innervating the torque producing muscles.

Chapters Eight A and Eight B were unable to directly explain the neural mechanisms underpinning the age-related differences in neuromuscular complexity, in addition to the age-dependent temporal structure revealed by the MSE curves. This was likely due to methodological (e.g., age group sample sizes and HD sEMG array only on the VL) and technological (e.g., size and density of the HD sEMG array) limitations. However, based on current findings, it is plausible that the strength of oscillations in common synaptic input may also be explanatory of the age-related differences in the complexity of KE torque, in addition to the age-dependent scale-to-scale entropic behaviour of the MSE curves.

Spatial structure of torque: *mechanisms that underpin the variability of isometric knee extensor torque signals.*

Stronger alpha band oscillations in common synaptic input were found to be significantly associated with greater targeting errors (i.e., higher RMSE) and greater absolute variability (i.e., higher SDT) in the KE torque signals during fresh isometric contractions (Chapter Eight A). Furthermore, the fatigue-related increases in the strength of alpha band oscillations in common synaptic input were significantly associated with the fatigue-related increase in the variability of isometric KE torque (Chapter Eight B). These findings highlight the involvement of alpha frequency band (physiological tremor band) oscillations in altering the spatial structure of isometric KE torque signals and therefore in modulating the precision of isometric KE muscle torque control.

The variability in low frequency oscillations in common synaptic input to the involved motor neurons (i.e., greater variability of smoothed CSTs) was found to be significantly associated with the variability in isometric KE torque signals (Chapter Eight A). In accordance, fatigue-related increases in the variability in low frequency oscillations in common synaptic input (effective neural drive) were significantly associated with fatigue-related increases in the variability of isometric KE torque signals (Chapter Eight B). Current thesis findings corroborate previous research which has shown the variability in low frequency oscillations in common synaptic input to be associated with the variability in isometric muscle force signals (Feeney et al., 2018; Germer et al., 2020; Mani et al., 2019). However, to the authors knowledge, current findings were the first to demonstrate that the spatial structure of isometric KE torque signals is attributable, in part, to the variability in low frequency oscillations in common synaptic input to the motor neurons innervating the VL muscle. Collectively, current thesis findings suggest that the spatial structure of an isometric KE torque signal is a function of alpha band oscillations in common synaptic input and the variability in low frequency oscillations in common synaptic input.

Notably, it was *not* possible to directly explain the neural mechanisms underpinning the age-related differences in the variability and accuracy of isometric KE torque from the MU data collected in Chapter Eight A. However, given current evidence, a plausible explanation for the age-related differences in KE torque control would be differences between the age groups in the strength and variability of oscillations in common synaptic input. This is supported by

previous research that found age-related increases in the muscle force variability to be associated with the increased strength of low-frequency oscillations in common synaptic input (Castronovo et al., 2018).

Temporospatial structure of torque

The temporospatial structure (the *complexity* and *variability*) of isometric KE torque signals has been found to be determined, in part, by the strength and variability of oscillations in common synaptic input. Importantly, this thesis provides the first experimental data that shows the complexity measures derived from isometric KE torque reflects the adaptive neural response, and thus, the neuromuscular system's strategy to meet task demands. Moreover, findings also support the theoretical framework of physiological complexity, that proposes the changes in a system on a component level (i.e., change in the strength and variability of common synaptic input), were reflected on a behavioural level in the *complexity* of a systems output (Vaillancourt & Newell, 2002; Sleimen-Malkoun et al., 2014).

Further research unconstrained by methodological and technological limitations is required to elucidate the remaining neuromuscular mechanism(s) that contribute to the temporal and spatial structure of muscle torque signals and importantly the age-dependent temporal structure of muscle torque signals.

9.7 - Thesis methodological considerations.

How physically active? *the impact of participant physical activity levels on neuromuscular complexity.*

There were many challenges and limitations to recruiting participants and controlling their physical activity levels. The most applicable to the current research were; the diverse range of participant physical activity modalities and levels within and between age groups (i.e., type, duration, intensity and frequency); regular physical activity in later life preceded by years of inactivity; the physical activity status reflecting or not reflecting the task demand; individual dose-response to physical activity in different age groups; and difficulties in matching age groups for physical activity status. All these factors contribute to the challenge of uncoupling the relative influence of age and physical activity levels on observed age-related differences in the neuromuscular complexity.

Across all experimental chapters participants were recruited to be physically active, performing levels of exercise consistent with the World Health Organisation guidelines for ≥ 2 years (i.e., 2.5 to 5 hours of moderate exercise per week; Bull et al. 2020). This approach to controlling participant physical activity levels is vulnerable to the limitations outlined above. Therefore, it is likely that the age-related differences in the complexity of isometric muscle torque observed within and between the experimental chapters represents the ageing process interacting with participant physical activity levels. However, this approach also ensured that all participants were at a minimum, recreationally active, while maintaining a wider inclusion criterion for physical activity levels and thus preserving the feasibility of recruitment.

In a cross-sectional research design, age-related differences in neuromuscular complexity were likely to always reflect, albeit to varying extents, age and physical activity status regardless of how closely participant physical activity levels can be controlled. In other words, it will be very difficult to uncouple the relative influence of physical activity on age-related differences in neuromuscular complexity. This underscores the importance of accounting for participant physical activity status in the interpretation of the study findings.

The methodologies in the current experimental chapters were not designed to conclusively uncouple the influences of age and physical activity status on the age-related differences in

neuromuscular complexity. Future research may aim to disentangle the relative influence of these factors on changes in neuromuscular complexity. However, this will be challenging in a cross-sectional research design due to the inter-individual variability in how physical activity likely affects muscle torque complexity across the lifespan. Therefore, research time and resources may be better used investigating the efficacy of exercise interventions in preserving and/or reversing the loss of complexity throughout life, and importantly, into older age.

Is age just a number? *the influence of the difference in participant ages across the experimental chapters.*

Across the experimental chapters that investigated the effect of age on the complexity of isometric KE torque signals, the age criteria for the older groups were gradually expanded from 50-70 years (Chapter Five) to 50-85 years (Chapter Six) and 50-90 years (Chapters Eight A and Eight B). In the first instance, the 50-70-year bracket was selected to be at the onset of progressive muscle ageing (~50 years; Janssen et al., 2000; Pabla et al., 2024) but prior to *older old* age and frailty (> 70 years; Carnavale et al., 2020). However, as noted in Chapter Five, the *younger* mean age of the middle age group (58.6 ± 5.1 years) provided an incomplete understanding of how the pathway to senescence effects the complexity of isometric KE torque. This influenced the subsequent increase in the maximum age for inclusion in the older groups in Chapters Six, Eight A and Eight B.

Despite increasing the maximum age for inclusion in the older groups, there were difficulties in recruiting older adults (> 70 years) who were regularly physically active, in addition to being absent of medical conditions and/or impairments to lower limb function. Consequently, across Chapters Six, Eight A and Eight B, there were only twelve volunteers aged > 70 years who were able to participate. Nevertheless, the change in the age criteria for the older groups resulted in the older group in Chapter Six being slightly *older* than the older group in Chapter Five (Chapter Five, 58.6 ± 5.1 years vs. Chapter Six, 64.9 ± 11.3 years). The *older* age of the older group in Chapter Six may explain why age-related differences in isometric KE torque complexity were observed in Chapter Six but not in Chapter Five.

Importantly, the increase in the maximum age of the older groups was sufficient to capture an age-related difference in the complexity of isometric KE torque (Chapter Six). However, current evidence was still unable to elucidate the effect of *older old* age (> 70 years) on the

complexity of isometric KE torque. The potential effect of *older old* age (> 70 years) on the neuromuscular complexity may be characterised by the suppression of the MSE curve across all time scales and the concurrent reduction in muscle torque steadiness and accuracy (Figures 9.1 and 9.2). This initial evidence necessitates further research to fully elucidate the effects of *older old* age on the complexity of isometric KE torque. Additionally, future research may look to elucidate the rate and magnitude of the age-related change in the complexity of isometric KE torque by recruiting participants across a wide spectrum of ages (e.g., 18 to 90 years). However, these approaches would necessitate large participant sample sizes, far in excess of what was feasible in the studies of the current thesis.

9.8 - Conclusion

In conclusion, the thesis demonstrates that older adults exhibit lower neuromuscular complexity and greater neuromuscular variability in both lower (knee extensor muscles) and upper (hand muscles) extremity muscle groups compared to younger adults. The observed age-group related differences in neuromuscular complexity and variability were likely attributable, in part, to alterations in the strength and variance of oscillations in common synaptic input. These findings highlight the potential of neuromuscular complexity and variability as reliable, functionally relevant, non-invasive biomarkers for assessing and monitoring age-related changes in the regulation of muscle torque and force.

The thesis introduced, for the first time using the MSE analysis, evidence that the temporal structure of isometric KE torque signals is influenced by age-group, neuromuscular fatigue, and contraction intensity. The scale-to-scale entropic behaviour observed in the MSE curves likely reflects the neuromuscular system's high dimensionality, arising from the interactions among multiple system components. These findings suggest that MSE analysis of isometric KE torque signals may be sensitive to both structural and functional changes within individual components, as well as broader systemic reorganisation of interactions between components due to age, fatigue, and contraction intensity.

01010100 01101000 01100101 00100000 01000101 01101110 01100100

Reference List

1. Abe, T., Loenneke, J. P., Thiebaud, R. S., & Fukunaga, T. (2014). Age-related site-specific muscle wasting of upper and lower extremities and trunk in Japanese men and women. *Age (Dordrecht, Netherlands), 36*(2), 813–821. https://doi.org/10.1007/s11357-013-9600-5

2. Abe, T., Sakamaki, M., Yasuda, T., Bemben, M. G., Kondo, M., Kawakami, Y., & Fukunaga, T. (2011). Age-related, site-specific muscle loss in 1507 Japanese men and women aged 20 to 95 years. *Journal of sports science & medicine, 10*(1), 145–150.

3. Adrian, E. D., & Bronk, D. W. (1929). The discharge of impulses in motor nerve fibres: Part II. The frequency of discharge in reflex and voluntary contractions. *The Journal of physiology, 67*(2), i3–i151.

4. Ahmadiahangar, A., Javadian, Y., Babaei, M., Heidari, B., Hosseini, S., & Aminzadeh, M. (2018). The role of quadriceps muscle strength in the development of falls in the elderly people, a cross-sectional study. *Chiropractic & manual therapies, 26,* 31. https://doi.org/10.1186/s12998-018-0195-x

5. Allen, M. D., Dalton, B. H., Gilmore, K. J., McNeil, C. J., Doherty, T. J., Rice, C. L., & Power, G. A. (2021). Neuroprotective effects of exercise on the aging human neuromuscular system. *Experimental gerontology, 152*, 111465. https://doi.org/10.1016/j.exger.2021.111465

6. Allison D. B. (1993). Limitations of coefficient of variation as index of measurement reliability. *Nutrition (Burbank, Los Angeles County, Calif.), 9*(6), 559–561.

7. Allman, B. L., & Rice, C. L. (2002). Neuromuscular fatigue and aging: central and peripheral factors. *Muscle & nerve, 25*(6), 785–796. https://doi.org/10.1002/mus.10116

8. Almuklass, A. M., Davis, L., Hamilton, L. D., Vieira, T. M., Botter, A., & Enoka, R. M. (2018a). Motor unit discharge characteristics and walking performance of individuals with multiple sclerosis. *Journal of neurophysiology, 119*(4), 1273–1282. https://doi.org/10.1152/jn.00598.2017

9. Almuklass, A. M., Feeney, D. F., Mani, D., Hamilton, L. D., & Enoka, R. M. (2018b). Peg-manipulation capabilities of middle-aged adults have a greater influence on pegboard times than those of young and old adults. *Experimental brain research, 236*(8), 2165–2172. https://doi.org/10.1007/s00221-018-5294-3

10. Almuklass, A. M., Price, R. C., Gould, J. R., & Enoka, R. M. (2016). Force steadiness as a predictor of time to complete a pegboard test of dexterity in young men and women. *Journal of applied physiology (Bethesda, Md. : 1985), 120*(12), 1410–1417. https://doi.org/10.1152/japplphysiol.01051.2015

11. Amirjani, N., Ashworth, N. L., Gordon, T., Edwards, D. C., & Chan, K. M. (2007). Normative values and the effects of age, gender, and handedness on the Moberg Pick-Up Test. *Muscle & nerve, 35*(6), 788–792. https://doi.org/10.1002/mus.20750

12. Arellano, C. J., Caha, D., Hennessey, J. E., Amiridis, I. G., Baudry, S., & Enoka, R. M. (2016). Fatigue-induced adjustment in antagonist coactivation by old adults during a steadiness task. *Journal of applied physiology (Bethesda, Md. : 1985), 120*(9), 1039–1046. https://doi.org/10.1152/japplphysiol.00908.2015

13. Arjunan, S. P., Kumar, D. K., & Bastos, T. (2012). Fractal based complexity measure and variation in force during sustained isometric muscle contraction: effect of aging. *Annual International Conference of the IEEE Engineering in Medicine and Biology Society. IEEE Engineering in Medicine and Biology Society. Annual International Conference, 2012*, 3484–3487. https://doi.org/10.1109/EMBC.2012.6346716

14. Ashendorf, L., Vanderslice-Barr, J. L., & McCaffrey, R. J. (2009). Motor tests and cognition in healthy older adults. *Applied neuropsychology, 16*(3), 171–176. https://doi.org/10.1080/09084280903098562

15. Atkinson, G., & Nevill, A. M. (1998). Statistical methods for assessing measurement error (reliability) in variables relevant to sports medicine. *Sports medicine (Auckland, N.Z.), 26*(4), 217–238. https://doi.org/10.2165/00007256-199826040-00002

16. Aubertin-Leheudre, M., Pion, C. H., Vallée, J., Marchand, S., Morais, J. A., Bélanger, M., & Robitaille, R. (2020). Improved Human Muscle Biopsy Method To Study Neuromuscular Junction Structure and Functions with Aging. *The journals of gerontology. Series A, Biological sciences and medical sciences, 75*(11), 2098–2102. https://doi.org/10.1093/gerona/glz292

17. Avrillon, S., Del Vecchio, A., Farina, D., Pons, J. L., Vogel, C., Umehara, J., & Hug, F. (2021). Individual differences in the neural strategies to control the lateral and medial head of the quadriceps during a mechanically constrained task. *Journal of applied physiology (Bethesda, Md. : 1985), 130*(1), 269–281. https://doi.org/10.1152/japplphysiol.00653.2020

18. Avrillon, S., Hug, F., Enoka, R., Caillet, A. H., & Farina, D. (2023). The decoding of extensive samples of motor units in human muscles reveals the rate coding of entire motor neuron pools. *eLife 13*:RP97085 https://doi.org/10.7554/eLife.97085.1

19. Baker, J. R., Davey, N. J., Ellaway, P. H., & Friedland, C. L. (1992). Short-term synchrony of motor unit discharge during weak isometric contraction in Parkinson's disease. *Brain : a journal of neurology, 115* Pt 1, 137–154. https://doi.org/10.1093/brain/115.1.137

20. Baltes, P. B., & Lindenberger, U. (1997). Emergence of a powerful connection between sensory and cognitive functions across the adult life span: a new window to the study of cognitive aging?. *Psychology and aging, 12*(1), 12–21. https://doi.org/10.1037//0882-7974.12.1.12

21. Bandholm, T., Rose, M. H., Sonne-Holm, S., & Jensen, B. R. (2008). Assessment of torque-steadiness reliability at the ankle level in healthy young subjects: implications for cerebral

palsy. *European journal of applied physiology, 104*(4), 609–615. https://doi.org/10.1007/s00421-008-0808-5

22. Barbosa, R. N., Silva, N. R. S., Santos, D. P. R., Moraes, R., & Gomes, M. M. (2018). The variability of the force produced by the plantar flexor muscles does not associate with postural sway in older adults during upright standing. *Human movement science, 60*, 115–121. https://doi.org/10.1016/j.humov.2018.05.009

23. Barbosa, R. N., Silva, N. R. S., Santos, D. P. R., Moraes, R., & Gomes, M. M. (2020). Force stability training decreased force variability of plantar flexor muscles without reducing postural sway in female older adults. *Gait & posture, 77*, 288–292. https://doi.org/10.1016/j.gaitpost.2020.02.015

24. Barry, B. K., Pascoe, M. A., Jesunathadas, M., & Enoka, R. M. (2007). Rate coding is compressed but variability is unaltered for motor units in a hand muscle of old adults. *Journal of neurophysiology, 97*(5), 3206–3218. https://doi.org/10.1152/jn.01280.2006

25. Bartko J. J. (1966). The intraclass correlation coefficient as a measure of reliability. *Psychological reports, 19*(1), 3–11. https://doi.org/10.2466/pr0.1966.19.1.3

26. Baudry, S., Penzer, F., & Duchateau, J. (2014). Input-output characteristics of soleus homonymous Ia afferents and corticospinal pathways during upright standing differ between young and elderly adults. *Acta physiologica (Oxford, England), 210*(3), 667–677. https://doi.org/10.1111/apha.12233

27. Baweja, H. S., Kwon, M., & Christou, E. A. (2012). Magnified visual feedback exacerbates positional variability in older adults due to altered modulation of the primary agonist muscle. *Experimental brain research, 222*(4), 355–364. https://doi.org/10.1007/s00221-012-3219-0

28. Bazzucchi, I., Felici, F., Macaluso, A., & De Vito, G. (2004). Differences between young and older women in maximal force, force fluctuations, and surface EMG during isometric knee extension and elbow flexion. *Muscle & nerve, 30*(5), 626–635. https://doi.org/10.1002/mus.20151

29. Bean, J. F., Kiely, D. K., Herman, S., Leveille, S. G., Mizer, K., Frontera, W. R., & Fielding, R. A. (2002). The relationship between leg power and physical performance in mobility-limited older people. *Journal of the American Geriatrics Society, 50*(3), 461–467. https://doi.org/10.1046/j.1532-5415.2002.50111.x

30. Beauchamp, J. A., Pearcey, G. E., Khurram, O. U., Negro, F., Dewald, J. P., & Heckman, C. J. (2023). Intrinsic properties of spinal motor neurons degrade ankle torque control in humans. *bioRxiv*, 2023-10.

31. Beaver, W. L., Wasserman, K., & Whipp, B. J. (1986). A new method for detecting anaerobic threshold by gas exchange. *Journal of applied physiology (Bethesda, Md. : 1985), 60*(6), 2020–2027. https://doi.org/10.1152/jappl.1986.60.6.2020

32. Beck, T. W., Defreitas, J. M., Stock, M. S., & Dillon, M. A. (2011). Effects of resistance training on force steadiness and common drive. *Muscle & nerve, 43*(2), 245–250. https://doi.org/10.1002/mus.21836

33. Beckerman, H., Roebroeck, M. E., Lankhorst, G. J., Becher, J. G., Bezemer, P. D., & Verbeek, A. L. (2001). Smallest real difference, a link between reproducibility and responsiveness. *Quality of life research : an international journal of quality of life aspects of treatment, care and rehabilitation, 10*(7), 571–578. https://doi.org/10.1023/a:1013138911638

34. Beckerman, Vogelaar, T. W., Lankhorst, G. J., & Verbeek, A. L. (1996). A criterion for stability of the motor function of the lower extremity in stroke patients using the Fugl-Meyer Assessment Scale. *Scandinavian journal of rehabilitation medicine, 28*(1), 3–7.

35. Bellew J. W. (2002). The effect of strength training on control of force in older men and women. *Aging clinical and experimental research, 14*(1), 35–41. https://doi.org/10.1007/BF03324415

36. Beretta-Piccoli, M., D'Antona, G., Barbero, M., Fisher, B., Dieli-Conwright, C. M., Clijsen, R., & Cescon, C. (2015). Evaluation of central and peripheral fatigue in the quadriceps using fractal dimension and conduction velocity in young females. *PloS one, 10*(4), e0123921. https://doi.org/10.1371/journal.pone.0123921

37. Berger, A., Steinberg, F., Thomas, F., & Doppelmayr, M. (2020). Neural Correlates of Age-Related Changes in Precise Grip Force Regulation: A Combined EEG-fNIRS Study. *Frontiers in aging neuroscience, 12*, 594810. https://doi.org/10.3389/fnagi.2020.594810

38. Bigger, J. T., Jr, Steinman, R. C., Rolnitzky, L. M., Fleiss, J. L., Albrecht, P., & Cohen, R. J. (1996). Power law behavior of RR-interval variability in healthy middle-aged persons, patients with recent acute myocardial infarction, and patients with heart transplants. *Circulation, 93*(12), 2142–2151. https://doi.org/10.1161/01.cir.93.12.2142

39. Bilodeau, M., Keen, D. A., Sweeney, P. J., Shields, R. W., & Enoka, R. M. (2000). Strength training can improve steadiness in persons with essential tremor. *Muscle & nerve, 23*(5), 771–778. https://doi.org/10.1002/(sici)1097-4598(200005)23:5<771::aid-mus15>3.0.co;2-9

40. Binder, M. D., Powers, R. K., & Heckman, C. J. (2020). Nonlinear Input-Output Functions of Motor neurons. *Physiology (Bethesda, Md.), 35*(1), 31–39. https://doi.org/10.1152/physiol.00026.2019

41. Bland, J. M., & Altman, D. G. (1986). Statistical methods for assessing agreement between two methods of clinical measurement. *Lancet (London, England), 1*(8476), 307–310.

42. Blomkvist, A. W., Eika, F., de Bruin, E. D., Andersen, S., & Jorgensen, M. (2018). Handgrip force steadiness in young and older adults: a reproducibility study. *BMC musculoskeletal disorders, 19*(1), 96. https://doi.org/10.1186/s12891-018-2015-9

43. Boehm, I., Miller, J., Wishart, T. M., Wigmore, S. J., Skipworth, R. J., Jones, R. A., & Gillingwater, T. H. (2020). Neuromuscular junctions are stable in patients with cancer cachexia. *The Journal of clinical investigation, 130*(3), 1461–1465. https://doi.org/10.1172/JCI128411

44. Booth, F. W., Laye, M. J., & Roberts, M. D. (2011). Lifetime sedentary living accelerates some aspects of secondary aging. *Journal of applied physiology (Bethesda, Md. : 1985), 111*(5), 1497–1504. https://doi.org/10.1152/japplphysiol.00420.2011

45. Bootsma, J. M., Caljouw, S. R., Veldman, M. P., Maurits, N. M., Rothwell, J. C., & Hortobágyi, T. (2021). Neural Correlates of Motor Skill Learning Are Dependent on Both Age and Task Difficulty. *Frontiers in aging neuroscience, 13*, 643132. https://doi.org/10.3389/fnagi.2021.643132

46. Bouchard, C., Blair, S. N., & Katzmarzyk, P. T. (2015). Less Sitting, More Physical Activity, or Higher Fitness?. *Mayo Clinic proceedings, 90*(11), 1533–1540. https://doi.org/10.1016/j.mayocp.2015.08.005

47. Bull, F. C., Al-Ansari, S. S., Biddle, S., Borodulin, K., Buman, M. P., Cardon, G., Carty, C., Chaput, J. P., Chastin, S., Chou, R., Dempsey, P. C., DiPietro, L., Ekelund, U., Firth, J., Friedenreich, C. M., Garcia, L., Gichu, M., Jago, R., Katzmarzyk, P. T., Lambert, E., … Willumsen, J. F. (2020). World Health Organization 2020 guidelines on physical activity and sedentary behaviour. *British journal of sports medicine, 54*(24), 1451–1462. https://doi.org/10.1136/bjsports-2020-102955

48. Burnett, R. A., Laidlaw, D. H., & Enoka, R. M. (2000). Coactivation of the antagonist muscle does not covary with steadiness in old adults. *Journal of applied physiology (Bethesda, Md. : 1985), 89*(1), 61–71. https://doi.org/10.1152/jappl.2000.89.1.61

49. Cabral, H. V., Cudicio, A., Bonardi, A., Del Vecchio, A., Falciati, L., Orizio, C., Martinez-Valdes, E., & Negro, F. (2024). Neural Filtering of Physiological Tremor Oscillations to Spinal Motor Neurons Mediates Short-Term Acquisition of a Skill Learning Task. *eNeuro, 11*(7), ENEURO.0043-24.2024. https://doi.org/10.1523/ENEURO.0043-24.2024

50. Caillet, A. H., Avrillon, S., Kundu, A., Yu, T., Phillips, A. T. M., Modenese, L., & Farina, D. (2023). Larger and Denser: An Optimal Design for Surface Grids of EMG Electrodes to Identify Greater and More Representative Samples of Motor Units. *eNeuro, 10*(9), ENEURO.0064-23.2023. https://doi.org/10.1523/ENEURO.0064-23.2023

51. Callahan, D. M., & Kent-Braun, J. A. (2011). Effect of old age on human skeletal muscle force-velocity and fatigue properties. *Journal of applied physiology (Bethesda, Md. : 1985), 111*(5), 1345–1352. https://doi.org/10.1152/japplphysiol.00367.2011

52. Callahan, D. M., Foulis, S. A., & Kent-Braun, J. A. (2009). Age-related fatigue resistance in the knee extensor muscles is specific to contraction mode. *Muscle & nerve, 39*(5), 692–702. https://doi.org/10.1002/mus.21278

53. Callahan, D. M., Umberger, B. R., & Kent, J. A. (2016). Mechanisms of in vivo muscle fatigue in humans: investigating age-related fatigue resistance with a computational model. *The Journal of physiology, 594*(12), 3407–3421. https://doi.org/10.1113/JP271400

54. Camacho-Villa, M. A., Giráldez-García, M. A., Sevilla-Sanchez, M., Rivera-Mejía, S. L., & Carballeira, E. (2025). Relationship Between Force Steadiness and Functionality in Older Adults: A Systematic Review With Meta-Analysis. *Scandinavian journal of medicine & science in sports, 35*(4), e70040. https://doi.org/10.1111/sms.70040

55. Campbell, M. J., McComas, A. J., & Petito, F. (1973). Physiological changes in ageing muscles. *Journal of neurology, neurosurgery, and psychiatry, 36*(2), 174–182. https://doi.org/10.1136/jnnp.36.2.174

56. Canepari, M., Pellegrino, M. A., D'Antona, G., & Bottinelli, R. (2010). Single muscle fiber properties in aging and disuse. *Scandinavian journal of medicine & science in sports, 20*(1), 10–19. https://doi.org/10.1111/j.1600-0838.2009.00965.x

57. Carey, L. M., Oke, L. E., & Matyas, T. A. (1997). Impaired touch discrimination after stroke: a quantiative test. *Journal of Neurologic Rehabilitation, 11*(4), 219-232.

58. Carmeli, E., Patish, H., & Coleman, R. (2003). The aging hand. *The journals of gerontology. Series A, Biological sciences and medical sciences, 58*(2), 146–152. https://doi.org/10.1093/gerona/58.2.m146

59. Carnavale, B. F., Fiogbé, E., Farche, A. C. S., Catai, A. M., Porta, A., & Takahashi, A. C. M. (2020). Complexity of knee extensor torque in patients with frailty syndrome: a cross-sectional study. *Brazilian journal of physical therapy, 24*(1), 30–38. https://doi.org/10.1016/j.bjpt.2018.12.004

60. Cartee, G. D., Hepple, R. T., Bamman, M. M., & Zierath, J. R. (2016). Exercise Promotes Healthy Aging of Skeletal Muscle. *Cell metabolism, 23*(6), 1034–1047. https://doi.org/10.1016/j.cmet.2016.05.007

61. Carville, S. F., Perry, M. C., Rutherford, O. M., Smith, I. C., & Newham, D. J. (2007). Steadiness of quadriceps contractions in young and older adults with and without a history of falling. *European journal of applied physiology, 100*(5), 527–533. https://doi.org/10.1007/s00421-006-0245-2

62. Carville, S. F., Rutherford, O. M., & Newham, D. J. (2006). Power output, isometric strength and steadiness in the leg muscles of pre- and postmenopausal women; the effects of hormone replacement therapy. *European journal of applied physiology, 96*(3), 292–298. https://doi.org/10.1007/s00421-005-0078-4

63. Caserta, F., Eldred, W. D., Fernandez, E., Hausman, R. E., Stanford, L. R., Bulderev, S. V., Schwarzer, S., & Stanley, H. E. (1995). Determination of fractal dimension of physiologically characterized neurons in two and three dimensions. *Journal of neuroscience methods, 56*(2), 133–144. https://doi.org/10.1016/0165-0270(94)00115-w

64. Cashaback, J. G., Cluff, T., & Potvin, J. R. (2013). Muscle fatigue and contraction intensity modulates the complexity of surface electromyography. *Journal of electromyography and*

kinesiology : official journal of the International Society of Electrophysiological Kinesiology, 23(1), 78–83. https://doi.org/10.1016/j.jelekin.2012.08.004

65. Castronovo, A. M., Mrachacz-Kersting, N., Stevenson, A. J. T., Holobar, A., Enoka, R. M., & Farina, D. (2018). Decrease in force steadiness with aging is associated with increased power of the common but not independent input to motor neurons. *Journal of neurophysiology, 120*(4), 1616–1624. https://doi.org/10.1152/jn.00093.2018

66. Castronovo, A. M., Negro, F., Conforto, S., & Farina, D. (2015). The proportion of common synaptic input to motor neurons increases with an increase in net excitatory input. *Journal of applied physiology (Bethesda, Md. : 1985), 119*(11), 1337–1346. https://doi.org/10.1152/japplphysiol.00255.2015

67. Cerella, J., & Hale, S. (1994). The rise and fall in information-processing rates over the life span. *Acta psychologica, 86*(2-3), 109–197. https://doi.org/10.1016/0001-6918(94)90002-7

68. Challis J. H. (2006). Aging, regularity and variability in maximum isometric moments. *Journal of biomechanics, 39*(8), 1543–1546. https://doi.org/10.1016/j.jbiomech.2005.04.008

69. Chen, Y. C., Lin, L. L., Lin, Y. T., Hu, C. L., & Hwang, I. S. (2017). Variations in Static Force Control and Motor Unit Behavior with Error Amplification Feedback in the Elderly. *Frontiers in human neuroscience, 11,* 538. https://doi.org/10.3389/fnhum.2017.00538

70. Christakos, C. N., Papadimitriou, N. A., & Erimaki, S. (2006). Parallel neuronal mechanisms underlying physiological force tremor in steady muscle contractions of humans. *Journal of neurophysiology, 95*(1), 53–66. https://doi.org/10.1152/jn.00051.2005

71. Christie, A., & Kamen, G. (2010). Short-term training adaptations in maximal motor unit firing rates and afterhyperpolarization duration. *Muscle & nerve, 41*(5), 651–660. https://doi.org/10.1002/mus.21539

72. Christie, A., Snook, E. M., & Kent-Braun, J. A. (2011). Systematic review and meta-analysis of skeletal muscle fatigue in old age. *Medicine and science in sports and exercise, 43*(4), 568–577. https://doi.org/10.1249/MSS.0b013e3181f9b1c4

73. Christou E. A. (2011). Aging and variability of voluntary contractions. *Exercise and sport sciences reviews, 39*(2), 77–84. https://doi.org/10.1097/JES.0b013e31820b85ab

74. Christou, E. A., & Carlton, L. G. (2001). Old adults exhibit greater motor output variability than young adults only during rapid discrete isometric contractions. *The journals of gerontology. Series A, Biological sciences and medical sciences, 56*(12), B524–B532. https://doi.org/10.1093/gerona/56.12.b524

75. Christou, E. A., & Carlton, L. G. (2002). Age and contraction type influence motor output variability in rapid discrete tasks. *Journal of applied physiology (Bethesda, Md. : 1985), 93*(2), 489–498. https://doi.org/10.1152/japplphysiol.00335.2001

76. Christou, E. A., Grossman, M., & Carlton, L. G. (2002). Modeling variability of force during isometric contractions of the quadriceps femoris. *Journal of motor behavior, 34*(1), 67–81. https://doi.org/10.1080/00222890209601932

77. Clark, B. C., Cook, S. B., & Ploutz-Snyder, L. L. (2007). Reliability of techniques to assess human neuromuscular function in vivo. *Journal of electromyography and kinesiology : official journal of the International Society of Electrophysiological Kinesiology, 17*(1), 90–101. https://doi.org/10.1016/j.jelekin.2005.11.008

78. Clark, B. C., Pierce, J. R., Manini, T. M., & Ploutz-Snyder, L. L. (2007). Effect of prolonged unweighting of human skeletal muscle on neuromotor force control. European journal of applied physiology, 100(1), 53–62. https://doi.org/10.1007/s00421-007-0399-6

79. Clark, N. C., Pethick, J., & Falla, D. (2023). Measuring complexity of muscle force control: Theoretical principles and clinical relevance in musculoskeletal research and practice. *Musculoskeletal science & practice, 64,* 102725. https://doi.org/10.1016/j.msksp.2023.102725

80. Cohen, J. (1988). Statistical Power Analysis for the Behavioral Sciences (2nd ed.). Hillsdale, NJ: Lawrence Erlbaum Associates, Publishers.

81. Connelly, D. M., Rice, C. L., Roos, M. R., & Vandervoort, A. A. (1999). Motor unit firing rates and contractile properties in tibialis anterior of young and old men. *Journal of applied physiology (Bethesda, Md. : 1985), 87*(2), 843–852. https://doi.org/10.1152/jappl.1999.87.2.843

82. Contessa, P., Adam, A., & De Luca, C. J. (2009). Motor unit control and force fluctuation during fatigue. *Journal of applied physiology (Bethesda, Md. : 1985), 107*(1), 235–243. https://doi.org/10.1152/japplphysiol.00035.2009

83. Conway, B. A., Halliday, D. M., Farmer, S. F., Shahani, U., Maas, P., Weir, A. I., & Rosenberg, J. R. (1995). Synchronization between motor cortex and spinal motor neuronal pool during the performance of a maintained motor task in man. *The Journal of physiology, 489* (Pt 3), 917–924. https://doi.org/10.1113/jphysiol.1995.sp021104

84. Costa, M., Goldberger, A. L., & Peng, C. K. (2002). Multiscale entropy analysis of complex physiologic time series. *Physical review letters, 89*(6), 068102. https://doi.org/10.1103/PhysRevLett.89.068102

85. Costa, M., Goldberger, A. L., & Peng, C. K. (2005). Multiscale entropy analysis of biological signals. *Physical review. E, Statistical, nonlinear, and soft matter physics, 71*(2 Pt 1), 021906. https://doi.org/10.1103/PhysRevE.71.021906

86. Craig, C. L., Marshall, A. L., Sjöström, M., Bauman, A. E., Booth, M. L., Ainsworth, B. E., Pratt, M., Ekelund, U., Yngve, A., Sallis, J. F., & Oja, P. (2003). International physical activity questionnaire: 12-country reliability and validity. *Medicine and science in sports and exercise, 35*(8), 1381–1395. https://doi.org/10.1249/01.MSS.0000078924.61453.FB

87. Cristea, A., Korhonen, M. T., Häkkinen, K., Mero, A., Alén, M., Sipilä, S., Viitasalo, J. T., Koljonen, M. J., Suominen, H., & Larsson, L. (2008). Effects of combined strength and sprint training on regulation of muscle contraction at the whole-muscle and single-fibre levels in elite master sprinters. *Acta physiologica (Oxford, England), 193*(3), 275–289. https://doi.org/10.1111/j.1748-1716.2008.01843.x

88. Critchley, K., Kokubu, M., Iemitsu, M., Fujita, S., & Isaka, T. (2014). Age-related differences in the availability of visual feedback during bimanual pinch. *European journal of applied physiology, 114*(9), 1925–1932. https://doi.org/10.1007/s00421-014-2916-8

89. Cruz-Jentoft, A. J., Bahat, G., Bauer, J., Boirie, Y., Bruyère, O., Cederholm, T., Cooper, C., Landi, F., Rolland, Y., Sayer, A. A., Schneider, S. M., Sieber, C. C., Topinkova, E., Vandewoude, M., Visser, M., Zamboni, M., & Writing Group for the European Working Group on Sarcopenia in Older People 2 (EWGSOP2), and the Extended Group for EWGSOP2 (2019). Sarcopenia: revised European consensus on definition and diagnosis. *Age and ageing, 48*(1), 16–31. https://doi.org/10.1093/ageing/afy169

90. D'Antona, G., Pellegrino, M. A., Adami, R., Rossi, R., Carlizzi, C. N., Canepari, M., Saltin, B., & Bottinelli, R. (2003). The effect of ageing and immobilization on structure and function of human skeletal muscle fibres. *The Journal of physiology, 552*(Pt 2), 499–511. https://doi.org/10.1113/jphysiol.2003.046276

91. Dalton, B. H., McNeil, C. J., Doherty, T. J., & Rice, C. L. (2008). Age-related reductions in the estimated numbers of motor units are minimal in the human soleus. *Muscle & nerve, 38*(3), 1108–1115. https://doi.org/10.1002/mus.20984

92. Dalton, B. H., Power, G. A., Vandervoort, A. A., & Rice, C. L. (2010). Power loss is greater in old men than young men during fast plantar flexion contractions. *Journal of applied physiology (Bethesda, Md. : 1985), 109*(5), 1441–1447. https://doi.org/10.1152/japplphysiol.00335.2010

93. Dalton, B. H., Power, G. A., Vandervoort, A. A., & Rice, C. L. (2012). The age-related slowing of voluntary shortening velocity exacerbates power loss during repeated fast knee extensions. *Experimental gerontology, 47*(1), 85–92. https://doi.org/10.1016/j.exger.2011.10.010

94. Daneshgar, S., Tvrdy, T., & Enoka, R. M. (2024). Explaining the influence of practice on the grooved pegboard times of older adults: role of force steadiness. *Experimental brain research, 242*(8), 1971–1982. https://doi.org/10.1007/s00221-024-06878-9

95. Davis, L. A., Allen, S. P., Hamilton, L. D., Grabowski, A. M., & Enoka, R. M. (2020). Differences in postural sway among healthy adults are associated with the ability to perform steady contractions with leg muscles. *Experimental brain research, 238*(2), 487–497. https://doi.org/10.1007/s00221-019-05719-4

96. de la Rocha, J., Doiron, B., Shea-Brown, E., Josić, K., & Reyes, A. (2007). Correlation between neural spike trains increases with firing rate. *Nature, 448*(7155), 802–806. https://doi.org/10.1038/nature06028

97. De Serres, S. J., & Enoka, R. M. (1998). Older adults can maximally activate the biceps brachii muscle by voluntary command. *Journal of applied physiology (Bethesda, Md. : 1985), 84*(1), 284–291. https://doi.org/10.1152/jappl.1998.84.1.284

98. Decorps, J., Saumet, J. L., Sommer, P., Sigaudo-Roussel, D., & Fromy, B. (2014). Effect of ageing on tactile transduction processes. *Ageing research reviews, 13*, 90–99. https://doi.org/10.1016/j.arr.2013.12.003

99. DeFreitas, J. M., Beck, T. W., Stock, M. S., Dillon, M. A., & Kasishke, P. R., 2nd (2011). An examination of the time course of training-induced skeletal muscle hypertrophy. *European journal of applied physiology, 111*(11), 2785–2790. https://doi.org/10.1007/s00421-011-1905-4

100. Degens, H., & Korhonen, M. T. (2012). Factors contributing to the variability in muscle ageing. *Maturitas, 73*(3), 197–201. https://doi.org/10.1016/j.maturitas.2012.07.015

101. Del Vecchio, A. D., & Farina, D. (2019). Interfacing the neural output of the spinal cord: robust and reliable longitudinal identification of motor neurons in humans. *Journal of neural engineering, 17*(1), 016003. https://doi.org/10.1088/1741-2552/ab4d05

102. Del Vecchio, A., Casolo, A., Negro, F., Scorcelletti, M., Bazzucchi, I., Enoka, R., Felici, F., & Farina, D. (2019b). The increase in muscle force after 4 weeks of strength training is mediated by adaptations in motor unit recruitment and rate coding. *The Journal of physiology, 597*(7), 1873–1887. https://doi.org/10.1113/JP277250

103. Del Vecchio, A., Germer, C. M., Elias, L. A., Fu, Q., Fine, J., Santello, M., & Farina, D. (2019a). The human central nervous system transmits common synaptic inputs to distinct motor neuron pools during non-synergistic digit actions. *The Journal of physiology, 597*(24), 5935–5948. https://doi.org/10.1113/JP278623

104. Del Vecchio, A., Holobar, A., Falla, D., Felici, F., Enoka, R. M., & Farina, D. (2020). Tutorial: Analysis of motor unit discharge characteristics from high-density surface EMG signals. *Journal of electromyography and kinesiology : official journal of the International Society of Electrophysiological Kinesiology, 53,* 102426. https://doi.org/10.1016/j.jelekin.2020.102426

105. Del Vecchio, A., Negro, F., Felici, F., & Farina, D. (2017). Associations between motor unit action potential parameters and surface EMG features. *Journal of applied physiology (Bethesda, Md. : 1985), 123*(4), 835–843. https://doi.org/10.1152/japplphysiol.00482.2017

106. Delbono, O., Renganathan, M., & Messi, M. L. (1997). Excitation-Ca2+ release-contraction coupling in single aged human skeletal muscle fiber. *Muscle & nerve. Supplement, 5,* S88–S92. https://doi.org/10.1002/(sici)1097-4598(1997)5+<88::aid-mus21>3.0.co;2-u

107. Delignieres, D., & Marmelat, V. (2012). Fractal fluctuations and complexity: current debates and future challenges. *Critical reviews in biomedical engineering, 40*(6), 485–500. https://doi.org/10.1615/critrevbiomedeng.2013006727

108. Deschenes M. R. (2011). Motor unit and neuromuscular junction remodeling with aging. *Current aging science, 4*(3), 209–220. https://doi.org/10.2174/1874609811104030209

109. Dewhurst, S., Graven-Nielsen, T., De Vito, G., & Farina, D. (2007). Muscle temperature has a different effect on force fluctuations in young and older women. *Clinical neurophysiology : official journal of the International Federation of Clinical Neurophysiology, 118*(4), 762–769. https://doi.org/10.1016/j.clinph.2006.12.006

110. Dictionary, O. E. (2024). Oxford English dictionary. URL: http://www.oed.com.

111. Dideriksen, J. L., Negro, F., Enoka, R. M., & Farina, D. (2012). Motor unit recruitment strategies and muscle properties determine the influence of synaptic noise on force steadiness. *Journal of neurophysiology, 107*(12), 3357–3369. https://doi.org/10.1152/jn.00938.2011

112. Dideriksen, J. L., Negro, F., Falla, D., Kristensen, S. R., Mrachacz-Kersting, N., & Farina, D. (2018). Coherence of the Surface EMG and Common Synaptic Input to Motor Neurons. *Frontiers in human neuroscience, 12,* 207. https://doi.org/10.3389/fnhum.2018.00207

113. Doherty, T. J., & Brown, W. F. (1993). The estimated numbers and relative sizes of thenar motor units as selected by multiple point stimulation in young and older adults. *Muscle & nerve, 16*(4), 355–366. https://doi.org/10.1002/mus.880160404

114. Dottor, A., Battista, S., Job, M., Sansone, L. G., & Testa, M. (2025). Force control of pinch grip: Normative data of a holistic evaluation. *Journal of hand therapy : official journal of the American Society of Hand Therapists, 38*(1), 129–142. https://doi.org/10.1016/j.jht.2024.06.001

115. Ebaid, D., Crewther, S. G., MacCalman, K., Brown, A., & Crewther, D. P. (2017). Cognitive Processing Speed across the Lifespan: Beyond the Influence of Motor Speed. *Frontiers in aging neuroscience, 9,* 62. https://doi.org/10.3389/fnagi.2017.00062

116. Eccles, J. C., & Sherrington, C. S. (1930). Numbers and contraction-values of individual motor-units examined in some muscles of the limb. *Proceedings of the Royal Society of London. Series B, Containing Papers of a Biological Character, 106*(745), 326-357.

117. Edelman, G. M., & Gally, J. A. (2001). Degeneracy and complexity in biological systems. *Proceedings of the National Academy of Sciences of the United States of America, 98*(24), 13763–13768. https://doi.org/10.1073/pnas.231499798

118. Eke, A., Herman, P., Kocsis, L., & Kozak, L. R. (2002). Fractal characterization of complexity in temporal physiological signals. *Physiological measurement, 23*(1), R1.

119. Elias, L. A., Watanabe, R. N., & Kohn, A. F. (2014). Spinal mechanisms may provide a combination of intermittent and continuous control of human posture: predictions from a biologically based neuromusculoskeletal model. *PLoS computational biology, 10*(11), e1003944. https://doi.org/10.1371/journal.pcbi.1003944

120. Ely, I. A., Jones, E. J., Inns, T. B., Dooley, S., Miller, S. B. J., Stashuk, D. W., Atherton, P. J., Phillips, B. E., & Piasecki, M. (2022). Training-induced improvements in knee extensor force accuracy are associated with reduced vastus lateralis motor unit firing variability. *Experimental physiology, 107*(9), 1061–1070. https://doi.org/10.1113/EP090367

121. Enoka R. M. (1995). Morphological features and activation patterns of motor units. *Journal of clinical neurophysiology : official publication of the American Electroencephalographic Society, 12*(6), 538–559. https://doi.org/10.1097/00004691-199511000-00002

122. Enoka, R. M., & Duchateau, J. (2017). Rate Coding and the Control of Muscle Force. *Cold Spring Harbor perspectives in medicine, 7*(10), a029702. https://doi.org/10.1101/cshperspect.a029702

123. Enoka, R. M., & Farina, D. (2021). Force Steadiness: From Motor Units to Voluntary Actions. *Physiology (Bethesda, Md.), 36*(2), 114–130. https://doi.org/10.1152/physiol.00027.2020

124. Enoka, R. M., Christou, E. A., Hunter, S. K., Kornatz, K. W., Semmler, J. G., Taylor, A. M., & Tracy, B. L. (2003). Mechanisms that contribute to differences in motor performance between young and old adults. *Journal of electromyography and kinesiology : official journal of the International Society of Electrophysiological Kinesiology, 13*(1), 1–12. https://doi.org/10.1016/s1050-6411(02)00084-6

125. Erim, Z., Beg, M. F., Burke, D. T., & de Luca, C. J. (1999). Effects of aging on motor-unit control properties. *Journal of neurophysiology, 82*(5), 2081–2091. https://doi.org/10.1152/jn.1999.82.5.2081

126. Falconer, J., Hughes, S. L., Naughton, B. J., Singer, R., Chang, R. W., & Sinacore, J. M. (1991). Self report and performance-based hand function tests as correlates of dependency in the elderly. *Journal of the American Geriatrics Society, 39*(7), 695–699. https://doi.org/10.1111/j.1532-5415.1991.tb03624.x

127. Farina, D., & Negro, F. (2015). Common synaptic input to motor neurons, motor unit synchronization, and force control. *Exercise and sport sciences reviews, 43*(1), 23–33. https://doi.org/10.1249/JES.0000000000000032

128. Farina, D., Negro, F., & Dideriksen, J. L. (2014). The effective neural drive to muscles is the common synaptic input to motor neurons. *The Journal of physiology, 592*(16), 3427–3441. https://doi.org/10.1113/jphysiol.2014.273581

129. Farina, D., Negro, F., Gizzi, L., & Falla, D. (2012). Low-frequency oscillations of the neural drive to the muscle are increased with experimental muscle pain. *Journal of neurophysiology, 107*(3), 958–965. https://doi.org/10.1152/jn.00304.2011

130. Farmer, S. F., Bremner, F. D., Halliday, D. M., Rosenberg, J. R., & Stephens, J. A. (1993). The frequency content of common synaptic inputs to motor neurones studied during voluntary isometric contraction in man. *The Journal of physiology, 470*, 127–155. https://doi.org/10.1113/jphysiol.1993.sp019851

131. Feeney, D. F., Mani, D., & Enoka, R. M. (2018). Variability in common synaptic input to motor neurons modulates both force steadiness and pegboard time in young and older adults. *The Journal of physiology, 596*(16), 3793–3806. https://doi.org/10.1113/JP275658

132. Feeney, D. F., Meyer, F. G., Noone, N., & Enoka, R. M. (2017). A latent low-dimensional common input drives a pool of motor neurons: a probabilistic latent state-space model. *Journal of neurophysiology, 118*(4), 2238–2250. https://doi.org/10.1152/jn.00274.2017

133. Feige, B., Aertsen, A., & Kristeva-Feige, R. (2000). Dynamic synchronization between multiple cortical motor areas and muscle activity in phasic voluntary movements. *Journal of neurophysiology, 84*(5), 2622–2629. https://doi.org/10.1152/jn.2000.84.5.2622

134. Fennell, C. R. J., Mauger, A. R., & Hopker, J. G. (2024). Inter-day reliability of heart rate complexity and variability metrics in healthy highly active younger and older adults. *European journal of applied physiology, 124*(5), 1409–1424. https://doi.org/10.1007/s00421-023-05373-3

135. Fiatarone, M. A., O'Neill, E. F., Ryan, N. D., Clements, K. M., Solares, G. R., Nelson, M. E., Roberts, S. B., Kehayias, J. J., Lipsitz, L. A., & Evans, W. J. (1994). Exercise training and nutritional supplementation for physical frailty in very elderly people. *The New England journal of medicine, 330*(25), 1769–1775. https://doi.org/10.1056/NEJM199406233302501

136. Fiogbé, E., Vassimon-Barroso, V., Catai, A. M., de Melo, R. C., Quitério, R. J., Porta, A., & Takahashi, A. C. M. (2021). Complexity of Knee Extensor Torque: Effect of Aging and Contraction Intensity. *Journal of strength and conditioning research, 35*(4), 1050–1057. https://doi.org/10.1519/JSC.0000000000002888

137. Fitts, R. H., Costill, D. L., & Gardetto, P. R. (1989). Effect of swim exercise training on human muscle fiber function. *Journal of applied physiology (Bethesda, Md. : 1985), 66*(1), 465–475. https://doi.org/10.1152/jappl.1989.66.1.465

138. Foldvari, M., Clark, M., Laviolette, L. C., Bernstein, M. A., Kaliton, D., Castaneda, C., Pu, C. T., Hausdorff, J. M., Fielding, R. A., & Singh, M. A. (2000). Association of muscle power with functional status in community-dwelling elderly women. *The journals of gerontology. Series A, Biological sciences and medical sciences, 55*(4), M192–M199. https://doi.org/10.1093/gerona/55.4.m192

139. Forrest, S. M., Challis, J. H., & Winter, S. L. (2014). The effect of signal acquisition and processing choices on ApEn values: towards a "gold standard" for distinguishing effort levels from isometric force records. *Medical engineering & physics, 36*(6), 676–683. https://doi.org/10.1016/j.medengphy.2014.02.017

140. Fox, E. J., Baweja, H. S., Kim, C., Kennedy, D. M., Vaillancourt, D. E., & Christou, E. A. (2013). Modulation of force below 1 Hz: age-associated differences and the effect of magnified visual feedback. *PloS one, 8*(2), e55970. https://doi.org/10.1371/journal.pone.0055970

141. Frontera, W. R., Hughes, V. A., Fielding, R. A., Fiatarone, M. A., Evans, W. J., & Roubenoff, R. (2000). Aging of skeletal muscle: a 12-yr longitudinal study. *Journal of applied physiology (Bethesda, Md. : 1985), 88*(4), 1321–1326. https://doi.org/10.1152/jappl.2000.88.4.1321

142. Frost, J., (2019). Regression analysis: An intuitive guide for using and interpreting linear models.

143. Fuglevand, A. J., Winter, D. A., & Patla, A. E. (1993). Models of recruitment and rate coding organization in motor-unit pools. *Journal of neurophysiology, 70*(6), 2470–2488. https://doi.org/10.1152/jn.1993.70.6.2470

144. Fuchs, C. J., Kuipers, R., Rombouts, J. A., Brouwers, K., Schrauwen-Hinderling, V. B., Wildberger, J. E., Verdijk, L. B., & van Loon, L. J. C. (2023). Thigh muscles are more susceptible to age-related muscle loss when compared to lower leg and pelvic muscles. *Experimental gerontology*, *175*, 112159. https://doi.org/10.1016/j.exger.2023.112159

145. Galea V. (1996). Changes in motor unit estimates with aging. *Journal of clinical neurophysiology : official publication of the American Electroencephalographic Society, 13*(3), 253–260. https://doi.org/10.1097/00004691-199605000-00010

146. Galganski, M. E., Fuglevand, A. J., & Enoka, R. M. (1993). Reduced control of motor output in a human hand muscle of elderly subjects during submaximal contractions. *Journal of neurophysiology, 69*(6), 2108–2115. https://doi.org/10.1152/jn.1993.69.6.2108

147. Garfinkel, A., Spano, M. L., Ditto, W. L., & Weiss, J. N. (1992). Controlling cardiac chaos. *Science (New York, N.Y.), 257*(5074), 1230–1235. https://doi.org/10.1126/science.1519060

148. Germer, C. M., Del Vecchio, A., Negro, F., Farina, D., & Elias, L. A. (2020). Neurophysiological correlates of force control improvement induced by sinusoidal vibrotactile stimulation. *Journal of neural engineering, 17*(1), 016043. https://doi.org/10.1088/1741-2552/ab5e08

149. Gershon, R. C., Cella, D., Fox, N. A., Havlik, R. J., Hendrie, H. C., & Wagster, M. V. (2010). Assessment of neurological and behavioural function: the NIH Toolbox. *The Lancet. Neurology, 9*(2), 138–139. https://doi.org/10.1016/S1474-4422(09)70335-7

150. Glenny R. W. (2011). Emergence of matched airway and vascular trees from fractal rules. *Journal of applied physiology (Bethesda, Md. : 1985), 110*(4), 1119–1129. https://doi.org/10.1152/japplphysiol.01293.2010

151. Goldberger A. L. (1996). Nonlinear dynamics for clinicians: chaos theory, fractals, and complexity at the bedside. *Lancet (London, England), 347*(9011), 1312–1314. https://doi.org/10.1016/s0140-6736(96)90948-4

152. Goldberger A. L. (2006). Giles f. Filley lecture. Complex systems. *Proceedings of the American Thoracic Society, 3*(6), 467–471. https://doi.org/10.1513/pats.200603-028MS

153. Goldberger, A. L., Amaral, L. A., Hausdorff, J. M., Ivanov, P. C.h, Peng, C. K., & Stanley, H. E. (2002a). Fractal dynamics in physiology: alterations with disease and aging. *Proceedings of the National Academy of Sciences of the United States of America, 99,* Suppl 1(Suppl 1), 2466–2472. https://doi.org/10.1073/pnas.012579499

154. Goldberger, A. L., Bhargava, V., West, B. J., & Mandell, A. J. (1985). On a mechanism of cardiac electrical stability. The fractal hypothesis. *Biophysical journal, 48*(3), 525–528. https://doi.org/10.1016/S0006-3495(85)83808-X

155. Goldberger, A. L., Peng, C. K., & Lipsitz, L. A. (2002b). What is physiologic complexity and how does it change with aging and disease?. *Neurobiology of aging, 23*(1), 23–26. https://doi.org/10.1016/s0197-4580(01)00266-4

156. Goldberger, A. L., Rigney, D. R., & West, B. J. (1990). Chaos and fractals in human physiology. *Scientific American, 262*(2), 42-49.

157. Gordon, A. M., Homsher, E., & Regnier, M. (2000). Regulation of contraction in striated muscle. *Physiological reviews, 80*(2), 853–924. https://doi.org/10.1152/physrev.2000.80.2.853

158. Gordon, T., Hegedus, J., & Tam, S. L. (2004). Adaptive and maladaptive motor axonal sprouting in aging and motoneuron disease. *Neurological research, 26*(2), 174–185. https://doi.org/10.1179/016164104225013806

159. Gow, B. J., Peng, C. K., Wayne, P. M., & Ahn, A. C. (2015). Multiscale entropy analysis of center-of-pressure dynamics in human postural control: methodological considerations. *Entropy, 17*(12), 7926-7947.

160. Graves, A. E., Kornatz, K. W., & Enoka, R. M. (2000). Older adults use a unique strategy to lift inertial loads with the elbow flexor muscles. *Journal of neurophysiology, 83*(4), 2030–2039. https://doi.org/10.1152/jn.2000.83.4.2030

161. Guo, Y., Jones, E. J., Škarabot, J., Inns, T. B., Phillips, B. E., Atherton, P. J., & Piasecki, M. (2024). Common synaptic inputs and persistent inward currents of vastus lateralis motor units are reduced in older male adults. *GeroScience, 46*(3), 3249–3261. https://doi.org/10.1007/s11357-024-01063-

162. Guo, Y., Jones, E. J., Smart, T. F., Altheyab, A., Gamage, N., Stashuk, D. W., Piasecki, J., Phillips, B. E., Atherton, P. J., & Piasecki, M. (2025). Sex disparities of human neuromuscular decline in older humans. *The Journal of physiology*, *603*(1), 151–165. https://doi.org/10.1113/JP285653

163. Hagio, S., & Kouzaki, M. (2015). Action Direction of Muscle Synergies in Three-Dimensional Force Space. *Frontiers in bioengineering and biotechnology, 3*, 187. https://doi.org/10.3389/fbioe.2015.00187

164. Hamilton, L. D., Thomas, E., Almuklass, A. M., & Enoka, R. M. (2017). A framework for identifying the adaptations responsible for differences in pegboard times between middle-

aged and older adults. *Experimental gerontology, 97,* 9–16. https://doi.org/10.1016/j.exger.2017.07.003

165. Hangelbroek, R. W. J., Knuiman, P., Tieland, M., & de Groot, L. C. P. G. M. (2018). Attenuated strength gains during prolonged resistance exercise training in older adults with high inflammatory status. *Experimental gerontology, 106*, 154–158. https://doi.org/10.1016/j.exger.2018.02.008

166. Hanson, M. R., Swanson, C. W., Whittier, T. T., & Fling, B. W. (2022). Inhibitory signaling as a predictor of leg force control in young and older adults. *Experimental brain research, 240*(4), 1005–1016. https://doi.org/10.1007/s00221-022-06321-x

167. Harridge, S. D., Bottinelli, R., Canepari, M., Pellegrino, M. A., Reggiani, C., Esbjörnsson, M., & Saltin, B. (1996). Whole-muscle and single-fibre contractile properties and myosin heavy chain isoforms in humans. *Pflugers Archiv : European journal of physiology, 432*(5), 913–920. https://doi.org/10.1007/s004240050215

168. Harridge, S. D., Kryger, A., & Stensgaard, A. (1999). Knee extensor strength, activation, and size in very elderly people following strength training. *Muscle & nerve, 22*(7), 831–839. https://doi.org/10.1002/(sici)1097-4598(199907)22:7<831::aid-mus4>3.0.co;2-3

169. Harvill, L. M. (1991). Standard error of measurement: an NCME instructional module on. *Educational Measurement: issues and practice, 10*(2), 33-41.

170. Heckman, C. J., & Enoka, R. M. (2012). Motor unit. *Comprehensive Physiology, 2*(4), 2629–2682. https://doi.org/10.1002/cphy.c100087

171. Heintz Walters, B., Huddleston, W. E., O'Connor, K., Wang, J., Hoeger Bement, M., & Keenan, K. G. (2021). The role of eye movements, attention, and hand movements on age-related differences in pegboard tests. *Journal of neurophysiology, 126*(5), 1710–1722. https://doi.org/10.1152/jn.00629.2020

172. Henneman, E., Somjen, G., & Carpenter, D. O. (1965). Functional significance of cell size in spinal motoneurons. *Journal of neurophysiology, 28*(3), 560-580. https://doi.org/10.1152/jn.1965.28.3.560

173. Henwood, T. R., Riek, S., & Taaffe, D. R. (2008). Strength versus muscle power-specific resistance training in community-dwelling older adults. *The journals of gerontology. Series A, Biological sciences and medical sciences, 63*(1), 83–91. https://doi.org/10.1093/gerona/63.1.83

174. Hepple R. T. (2003). Sarcopenia--a critical perspective. *Science of aging knowledge environment : SAGE KE, 2003*(46), pe31. https://doi.org/10.1126/sageke.2003.46.pe31

175. Hepple, R. T., & Rice, C. L. (2016). Innervation and neuromuscular control in ageing skeletal muscle. *The Journal of physiology, 594*(8), 1965–1978. https://doi.org/10.1113/JP270561

176. Hernandez, L. R., & Camic, C. L. (2019). Fatigue-Mediated Loss of Complexity is Contraction-Type Dependent in Vastus Lateralis Electromyographic Signals. *Sports (Basel, Switzerland), 7*(4), 78. https://doi.org/10.3390/sports7040078

177. Hirono, T., Ikezoe, T., Taniguchi, M., Yamagata, M., Miyakoshi, K., Umehara, J., & Ichihashi, N. (2020). Relationship between ankle plantar flexor force steadiness and postural stability on stable and unstable platforms. *European journal of applied physiology, 120*(5), 1075–1082. https://doi.org/10.1007/s00421-020-04346-0

178. Hirono, T., Ikezoe, T., Yamagata, M., Kato, T., Kimura, M., & Ichihashi, N. (2021). Relationship between postural sway on an unstable platform and ankle plantar flexor force steadiness in community-dwelling older women. *Gait & posture, 84,* 227–231. https://doi.org/10.1016/j.gaitpost.2020.12.023

179. Ho, K. K., Moody, G. B., Peng, C. K., Mietus, J. E., Larson, M. G., Levy, D., & Goldberger, A. L. (1997). Predicting survival in heart failure case and control subjects by use of fully automated methods for deriving nonlinear and conventional indices of heart rate dynamics. *Circulation, 96*(3), 842–848. https://doi.org/10.1161/01.cir.96.3.842

180. Holmes, M. R., Gould, J. R., Peña-González, I., & Enoka, R. M. (2015). Force steadiness during a co-contraction task can be improved with practice, but only by young adults and not by middle-aged or old adults. *Experimental physiology, 100*(2), 182–192. https://doi.org/10.1113/expphysiol.2014.083741

181. Hong, Z., Ng, K. K., Sim, S. K., Ngeow, M. Y., Zheng, H., Lo, J. C., Chee, M. W., & Zhou, J. (2015). Differential age-dependent associations of gray matter volume and white matter integrity with processing speed in healthy older adults. *NeuroImage, 123*, 42–50. https://doi.org/10.1016/j.neuroimage.2015.08.034

182. Höök, P., Sriramoju, V., & Larsson, L. (2001). Effects of aging on actin sliding speed on myosin from single skeletal muscle cells of mice, rats, and humans. *American journal of physiology. Cell physiology, 280*(4), C782–C788. https://doi.org/10.1152/ajpcell.2001.280.4.C782

183. Hopkins W. G. (2000). Measures of reliability in sports medicine and science. *Sports medicine (Auckland, N.Z.), 30*(1), 1–15. https://doi.org/10.2165/00007256-200030010-00001

184. Hortobágyi, T., Tunnel, D., Moody, J., Beam, S., & DeVita, P. (2001). Low- or high-intensity strength training partially restores impaired quadriceps force accuracy and steadiness in aged adults. *The journals of gerontology. Series A, Biological sciences and medical sciences, 56*(1), B38–B47. https://doi.org/10.1093/gerona/56.1.b38

185. Horwath, O., Moberg, M., Edman, S., Philp, A., & Apró, W. (2025). Ageing leads to selective type II myofibre deterioration and denervation independent of reinnervative capacity in human skeletal muscle. *Experimental physiology, 110*(2), 277–292. https://doi.org/10.1113/EP092222

186. Hourigan, M. L., McKinnon, N. B., Johnson, M., Rice, C. L., Stashuk, D. W., & Doherty, T. J. (2015). Increased motor unit potential shape variability across consecutive motor unit

discharges in the tibialis anterior and vastus medialis muscles of healthy older subjects. *Clinical neurophysiology : official journal of the International Federation of Clinical Neurophysiology, 126*(12), 2381–2389. https://doi.org/10.1016/j.clinph.2015.02.002

187. Hu, X., & Newell, K. M. (2011). Aging, visual information, and adaptation to task asymmetry in bimanual force coordination. *Journal of applied physiology (Bethesda, Md. : 1985), 111*(6), 1671–1680. https://doi.org/10.1152/japplphysiol.00760.2011

188. Huddleston, W. E., Ernest, B. E., & Keenan, K. G. (2014). Selective Age Effects on Visual Attention and Motor Attention during a Cued Saccade Task. *Journal of ophthalmology, 2014,* 860493. https://doi.org/10.1155/2014/860493

189. Hug, F., Del Vecchio, A., Avrillon, S., Farina, D., & Tucker, K. (2021). Muscles from the same muscle group do not necessarily share common drive: evidence from the human triceps surae. *Journal of applied physiology (Bethesda, Md. : 1985), 130*(2), 342–354. https://doi.org/10.1152/japplphysiol.00635.2020

190. Hunter, Robert (2023) Investigating the Neural Control of Muscle Torque Using High-Density Surface Electromyography. Doctor of Philosophy (PhD) thesis, University of Kent,. (doi:10.22024/UniKent/01.02.100906) (KAR id:100906)

191. Hunter, S. K., Critchlow, A., & Enoka, R. M. (2005). Muscle endurance is greater for old men compared with strength-matched young men. *Journal of applied physiology (Bethesda, Md. : 1985), 99*(3), 890–897. https://doi.org/10.1152/japplphysiol.00243.2005

192. Hunter, S. K., Pereira, H. M., & Keenan, K. G. (2016). The aging neuromuscular system and motor performance. *Journal of applied physiology (Bethesda, Md. : 1985), 121*(4), 982–995. https://doi.org/10.1152/japplphysiol.00475.2016

193. Hunter, S. K., Thompson, M. W., Ruell, P. A., Harmer, A. R., Thom, J. M., Gwinn, T. H., & Adams, R. D. (1999). Human skeletal sarcoplasmic reticulum Ca2+ uptake and muscle function with aging and strength training. *Journal of applied physiology (Bethesda, Md. : 1985), 86*(6), 1858–1865. https://doi.org/10.1152/jappl.1999.86.6.1858

194. Hunter, S. K., Todd, G., Butler, J. E., Gandevia, S. C., & Taylor, J. L. (2008). Recovery from supraspinal fatigue is slowed in old adults after fatiguing maximal isometric contractions. *Journal of applied physiology (Bethesda, Md. : 1985), 105*(4), 1199–1209. https://doi.org/10.1152/japplphysiol.01246.2007

195. Haynes, E. M. K., Neubauer, N. A., Cornett, K. M. D., O'Connor, B. P., Jones, G. R., & Jakobi, J. M. (2020). Age and sex-related decline of muscle strength across the adult lifespan: a scoping review of aggregated data. *Applied physiology, nutrition, and metabolism = Physiologie appliquee, nutrition et metabolisme*, *45*(11), 1185–1196. https://doi.org/10.1139/apnm-2020-0081

196. Huxley A. F. (1957). Muscle structure and theories of contraction. *Progress in biophysics and biophysical chemistry, 7*, 255–318.

197. Inglis, J. G., Cabral, H. V., Cosentino, C., Bonardi, A., & Negro, F. (2025). Motor unit discharge behavior in human muscles throughout force gradation: a systematic review and meta-analysis with meta-regression. *Journal of applied physiology (Bethesda, Md. : 1985), 138*(4), 1050–1065. https://doi.org/10.1152/japplphysiol.00863.2024

198. Jang, Y. C., & Van Remmen, H. (2011). Age-associated alterations of the neuromuscular junction. *Experimental gerontology, 46*(2-3), 193–198. https://doi.org/10.1016/j.exger.2010.08.029

199. Janssen, I., Heymsfield, S. B., Wang, Z. M., & Ross, R. (2000). Skeletal muscle mass and distribution in 468 men and women aged 18-88 year. *Journal of applied physiology (Bethesda, Md. : 1985), 89*(1), 81–88. https://doi.org/10.1152/jappl.2000.89.1.81

200. Jette, A. M., Branch, L. G., & Berlin, J. (1990). Musculoskeletal impairments and physical disablement among the aged. *Journal of gerontology, 45*(6), M203–M208. https://doi.org/10.1093/geronj/45.6.m203

201. Jiang, B. C., Yang, W. H., Shieh, J. S., Fan, J. Z., & Peng, C. K. (2013). Entropy-based method for COP data analysis. *Theoretical Issues in Ergonomics Science, 14*(3), 227-246.

202. Johansson, J., Nordström, A., Gustafson, Y., Westling, G., & Nordström, P. (2017). Increased postural sway during quiet stance as a risk factor for prospective falls in community-dwelling elderly individuals. *Age and ageing, 46*(6), 964–970. https://doi.org/10.1093/ageing/afx083

203. Jones, E. J., Chiou, S. Y., Atherton, P. J., Phillips, B. E., & Piasecki, M. (2022). Ageing and exercise-induced motor unit remodelling. *The Journal of physiology, 600*(8), 1839–1849. https://doi.org/10.1113/JP281726

204. Jordan, K., Jesunathadas, M., Sarchet, D. M., & Enoka, R. M. (2013). Long-range correlations in motor unit discharge times at low forces are modulated by visual gain and age. *Experimental physiology, 98*(2), 546–555. https://doi.org/10.1113/expphysiol.2012.067975

205. Justice, J. N., Mani, D., Pierpoint, L. A., & Enoka, R. M. (2014). Fatigability of the dorsiflexors and associations among multiple domains of motor function in young and old adults. *Experimental gerontology, 55,* 92–101. https://doi.org/10.1016/j.exger.2014.03.018

206. Kallio, J., Søgaard, K., Avela, J., Komi, P., Selänne, H., & Linnamo, V. (2012). Age-related decreases in motor unit discharge rate and force control during isometric plantar flexion. *Journal of electromyography and kinesiology : official journal of the International Society of Electrophysiological Kinesiology, 22*(6), 983–989. https://doi.org/10.1016/j.jelekin.2012.05.009

207. Kamen, G., & Knight, C. A. (2004). Training-related adaptations in motor unit discharge rate in young and older adults. *The journals of gerontology. Series A, Biological sciences and medical sciences, 59*(12), 1334–1338. https://doi.org/10.1093/gerona/59.12.1334

208. Kamen, G., Sison, S. V., Du, C. C., & Patten, C. (1995). Motor unit discharge behavior in older adults during maximal-effort contractions. *Journal of applied physiology (Bethesda, Md. : 1985), 79*(6), 1908–1913. https://doi.org/10.1152/jappl.1995.79.6.1908

209. Kang, H. G., Quach, L., Li, W., & Lipsitz, L. A. (2013). Stiffness control of balance during dual task and prospective falls in older adults: the MOBILIZE Boston Study. *Gait & posture, 38*(4), 757–763. https://doi.org/10.1016/j.gaitpost.2013.03.022

210. Kaplan, D. T., Furman, M. I., Pincus, S. M., Ryan, S. M., Lipsitz, L. A., & Goldberger, A. L. (1991). Aging and the complexity of cardiovascular dynamics. *Biophysical journal, 59*(4), 945–949. https://doi.org/10.1016/S0006-3495(91)82309-8

211. Kavanagh, J. J., Wedderburn-Bisshop, J., & Keogh, J. W. (2016). Resistance Training Reduces Force Tremor and Improves Manual Dexterity in Older Individuals With Essential Tremor. *Journal of motor behavior, 48*(1), 20–30. https://doi.org/10.1080/00222895.2015.1028583

212. Keen, D. A., Yue, G. H., & Enoka, R. M. (1994). Training-related enhancement in the control of motor output in elderly humans. *Journal of applied physiology (Bethesda, Md. : 1985), 77*(6), 2648–2658. https://doi.org/10.1152/jappl.1994.77.6.2648

213. Keenan, K. G., Huddleston, W. E., & Ernest, B. E. (2017). Altered visual strategies and attention are related to increased force fluctuations during a pinch grip task in older adults. *Journal of neurophysiology, 118*(5), 2537–2548. https://doi.org/10.1152/jn.00928.2016

214. Kent-Braun J. A. (2009). Skeletal muscle fatigue in old age: whose advantage?. *Exercise and sport sciences reviews, 37*(1), 3–9. https://doi.org/10.1097/JES.0b013e318190ea2e

215. Kenway, L. C., Bisset, L. M., & Kavanagh, J. J. (2016). Visually guided targeting enhances bilateral force variability in healthy older adults. *Neurobiology of aging, 37*, 127–137. https://doi.org/10.1016/j.neurobiolaging.2015.10.003

216. Keogh, J. W., Morrison, S., & Barrett, R. (2007). Strength training improves the tri-digit finger-pinch force control of older adults. *Archives of physical medicine and rehabilitation, 88*(8), 1055–1063. https://doi.org/10.1016/j.apmr.2007.05.014

217. Keogh, J., Morrison, S., & Barrett, R. (2006). Age-related differences in inter-digit coupling during finger pinching. *European journal of applied physiology, 97*(1), 76–88. https://doi.org/10.1007/s00421-006-0151-7

218. Kent, M. (2006). *The Oxford dictionary of sports science & medicine* (3rd ed.). Oxford University Press. https://doi.org/10.1093/acref/9780198568506.001.0001

219. Klass, M., Baudry, S., & Duchateau, J. (2007). Voluntary activation during maximal contraction with advancing age: a brief review. *European journal of applied physiology, 100*(5), 543–551. https://doi.org/10.1007/s00421-006-0205-x

220. Klein, C. S., Marsh, G. D., Petrella, R. J., & Rice, C. L. (2003). Muscle fiber number in the biceps brachii muscle of young and old men. *Muscle & nerve, 28*(1), 62–68. https://doi.org/10.1002/mus.10386

221. Klotz, T., Lehmann, L., Negro, F., & Röhrle, O. (2023). High-density magnetomyography is superior to high-density surface electromyography for motor unit decomposition: a simulation study. *Journal of neural engineering, 20*(4), 10.1088/1741-2552/ace7f7. https://doi.org/10.1088/1741-2552/ace7f7

222. Knight, C. A., & Kamen, G. (2008). Relationships between voluntary activation and motor unit firing rate during maximal voluntary contractions in young and older adults. *European journal of applied physiology, 103*(6), 625–630. https://doi.org/10.1007/s00421-008-0757-z

223. Knol, H., Huys, R., Temprado, J. J., & Sleimen-Malkoun, R. (2019). Performance, complexity and dynamics of force maintenance and modulation in young and older adults. *PloS one, 14*(12), e0225925. https://doi.org/10.1371/journal.pone.0225925

224. Kobayashi, H., Koyama, Y., Enoka, R. M., & Suzuki, S. (2014). A unique form of light-load training improves steadiness and performance on some functional tasks in older adults. *Scandinavian journal of medicine & science in sports, 24*(1), 98–110. https://doi.org/10.1111/j.1600-0838.2012.01460.x

225. Koo, T. K., & Li, M. Y. (2016). A Guideline of Selecting and Reporting Intraclass Correlation Coefficients for Reliability Research. *Journal of chiropractic medicine, 15*(2), 155–163. https://doi.org/10.1016/j.jcm.2016.02.012

226. Korhonen, M. T., Cristea, A., Alén, M., Häkkinen, K., Sipilä, S., Mero, A., Viitasalo, J. T., Larsson, L., & Suominen, H. (2006). Aging, muscle fiber type, and contractile function in sprint-trained athletes. *Journal of applied physiology (Bethesda, Md. : 1985), 101*(3), 906–917. https://doi.org/10.1152/japplphysiol.00299.2006

227. Kostka T. (2005). Quadriceps maximal power and optimal shortening velocity in 335 men aged 23-88 years. *European journal of applied physiology, 95*(2-3), 140–145. https://doi.org/10.1007/s00421-005-1390-8

228. Kouzaki, M., & Shinohara, M. (2010). Steadiness in plantar flexor muscles and its relation to postural sway in young and elderly adults. *Muscle & nerve, 42*(1), 78–87. https://doi.org/10.1002/mus.21599

229. Krishnamoorthy, V., Goodman, S., Zatsiorsky, V., & Latash, M. L. (2003). Muscle synergies during shifts of the center of pressure by standing persons: identification of muscle modes. *Biological cybernetics, 89*(2), 152–161. https://doi.org/10.1007/s00422-003-0419-5

230. Krishnamoorthy, V., Latash, M. L., Scholz, J. P., & Zatsiorsky, V. M. (2004). Muscle modes during shifts of the center of pressure by standing persons: effect of instability and additional support. *Experimental brain research, 157*(1), 18–31. https://doi.org/10.1007/s00221-003-1812-y

231. Kudina L. P. (1999). Analysis of firing behaviour of human motor neurones within 'subprimary range'. *Journal of physiology, Paris, 93*(1-2), 115–123. https://doi.org/10.1016/s0928-4257(99)80142-9

232. Kutch, J. J., Kuo, A. D., Bloch, A. M., & Rymer, W. Z. (2008). Endpoint force fluctuations reveal flexible rather than synergistic patterns of muscle cooperation. *Journal of neurophysiology, 100*(5), 2455–2471. https://doi.org/10.1152/jn.90274.2008

233. Kwon, M., & Christou, E. A. (2018). Visual information processing in older adults: reaction time and motor unit pool modulation. *Journal of neurophysiology, 120*(5), 2630–2639. https://doi.org/10.1152/jn.00161.2018

234. Kim, K. M., Lim, S., Oh, T. J., Moon, J. H., Choi, S. H., Lim, J. Y., Kim, K. W., Park, K. S., & Jang, H. C. (2018). Longitudinal Changes in Muscle Mass and Strength, and Bone Mass in Older Adults: Gender-Specific Associations Between Muscle and Bone Losses. *The journals of gerontology. Series A, Biological sciences and medical sciences*, *73*(8), 1062–1069. https://doi.org/10.1093/gerona/glx188

235. La Rovere, M. T., Bigger, J. T., Jr, Marcus, F. I., Mortara, A., & Schwartz, P. J. (1998). Baroreflex sensitivity and heart-rate variability in prediction of total cardiac mortality after myocardial infarction. ATRAMI (Autonomic Tone and Reflexes After Myocardial Infarction) Investigators. *Lancet (London, England), 351*(9101), 478–484. https://doi.org/10.1016/s0140-6736(97)11144-8

236. Laidlaw, D. H., Bilodeau, M., & Enoka, R. M. (2000). Steadiness is reduced and motor unit discharge is more variable in old adults. *Muscle & nerve, 23*(4), 600–612. https://doi.org/10.1002/(sici)1097-4598(200004)23:4<600::aid-mus20>3.0.co;2-d

237. Laidlaw, D. H., Kornatz, K. W., Keen, D. A., Suzuki, S., & Enoka, R. M. (1999). Strength training improves the steadiness of slow lengthening contractions performed by old adults. *Journal of applied physiology (Bethesda, Md. : 1985), 87*(5), 1786–1795. https://doi.org/10.1152/jappl.1999.87.5.1786

238. Laine, C. M., & Valero-Cuevas, F. J. (2017). Intermuscular coherence reflects functional coordination. *Journal of neurophysiology, 118*(3), 1775–1783. https://doi.org/10.1152/jn.00204.2017

239. Laine, C. M., Martinez-Valdes, E., Falla, D., Mayer, F., & Farina, D. (2015). Motor Neuron Pools of Synergistic Thigh Muscles Share Most of Their Synaptic Input. *The Journal of neuroscience : the official journal of the Society for Neuroscience, 35*(35), 12207–12216. https://doi.org/10.1523/JNEUROSCI.0240-15.2015

240. Laine, C. M., Nagamori, A., & Valero-Cuevas, F. J. (2016). The Dynamics of Voluntary Force Production in Afferented Muscle Influence Involuntary Tremor. *Frontiers in computational neuroscience, 10,* 86. https://doi.org/10.3389/fncom.2016.00086

241. Lamboley, C. R., Wyckelsma, V. L., Dutka, T. L., McKenna, M. J., Murphy, R. M., & Lamb, G. D. (2015). Contractile properties and sarcoplasmic reticulum calcium content in type I and type II skeletal muscle fibres in active aged humans. *The Journal of physiology, 593*(11), 2499–2514. https://doi.org/10.1113/JP270179

242. Lanza, I. R., Larsen, R. G., & Kent-Braun, J. A. (2007). Effects of old age on human skeletal muscle energetics during fatiguing contractions with and without blood flow. *The Journal of physiology, 583*(Pt 3), 1093–1105. https://doi.org/10.1113/jphysiol.2007.138362

243. Larsson, L. (1990). A technique for measuring contractile properties in single chemically skinned human muscle fibres obtained from percutaneous biopsies. *Journal of the neurological sciences, 98*, 430.

244. Larsson, L., & Moss, R. L. (1993). Maximum velocity of shortening in relation to myosin isoform composition in single fibres from human skeletal muscles. *The Journal of physiology, 472,* 595–614. https://doi.org/10.1113/jphysiol.1993.sp019964

245. Larsson, L., Degens, H., Li, M., Salviati, L., Lee, Y. I., Thompson, W., Kirkland, J. L., & Sandri, M. (2019). Sarcopenia: Aging-Related Loss of Muscle Mass and Function. *Physiological reviews, 99*(1), 427–511. https://doi.org/10.1152/physrev.00061.2017

246. Laughton, C. A., Slavin, M., Katdare, K., Nolan, L., Bean, J. F., Kerrigan, D. C., Phillips, E., Lipsitz, L. A., & Collins, J. J. (2003). Aging, muscle activity, and balance control: physiologic changes associated with balance impairment. *Gait & posture, 18*(2), 101–108. https://doi.org/10.1016/s0966-6362(02)00200-x

247. Lavender, A. P., & Nosaka, K. (2007). Fluctuations of isometric force after eccentric exercise of the elbow flexors of young, middle-aged, and old men. *European journal of applied physiology, 100*(2), 161–167. https://doi.org/10.1007/s00421-007-0418-7

248. Lawrence, E. L., Dayanidhi, S., Fassola, I., Requejo, P., Leclercq, C., Winstein, C. J., & Valero-Cuevas, F. J. (2015). Outcome measures for hand function naturally reveal three latent domains in older adults: strength, coordinated upper extremity function, and sensorimotor processing. *Frontiers in aging neuroscience, 7,* 108. https://doi.org/10.3389/fnagi.2015.00108

249. Lecce, E., Nuccio, S., Del Vecchio, A., Conti, A., Nicolò, A., Sacchetti, M., Felici, F., & Bazzucchi, I. (2023). Sensorimotor integration is affected by acute whole-body vibration: a coherence study. *Frontiers in physiology, 14,* 1266085. https://doi.org/10.3389/fphys.2023.1266085

250. Lexell J. (1995). Human aging, muscle mass, and fiber type composition. *The journals of gerontology. Series A, Biological sciences and medical sciences, 50* Spec No, 11–16. https://doi.org/10.1093/gerona/50a.special_issue.11

251. Lexell, J., Henriksson-Larsén, K., Winblad, B., & Sjöström, M. (1983). Distribution of different fiber types in human skeletal muscles: effects of aging studied in whole muscle cross sections. *Muscle & nerve, 6*(8), 588–595. https://doi.org/10.1002/mus.880060809

252. Lexell, J., Taylor, C. C., & Sjöström, M. (1988). What is the cause of the ageing atrophy? Total number, size and proportion of different fiber types studied in whole vastus lateralis

muscle from 15- to 83-year-old men. *Journal of the neurological sciences, 84*(2-3), 275–294. https://doi.org/10.1016/0022-510x(88)90132-3

253. Libchaber, A., Laroche, C., & Fauve, S. (1982). Period doubling cascade in mercury, a quantitative measurement. *Journal de Physique Lettres, 43*(7), 211-216.

254. Liebovitch, L. S., Fischbarg, J., & Koniarek, J. P. (1987). Ion channel kinetics: a model based on fractal scaling rather than multistate Markov processes. *Mathematical Biosciences, 84*(1), 37-68.

255. Lindle, R. S., Metter, E. J., Lynch, N. A., Fleg, J. L., Fozard, J. L., Tobin, J., Roy, T. A., & Hurley, B. F. (1997). Age and gender comparisons of muscle strength in 654 women and men aged 20-93 yr. *Journal of applied physiology (Bethesda, Md. : 1985), 83*(5), 1581–1587. https://doi.org/10.1152/jappl.1997.83.5.1581

256. Lippold O. (1971). Physiological tremor. *Scientific American, 224*(3), 65–73. https://doi.org/10.1038/scientificamerican0371-65

257. Lippold O. C. (1970). Oscillation in the stretch reflex arc and the origin of the rhythmical, 8-12 C-S component of physiological tremor. *The Journal of physiology, 206*(2), 359–382. https://doi.org/10.1113/jphysiol.1970.sp009018

258. Lipsitz L. A. (2002). Dynamics of stability: the physiologic basis of functional health and frailty. *The journals of gerontology. Series A, Biological sciences and medical sciences, 57*(3), B115–B125. https://doi.org/10.1093/gerona/57.3.b115

259. Lipsitz, L. A., & Goldberger, A. L. (1992). Loss of 'complexity' and aging. Potential applications of fractals and chaos theory to senescence. *JAMA, 267*(13), 1806–1809.

260. Liu, P., Hao, Q., Hai, S., Wang, H., Cao, L., & Dong, B. (2017). Sarcopenia as a predictor of all-cause mortality among community-dwelling older people: A systematic review and meta-analysis. *Maturitas, 103,* 16–22. https://doi.org/10.1016/j.maturitas.2017.04.007

261. Lodha, N., Moon, H., Kim, C., Onushko, T., & Christou, E. A. (2016). Motor Output Variability Impairs Driving Ability in Older Adults. *The journals of gerontology. Series A, Biological sciences and medical sciences, 71*(12), 1676–1681. https://doi.org/10.1093/gerona/glw013

262. Loram, I. D., & Lakie, M. (2002). Human balancing of an inverted pendulum: position control by small, ballistic-like, throw and catch movements. *The Journal of physiology, 540*(Pt 3), 1111–1124. https://doi.org/10.1113/jphysiol.2001.013077

263. Lorenz, E. N. (1963). Deterministic nonperiodic flow. *Journal of atmospheric sciences, 20*(2), 130-141.

264. Lorenz, E. N., & Haman, K. (1996). The essence of chaos. *Pure and Applied Geophysics, 147*(3), 598-599.

265. Lowe, D. A., Surek, J. T., Thomas, D. D., & Thompson, L. V. (2001). Electron paramagnetic resonance reveals age-related myosin structural changes in rat skeletal muscle fibers. American journal of physiology. *Cell physiology, 280*(3), C540–C547. https://doi.org/10.1152/ajpcell.2001.280.3.C540

266. Lucía, A., Sánchez, O., Carvajal, A., & Chicharro, J. L. (1999). Analysis of the aerobic-anaerobic transition in elite cyclists during incremental exercise with the use of electromyography. *British journal of sports medicine, 33*(3), 178–185. https://doi.org/10.1136/bjsm.33.3.178

267. Luu, B. L., Inglis, J. T., Huryn, T. P., Van der Loos, H. F., Croft, E. A., & Blouin, J. S. (2012). Human standing is modified by an unconscious integration of congruent sensory and motor signals. *The Journal of physiology, 590*(22), 5783–5794. https://doi.org/10.1113/jphysiol.2012.230334

268. Maden-Wilkinson, T. M., Degens, H., Jones, D. A., & McPhee, J. S. (2013). Comparison of MRI and DXA to measure muscle size and age-related atrophy in thigh muscles. *Journal of musculoskeletal & neuronal interactions, 13*(3), 320–328.

269. Mandelbrot B. (1967). How long is the coast of britain? Statistical self-similarity and fractional dimension. *Science (New York, N.Y.), 156*(3775), 636–638. https://doi.org/10.1126/science.156.3775.636

270. Mandelbrot, B. (1977). Fractals (p. 24). San Francisco: Freeman.

271. Mandelbrot, B. (1982). The fractal geometry of nature (Vol. 1). New York: WH, Freeman.

272. Mani, D., Almuklass, A. M., Hamilton, L. D., Vieira, T. M., Botter, A., & Enoka, R. M. (2018). Motor unit activity, force steadiness, and perceived fatigability are correlated with mobility in older adults. *Journal of neurophysiology, 120*(4), 1988–1997. https://doi.org/10.1152/jn.00192.2018

273. Mani, D., Feeney, D. F., & Enoka, R. M. (2019). The modulation of force steadiness by electrical nerve stimulation applied to the wrist extensors differs for young and older adults. *European journal of applied physiology, 119*(1), 301–310. https://doi.org/10.1007/s00421-018-4025-6

274. Manini, T. M., Clark, B. C., Tracy, B. L., Burke, J., & Ploutz-Snyder, L. (2005). Resistance and functional training reduces knee extensor position fluctuations in functionally limited older adults. *European journal of applied physiology, 95*(5-6), 436–446. https://doi.org/10.1007/s00421-005-0048-x

275. Manor, B., & Lipsitz, L. A. (2013). Physiologic complexity and aging: implications for physical function and rehabilitation. *Progress in neuro-psychopharmacology & biological psychiatry, 45,* 287–293. https://doi.org/10.1016/j.pnpbp.2012.08.020

276. Manor, B., Costa, M. D., Hu, K., Newton, E., Starobinets, O., Kang, H. G., Peng, C. K., Novak, V., & Lipsitz, L. A. (2010). Physiological complexity and system adaptability: evidence from postural control dynamics of older adults. *Journal of applied physiology*

(Bethesda, Md. : 1985), 109(6), 1786–1791. https://doi.org/10.1152/japplphysiol.00390.2010

277. Marchini, A., Pereira, R., Pedroso, W., Christou, E., & Neto, O. P. (2017). Age-associated differences in motor output variability and coordination during the simultaneous dorsiflexion of both feet. *Somatosensory & motor research, 34*(2), 96–101. https://doi.org/10.1080/08990220.2017.1313220

278. Marmon, A. R., Gould, J. R., & Enoka, R. M. (2011a). Practicing a functional task improves steadiness with hand muscles in older adults. *Medicine and science in sports and exercise, 43*(8), 1531–1537. https://doi.org/10.1249/MSS.0b013e3182100439

279. Marmon, A. R., Pascoe, M. A., Schwartz, R. S., & Enoka, R. M. (2011b). Associations among strength, steadiness, and hand function across the adult life span. *Medicine and science in sports and exercise, 43*(4), 560–567. https://doi.org/10.1249/MSS.0b013e3181f3f3ab

280. Martinez-Valdes, E., Enoka, R. M., Holobar, A., McGill, K., Farina, D., Besomi, M., Hug, F., Falla, D., Carson, R. G., Clancy, E. A., Disselhorst-Klug, C., van Dieën, J. H., Tucker, K., Gandevia, S., Lowery, M., Søgaard, K., Besier, T., Merletti, R., Kiernan, M. C., Rothwell, J. C., … Hodges, P. W. (2023). Consensus for experimental design in electromyography (CEDE) project: Single motor unit matrix. *Journal of Electromyography and Kinesiology, 68,* 102726. https://doi.org/10.1016/j.jelekin.2022.102726.

281. Martinez-Valdes, E., Guzman-Venegas, R. A., Silvestre, R. A., Macdonald, J. H., Falla, D., Araneda, O. F., & Haichelis, D. (2016). Electromyographic adjustments during continuous and intermittent incremental fatiguing cycling. *Scandinavian journal of medicine & science in sports, 26*(11), 1273–1282. https://doi.org/10.1111/sms.12578

282. Masani, K., Popovic, M. R., Nakazawa, K., Kouzaki, M., & Nozaki, D. (2003). Importance of body sway velocity information in controlling ankle extensor activities during quiet stance. *Journal of neurophysiology, 90*(6), 3774–3782. https://doi.org/10.1152/jn.00730.2002

283. May, R. M. (1976). Simple mathematical models with very complicated dynamics. *Nature, 261*(5560), 459-467.

284. May, R. M. (1987). Chaos and the dynamics of biological populations. *Proceedings of the Royal Society of London. A. Mathematical and Physical Sciences, 413*(1844), 27-44.

285. May, R. M., & Oster, G. F. (1976). Bifurcations and dynamic complexity in simple ecological models. *The American Naturalist, 110*(974), 573-599.

286. Mazzo, M. R., Holobar, A., & Enoka, R. M. (2022). Association between effective neural drive to the triceps surae and fluctuations in plantar-flexion torque during submaximal isometric contractions. *Experimental physiology, 107*(5), 489–507. https://doi.org/10.1113/EP090228

287. McAuley, J. H., & Marsden, C. D. (2000). Physiological and pathological tremors and rhythmic central motor control. *Brain : a journal of neurology, 123* (Pt 8), 1545–1567. https://doi.org/10.1093/brain/123.8.1545

288. McAuley, J. H., Corcos, D. M., Rothwell, J. C., Quinn, N. P., & Marsden, C. D. (2001). Levodopa reversible loss of the Piper frequency oscillation component in Parkinson's disease. *Journal of neurology, neurosurgery, and psychiatry, 70*(4), 471–476. https://doi.org/10.1136/jnnp.70.4.471

289. McAuley, J. H., Rothwell, J. C., & Marsden, C. D. (1997). Frequency peaks of tremor, muscle vibration and electromyographic activity at 10 Hz, 20 Hz and 40 Hz during human finger muscle contraction may reflect rhythmicities of central neural firing. *Experimental brain research, 114*(3), 525–541. https://doi.org/10.1007/pl00005662

290. McGinnis, S. M., Brickhouse, M., Pascual, B., & Dickerson, B. C. (2011). Age-related changes in the thickness of cortical zones in humans. *Brain topography, 24*(3-4), 279–291. https://doi.org/10.1007/s10548-011-0198-6

291. McGraw, K. O., & Wong, S. P. (1996). Forming inferences about some intraclass correlation coefficients. *Psychological methods, 1*(1), 30.

292. McIntosh, A. R., Vakorin, V., Kovacevic, N., Wang, H., Diaconescu, A., & Protzner, A. B. (2014). Spatiotemporal dependency of age-related changes in brain signal variability. *Cerebral cortex (New York, N.Y. : 1991), 24*(7), 1806–1817. https://doi.org/10.1093/cercor/bht030

293. McKinnon, N. B., Connelly, D. M., Rice, C. L., Hunter, S. W., & Doherty, T. J. (2017). Neuromuscular contributions to the age-related reduction in muscle power: Mechanisms and potential role of high velocity power training. *Ageing research reviews, 35,* 147–154. https://doi.org/10.1016/j.arr.2016.09.003

294. McManus, L., Hu, X., Rymer, W. Z., Suresh, N. L., & Lowery, M. M. (2016). Muscle fatigue increases beta-band coherence between the firing times of simultaneously active motor units in the first dorsal interosseous muscle. *Journal of neurophysiology, 115*(6), 2830-2839.

295. McNeil, C. J., & Rice, C. L. (2007). Fatigability is increased with age during velocity-dependent contractions of the dorsiflexors. *The journals of gerontology. Series A, Biological sciences and medical sciences, 62*(6), 624–629. https://doi.org/10.1093/gerona/62.6.624

296. McNeil, C. J., Doherty, T. J., Stashuk, D. W., & Rice, C. L. (2005). Motor unit number estimates in the tibialis anterior muscle of young, old, and very old men. *Muscle & nerve, 31*(4), 461–467. https://doi.org/10.1002/mus.20276

297. McNeil, C. J., Vandervoort, A. A., & Rice, C. L. (2007). Peripheral impairments cause a progressive age-related loss of strength and velocity-dependent power in the dorsiflexors. *Journal of applied physiology (Bethesda, Md. : 1985), 102*(5), 1962–1968. https://doi.org/10.1152/japplphysiol.01166.2006

298. McCrum, C., Leow, P., Epro, G., König, M., Meijer, K., & Karamanidis, K. (2018). Alterations in Leg Extensor Muscle-Tendon Unit Biomechanical Properties With Ageing and Mechanical Loading. *Frontiers in physiology*, *9*, 150. https://doi.org/10.3389/fphys.2018.00150

299. Mear, E., Gladwell, V., & Pethick, J. (2023). Knee extensor force control as a predictor of dynamic balance in healthy adults. *Gait & posture, 100*, 230–235. https://doi.org/10.1016/j.gaitpost.2023.01.004

300. Mehrkanoon, S., Breakspear, M., & Boonstra, T. W. (2014). The reorganization of corticomuscular coherence during a transition between sensorimotor states. *NeuroImage, 100*, 692–702. https://doi.org/10.1016/j.neuroimage.2014.06.050

301. Melzer, I., Benjuya, N., & Kaplanski, J. (2004). Postural stability in the elderly: a comparison between fallers and non-fallers. *Age and ageing, 33*(6), 602–607. https://doi.org/10.1093/ageing/afh218

302. Metter, E. J., Talbot, L. A., Schrager, M., & Conwit, R. A. (2004). Arm-cranking muscle power and arm isometric muscle strength are independent predictors of all-cause mortality in men. *Journal of applied physiology (Bethesda, Md. : 1985), 96*(2), 814–821. https://doi.org/10.1152/japplphysiol.00370.2003

303. Miljkovic, I., & Zmuda, J. M. (2010). Epidemiology of myosteatosis. *Current opinion in clinical nutrition and metabolic care, 13*(3), 260–264. https://doi.org/10.1097/MCO.0b013e328337d826

304. Milligan, R. A., & Flicker, P. F. (1987). Structural relationships of actin, myosin, and tropomyosin revealed by cryo-electron microscopy. *Journal of Cell Biology, 105*(1), 29-39.

305. Milner-Brown, H. S., Stein, R. B., & Yemm, R. (1973). The orderly recruitment of human motor units during voluntary isometric contractions. *The Journal of physiology, 230*(2), 359–370. https://doi.org/10.1113/jphysiol.1973.sp010192

306. Mitchell, W. K., Williams, J., Atherton, P., Larvin, M., Lund, J., & Narici, M. (2012). Sarcopenia, dynapenia, and the impact of advancing age on human skeletal muscle size and strength; a quantitative review. *Frontiers in physiology, 3,* 260. https://doi.org/10.3389/fphys.2012.00260

307. Molenaar, J. P., McNeil, C. J., Bredius, M. S., & Gandevia, S. C. (2013). Effects of aging and sex on voluntary activation and peak relaxation rate of human elbow flexors studied with motor cortical stimulation. *Age (Dordrecht, Netherlands), 35*(4), 1327–1337. https://doi.org/10.1007/s11357-012-9435-5

308. Monte, A., Benamati, A., Pavan, A., d'Avella, A., & Bertucco, M. (2024). Muscle synergies for multidirectional isometric force generation during maintenance of upright standing posture. *Experimental brain research, 242*(8), 1881–1902. https://doi.org/10.1007/s00221-024-06866-z

309. Moritz, C. T., Barry, B. K., Pascoe, M. A., & Enoka, R. M. (2005). Discharge rate variability influences the variation in force fluctuations across the working range of a hand muscle. *Journal of neurophysiology, 93*(5), 2449–2459. https://doi.org/10.1152/jn.01122.2004

310. Moro, T., Tinsley, G., Bianco, A., Gottardi, A., Gottardi, G. B., Faggian, D., Plebani, M., Marcolin, G., & Paoli, A. (2017). High intensity interval resistance training (HIIRT) in older adults: Effects on body composition, strength, anabolic hormones and blood lipids. *Experimental gerontology, 98*, 91–98. https://doi.org/10.1016/j.exger.2017.08.015

311. Morrison, S., & Newell, K. M. (2012). Aging, neuromuscular decline, and the change in physiological and behavioral complexity of upper-limb movement dynamics. *Journal of aging research, 2012,* 891218. https://doi.org/10.1155/2012/891218

312. Mosole, S., Carraro, U., Kern, H., Loefler, S., Fruhmann, H., Vogelauer, M., Burggraf, S., Mayr, W., Krenn, M., Paternostro-Sluga, T., Hamar, D., Cvecka, J., Sedliak, M., Tirpakova, V., Sarabon, N., Musarò, A., Sandri, M., Protasi, F., Nori, A., Pond, A., … Zampieri, S. (2014). Long-term high-level exercise promotes muscle reinnervation with age. *Journal of neuropathology and experimental neurology, 73*(4), 284–294. https://doi.org/10.1097/NEN.0000000000000032

313. Myers, L. J., Erim, Z., & Lowery, M. M. (2004). Time and frequency domain methods for quantifying common modulation of motor unit firing patterns. *Journal of neuroengineering and rehabilitation, 1*(1), 2. https://doi.org/10.1186/1743-0003-1-2

314. Mynark, R. G., & Koceja, D. M. (2001). Effects of age on the spinal stretch reflex. *Journal of applied biomechanics, 17*(3), 188-203

315. Mlinac, M. E., & Feng, M. C. (2016). Assessment of Activities of Daily Living, Self-Care, and Independence. *Archives of clinical neuropsychology : the official journal of the National Academy of Neuropsychologists*, *31*(6), 506–516. https://doi.org/10.1093/arclin/acw049

316. Martien, S., Delecluse, C., Boen, F., Seghers, J., Pelssers, J., Van Hoecke, A. S., & Van Roie, E. (2015). Is knee extension strength a better predictor of functional performance than handgrip strength among older adults in three different settings?. *Archives of gerontology and geriatrics*, *60*(2), 252–258. https://doi.org/10.1016/j.archger.2014.11.010

317. Narici, M. V., Maffulli, N., & Maganaris, C. N. (2008). Ageing of human muscles and tendons. *Disability and rehabilitation, 30*(20-22), 1548–1554. https://doi.org/10.1080/09638280701831058

318. Negro, F., & Farina, D. (2011). Linear transmission of cortical oscillations to the neural drive to muscles is mediated by common projections to populations of motor neurons in humans. *The Journal of physiology, 589*(Pt 3), 629–637. https://doi.org/10.1113/jphysiol.2010.202473

319. Negro, F., & Farina, D. (2012). Factors influencing the estimates of correlation between motor unit activities in humans. *PloS one, 7*(9), e44894. https://doi.org/10.1371/journal.pone.0044894

320. Negro, F., Holobar, A., & Farina, D. (2009). Fluctuations in isometric muscle force can be described by one linear projection of low-frequency components of motor unit discharge rates. *The Journal of physiology, 587*(Pt 24), 5925–5938. https://doi.org/10.1113/jphysiol.2009.178509

321. Negro, F., Muceli, S., Castronovo, A. M., Holobar, A., & Farina, D. (2016a). Multi-channel intramuscular and surface EMG decomposition by convolutive blind source separation. *Journal of neural engineering, 13*(2), 026027. https://doi.org/10.1088/1741-2560/13/2/026027

322. Negro, F., Yavuz, U. Ş., & Farina, D. (2016b). The human motor neuron pools receive a dominant slow-varying common synaptic input. *The Journal of physiology, 594*(19), 5491–5505. https://doi.org/10.1113/JP271748

323. Newell, K. M. (2020). What are Fundamental Motor Skills and What is Fundamental About Them?. *Journal of Motor Learning and Development, 8*(2), 280-314. https://doi.org/10.1123/jmld.2020-0013

324. Ochala, J., Frontera, W. R., Dorer, D. J., Van Hoecke, J., & Krivickas, L. S. (2007). Single skeletal muscle fiber elastic and contractile characteristics in young and older men. *The journals of gerontology. Series A, Biological sciences and medical sciences, 62*(4), 375–381. https://doi.org/10.1093/gerona/62.4.375

325. Ofori, E., Samson, J. M., & Sosnoff, J. J. (2010). Age-related differences in force variability and visual display. *Experimental brain research, 203*(2), 299–306. https://doi.org/10.1007/s00221-010-2229-z

326. Oomen, N. M., & van Dieën, J. H. (2017). Effects of age on force steadiness: A literature review and meta-analysis. *Ageing research reviews, 35,* 312–321. https://doi.org/10.1016/j.arr.2016.11.004

327. Orssatto, L. B. R., Borg, D. N., Pendrith, L., Blazevich, A. J., Shield, A. J., & Trajano, G. S. (2022). Do motor neuron discharge rates slow with aging? A systematic review and meta-analysis. *Mechanisms of ageing and development, 203,* 111647. https://doi.org/10.1016/j.mad.2022.111647

328. Oshita, K., & Yano, S. (2010). Relationship between force fluctuation in the plantar flexor and sustainable time for single-leg standing. *Journal of physiological anthropology, 29*(3), 89–93. https://doi.org/10.2114/jpa2.29.89

329. Oshita, K., & Yano, S. (2012). Association of force steadiness of plantar flexor muscles and postural sway during quiet standing by young adults. *Perceptual and motor skills, 115*(1), 143–152. https://doi.org/10.2466/15.26.29.PMS.115.4.143-152

330. Ostwald, S. K., Snowdon, D. A., Rysavy, D. M., Keenan, N. L., & Kane, R. L. (1989). Manual dexterity as a correlate of dependency in the elderly. *Journal of the American Geriatrics Society, 37*(10), 963–969. https://doi.org/10.1111/j.1532-5415.1989.tb07282.x

331. Ott, E. (2002). Chaos in Dynamical Systems (2nd ed.). Cambridge: Cambridge University Press.

332. Overend, T. J., Cunningham, D. A., Paterson, D. H., & Lefcoe, M. S. (1992). Thigh composition in young and elderly men determined by computed tomography. *Clinical physiology (Oxford, England), 12*(6), 629–640. https://doi.org/10.1111/j.1475-097x.1992.tb00366.x

333. Pabla, P., Jones, E. J., Piasecki, M., & Phillips, B. E. (2024). Skeletal muscle dysfunction with advancing age. *Clinical science (London, England : 1979), 138*(14), 863–882. https://doi.org/10.1042/CS20231197

334. Pajala, S., Era, P., Koskenvuo, M., Kaprio, J., Törmäkangas, T., & Rantanen, T. (2008). Force platform balance measures as predictors of indoor and outdoor falls in community-dwelling women aged 63-76 years. *The journals of gerontology. Series A, Biological sciences and medical sciences, 63*(2), 171–178. https://doi.org/10.1093/gerona/63.2.171

335. Pallarés, J. G., Morán-Navarro, R., Ortega, J. F., Fernández-Elías, V. E., & Mora-Rodriguez, R. (2016). Validity and Reliability of Ventilatory and Blood Lactate Thresholds in Well-Trained Cyclists. *PloS one, 11*(9), e0163389. https://doi.org/10.1371/journal.pone.0163389

336. Patten, C., Kamen, G., & Rowland, D. M. (2001). Adaptations in maximal motor unit discharge rate to strength training in young and older adults. *Muscle & nerve, 24*(4), 542–550. https://doi.org/10.1002/mus.1038

337. Peng, C. K., Buldyrev, S. V., Havlin, S., Simons, M., Stanley, H. E., & Goldberger, A. L. (1994). Mosaic organization of DNA nucleotides. *Physical review. E, Statistical physics, plasmas, fluids, and related interdisciplinary topics, 49*(2), 1685–1689. https://doi.org/10.1103/physreve.49.1685

338. Peng, C. K., Costa, M., & Goldberger, A. L. (2009). Adaptive data analysis of complex fluctuations in physiologic time series. *Advances in adaptive data analysis, 1*(1), 61–70. https://doi.org/10.1142/S1793536909000035

339. Peng, C. K., Hausdorff, J. M., & Goldberger, A. L. (2000). Fractal mechanisms in neuronal control: human heartbeat and gait dynamics in health and disease. Self-organized biological dynamics and nonlinear control: Toward understanding complexity, chaos and emergent function in living systems, 66-96.

340. Peng, C. K., Havlin, S., Stanley, H. E., & Goldberger, A. L. (1995). Quantification of scaling exponents and crossover phenomena in nonstationary heartbeat time series. *Chaos (Woodbury, N.Y.), 5*(1), 82–87. https://doi.org/10.1063/1.166141

341. Peng, C. K., Mietus, J. E., Liu, Y., Lee, C., Hausdorff, J. M., Stanley, H. E., Goldberger, A. L., & Lipsitz, L. A. (2002). Quantifying fractal dynamics of human respiration: age and gender effects. *Annals of biomedical engineering, 30*(5), 683–692. https://doi.org/10.1114/1.1481053

342. Pereira, H. M., Schlinder-DeLap, B., Keenan, K. G., Negro, F., Farina, D., Hyngstrom, A. S., Nielson, K. A., & Hunter, S. K. (2019). Oscillations in neural drive and age-related reductions in force steadiness with a cognitive challenge. *Journal of applied physiology (Bethesda, Md. : 1985), 126*(4), 1056–1065. https://doi.org/10.1152/japplphysiol.00821.2018

343. Pereira, H. M., Schlinder-Delap, B., Nielson, K. A., & Hunter, S. K. (2018). Force Steadiness During a Cognitively Challenging Motor Task Is Predicted by Executive Function in Older Adults. *Frontiers in physiology, 9,* 1316. https://doi.org/10.3389/fphys.2018.01316

344. Pereira, H. M., Spears, V. C., Schlinder-Delap, B., Yoon, T., Nielson, K. A., & Hunter, S. K. (2015). Age and sex differences in steadiness of elbow flexor muscles with imposed cognitive demand. *European journal of applied physiology, 115*(6), 1367–1379. https://doi.org/10.1007/s00421-015-3113-0

345. Perry, M. C., Carville, S. F., Smith, I. C., Rutherford, O. M., & Newham, D. J. (2007). Strength, power output and symmetry of leg muscles: effect of age and history of falling. *European journal of applied physiology, 100*(5), 553–561. https://doi.org/10.1007/s00421-006-0247-0

346. Peterka R. J. (2018). Sensory integration for human balance control. *Handbook of clinical neurology, 159,* 27–42. https://doi.org/10.1016/B978-0-444-63916-5.00002-1

347. Pethick, J. (2023). The effect of lifelong physical (in) activity on knee extensor force control. *bioRxiv,* 2023-02.

348. Pethick, J., & Piasecki, M. (2022). Alterations in Muscle Force Control With Aging: Is There a Modulatory Effect of Lifelong Physical Activity?. *Frontiers in sports and active living, 4,* 817770. https://doi.org/10.3389/fspor.2022.817770

349. Pethick, J., & Tallent, J. (2022). The Neuromuscular Fatigue-Induced Loss of Muscle Force Control. *Sports (Basel, Switzerland), 10*(11), 184. https://doi.org/10.3390/sports10110184

350. Pethick, J., Taylor, M. J. D., & Harridge, S. D. R. (2022). Aging and skeletal muscle force control: Current perspectives and future directions. *Scandinavian journal of medicine & science in sports, 32*(10), 1430–1443. https://doi.org/10.1111/sms.14207

351. Pethick, J., Winter, S. L., & Burnley, M. (2015). Fatigue reduces the complexity of knee extensor torque fluctuations during maximal and submaximal intermittent isometric contractions in man. *The Journal of physiology, 593*(8), 2085–2096. https://doi.org/10.1113/jphysiol.2015.284380

352. Pethick, J., Winter, S. L., & Burnley, M. (2016). Loss of knee extensor torque complexity during fatiguing isometric muscle contractions occurs exclusively above the critical torque. *American journal of physiology. Regulatory, integrative and comparative physiology, 310*(11), R1144–R1153. https://doi.org/10.1152/ajpregu.00019.2016

353. Pethick, J., Winter, S. L., & Burnley, M. (2018a). Caffeine Ingestion Attenuates Fatigue-induced Loss of Muscle Torque Complexity. *Medicine and science in sports and exercise, 50*(2), 236–245. https://doi.org/10.1249/MSS.0000000000001441

354. Pethick, J., Winter, S. L., & Burnley, M. (2018b). Effects of ipsilateral and contralateral fatigue and muscle blood flow occlusion on the complexity of knee-extensor torque output in humans. *Experimental physiology, 103*(7), 956–967. https://doi.org/10.1113/EP086960

355. Pethick, J., Winter, S. L., & Burnley, M. (2019). Fatigue reduces the complexity of knee extensor torque during fatiguing sustained isometric contractions. *European journal of sport science, 19*(10), 1349–1358. https://doi.org/10.1080/17461391.2019.1599450

356. Pethick, J., Winter, S. L., & Burnley, M. (2021a). Did you know? Using entropy and fractal geometry to quantify fluctuations in physiological outputs. *Acta physiologica (Oxford, England), 233*(4), e13670. https://doi.org/10.1111/apha.13670

357. Pethick, J., Winter, S. L., & Burnley, M. (2021b). Physiological complexity: influence of ageing, disease and neuromuscular fatigue on muscle force and torque fluctuations. *Experimental physiology, 106*(10), 2046–2059. https://doi.org/10.1113/EP089711

358. Petrella, J. K., Kim, J. S., Tuggle, S. C., Hall, S. R., & Bamman, M. M. (2005). Age differences in knee extension power, contractile velocity, and fatigability. *Journal of applied physiology (Bethesda, Md. : 1985), 98*(1), 211–220. https://doi.org/10.1152/japplphysiol.00294.2004

359. Piasecki, J., Inns, T. B., Bass, J. J., Scott, R., Stashuk, D. W., Phillips, B. E., Atherton, P. J., & Piasecki, M. (2021a). Influence of sex on the age-related adaptations of neuromuscular function and motor unit properties in elite masters athletes. *The Journal of physiology, 599*(1), 193–205. https://doi.org/10.1113/JP280679

360. Piasecki, M., Garnés-Camarena, O., & Stashuk, D. W. (2021b). Near-fiber electromyography. *Clinical neurophysiology : official journal of the International Federation of Clinical Neurophysiology, 132*(5), 1089–1104. https://doi.org/10.1016/j.clinph.2021.02.008

361. Piasecki, M., Ireland, A., Jones, D. A., & McPhee, J. S. (2016a). Age-dependent motor unit remodelling in human limb muscles. *Biogerontology, 17*(3), 485–496. https://doi.org/10.1007/s10522-015-9627-3

362. Piasecki, M., Ireland, A., Stashuk, D., Hamilton-Wright, A., Jones, D. A., & McPhee, J. S. (2016b). Age-related neuromuscular changes affecting human vastus lateralis. *The Journal of physiology, 594*(16), 4525–4536. https://doi.org/10.1113/JP271087

363. Piasecki, M., Ireland, A., Coulson, J., Stashuk, D. W., Hamilton-Wright, A., Swiecicka, A., Rutter, M. K., McPhee, J. S., & Jones, D. A. (2016c). Motor unit number estimates and neuromuscular transmission in the tibialis anterior of master athletes: evidence that athletic older people are not spared from age-related motor unit remodeling. *Physiological reports, 4*(19), e12987. https://doi.org/10.14814/phy2.12987

364. Piasecki, M., Ireland, A., Piasecki, J., Degens, H., Stashuk, D. W., Swiecicka, A., Rutter, M. K., Jones, D. A., & McPhee, J. S. (2019). Long-Term Endurance and Power Training May Facilitate Motor Unit Size Expansion to Compensate for Declining Motor Unit Numbers in Older Age. *Frontiers in physiology, 10,* 449. https://doi.org/10.3389/fphys.2019.00449

365. Pincus S. (1995). Approximate entropy (ApEn) as a complexity measure. *Chaos (Woodbury, N.Y.), 5*(1), 110–117. https://doi.org/10.1063/1.166092

366. Pincus S. M. (1991). Approximate entropy as a measure of system complexity. *Proceedings of the National Academy of Sciences of the United States of America, 88*(6), 2297–2301. https://doi.org/10.1073/pnas.88.6.2297

367. Pincus, S. M., & Goldberger, A. L. (1994). Physiological time-series analysis: what does regularity quantify?. *The American journal of physiology, 266*(4 Pt 2), H1643–H1656. https://doi.org/10.1152/ajpheart.1994.266.4.H1643

368. Poincaré, H. (2017). On the Three-Body Problem and the Equations of Dynamics. (B. D. Popp, Trans. Poincaré, H. (1890). On the three-body problem and the equations of dynamics. Acta Math, 13(1).

369. Power, G. A., Allen, M. D., Gilmore, K. J., Stashuk, D. W., Doherty, T. J., Hepple, R. T., Taivassalo, T., & Rice, C. L. (2016). Motor unit number and transmission stability in octogenarian world class athletes: Can age-related deficits be outrun?. *Journal of applied physiology (Bethesda, Md. : 1985), 121*(4), 1013–1020. https://doi.org/10.1152/japplphysiol.00149.2016

370. Power, G. A., Dalton, B. H., & Rice, C. L. (2013). Human neuromuscular structure and function in old age: A brief review. *Journal of sport and health science, 2*(4), 215–226. https://doi.org/10.1016/j.jshs.2013.07.001

371. Power, G. A., Dalton, B. H., Behm, D. G., Doherty, T. J., Vandervoort, A. A., & Rice, C. L. (2012). Motor unit survival in lifelong runners is muscle dependent. *Medicine and science in sports and exercise, 44*(7), 1235–1242. https://doi.org/10.1249/MSS.0b013e318249953c

372. Power, G. A., Dalton, B. H., Behm, D. G., Vandervoort, A. A., Doherty, T. J., & Rice, C. L. (2010). Motor unit number estimates in masters runners: use it or lose it?. *Medicine and science in sports and exercise, 42*(9), 1644–1650. https://doi.org/10.1249/MSS.0b013e3181d6f9e9

373. Purves-Smith, F. M., Sgarioto, N., & Hepple, R. T. (2014). Fiber typing in aging muscle. *Exercise and sport sciences reviews, 42*(2), 45–52. https://doi.org/10.1249/JES.0000000000000012

374. Purves, D. (2018). Neuroscience. 6th Edition.

375. R.Shaw:The Dripping Faucet as a Model Chaotic System (Aerial Press, Santa Cruz, 1984).

376. Raffalt, P. C., Yentes, J. M., & Spedden, M. E. (2023). Isometric force complexity may not fully originate from the nervous system. *Human movement science, 90*, 103111. https://doi.org/10.1016/j.humov.2023.103111

377. Ranganathan, V. K., Siemionow, V., Sahgal, V., & Yue, G. H. (2001). Effects of aging on hand function. *Journal of the American Geriatrics Society, 49*(11), 1478–1484. https://doi.org/10.1046/j.1532-5415.2001.4911240.x

378. Reid, K. F., & Fielding, R. A. (2012). Skeletal muscle power: a critical determinant of physical functioning in older adults. *Exercise and sport sciences reviews, 40*(1), 4–12. https://doi.org/10.1097/JES.0b013e31823b5f13

379. Reuben, D. B., Magasi, S., McCreath, H. E., Bohannon, R. W., Wang, Y. C., Bubela, D. J., Rymer, W. Z., Beaumont, J., Rine, R. M., Lai, J. S., & Gershon, R. C. (2013). Motor assessment using the NIH Toolbox. *Neurology, 80*(11 Suppl 3), S65–S75. https://doi.org/10.1212/WNL.0b013e3182872e01

380. Rey-Robert, B., Temprado, J. J., & Berton, E. (2011). Aging and changes in complexity in the neurobehavioral system. *Medicina (Kaunas, Lithuania), 47*(1), 1–10.

381. Richman, J. S., & Moorman, J. R. (2000). Physiological time-series analysis using approximate entropy and sample entropy. *American journal of physiology. Heart and circulatory physiology, 278*(6), H2039–H2049. https://doi.org/10.1152/ajpheart.2000.278.6.H2039

382. Rivner, M. H., Swift, T. R., & Malik, K. (2001). Influence of age and height on nerve conduction. *Muscle & nerve, 24*(9), 1134–1141. https://doi.org/10.1002/mus.1124

383. Røgind, H., Lykkegaard, J. J., Bliddal, H., & Danneskiold-Samsøe, B. (2003). Postural sway in normal subjects aged 20-70 years. *Clinical physiology and functional imaging, 23*(3), 171–176. https://doi.org/10.1046/j.1475-097x.2003.00492.x

384. Röhrle, O., Yavuz, U. Ş., Klotz, T., Negro, F., & Heidlauf, T. (2019). Multiscale modeling of the neuromuscular system: Coupling neurophysiology and skeletal muscle mechanics. Wiley interdisciplinary reviews. *Systems biology and medicine, 11*(6), e1457. https://doi.org/10.1002/wsbm.1457

385. Rossato, J., Tucker, K., Avrillon, S., Lacourpaille, L., Holobar, A., & Hug, F. (2022). Less common synaptic input between muscles from the same group allows for more flexible coordination strategies during a fatiguing task. *Journal of neurophysiology, 127*(2), 421–433. https://doi.org/10.1152/jn.00453.2021

386. Sahinis, C., Amiridis, I. G., Varvariotis, N., Lykidis, A., Kannas, T. M., Negro, F., & Enoka, R. M. (2024). Foot-dominance does not influence force variability during ankle dorsiflexion and foot adduction. *Journal of sports sciences,* 1–11. Advance online publication. https://doi.org/10.1080/02640414.2024.2379699

387. Salat, D. H., Buckner, R. L., Snyder, A. Z., Greve, D. N., Desikan, R. S., Busa, E., Morris, J. C., Dale, A. M., & Fischl, B. (2004). Thinning of the cerebral cortex in aging. *Cerebral cortex (New York, N.Y. : 1991), 14*(7), 721–730. https://doi.org/10.1093/cercor/bhh032

388. Sandow A. (1952). Excitation-contraction coupling in muscular response. *The Yale journal of biology and medicine, 25*(3), 176–201.

389. Schmied, A., & Descarreaux, M. (2010). Influence of contraction strength on single motor unit synchronous activity. *Clinical neurophysiology : official journal of the International Federation of Clinical Neurophysiology, 121*(10), 1624–1632. https://doi.org/10.1016/j.clinph.2010.02.165

390. Seely, A. J., & Macklem, P. T. (2004). Complex systems and the technology of variability analysis. *Critical care (London, England), 8*(6), R367–R384. https://doi.org/10.1186/cc2948

391. Seidler, R. D., Alberts, J. L., & Stelmach, G. E. (2002). Changes in multi-joint performance with age. *Motor control, 6*(1), 19–31. https://doi.org/10.1123/mcj.6.1.19

392. Seidler, R. D., Bernard, J. A., Burutolu, T. B., Fling, B. W., Gordon, M. T., Gwin, J. T., Kwak, Y., & Lipps, D. B. (2010). Motor control and aging: links to age-related brain structural, functional, and biochemical effects. *Neuroscience and biobehavioral reviews, 34*(5), 721–733. https://doi.org/10.1016/j.neubiorev.2009.10.005

393. Selen, L. P., Beek, P. J., & van Dieën, J. H. (2005). Can co-activation reduce kinematic variability? A simulation study. *Biological cybernetics, 93*(5), 373–381. https://doi.org/10.1007/s00422-005-0015-y

394. Semmler, J. G., Steege, J. W., Kornatz, K. W., & Enoka, R. M. (2000). Motor-unit synchronization is not responsible for larger motor-unit forces in old adults. *Journal of neurophysiology, 84*(1), 358–366. https://doi.org/10.1152/jn.2000.84.1.358

395. Seynnes, O., Hue, O. A., Garrandes, F., Colson, S. S., Bernard, P. L., Legros, P., & Fiatarone Singh, M. A. (2005). Force steadiness in the lower extremities as an independent predictor of functional performance in older women. *Journal of aging and physical activity, 13*(4), 395–408. https://doi.org/10.1123/japa.13.4.395

396. Shaffer, S. W., & Harrison, A. L. (2007). Aging of the somatosensory system: a translational perspective. *Physical therapy, 87*(2), 193–207. https://doi.org/10.2522/ptj.20060083

397. Shannon, C. E. (1948). A mathematical theory of communication. *The Bell system technical journal, 27*(3), 379-423.

398. Sherrington, C. S. (1925). Remarks on some aspects of reflex inhibition. *Proceedings of the Royal Society of London. Series B, Containing Papers of a Biological Character, 97*(686), 519-545.

399. Shim, J. K., Lay, B. S., Zatsiorsky, V. M., & Latash, M. L. (2004). Age-related changes in finger coordination in static prehension tasks. *Journal of applied physiology (Bethesda, Md. : 1985), 97*(1), 213–224. https://doi.org/10.1152/japplphysiol.00045.2004

400. Shinohara, M., Keenan, K. G., & Enoka, R. M. (2005). Fluctuations in motor output during steady contractions are weakly related across contraction types and between hands. *Muscle & nerve, 31*(6), 741–750. https://doi.org/10.1002/mus.20326

401. Shrout, P.E. and Fleiss, J.L., (1979). Intraclass correlations: Uses in assessing rater reliability. *PsychologicalBulletin, 86,* 420-428. https://doi.org/10.1037//0033-2909.86.2.420.

402. Sienko, K. H., Seidler, R. D., Carender, W. J., Goodworth, A. D., Whitney, S. L., & Peterka, R. J. (2018). Potential Mechanisms of Sensory Augmentation Systems on Human Balance Control. *Frontiers in neurology, 9,* 944. https://doi.org/10.3389/fneur.2018.00944

403. Singh, N. B., Arampatzis, A., Duda, G., Heller, M. O., & Taylor, W. R. (2010). Effect of fatigue on force fluctuations in knee extensors in young adults. *Philosophical transactions. Series A, Mathematical, physical, and engineering sciences, 368*(1920), 2783–2798. https://doi.org/10.1098/rsta.2010.0091

404. Skelton, D. A., Greig, C. A., Davies, J. M., & Young, A. (1994). Strength, power and related functional ability of healthy people aged 65-89 years. *Age and ageing, 23*(5), 371–377. https://doi.org/10.1093/ageing/23.5.371

405. Skelton, D. A., Kennedy, J., & Rutherford, O. M. (2002). Explosive power and asymmetry in leg muscle function in frequent fallers and non-fallers aged over 65. *Age and ageing, 31*(2), 119–125. https://doi.org/10.1093/ageing/31.2.119

406. Sleimen-Malkoun, R., Temprado, J. J., & Hong, S. L. (2014). Aging induced loss of complexity and dedifferentiation: consequences for coordination dynamics within and between brain, muscular and behavioral levels. *Frontiers in aging neuroscience, 6,* 140. https://doi.org/10.3389/fnagi.2014.00140

407. Slifkin, A. B., & Newell, K. M. (1999). Noise, information transmission, and force variability. *Journal of experimental psychology. Human perception and performance, 25*(3), 837–851. https://doi.org/10.1037//0096-1523.25.3.837

408. Smart, R. R., Kohn, S., Richardson, C. M., & Jakobi, J. M. (2018). Influence of forearm orientation on biceps brachii tendon mechanics and elbow flexor force steadiness. *Journal of biomechanics, 76,* 129–135. https://doi.org/10.1016/j.jbiomech.2018.05.039

409. Soderberg, G. L., Minor, S. D., & Nelson, R. M. (1991). A comparison of motor unit behaviour in young and aged subjects. *Age and ageing, 20*(1), 8–15. https://doi.org/10.1093/ageing/20.1.8

410. Sosnoff, J. J., & Newell, K. M. (2006a). Aging, visual intermittency, and variability in isometric force output. *The journals of gerontology. Series B, Psychological sciences and social sciences, 61*(2), P117–P124. https://doi.org/10.1093/geronb/61.2.p117

411. Sosnoff, J. J., & Newell, K. M. (2006b). The generalization of perceptual-motor intra-individual variability in young and old adults. *The journals of gerontology. Series B, Psychological sciences and social sciences, 61*(5), P304–P310. https://doi.org/10.1093/geronb/61.5.p304

412. Sosnoff, J. J., & Newell, K. M. (2006c). Are age-related increases in force variability due to decrements in strength?. *Experimental brain research, 174*(1), 86–94. https://doi.org/10.1007/s00221-006-0422-x

413. Sosnoff, J. J., & Newell, K. M. (2006d). Information processing limitations with aging in the visual scaling of isometric force. *Experimental brain research, 170*(3), 423–432. https://doi.org/10.1007/s00221-005-0225-5

414. Sosnoff, J. J., & Newell, K. M. (2007). Are visual feedback delays responsible for aging-related increases in force variability?. *Experimental aging research, 33*(4), 399–415. https://doi.org/10.1080/03610730701525311

415. Sosnoff, J. J., & Newell, K. M. (2008). Age-related loss of adaptability to fast time scales in motor variability. *The journals of gerontology. Series B, Psychological sciences and social sciences, 63*(6), P344–P352. https://doi.org/10.1093/geronb/63.6.p344

416. Sosnoff, J. J., & Newell, K. M. (2011). Aging and motor variability: a test of the neural noise hypothesis. *Experimental aging research, 37*(4), 377–397. https://doi.org/10.1080/0361073X.2011.590754

417. Sosnoff, J. J., & Voudrie, S. J. (2009). Practice and age-related loss of adaptability in sensorimotor performance. *Journal of motor behavior, 41*(2), 137–146. https://doi.org/10.3200/JMBR.41.2.137-146

418. Sosnoff, J. J., Vaillancourt, D. E., & Newell, K. M. (2004). Aging and rhythmical force output: loss of adaptive control of multiple neural oscillators. *Journal of neurophysiology, 91*(1), 172–181. https://doi.org/10.1152/jn.00613.2003

419. Spiegel, K. M., Stratton, J., Burke, J. R., Glendinning, D. S., & Enoka, R. M. (1996). The influence of age on the assessment of motor unit activation in a human hand muscle. *Experimental physiology, 81*(5), 805–819. https://doi.org/10.1113/expphysiol.1996.sp003978

420. Spiering, B. A., Lee, S. M., Mulavara, A. P., Bentley, J. R., Buxton, R. E., Lawrence, E. L., Sinka, J., Guilliams, M. E., Ploutz-Snyder, L. L., & Bloomberg, J. J. (2011). Test battery designed to quickly and safely assess diverse indices of neuromuscular function after unweighting. *Journal of strength and conditioning research, 25*(2), 545–555. https://doi.org/10.1519/JSC.0b013e3181f56780

421. Stålberg, E. V., & Sonoo, M. (1994). Assessment of variability in the shape of the motor unit action potential, the "jiggle," at consecutive discharges. *Muscle & nerve, 17*(10), 1135–1144. https://doi.org/10.1002/mus.880171003

422. Stec, M. J., Thalacker-Mercer, A., Mayhew, D. L., Kelly, N. A., Tuggle, S. C., Merritt, E. K., Brown, C. J., Windham, S. T., Dell'Italia, L. J., Bickel, C. S., Roberts, B. M., Vaughn, K. M., Isakova-Donahue, I., Many, G. M., & Bamman, M. M. (2017). Randomized, four-arm, dose-response clinical trial to optimize resistance exercise training for older adults with age-related muscle atrophy. *Experimental gerontology, 99,* 98–109. https://doi.org/10.1016/j.exger.2017.09.018

423. Stergiou, N., & Decker, L. M. (2011). Human movement variability, nonlinear dynamics, and pathology: is there a connection?. *Human movement science, 30*(5), 869–888. https://doi.org/10.1016/j.humov.2011.06.002

424. Stijic, M., Petrovic, K., Schwingenschuh, P., Koini, M., & Schmidt, R. (2023). The Purdue Pegboard Test: Normative Data From 1,355 Healthy People From Austria. *The American journal of occupational therapy : official publication of the American Occupational Therapy Association, 77*(3), 7703205030. https://doi.org/10.5014/ajot.2023.050023

425. Sturnieks, D. L., George, R, St., & Lord, S. R. (2008). Balance disorders in the elderly. *Clinical Neurophysiology, 38*(6), 467-478. https://doi.org/10.1016/j.neucli.2008.09.001

426. Sundberg, C. W., Teigen, L. E., Hunter, S. K., & Fitts, R. H. (2025). Cumulative effects of H+ and Pi on force and power of skeletal muscle fibres from young and older adults. *The Journal of physiology, 603*(1), 187–209. https://doi.org/10.1113/JP286938

427. Tam, S. L., & Gordon, T. (2003). Mechanisms controlling axonal sprouting at the neuromuscular junction. *Journal of neurocytology, 32*(5-8), 961–974. https://doi.org/10.1023/B:NEUR.0000020635.41233.0f

428. Tang, S., & Chen, L. (2002). Density-dependent birth rate, birth pulses and their population dynamic consequences. *Journal of Mathematical Biology, 44*(2), 185-199.

429. Taylor, J. L., & Gandevia, S. C. (2008). A comparison of central aspects of fatigue in submaximal and maximal voluntary contractions. *Journal of applied physiology (Bethesda, Md. : 1985), 104*(2), 542–550. https://doi.org/10.1152/japplphysiol.01053.2007

430. Taylor, J. L., Butler, J. E., & Gandevia, S. C. (2000). Changes in muscle afferents, motor neurons and motor drive during muscle fatigue. *European journal of applied physiology, 83*(2-3), 106–115. https://doi.org/10.1007/s004210000269

431. Thompson, C. K., Negro, F., Johnson, M. D., Holmes, M. R., McPherson, L. M., Powers, R. K., Farina, D., & Heckman, C. J. (2018). Robust and accurate decoding of motor neuron behaviour and prediction of the resulting force output. *The Journal of physiology, 596*(14), 2643–2659. https://doi.org/10.1113/JP276153

432. Tiffin, J., & Asher, E. J. (1948). The Purdue pegboard; norms and studies of reliability and validity. *The Journal of applied psychology, 32*(3), 234–247. https://doi.org/10.1037/h0061266

433. Tikkanen, O., Sipilä, S., Kuula, A. S., Pesola, A., Haakana, P., & Finni, T. (2016). Muscle activity during daily life in the older people. *Aging clinical and experimental research, 28*(4), 713–720. https://doi.org/10.1007/s40520-015-0482-5

434. Tomlinson, B. E., & Irving, D. (1977). The numbers of limb motor neurons in the human lumbosacral cord throughout life. *Journal of the neurological sciences, 34*(2), 213–219. https://doi.org/10.1016/0022-510x(77)90069-7

435. Tracy B. L. (2007). Force control is impaired in the ankle plantarflexors of elderly adults. *European journal of applied physiology, 101*(5), 629–636. https://doi.org/10.1007/s00421-007-0538-0

436. Tracy, B. L., & Enoka, R. M. (2002). Older adults are less steady during submaximal isometric contractions with the knee extensor muscles. *Journal of applied physiology (Bethesda, Md. : 1985), 92*(3), 1004–1012. https://doi.org/10.1152/japplphysiol.00954.2001

437. Tracy, B. L., & Enoka, R. M. (2006). Steadiness training with light loads in the knee extensors of elderly adults. *Medicine and science in sports and exercise, 38*(4), 735–745. https://doi.org/10.1249/01.mss.0000194082.85358.c4

438. Tracy, B. L., Byrnes, W. C., & Enoka, R. M. (2004). Strength training reduces force fluctuations during anisometric contractions of the quadriceps femoris muscles in old adults. *Journal of applied physiology (Bethesda, Md. : 1985), 96*(4), 1530–1540. https://doi.org/10.1152/japplphysiol.00861.2003

439. Tracy, B. L., Dinenno, D. V., Jorgensen, B., & Welsh, S. J. (2007a). Aging, visuomotor correction, and force fluctuations in large muscles. *Medicine and science in sports and exercise, 39*(3), 469–479. https://doi.org/10.1249/mss.0b013e31802d3ad3

440. Tracy, B. L., Hitchcock, L. N., Welsh, S. J., Paxton, R. J., & Feldman-Kothe, C. E. (2015). Visuomotor Correction is a Robust Contributor to Force Variability During Index Finger Abduction by Older Adults. *Frontiers in aging neuroscience, 7,* 229. https://doi.org/10.3389/fnagi.2015.00229

441. Tracy, B. L., Maluf, K. S., Stephenson, J. L., Hunter, S. K., & Enoka, R. M. (2005). Variability of motor unit discharge and force fluctuations across a range of muscle forces in older adults. *Muscle & nerve, 32*(4), 533–540. https://doi.org/10.1002/mus.20392

442. Tracy, B. L., Mehoudar, P. D., & Ortega, J. D. (2007b). The amplitude of force variability is correlated in the knee extensor and elbow flexor muscles. *Experimental brain research, 176*(3), 448–464. https://doi.org/10.1007/s00221-006-0631-3

443. Vaillancourt, D. E., & Newell, K. M. (2000). Amplitude changes in the 8-12, 20-25, and 40 Hz oscillations in finger tremor. *Clinical neurophysiology : official journal of the International Federation of Clinical Neurophysiology, 111*(10), 1792–1801. https://doi.org/10.1016/s1388-2457(00)00378-3

444. Vaillancourt, D. E., & Newell, K. M. (2002). Changing complexity in human behavior and physiology through aging and disease. *Neurobiology of aging, 23*(1), 1–11. https://doi.org/10.1016/s0197-4580(01)00247-0

445. Vaillancourt, D. E., & Newell, K. M. (2003). Aging and the time and frequency structure of force output variability. *Journal of applied physiology (Bethesda, Md. : 1985), 94*(3), 903–912. https://doi.org/10.1152/japplphysiol.00166.2002

446. Vaillancourt, D. E., Larsson, L., & Newell, K. M. (2003). Effects of aging on force variability, single motor unit discharge patterns, and the structure of 10, 20, and 40 Hz

EMG activity. *Neurobiology of aging, 24*(1), 25–35. https://doi.org/10.1016/s0197-4580(02)00014-3

447. Vaillancourt, D. E., Slifkin, A. B., & Newell, K. M. (2002). Inter-digit individuation and force variability in the precision grip of young, elderly, and Parkinson's disease participants. *Motor control, 6*(2), 113–128. https://doi.org/10.1123/mcj.6.2.113

448. Vaillancourt, D. E., Sosnoff, J. J., & Newell, K. M. (2004). Age-related changes in complexity depend on task dynamics. *Journal of applied physiology (Bethesda, Md. : 1985), 97*(1), 454–455. https://doi.org/10.1152/japplphysiol.00244.2004

449. Vanden Noven, M. L., Pereira, H. M., Yoon, T., Stevens, A. A., Nielson, K. A., & Hunter, S. K. (2014). Motor Variability during Sustained Contractions Increases with Cognitive Demand in Older Adults. *Frontiers in aging neuroscience, 6,* 97. https://doi.org/10.3389/fnagi.2014.00097

450. Vandervoort A. A. (2002). Aging of the human neuromuscular system. *Muscle & nerve, 25*(1), 17–25. https://doi.org/10.1002/mus.1215

451. Vieluf, S., Mora, K., Gölz, C., Reuter, E. M., Godde, B., Dellnitz, M., Reinsberger, C., & Voelcker-Rehage, C. (2018). Age- and Expertise-Related Differences of Sensorimotor Network Dynamics during Force Control. *Neuroscience, 388,* 203–213. https://doi.org/10.1016/j.neuroscience.2018.07.025

452. Vieluf, S., Temprado, J. J., Berton, E., Jirsa, V. K., & Sleimen-Malkoun, R. (2015). Effects of task and age on the magnitude and structure of force fluctuations: insights into underlying neuro-behavioral processes. *BMC neuroscience, 16,* 12. https://doi.org/10.1186/s12868-015-0153-7

453. Voelcker-Rehage, C., Stronge, A. J., & Alberts, J. L. (2006). Age-related differences in working memory and force control under dual-task conditions. *Neuropsychology, development, and cognition. Section B, Aging, neuropsychology and cognition, 13*(3-4), 366–384. https://doi.org/10.1080/138255890969339

454. Valenčič, T., Ansdell, P., Brownstein, C. G., Spillane, P. M., Holobar, A., & Škarabot, J. (2024). Motor unit discharge rate modulation during isometric contractions to failure is intensity- and modality-dependent. *The Journal of physiology*, *602*(10), 2287–2314. https://doi.org/10.1113/JP286143

455. Walker, S., Avela, J., Wikgren, J., Meeusen, R., Piitulainen, H., Baker, S. N., & Parviainen, T. M. (2019). Aging and Strength Training Influence Knee Extensor Intermuscular Coherence During Low- and High-Force Isometric Contractions. *Frontiers in physiology, 9,* 1933. https://doi.org/10.3389/fphys.2018.01933

456. Wallace, J. W., Power, G. A., Rice, C. L., & Dalton, B. H. (2016). Time-dependent neuromuscular parameters in the plantar flexors support greater fatigability of old compared with younger males. *Experimental gerontology, 74,* 13–20. https://doi.org/10.1016/j.exger.2015.12.001

457. Wang, Y. C., Magasi, S. R., Bohannon, R. W., Reuben, D. B., McCreath, H. E., Bubela, D. J., Gershon, R. C., & Rymer, W. Z. (2011). Assessing dexterity function: a comparison of two alternatives for the NIH Toolbox. *Journal of hand therapy : official journal of the American Society of Hand Therapists, 24*(4), 313–321. https://doi.org/10.1016/j.jht.2011.05.001

458. Watanabe, K., Holobar, A., Kouzaki, M., Ogawa, M., Akima, H., & Moritani, T. (2016). Age-related changes in motor unit firing pattern of vastus lateralis muscle during low-moderate contraction. *Age (Dordrecht, Netherlands), 38*(3), 48. https://doi.org/10.1007/s11357-016-9915-0

459. Watanabe, R. N., & Kohn, A. F. (2015). Fast Oscillatory Commands from the Motor Cortex Can Be Decoded by the Spinal Cord for Force Control. *The Journal of neuroscience : the official journal of the Society for Neuroscience, 35*(40), 13687–13697. https://doi.org/10.1523/JNEUROSCI.1950-15.2015

460. Webber, C. L., Jr, & Zbilut, J. P. (1994). Dynamical assessment of physiological systems and states using recurrence plot strategies. *Journal of applied physiology (Bethesda, Md. : 1985), 76*(2), 965–973. https://doi.org/10.1152/jappl.1994.76.2.965

461. Weibel, E. R., & Gomez, D. M. (1962). Architecture of the human lung. Use of quantitative methods establishes fundamental relations between size and number of lung structures. *Science (New York, N.Y.), 137*(3530), 577–585. https://doi.org/10.1126/science.137.3530.577

462. Weir J. P. (2005). Quantifying test-retest reliability using the intraclass correlation coefficient and the SEM. *Journal of strength and conditioning research, 19*(1), 231–240. https://doi.org/10.1519/15184.1

463. Welsh, S. J., Dinenno, D. V., & Tracy, B. L. (2007). Variability of quadriceps femoris motor neuron discharge and muscle force in human aging. *Experimental brain research, 179*(2), 219–233. https://doi.org/10.1007/s00221-006-0785-z

464. Westgaard, R. H., & De Luca, C. J. (2001). Motor control of low-threshold motor units in the human trapezius muscle. *Journal of neurophysiology, 85*(4), 1777–1781. https://doi.org/10.1152/jn.2001.85.4.1777

465. Whipp, B. J., Davis, J. A., & Wasserman, K. (1989). Ventilatory control of the 'isocapnic buffering' region in rapidly-incremental exercise. *Respiration physiology, 76*(3), 357–367. https://doi.org/10.1016/0034-5687(89)90076-5

466. Williams, M. E., Hadler, N. M., & Earp, J. A. (1982). Manual ability as a marker of dependency in geriatric women. *Journal of chronic diseases, 35*(2), 115–122. https://doi.org/10.1016/0021-9681(82)90112-6

467. Winter, D. A. (1995). Human balance and posture control during standing and walking. *Gait & posture, 3*(4), 193-214.

468. Winter, D. A., Patla, A. E., Ishac, M., & Gage, W. H. (2003). Motor mechanisms of balance during quiet standing. *Journal of electromyography and kinesiology : official journal of the International Society of Electrophysiological Kinesiology, 13*(1), 49–56. https://doi.org/10.1016/s1050-6411(02)00085-8

469. Wroblewski, A. P., Amati, F., Smiley, M. A., Goodpaster, B., & Wright, V. (2011). Chronic exercise preserves lean muscle mass in masters athletes. *The Physician and sports medicine, 39*(3), 172–178. https://doi.org/10.3810/psm.2011.09.193

470. Wu, R., Delahunt, E., Ditroilo, M., Ferri Marini, C., & De Vito, G. (2019a). Torque steadiness and neuromuscular responses following fatiguing concentric exercise of the knee extensor and flexor muscles in young and older individuals. *Experimental gerontology, 124,* 110636. https://doi.org/10.1016/j.exger.2019.110636

471. Wu, R., Delahunt, E., Ditroilo, M., Lowery, M. M., Segurado, R., & De Vito, G. (2019b). Changes in knee joint angle affect torque steadiness differently in young and older individuals. *Journal of electromyography and kinesiology : official journal of the International Society of Electrophysiological Kinesiology, 47,* 49–56. https://doi.org/10.1016/j.jelekin.2019.05.010

472. Yao, W., Fuglevand, R. J., & Enoka, R. M. (2000). Motor-unit synchronization increases EMG amplitude and decreases force steadiness of simulated contractions. *Journal of neurophysiology, 83*(1), 441–452. https://doi.org/10.1152/jn.2000.83.1.441

473. Yentes, J. M., & Raffalt, P. C. (2021). Entropy Analysis in Gait Research: Methodological Considerations and Recommendations. *Annals of biomedical engineering, 49*(3), 979–990. https://doi.org/10.1007/s10439-020-02616-8

474. Yeung, S. S. Y., Reijnierse, E. M., Pham, V. K., Trappenburg, M. C., Lim, W. K., Meskers, C. G. M., & Maier, A. B. (2019). Sarcopenia and its association with falls and fractures in older adults: A systematic review and meta-analysis. *Journal of cachexia, sarcopenia and muscle, 10*(3), 485–500. https://doi.org/10.1002/jcsm.12411

475. Yoon, T., Vanden Noven, M. L., Nielson, K. A., & Hunter, S. K. (2014). Brain areas associated with force steadiness and intensity during isometric ankle dorsiflexion in men and women. *Experimental brain research, 232*(10), 3133–3145. https://doi.org/10.1007/s00221-014-3976-z

476. Yoshimura, Y., Wakabayashi, H., Bise, T., & Tanoue, M. (2018). Prevalence of sarcopenia and its association with activities of daily living and dysphagia in convalescent rehabilitation ward inpatients. *Clinical nutrition (Edinburgh, Scotland), 37*(6 Pt A), 2022–2028. https://doi.org/10.1016/j.clnu.2017.09.009

477. Young, A., Stokes, M., & Crowe, M. (1984). Size and strength of the quadriceps muscles of old and young women. *European journal of clinical investigation, 14*(4), 282–287. https://doi.org/10.1111/j.1365-2362.1984.tb01182.x

478. Yu, F., Hedström, M., Cristea, A., Dalén, N., & Larsson, L. (2007). Effects of ageing and gender on contractile properties in human skeletal muscle and single fibres. *Acta*

physiologica (Oxford, England), 190(3), 229–241. https://doi.org/10.1111/j.1748-1716.2007.01699.x

479. Zampieri, S., Pietrangelo, L., Loefler, S., Fruhmann, H., Vogelauer, M., Burggraf, S., Pond, A., Grim-Stieger, M., Cvecka, J., Sedliak, M., Tirpáková, V., Mayr, W., Sarabon, N., Rossini, K., Barberi, L., De Rossi, M., Romanello, V., Boncompagni, S., Musarò, A., Sandri, M., … Kern, H. (2015). Lifelong physical exercise delays age-associated skeletal muscle decline. *The journals of gerontology. Series A, Biological sciences and medical sciences, 70*(2), 163–173. https://doi.org/10.1093/gerona/glu006

480. Zhou, J., Habtemariam, D., Iloputaife, I., Lipsitz, L. A., & Manor, B. (2017). The Complexity of Standing Postural Sway Associates with Future Falls in Community-Dwelling Older Adults: The MOBILIZE Boston Study. *Scientific reports, 7*(1), 2924. https://doi.org/10.1038/s41598-017-03422-

Appendix

Chapter Seven

Part A

Digital filtering of isometric precision pinch grip force signals.

7.1a - Introduction

The miniature button load cell system (Applied Measurements Ltd, Berkshire, UK), used for the measurement of isometric precision PG muscle force signals during the experimental Chapter Seven, produced a signal with baseline noise around the frequencies of 50 Hz, 150 Hz and between 200 and 250 Hz (Figure 7.1a.A). Therefore, to ensure the complexity, entropy and variability of the signals collected during the experimental trial were physiological in nature and not altered by artificial system noise, the isometric PG force signals were digitally filtered with a low-pass 2nd order Butterworth filter prior to analysis.

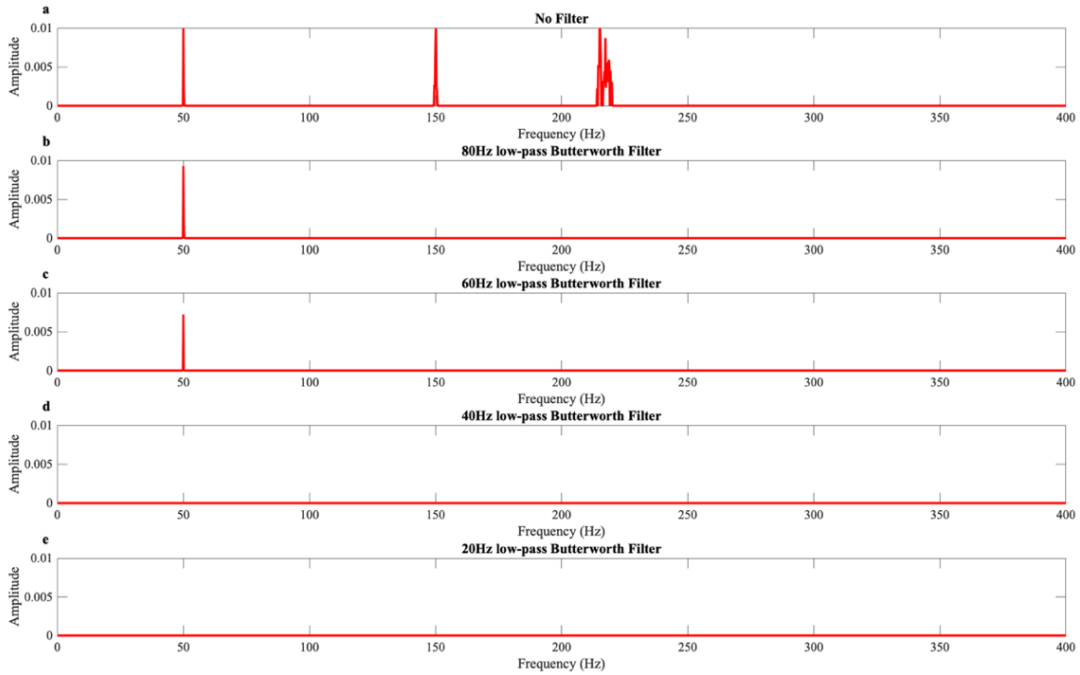

Figure 7.1a. Frequency spectrums derived from the miniature button load cell system at baseline **(A)** No filter, **(B)** 80Hz low-pass Butterworth filter, **(C)** 60Hz low-pass Butterworth filter, **(D)** 40Hz low-pass Butterworth filter, **(E)** 20Hz low-pass Butterworth filter.

Butterworth filters are commonly used on force signals to attenuate or reduce certain frequencies in the signal, while maintaining a relatively constant amplitude for signal frequencies within the passband. The low-pass cut-off frequencies applied to force signals in the literature generally range from 25.6 Hz to 80 Hz (Forrest et al., 2014) and is likely determined by the baseline system noise of the measurement device and the desired frequency the researchers are looking to capture in their subsequent analysis of the signal. However, it is important to note the application of a filter to a force signal has been shown to change the ApEn of the signal (Forrest et al., 2014). Indeed, over filtering a physiological signal could also potentially remove important physiological information and likely influence the outcome of a study.

The aim of the current study was to assess the effect of filtering frequency on the complexity, entropy and variability of the isometric precision PG force signals and therefore determine the appropriate cut-off frequency for the Butterworth filter in experimental Chapter Seven. The precision PG force data of $N = 64$ participants collected during experimental Chapter Seven were analysed at four low-pass cut-off frequencies using a Butterworth filter. The frequencies applied were 80 Hz and 60 Hz, chosen to allow some system noise to pass through the filter (as shown by the frequency spectrums in figures 7.1a.B and 7.1a.C) and 40 Hz and 20 Hz chosen to attenuate all system noise (as shown by the frequency spectrums in figures 7.1a.D and 7.1a.E). Figures 7.2a.A to C illustrate how the force signal is "cleaned" of system noise by the application of the Butterworth filters.

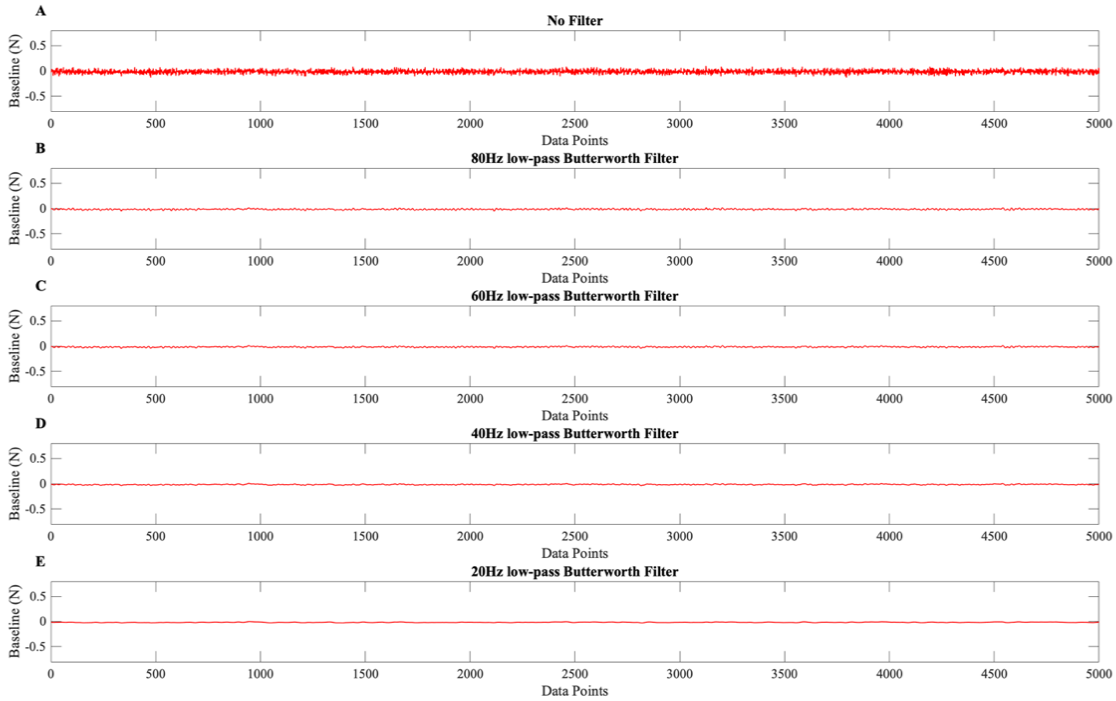

Figure 7.2a. Baseline signal from the miniature button load cell system **(A)** No filter, **(B)** 80Hz low-pass Butterworth filter, **(C)** 60Hz low-pass Butterworth filter, **(D)** 40Hz low-pass Butterworth filter, **(E)** 20Hz low-pass Butterworth filter.

Aims and Hypothesis.

The study aimed to assess the effect of the digital filtering frequency cut-off on the complexity entropy and variability of isometric precision PG force signals. It was hypothesised that lowering the frequency cut-off of the Butterworth filter would reduce the complexity, entropy and variability of the isometric precision PG force signals.

7.2a - Methods

7.2.1. Participants.

The data from sixty-four healthy individuals (38 male; 26 female) recruited to participate in the study of Chapter Seven were used in the current study. Participants were divided into four age groups, the YG were aged 18 to 30 years (N = 16; 10M, 6F), the 50 year old group were aged 50 to 59 years (N = 16; 6M, 10F), the 60 year old group were aged 60 to 69 years (N = 16; 10M, 6F) and the 70 year old group were aged 70 to 85 years (N = 16; 12M, 4F).

7.2.2. Experimental Design.

Participants completed four isometric precision PG contractions at eight relative contraction intensities (5, 10, 15, 20, 30, 40, 50 and 60% MVF). From the isometric precision PG force control tasks, the force signal complexity, entropy and variability metrics were calculated. See Chapter Seven for full methods.

7.2.3. Digital filtering of the precision pinch grip force signals.

Prior to the calculation of the complexity, entropy and variability metrics, a 2nd order Butterworth filter with a low-pass cut-off at either 80 Hz, 60 Hz, 40 Hz and 20 Hz was applied to the isometric precision PG muscle force signals

7.2.4. Force signal complexity, entropy, and variability metric analysis.

The steadiest 5 seconds of each contraction was then identified as the 5 seconds with the lowest SD from which the complexity, entropy and variability metrics were calculated. The SDF and CVF which quantify the variability of force signal were calculated as outlined in Chapter Three - General Methods - Section 3.8. The complexity and entropy metrics, SampEn, DFA, MSE and CI-28 were calculated as outlined in Chapter Three - General Methods - Section 3.9. For each contraction intensity, the two most accurate contractions (identified as the contractions with the lowest RMSE) were selected. The mean of these two contractions was then calculated and used as the participant's complexity, entropy and variability metric values for statistical analysis.

7.2.5. Statistical analysis.

The effect of Butterworth filter frequency (80, 60, 40 and 20 Hz) at each precision PG contraction intensity (5, 10, 15, 20, 30, 40, 50 and 60% MVF) on the complexity, entropy and variability metrics were assessed using a two-way repeated measures ANOVA.

The effect of filter frequency on the behaviour of the MSE curves was assessed using a three-way ANOVA, Butterworth filter frequency (80, 60, 40 and 20 Hz) by coarse-grained scale (1 to 28) by precision PG contraction intensity (5, 10, 15, 20, 30, 40, 50 and 60% MVF).

To assess whether filter frequency affected the behaviour of each age groups MSE curves at each contraction intensity, mixed-design three-way ANOVAs were performed, with Butterworth filter frequency (80, 60, 40 and 20 Hz) by coarse-grained scale (1 to 28) as the within-subjects factor and age-group (YG vs. 50 year vs. 60 year vs. 70 year) as the between-subjects factor.

Partial eta squared (η_p^2; interpreted as: 0.01 small effect, 0.06 medium effect, 0.14 large effect) was used to assess effect sizes. Bonferroni *post hoc* comparisons were used when a main effect or interaction was significant. The significance level was set at $P < 0.05$ in all cases. Statistical analyses were performed in IBM SPSS statistics 29 (IBM Corp., Armonk, NY, United States).

7.3a - Results

Table 7.1a displays the descriptive statistics and ANOVA for the effect of Butterworth filter frequency and contraction intensity on the complexity, entropy and variability of the isometric precision PG force signals.

There was a significant main effect of Butterworth filter frequency on the SDF ($P = 0.026$), SampEn ($P < 0.001$), DFA ($P < 0.001$), and CI-28 ($P < 0.001$; Table 7.1a). There was no significant main effect of Butterworth filter frequency on PG force ($P = 0.607$) and the CVF ($P = 0.056$; Table 7.1a). Across all contraction intensities lowering the Butterworth filter frequency resulted in a lower SampEn and CI-28, and a higher DFA. There was a significant main effect of contraction intensity on all complexity, entropy and variability metrics ($P < 0.001$; Table 7.1a).

There was a significant Butterworth filter frequency by contraction intensity interaction for the SDF ($P = 0.048$), CVF ($P < 0.001$), SampEn ($P < 0.001$), DFA ($P < 0.001$), and CI-28 ($P < 0.001$; Table 7.1a). In all cases the Butterworth filter frequency resulted in a greater absolute change in all metrics at lower contraction intensities, in comparison to higher contraction intensities. There was no Butterworth filter frequency by contraction intensity interaction for PG force ($P = 0.245$; Table 7.1a).

The analysis of the MSE curves revealed a significant main effect of Butterworth filter frequency ($F = 117.729$; $P < 0.001$; $\eta_p^2 = 0.194$; Figure 7.3a), a significant Butterworth filter frequency by coarse-grained scale interaction ($F = 16.194$; $P < 0.001$; $\eta_p^2 = 0.032$), and a significant Butterworth filter frequency by contraction intensity interaction ($F = 1.578$; $P = 0.047$; $\eta_p^2 = 0.022$). *Post hoc* pairwise comparisons revealed the 20 Hz filter to present with significantly lower SampEn across all coarse-grained scales and at all contraction intensities in comparison to the 40 Hz filter ($P < 0.001$), 60 Hz filter ($P < 0.001$) and 80 Hz filter ($P < 0.001$). The SampEn of the 40 Hz filter was significantly lower from scales 13 to 15 in comparison to the 80 Hz filter ($P < 0.05$). There were no significant differences between the 60 and 80 Hz filters at all coarse-grained scales and all contraction intensities ($P > 0.05$).

Table 7.1a Descriptive statistics and ANOVA results for the effect of Butterworth filter frequency and contraction intensity on the complexity, entropy and variability of the isometric precision pinch grip force signals.

		Contraction Intensity								*F, P* and η_p^2 values			
		5% MVF	10% MVF	15% MVF	20% MVF	30% MVF	40% MVF	50% MVF	60% MVF		Main effect of filter	Main effect of intensity	Filter by Intensity Interaction
Force (N)	80 Hz	0.56±0.20	1.17±0.39	1.77±0.58	2.36±0.78	3.54±1.19	4.72±1.60	5.90±2.00	7.05±2.42	*F*	0.613	470.464	1.417
	60 Hz	0.57±0.20	1.17±0.39	1.77±0.58	2.36±0.78	3.55±1.17	4.72±1.59	5.90±1.98	7.06±2.44	*P*	0.607	**< 0.001**	0.245
	40 Hz	0.56±0.20	1.17±0.39	1.77±0.58	2.36±0.78	3.54±1.19	4.72±1.60	5.89±1.99	7.06±2.43	η_p^2	0.010	0.889	0.023
	20 Hz	0.56±0.20	1.17±0.39	1.77±0.58	2.36±0.78	3.54±1.19	4.72±1.60	5.89±1.99	7.06±2.43				
SDF (N)	80 Hz	0.04±0.01	0.05±0.02	0.05±0.02	0.07±0.04	0.11±0.06	0.15±0.09	0.18±0.11	0.22±0.12	*F*	5.118	86.043	3.016
	60 Hz	0.04±0.02	0.05±0.02	0.05±0.02	0.07±0.04	0.11±0.06	0.16±0.09	0.20±0.13	0.23±0.12	*P*	**0.026**	**< 0.001**	**0.048**
	40 Hz	0.03±0.02	0.05±0.02	0.05±0.02	0.07±0.04	0.11±0.06	0.16±0.09	0.20±0.13	0.23±0.12	η_p^2	0.080	0.593	0.049
	20 Hz	0.03±0.02	0.04±0.02	0.05±0.02	0.07±0.04	0.11±0.06	0.16±0.09	0.19±0.13	0.23±0.12				
CVF (%)	80 Hz	7.05±3.25	4.25±2.03	3.28±1.49	3.13±1.43	3.19±1.53	3.31±1.70	3.22±1.80	3.36±1.84	*F*	3.395	44.846	6.509
	60 Hz	7.21±3.71	4.30±1.94	3.31±1.37	3.22±1.38	3.35±1.67	3.36±1.50	3.45±1.99	3.51±1.80	*P*	0.056	**< 0.001**	**< 0.001**
	40 Hz	6.56±2.91	4.16±1.87	3.27±1.39	3.18±1.38	3.23±1.50	3.42±1.66	3.46±1.99	3.49±1.80	η_p^2	0.054	0.432	0.099
	20 Hz	6.34±2.85	4.10±1.86	3.23±1.39	3.15±1.38	3.22±1.50	3.41±1.66	3.45±1.99	3.48±1.81				
SampEn	80 Hz	0.64±0.09	0.58±0.10	0.54±0.11	0.47±0.14	0.38±0.14	0.31±0.15	0.27±0.13	0.23±0.12	*F*	763.153	187.495	99.639
	60 Hz	0.56±0.10	0.48±0.11	0.44±0.13	0.37±0.15	0.27±0.13	0.23±0.13	0.19±0.10	0.16±0.09	*P*	**< 0.001**	**< 0.001**	**< 0.001**
	40 Hz	0.38±0.12	0.29±0.12	0.26±0.12	0.21±0.12	0.15±0.10	0.12±0.08	0.11±0.06	0.09±0.04	η_p^2	0.928	0.761	0.628
	20 Hz	0.12±0.06	0.08±0.03	0.08±0.05	0.07±0.04	0.06±0.03	0.06±0.03	0.06±0.03	0.06±0.03				
DFA α	80 Hz	1.17±0.11	1.27±0.11	1.31±0.11	1.37±0.11	1.44±0.10	1.47±0.11	1.48±0.10	1.50±0.10	*F*	451.439	94.409	114.556
	60 Hz	1.23±0.10	1.33±0.10	1.37±0.11	1.42±0.11	1.49±0.10	1.51±0.11	1.51±0.10	1.53±0.10	*P*	**< 0.001**	**< 0.001**	**< 0.001**
	40 Hz	1.31±0.10	1.41±0.09	1.44±0.10	1.48±0.10	1.54±0.10	1.56±0.11	1.55±0.10	1.56±0.10	η_p^2	0.884	0.615	0.660
	20 Hz	1.45±0.10	1.53±0.08	1.55±0.10	1.58±0.09	1.61±0.10	1.61±0.11	1.59±0.10	1.59±0.10				
CI-28	80 Hz	50.22±9.12	43.83±8.33	41.41±8.87	37.32±9.90	31.75±9.23	29.36±9.31	28.72±8.89	26.63±8.20	*F*	633.612	73.768	132.457
	60 Hz	45.96±8.69	39.81±7.96	37.69±8.64	33.55±9.83	28.17±8.66	26.58±8.58	25.97±8.71	24.09±7.81	*P*	**< 0.001**	**< 0.001**	**< 0.001**
	40 Hz	40.79±8.74	34.47±7.64	32.55±8.18	28.92±9.02	24.73±8.09	23.30±7.77	23.28±8.17	21.95±7.25	η_p^2	0.915	0.556	0.692
	20 Hz	28.36±7.38	23.57±5.69	22.83±6.51	20.64±6.85	18.73±6.66	18.67±6.62	19.45±6.96	19.11±6.57				

Abbreviations: CI-28 = complexity index under 28 scales; CVF = coefficient of variation of force; DFA = detrended fluctuation analysis scaling exponent α; MVF = maximal voluntary force; SampEn = sample entropy; SDF = standard deviation of force; Significant *P* values highlighted by bold font; data are mean ± SD.

There was a significant main effect of coarse-grained scale (F = 1440.813; P < 0.001; η_p^2 = 0.747), and a significant main effect of contraction intensity (F = 54.177; P < 0.001; η_p^2 = 0.437) on SampEn (Figures 7.3a and 7.4a). There was significant coarse-grained scale by contraction intensity interaction (F = 13.222; P < 0.001; η_p^2 = 0.159), and a significant Butterworth filter frequency by coarse-grained scale interaction by contraction intensity interaction (F = 1.525; P = 0.020; η_p^2 = 0.021). Figure 7.3a. presents MSE curves calculated from all participants (N = 64) precision PG force signals at all contraction intensities filtered at 80, 60, 40 and 20 Hz.

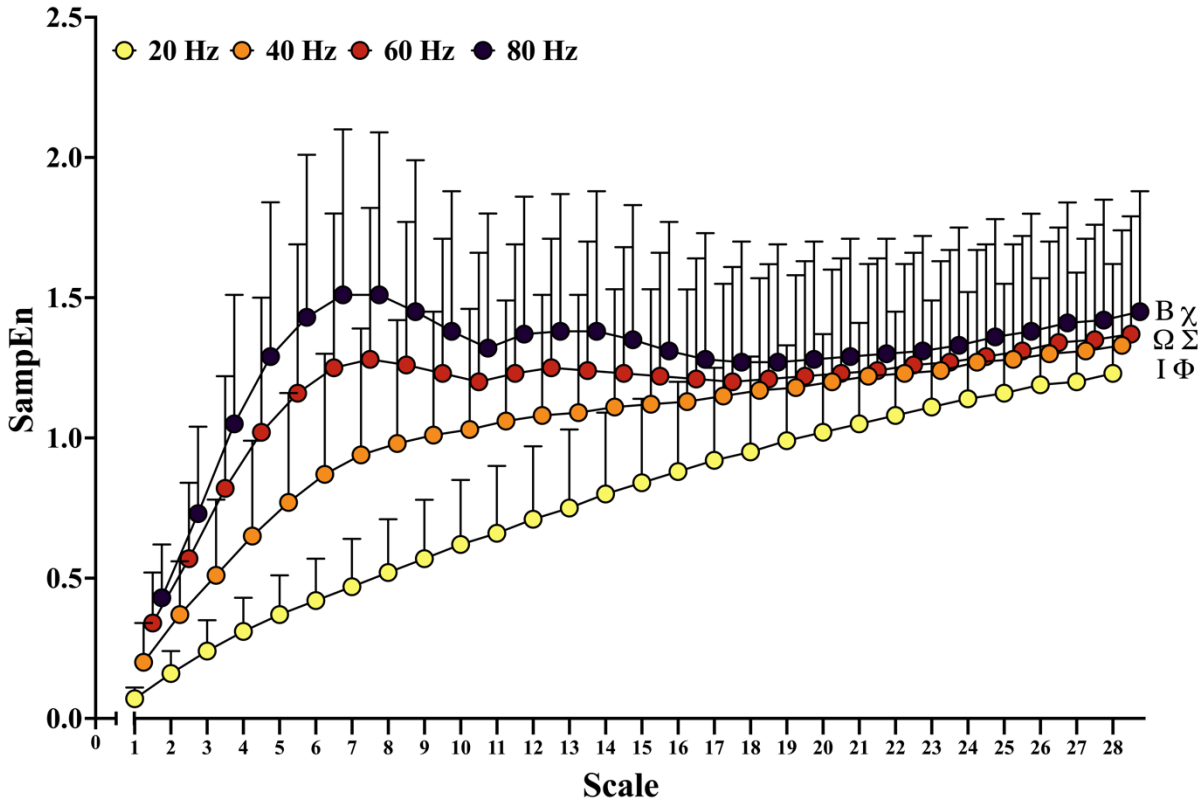

Figure 7.3a. Multiscale entropy curves derived from precision pinch grip force at all contraction intensities Butterworth filtered at 80, 60, 40 and 20 Hz (SampEn = Sample Entropy; B = main effect of Butterworth filter frequency; I = significant main effect of contraction intensity; Ω = significant main effect of coarse-grained scale; χ = significant Butterworth filter frequency by coarse-grained scale interaction; Φ = significant coarse-grained scale by contraction intensity interaction; Σ = significant Butterworth filter frequency by contraction intensity interaction).

Figure 7.4a. presents individual MSE curves for each contraction intensity derived from the precision PG force signals low-pass Butterworth filtered at the 80, 60, 40 and 20 Hz cut-offs.

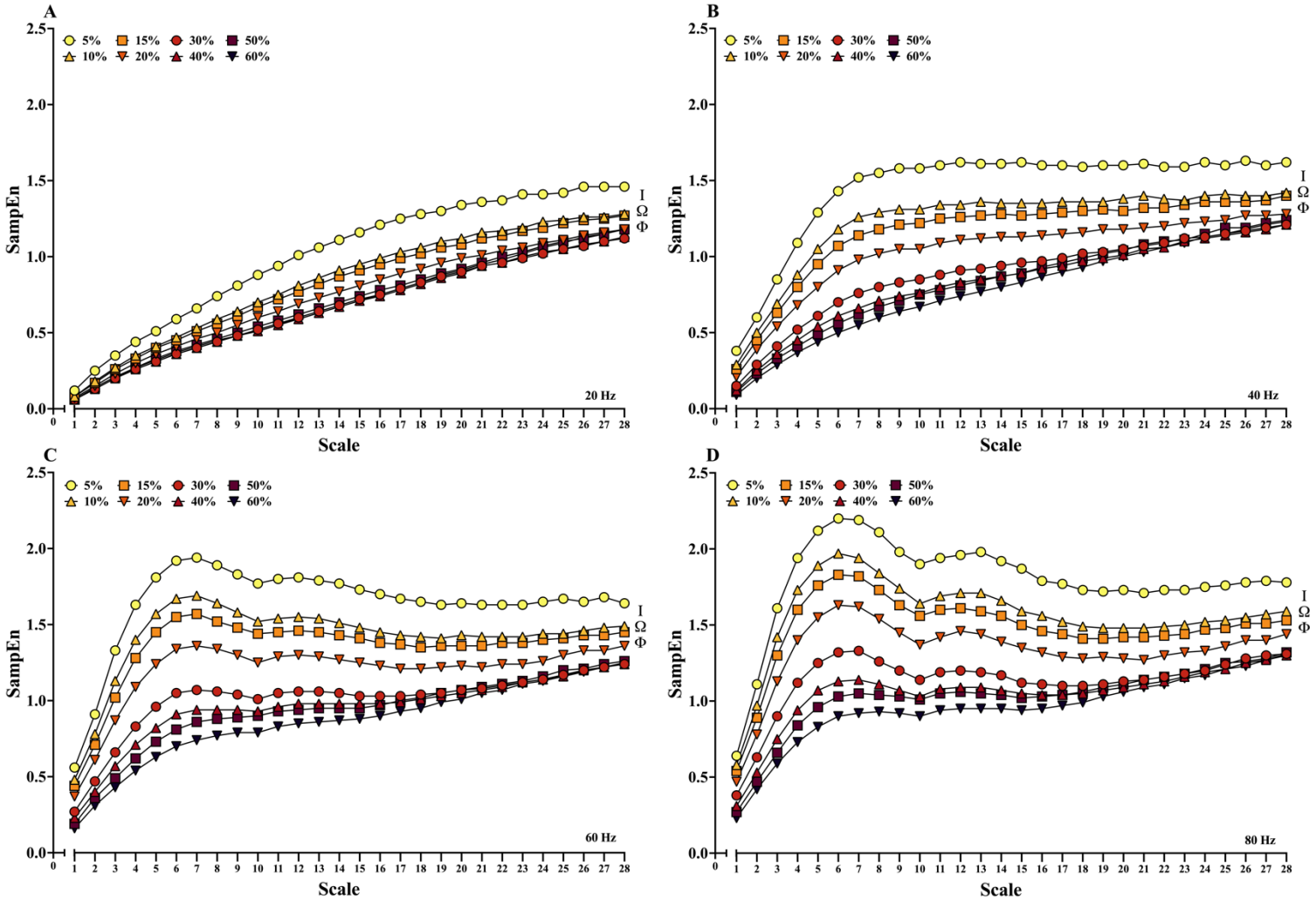

Figure 7.4a. Multiscale entropy curves at each contraction intensity derived from precision pinch grip force data low-pass Butterworth filtered at **(A)** 20 Hz, **(B)** 40 Hz, **(C)** 60 Hz, **(D)** 80 Hz (error bars were removed for clarity; SampEn = Sample Entropy; I = significant main effect of contraction intensity; Ω = significant main effect of coarse-grained scale; Φ = significant coarse-grained scale by contraction intensity interaction).

The Butterworth filter frequencies had the same effect on the behaviour of each age groups MSE curves (i.e., filter frequency by coarse-grained scale by age group interaction) at 5% MVF ($F = 0.978$; $P = 0.583$; $\eta_p^2 = 0.047$), 10% MVF ($F = 1.583$; $P = 0.089$; $\eta_p^2 = 0.076$), 15% MVF ($F = 1.294$; $P = 0.215$; $\eta_p^2 = 0.061$), 20% MVF ($F = 1.215$; $P = 0.280$; $\eta_p^2 = 0.057$), 30% MVF ($F = 0.978$; $P = 0.461$; $\eta_p^2 = 0.047$), 40% MVF ($F = 1.148$; $P = 0.337$; $\eta_p^2 = 0.054$), 50% MVF ($F = 1.271$; $P = 0.270$; $\eta_p^2 = 0.062$), and 60% MVF ($F = 1.482$; $P = 0.188$; $\eta_p^2 = 0.071$).

7.4a - Discussion

To establish an appropriate Butterworth filter cut-off frequency for the isometric precision PG force derived from the miniature button load cell system, the isometric precision PG force data of $N = 64$ participants collected during the study presented in Chapter Seven was analysed using four low-pass cut-off frequencies, 80, 60, 40 and 20 Hz. Main findings show that Butterworth filter frequency significantly changes all complexity, entropy and variability metrics, apart from the CVF (Table 7.1a).

The 80 and 60 Hz Butterworth filters allowed some major system noise (50 Hz) to pass through into the signal, therefore the higher complexity and entropy (i.e., lower DFA and higher mean CI-28 and SampEn) in comparison to the 40 and 20 Hz filters can most likely be attributed to the system noise artificially altering the information content and structure of the signal. Indeed, the effect of allowing the noise at 50 Hz into the signal by using the 80 and 60 Hz filter can be seen in MSE curves presented Figures 7.3a and 7.4a, whereby the 80 and 60 Hz filters have a notably higher SampEn up to scale 20, in comparison to the 40 and 20 Hz filters. The coarse-graining procedure used in the MSE analysis effectively acts as a low-pass filter, therefore at shorter scales (i.e., < 20 scales) the SampEn derived from the force signals filtered at 80 and 60 Hz were likely being artificially elevated by the system noise. However, coarse graining above scale 20 (when sampling force output at 1000 Hz) will begin to attenuate fluctuations in the signal greater than 50 Hz. Hence why the 80, 60 and 40 Hz MSE curves converge beyond scale 20 (Figure 7.3a).

The 40 and 20 Hz filters should have attenuated all major system noise (as shown by the frequency spectrums in Figures 7.1a.D and 7.1a.E). The lower complexity and entropy metrics derived from the force signals filtered at 20 Hz when compared to the force signals filtered at 40 Hz (Table 7.1a) is therefore likely explained by the removal of important information and structure in the force signals, which should theoretically be physiological in nature. Low-pass filters in the 20 Hz range could be applied to the force signals, based on the rationale that they still capture the dominant physiological fluctuations in force output signals which were in the low frequency range (> 20 Hz), with fluctuations between 0 and 4 Hz related to sensorimotor processing in force control (Vaillancourt & Newell, 2003). However, based on current data it is possible that the use of the 20 Hz filter results in *over-filtering* and the likelihood of removing physiological information and structure from the signal.

7.5a - Conclusion

Choosing the appropriate digital filter cut-off frequency to *clean* physiological signals of artificial system noise is essential to ensure the complexity, entropy and variability metrics primarily capture physiological information and temporospatial structure present within the signal. The current analysis shows that the Butterworth filter cut-off frequency applied to force data collected using the miniature button load cell system significantly changes the complexity, entropy and variability metrics derived from the force signals. Based on current evidence the Butterworth low-pass cut-off filter frequency applied to the PG force data in Chapter Seven of the thesis will be 40 Hz. This is to confirm all major artificial system noise is attenuated, while ensuring that potentially important physiological information and structure in the force signals is preserved.